ADVANCES IN EXPERIMENTAL MEDICINE AND BIOLOGY

Volume 605

INTEGRATION IN RESPIRATORY CONTROL

From Genes to Systems

Edited by
Marc J. Poulin
and
Richard J. A. Wilson

Springer

Integration in Respiratory Control

ADVANCES IN EXPERIMENTAL MEDICINE AND BIOLOGY

Recent Volumes in this Series

Volume 597
TNF RECEPTOR ASSOCIATED FACTORS (TRAFs)
Edited by Hao Wu

Volume 598
INNATE IMMUNITY
Edited by John D. Lambris

Volume 599
OXYGEN TRANSPORT TO TISSUE XXVIII
Edited by David Maguire, Duane F. Bruley and David K. Harrison

Volume 600
SEMAPHORINS: RECEPTOR AND INTRACELLULAR SIGNALING MECHANISMS
Edited by R. Jeroen Pasterkamp

Volume 601
IMMUNE MEDIATED DISEASES: FROM THEORY TO THERAPY
Edited by Michael R. Shurin

Volume 602
OSTEOIMMUNOLOGY: INTERACTIONS OF THE IMMUNE AND SKELETAL SYSTEMS
Edited by Yongwon Choi

Volume 603
THE GENUS YERSINIA: FROM GENOMICS TO FUNCTION
Edited by Robert D. Perry and Jacqueline D. Fetherson

Volume 604
ADVANCES IN MOLECULAR ONCOLOGY
Edited by Fabrizio d'Adda di Gagagna, Susanna Chiocca, Fraser McBlane and Ugo Cavallaro

Volume 605
INTEGRATION IN RESPIRATORY CONTROL: FROM GENES TO SYSTEMS
Edited by Marc Poulin and Richard Wilson

Marc J. Poulin Richard J.A. Wilson
Editors

Integration in Respiratory Control

From Genes to Systems

Springer

Marc J. Poulin
University of Calgary
3330 Hospital Drive NW
Calgary T2N 4N1
Canada
poulin@ucalgary.edu

Richard J.A. Wilson
University of Calgary
3330 Hospital Drive NW
Calgary T2N 4N1
Canada
wilsonr@ucalgary.edu

ISBN-13: 978-0-387-73692-1 e-ISBN-13: 978-0-387-73693-8

Library of Congress Control Number: 2007933492

Printed on acid-free paper

9 8 7 6 5 4 3 2 1

springer.com

Preface

Like the geological treasures that surely must lie below the Athabasca glacier, some of the answers to key questions about the control of respiration remain buried. But bit by bit, year by year the ice is melting and perhaps in some areas the rocks are starting to be revealed. With a mission to advance our understanding of the emerging gems of respiration, the Xth Oxford Conference was held between 19–24th September (2006) next to the turquoise and tranquil waters of Lake Louise, in the middle of Banff National Park, Alberta, Canada.

Since its inauguration 30 years ago in Oxford, the Oxford Conference on modeling and control of breathing has been held every three years in locations spanning the globe (a list of past conferences and publications that have emerged is included in the pages that follow). The series has provided key opportunities for respiratory scientists to meet with colleagues, discuss recent advances and celebrate their field. The 2006 Lake Louise meeting was Canada's second Oxford Conference; the previous Canadian meeting (the VIIth Oxford Conference) was held in 1997 at the Grandview Inn in Huntsville (Ontario) and was chaired by Richard Hughson, David Cunningham and Jim Duffin.

In total, 277 people from 16 different countries attended the Xth Oxford Conference. Of those, 170 were full delegates (82 invited speakers), 65 were trainees (students and postdoctoral fellows), 7 were exhibitors, and 35 were guests (accompanying people and children). The attendees came from Australia, Canada, Chile, Denmark, England, France, Germany, Ireland, Japan, Mexico, The Netherlands, New Zealand, Scotland, Sweden, Switzerland, and the United States of America.

A common theme of Oxford meetings is the integration of various aspects of respiratory physiology. Thirty years ago, electrophysiology and molecular biology were in their infancy. One of the few integrative approaches available was the melding of human respiratory physiology with mathematical modeling. The first Oxford Conference brought together scientists from various parts of the world with a wide variety of experimental and theoretical approaches to the problem of the regulation of breathing. Today, many scientists work on genetic models and animal preparations to better understand the regulation of breathing. These new approaches have allowed impressive advances, providing essential tools to study aspects of breathing

ranging from genes to system. However, as our field expands into these new realms, the need to relate disparate measurements in an integrative framework is as important today as it was in those early days in Oxford.

The Xth Oxford Conference offered a unique forum for respiratory physiologists, clinicians, neurobiologists, modelers, geneticists and biomedical engineers from around the world to exchange ideas and present their latest genomic perspectives. Indeed, the importance of integration was apparent in many of the sessions at the Xth Oxford Conference. We heard, for example, how there might be multiple oxygen sensing mechanisms. Three somewhat competing hypotheses were proposed regarding the identity of the central respiratory chemoreceptor(s). There was compelling evidence to suggest generation of the respiratory rhythm might extend beyond the PreBötzinger Complex and involve more than one cellular mechanism. Ultimately, only multiple disciplinary studies, similar to those that inspired the founders of the original Oxford Conference will resolve these issues.

At the beginning of the conference we heard about the complex genetics and physiology of Rett Syndrome, a disease causing severe respiratory dysfunction. We closed with a session on clinical perspectives of breathing disordered during sleep, a phenomenon that will become all too commonplace as the obesity epidemic mounts. Both sessions serve as a reminder as to the urgency of our work and how much is still to be done.

Oxford Conferences are an important ingredient to the future success of our field. Essential to such success, will be our ability to promote the careers of our trainees. At the Xth Oxford Conference, we held a competition to select trainees to present their work orally in a special symposium. An international panel of senior researchers served as judge and jury (the names of those on the selection committee are listed in the pages that follow). The six finalists included Trevor Day (University of Calgary, Calgary, Canada; 1st place), Harold Bell (University of Calgary, Calgary, Canada; 2nd place), Christopher Wyatt (St. Andrews University, St. Andrews, Scotland, 3rd place), Glen Foster (University of Calgary, Calgary, Canada; finalist), Lynn Hartzler (Wright State University, Dayton, USA; finalist) and Jun Ren (University of Alberta, Edmonton, Canada; finalist). We would like to congratulate and thank each of the 62 trainee participants: the standard was remarkable.

The success of the Xth meeting was the direct result of the hard work of our dedicated staff which included Linda Brigan (conference coordinator), Carly McMorris, Sherry Moore and Cherise Klotz. Special thanks to the members of the local and international organizing committees for their support and guidance and to Linda Brigan and Marnie Cudmore for editorial assistance in the production of this book.

We look forward to seeing you all at the XIth Oxford Conference that will take place in Nara City, near Kyoto, Japan in 2009!

Co-Chairs, Xth Oxford Conference Marc Poulin and Richard Wilson

Conference Proceedings

19–24 September 2006
Fairmont Chateau Lake Louise
Lake Louise, Alberta, Canada

Conference Co-Chairs : Marc J. Poulin (Calgary, Canada)
Richard J.A. Wilson (Calgary, Canada)

The Xth Oxford Conference: International Organizing Committee

Pierre Baconnier
Faculté de Médecine
Univ. Joseph Fourier Grenoble
Domaine de la Merci
La Tronche, 38700, France

Jean Champagnat
Neurobiologie Génétique et
Intégrative, C.N.R.S.
1 Avenue de la Terrasse
91 198, Gif-sur-Yvette, France

Ikuo Homma
Department of Physiology
Showa University School of Medicine
Hatanodai 1-5-8, Shinagawa-Ku
Tokyo 142-8555, Japan

Richard L. Hughson
Faculty of Applied Health Sciences
University of Waterloo
Waterloo, Ontario
Canada

Homayoun Kazemi
Pulmonary and Critical Care Unit
Harvard Medical School
Bulfinch 148
Massachusetts General Hospital
Boston, MA, 02114, USA

Chi-Sang Poon
Harvard-MIT Division of Health
Sciences & Technology
Bldg. E25-501, Massachusetts
Institute of Technology
77 Massachusetts Avenue
Cambridge, MA, 02139, USA

Marc J. Poulin
Department of Physiology &
Biophysics
Faculty of Medicine, University
of Calgary
3330 Hospital Drive NW
Calgary, Alberta
T2N 4N1, Canada

Peter A. Robbins
University Laboratory of Physiology
University of Oxford
Parks Road
Oxford OX1 3PT,
United Kingdom

Peter Scheid
Institute für Physiologie
Ruhr-Universität Bochum
In Der Russbreite 10
Goettingen 37077, Germany

John W. Severinghaus
Department of Anesthesiology
University of California Medical School
PO Box 974
Ross, CA 94957,
USA

Susan A. Ward
Institute of Membrane & Systems Biology
Sport & Exercise Sciences
University of Leeds
Leeds, LS2 9JT, United Kingdom

Brian J. Whipp
Institute of Membrane & Systems Biology
Sport & Exercise Sciences
University of Leeds
Leeds, LS2 9JT, United Kingdom

Richard J.A. Wilson
Department of Physiology & Biophysics
Faculty of Medicine, University of Calgary
3330 Hospital Drive NW
Calgary, Alberta
T2N 4N1, Canada

The Xth Oxford Conference: Local Organizing Committee

Dr. Klaus Ballanyi
Department of Physiology
University of Alberta
HMRC Room 232D
Edmonton, Alberta
T6G 2S2, Canada

Dr. Gordon Ford
Faculty of Medicine
University of Calgary
Calgary, Alberta,
Canada

Dr. Greg Funk
Department of Physiology
University of Alberta
Rm 7-50 Medical Science Bldg
Edmonton, Alberta
T6G 2H7, Canada

Dr. John Greer
Department of Physiology
University of Alberta
513 HMRC Bldg
Edmonton, Alberta
T6G 2S2, Canada

Dr. Richard Leigh
Faculty of Medicine
University of Calgary
Calgary, Alberta, Canada

Dr. Marc Poulin
Co-Chair – Xth Oxford Conference
Department of Physiology & Biophysics
Faculty of Medicine
University of Calgary
3330 Hospital Drive NW
Calgary, Alberta
T2N 4N1, Canada

Dr. Neal Skjodt
Faculty of Medicine
University of Alberta
2E4.43 WMC
Edmonton, Alberta
T6G 2B7 Canada

Dr. Richard Wilson
Co-Chair - Xth Oxford Conference
Department of Physiology & Biophysics
Faculty of Medicine
University of Calgary
3330 Hospital Drive NW
Calgary, Alberta
T2N 4N1, Canada

CONFERENCE COORDINATOR

Mrs. Linda Brigan
University of Calgary

CONFERENCE ASSISTANTS

Ms. Carly McMorris
University of Calgary

Ms. Jane Dunstan
AHFMR Summer Student (2006)
Dalhousie University

Ms. Cherise Klotz
University of Calgary

Ms. Sherry Moore
University of Calgary

WEBSITE COORDINATOR

Mr. Kevin Ho
University of Calgary

SPECIAL LIAISONS

Dr. Serdia Mack
Department of Physiology and Biophysics, Howard University
520 W Street NW
Washington, DC 20059
USA

Dr. Musa Haxhiu
Department of Pediatrics
Case Western Reserve University
11100 Euclid Ave
Cleveland, OH 44106
USA

The Xth Oxford Conference: Young Investigator Awards Selection Committee

Dr. Gerald Bisgard (Chair)
Department of Comparative Biosciences
University of Wisconsin-Madison
2015 Linden Dr.
Madison, Wisconsin
53706, USA

Dr. Jerome Dempsey
Department of Population Health Science
University of Wisconsin
1300 University Ave
Madison, Wisconsin
53706, USA

Dr. Hubert Forster
Department of Physiology
Wisconsin Medical College
8701 Watertown Plank Road
Milwaukee, Wisconsin
53226, USA

Dr. Bruce Lindsey
Department of Molecular Pharmacology and Physiology
University of Southern Florida Health
12901 Bruce B Downs Blvd
Tampa, Florida
33612, USA

Dr. Peter Scheid
Department of Physiology
Ruhr-Universitaët Bochum
In Der Russbreite 10
Goettingen 37077
Germany

Dr. Greg Funk
Department of Physiology
University of Alberta
Rm 7-50 Medical Science Bldg
Edmonton, Alberta
T6G 2H7, Canada

Acknowledgements

The Xth Oxford Conference was hosted by the University of Calgary and the University of Alberta

The Organizing Committee gratefully acknowledges the valuable support from the following groups:

Universities
Faculty of Medicine, University of Calgary
Respiratory Research Group, University of Calgary
Hotchkiss Brain Institute, University of Calgary
Faculty of Medicine, University of Alberta
Perinatal Research Centre, University of Alberta
Centre for Neuroscience, University of Alberta
University of Alberta Conference Fund

Foundations, Granting Agencies and Societies
Alberta Heritage Foundation for Medical Research
Centre National de la Recherche Scientifique (CNRS, France)
Institute of Circulatory and Respiratory Health, Canadian Institutes of Health Research
Institute of Genetics, Canadian Institutes of Health Research
NIH/NHLBI (Conference Grant HL084900)
Rett Syndrome Research Foundation
The Physiological Society of Great Britain

Corporate Sponsors
AD Instruments
AEI Technologies
AstraZeneca
AnaSpec
Apex Audio Visual Systems Integration (AVSI)
Boehringer Ingelheim (Canada) Ltd/Ltée and Pfizer
CWE, Inc.
Elsevier Inc.

Corporate Sponsors—continued
GlaxoSmithKline Inc.
Medigas
Merck Frosst Canada & Co.
National Research Council Research Press (Canada)
Novus Biologicals, Inc.
Physiological Measurement
Springer Publishing
STARR Life Sciences Corp

Xth Oxford Conference Participants (see Color Plates)

Past Oxford Conferences

Ist Oxford Conference
University Laboratory of Physiology, Oxford, United Kingdom (September 1978)

Publication: *Modelling of a Biological Control System: The Regulation of Breathing. E.R. Carson, D.J.C. Cunningham, R. Herczynski, D.J. Murray-Smith and E.S. Peterson, eds., Oxford: Institute of Measurement and Control, 1978*

IInd Oxford Conference
University of California Conference Centre at Lake Arrowhead California, USA (13–16 September, 1982)

Publication: *Modelling and the Control of Breathing. B.J. Whipp and D.M. Wiberg, eds., Elsevier Press, New York, 1983.*

IIIrd Oxford Conference
Medieval Abbey of Solignac, Solignac, France (September 1985)

Publication: *Concepts and Formalizations in the Control of Breathing. G. Benchetrit, P. Baconnier and J. Demongeot, eds., Manchester University Press, 1987.*

IVth Oxford Conference
Shadow Cliff Life Centre at Grand Lake, Grand Lake, Colorado, USA (September 1988)

Publication: *Respiratory Control: A Modeling Perspective, G.D. Swanson, F.S. Grodins, and R.L. Hughson, eds., Plenum Press, New York, 1989.*

Vth Oxford Conference
Fuji Institute, Fuji, Japan (1991)

Publication: *Control of Breathing and its Modelling Perspective Y. Honda, Y.Miyamoto, K. Konno and J. Widdicombe, eds., Plenum Press, New York. 1992.*

VIth Oxford Conference
Royal Holloway College, Egham, Surrey, United Kingdom (September, 1994)

Publication: *Modeling and Control of Ventilation (Advances in Experimental Medicine and Biology series, Vol. 393). S.J.G. Semple, L. Adams, and B.J. Whipp, eds., Plenum Press, New York, 1995.*

VIIth Oxford Conference
Grandview Inn, Huntsville, Ontario, Canada (September, 1997)

Publication: *Advances in Modeling and Control of Ventilation (Advances in Experimental Medicine and Biology series, Vol. 450). R.L. Hughson, D.A. Cunningham, and J. Duffin, eds., Plenum Press, New York, 1998.*

VIIIth Oxford Conference
North Falmouth, Cape Cod, Massachusetts, USA (11–15 October, 2000)

Publication: *Frontiers in Modeling and Control of Breathing: Integration at Molecular, Cellular, and Systems Levels (Advances in Experimental Medicine and Biology series, Vol. 499). C.-S. Poon and H. Kazemi, eds., Kluwer Academic/ Plenum Publishers, New York, 2001.*

IXth Oxford Conference
Paris, France (September, 2003)

Publication: *Post-Genomic Perspectives in Modeling and Control of Breathing (Advances in Experimental Medicine and Biology series, Vol. 551). J. Champagnat, M. Denavit-Saubié, G. Fortin, A.S. Foutz, M. Thoby-Brisson, eds., Kluwer Academic/Plenum Publishers, New York, 2004.*

Xth Oxford Conference
Chateau Lake Louise, Lake Louise, Alberta, Canada (19–24 September, 2006)

Contents

Erratum

The article “The Cell-Vessel Architecture Model for the Central Respiratory Chemoreceptor,” published in volume 580 of Advances in Experimental Medicine and Biology (2006; pp 233–238), contained an error in the names of the article authors. The correct spelling of the authors’ names are Yasumasa Okada, Shun-ichi Kuwana, Yoshitaka Oyamada, and Zibin Chen.

Part I
Historical and Future Perspectives of the Control of Breathing

1
History of Measuring O_2 and CO_2 Responses

John W. Severinghaus

Abstract Quantitative analysis of the chemical interactions of CO_2 and O_2 on ventilation from early 20th century to the present start with the amazingly steep CO_2 response found by Haldane and his pupils, proceed through discovery of the prime role of the H^+ ion and the discovery of carotid body chemoreception. The interaction of central and peripheral drives and changes with time and acute and chronic altitude exposure are still under investigation.

1 The Steep CO_2 Response to Falling PO_2

For early references here see Kellogg's review of the history of regulation on respiration (1981). Haldane and Priestley showed the steep relation of ventilation (V_E) to PCO_2, about 3 liters per min per mm Hg. Heymans discovered peripheral hypoxic chemosensitivity. Nielsen and Smith found that hypoxia at 37 mm Hg $P_{ET}O_2$ quadrupled the CO_2 response slope. The Oxford group computed the hyperbolic effect of hypoxia on CO_2 slope. Weil, Byrne-Quinn, Sodal, Friesen, Underhill, Filley and Grover, (1970) assumed a hyperbolic asymptote at PO_2 = 32 torr, writing $V_E = A/(PaO_2\text{-}32) + B$ (resting V_E). A is V_E at PaO_2 = 33 torr, measurable as ΔV_E at PaO_2 = 40 torr (A = 8ΔV40).

2 Oximetry and the Switch to V_E vs. SaO_2

When accurate arterial blood oximetry became available, Rebuck and Campbell (1974) noted that the ventilatory response to isocapnic hypoxia was linear from 100% to 70% SaO_2. Isocapnic HVR (Hypoxic Ventilatory Response) is now defined as $\Delta V_E/\Delta SaO_2$, L/min/%, normal mean value of 1.0. If hypoxic $P_{ET}CO_2$ is

University of California San Francisco, Department of Anesthesia, jwseps@comcast.net

M.J. Poulin and R.J.A. Wilson (eds.), *Integration in Respiratory Control: From Genes to Systems*. © Springer 2008

not controlled (poikilocapnic), after 10 min of acute hypoxia at SaO_2 = 80% PCO_2 falls ~ 5 torr due to a 1 L/min rise of VE. This poikilocapnic HVR is only 1/20 of isocapnic HVR because hypocapnia inhibits about 95% of the hypoxic drive.

3 Discovery of Ventral Medullary ECF H^+ Chemoreceptors

Leusen (1954) demonstrated that perfusion of dog cerebral ventricles with a low-bicarbonate mock spinal fluid stimulated ventilation. Loeschcke, Koepchen and Gertz (1958) located maximum chemosensitivity in the lateral recesses of the 4th ventricle. Mitchell (unpublished, ~ 1957) demonstrated that $PaCO_2$ fell to normal in two patients with COPD after reduction of their elevated CSF bicarbonate using an acidified mock CSF. A new surgical approach to the ventral surface of the brain stem pioneered by Mitchell, Loeschcke, Severinghaus and Massion (1963) located the regions sensing ECF H^+. Response to ECF acid due to low HCO_3^- was greater than to high PCO_2. Topical procaine caused apnea despite penetration less than 0.35 mm.

Schlaefke, See and Loeschcke (1971) discovered a small area (S) caudal to Mitchell's area (M) lacking chemosensitivity but in which topical anesthesia or cauterization produced apnea at any PCO_2 and a second more caudal chemosensitive region (L). Recently, pH or PCO_2 sensitive ventilatory response areas have been found in several other regions of pons or medulla, but their quantitative role is not established.

Hypoxemia results in greater fall of pH on the surface over the medullary chemosensitive areas than other surfaces of the brain stem or cortex (Xu, Spellman, Sato, Baumgartner, Ciricillo and Severinghaus 1991), suggesting that the chemosensory cells do not respond to intracellularly generated (lactic) acid, and that this area has an unusually high metabolic rate.

4 Acute Hypoxic Decline (HVD, Formerly Depression)

The acute ventilatory response to isocapnic hypoxia fades over ~20 min to about half the 5 min peak response (Fig. 1) (Steinback and Poulin, 2007). This is partly due to increased medullary chemoreceptor tissue blood flow, lowering the arterial-tissue PCO_2 difference and perhaps to hypoxic chemosensor intracellular lactic acid: both effects reset the HVR control set point. HVD is reversed after 5 min of hyperoxia.

Testing of HVR should include both a 5 min isocapnic test (iHVR) to define peripheral sensitivity before HVD and a 20 min poikilocapnic test (pHVR) to simulate acclimatization (Fig. 1). After 20 min without added CO_2, the rise of ventilation is so small (~ 1 L/min) that a more robust index may be defined as $pHVR = \Delta PCO_2/\Delta SaO_2$ torr/%, with an expected normal value of about 0.25 torr/%.

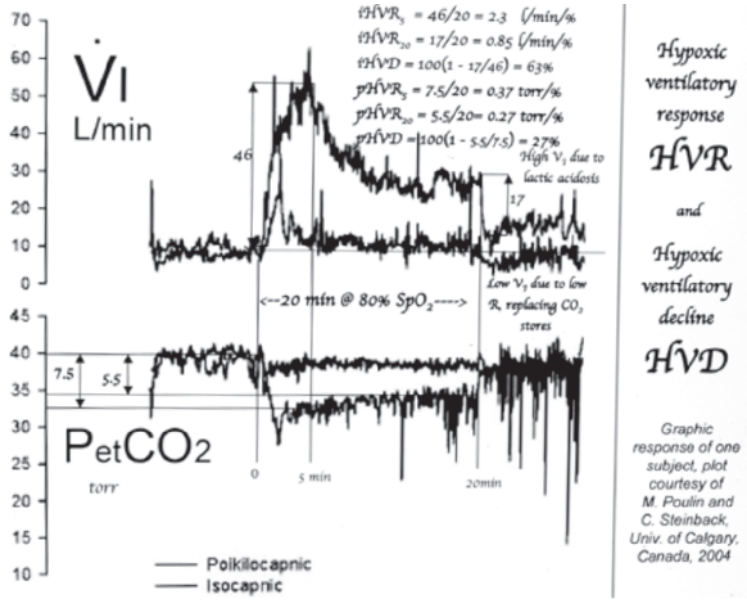

Fig. 1 Example of analysis of isocapnic and poikilocapnic hypoxic ventilatory response

5 Post Altitude Persisting Hyperventilation and CSF pH

The persistence of hyperventilation after descending from high altitude was first noted in 1908 and documented by Riley and Houston (1949) in the volunteers of the first Operation Everest. To test whether this is due to persisting reduction of CSF HCO_3^-, a metabolic acidosis induced by hypoxic respiratory alkalosis, we recruited two anesthesia research fellows who agreed to join us in having lumbar spinal taps at 3810 m altitude (Severinghaus, Mitchell, Richardson and Singer 1963). CSF HCO_3^- fell more rapidly than in blood, and CSF pH rose about 0.03. We initially incorrectly thought that pH of CSF was returning to normal at altitude. Several groups in the succeeding years found that CSF pH rises within minutes from about 7.32 to 7.36 in acute hypoxic hypocapnia, where it remains or possibly rises further over days to weeks at altitude as peripheral carotid chemosensitivity increases slowly. Crawford and Severinghaus (1978) reported that lumbar CSF pH, sampled after several days at altitude and after 45 min of hyperoxia, had returned to sea level control, while ventilation remained high and $PaCO_2$ low. This conclusion was challenged by Dempsey, Forster, Bisgard, Chosy, Hanson, Kiorpes and Pelligrino (1979), who found that CSF pH fell promptly to control shortly after restoration of normoxia but over hours to days fell below control. They concluded that low CSF HCO_3^- failed to explain persistent hyperventilation post altitude.

In unbuffered CSF and ECF, $\Delta pH/\Delta \log PCO_2 = 1.0$. At $PCO_2 = 40$ torr, 1 torr rise of PCO_2 reduces pH by 0.01. Thus $\Delta VE/\Delta pH_{ECF} = 3$ L/min/0.01 CSF pH. The pH fall needed to drive ventilation enough to reduce $PaCO_2$ by 1 torr in CSF metabolic acidosis (low HCO_3^-), computed as $\Delta pH_{CSF}/\Delta VE$, is 0.0005. This is a negative feedback gain of −20. The hypoxic ventilatory drive needed to increase CSF pH from 7.32 to 7.36 at 3500–4000 m is equivalent to about 12 L/min, the drive transferred from the central to peripheral chemosensors (computed as 3 L/min/torr × 4 torr).

6 Peripheral Chemosensitivity Fall in Long-term Hypoxia

Chiodi (1957) showed that natives of high altitude have higher PCO_2 than acclimatized lowlanders. Severinghaus and Carcelen (1964) found normal lumbar CSF pH (7.33) in altiplano natives at $PaCO_2 = 32.4 \pm 0.5$, independent of altitude from 3720 m to 4820 m. At 4330 m altitude, Severinghaus, Bainton and Carcelen (1966) reported hypoxic response (ΔV40) ranged from 1/4 of sea level normal in normal altitude dwellers to about 1/8 of normal in 6 natives with chronic mountain polycythemia (Hct > 70%). Sørensen and Severinghaus (1968) found most high altitude natives do not recover normal hypoxic chemosensitivity after years at sea level. However, such natives do acclimatize normally (Rivera-Ch, Gamboa, Leon-Velarde, Palacios, O'Connor and Robbins 2003).

7 Peripheral Chemoreceptor Sensitization in Chronic Hypoxia

The carotid bodies show both hypertrophy and hyperplasia after long-term hypoxia, and the sensitivity increases gradually. At 3810 m altitude, Sato, Severinghaus and Bickler (1994) reported that isocapnic HVR was constant for about 40 hr and then gradually doubled over two weeks (Fig. 2). They used a control (hyperoxic) PCO_2 generating the same resting ventilation at both low and high altitude. Acclimatization resulted in mild arterial alkalinity at altitude. Ren, Fatemian, and Robbins (2000) reported rises of HVR even after 8 hr of hypoxia. HVR was tested using the pre-hypoxic isocapnic control $P_{ET}CO_2$ after hypoxic exposure (despite acclimatization), resulting in higher post-hypoxic control normoxic ventilation and lower pH. That method may result in the early observed HVR rise. To determine the rate of rise of peripheral chemosensitivity in hypoxia will require brief correction of arterial alkalosis before testing with a hyperoxic control PCO_2 providing equal central drive before and after acclimatization.

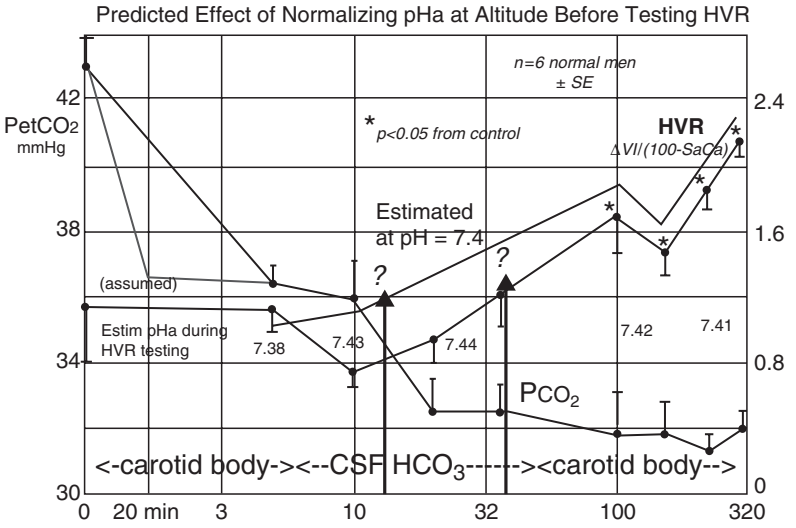

Fig. 2 HVR vs. hours at 3810 m altitude with estimated and proposed test of pH effect

References

Chiodi, H. (1957) Respiratory adaptations to chronic high altitude hypoxia. J. Appl. Physiol. 10, 81–87.

Crawford R.D. and Severinghaus J.W (1978) CSF pH and ventilatory acclimatization to altitude. J. Appl. Physiol. 45, 275–283.

Dempsey, J.A., Forster, H.V., Bisgard, G.E., Chosy, L.W., Hanson, P.G., Kiorpes, A.L. and Pelligrino, D.A. (1979) Role of cerebrospinal fluid [H^+] in ventilatory deacclimatization from chronic hypoxia. J. Clin. Invest. 64, 199–205.

Kellogg, R.H. (1981) Historical perspectives. In: T. F. Hornbein, (Ed.), *Regulation of Breathing,* Vol. 17 Part 1, in C. Lenfant, (Sr. Ed.), *Lung Biology in Health and Disease,* Marcel Dekker, New York, pp. 3–66.

Leusen, I.R. (1954) Chemosensitivity of the respiratory center influence of changes in the H^+ and total buffer concentrations in the cerebral ventricles on respiration. Am. J. Physiol. 176, 45–51.

Loeschcke, H.H., Koepchen, H.P. and Gertz, K.H. (1958) Effect of hydrogen ion concentration and carbon dioxide pressure in the cerebrospinal fluid on respiration. German. Pflügers Arch. 266, 569–585.

Mitchell, R.A., Loeschcke, H.H., Severinghaus, J.W. and Massion, W.H. (1963) Respiratory responses mediated through superficial chemosensitive areas on the medulla. J. Appl. Physiol. 18, 523–533.

Rebuck, A.S. and Campbell, E.J. (1974) A clinical method for assessing the ventilatory response to hypoxia. Am. Rev. Respir. Dis. 109, 345–350.

Ren, X., Fatemian, M. and Robbins, P.A. (2000) Changes in respiratory control in humans induced by 8 hr of hyperoxia. J. Appl. Physiol. 89, 655–662.

Riley, R.L. and Houston, C.S. (1951) Composition of alveolar air and volume of pulmonary ventilation during long exposure to high altitude. J. Appl. Physiol. 3, 526–534.

Rivera-Ch, M., Gamboa, A., Leon-Velarde, F., Palacios, J.A., O'Connor, D.F. and Robbins, P.A. (2003) High-altitude natives living at sea level acclimatize to high altitude like sea level natives. J. Appl. Physiol. 94, 1263–1268.

Sato, M., Severinghaus, J.W. and Bickler, P.E. (1994) Time course of augmentation and depression of hypoxic ventilatory responses at altitude. J. Appl. Physiol. 76, 313–316.

Schlaefke, M.E., See, W.R. and Loeschcke, H.H. (1970) Ventilatory response to alterations of H^+ ion concentration in small areas of the ventral medullary surface. Respir. Physiol. 10, 198–212.

Severinghaus, J.W., Bainton, C.R. and Carcelen, A. (1966) Respiratory insensitivity to hypoxia in chronically hypoxic man. Resp. Physiol. 1, 308–334.

Severinghaus, J.W. and Carcelen, A.B. (1964) Cerebrospinal fluid in man native to high altitude. J. Appl. Physiol. 19, 319–321.

Severinghaus, J.W., Mitchell, R.A., Richardson, B.W. and Singer, M.M. (1963) Respiratory control at high altitude suggesting active transport regulation of CSF pH. J. Appl. Physiol. 18, 1155–1166.

Sørensen, S.C. and Severinghaus, J.W. (1968) Irreversible respiratory insensitivity to acute hypoxia in man born at high altitude. J. Appl. Physiol. 25, 217–220.

Steinbeck, C.D. and Poulin, M.J. (2007) Ventilatory responses to isocapnic and poikilcapnic hypoxia in humans. Respiratory Physiology and Neurobiology 155, 104–113.

Weil, J.V., Byrne-Quinn, E., Sodal, I.E., Friesen, W.O., Underhill, B., Filley, G.F. and Grover, R.F. (1970) Hypoxic ventilatory drive in normal man. J. Clin. Invest. 49, 1061–1072.

Xu, F., Spellman, M.J., Jr., Sato, M., Baumgartner, J.E., Ciricillo, S.F. and Severinghaus, J.W. (1991) Anomalous hypoxic acidification of medullary ventral surface. J. Appl. Physiol. 71, 2211–2217.

2
J.S. Haldane and Some of His Contributions to Physiology

John B. West

Abstract Although the Oxford Conferences began in 1978 as a result of the inspiration of Dan Cunningham and others at the University Laboratory of Physiology in Oxford, the roots of the meetings can be traced to John Scott Haldane (1860–1936) and his colleagues at the turn of the century. Indeed, the Laboratory (or its predecessor) has had an exemplary persistence (some might say an obsession) with the role of oxygen and, particularly, carbon dioxide in the control of breathing for over 100 years. An early key paper was that by Haldane and J.G. Priestley in 1905, "The regulation of the lung ventilation," where careful measurements of the P_{CO_2} in alveolar gas under a variety of conditions showed its critical role in control. But, Haldane was a man of very wide interests and enormous energy, and he made many other contributions, some of which are discussed here. On the one hand, he had an intense interest in very practical issues, for example, the dangers of mine gases and, on the other, he had a distinctly philosophical, vitalist bent which colored his views of physiology.

1 Introduction

The Oxford Conferences on the control of ventilation have been held every three years since they were inaugurated in 1978 as a result of the inspiration of Dan Cunningham and others at the University Laboratory of Physiology in Oxford. However, the roots of the meetings can be traced back to John Scott Haldane (1860–1936) and his colleagues at the turn of the century. Indeed the Laboratory has maintained a continuous interest in the control of ventilation, particularly the roles of carbon dioxide and oxygen, and remarkably this still exists after 100 years. One of the most influential papers titled, "The regulation of the lung ventilation," was published in 1905 (Haldane and Priestley 1905), and exactly 100 years later a paper on ventilatory acclimatization in response to small changes in P_{O_2} appeared from the same laboratory (Donoghue *et al*. 2005). This extraordinary focus on the

University of California, San Diego, Department of Medicine, jwest@ucsd.edu

M.J. Poulin and R.J.A. Wilson (eds.), *Integration in Respiratory Control: From Genes to Systems*.

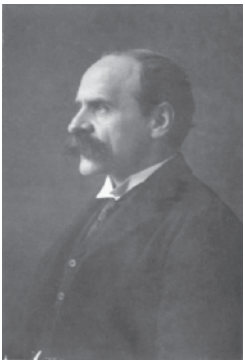

Fig. 1 John Scott Haldane (1860–1936) who, with Priestley, discovered the role of carbon dioxide in the control of ventilation (from Cunningham and Lloyd 1963)

effects of oxygen and carbon dioxide on the control of ventilation can be viewed as an exemplary persistence or possibly an unfortunate obsession!

J.S. Haldane (Fig. 1) was a giant in the history of physiology in the early twentieth century and the present-day historian enjoys a wealth of available information. An important source is the Proceedings of the Haldane Centenary Symposium held in Oxford in 1961 (Cunningham and Lloyd 1963). This begins with a reprint of the obituary notice written in 1936 for the Royal Society (Douglas 1936) and includes a complete bibliography of Haldane's publications. There is also a splendid photograph of the conference participants, which includes many of the major figures in respiratory physiology in 1961 and also Haldane's son, J.B.S. Haldane (1892–1964), who was an evolutionary biologist and Marxist. In many people's view, the son was an even more eminent scientist than his famous father. Additional information about J.S. Haldane can be found in the publications by Sturdy (1987; 1998).

2 The Role of Carbon Dioxide in the Control of Ventilation

In the context of the Oxford Conferences, one of Haldane's most important contributions was his paper cited above on the importance of the P_{CO_2} in the control of ventilation (Haldane and Priestley 1905). The investigators used the alveolar P_{O_2} and P_{CO_2} as a measure of the arterial values. Alveolar gas samples were collected by the simple yet ingenious technique of having the subject exhale into a rubber tube about 1 inch in diameter and 4 feet long, the last-expired gas being obtained by opening the tap of a pre-evacuated glass sampling tube situated close to the mouth. The gas was subsequently analyzed using equipment developed by Haldane, which was a standard method of gas analysis for many years and is still occasionally used (Haldane 1898).

Typical of Haldane's emphasis on precision was that two methods of delivering the alveolar gas sample were used. In the first, the subject made a rapid full expiration at the end of a normal inspiration and, in the second, the expiration was made

at the end of a normal expiration, and the means of the two values were taken. The mean differences between the two P_{CO_2} values was 1–2 mm Hg. Subsequently, Rahn and colleagues (1946) showed that end-tidal gas obtained continuously from an automated sampler gave similar results. It is interesting that in experiments done at sea level, the alveolar P_{CO_2} values for both Haldane and Priestley were remarkably constant, but that the mean value for Haldane was 39.7 mm Hg and that for Priestley was 44.5 mm Hg. Thus, the two scientists apparently had different CO_2 set points.

Haldane and Priestley then investigated the effects of changing the barometric pressure on the alveolar P_{O_2} and P_{CO_2}. To do this, they first went into the Dolcoath Mine in Cornwall where measurements were made 2,240 feet (683 m) below sea level and the barometric pressure was 832 mm Hg. Next they went to the summit of Ben Nevis, altitude 4,406 feet (1343 m), barometric pressure 646.5 mm Hg. Finally, they carried out experiments in a pressure chamber at the Brompton Hospital in London, where the barometric pressure was increased to about 1260 mm Hg.

The striking finding was that the alveolar P_{CO_2} remained remarkably constant in spite of these large variations in barometric pressure. For example, for Haldane the mean P_{CO_2} at sea level, in the mine, on the mountain and in the pressure chamber were 40, 39, 37 and 42 mm Hg, respectively. For Priestley, the values in the four locations were 45, 40, 42 and 44 mm Hg, respectively (Fig. 2). These nearly constant values for P_{CO_2} contrasted dramatically with the very large changes in alveolar P_{O_2} resulting from the alterations in barometric pressure. The conclusion was that ventilation was being regulated by the level of alveolar and therefore arterial P_{CO_2}. In addition, the investigators showed that the alveolar P_{O_2} had to be reduced from its normal value of about 100 mm Hg to less than 60 mm Hg before any increase in ventilation was observed.

An additional finding was that when the alveolar P_{CO_2} was raised by adding CO_2 to inspired air, there was a dramatic increase in ventilation. For example, an increase in

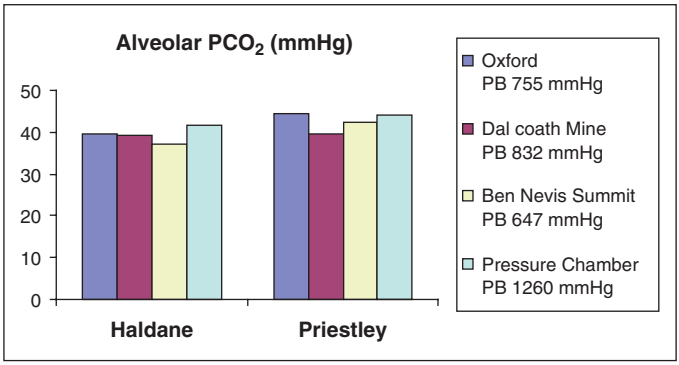

Fig. 2 Mean alveolar P_{CO_2} values for Haldane and Priestley at the four locations where measurements were made. Note the nearly constant P_{CO_2} values for each person in spite of very large changes in P_{O_2}

alveolar P_{CO_2} of about 1.4 mm Hg was sufficient to double the alveolar ventilation at rest. The general conclusion was summed up at the end of the paper as follows:

The evidence furnished by our experiments, taken in conjunction with facts ascertained by previous observers, points to the general conclusion that the regulation of the rate of alveolar ventilation in breathing depends, under normal conditions, exclusively on CO_2 pressure in the respiratory centre.

This conclusion remains true 100 years later although we would now use the term central chemoreceptor rather than respiratory center. The role of hypoxia in the control of ventilation had to wait for 20 years after the publication by Haldane and Priestley when Heymans and Heymans (1927) clarified the mechanism by which hypoxia stimulated ventilation, and De Castro (1928) showed histological evidence of chemoreceptive tissue in the carotid body.

3 Research on Ventilation of Rooms, Air in Mines and Diving

A remarkable feature of Haldane's research career was his important contributions to very practical issues, such as the ventilation of buildings, the air in mines and the pathological consequences of deep diving. In fact, the first scientific articles that he wrote after graduating in medicine from Edinburgh University and becoming a research worker at University College, Dundee, were on "The air of buildings and sewers" (Haldane 1887) and "The air of sewers" (Carnelly and Haldane 1887). The latter begins disarmingly, "Owning to the complaints which have been made of bad smells in the House of Commons, a Select Committee was appointed in the spring of 1886 to inquire into the ventilation of the House." An unexpected conclusion from these studies was that "the air of the sewers was in very much better condition than that of naturally ventilated schools" (Carnelly and Haldane 1887). Haldane maintained his research interests in these practical matters throughout his life. A continuing concern was the so-called "vitiated air" in buildings, for example, classrooms where the inadequate ventilation led to an increased carbon dioxide concentration and bacterial content.

The air in coal mines at that time was frequently toxic and he investigated the so-called "black damp" which was caused by spontaneous oxidation of the coal and resulted in an atmosphere of about 87% nitrogen and 13% carbon dioxide. Another toxic atmosphere was a high concentration of carbon monoxide following a mine explosion known as "after damp." The recent tragedy in West Virginia reminds us that this problem is still potentially with us. Another area of investigation in mines was the physiological consequences of high temperatures where he recognized that strenuous physical activity in a very humid atmosphere could result in heat stroke. Some of this research was carried out in Turkish Baths. Haldane also concerned himself with the general health of miners, pointing out the importance of dust as a cause of pneumoconiosis, the high prevalence of tuberculosis in this group of workers and the condition known as miner's nystagmus, which was apparently mainly caused by poor lighting conditions.

My husband

Fig. 3 J.S. Haldane at work in a mine. The only photograph in Louisa Haldane's book of her husband and one suspects she was not especially proud of his profession (from Haldane 1961). The words under the photograph are "My husband"

As an aside, there is a suggestion that his interests in adequate ventilation were perhaps an embarrassment to his family at times. One can imagine the reaction at a dinner party when asked what he was presently working on Haldane replied, "The air of sewers!" In fact, his wife, Louisa Haldane, wrote an interesting book about her family (Haldane 1961), which contains surprisingly little about her husband, and the only photograph of him (Fig. 3) hardly does him justice.

Some of Haldane's most important applied research was in the area of decompression sickness following diving. Together with Boycott and Damant he carried out a series of very influential experiments in a compressed air chamber at the Lister Institute in London using goats as the experimental animal (Boycott *et al.* 1908). It was known from the experience of caisson workers that decompression sickness almost never occurred in spite of rapid decompression if the worker had been exposed to two atmospheres of pressure and returned to the normal one. Haldane recognized that if it was safe to decompress from two atmospheres to one, it should also be safe to go from four to two or six to three. With these assumptions and numerous experiments with goats, Haldane generated a series of decompression tables, which proved to be of immense practical value in commercial diving and, indeed, the tables used by the U.S. Navy and others today are largely based on his work.

4 Philosophy and Vitalism

Another notable feature of Haldane's career was his interest in the philosophy of life and what might be called vitalism. The following quotation from the preface of the first edition of his textbook, *Respiration* (Haldane 1922), summarizes his views:

> The mechanistic theory of life is now outworn and must soon take its place in history as a passing phase in the development of biology. … The time has come for a far more clear realization of what life implies. The bondage of biology to the physical sciences has lasted more thanhalf a century. It is now time for biology to take her rightful place as an inexact science to speak her own language, and not that of other sciences.

It is perhaps something of a paradox that a man with such immensely practical interests in applied physiology should question the application of the physical sciences to biology. In fact, although I stated earlier that the first scientific paper by Haldane was on "The air of buildings and sewers" (Haldane 1887), he actually published a more philosophical paper, "On life and mechanism" three years before this (Haldane 1884). Remarkably, the 20-page publication, which appeared in the prestigious journal, *Mind,* was written while Haldane was a medical student. It is droll that his first two publications were on philosophy and sewers, respectively.

It could be argued that an unfortunate example of Haldane's preoccupation with vitalism was his stubborn support throughout his life of the theory of oxygen secretion by the lungs. This interest apparently began after a visit to the physiologist, Christian Bohr, in Copenhagen in the 1890s. Bohr had made measurements showing that the arterial P_{O_2} could exceed the alveolar P_{O_2} in anesthetized animals. Haldane subsequently carried out additional animal experiments in Oxford finding the same results. He then collaborated with C.G. Douglas on human experiments, where he modified his views somewhat. He found that there was no evidence for oxygen secretion at rest, but that the arterial P_{O_2} exceeded the alveolar value under three conditions: namely, inspiring a low oxygen mixture, during carbon monoxide inhalation and with muscular work. The conclusion from these experiments was that although the lung does not make use of oxygen secretion under resting conditions, when an abnormal stress is faced upon it, oxygen secretion is called into action.

The most elaborate investigation of oxygen secretion carried out by Haldane and his colleagues was during the Anglo-American Pikes Peak Expedition of 1911. This has been described in detail elsewhere (West 1998). A carbon monoxide equilibration technique was used to measure the arterial P_{O_2}, and it was found that once acclimatization to the low barometric pressure was established, the arterial P_{O_2} was as much as 70% above the alveolar value (Douglas *et al*. 1913). These results led Haldane to conclude that, although the lung might not secrete oxygen under normal resting conditions, this was a strategy that it adopted following acclimatization to high altitude.

Haldane clung doggedly to his theory of oxygen secretion throughout his life in spite of overwhelming evidence from August Krogh, Joseph Barcroft and others that it did not occur either at sea level or at high altitude. In fact, the second edition of Haldane's book, *Respiration* (Haldane and Priestley 1935), includes a whole chapter devoted to oxygen secretion in the lungs, and Haldane died only one year later. The chapter makes interesting reading even today. Haldane pointed out that the swim bladder of fishes often contains gas with a P_{O_2} far higher than that in the surrounding water, and that since the swim bladder is derived from the primitive gut, as is the lung, it was not a big step to envisage oxygen secretion by the lungs. Incidentally, we now know now that the high partial pressure of oxygen in the fish swim bladder is developed by a countercurrent system not active secretion.

In conclusion, J.S. Haldane was one of the giants in respiratory physiology in the early part of the 20th Century. Although his contributions to the control of ventilation were seminal and probably of most interest to people at this meeting, he was also enormously productive in areas of environmental and occupational physiology, including high altitude, deep diving, mining and ventilation of closed spaces. His erroneous support of the theory of oxygen secretion is often emphasized, but this was a small part of his research output and may well have stemmed from his belief in the special characteristics of living organisms.

Acknowledgement The work was supported by NIH grant RO1 HL 60968.

References

Boycott, A.E., Damant, G.C.C. and Haldane, J.S. (1908) The prevention of compressed air illness. J. Hyg. 8, 342–443.

Carnelly, T. and Haldane, J.S. (1887) The air of sewers. Proc. Roy. Soc. 42, 501–522.

Cunningham, D.J.C. and Lloyd, B.B. (Eds). (1963) *The Regulation of Human Respiration: The Proceedings of the J.S. Haldane Centenary Symposium*. Blackwell, Oxford.

De Castro, F. (1928) Sur la structure et l'innervation du sinus carotidien de l'homme et des mammifères. Nouveaux faits sur l'innervation et la fonction du glomus caroticum. Trab. Lab. Invest. Biol. Univ. Madr. 25, 331.

Donoghue, S., Fatemian, M., Balanos, G.M., Crosby, A., Liu, C., O'Connor, D., Talbot, N.P. and Robbins, P.A. (2005) Ventilatory acclimatization in response to very small changes in PO_2 in humans. J. Appl. Physiol. 98, 1587–1591.

Douglas, C.G. (1936) John Scott Haldane, 1860–1936. Obituary Notices of Fellows of the Royal Society 2, 115–139.

Douglas, C.G., Haldane, J.S., Henderson, Y. and Schneider, E.C. (1913) Physiological observations made on Pikes Peak, Colorado, with special reference to adaptation to low barometric pressures. Phil. Trans. Roy. Soc. Lond. Ser. B 203, 185–381.

Haldane, J.S. (1884) Life and mechanism. Mind 9, 27–47.

Haldane, J.S. (1887) The air of buildings and sewers. Sanit. Rec. 9, 152–158.

Haldane, J.S. (1898) Some improved methods of gas analysis. J. Physiol. (London) 22, 465–460.

Haldane, J.S. (1922) *Respiration*. Yale University Press, New Haven, CT.

Haldane, J.S. and Priestley, J.G. (1905) The regulation of the lung ventilation. J. Physiol. (London) 32, 225–266.

Haldane, J.S. and Priestley, J.G. (1935) *Respiration*. Oxford University Press, London.

Haldane, L.K. (1961) *Friends and Kindred*. Faber and Faber, London.

Heymans, J. and Heymans, C. (1927) Sur les modifications directes et sur la regulation reflexe de l'activité du centre respiratoire de la tête isolée du chien. Arch. Intern. Pharmacodyn. 33, 273–370.

Rahn, H., Mohney, J., Otis, A.B. and Fenn, W.O. (1946) A method for the continuous analysis of alveolar air. J. Aviat. Med. 17, 173–179.

Sturdy, S.W. (1997) *A Co-ordinated Whole. The life and work of John Scott Haldane*. Ph.D. Thesis, Edinburgh University. [cited in Chapter 4]

Sturdy, S.W. (1998) Biology as a social theory: John Scott Haldane and physiological regulation. Brit. J. Hist. Science 21, 315–340.

West, J.B. (1998) *High Life: A History of High-Altitude Physiology and Medicine*. Oxford University Press, New York.

3
Control of the Exercise Hyperpnea: The Unanswered Question

Brian J. Whipp

1 Introduction

At the first of what is now known as, the "Oxford Conferences," Fred Grodins referred to the mechanism of the exercise hyperpnea, as "The Ultra Secret." I have chosen to sub-title my presentation, "The Unanswered Question" (with apologies to Charles Ives) in the hope that even if the answer does not eventuate then at least the nature of the essential question will. But space constraints allow only one theme to be developed and that only for moderate exercise. And, as it is the "Oxford Conference," I have chosen one initially adumbrated by one of Oxford's luminaries, C.G. Douglas; one, in my judgment, that is under-appreciated. In his 1927 Lancet review, Douglas (1927) describes an important study: *"in which we followed in detail the behaviour of the breathing after the ingestion of a considerable quantity of sugar by a person at complete rest … The volume of air breathed per minute showed a perfectly definite rise and fall which ran closely parallel to the change in CO_2 production, and the parallelism became still more obvious if the effective amount of air was calculated as distinguished from the total amount of air breathed."*

This was clearly suggestive of a CO_2-related mechanism and possibly an arterial PCO_2 ($PaCO_2$) regulatory one. Taylor and Jones (1979) addressed the same issue but in exercise. Utilizing endurance training to reduce the respiratory quotient associated with two constant work rates (WR), they demonstrated that while there was no consistent relationship between the training-induced changes in ventilation ($\dot{V}E$) and O_2 consumption ($\dot{V}O2$), $\dot{V}E$ was reduced in close proportion to the reduced CO_2 production ($\dot{V}CO2$), the result of a greater fatty-acid contribution to substrate catabolism. Thus, not only did $\dot{V}E$ change as a linear function of $\dot{V}CO2$ during the exercise, but it *didn't* change, in the same proportion, to the CO_2 that *wasn't* produced.

The implications for the operation of a "CO_2-linked" mechanism are, perhaps, even stronger when the nonsteady-state response profiles are considered, *i.e.*, conditions in which blood and skeletal muscle tissue capacitance (Farhi and Rahn 1955)

University of Leeds, Institute of Membrane and Systems Biology, b.whipp@leeds.ac.uk

M.J. Poulin and R.J.A. Wilson (eds.), *Integration in Respiratory Control: From Genes to Systems*.

dissociate pulmonary gas exchange transients from those of muscle metabolism. In addition to the normal CO_2 capacitance of blood being several-fold greater than for O_2, the net proton trapping associated with phosphocreatine splitting during skeletal muscle contraction results in a transient metabolic alkalosis in the force-generating units (Kemp 2005) and in the venous effluent of the exercising muscle (Wasserman *et al*. 1997). A component of the metabolically-produced CO_2 is therefore retained within the muscle, such that the $\dot{V}CO_2$ time course is slow relative to that of $\dot{V}O_2$ during the nonsteady-state. The difference between $\tau\,\dot{V}CO_2$ and $\tau\,\dot{V}O_2$ is evident for the first of the two-step, constant-WR test in Fig 1 (Brittain *et al*. 2001). As $\tau\,\dot{V}E$ is appreciably longer than $\tau\,\dot{V}O_2$, alveolar and arterial PO_2 fall transiently. But, owing to the relatively small kinetic dissociation between $\dot{V}E$ and $\dot{V}CO_2$, the $PaCO_2$ increase is only a mmHg or so (*e.g*., Whipp and Ward 1991) and, usually, only in the transient.

Note (Fig. 1), however, that the degree of dissociation between $\dot{V}CO_2$ and $\dot{V}O_2$ during the on-transient of the higher step is appreciably less (Hughson and Morrissey 1982; Whipp and Ward 1991). $\dot{V}CO_2$ kinetics are speeded both in absolute terms and relative to those of $\dot{V}O_2$, presumably because the muscle CO_2 capacitance is already partially charged. $\dot{V}E$ "tracks" the altered $\dot{V}CO_2$ kinetics such that the linear steady-state $\dot{V}E$-$\dot{V}CO_2$ relationship (with a positive $\dot{V}E$-intercept) is maintained throughout each WR transient despite the markedly-changed $\dot{V}CO_2$ kinetics. This demonstrates that *if* $\dot{V}E$ is, somehow "CO_2 coupled," it is not with the muscle CO_2 production rate but with its exchange rate at the lung.

Also, when WR is "forced" sinusoidally over a range of increasing input frequencies (Fig. 2), the $\dot{V}E$ response amplitude decreases as a close linear function of the decrease of that of $\dot{V}CO_2$ (*e.g*., Casaburi *et al*. 1978). Importantly, however, the relationship extrapolates to the origin at high frequencies (*i.e*., *along* the slope of the transient and steady-state $\dot{V}E$- $\dot{V}CO_2$ relationship, Fig. 1). Consequently, central command, which continues to drive the force-generating muscle units over the same amplitude range and the neurogenic feedback mechanisms from them, either subserve a trivially small role in $\dot{V}E$ control under these nonsteady-state conditions or these mechanisms themselves exhibit slow neural dynamics (Eldridge and Waldrop 1991), but somehow closely proportional to those of $\dot{V}CO_2$.

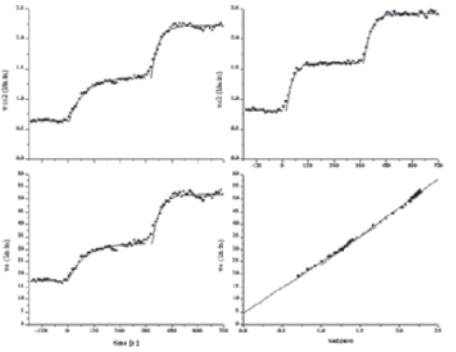

Fig. 1 Responses to moderate two-step (equal step) exercise test from 20 W: $\dot{V}O_2$ vs. time (*upper right*), $\dot{V}CO_2$ vs. time (*upper left*), $\dot{V}E$ vs. time (*lower left*), and $\dot{V}E$ vs. $\dot{V}CO_2$ (*lower right*) (Rossiter, Brittain, Kowalchuk and Whipp, unpublished)

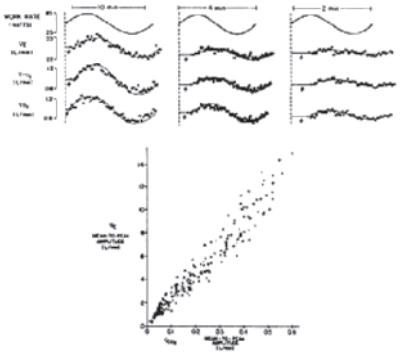

Fig. 2 Responses to sinusoidal exercise. (*Upper*: $\dot{V}_E$, $\dot{V}_{CO2}$ and $\dot{V}_{O2}$ vs. time for three different frequencies; *lower*: peak-mean amplitude of $\dot{V}_E$ vs. $\dot{V}_{CO2}$ across all forcings (from Casaburi *et al*. 1978)

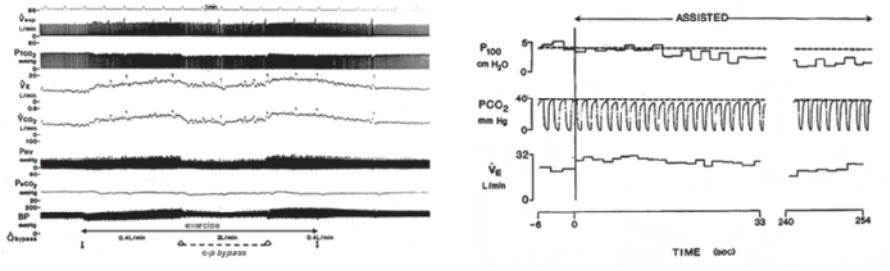

Fig. 3 ***Top***: Responses to proportional venous return diversion through an extracorporeal gas exchanger to the systemic arterial circulation (anesthetized dog) during electrically-induced, hind-limb exercise (from Huszczuk *et al*. 1986). ***Bottom:*** Inspiratory occlusion pressure (P100), respired PCO_2 and $\dot{V}_E$ responses to inspiratory proportional-assist ventilation in moderate exercise (from Poon *et al*. 1986)

Furthermore, electrically-induced exercise in subjects with clinically complete spinal cord transection, results in a $\dot{V}_E$ response that is essentially normal with respect to $\dot{V}_{CO2}$ (Adams *et al*. 1984) both in magnitude and time course (albeit over a restricted range of metabolic rate). These observations support the argument against a major obligatory involvement of central command in $\dot{V}_E$ control during moderate exercise.

Huszczuk and associates (1986) took a next logical step in considering this control behavior: diverting a fraction of the venous return from the inferior vena cava to the descending aorta in the steady-state of electrically-induced exercise in the anaesthetized dog, having "cleared" the appropriate amount of CO_2 via an extra-corporeal gas exchanger. $\dot{V}_E$ decreased in appropriate proportion to the reduced $\dot{V}_{CO2}$ demands at the lung, maintaining arterial isocapnia (Fig. 3, top). Similar results have also been demonstrated in a range of experimental paradigms (reviewed in Haouzi 2006). This large body of correlative evidence has enticed several investigators to hypothesize "CO_2-coupled" control of the exercise hyperpnea, such as: *"A natural corollary to this is the proposition that the activity of the respiratory centre is proportional to the mass of CO_2 produced by the body and carried to the lungs"* (Douglas 1927) or that

"CO_2 flux to the lung" was a determinant of the hyperpnea (Wasserman *et al*. 1977). Such proposals, however, fail to meet the $PaCO_2$-regulatory demands of the control. That is, any such control link will depend not on the rate at which CO_2 is brought to the lung per unit time but that *minus* the rate at which CO_2 leaves the lung in the pulmonary arterial blood.

But there is another concern regarding the $PaCO_2$ regulatory demands of any coupling between $\dot{V}E$ and $\dot{V}CO2$, as evident in the mass balance equation:

$$PaCO_2 = 863/[(\dot{V}E/\dot{V}CO2)\cdot (1\text{-}VD/VT)] \quad (1)$$

$PaCO_2$ regulation during exercise therefore depends on the relationship between two compound variables (the ventilatory equivalent for CO_2 ($\dot{V}E/\dot{V}CO2$) and the physiological dead space fraction of the tidal volume (V_D/V_T)), but *only* two! And as, over the range of exercise intensities, arterial pH appears to be the more closely regulated variable, then "replacing" $PaCO_2$ in the Henderson-Hasselbalch equation (*i.e*., $pH = pK + \log[HCO_3^-]/\alpha \cdot PaCO_2]$) yields the instructive equation:

$$pH = pK + \log\{[HCO_3^-]/25.9] \cdot [\dot{V}E/\dot{V}CO2] \cdot [1\text{-}VD/VT]\} \quad (2)$$

This characterises how the ventilatory-related variables must interact to provide: (a) pH stability during moderate exercise (*i.e*., $[HCO_3^-]$ constant) and (b) respiratory compensation for the metabolic acidosis at higher exercise intensities (*i.e*., $[HCO_3^-]$ being decreased). But the relationship, or what has been termed "coupling," between $\dot{V}E$ and $\dot{V}CO2$ has dominated the literature of $PaCO_2$ and pH regulation during exercise; the role of V_D/V_T has, in effect, been neglected. Therefore, a brief consideration seems justified.

In normal subjects (with little difference between anatomical (or series) and physiological dead space), V_D normally increases as a linear function of V_T with a positive intercept on the V_T axis (Lamarra *et al*. 1988); V_D/V_T therefore decreases as a hyperbolic function of increasing V_T. To regulate $PaCO_2$ and pH, $\dot{V}E/\dot{V}CO2$ must decrease with an appropriately-proportional profile. This it does; note the positive intercept on the linear $\dot{V}E$ - $\dot{V}CO2$ relationship in Fig. 1 (Whipp and Ward 1991)! The linear $\dot{V}E$ - $\dot{V}CO2$ relationship during exercise is therefore a result of the regulatory behaviour and not a cause. In crude terms, the system seems to "know" that when V_D/V_T is reduced (making $\dot{V}E$ more efficient with respect to alveolar ventilation) $\dot{V}E$ "needs" to increase less per unit $\dot{V}CO2$ to effect its regulatory function, with the necessary logical assumption, of course, that there is such regulation. But unless one is badly confusing subsequence and consequence, it is hard to believe, in the light of the evidence cited above, that there is not.

Further to the issue of the respiratory motor output under conditions of altered demand for achieving a regulatory-necessary level of $\dot{V}E$ is the compelling evidence provided by studies in which a servo-assisted positive-pressure ventilator has been used as a means of dissociating a subject's intrinsic ventilatory motor output from the achieved ventilation during moderate (Poon *et al*. 1987) and even very heavy intensity (Krishnan *et al*. 1996) exercise in normal subjects. That is, increased

inspiratory pressure is applied, carefully synchronized with the respiratory cycle, to "take over" a proportion of the normal inspiratory flow. Were $\dot{V}_E$ to be dictated wholly by central command and/or neurogenic feedback from the limbs, then the subject's intrinsic ventilatory drive would be expected to remain unchanged despite the proportional-flow assistance. Total $\dot{V}_E$ would, consequently, be expected to increase, resulting in a sustained hypocapnia. This is *not* the case, however, despite neither "central command" nor mechanical feedback from the exercising muscles, presumably, being altered. Rather, there is a proportional compensatory reduction in the intrinsic ventilatory drive (which, in the study of Krishnan *et al*. 1996 accounted for approximately a third of the hyperpneic drive), the result being an unchanged level of $\dot{V}_E$ (Fig. 3, bottom).

In 1991 Sue Ward and I (Whipp and Ward 1991) thought that the appropriate core question to be resolved was that: "… although many mechanisms have been demonstrated which can increase ventilation during exercise, the essential challenge which remains is why, for moderate exercise, does ventilation only increase to levels commensurate with the level of pulmonary CO_2 exchange?"

And in a recent review-and-preview of exercise hyperpnea research, Dempsey similarly judged that: "This is clearly an issue for a multitalented team of visionaries, preferably those who are willing to start with the belief that CO_2 exchange is truly the underpinning to ventilatory control and that ''somewhere out there'' exist the appropriate receptor sites, specific stimuli, and the neural pathways."

It remains the unanswered question. Not providing *the* answer to the *entire* exercise hyperpnea but perhaps the crucial core or fundamental feature upon which factors such as volition, emotion, short-, and/or long-term potentiation, mechanical constraint and limitation, among others, provide modulating influences.

References

Adams, L., Frankel, H., Garlick, J., Guz, A., Murphy, K. and Semple, S.J. (1984) The role of spinal cord transmission in the ventilatory response to exercise in man. J. Physiol. 355, 85–97.

Brittain, C.J., Rossiter, H.B., Kowalchuk, J.M. and Whipp, B.J. (2001) Effect of prior metabolic rate on the kinetics of oxygen uptake during moderate-intensity exercise. Eur. J. Appl. Physiol. 86, 125–134.

Casaburi, R., Whipp, B.J., Wasserman, K. and Stremel, R.W. (1978) Ventilatory control characteristics of the exercise hyperpnea as discerned from dynamic forcing techniques. Chest 73S, 280–283.

Dempsey, J.A. (2006) Challenges for future research in exercise physiology as applied to the respiratory system. Exerc. Sport Sci. Rev. 34, 92–98.

Douglas, C.G. (1927) Co-ordination of the respiration and circulation with variations in bodily activity. Lancet 2, 213–218.

Eldridge, F.L. and Waldrop, T.G. (1991) Neural control of breathing. In: B.J. Whipp and K. Wasserman (Eds.), *Pulmonary Physiology and Pathophysiology of Exercise*. Dekker, New York, pp. 309–370.

Farhi, L.E. and Rahn H. (1955) Gas stores in the body and the unsteady state. J. Appl. Physiol. 7, 472–484.

Haouzi, P. (2006) Theories on the nature of the coupling between ventilation and gas exchange during exercise. Resp. Physiol. Neurobiol. 151, 267–279.

Hughson, R.L., and Morrissey, M. (1982) Delayed kinetics of respiratory gas exchange in the transition from prior exercise. J. Appl. Physiol. 52, 921–929.

Huszczuk, A., Whipp, B.J., Oren, A., Shors, E.C., Pokorski, M., Nery, L.E. and Wasserman, K. (1986) Ventilatory responses to partial cardiopulmonary bypass at rest and exercise in the dog. J. Appl. Physiol. 61, 575–583.

Kemp, G. (2005) Lactate accumulation, proton buffering and ph change in ischemically exercising muscle. Am. J. Physiol. 289, R895–R901.

Krishnan, B., Zintel, T., McParland, C. and Gallagher, C.G. (1996) Lack of importance of respiratory muscle load in ventilatory regulation during heavy exercise in humans. J. Physiol. 490, 537–50.

Lamarra, N., Whipp, B.J. and Ward, S.A. (1988) Physiological inferences from intra-breath measurement of pulmonary gas exchange. Proc. Ann. Internat. Conf. I.E.E.E. Eng. Med. Biol. Soc., New Orleans, pp. 825–826.

Poon, C.S., Ward, S.A. and Whipp B.J. (1987) Influence of inspiratory assistance on ventilatory control during moderate exercise. J. Appl. Physiol. 62, 551–560.

Taylor, R. and Jones, N.L. (1979) The reduction by training of CO_2 output during exercise. Eur. J. Cardiol. 9, 53–62.

Wasserman, K., Stringer, W., Casaburi, R. and Zhang, Y.Y. (1997) Mechanism of exercise hyperkalemia: an alternate hypothesis J. Appl. Physiol. 83, 631–643.

Wasserman, K., Whipp, B.J., Casaburi, R., Beaver, W.L. and Brown, H.V. (1977) CO_2 flow to the lungs and ventilatory control. In: J.A. Dempsey and C.E. Reed (Eds.), *Muscular Exercise and the Lung*. University of Wisconsin Press, Madison, pp. 105–135.

Whipp, B.J. and Ward, S.A. (1982) Cardiopulmonary coupling during exercise. J. Exp. Biol. 100, 175–193.

Whipp, B.J. and Ward, S.A. (1991) The coupling of ventilation to pulmonary gas exchange during exercise. In: B.J. Whipp and K. Wasserman (Eds.), *Pulmonary Physiology and Pathophysiology of Exercise*. Dekker, New York, pp. 271–307.

Part II
Oxygen Sensing and the Carotid Body

4
A Peripheral Oxygen Sensor Provides Direct Activation of an Identified Respiratory CPG Neuron in *Lymnaea*

Harold J. Bell[1], Takuya Inoue[2] and Naweed I. Syed[3]

Abstract The mechanisms by which peripheral, hypoxia-sensitive chemosensory cells modulate the output from the respiratory central pattern generator (CPG) remain largely unknown. In order to study this topic at a fundamental level, we have developed a simple invertebrate model system, *Lymnaea stagnalis* wherein we have identified peripheral chemoreceptor cells (PCRCs) that relay hypoxia-sensitive chemosensory information to a known respiratory CPG neuron, right pedal dorsal 1 (RPeD1). Significance of this chemosensory drive was confirmed via denervation of the peripheral sensory organ containing the PCRCs, and subsequent behavioral observation. This study provides evidence for direct synaptic connectivity between oxygen sensing PCRCs and a CPG neuron, and describes a unique model system appropriate for studying mechanisms of hypoxia-induced, respiratory plasticity from the level of an identified synapse to whole animal behavior.

1 Introduction

Despite recent advances in our understanding of respiratory control ((Ramirez, Zuperku, Alheid, Lieske, Ptak and McCrimmon, 2002; Feldman and Del Negro 2006), the fundamental mechanisms by which respiratory rhythm is generated and then subsequently modulated by inputs or 'drives to breathe' remain largely undefined. To achieve a better comprehension of the basic mechanisms underlying respiratory rhythm generation, modulation and plasticity, we have developed an invertebrate model system using the fresh water pond snail, *Lymnaea stagnalis*.

Lymnaea are pulmonate bimodal breathers; they can exchange respiratory gases in water via simple diffusion across their body surface, but may also exhibit aerial breathing via their respiratory orifice, the pneumostome, at the water surface. Surface breathing in *Lymnaea* is a simple, hypoxia-driven behavior (Jones 1961); animals breathe more often and for longer periods of time when oxygen content in

[1–3]University of Calgary, Department of Cell Biology and Anatomy, harold.bell@ucalgary.ca

M.J. Poulin and R.J.A. Wilson (eds.), *Integration in Respiratory Control: From Genes to Systems*. © Springer 2008

their aquatic environment is low. This surface breathing behavior is known to be governed by a 3-cell central pattern generator (CPG) which has been well described elsewhere (Syed, Bulloch and Lukowiak 1990).

The initiation of rhythmic patterned activity in this CPG requires an excitatory input to one of the three cells in this network, specifically the neuron right pedal dorsal 1 (RPeD1). Since aerial respiratory activity in *Lymnaea* is a hypoxia-driven behavior, we supposed that the excitatory input to RPeD1 may arise from a chemoreceptor site which senses oxygen status and drives the respiratory CPG appropriately. Since our laboratory has previously demonstrated that the source of the hypoxic signal resides in the periphery of *Lymnaea* (Inoue, Haque, Lukowiak and Syed 2001), the purpose of this study was to identify and characterize the nature of the hypoxia-driven, excitatory input to the respiratory neuron RPeD1.

As a potential locus for this input to the CPG, we focused upon the osphradium, a peripheral sensory organ located adjacent to the pneumostome, which has been implicated in the regulation of multiple behaviors such as feeding and respiration (Wedemeyer and Schild 1995; Kamardin, Shalanki, Rozha and Nozdrachev 2001). Based upon the anatomical location of the organ and its known sensory function, we hypothesized that neurons within the osphradium might provide a hypoxia-related respiratory drive to the respiratory CPG via the neuron RPeD1.

2 Methods

Lymnaea stagnalis L. were raised, maintained and prepared for dissection as described previously (Inoue *et al*. 2001). A semi-intact preparation was extracted which included the central ring ganglia along with the pneumostome tissue, wherein the osphradium is located. The internal right parietal nerve and osphradial nerve were left intact thereby preserving connectivity between the central ring ganglia and the osphradium.

The preparation was then pinned to the bottom of a recording dish layered with black siliconized rubber (RTV616, General Electric) and bathed in normal *Lymnaea* saline. A physical separation isolated the central ring ganglia from the pneumostome tissue and osphradium, and each compartment could be independently superfused with solutions. Neurons in the osphradium and RPeD1 in the central ring were exposed to permit sharp electrode intracellular recording, as has been described elsewhere (Haque, Lee, Inoue, Luk, Hasan, Lukowiak and Syed 2006).

Normoxic (PO_2 ~ 140 mmHg) and hypoxic (PO_2 ~ 70 mmHg) salines were delivered directly to the recording chamber containing the pneumostome and osphradium via a perfusion system (flow ~ 25 ml/min). The chambers of the recording dish were sealed using parafilm, the exception being a small opening to allow for cell penetration, thereby limiting contamination of the recording bath. Modified salines were also used to examine the synaptic connections between RPeD1 and osphradial neurons. Specifically, to attenuate polysynaptic transmission, HiDi (6x Ca^{2+}/6x Mg^{2+}; in mM: 35.0 NaCl, 1.7 KCl, 24.0 $CaCl_2$, and 9.0 $MgCl_2$) saline was used.

To avert chemical transmission between cells, zero calcium (in mM: 42.8 NaCl, 1.7 KCl, and 14.0 $MgCl_2$) saline was used.

To denervate the osphradium, animals were anaesthetized (140 mM $MgCl_2$, 0.5–1.0 ml injection) and the osphradial nerve (Osn) was cut proximal to the organ through a small opening in the skin. Sham animals were prepared using an identical procedure, with the exception that ultimately the Osn was left intact.

Behavioral observations were made 3 to 10 days post-recovery on one pair of size-matched denervated and control animals, placed in 500 ml containers in 250 ml of pond water. Observation was started 20 min after the animals were transferred to the container, and lasted for 60 minutes. The animals were observed under two conditions, normoxia (20.9% O_2, PO_2 ~ 140 mmHg) and hypoxia (7.88% O_2, PO_2 ~ 55 mmHg). Custom-written software (Labview, National Instruments, Austin) was informed of the status of the snail at any time during the 60-minute observation period, status being: submerged, surfaced but not breathing, or surfaced with pneumostome open.

Statistical comparisons were made using analysis of variance tests (one- or two-way, depending on the number of experimental factors influencing outcomes), and where indicated, *post-hoc* testing consisted of applying Tukey's t-testing procedure. The value for was set *a priori* at 0.05.

Experiments were performed at room temperature, controlled to 22–24°C, RH ~ 30%. Chemicals were purchased from Sigma (MO, USA), unless stated otherwise.

3 Results

To test whether osphradial neurons (ONs) demonstrate oxygen-sensitivity, direct intracellular recordings were made from them under both normoxic (PO_2 ~ 140 mmHg) and hypoxic (PO_2 ~ 65–69 mmHg) conditions (see Fig. 1).

Resting membrane potentials typically ranged from −40 to −60 mV. Exposure to hypoxic saline elicited burst-like activity in the ONs, which terminated upon washout with normoxic saline. When examined over a standardized 2-minute interval during exposure to hypoxia (PO_2 ~ 65–69 mmHg), there were an average of 4 bursts observed (3.9 ± 0.4 bursts) with an interburst interval of 25.9 ± 1.6 seconds (8 cells from 5 preparations). The first burst was composed of 14 ± 1.1 action potentials, while the last burst in the 2-minute observation period exhibited 12 ± 0.9 action potentials; this decrement was significant and observed in 7 of 8 cells ($p = 0.026$).

Simultaneous intracellular recordings were made from ON and RPeD1 in the semi-intact preparation. Induced burst activity in the ON triggered spike activity in a normally quiescent RPeD1 (see Fig. 2), and this relationship remained in the presence of high divalent cation (HiDi) saline ($n = 11$). Conversely, in the background presence of a zero-calcium, high Mg^{2+} saline, activity induced by current injection in the PCRCs failed to trigger spike activity in RPeD1 ($n = 6$). Washout with normal saline restored synaptic transmission between the PCRC and RPeD1.

In an effort to confirm a physiological role for PCRC input to the respiratory CPG, we performed behavioral analysis on animals wherein input to the respiratory

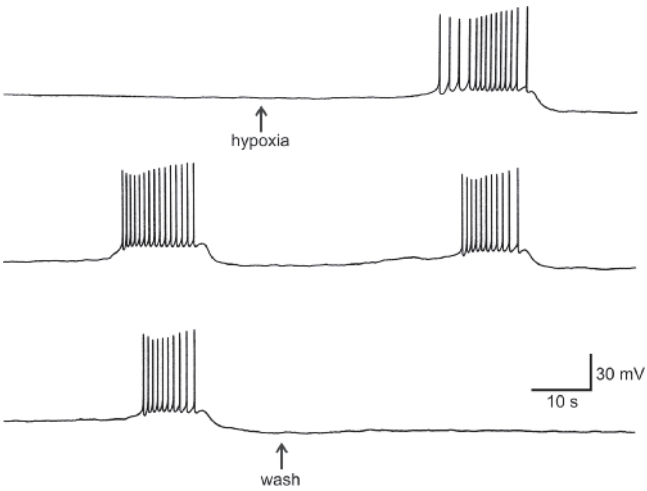

Fig. 1 Burst activity in a chemosensory osphradial neuron elicited by hypoxic exposure (n = 23 cells from 11 preparations). Above, RMP pre-hypoxia = − 46 mV

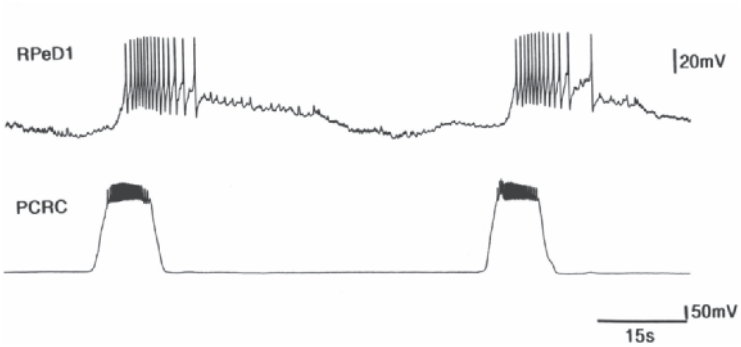

Fig. 2 Induced activity in a PCRC, via direct depolarizing current injection, elicits spike activity in the CPG neuron RPeD1 (RMP = −57 mV, held to −70 mV)

CPG neurons was removed via surgical denervation of the osphradium. There were significant effects of both experimental condition (hypoxia versus normoxia) and experimental group (denervated versus sham animals) on measured indicators of breathing activity (n = 7).

Hypoxia had an independent influence over breathing behavior when expressed as amount of time spent submerged, at the surface, and breathing (all, $p \leq 0.001$). Denervation also had an effect upon breathing activity independent of background PO_2; the denervated animals spent more time submerged ($p = 0.018$), came to the surface less often ($p = 0.038$), and breathed less whether expressed as number of breaths ($p = 0.027$) or total breathing time ($p = 0.032$). No interaction effects were resolved between factors of condition and experimental group. Together, these

behavioral data show that while PCRC input to the respiratory CPG is not essential for respiratory behavior, in its absence, respiratory drive significantly reduced.

4 Discussion

We have identified peripheral chemosensory neurons located in the osphradium, which demonstrate hypoxia-induced burst activity and form direct chemical synapses with the respiratory CPG neuron RPeD1. We found that, although PCRCs are not essential for normal respiratory function in *Lymnaea*, eliminating their input to the respiratory CPG significantly reduced surface breathing activity in the freely-behaving animal, attesting to the physiological relevance of this chemosensory input. The PCRC-RPeD1 synapse therefore provides us with a simple model system where the fundamental mechanisms by which a physiologically relevant, peripheral chemosensory element may effect a change in respiratory CPG activity. This identified synapse provides us with an unprecedented opportunity to better understand those cellular processes, which lead to modulation and plasticity in the respiratory control system.

Acknowledgements This research was funded by the Canadian Institutes of Health Research (CIHR grant # 691402). HJB is an Alberta Heritage Foundation for Medical Research (AHFMR) fellow. NIS is a CIHR Investigator and a (AHFMR) Medical Scientist. We acknowledge the excellent technical support provided by Wali Zaidi and Ishrat Hussain.

References

Feldman, J.L. and Del Negro, C.A. (2006) Looking for inspiration: new perspectives on respiratory rhythm. Nat. Rev. Neurosci. 7, 232–242.

Haque, Z., Lee, T.K., Inoue, T., Luk, C., Hasan, S.U., Lukowiak, K. and Syed, N.I. (2006) An identified central pattern-generating neuron co-ordinates sensory-motor components of respiratory behavior in *Lymnaea*. Eur. J. Neurosci. 23, 94–104.

Inoue, T., Haque, Z., Lukowiak, K. and Syed, N.I. (2001) Hypoxia-induced respiratory patterned activity in *Lymnaea* originates at the periphery. J. Neurophysiol. 86, 156–163.

Jones, J.D. (1961) Aspects of respiration in *Planorbis corneus L.* and *Lymnaea stagnalis L.* (*gastropoda: pulmonata*). Comparative Biochem. Physiol. 4, 1–29.

Kamardin, N.N., Shalanki, Y., Rozha, K.S. and Nozdrachev, A.D. (2001) Studies of chemoreceptor perception in mollusks. Neurosci. Behav. Physiol. 31, 227–235.

Ramirez, J.M., Zuperku, E.J., Alheid, G.F., Lieske, S.P., Ptak, K. and McCrimmon, D.R. (2002) Respiratory rhythm generation: converging concepts from *in vitro* and *in vivo* approaches? Respir. Physiol. Neurobiol. 131, 43–56.

Syed, N.I., Bulloch, A.G. and Lukowiak, K. (1990) *In vitro* reconstruction of the respiratory central pattern generator of the mollusk *Lymnaea*. Science 250, 282–285.

Wedemeyer, H. and Schild, D. (1995) Chemosensitivity of the osphradium of the pond snail *Lymnaea stagnalis*. J. Exp. Biol. 198, 1743–1754.

5
Environmental Hyperoxia and Development of Carotid Chemoafferent Function

Gerald Bisgard[1], Julie Wenninger[2], Zunyi Wang[3] and E. Burt Olson, Jr.[4]

Abstract Exposure to hyperoxia in the first few weeks of life causes life-long impairment of carotid chemoreceptor function in rats, *e.g.,* depressed carotid sinus nerve (CSN) and phrenic nerve responses to acute hypoxia. We determined the maximal CSN responses of anesthetized adult rats to severe hypoxia (ventilation with 100% N_2) or asphyxia (stopped ventilator) after 1, 2, and 4 weeks of postnatal hyperoxia (60% O_2) (PNH). As with acute responses to hypoxic stimuli, we find that maximal CSN responses are significantly attenuated with severity of attenuation dependent on duration of PNH. We suggest that impaired carotid chemoafferent input produced by PNH could play a role in failure of arousal in severely hypoxic states occurring in infants and adults.

1 Introduction

It has been well established that developmental hyperoxia results in deficient function of carotid body chemoreceptor input during hypoxic stimulation. This has been demonstrated by exposing rats to 60% O_2 during the first 4 weeks of postnatal life, termed postnatal hyperoxia (PNH). The most commonly used model is to expose pregnant females to 60% O_2 beginning 2–4 days before parturition and confine the mothers with their pups for 1–4 weeks in the hyperoxic chamber. The rat pups are then raised to adults in normoxia.

[1] University of Wisconsin Madison, Department of Comparative Biosciences, bisgardg@svm.vetmed.wisc.edu

[2] University of Wisconsin Madison, Department of Comparative Biosciences, wenninger@svm.vetmed.wisc.edu

[3] University of Wisconsin Madison, Department of Surgical Sciences, wangz @svm.vetmed.wisc.edu

[4] University of Wisconsin Madison, Department of Population Health Sciences, ebolson@facstaff.wisc.edu

M.J. Poulin and R.J.A. Wilson (eds.), *Integration in Respiratory Control: From Genes to Systems*.

In previous studies it, has been shown that 2–4 weeks of PNH causes attenuated development and life-long depression of ventilatory and carotid chemoafferent responses to acute hypoxia in adult rats with no evidence of spontaneous recovery of this function (Bavis, Olson and Mitchell 2002; Bisgard, Olson, Wang, Bavis, Fuller and Mitchell 2003; Fuller, Bavis, Vidruk, Wang, Olson, Bisgard and Mitchell 2002).

Infants exposed to oxygen therapy for bronchopulmonary dysplasia or for other disease states have been shown to have depressed chemoreflex responses and may be at greater risk for apnea and deficient hypoxia arousal mechanisms during sleep (Cohen and Katz-Salamon 2005; Gauda, McLemore, Tolosa, Marston-Nelson and Kwak 2004).

Depressed carotid chemoafferent function is also present in newborn rats following PNH (Donnelly, Kim, Carle and Carroll 2005). Recent studies indicate that PNH impairs the normally vigorous type 1 cell division within the carotid body of newborn rats and depresses the development of chemoreceptor afferent neurons in the carotid sinus nerve (CSN) (Erickson, Nayer, Jawa, Ling, Olson, Vidruk, Mitchell and Katz 1998; Wang and Bisgard 2005). Carotid chemoreceptor stimulation is thought to play a crucial role in arousal from asphyxic and hypoxic states. Therefore, we wished to determine the CSN chemoafferent frequency responses to maximal hypoxic and asphyxic stimuli in PNH-treated adult rats. We also compared these maximal responses to the CSN responses to moderate hypoxic stimuli.

2 Methods

All experimental procedures were approved by the Animal Care and Use Committee of the School of Veterinary Medicine at the University of Wisconsin.

Two to four days prior to projected delivery date, pregnant female Harlan Sprague Dawley rats were placed into a hyperoxic (60% O_2 + balance N_2) environmental chamber with the remaining rats housed nearby in room air (control). Rat pups were born into and maintained in these ambient conditions for 1, 2 or 4 weeks. After hyperoxic exposure (or normoxia), all mothers and pups were returned to (or maintained at) room air, and returned to standard animal quarters until studied at 3 to 5 months of age.

Body weights at the time of study in adult rats were 429.2 ± 8.0 g (mean ± SEM, n = 18) for control vs. 402.6 ± 8.0 g for PNH-treated rats (n = 32) (NS). Methods and limitations of CSN recording under general anesthesia have been described in detail elsewhere (Bisgard *et al*. 2003).

3 Results

The responses to NaCN injection and to sustained 100% N_2 (max N_2) in a normal control rat are presented in Fig. 1. The time to reach maximal N_2 response in all rats was 35–40 sec and was not different between PNH vs. control rats. Rats subjected

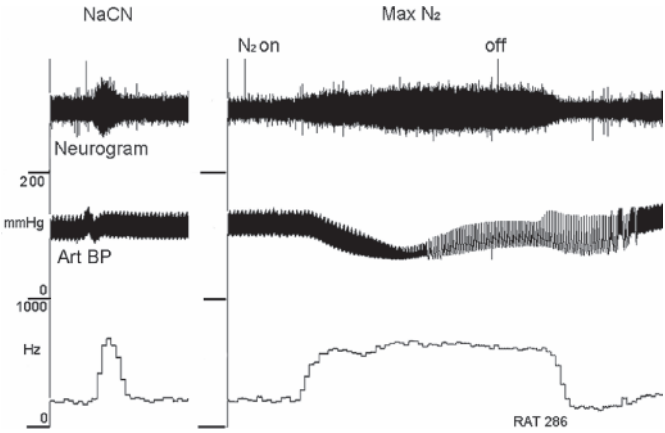

Fig. 1 Response to 40 µg·kg^{-1} NaCN *i.v.* and maximal response to ventilation with 100% N_2 (control rat)

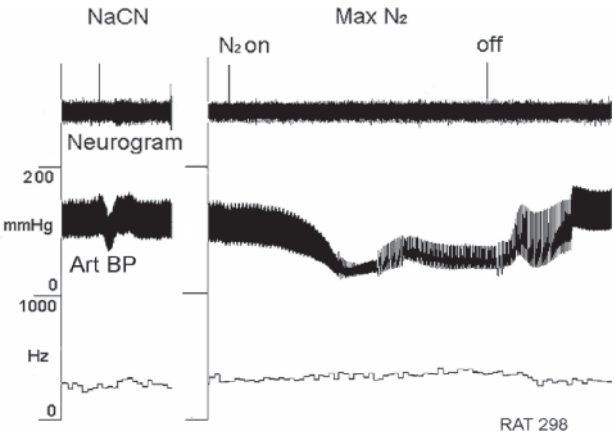

Fig. 2 CSN response to 40 µg·kg $^{-1}$ NaCN *i.v.* and maximal response to ventilation with 100% N_2 (2-week PNH rat)

to PNH had a diminished CSN response to max N_2 (Fig. 2). Mean values for all groups are presented in Fig. 3.

Arterial blood gas measurements indicated that severe hypoxemia and moderate respiratory alkalosis was induced by max N_2 to a similar extent in normal controls and in PNH-treated rats (Table 1).

Responses to max asphyxia were carried out in 9 rats (6 normal controls + 3 two-week PNH rats) that were also subjected to max N_2. The CSN response to max asphyxia was the same as that attained with max N_2 (mean normal control max N_2 frequency increase was 347 Hz, for max asphyxia 332 Hz); while in 2-week PNH rats max N_2 frequency increased 115 Hz, for max asphyxia 130 Hz.

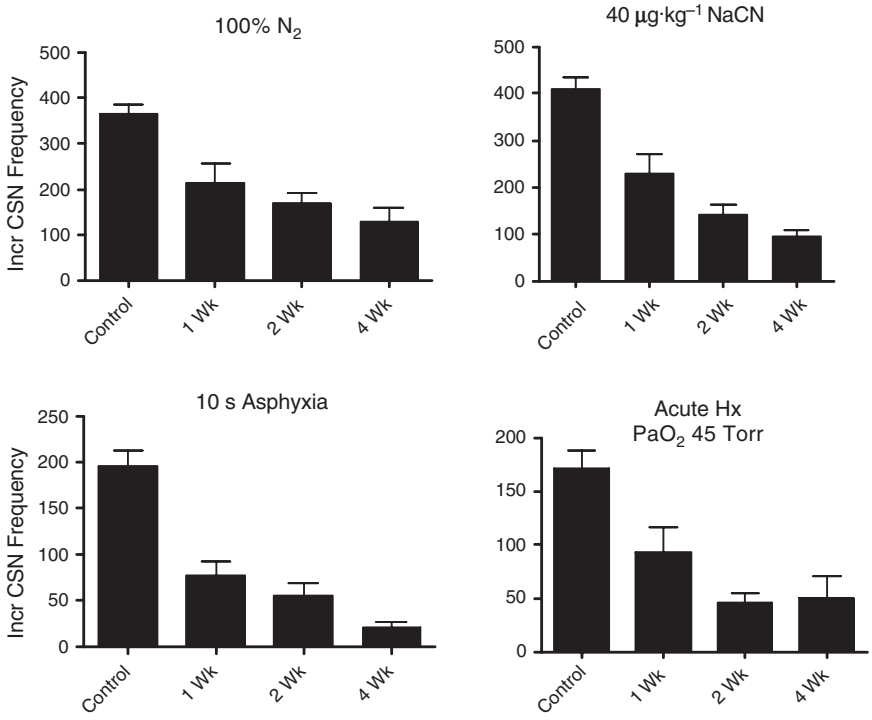

Fig. 3 Mean ± SE responses to acute stimuli (NaCN, 10 sec asphyxia, acute moderate hypoxia) compared to maximal N_2 (100% N_2) in control animals and after 1, 2 and 4 weeks of PNH

Table 1 Mean arterial blood gases and pH (* different from normoxia, $p < 0.001$)

Normal Rats, n = 11	pH	Pco_2, Torr	Po_2, Torr
Normoxia	7.39	37.2	108
Max N_2	7.50*	26.2*	16.8*
PNH Rats, n = 16			
Normoxia	7.41	37.0	105
Max N_2	7.52*	24.1*	17.1*

The mean responses to NaCN, moderate hypoxia and 10 sec asphyxia are summarized in Fig. 3. These results are similar to those previously reported (Bisgard *et al*. 2003). The responses of all PNH treated groups were significantly depressed compared to untreated controls and show the general pattern of similar reduction in CSN response depending on duration of PNH.

4 Discussion

Our findings indicate that PNH significantly attenuates the CSN response to maximal sustained hypoxic and asphyxic stimulation. The responses between these two stimuli were similar in magnitude to a high dose ($40\,\mu g \cdot kg^{-1}$) of NaCN injected IV. The responses to maximal stimuli exhibited the same pattern of reduction depending on the duration of PNH. Depressed CSN responses after PNH likely reflect both reduced chemoafferent hypoxic sensitivity and a lower number of afferent fibers (Donnelly *et al*. 2005; Erickson *et al*. 1998).

Depressed function of peripheral chemoreception may impair ability to respond appropriately in hypoxic episodes by arousal in both adults and infants. Diminished chemoreceptor function after maternal use of nicotine or following prolonged O_2 therapy (*e.g*., in infants with bronchopulmonary dysplasia) may play a role in vulnerability to hypoxia and sudden infant death syndrome (Cohen and Katz-Salamon 2005; Gauda *et al*. 2004).

Acknowledgements The authors thank Gordon Johnson for excellent technical assistance. This research was supported by NIH grants HL68255 and HL07654.

References

Bavis, R.W., Olson E.B. Jr. and Mitchell, G.S. (2002) Critical developmental period for hyperoxia-induced blunting of hypoxic phrenic responses in rats. J. Appl. Physiol. 92, 1013–1018.

Bisgard, G.E., Olson, E.B. Jr., Wang, Z.-Y., Bavis, R.W., Fuller, D.D. and Mitchell, G.S. (2003) Adult carotid chemoafferent responses to hypoxia after 1, 2, and 4 wk of postnatal hyperoxia. J. Appl. Physiol. 95, 946–952.

Cohen, G. and Katz-Salamon, M. (2005) Development of chemoreceptor responses in infants. Resp. Physiol. Neurobiol. 149, 233–242.

Donnelly, D.F., Kim, I., Carle, C. and Carroll, J.L. (2005) Perinatal hyperoxia for 14 days increases nerve conduction time and the unitary response to hypoxia of rat carotid body chemoreceptors. J. Appl. Physiol. 99, 114–119.

Erickson, J.T., Mayer, C., Jawa, A., Ling, L., Olson, E.R. Jr., Vidruk, E.H., Mitchell, G.S. and Katz, D.M. (1998) Chemoafferent degeneration and carotid body hypoplasia following chronic hyperoxia in newborn rats. J. Physiol. (Lond.) 509, 519–526.

Fuller, D.D., Bavis, R.W., Vidruk, E.H., Wang, Z.-Y., Olson, E.B. Jr., Bisgard, G.E. and Mitchell, G.S. (2002) Life-long impairment of hypoxic phrenic responses in rats following 1 month of developmental hyperoxia. J. Physiol. (Lond.) 538.3: 947–955.

Gauda, E.B., McLemore, G.L., Tolosa, J., Marston-Nelson, J. and Kwak, D. (2004) Maturation of peripheral arterial chemoreceptors in relation to neonatal apnoea. Sem. Neonatol. 9, 181–194.

Wang, Z.-Y., Bisgard, G.E. (2005) Postnatal growth of the carotid body. Resp. Physiol. Neurobiol. 149, 181–190.

6
HSP70 Reduces Chronic Hypoxia-Induced Neural Suppression via Regulating Expression of Syntaxin

Guanghe Fei[1,2], Conghui Guo[1], Hong-Shuo Sun[1] and Zhong-Ping Feng[1,*]

Abstract Long-term exposure to modest hypoxia conditions may result in neural dysfunction; however, the involvement of presynaptic proteins has not been tested directly. Here, we reported that adult snails, *Lymnaea stagnalis,* developed a slow righting movement after placement in low O_2 (~ 5%) for 4 days. Semi-quantitative Western blot analysis showed that hypoxia induced heat shock protein 70 (HSP70) up-regulation and a reduction of syntaxin I. The inducible HSP70 occurs within 6 hours preceding the down-regulation of syntaxin I, suggesting that HSP70 may be involved in regulation of syntaxin expression. Injecting directly double-stranded RNAs (dsRNA) into the center ganglia region, we found that dsRNA *HSP70*, not the scrambled RNA, prevented the hypoxia-induced HSP70 expression, enhanced the hypoxia-dependent down-regulation of syntaxin I, and aggravated motor suppression. We thus provided the first evidence that early induction of HSP70 by chronic hypoxia is critical for maintaining expression levels of presynaptic proteins and neural function. These findings implicate a new molecular mechanism underlying chronic hypoxia-induced neurobehavioral adaptation and impairment.

1 Introduction

Long-term oxygen deficiency occurs commonly at high altitudes, and in many chronic diseases which are characterized by insufficient respiration and/or decreased in oxygen delivery. Chronic hypoxia exposure can result in atypical neural behavior such as deficits in neurocognitive and learning abilities (Gozal, Daniel and Dohanich 2001) and motor/sensorimotor restriction (Strata, Coq, Byl and Merzenich 2004). Proper neural behaviors require optimal synaptic activities of neuronal networks,

[1] Department of Physiology, Faculty of Medicine, University of Toronto, Toronto, ON M5S 1A8, Canada

[2] First Affiliated Hospital of Anhui Medical University, Hefei, Anhui 230022, China

* Correspondence should be addressed to Z.P.F. email: zp.feng@utoronto.ca, Tel: (416) 946-5506, Fax: (416) 978-4940)

M.J. Poulin and R.J.A. Wilson (eds.), *Integration in Respiratory Control: From Genes to Systems*. © Springer 2008

including neurotransmitter release from the presynaptic terminals; however, relatively little is known whether and for how long (days) hypoxia affects the release machinery. Heat shock protein 70 (HSP70) is up-regulated by hypoxia exposure, and the inducible HSP70 serves as a useful marker of cellular response to hypoxic insult (Das, Maulik and Moraru 1995). Whether the inducible HSP70 is involved in the presynaptic protein regulation has not been tested directly. *Lymnaea stagnalis* (*L. stagnalis*), a fresh water pond snail, is a bimodal breather. The breathing pattern of the snail changes in responding to O_2 levels in water (Hermann, Wildering and Bulloch 2000; Inoue, Haque, Lukowiak and Syed 2001). Here, we used this simple model to examine the effects of chronic hypoxia on righting behavior and expression level of an exocytotic protein, syntaxin I. Double-stranded RNAi approach was used to determine the role of the inducible HSP70 in such effects.

2 Materials and Methods

2.1 Animals and Righting Behavioral Assessments

L. stagnalis, obtained from an inbred culture at the Free University in Amsterdam, were raised and maintained at 18°C–20°C on a 12 hr light/12 hr dark cycle in aquaria at the University of Toronto. Adult snails were used in all experiments. A control normoxia group of snails was placed in well-aerated water; the hypoxia group was forced to submerge in water equilibrated with ~ 5% O_2 (pH: 7).

To assess righting behavioral activities, individual snails were placed upside down onto their backs; the time required for the snail to resume its upright posture was recorded and compared between the control and hypoxia groups. The experiment was repeated 3 times at 5-minute intervals.

2.2 Western Blots

Snail ganglia proteins were prepared and Western blots performed following the standard protocols. Primary antibodies used were HSP70 (Santa Cruz); syntaxin I (Chemicon); and β-actin (Chemicon). Proteins were visualized using ECL and detected using Kodak Image Station. The data were analyzed using Kodak 1D image analysis DC290 software and normalized by the ratio of specific protein to β-actin.

2.3 Double-Stranded RNA (dsRNA) Synthesis and Delivery

The dsRNA (321 bp) specific to *Lymnaea* HSP70 (DQ206432) was produced using standard PCR (the forward primer: 5′-CCAAGAGGCGTCCCAC-3′, the reverse

primer: 5′-CTTGGACGCCTCTTGG -3′). Each strand was purified using LiCl and dsRNA was generated by combining equal molar amounts of sense and anti-sense transcripts. Scrambled dsRNA (scrRNA, 320 bp) was produced using the same protocol. RNA_{HSP70}, scrRNA, or snail saline (control) was injected into the snail ganglia.

2.4 Data Analysis

The data are presented as the mean ± S.E.M. Statistical analysis was carried out using SigmaStat 3.0 (Jandel Scientific). Differences between mean values from each experimental group were tested using one-way analysis of variance (ANOVA). Differences were considered significant if $p < 0.05$.

3 Results

3.1 Righting Behavior Suppression in Chronic Hypoxia Conditions

To study whether the motor activity is suppressed by hypoxia exposure, we studied the righting behavior of the animal. Figure 1A shows that the time required for the control animals to right themselves was 120.8 ± 10.0 s (n = 8), and it increased significantly as the duration of hypoxic exposure prolonged, reaching a maximal level on the sixth day (227.5 ± 22.8 s; n = 8; $p < 0.05$). Our results demonstrated that the righting motor activity was suppressed under long-term hypoxia treatment.

3.2 Time Dependence of Hypoxia-Induced Molecular Alteration

The expression levels of HSP70 and syntaxin I under hypoxia conditions were then determined using semi-quantitative Western blot analyses. Figures 1B1 and 1B2 show that the relative HSP70 expression progressively increased from 6 hours to 6 days of exposure to hypoxia. The increase at all stages was significant as compared to expression levels in the normoxia group. A 7.21 ± 0.75 fold increase of HSP at 6 days of hypoxia was coincident with righting suppression (Fig. 1A). Syntaxin level, however, decreased significantly after one day of treatment (Fig. 2C1 and 2C2), and was maintained at a relatively stable level up to 6 post-hypoxia days. The modest hypoxia-induced HSP70 expression preceded syntaxin down regulation and thus may play a role in preventing reduction of syntaxin I to maintain neural function.

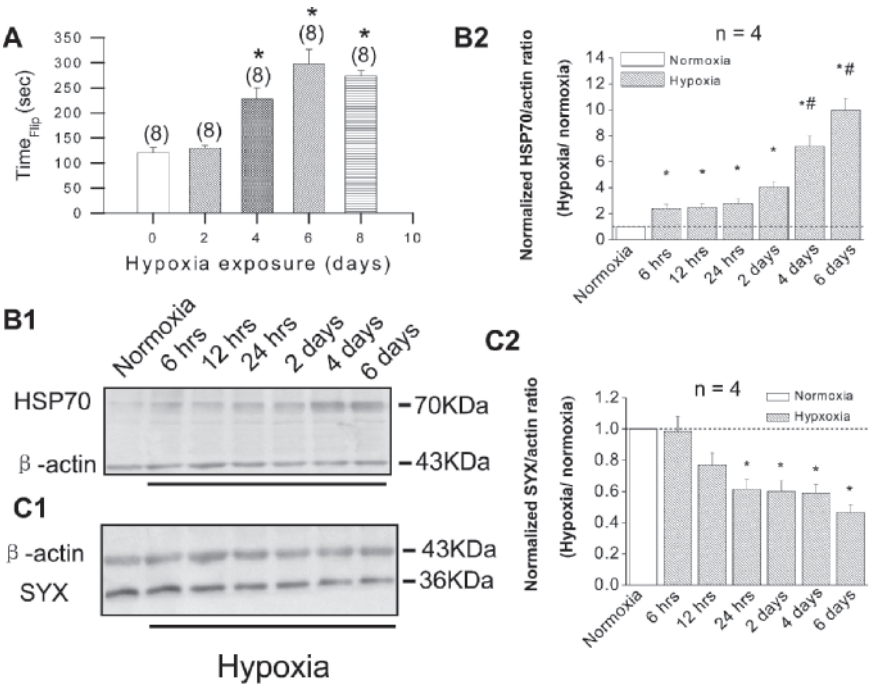

Fig. 1 Chronic hypoxic exposure suppressed righting reflex, increased neuronal HSP70 and reduced syntaxin I expression. (A) Hypoxia prolonged the time required for the snails to return to their upright position after being flipped upside down. Representative semi-quantitative Western blots of HSP70 (B1), SYX (C1), and β-actin (B1, C1) from the central ganglia of normoxic and hypoxic snails at the different times after exposure to low O_2. The summary of normalized intensity for HSP70 (B2) and SYX (C2) to β-actin. * Statistical significance ($p < 0.05$) as compared to the normoxia group

3.3 The Role of HSP70 dsRNA in Syntaxin I Expression and the Right ing Behavior

To determine the role of HSP70 in chronic hypoxia-induced neural suppression and reduction of syntaxin I expression, dsRNAi approach was used to prevent HSP70 induction. Fig. 2A1 shows that RNA_{HSP70}-treated animal failed to induce HSP70 in response to hypoxia, in contrast to the srcRNA-treated and the control hypoxia groups. The relative expression level of syntaxin (Fig. 2A2) in the RNA_{HSP70}-treated group (0. 35 ± 0.04, n = 4) was significantly lower than that of the control (0.60 ± 0.07, n = 4) or the scrRNA-treated hypoxia (0.62 ± 0.08, n = 4) groups. These data indicate that HSP70 may contribute to prevent syntaxin I from degradation under hypoxic conditions. Moreover, the time required for snails to right themselves (Fig. 2B) was significantly increased in the RNA_{HSP70}-treated hypoxia group (316.27 ± 29.56 s) compared

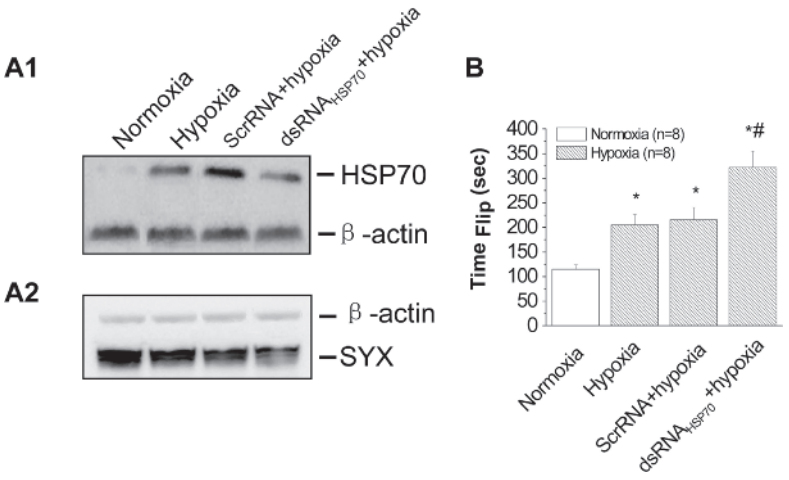

Fig. 2 ***HSP70*** dsRNAi affected syntaxin I expression and righting behavior in chronic hypoxia *L. stagnalis*. Representatives of semi-quantitative immunoblots of HSP70 (**A1**), syntaxin I (**A2**), and β-actin from the control, scrRNA and RNA_{HSP70} treated animals under indicated conditions. (**B**) The time required for the snails to return to their upright position from upside down in indicated groups following exposure to hypoxic conditions for 4 days. *, # Statistical significance ($p < 0.05$) to the normoxia group and to other hypoxia groups

to the control hypoxia (227.54 ± 22.76 s) or the srcRNA-treated hypoxia group (230.56 ± 23.71 s), indicating that the righting ability was further reduced in the absence of inducible HSP70.

4 Discussion

Hypoxia stimulation causes an immediate compensatory and a delayed adaptive alteration in metabolism, respiratory ventilation, cardiac output and neuromuscular activity (Powell, Milsom and Mitchell 1998; Prabhakar, Fields, Baker and Fletcher 2001). We found that the righting activities of snails were suppressed by extending exposure to hypoxic conditions. The observed behavioral suppression may result from a deficiency in either muscle and/or neuronal functions; however, we showed that ganglial expression of syntaxin I was co-incidentally reduced. This indicates that the reduced availability of syntaxin I may contribute, at least in part, to hypoxia-induced behavioral suppression.

Cells transactivate HSP70 in response to environment alterations (Semenza 1999). Our finding of the early induction of HSP70 by hypoxia is consistent with the previous reports. Injection of synthesized dsRNA into the invertebrates results in the gene-specific interference (*C elegans*: Fire, Xu, Montgomery, Kostas, Driver

and Mello 1998). We used a similar approach and showed that injecting dsRNA into ganglia of adult snails prevented the hypoxia-induced expression of HSP70. In our hands, the RNAi effect was consistent and reproducible. HSPs function as molecular chaperones that recognize and interact with target proteins in non-native conformations (Somero 1995). Our observations of a positive correlation between HSP induction and syntaxin I expression provide the first evidences that HSP70 may serve as a chaperone involving in the presynaptic protein regulation. However, the potential conformational effects of the chaperone machinery of HSP on SNARE complex formation remain to be investigated.

References

Das, D.K., Maulik, N. and Moraru, I.I. (1995) Gene expression in acute myocardial stress. Induction by hypoxia, ischemia, reperfusion, hyperthermia and oxidative stress. J. Mol. Cell Cardiol. 27, 181–193.

Fire, A., Xu, S., Montgomery, M.K., Kostas, S.A., Driver, S.E. and Mello, C.C. (1998) Potent and specific genetic interference by double-stranded RNA in *Caenorhabditis elegans*. Nature 391, 806–811.

Gozal, D., Daniel, J.M. and Dohanich, G.P. (2001) Behavioral and anatomical correlates of chronic episodic hypoxia during sleep in the rat. J. Neurosci. 21, 2442–2450.

Hermann, P.M., Wildering, W.C. and Bulloch, A.G. (2000) Functional recovery of respiratory behavior during axonal regeneration in snails (*Lymnaea stagnalis*) is experience dependent. Behav. Neurosci. 114, 410–423.

Inoue, T., Haque, Z., Lukowiak, K. and Syed, N.I. (2001) Hypoxia-induced respiratory patterned activity in *Lymnaea* originates at the periphery. J. Neurophysiol. 86, 156–163.

Powell, F.L., Milsom, W.K. and Mitchell, G.S. (1998) Time domains of the hypoxic ventilatory response. Respir. Physiol. 112, 123–134.

Prabhakar, N.R., Fields, R.D., Baker, T. and Fletcher, E.C. (2001) Intermittent hypoxia: cell to system. Am. J. Physiol. Lung Cell Mol. Physiol. 281, L524–L528.

Semenza, G.L. (1999) Perspectives on oxygen sensing. Cell 98, 281–284.

Somero, G.N. (1995) Proteins and temperature. Annu. Rev. Physiol. 57, 43–68.

Strata, F., Coq, J.O., Byl, N. and Merzenich, M.M. (2004) Effects of sensorimotor restriction and anoxia on gait and motor cortex organization: implications for a rodent model of cerebral palsy. Neuroscience 129, 141–156.

7
Effect of Systemic Administration of the Nitric Oxide Synthase Inhibitor L-NMMA on the Human Ventilatory Response to Hypoxia

Kojiro Ide[1], Matthew Worthley[3,4], Todd Anderson[3,4] and Marc J. Poulin[1,2,4,5,6]

1 Introduction

Although it is well known that nitric oxide (NO) production is involved in several physiological functions (*e.g.*, vasodilatation, platelet inhibition, immune responses, cell adhesion and neurotransmission), its role in the regulation of respiration is less clear. In carotid body studies, most studies indicate that NO appears to play an inhibitory role in response to hypoxia (Gozal, Gozal, Gozal and Torres 1996a; Gozal, Torres, Gozal and Littwin 1996b; Iturriaga, Villanueva and Mosqueira 2000; Trzebski, Sato, Suzuki and Sato 1995; Valdes, Mosqueira, Rey, Del Rio and Iturriaga 2003). However, there is less agreement for studies carried out in the nucleus tractus solitarius (NTS), with some studies indicating that NO may play an excitatory role in response to hypoxia (Kline, Yang, Huang and Prabhakar 1998; Vitagliano, Berrino, D'Amico, Maione, De Novallis and Rossi 1996) and others suggesting that NO plays an inhibitory role (Haxhiu, Chang, Dreshaj, Erokwu, Prabhakar and Cherniack 1995; Ogawa, Mizusawa, Kikuchi, Hida, Miki and Shirato 1995). Further, the aforementioned studies have been carried out in experimental animal models and it is unclear whether NO is involved in the regulation of respiration in humans. Thus, we sought to elucidate the effects of systemic administration of N^G-Monomethyl-L-arginine (L-NMMA) on the response of ventilation ($\dot{V}_E$) to 20 min of isocapnic hypoxia in human volunteers.

2 Methods

Subjects visited the laboratory on a *Control Day* (no infusion) and on an *L-NMMA Day* (L-NMMA infusion). Nitric oxide synthase (NOS) inhibition was instituted by L-NMMA (Clinalfa AG, Läufelfingen Switzerland) and administered intravenously;

[1] University of Calgary, Departments of Physiology & Biophysics, [2] Clinical Neurosciences, and [3] Cardiac Sciences, [4] Libin Cardiovascular Institute and [5] Hotchkiss Brain Institute, [6] Faculty of Medicine and Faculty of Kinesiology, poulin@ucalgary.ca

M.J. Poulin and R.J.A. Wilson (eds.), *Integration in Respiratory Control: From Genes to Systems*.

first by a bolus (5 mg kg^{-1}; concentration range = 183–270 mg 50 ml^{-1} over 5 min; 10 ml min^{-1}), then by infusion (50 µg kg^{-1} min^{-1}; concentration range = 732–1080 mg 250 ml^{-1} over 240 min; 1.0 ml min^{-1}). End-tidal gases were controlled using the technique of dynamic end-tidal forcing (Ide, Eliasziw and Poulin 2003; Poulin and Robbins 1998).

The protocol started with a 10-min period during which end-tidal PO_2 ($PETO_2$) was maintained at 88 Torr and end-tidal PCO_2 ($PETCO_2$) was held at 1.5 Torr above the subject's natural value as determined on that day. Then, $PETO_2$ was lowered to 50 Torr (over 2–3 breaths) and maintained constant for 20 min. Finally, $PETO_2$ was returned (again within 2–3 breaths) to its initial euoxic value and maintained constant for a further 10 min. Throughout, $PETCO_2$ was maintained constant at 1.5 Torr above the subject's normal value.

3 Results

During air breathing, there were no effect of L-NMMA administration on $PETCO_2$ and $PETO_2$, whereas mean arterial pressure increased (MAP; 80.0 ± 13.9 to 87.6 ± 15.3 mmHg, 7.3%, $p < 0.01$) and heart rate decreased (HR; 57.5 ± 10.9 to 51.6 ± 10.6 beats min^{-1}, 10.3%, $p < 0.01$) (Fig. 1).

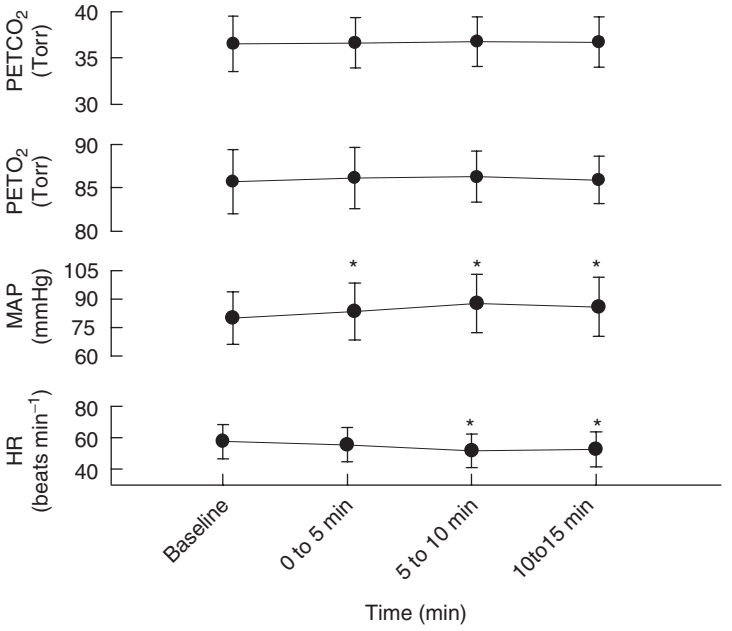

Fig. 1 Changes in end-tidal PCO_2 (PET_{CO_2}) and PO_2 (PET_{O_2}), mean arterial blood pressure (MAP) and heart rate (HR) before and after L-NMMA administration during air breathing. Each symbol represents a group mean (n = 10 subjects) ± SD. *, significant differences from Baseline at $p < 0.05$

When the end-tidal gases were regulated near-resting values (*i.e.*, isocapnia and euoxia), there was a significant effect of L-NMMA administration on MAP, HR and $\dot{V}_E$. Compared with the *Control Day*: (a) MAP was higher (76.3 ± 7.5 *vs* 86.7 ± 3.8 mmHg, n = 8, p = 0.004), (b) HR was lower (59.5 ± 8.8 *vs* 55.8 ± 10.9 bpm, p = 0.018), and $\dot{V}_E$ was lower (12.6 ± 3.9 *vs* 10.1 ± 2.0 $l \cdot min^{-1}$, p = 0.043, GLM, SPSS v. 14.01).

On the *Control Day*, $\dot{V}_E$ increased from 12.6 ± 3.9 to 43.4 ± 17.2 $l \cdot min^{-1}$ during the initial 5 min of hypoxia and gradually decreased to 27.5 ± 11.7 $l \cdot min^{-1}$ during the last min of hypoxic period and then returned to 13.3 ± 4.6 $l \cdot min^{-1}$ during the fifth min of recovery (eucapnic euoxia). During the systemic administration of L-NMMA, $\dot{V}_E$ increased from 10.1 ± 2.0 to 37.7 ± 16.0 $l \cdot min^{-1}$ during the initial 5 min of hypoxia and gradually decreased to 24.2 ± 18.6 $l \cdot min^{-1}$ during the last min of hypoxic period and then returned to 11.5 ± 5.8 $l \cdot min^{-1}$ during the fifth min of recovery (Fig. 2 and Table 1).

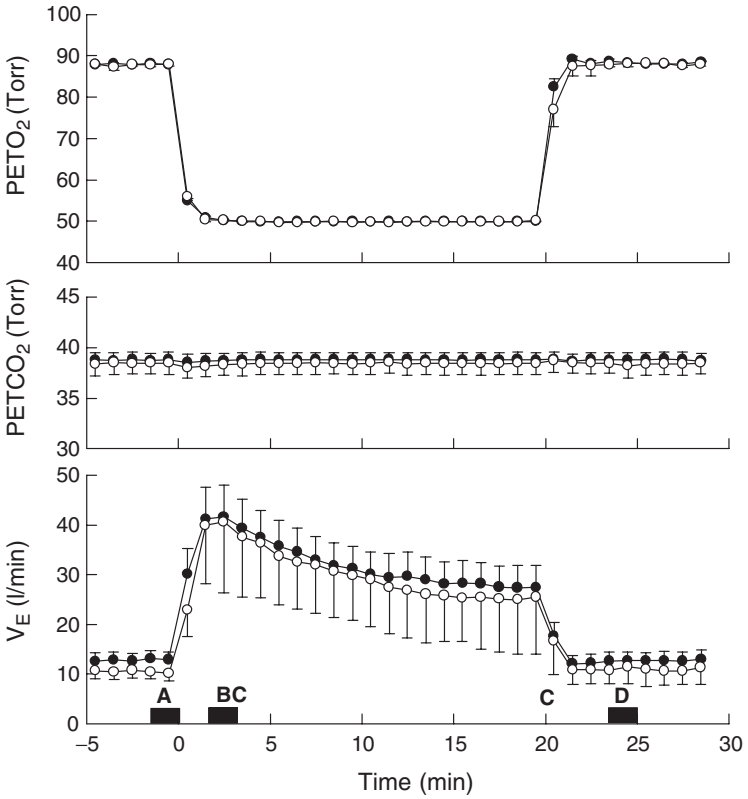

Fig. 2 Ensemble-averages of the time-related changes in end-tidal PO_2 ($P_{ET_{O_2}}$) and PCO_2 ($P_{ET_{CO_2}}$), and the ventilatory responses ($\dot{V}_E$) to hypoxia. Profiles represent group averages (n = 10 subjects) for control (solid circles) and L-NMMA (open circles) days. Each symbol and error bar represents a 60-sec mean ± SD

Table 1 Ventilatory responses to isocapnic hypoxia with and without L-NMMA

Time Period*	Control	L-NMMA	p-value
A	12.6± 3.9	10.1± 2.0	0.043
B	43.4±17.2	37.7±16.0	0.055
C	27.5±11.7	24.2±18.6	0.443
D	13.3± 4.6	11.5±5.8	0.331
B – A (AHVR)	30.8±15.0	27.6±14.9	0.093
B – C (HVD)	15.9± 7.4	13.5± 8.7	0.476

Values are means ± SD (l min^{-1}).

* Time periods correspond to those indicated by solid bars in Fig. 2 (A, isocapnic euoxia; B, acute hypoxic ventilatory responses (AHVR); C, last min of hypoxia; D, fifth minute of the recovery period from isocapnic hypoxia; B – A, AHVR; B – C, hypoxic ventilatory decline (HVD).

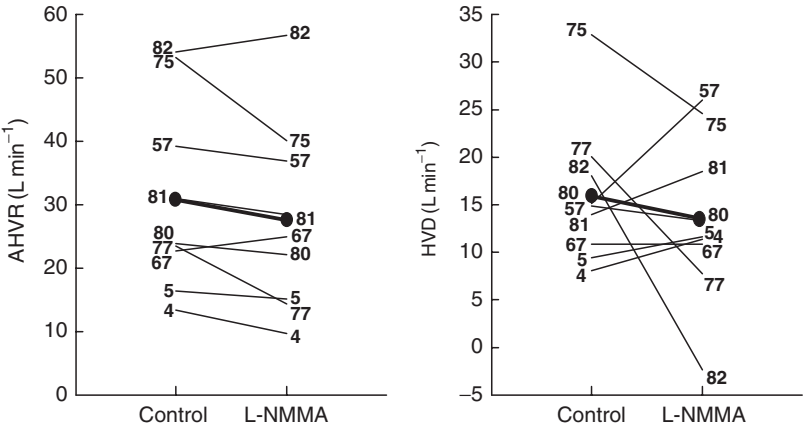

Fig. 3 Acute hypoxic ventilatory response (AHVR) and hypoxic ventilatory decline (HVD) for control and L-NMMA days. Individual data are illustrated by numbers (subject ID numbers) while the group means (n = 9) are illustrated by solid circles

The peak $\dot{V}_E$ response to the initial 5 min of hypoxia showed a lower tendency with L-NMMA (37.7 ± 16.0 *vs* 43.4 ± 17.2 l·min^{-1}). This trend was also apparent in the acute hypoxic ventilatory responses after correction for the lower baseline $\dot{V}_E$ (values during isocapnia and euoxia) (30.8 ± 15.0 *vs* 27.6 ± 14.9 l·min^{-1}, Table 1).

There was no effect of L-NMMA on the hypoxic ventilatory dec line (HVD) or ventilatory off-response (Fig. 3).

4 Discussion

It has not been known whether NO is involved in the regulation of hypoxic or hypercapnic respiration in humans. This study was the first attempt to investigate how the systemic administration of the non-selective NOS inhibitor, L-NMMA

would affect the acute hypoxic ventilatory response (AHVR). Following the L-NMMA, $\dot{V}_E$ during isocapnic euoxia decreased significantly and also there was a lower tendency in the peak $\dot{V}_E$ response to the initial 5 min of hypoxia, resulting in a lower tendency in AHVR. The exact mechanism responsible for the lower tendency in AHVR following the L-NMMA is unclear in this study. Peripheral chemoreceptor sensitivity may be responsible for altering the magnitude of AHVR. In carotid body studies (animal model), it was shown that NO appears to play an inhibitory role in the hypoxic response (Gozal *et al*. 1996a; Gozal *et al*. 1996b; Iturriaga *et al*. 2000; Trzebski *et al*. 1995; Valdes *et al*. 2003). However, those observations in the animal models contradict the results in humans (this study). It is not clear whether the lower tendency of AHVR would reflect changes in peripheral chemoreceptor sensitivity or central effect of L-NMMA.

Acknowledgements This project was supported by the Alberta Heritage Foundation for Medical Research (AHFMR), Heart and Stroke Foundation of Alberta, NWT, & Nunavut, the Canadian Institutes of Health Research (CIHR) and the Canada Foundation for Innovation (CFI). KI was supported by an AHFMR Postdoctoral Fellowship. TJA and MJP are AHFMR Senior Medical Scholars.

References

Gozal, D., Gozal, E., Gozal, Y.M. and Torres, J.E. (1996a) Nitric oxide synthase isoforms and peripheral chemoreceptor stimulation in conscious rats. Neuroreport 7, 1145–1148.

Gozal, D., Torres, J.E., Gozal, Y.M. and Littwin, S.M. (1996b) Effect of nitric oxide synthase inhibition on cardiorespiratory responses in the conscious rat. J. Appl. Physiol. 81, 2068–2077.

Haxhiu, M.A., Chang, C.H., Dreshaj, I.A., Erokwu, B., Prabhakar, N.R. and Cherniack, N.S. (1995) Nitric oxide and ventilatory response to hypoxia. Respir. Physiol. 101, 257–266.

Ide, K., Eliasziw, M. and Poulin, M.J. (2003) The relationship between middle cerebral artery blood velocity and end-tidal PCO_2 in the hypocapnic-hypercapnic range in humans. J. Appl. Physiol. 95, 129–137.

Iturriaga, R., Villanueva, S. and Mosqueira, M. (2000) Dual effects of nitric oxide on cat carotid body chemoreception. J. Appl. Physiol. 89, 1005–1012.

Kline, D.D., Yang, T., Huang, P.L. and Prabhakar, N.R. (1998) Altered respiratory responses to hypoxia in mutant mice deficient in neuronal nitric oxide synthase. J. Physiol. 511.1, 273–287.

Ogawa, H., Mizusawa, A., Kikuchi, Y., Hida, W., Miki, H. and Shirato, K. (1995) Nitric oxide as a retrograde messenger in the nucleus tractus solitarii of rats during hypoxia. J. Physiol. 486.2, 495–504.

Poulin, M.J. and Robbins, P.A. (1998) Influence of cerebral blood flow on the ventilatory response to hypoxia in humans. Experim. Physiol. 83, 95–106.

Trzebski, A., Sato, Y., Suzuki, A. and Sato, A. (1995) Inhibition of nitric oxide synthesis potentiates the responsiveness of carotid chemoreceptors to systemic hypoxia in the rat. Neurosci. Lett. 190, 29–32.

Valdes, V., Mosqueira, M., Rey, S., Del Rio, R. and Iturriaga, R. (2003) Inhibitory effects of NO on carotid body: contribution of neural and endothelial nitric oxide synthase isoforms. Am. J. Physiol. 284, L57–L68.

Vitagliano, S., Berrino, L., D'Amico, M., Maione, S., De Novallis, V. and Rossi, F. (1996) Involvement of nitric oxide in cardiorespiratory regulation in the nucleus tractus solitarii. Neuropharmacology 35, 625–631.

8
Effects of Volatile Anesthetics on Carotid Body Response to Hypoxia in Animals

Jaideep J. Pandit[1] and Kevin O'Gallagher[2]

Abstract This study was a systematic review of the anesthetic effect on carotid body response to hypoxia. We undertook a systematic literature search (electronic plus manual) for full-paper articles in English that used methodologies enabling any anesthetic effect to be located to the carotid body. We found just 7 articles that met our inclusion criteria, incorporating 16 separate studies. Anesthetic (mean dose ± SD 0.70 ± 0.33 MAC) significantly depressed carotid body response by 24% ($p = 0.041$). There were no differences between individual agents (halothane, enflurane, isoflurane) and no influence of the use of neuromuscular blockade or of species (although the data were sufficiently sparse to interpret such sub-group analysis with caution).

1 Introduction

In humans, volatile anesthetics in low dose (< 0.2 minimum alveolar concentration, MAC) significantly depress the ventilatory response to hypoxia by up to 70% (Pandit 2002). The depressive action may occur at the level of the carotid body: when ventilatory responses to hypoxia in humans are analysed mathematically into 'fast' and 'slow' components (corresponding to peripheral chemoreceptor and central effects, respectively), the fast component is preferentially affected by volatile agents (Dahan, van den Elsen, Berkenbosch, de Goede, Olievier, van Kleef and Bovill 1994). Buckler, Williams and Honore (2000) have described a potassium channel in the carotid body glomus cell, sensitive to hypoxia, acid and halothane, potentially making it a candidate mechanism for the effects described.

Nonetheless, a review of the effect of anesthetics on the carotid body (Eriksson, 1999) concluded that "the carotid body chemoreceptors are minimally affected by inhaled anesthetics, even at anesthetic levels of the vapor [and] function is well-maintained at sub-anesthetic end-tidal concentrations." This assertion implies that

[1] University of Oxford, Nuffield Department of Anaesthetics, John Radcliffe Hospital, jaideep.pandit@physiol.ox.ac.uk

[2] University of Oxford, Nuffield Department of Anaesthetics, John Radcliffe Hospital, kevin.ogallagher@jesus.ac.uk

M.J. Poulin and R.J.A. Wilson (eds.), *Integration in Respiratory Control: From Genes to Systems*.

the anesthetic depressive effect is located more centrally in the hypoxic chemoreflex loop (presumably in the brain) and not at the carotid body.

However, Eriksson's review was not *systematic* (*i.e.*, it did not define explicit search strategies or specific criteria for accepting or rejecting data); and only seven animal reports (and one abstract) were quoted. This may have reflected the true paucity of data in the field but, in the absence of a systematic approach, it is difficult to be confident that this was the case. The purpose of our study was to address these shortcomings. We wished to conduct a quantitative, systematic review to assess more precisely the extent to which volatile anesthetics depress (or not) the response of the carotid body to hypoxia.

2 Methods

2.1 Data Retrieval and Inclusion Criteria

We conducted a formal search of Medline and PubMed using explicit search terms, supplemented this by a manual search of the reference lists of the initially retrieved papers. An article was accepted if: (a) it was a full paper and not an abstract or letter; (b) it was in English (or with a co-translation); and (c) it concerned animal investigation.

We assessed each retrieved paper on its ability to isolate the anesthetic effect to the carotid body itself. Thus, we determined that the following experimental preparations were acceptable:

(1) any study in which recordings were taken from the carotid sinus nerve (the anesthetic being administered either to an isolated, separately perfused carotid body or to the whole animal);
(2) any study in which the carotid body was isolated and so could be separately perfused and so separately exposed to anesthetic and hypoxia. Recordings might be taken either from the carotid sinus nerve or from the phrenic nerve or from the minute ventilation of the animal. Such methods might include methods that separately perfused the carotid body from the systemic circulation or artificial brainstem perfusion techniques that separated the brain's circulation from that of the body (including from that of the carotid body).

2.2 Data Formatting

For each article accepted, we recorded: the animal species (and number), whether neuromuscular blockade was used, the anesthetic used (and dose). If an article presented only a range of doses and did not specify the exact dose administered, we used the middle of range of doses presented. Where a published article contained

data from more than one agent, or the same agent at more than one dose or had examined more than one species of animal, we regarded each as a separate study.

The 'response' to hypoxia in the presence of anesthetic was expressed as a fraction of the 'response' without anesthetic (the 'standardised hypoxic response,' SHR). The nature of the 'response' varied and was (a) carotid sinus or phrenic nerve activity, (b) minute ventilation, or (c) as either of (a) or (b) per % hemoglobin desaturation with hypoxia.

In summary, each published *article* we accepted yielded one or more *studies*. Each *study* yielded a *standardised hypoxic response* reflecting anesthetic effect. The SHRs for all studies were averaged (with weighting) and analysis undertaken on these weighted means.

2.3 Statistical Analysis

Values for SHR were subjected to analysis of variance (with the factors being 'agent', 'species', 'neuromuscular blockade') and *post hoc* t-tests.

3 Results

For all agents combined, the weighted SHR was 0.76 ± 0.43 (Table 1), which indicates that on average anesthetics significantly depressed carotid body hypoxic response by 24% ($p = 0.041$). SHRs for different agents were similar: halothane 0.73

Table 1 SHR values from each study from each article accepted. Also shown is the agent used, its dose (MAC), the number (n) and type of animal used and whether neuromuscular blockade was used (NMB)

Study from	Agent	Dose (MAC)	NMB	Animal	n	SHR
Biscoe and Purves	halothane	1.250	Y	cat	1	1.04
Biscoe and Purves	halothane	2.500	Y	cat	1	0.69
Davies et al.	halothane	0.625	Y	cat	6	0.58
Van Dissel et al.	halothane	1.250	N	cat	6	0.54
Morray et al.	halothane	0.625	Y	cat	6	1.84
Morray et al.	halothane	1.250	Y	cat	6	0.20
Ide et al.	halothane	0.125	Y	cat	10	0.94
Ide et al.	halothane	1.000	Y	cat	10	0.11
Ponte and Sadler	halothane	0.938	Y	rabbit	5	1.00
Ponte and Sadler	halothane	0.938	Y	cat	5	0.92
Ponte and Sadler	enflurane	0.500	Y	rabbit	4	0.67
Ponte and Sadler	enflurane	0.500	Y	cat	7	0.96
Ponte and Sadler	isoflurane	0.682	Y	rabbit	4	0.89
Ponte and Sadler	isoflurane	0.682	Y	cat	8	0.67
Joensen et al.	isoflurane	0.909	N	rabbit	6	0.92
Joensen et al.	isoflurane	0.091	N	rabbit	3	0.69

± 0.53, enflurane 0.85 ± 0.23, isoflurane 0.79 ± 0.11 (ANOVA, p = 0.96). The weighted mean dose of anesthetics used in all studies combined was 0.70 ± 0.33 MAC. SHR was not influenced by use of neuromuscular blockade, or by the species studied (ANOVA: p = 0.70 and p = 0.91, respectively). Thus, the mean result of studies using neuromuscular blockade (0.72 ± 0.23, n = 3) was similar to that of studies using no blockade (0.76 ± 0.47, n = 13); and the mean result of studies in cats (0.77 ± 0.47, n = 11) was similar to that of studies in rabbits (0.83 ± 0.15, n = 5).

4 Discussion

Our main finding is that volatile anesthetics modestly but significantly depress the carotid body response to hypoxia. We found no evidence that either use of neuromuscular blockade or species influences this result. When we compare the available data for anesthetic effect in humans with our data for effect on carotid bodies (Pandit 2002), the striking result is the exquisite sensitivity of whole-body response versus the insensitivity of the carotid body response. Thus, in humans, approximately 0.1–0.2 MAC anesthetic halves the hypoxic response. In animal carotid bodies (Table 1), a dose ~ 0.7 MAC on average reduces carotid body hypoxic response by just a quarter (~ 24%). We summarize these differences in Fig. 1. The difference in sensitivity may reflect ‘species differences’ between humans and animals. The cellular basis of such ‘species difference’ may lie with differences in transduction mechanisms within the carotid body. Alternatively, human and animal carotid bodies may employ the same transduction processes, but there may be important differences in structure of the proteins or channels involved that lead to a differential sensitivity to anesthetics.

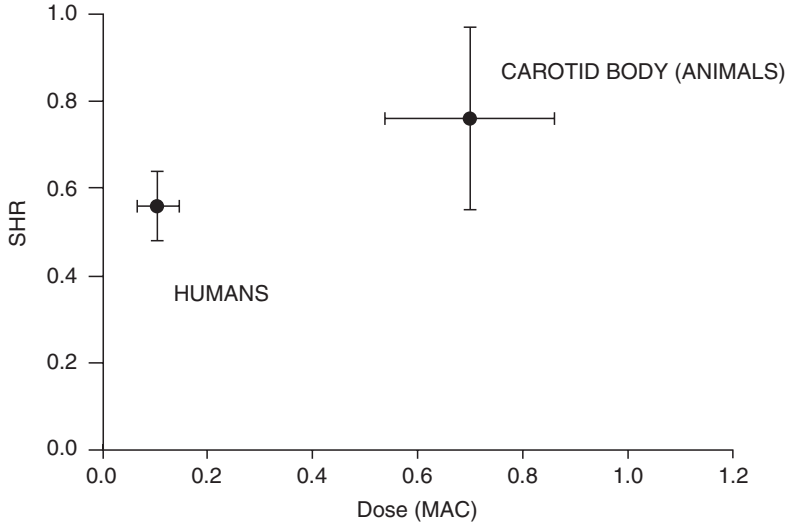

Fig. 1 Summary of SHR vs anesthetic dose (MAC) for human studies (data from Pandit 2000) and carotid body animal studies (this review). Means ± 95% confidence intervals

In summary, there have been remarkably few studies addressing the question of volatile anesthetics and the carotid body, and there is still place for a carefully conducted animal carotid body study. Our review highlights what might be learned from focusing future research on the specific cellular/molecular mechanisms that underlie the transduction process.

Acknowledgements This work was supported by a grant jointly from the British Journal of Anaesthesia and Royal College of Anaesthetists of the United Kingdom.

References

Biscoe, T.J. and Millar, R.A. (1968) Effects of inhalation anaesthetics on carotid body chemoreceptor activity. Br. J. Anaesth. 40, 2–12.

Buckler, K.J., Williams, B.A. and Honore, E. (2000) An oxygen-, acid- and anaesthetic-sensitive TASK-like background potassium channel in rat arterial chemoreceptor cells. J. Physiol. 525, 135–142.

Dahan, A, van den Elsen, M.J.L.J., Berkenbosch, A., de Goede, J., Olievier, I.C., van Kleef, J.W. and Bovill, J.G. (1994) Effects of subanesthetic halothane on the ventilatory responses to hyercapnia and acute hypoxia in healthy volunteers. Anesthesiology 80, 727–738.

Davies, R.O., Edwards, M.W. and Lahiri, S. (1982) Halothane depresses the response of carotid body chemoreceptors to hypoxia and hypercapnia in the cat. Anesthesiology 57, 153–159.

Eriksson, L.I. (1999) The effects of residual neuromuscular blockade and volatile anaesthetics on the control of ventilation. Anesth. Analg. 89, 243–251.

Ide, T., Sakurai, Y., Aono, M. and Nishino, T. (1999) Contribution of peripheral chemoreception to the depression of the hypoxic ventilatory response during halothane anesthesia in cats. Anesthesiology 90, 1084–1091.

Joensen, H., Sadler, C.L., Ponte, J., Yamamoto, Y., Lindahl, S.G.E. and Eriksson, L.I. (2000) Isoflurane does not depress the hypoxic response of rabbit carotid chemoreceptors. Anesth. Analg. 91, 480–485.

Morray, J.P., Nobel, R., Bennet, L. and Hanson, M.A. (1996) The effect of halothane on phrenic and chemoreceptor responses to hypoxia in anesthetized kittens. Anesth. Analg. 83, 329–335.

Pandit, J.J. (2002) The variable effect of low-dose volatile anaesthetics on the acute ventilatory response to hypoxia in humans: a quantitative review. Anaesthesia 57, 632–643.

Ponte, J. and Sadler, C.L. (1989) Effect of halothane, enflurane and isoflurane on carotid body chemoreceptor activity in the rabbit and the cat. Br. J. Anaesth. 62, 33–40.

Van Dissel, J., Berkenbosch, A., Olievier, C.N., de Goede, J. and Quanjer, Ph. H. (1985) Effects of halothane on the ventilatory response to hypoxia and hypercapnia in cats. Anesthesiology 62, 448–456.

9
Mutation of the von Hippel-Lindau Gene Alters Human Cardiopulmonary Physiology

T.G. Smith[1], J.T. Brooks[1], G.M. Balanos[2], T.R. Lappin[3], D.M. Layton[4], D.L. Leedham[5], C. Liu[1], P.H. Maxwell[6], M.F. McMullin[7], C.J. McNamara[8], M.J. Percy[7], C.W. Pugh[9], P.J. Ratcliffe[9], N.P. Talbot[1], M. Treacy[5] and P.A. Robbins[1]

Abstract Intracellular responses to hypoxia are coordinated by the von Hippel-Lindau – hypoxia-inducible factor (VHL-HIF) transcriptional system. This study investigated the potential role of the VHL-HIF pathway in human systems-level physiology. Patients diagnosed with Chuvash polycythaemia, a rare disorder in which VHL signalling is specifically impaired, were studied during acute hypoxia and hypercapnia. Subjects breathed through a mouthpiece and ventilation was measured while pulmonary vascular tone was assessed echocardiographically. The patients were found to have elevated basal ventilation and pulmonary vascular tone, and ventilatory, pulmonary vasoconstrictive and heart rate responses to acute hypoxia were greatly increased, as were heart rate responses to hypercapnia. The patients also had abnormal pulmonary function on spirometry. This study's findings demonstrate that the VHL-HIF signalling pathway, which is so central to intracellular oxygen sensing, also regulates the organ systems upon which cellular oxygen delivery ultimately depends.

[1] University of Oxford, Department of Physiology, Anatomy and Genetics, peter.robbins@physiol.ox.ac.uk

[2] University of Birmingham, School of Sport and Exercise Sciences

[3] Belfast City Hospital, Queen's University, Centre for Cancer Research and Cell Biology

[4] Imperial College of Science, Technology and Medicine, Department of Haematology

[5] Chase Farm Hospital, Diagnostics, Therapies and Cancer Division

[6] Imperial College of Science, Technology and Medicine, Renal Section

[7] Belfast City Hospital, Queen's University, Department of Haematology

[8] The Royal Free Hospital, Department of Haematology

[9] University of Oxford, Nuffield Department of Clinical Medicine

M.J. Poulin and R.J.A. Wilson (eds.), *Integration in Respiratory Control: From Genes to Systems*.

1 Introduction

Intracellular responses to hypoxia are coordinated by the hypoxia-inducible factor (HIF) family of transcription factors (Semenza 2004). HIF is primarily regulated via its interaction with the von Hippel-Lindau tumour suppressor protein (VHL) (Maxwell *et al*. 1999). Oxygen-dependent hydroxylation of HIF increases its affinity for VHL (Jaakkola *et al*. 2001) which then binds to HIF, so targeting it for proteasomal degradation. Under hypoxic conditions this hydroxylation and degradation are slowed, resulting in accumulation of HIF and up-regulation of HIF-dependent genes.

Chuvash polycythaemia (CP) is a rare disorder caused by a point mutation in VHL that diminishes its binding affinity for hydroxylated HIF (Ang *et al*. 2002). HIF target genes including erythropoietin are pathologically up-regulated, resulting in congenital erythrocytosis. CP provides a unique opportunity to explore the molecular mechanisms underlying cardiopulmonary physiology. A recent publication reported this study's major findings and included data not shown here (Smith *et al*. 2006). The spirometry and hypercapnia protocol data have not previously been published.

2 Methods

These methods have been described in detail elsewhere (Smith *et al*. 2006). Three patients with CP were compared with a normal control group (six age- and sex-matched healthy volunteers) and a polycythaemia control group (three sex-matched patients with polycythaemia unrelated to VHL). The CP patients and polycythaemia control subjects had been chronically venesected to a normal haematocrit and were iron-deficient, although none had recently been venesected. The CP patients (age 22.3 ± 5 yr) did not differ significantly in age, height, weight or BMI from the normal control group (24.2 ± 5 yr). The study was approved by the Oxfordshire Clinical Research Ethics Committee, and each participant provided written informed consent.

Pulmonary function tests were performed using a handheld spirometer (Micro Medical Ltd, Kent, UK) and peak flow meter (Vitalograph Ltd, Buckingham, UK). Each subject then undertook six protocols. The first two protocols determined responses to very mild hypoxia. An initial five min of euoxia (end-tidal partial pressure of oxygen, $P_{ET_{O_2}}$, of 100 mmHg) preceded 10 min hypoxia at $P_{ET_{O_2}}$ 70 mmHg, followed by a final 5 min of euoxia. The second two protocols determined responses to moderate hypoxia using a stimulus $P_{ET_{O_2}}$ of 50 mmHg. The end-tidal partial pressure of carbon dioxide, $P_{ET_{CO_2}}$, was maintained close to each subject's baseline air-breathing value throughout the hypoxia protocols. The final two protocols determined responses to euoxic hypercapnia ($P_{ET_{CO_2}}$ 5 mmHg above each subject's baseline value).

Gas control was achieved using dynamic end-tidal forcing (Robbins *et al*. 1982). Subjects breathed through a mouthpiece and ventilation was measured using a

turbine volume-measuring device. During the first of each pair of protocols, pulmonary vascular tone was assessed continuously by echocardiography (Smith *et al*. 2006). In this technique, Doppler measurements are used to determine the maximum systolic pressure gradient across the tricuspid valve (ΔP_{max}), a standard index of pulmonary vascular tone. Cardiac output was determined echocardiographically during the second protocol in each pair.

Differences between groups were assessed using Student's unpaired t-test (Microsoft Excel) and univariate repeated measures ANOVA (SPSS statistical package), and were considered significant at the $p < 0.05$ level.

3 Results

3.1 Pulmonary Function Tests

Mean arterial P_{CO_2} was 6 mmHg lower in the CP patient group than in the normal control group (data not shown; $p < 0.05$). In the CP patients, forced expiratory volume in one second (FEV_1), forced vital capacity (FVC) and peak expiratory flow rate (PEFR) were all approximately 80% of predicted values (adjusted for age, sex, height and ethnicity), and were significantly lower than for the normal controls (Table 1; $p < 0.05$). However, the FEV_1/FVC ratio was preserved in the CP patients.

3.2 Hypoxia Protocols

These results have been reported previously (Smith *et al*. 2006). Both mild and moderate hypoxia provoked a greater increase in ventilation in CP patients than in normal control subjects ($p < 0.05$). Baseline pulmonary arterial pressure in the CP patients was almost double that of the control group ($p < 0.01$). The ΔP_{max} response was much more vigorous in the CP patient group with both mild and moderate hypoxia ($p < 0.01$). Upon transition to mild hypoxia, heart rate increased 3.2-fold more in the CP patient group ($p < 0.01$); the corresponding difference was not statistically significant with moderate hypoxia. Changes in cardiac output did not differ significantly between the two groups.

Table 1 Pulmonary function tests. Values are mean ± SD. Asterisks indicate significant differences between each control group and the CP patient group (*, $p < 0.05$; **, $p < 0.01$)

	CP Patients (n = 3)	Normal Controls (n = 6)	Polycythaemia Controls (n = 3)
FEV_1 (% predicted)	80.4 ± 6.5	98.4 ± 6.5 **	99.4 ± 6.3 *
FVC (% predicted	80.8 ± 4.8	99.3 ± 9.3 *	102.8 ± 3.4 **
FEV_1/FVC ratio	0.85 ± 0.01	0.85 ± 0.05	0.81 ± 0.04
PEFR (% predicted)	83.6 ± 9.5	102.6 ± 7.0 *	99.3 ± 11.6

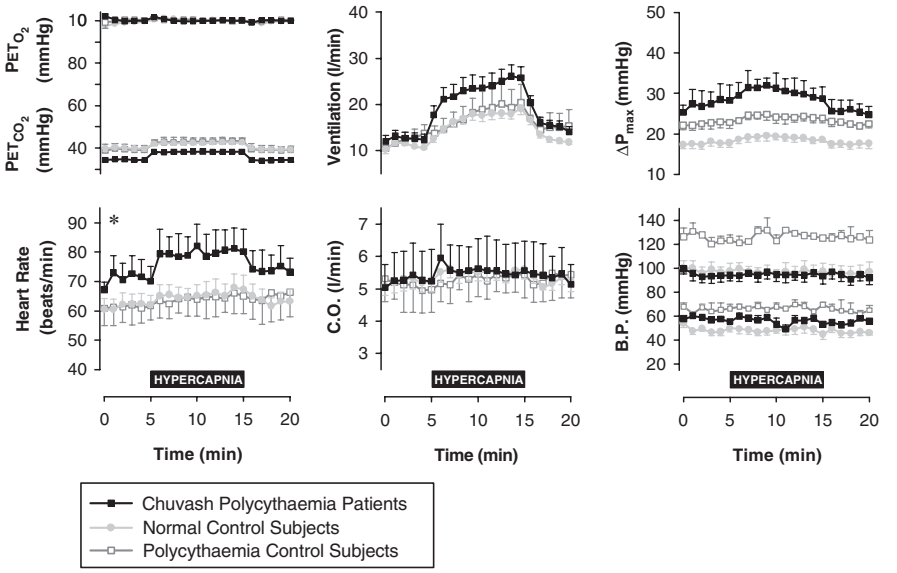

Fig. 1 Hypercapnia Protocol: End-tidal Gas Control and Physiological Responses. The baseline air-breathing $P_{ET_{CO2}}$ was lower in the CP patient group. ΔP_{max} is a standard echocardiographic index of pulmonary vascular tone. C.O., cardiac output. B.P., blood pressure. Systolic (upper plot) and diastolic blood pressure (lower plot) are shown. Values are mean ± SEM. Asterisk (*) indicates a significantly greater response in the CP patient group than in the normal control group ($p < 0.05$)

3.3 Hypercapnia Protocols

The changes in ventilation, ΔP_{max} and cardiac output stimulated by hypercapnia did not differ significantly between the groups (Fig. 1). However, hypercapnia provoked a 3.7-fold greater rise in heart rate in CP patients than in normal controls ($p < 0.05$).

3.4 Polycythaemia Control Subjects

The polycythaemia control subjects had normal pulmonary function tests (Table 1). The major physiological abnormalities present in the CP patients were not present in the polycythaemia control subjects (Fig. 1; repeated measures ANOVA).

4 Discussion

It is striking that CP patients had elevated basal ventilation (as evidenced by arterial hypocapnia whilst breathing air) and baseline pulmonary arterial hypertension, as well as displaying extremely high ventilatory and pulmonary vascular sensitivities

to acute hypoxia, as together these are characteristic features of acclimatisation to the hypoxia of high altitude. As discussed previously (Smith *et al*. 2006), these findings strongly implicate the VHL-HIF system in human acclimatisation to hypoxia and establish an important role for VHL in regulating cardiopulmonary control in hypoxia-naïve individuals.

CP is inherited recessively and thus VHL signalling is impaired from conception. It is therefore remarkable that CP patients do not resemble individuals born and raised at high altitude, in whom physiological responses to hypoxia are blunted (reviewed by Rupert and Hochachka 2001), but rather resemble individuals who are acutely acclimatised to hypoxia. Furthermore, whereas high altitude natives tend to develop large lungs (Rupert and Hochachka 2001), the pulmonary function test results reported in this study suggest the opposite is true of CP patients. This aspect of the CP phenotype may reflect a lung-specific role of HIF in foetal development, in which HIF is known to perform critically important functions (Semenza 2004).

Involvement of VHL-HIF in cardiopulmonary control is consistent with the nature of some of the genes HIF is known to regulate including tyrosine hydroxylase, endothelin-1, endothelial nitric-oxide synthase, $\alpha_{1\beta}$-adrenergic receptor, adrenomedullin, heme oxygenase-1 and atrial natriuretic peptide (Schofield and Ratcliffe 2004). It is interesting that CP patients had increased heart rate sensitivity to both hypoxia and hypercapnia. One theoretical explanation is that pathological up-regulation of tyrosine hydroxylase, the rate-limiting enzyme in catecholamine biosynthesis, contributes to a state of heightened sympathetic activation.

In conclusion, our findings demonstrate that a subtle disorder of HIF degradation profoundly alters human cardiopulmonary physiology. Thus, it appears that the VHL-HIF transcriptional signalling pathway, which is so central to intracellular oxygen sensing, also plays a major role in calibrating the organ systems upon which cellular oxygen delivery ultimately depends. This has important implications for nascent therapies directed towards manipulation of the VHL-HIF pathway as a treatment for cancer and ischaemic/hypoxic vascular disease.

Acknowledgements Thomas G. Smith is supported by a Rhodes Scholarship. This work was funded by the Wellcome Trust. We thank David O'Connor for expert technical assistance, and the patients and volunteers who took part in this study.

References

Ang, S.O., Chen, H., Hirota, K., Gordeuk, V.R., Jelinek, J., Guan, Y., Liu, E., Sergueeva, A.I., Miasnikova, G.Y., Mole, D., Maxwell, P.H., Stockton, D.W., Semenza, G.L. and Prchal, J.T. (2002) Disruption of oxygen homeostasis underlies congenital Chuvash polycythemia. Nat. Genet. 32, 614–621.

Jaakkola, P., Mole, D.R., Tian, Y.M., Wilson, M.I., Gielbert, J., Gaskell, S.J., Kriegsheim, A.V., Hebestreit, H.F., Mukherji, M., Schofield, C.J., Maxwell, P.H., Pugh, C.W. and Ratcliffe, P.J. (2001) Targeting of HIF-α to the von Hippel-Lindau ubiquitylation complex by O_2-regulated prolyl hydroxylation. Science 292, 468–472.

Maxwell, P.H., Wiesener, M.S., Chang, G.W., Clifford, S.C., Vaux, E.C., Cockman, M.E., Wykoff, C.C., Pugh, C.W., Maher, E.R. and Ratcliffe, P.J. (1999) The tumour suppressor protein VHL targets hypoxia-inducible factors for oxygen-dependent proteolysis. Nature 399, 271–275.

Robbins, P.A., Swanson, G.D. and Howson, M.G. (1982) A prediction-correction scheme for forcing alveolar gases along certain time courses. J. Appl. Physiol. 52, 1353–1357.

Rupert, J.L. and Hochachka, P.W. (2001) The evidence for hereditary factors contributing to high altitude adaptation in Andean natives: a review. High Alt. Med. Biol. 2(2), 235–256.

Schofield, C.J. and Ratcliffe, P.J. (2004) Oxygen sensing by HIF hydroxylases. Nat. Rev. Mol. Cell Biol. 5, 343–354.

Semenza, G.L. (2004) Hydroxylation of HIF-1: oxygen sensing at the molecular level. Physiology (Bethesda) 19, 176–182.

Smith, T.G., Brooks, J.T., Balanos, G.M., Lappin, T.R., Layton, D.M., Leedham, D.L., Liu, C., Maxwell, P.H., McMullin, M.F., McNamara, C.J., Percy, M.J., Pugh, C.W., Ratcliffe, P.J., Talbot, N.P., Treacy, M. and Robbins, P.A. (2006) Mutation of von Hippel–Lindau tumour suppressor and human cardiopulmonary physiology. PLoS Med. 3(7), e290.

10
Intravenous Endothelin-1 and Ventilatory Sensitivity to Hypoxia in Humans

Nick P. Talbot[1], George M. Balanos[2], Peter A. Robbins[1] and Keith L Dorrington[1]

Abstract The effects of intravenous endothelin-1 (ET-1) on the ventilatory response to hypoxia were studied in healthy humans. Nine volunteers were each exposed twice to 4 hr eucapnic hypoxia. They received a continuous infusion of ET-1 during the ET-1 protocol and an infusion of saline during the control protocol. Plasma ET-1 levels and an index of ventilation were measured regularly. Hypoxia caused a rise in plasma ET-1 in the control protocol. Hypoxia also caused the index of ventilation to increase in both protocols, and this increase was greater in the ET-1 protocol than in the control protocol. These results are consistent with the hypothesis that ET-1 plays a role in controlling the ventilatory response to hypoxia in man.

1 Introduction

There is evidence to suggest that sustained hypoxia enhances the chemo-sensitivity of the carotid body, and that this process contributes to ventilatory acclimatisation (Howard and Robbins 1995). However, the cellular mechanisms underlying this process remain unclear.

Since the characterisation of the transcription factor hypoxia-inducible factor-1 (HIF-1) as a regulator of responses to sustained hypoxia in man, there has been interest in its potential role in the regulation of ventilation. In support of such a role, impaired ventilatory acclimatisation to chronic hypoxia has been reported in mice deficient in the alpha subunit of HIF-1 (HIF-1α; Kline *et al*. 2002), and more recently, exaggerated ventilatory responses to acute hypoxia have been reported in patients with congenital upregulation of HIF-1α (Smith *et al*. 2006).

Endothelin-1 (ET-1) is a 21-amino acid peptide whose expression is increased during hypoxia, at least in part by HIF-1 (Yamashita *et al*. 2001). Originally described as a potent systemic vasoconstrictor, the peptide has emerged as a

[1] University of Oxford, Department of Physiology, Anatomy and Genetics, UK, keith.dorrington@physiol.ox.ac.uk

[2] University of Birmingham, School of Sport and Exercise Sciences, UK

M.J. Poulin and R.J.A. Wilson (eds.), *Integration in Respiratory Control: From Genes to Systems*.

potential mediator of ventilatory acclimatisation. In rabbit isolated carotid bodies, ET-1 had no effect during hyperoxia but augmented carotid sinus nerve discharge during acute reductions of superfusate oxygen tension (Chen *et al*. 2000). In addition, the expression of both ET-1 and its receptor (ET_A) in rat carotid body was greatly upregulated during chronic hypoxia, and was accompanied by an increased sensitivity to reduced oxygen tension that could be inhibited by an ET_A antagonist (Chen *et al*. 2002).

To address the hypothesis that increased plasma ET-1 would enhance the ventilatory response to hypoxia in man, we measured ET-1 levels and an index of ventilation in volunteers exposed to 4 hr of hypoxia with and without an intravenous ET-1 infusion. This exposure was part of a separate study designed to investigate the effects of ET-1 on pulmonary and systemic haemodynamics during hypoxia, the detailed results of which will be reported elsewhere.

2 Methods

Nine healthy volunteers (2 female, 7 males, age 24 ± 3 years, mean ± SD) took part in the study. The study received ethical approval and volunteers gave informed consent. Each volunteer undertook two 7-hr protocols, separated by at least one week. ET-1 was administered intravenously during one protocol, and saline during the other. In all other respects, the protocols were identical, and volunteers were unaware which protocol they were undertaking on each day.

2.1 End-tidal Gas Control

Experiments took place in a purpose-built chamber in which respired gas was sampled using a nasal catheter. Inspired and end-tidal values were recorded breath-by-breath (Datex Engstrom gas analyzer, Finland), and control of end-tidal gases was achieved using computer-automated adjustment of chamber gas composition, as described elsewhere (Howard *et al*. 1995). Protocols consisted of 1 hr of air breathing, followed by 4 hr of eucapnic hypoxia (end-tidal P_{O_2}, 50 Torr) and then 2 hr of eucapnic euoxia (end-tidal P_{O_2}, 100 Torr). During eucapnic periods, end-tidal P_{CO_2} was maintained at each volunteer's normal value, measured at the start of each protocol.

2.2 Endothelin-1 Infusion

Human ET-1 (Clinalfa AG, Switzerland) was infused for 7 hr through an indwelling venous cannula in the forearm. The rate was 1.0 ng kg^{-1} min^{-1} for the first 30 min, but

was then increased gradually to a maximum of 2.5 ng kg^{-1} min^{-1} over the next 30 min. In some volunteers, ET-1 produced a mild inflammatory response or stiffness at or near the infusion site and, when necessary, the rate was varied to control these symptoms. The total volume of infusion was 59 ± 15 ml (mean ± SD). During the control protocol, a similar volume of normal saline was infused at a constant rate.

2.3 Physiological Measurements

Ventilation was not measured directly in this study, but an index of ventilation was calculated retrospectively by taking the reciprocal of the difference between inspired and end-tidal P_{CO_2}, both of which were recorded continuously during each protocol.

Small (5 ml) venous blood samples were obtained every 60 min from a forearm vein, anticoagulated with EDTA and spun for 15 min at 3000 rpm to obtain plasma. Plasma was stored at −20°C for subsequently determination of ET-1 concentration by enzyme-linked immunosorbent assay (ELISA; QuantiGlo human ET-1 immunoassay, R&D systems, UK).

Additional measurements were made during both protocols as part of another study. These data will be reported in detail elsewhere, but mean values for some parameters during hypoxia are shown in Fig. 1.

2.4 Statistical Analysis

Repeated measures analysis of variance (ANOVA) was used to determine whether exogenous ET-1 altered the effect of hypoxia on the index of ventilation in this study. This analysis used data from the periods 0–1 hr (euoxia), 4–5 hr (hypoxia)

	ET-1	Control
Cardiac output (L min^{-1})	5.38 ± 0.25	6.06 ± 0.23 *
Mean arterial pressure (mmHg)	85.1 ± 2.1	81.4 ± 1.8
Arterial oxygen saturation (%)	83.2 ± 0.2	82.9 ± 0.2
Plasma ET-1 (pg ml^{-1})	17.4 ± 2.8	1.7 ± 0.1 *

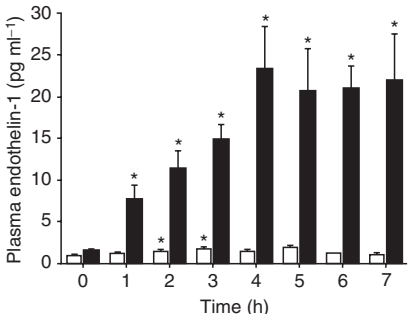

Fig 1 *Left*: Mean cardiac output, arterial pressure, arterial oxygen saturation and plasma ET-1 during hypoxia. Asterisks indicate significant difference between ET-1 and control protocols ($p < 0.05$). *Right*: plasma ET-1 during ET-1 (*black bars*) and control (*open bars*) protocols. Asterisks indicate significant difference from baseline (0 hr, $p < 0.02$). Data are presented as mean ± SEM, n = 9

and 6–7 hr (euoxia). Paired Student's *t*-tests were used for all other comparisons. Statistical significance was assumed if $p < 0.05$. Values are given as mean ± SEM, unless stated.

3 Results

3.1 Plasma ET-1 Concentration

Venous plasma ET-1 concentration during each protocol is shown in Fig. 1. At baseline (0 hr), plasma ET-1 was 1.0 ± 0.1 pg ml^{-1} in the ET-1 protocol and 1.3 ± 0.2 pg ml^{-1} in the control protocol ($p > 0.07$). These values are in good accord with the normal range quoted by the assay manufacturer (range 0.5–2.3, mean 1.1 pg ml^{-1}, n = 66 healthy humans).

In the control protocol, ET-1 levels were elevated above baseline within 1 hr of hypoxia onset ($p < 0.02$), rising to reach a mean of 1.7 ± 0.1 pg ml^{-1} during the final 2 hr of hypoxia. On return to euoxia, ET-1 levels returned to baseline within 1 hr.

In the ET-1 protocol, ET-1 levels were greater than baseline at every time-point following the onset of infusion ($p < 0.02$), and were at every point substantially higher than in the control protocol ($p < 0.02$). A steady state of plasma ET-1 appeared to occur approximately 4 hr after the onset of infusion.

3.2 Ventilatory Response to Hypoxia

Changes in our index of ventilation during both protocols are shown in Fig. 2.

Before hypoxia, there was no difference between the two protocols. Ventilation increased rapidly during the first 30 min of hypoxia and more gradually for the remainder of the exposure. There was no clear difference between the two protocols for the first 1–2 hr of hypoxia, but thereafter ventilation appeared to be enhanced in the ET-1 protocol. ANOVA suggested that the effect of hypoxia on ventilation was indeed increased in the ET-1 protocol, compared with the control protocol ($p < 0.05$).

Upon returning to euoxia, ventilation initially fell rapidly toward baseline. However, this rapid response was followed in both protocols by a more complex change in ventilation during the final 90 min of the protocol.

4 Discussion

This study has two main findings, both of which are consistent with a possible role for ET-1 in the control of ventilation during hypoxia in man. First, we report a progressive rise in plasma ET-1 levels during eucapnic hypoxia. Second, we report that

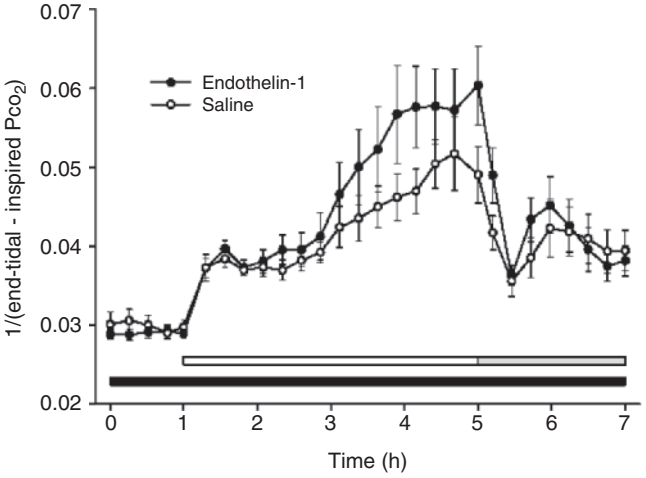

Fig. 2 Reciprocal of the difference between end-tidal and inspired P_{CO_2} during 4 hr eucapnic hypoxia (*white bar*, end-tidal P_{O_2}=50 Torr) followed by 2 hr eucapnic euoxia (*grey bar*, end-tidal P_{O_2} = 100 Torr). *Black bar* indicates 7 hr infusion of ET-1 or normal saline (control). Symbols represent mean ± SEM of previous 15 min, n = 9

exogenous ET-1 enhanced the effect of hypoxia on an indirect index of ventilation. There are several possible explanations for this result, including the following:

(i) One possibility is that exogenous ET-1 may directly enhance the sensitivity of the carotid body to hypoxia. A role for both endogenous and exogenous ET-1 in enhancing carotid body chemo-sensitivity during hypoxia is supported by previous observations in animals (Chen *et al*. 2000; Chen *et al*. 2002). The reason for the apparent delay between the onset of hypoxia and an effect of ET-1 in the current study is unclear, but it may represent the time required for other biochemical effects of hypoxia, such as upregulation of ET_A receptor expression in the carotid body.

(ii) An alternative explanation is that ET-1 had no specific effect on ventilation, but instead caused a reduction in metabolic rate (*i.e.,* rate of CO_2 production). We did not measure metabolic rate directly, but a significantly lower cardiac output during hypoxia in the ET-1 protocol, compared with the control protocol (Fig. 1), would be consistent with this explanation.

(iii) A third possibility is that ET-1 had no direct effect on carotid body type I cells, but altered their activity via an effect on blood supply. Mean arterial pressure during hypoxia appeared to be slightly higher in the ET-1 protocol than in the control protocol (Fig. 1), suggesting that the peptide did mediate some vasoactive effects.

In summary, our results are consistent with the hypothesis that ET-1 may enhance the sensitivity of the carotid body during sustained hypoxia. This may represent a mechanism for modulation of ventilation by HIF-1 during sustained hypoxia.

However, further studies are required to confirm these preliminary results and to distinguish between the various possible interpretations of our current findings.

Acknowledgement This work was supported by the Dunhill Medical Trust and the Wellcome Trust.

References

Chen, J., He, L., Dinger, B., Stensaas, L. and Fidone, S. (2002). Role of endothelin and endothelin A-type receptor in adaptation of the carotid body to chronic hypoxia. Am. J. Physiol. 282, L1314–L1323.

Chen, J., He, L., Dinger, B. and Fidone, S. (2000) Cellular mechanisms involved in rabbit carotid body excitation elicited by endothelin peptides. Resp. Physiol. 121, 13–23.

Howard, L.S. and Robbins, P.A. (1995). Alterations in respiratory control during 8 hr of isocapnic and poikilocapnic hypoxia in humans. J. Appl. Physiol. 78, 1098–1107.

Howard, L.S., Barson, R.A, Howse, B.P., McGill, T.R, McIntyre, M.E., O'Connor, D.F. and Robbins, P.A. (1995). Chamber for controlling end-tidal gas tensions over sustained periods in humans. J. Appl. Physiol. 78, 1088–1091.

Kline, D.D., Peng, Y., Manalo, D.J., Semenza, G.L. and Prabhaker, N.R. (2002) Defective carotid body function and impaired ventilatory responses to chronic hypoxia in mice partially deficient for hypoxia-inducible factor 1α. PNAS 99, 821–826.

Smith, T.G., Brooks, J.T., Balanos, G.M., Lappin, T.R., Layton, D.M., Leedham, D.L., Liu, C., Maxwell, P.H., McMullin, M.F., McNamara, C.J., Percy, M.L., Pugh, C.W., Ratcliffe, P.J., Talbot, N.P., Treacy, M. and Robbins, P.A. (2006) Mutation of von Hippel-Lindau tumour suppressor and human cardiopulmonary physiology. PLoS Med. 3(7), e290.

Yamashita, K., Discher, D.J, Hu, J. Bishopric, N.H. and Webster, K.A. (2001) Molecular regulation of the endothelin-1 gene by hypoxia. Contributions of hypoxia-inducible factor-1, activator protein-1, GATA-2 and p300/CBP. J. Biol. Chem. 276, 12645–12653.

11
Key Roles for AMP-activated Protein Kinase in the Function of the Carotid Body?

Christopher N. Wyatt[1], Selina A. Pearson[2], Prem Kumar[2], Chris Peers[3], D. Grahame Hardie[4] and A. Mark Evans[1]

Abstract The carotid bodies play a critical role in initiating compensatory ventilatory responses to hypoxia. However, the complete mechanism by which hypoxia excites the oxygen-sensing carotid body type 1 cells has not been fully defined. We have previously proposed that the enzyme adenosine monophosphate-activated protein kinase (AMPK) may couple hypoxic inhibition of mitochondrial oxidative phosphorylation to carotid body type I cell excitation (Evans, Mustard, Wyatt, Peers, Dipp, Kumar, Kinnear and Hardie 2005). Here we discuss evidence that AMPK is a key requirement for hypoxic chemotransduction by the carotid body. In addition, we postulate upon a role for AMPK in the plasticity observed in the carotid body during both chronic and chronic intermittent hypoxia.

1 Introduction

During the last 21 years the mechanisms by which hypoxia excites the type I cells of the carotid body have been studied in tremendous detail by multiple researchers worldwide. It has been established that when carotid body microvascular pO_2 falls from approximately 50 Torr (normoxia) to 20–30 Torr (hypoxia) chemoreceptor output increases dramatically (Lahiri, Rumsey, Wilson and Iturriaga 1993) leading to an increase in ventilation. The underlying process by which this occurs involves inhibition of O_2-sensitive K^+ channels in the type I cell (Lopez-Barneo, Lopez-Lopez, Urena and Gonzalez 1988; Hescheler, Delpiano, Acker and Pietruschka 1989; Peers 1990; Stea and Nurse 1991; Buckler 1997; Perez-Garcia, Colinas, Miguel-Velado,

[1] University of St Andrews, Division of Biomedical Sciences, School of Biology. ame3@st-andrews.ac.uk

[2] University of Birmingham, Department of Physiology, The Medical School. P.Kumar@bham.ac.uk

[3] University of Leeds, Department of Medicine. c.s.peers@leeds.ac.uk

[4] University of Dundee, Division of Molecular Physiology, School of Life Sciences. d.g.hardie@dundee.ac.uk

M.J. Poulin and R.J.A. Wilson (eds.), *Integration in Respiratory Control: From Genes to Systems*.

Moreno-Dominguez and Lopez-Lopez 2004) which initiate voltage-gated calcium entry (Buckler and Vaughan-Jones 1994) thereby evoking neurotransmitter release (Eyzaguirre, Koyano and Taylor 1965; Fidone, Gonzalez, Dinger and Hanson 1988) with resultant increase in sensory afferent discharge to the brainstem.

Despite agreement on this basic cascade for hypoxic chemotransduction the precise means by which hypoxia brings about inhibition of K^+ channels remains speculative with multiple mechanisms proposed. However, perhaps the most outstanding feature of the carotid body is its O_2-sensitivity. Relatively mild hypoxia (Lahiri *et al*. 1993) excites the carotid body, and it is known that this level of hypoxia will cause the mitochondria of the type I cells to depolarize and NAD(P)H levels to rise (Duchen and Biscoe 1992a, b). This phenomenon occurs over a range of pO_2 values that evoke no such response in other cell types (Duchen and Biscoe 1992a) and therefore provides strong supporting evidence for the hypothesis that mitochondrial oxidative phosphorylation is unusually sensitive to hypoxia in the carotid body (Mills and Jobsis 1970, 1972). Further studies have demonstrated that a wide spectrum of mitochondrial inhibitors not only mimic hypoxia in the intact carotid body and isolated type I cell but that they occlude any further effect of hypoxia (Mulligan, Lahiri and Storey 1981; Buckler and Vaughan-Jones 1998; Mosqueira and Iturriaga 2002; Wyatt and Buckler 2004). Thus, mitochondrial inhibition and hypoxia must be acting on the type 1 cell by a common or convergent mechanism (see Wyatt and Buckler 2004). Taken together, these data suggest that relatively mild hypoxia will inhibit type I cell mitochondrial oxidative phosphorylation and that this couples to K^+ channel inhibition with consequent initiation of the chemotransduction cascade.

1.1 Could AMPK Underpin Hypoxic Chemotransduction?

Our recent research has demonstrated that the 'energy-sensing' enzyme AMP-activated protein kinase may provide the direct coupling mechanism necessary to link hypoxic inhibition of mitochondrial oxidative phosphorylation to K^+ channel inhibition (Evans *et al*. 2005; Wyatt, Kumar, Aley, Peers, Hardie and Evans 2006a; Wyatt, Peers, Kumar, Hardie and Evans 2006b).

Hypoxic attenuation of mitochondrial oxidative phosphorylation will result in a fall in the cellular energy status and a rise in the cellular ADP/ATP ratio. Consequently, adenylate kinase will catalyse a reaction that converts 2 molecules of ADP to AMP and ATP in order to maintain cellular ATP levels. The resultant rise in the AMP/ATP ratio will activate AMPK, a serine threonine kinase comprising a catalytic α subunit and regulatory β and γ subunits (Hardie 2004). Previously, we have shown that hypoxia increased the AMP/ATP ratio in O_2-sensing cells with a resultant increase in AMPK activity (Evans *et al*. 2005). Additionally, this preliminary study ascertained that, like hypoxia, activation of AMPK evoked calcium influx into carotid body type I cells and increased afferent fibre discharge from the carotid body. However,

whether these effects occurred via the same mechanisms engaged by hypoxia was not established. Our most recent data now suggest that this is the case.

2 Methods

Neonatal (10–21 days) rat carotid body type I cells were isolated as previously described (Wyatt and Buckler 2004). Cells were allowed to adhere to poly-d-lysine coated coverslips before being used for immunofluorescent imaging, calcium imaging or electrophysiology. Carotid sinus nerve recordings were made from an *in vitro* carotid body preparation as previously described. (Pepper, Landauer and Kumar 1995) Extracellular recordings of single or few afferent fibre action potentials were recorded on videotape and sampled digitally via Spike2 software (CED) for analysis of discharge frequency. All methods for immunofluorescent imaging and calcium imaging have been described in full previously (Evans *et al*. 2005). Electrophysiological recordings were made using the amphotericin perforated-patch configuration of the whole–cell patch-clamp technique at 37°C.

3 Results

Immunofluorescent imaging revealed that the AMPKα1 catalytic subunit isoform was predominantly targeted to the plasma membrane, with approximately 75% of the total AMPKα1 subunit staining within 1 µm of the plasma membrane. This localisation of AMPKα1 is entirely consistent with it targeting O_2-sensitive K^+ channels located in the plasma membrane. Indeed, like hypoxia, AMPK activation by 5-aminoimidazole-4-carboxamide riboside (AICAR) induced a reversible depolarisation of the membrane potential (Wyatt *et al*. 2006a; Wyatt *et al*. 2007). This depolarization was mediated by inhibition of the O_2-sensitive K^+ currents carried by TASK-like K^+ channels and large conductance Ca^{2+}-activated (BK_{Ca}) K^+ channels but not the O_2-insensitive voltage-gated (Kv) K^+ channel current. As a result of consequent depolarization, voltage-gated Ca^{2+} entry was evoked via Ni^{2+}- and Cd^{2+}-sensitive influx pathways ultimately leading to an increase in sensory afferent discharge from the carotid body (Evans *et al*. 2005; Wyatt *et al*. 2006b). Thus, AMPK activation precisely mimics the excitatory effects of hypoxia on isolated type I cells and on an *in vitro* carotid body preparation.

The concept that AMPK is *required* for hypoxic chemotransduction to occur is supported by our most recent investigations. The AMPK antagonist compound C reverses the increase in intracellular Ca^{2+} concentration evoked by both hypoxia and AICAR in isolated carotid body type I cells and the increase in sensory afferent discharge elicited from the *in vitro* carotid body by each of these stimuli (Wyatt *et al*. 2007).

4 Conclusion and Discussion

Our data demonstrate that hypoxic inhibition of mitochondrial oxidative phosphorylation may couple to inhibition of O_2-sensitive TASK-like and BK_{Ca} K^+ channels via the activation of AMPK. Thus, activation of AMPK precisely mimics hypoxia in isolated type I cells and an *in vitro* carotid body preparation. Furthermore, the AMPK antagonist reversed the effects of hypoxia and AICAR in both preparations demonstrating that AMPK is both necessary and sufficient for hypoxic chemotransduction.

The exact molecular makeup of AMPK heterotrimers in carotid body type I cells remains to be established. However, it is known that the subunit isoform combination of AMPK heterotrimers may determine the subcellular targeting of AMPK (Salt, Celler, Hawley, Prescott, Woods, Carling and Hardie 1998). Thus, whilst the targeting of AMPKα1 subunits to the type I cell membrane provides the perfect mechanism for mediating acute hypoxic chemotransduction, it may yet be found that other subunit combinations of AMPK play fundamental roles in the adaptations observed in the carotid body to both chronic and intermittent hypoxia. Indeed, it is known that AMPK can elevate the expression and activity of Hypoxia Inducible Factor-1α (Hwang, Lee, Jung, Lee, Kang, Kim and Ha 2004) the regulatory subunit of a dimeric transcription factor that is vital for hypoxic induction of physiologically important genes (Lee, Hwang, Lee, Jung, Kang, Chi, Kim and Ha 2003). These observations have important ramifications for AMPK with regard to the blunting of the hypoxic response following exposure to chronic hypoxia (Wyatt, Wright, Bee and Peers 1995) and the enhanced response of the carotid body following intermittent hypoxia (Prabhakar, Peng, Jacono, Kumar and Dick 2005). Further research is required to confirm any role of AMPK in these processes but it may be that we are at the beginning of an exciting new chapter on the control of breathing.

Acknowledgement This work was supported by the Wellcome Trust (Grant Ref: 070772).

References

Buckler, K.J. (1997) A novel oxygen-sensitive potassium current in rat carotid body type I cells. J. Physiol. 498 (Pt. 3), 649–662.

Buckler, K.J. and Vaughan-Jones, R.D. (1994) Effects of hypoxia on membrane potential and intracellular calcium in rat neonatal carotid body type I cells. J. Physiol. 476, 423–428.

Buckler, K.J. and Vaughan-Jones, R.D. (1998) Effects of mitochondrial uncouplers on intracellular calcium, pH and membrane potential in rat carotid body type I cells. J. Physiol. 513 (Pt. 3), 819–833.

Duchen, M.R. and Biscoe, T.J. (1992a) Mitochondrial function in type I cells isolated from rabbit arterial chemoreceptors. J. Physiol. 450, 13–31.

Duchen, M.R. and Biscoe, T.J. (1992b) Relative mitochondrial membrane potential and [Ca2+]i in type I cells isolated from the rabbit carotid body. J. Physiol. 450, 33–61.

Evans, A.M., Mustard, K.J., Wyatt, C.N., Peers, C., Dipp, M., Kumar, P., Kinnear, N.P. and Hardie, D.G. (2005) Does AMP-activated protein kinase couple inhibition of mitochondrial oxidative phosphorylation by hypoxia to calcium signaling in O_2-sensing cells? J. Biol. Chem. 280, 41504–41511.

Eyzaguirre, C., Koyano, H. and Taylor, J.R. (1965) Presence of acetylcholine and transmitter release from carotid body chemoreceptors. J. Physiol. 178, 463–476.

Fidone, S.J., Gonzalez, C., Dinger, B.G. and Hanson, G.R. (1988) Mechanisms of chemotransmission in the mammalian carotid body. Prog. Brain Res. 74, 169–179.

Hardie, D.G. (2004). The AMP-activated protein kinase pathway–new players upstream and downstream. J. Cell Sci. 117, 5479–5487.

Hescheler, J., Delpiano, M.A., Acker, H. and Pietruschka, F. (1989) Ionic currents on type-I cells of the rabbit carotid body measured by voltage-clamp experiments and the effect of hypoxia. Brain Res. 486, 79–88.

Hwang, J.T., Lee, M., Jung, S.N., Lee, H.J., Kang, I., Kim, S.S. and Ha, J. (2004) AMP-activated protein kinase activity is required for vanadate-induced hypoxia-inducible factor 1alpha expression in DU145 cells. Carcinogenesis 25, 2497–2507.

Lahiri, S., Rumsey, W.L., Wilson, D.F. and Iturriaga, R. (1993) Contribution of *in vivo* microvascular PO_2 in the cat carotid body chemotransduction. J. Appl. Physiol. 75, 1035–1043.

Lee, M., Hwang, J.T., Lee, H.J., Jung, S.N., Kang, I., Chi, S.G., Kim, S.S. and Ha, J. (2003) AMP-activated protein kinase activity is critical for hypoxia-inducible factor-1 transcriptional activity and its target gene expression under hypoxic conditions in DU145 cells. J. Biol. Chem. 278, 39653–39661.

Lopez-Barneo, J., Lopez-Lopez, J.R., Urena, J. and Gonzalez, C. (1988) Chemotransduction in the carotid body: K+ current modulated by PO2 in type I chemoreceptor cells. Science 241, 580–582.

Mills, E. and Jobsis, F.F. (1970) Simultaneous measurement of cytochrome a3 reduction and chemoreceptor afferent activity in the carotid body. Nature 225, 1147–1149.

Mills, E. and Jobsis, F.F. (1972). Mitochondrial respiratory chain of carotid body and chemoreceptor response to changes in oxygen tension. J. Neurophysiol. 35, 405–428.

Mosqueira, M. and Iturriaga, R. (2002). Carotid body chemosensory excitation induced by nitric oxide: involvement of oxidative metabolism. Respir. Physiol. Neurobiol. 131, 175–187.

Mulligan, E., Lahiri, S. and Storey, B.T. (1981) Carotid body O_2 chemoreception and mitochondrial oxidative phosphorylation. J. Appl. Physiol. 51, 438–446.

Peers, C. (1990) Hypoxic suppression of K+ currents in type I carotid body cells: selective effect on the Ca2(+)-activated K+ current. Neurosci. Lett. 119, 253–256.

Pepper, D.R., Landauer, R.C. and Kumar, P. (1995) Postnatal development of CO_2-O_2 interaction in the rat carotid body *in vitro*. J. Physiol. 485 (Pt. 2), 531–541.

Perez-Garcia, M.T., Colinas, O., Miguel-Velado, E., Moreno-Dominguez, A. and Lopez-Lopez, J.R. (2004) Characterization of the Kv channels of mouse carotid body chemoreceptor cells and their role in oxygen sensing. J. Physiol. 557, 457–471.

Prabhakar, N.R., Peng, Y.J., Jacono, F.J., Kumar, G.K. and Dick, T.E. (2005) Cardiovascular alterations by chronic intermittent hypoxia: importance of carotid body chemoreflexes. Clin. Exp. Pharmacol. Physiol. 32, 447–449.

Salt, I., Celler, J.W., Hawley, S.A., Prescott, A., Woods, A., Carling, D. and Hardie, D.G. (1998) AMP-activated protein kinase: greater AMP dependence, and preferential nuclear localization, of complexes containing the alpha2 isoform. Biochem. J. 334 (Pt. 1), 177–187.

Stea, A. and Nurse, C.A. (1991) Whole-cell and perforated-patch recordings from O_2-sensitive rat carotid body cells grown in short- and long-term culture. Pflugers Arch. 418, 93–101.

Wyatt, C.N. and Buckler, K.J. (2004) The effect of mitochondrial inhibitors on membrane currents in isolated neonatal rat carotid body type I cells. J. Physiol. 556, 175–191.

Wyatt, C.N., Kumar, P., Aley, P., Peers, C., Hardie, D.G. and Evans, A.M. (2006a) Does AMP-activated protein kinase couple hypoxic inhibition of oxidative phosphorylation to carotid body excitation? Adv. Exp. Med. Biol. 580, 191–196; discussion 351–199.

Wyatt, C.N., Mustard, K.J., Pearson, S.A., Dallas, M.L., Atkinson, L., Kumar, P., Peers, C,, Hardie, D.G. and Evans, A.M. (2007) AMP-activated protein kinase mediates carotid body excitation by hypoxia. J. Biol. Chem. 282, 8092–8098.

Wyatt, C.N., Peers, C., Kumar, P., Hardie, D.G. and Evans, A.M. (2006b) The effect of AMP-kinase activators on oxygen-sensing type-I cells of the rat carotid body. British Journal of Pharmacology pA23, 049P.

Wyatt, C.N., Wright, C., Bee, D. and Peers, C. (1995) O_2-sensitive K+ currents in carotid body chemoreceptor cells from normoxic and chronically hypoxic rats and their roles in hypoxic chemotransduction. Proc. Natl. Acad. Sci. USA 92, 295–299.

12
Stimulatory Actions of Pituitary Adenylate Cyclase-Activating Polypeptide (PACAP) in Rat Carotid Glomus Cells

Fenglian Xu[1], Frederick W. Tse[2] and Amy Tse[3]

Abstract The carotid bodies are the major peripheral chemoreceptors that detect changes in arterial blood oxygen level. PACAP-deficient mice are prone to sudden neonatal death and have reduced respiratory response to hypoxia and hypercapnia. To investigate whether PACAP contributes to the chemotransduction in carotid body, we studied the action of PACAP on glomus cells isolated from rat carotid body. We found that PACAP triggered cytosolic $[Ca^{2+}]$ ($[Ca^{2+}]_i$) rise in glomus cells. Removal of extracellular Ca^{2+} reversibly inhibited the PACAP-mediated $[Ca^{2+}]_i$ rise. Under voltage clamp conditions and in the presence of tetraethylammonium (TEA) and Cd^{2+}, PACAP reduced the outward current evoked at positive potentials. We suggest that the inhibition of a TEA-insensitive current is a mechanism underlying the PACAP-mediated $[Ca^{2+}]_i$ rise in glomus cells. The loss of the stimulatory action of PACAP in glomus cells may partly account for the reduction in chemoresponse in the PACAP-deficient mice.

1 Introduction

PACAP, which is widely distributed in the body, has many important physiological functions, including respiration (Sherwood *et al*. 2000). PACAP receptors are present in the respiratory tract (Vaudry *et al*. 2000) and in brain areas involved in the regulation of respiratory rhythm and chemosensitivity (Hannibal 2002). PACAP may also be involved in the regulation of chemosensing in the carotid body. Intravenous injection of PACAP increased ventilation and this effect was abolished by the cutting of the carotid sinus nerve (Runcie *et al*. 1995). PACAP-deficient mice exhibited reduced respiratory response to hypoxia and hypercapnia and were more prone to sudden

[1] University of Alberta, Centre for Neurosciences, fenglianx@yahoo.com

[2] University of Alberta, Department of Pharmacology, Centre for Neurosciences, fred.tse@ualberta.ca

[3] University of Alberta, Department of Pharmacology, Centre for Neurosciences, amy.tse@ualberta.ca

M.J. Poulin and R.J.A. Wilson (eds.), *Integration in Respiratory Control: From Genes to Systems*.

neonatal death (Cummings *et al*. 2004). Since glomus cells are the initial sites of oxygen sensing, we examined the action of PACAP in carotid glomus cells.

2 Methods

2.1 Preparation of Glomus Cells

The carotid bifurcation was removed from male Sprague-Dawley rats (age: 6–7 weeks) euthanized in accordance with the standards of the Canadian Council on Animal Care. The procedures for cell isolation and culture have been described (Xu *et al*. 2003; Xu *et al*. 2005). Cells were cultured for 2–6 hours before recordings.

2.2 Measurement of $[Ca^{2+}]_I$

$[Ca^{2+}]_i$ was monitored at 20–23°C with fura-2 digital imaging as described previously (Xu *et al*. 2003; Xu *et al*. 2005). The standard bath solution contained (in mM): 117 NaCl, 4.5 KCl, 23 $NaHCO_3$, 5 sucrose, 5 glucose, 2.5 $CaCl_2$ and 1 $MgCl_2$ (pH 7.4 when bubbled with 5% CO_2).

2.3 Electrophysiology

Single cells were recorded at 20–23°C with the perforated patch clamp technique as described previously (Xu *et al*. 2006). No correction for junction potential was applied. The pipette solution (pH 7.2) contained (in mM): 140 K-gluconate, 10 K-Hepes, 5 $MgCl_2$, 1 EGTA and amphotericin B (250 g/ml). Cells were perfused with bath solution bubbled continuously with 5% CO_2 - 95% air. Hypoxia was induced by perfusing the cells with bath solution bubbled with 5% CO_2 - 95% N_2 (pO_2 of the bath solution = ~ 40 mm Hg).

3 Results

3.1 PACAP Triggered $[Ca^{2+}]_i$ Rise in Glomus Cells via Extracellular Ca^{2+} Entry

In all our experiments, PACAP-38 was employed. Since only glomus cells have Ca^{2+} response to hypoxia challenge (Buckler and Vaughan-Jones 1994; Xu *et al*. 2005), we identified individual glomus cells based on their Ca^{2+} response to

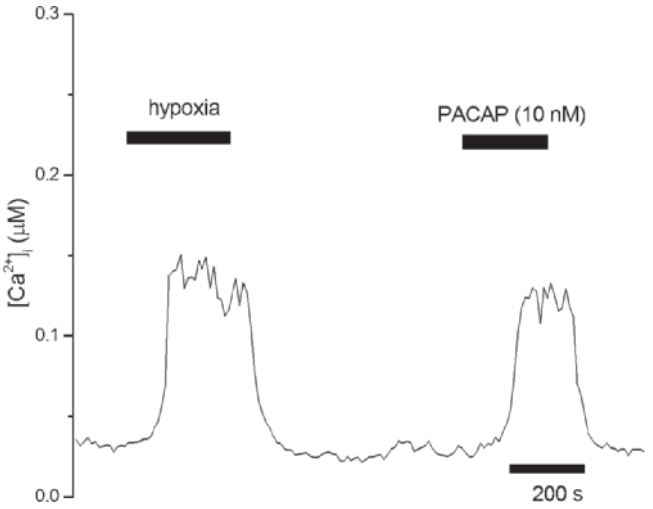

Fig. 1 PACAP induced $[Ca^{2+}]_i$ rise in the oxygen sensing glomus cell

hypoxia. As shown in Fig. 1, moderate hypoxia induced $[Ca^{2+}]_i$ rise in glomus cell. Application of PACAP to the same cell also triggered a rise in $[Ca^{2+}]_i$.

To determine whether the PACAP-mediated $[Ca^{2+}]_i$ rise in glomus cells involved extracellular Ca^{2+} entry, we examined whether the removal of extracellular Ca^{2+} affected the PACAP response. Following the PACAP-mediated $[Ca^{2+}]_i$ rise, the standard bath solution was replaced by a Ca^{2+}-free solution which contained the same concentration of PACAP as well as 1 mM of the Ca^{2+} chelator, EGTA. Fig. 2 shows that the removal of extracellular Ca^{2+} reversibly abolished the PACAP-mediated $[Ca^{2+}]_i$ rise.

3.2 PACAP Reduced a TEA-insensitive Outward Current

The strong dependence of the PACAP-mediated $[Ca^{2+}]_i$ rise on extracellular Ca^{2+} (Fig. 2) suggests the involvement of depolarization and activation of voltage-gated Ca^{2+} entry. Rat glomus cells express a variety of K^+ channels, including the delayed rectifier K^+ channels, the TASK-like K^+ channels, the large conductance Ca^{2+}-activated K^+ (BK) channels and the 4-aminopyridine (4-AP) sensitive K^+ channels (Buckler 1997; Riesco-Fagundo *et al*. 2001; Vandier *et al*. 1999; Williams *et al*. 2004). Inhibition of the TASK-like K^+ channels or the BK channels has been associated with an increase in cell excitability and $[Ca^{2+}]_i$ in glomus cells (Buckler 1997; Riesco-Fagundo *et al*. 2001). This raises the possibility that the action of PACAP may involve inhibition of the TASK-like K^+ channel or BK channels. Since TEA inhibits the BK channels (Pardal *et al*. 2000) but not the TASK-like K^+ channels (Buckler 1999), we examined whether PACAP affected

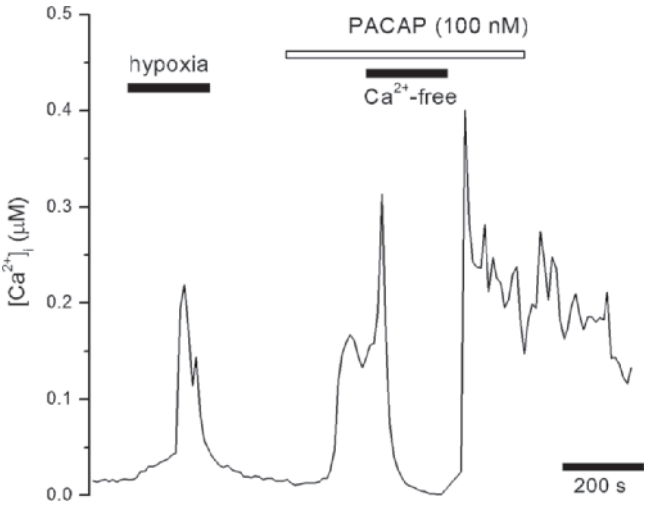

Fig. 2 The PACAP-mediated $[Ca^{2+}]_i$ rise required the presence of extracellular Ca^{2+}

the K^+ current in glomus cells when TEA (10 mM) was present in the bath solution. We also included Cd^{2+} (0.2 mM) in the standard bath solution to block any other Ca^{2+}-activated channels. Single glomus cell was voltage clamped at −60 mV and voltage steps (200 ms in duration) to potentials between −70 and +50 mV were applied. Fig. 3A shows the family of current elicited before and in the presence of PACAP (100 nM). The current amplitude at different potentials was measured by averaging the current during the last 20 ms of the voltage step. The current voltage relations for the same cell before and in the presence of PACAP were plotted in Fig. 3B. Note that PACAP reduced the outward current evoked at potentials more positive than 0 mV. This result suggests that the reduction of a TEA-insensitive current may be a mechanism underlying the PACAP-mediated $[Ca^{2+}]_i$ rise in glomus cells.

4 Discussion

Our finding demonstrates that PACAP stimulates $[Ca^{2+}]_i$ rise in carotid glomus cells (Fig. 1). The actions of PACAP in glomus cells bear some similarities to those mediated by hypoxia. Both the hypoxia- and PACAP-mediated $[Ca^{2+}]_i$ rise were dependent on the presence of extracellular Ca^{2+}. Similar to hypoxia, PACAP reduced a TEA-insensitive current (Fig. 3), suggesting the possible involvement of the TASK-like K^+ current. The amplitude of the Ca^{2+} signal triggered by PACAP was comparable to that triggered by moderate hypoxia (Fig. 1 and 2). This raises the possibility that PACAP may augment the hypoxia-mediated

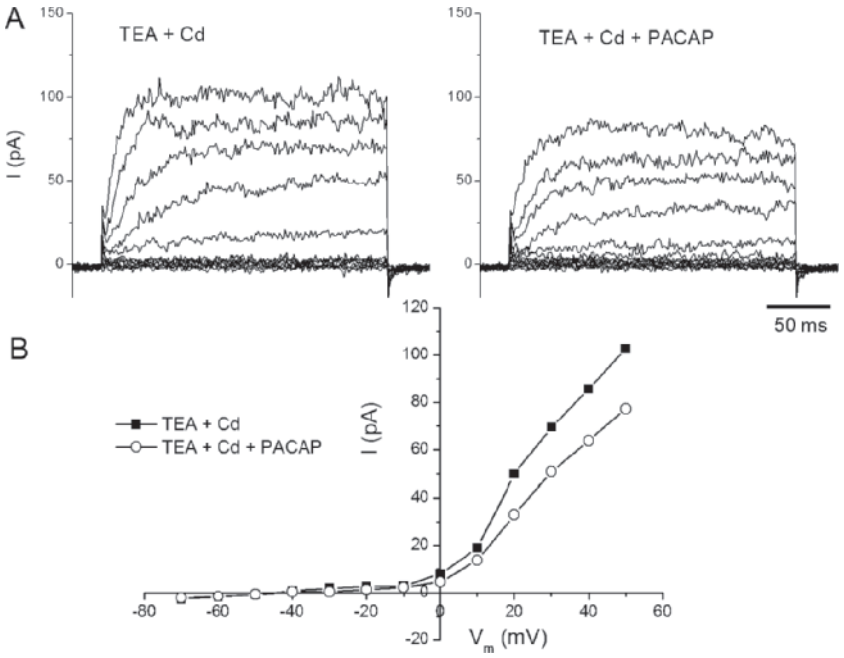

Fig. 3 PACAP reduced a TEA-insensitive current in glomus cells

$[Ca^{2+}]_i$ rise in glomus cells. The loss of the stimulatory action of PACAP in carotid glomus cells may partly account for the reduction in chemoresponse in the PACAP-deficient mice.

Acknowledgement This work is supported by grants from the Heart and Stroke Foundation of Canada, Canadian Institute of Health Research (CIHR) and the Alberta Heritage Foundation for Medical Research (AHFMR).

References

Buckler, K.J. (1997) A novel oxygen-sensitive potassium current in rat carotid body type I cells. J. Physiol. 498 (Pt. 3), 649–662.

Buckler, K.J. (1999) Background leak K+-currents and oxygen sensing in carotid body type 1 cells. Respir. Physiol. 115, 179–187.

Buckler, K.J. and Vaughan-Jones, R.D. (1994) Effects of hypoxia on membrane potential and intracellular calcium in rat neonatal carotid body type I cells. J. Physiol. 476, 423–428.

Cummings, K.J., Pendlebury, J.D., Sherwood, N.M. and Wilson, R.J. (2004) Sudden neonatal death in PACAP-deficient mice is associated with reduced respiratory chemoresponse and susceptibility to apnoea. J. Physiol. 555, 15–26.

Hannibal, J. (2002) Pituitary adenylate cyclase-activating peptide in the rat central nervous system: an immunohistochemical and *in situ* hybridization study. J. Comp Neurol. 453, 389–417.

Pardal, R., Ludewig, U., Garcia-Hirschfeld, J. and Lopez-Barneo, J. (2000) Secretory responses of intact glomus cells in thin slices of rat carotid body to hypoxia and tetraethylammonium. Proc. Natl. Acad. Sci. USA 97, 2361–2366.

Riesco-Fagundo, A.M., Perez-Garcia, M.T., Gonzalez, C. and Lopez-Lopez, J.R. (2001) O(2) modulates large-conductance Ca(2+)-dependent K(+) channels of rat chemoreceptor cells by a membrane-restricted and CO-sensitive mechanism. Circ. Res. 89, 430–436.

Runcie, M.J., Ulman, L.G. and Potter, E.K. (1995) Effects of pituitary adenylate cyclase-activating polypeptide on cardiovascular and respiratory responses in anaesthetised dogs. Regul. Pept. 60, 193–200.

Sherwood, N.M., Krueckl, S.L. and McRory, J.E. (2000) The origin and function of the pituitary adenylate cyclase-activating polypeptide (PACAP)/glucagon superfamily. Endocr. Rev. 21, 619–670.

Vandier, C., Conway, A.F., Landauer, R.C. and Kumar, P. (1999) Presynaptic action of adenosine on a 4-aminopyridine-sensitive current in the rat carotid body. J. Physiol. 515 (Pt. 2), 419–429.

Vaudry, D., Gonzalez, B.J., Basille, M., Yon, L., Fournier, A. and Vaudry, H. (2000) Pituitary adenylate cyclase-activating polypeptide and its receptors: from structure to functions. Pharmacol. Rev. 52, 269–324.

Williams, S.E., Wootton, P., Mason, H.S., Bould, J., Iles, D.E., Riccardi, D., Peers, C. and Kemp, P.J. (2004) Hemoxygenase-2 is an oxygen sensor for a calcium-sensitive potassium channel. Science 306, 2093–2097.

Xu, F., Xu, J., Tse, F.W. and Tse, A. (2006) Adenosine stimulates depolarization and rise in cytoplasmic [Ca2+] in type I cells of rat carotid bodies. Am. J. Physiol. Cell Physiol. 290, C1592–C1598.

Xu, J., Tse, F.W. and Tse, A. (2003) ATP triggers intracellular Ca^{2+} release in type II cells of the rat carotid body. J. Physiol. 549, 739–747.

Xu, J., Xu, F., Tse, F.W. and Tse, A. (2005) ATP inhibits the hypoxia response in type I cells of rat carotid bodies. J. Neurochem. 92, 1419–1430.

13
Post-hypoxic Unstable Breathing in the C57BL/6J Mouse: Effects of Acetazolamide

Motoo Yamauchi[1], Jesse Dostal[2] and Kingman P. Strohl[3]

Abstract We examined whether acetazolamide (ACZ), a carbonic anhydrase inhibitor, would alter post-hypoxic ventilatory behavior and periodic breathing in the C57BL/6J (B6) mouse. Experiments were performed with unanaesthetized, awake adult male B6 mice (n = 5, 2.5 months old, 21.3 ± 1.5 g, mean ± SD) and ventilatory behavior was measured using a flow through body plethysmography. Mice were given an intraperitoneal injection of either vehicle or ACZ (40 mg/kg) and one hour later exposed to 1 min of 8% O2-balance N2 (poikilocapnic hypoxia) or 12%-O2, 3% CO2-balance N2 (non-poikilocapnic hypoxia) followed by rapid reoxygenation (100% O2) of 5 minutes. One minute after reoxygenation, ACZ-treated animals exhibited post-hypoxic frequency decline ($p < 0.05$), a lower coefficient of variability for frequency ($p < 0.001$) and no tendency towards periodic breathing ($p < 0.05$), as compared to vehicle-treated animals. ACZ improves unstable breathing in the B6 model of periodic breathing, despite producing post-hypoxic frequency decline. Our speculation is that periodic breathing occurs through pathways independent of the A5 pontine area.

1 Introduction

Periodic breathing (PB; the waxing and waning of ventilation) is common among heart failure patients. The presence of PB during the night worsens the symptoms and prognoses of patients with these illnesses (Leung and Bradley 2001). One proposed mechanism for initiation and propagation of apneas is said to be the balance between two different post-hypoxic breathing patterns: short-term potentiation (STP) and post-hypoxic frequency decline (PHFD). The absence of STP and, conversely, the presence of PHFD is reasoned to promote recurrent apneas and unstable breathing (Younes 1989; Ahmed, Serrette, Kryger and Anthonisen 1994; Dempsey, Smith, Harms, Chow and Saupe 1996; Powell, Milsom and Mitchell 1998) and seems to be a property of pontine A5 neurons (Dick and Coles 2000).

[1–3]Department of Medicine, Case Western Reserve University, Cleveland VA Medical Center, mountain@pastel.ocn.ne.jp

M.J. Poulin and R.J.A. Wilson (eds.), *Integration in Respiratory Control: From Genes to Systems*. © Springer 2008

Former studies from our laboratory have demonstrated that C57BL/6J (B6) mice exhibit post-hypoxic PB compared to A/J mice (Han, Subramanian, Price, Nadeau and Strohl 2002). Acetazolamide (ACZ), which is a carbonic anhydrase inhibitor, is commonly used to manage PB (Javaheri 2006). The hypothesis of this study was that ACZ would modulate post-hypoxic unstable breathing and PB by producing STP.

2 Methods

2.1 Animals

Experiments were performed on adult male B6 mice (n = 5, 2.5 months old, 21.3 ± 1.5 g, mean ± SD). Experimental protocols used were approved by the Louis Stokes Department of Veterans Affairs Medical Center Animal Care and Use Committee and were in agreement with the National Institutes of Health Guide for the Care and Use of Laboratory Animals.

2.2 Experimental Protocols

All experiments were carried out when the animals appeared awake, as determined by behavioral observation. The mice received an intraperitoneal injection of either vehicle (saline) or ACZ dissolved in saline at a dose of 40 mg/kg; pH was adjusted to be similar. The volume of each injection was 0.02 ml per body weight (g). One hour later, the animals underwent a 5-min recording of baseline breathing, followed by a 1-min poikilocapnic hypoxia challenge (8% O_2-balance N_2). The hypoxic gas was then flushed out of the chamber and replaced with 100% O_2 for 5 min. After a 20-min interval, the same protocol was performed but using a non-poikilocapnic hypoxia challenge (3% CO_2- 12% O_2- balance N_2).

2.3 Measurements of Ventilatory Behavior

Ventilatory behavior (frequency, tidal volume and minute ventilation) was measured using a flow through body plethysmography (Han, Subramanian, Dick, Dreshaj and Strohl 2001). Ventilatory parameters were measured continuously throughout the testing period and scored by computer using a respiratory-based software program (LabView programming by I.C.E). For each animal, ventilatory parameters were obtained from the mean of consecutive breaths for 30 s during baseline and first 60 s after reoxygenation with 100% O_2. Sighs and sniffs were excluded from the analysis.

To quantify breathing stability after reoxygenation, we calculated the coefficient of variation (CV). We also investigated the existence of PB. PB was defined as cyclic fluctuations in frequency of respiration interrupted by periods of apnea or near apnea. In this study, apnea was defined as an end-expiratory pause of ≥ 2 average breath durations. A minimum of three instances of apnea were needed to classify a given set of breaths as PB (Han *et al*. 2002).

3 Results

3.1 Post-hypoxic Ventilatory Behavior

In comparison to ventilatory behavior upon reoxygenation to pre-hypoxic baseline, B6 mice with ACZ showed PHFD (Fig. 1) as well as post-hypoxic ventilatory decline (data not shown) with reoxygenation after both poikilocapnic and non-poikilocapnic hypoxic challenges.

3.2 Effects of ACZ on Unstable Breathing

To assess the stability of respiratory frequency, we analyzed the first one-min duration during reoxygenation and calculated the coefficients of variability (CVs) for frequency. The frequency CVs for mice treated with ACZ were significantly lower than with the frequency CVs for vehicle for both the poikilocapnic and

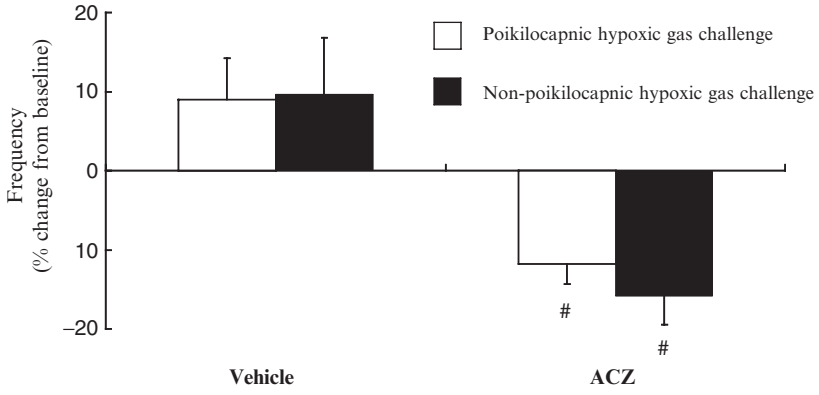

Fig. 1 The effect of ACZ on post-hypoxic ventilatory behavior compared with vehicle. Values are mean ± SEM. Results are presented as percent change from baseline resting breathing to the first minute of breathing after reoxygenation. Pound signs denote significant differences between treatments (#: $p < 0.05$)

Table 1 Coefficient of variation (CV) for frequency and presence of periodic breathing (PB) in the first one minute after reoxygenation

Poikilocapnic hypoxic gas challenge		Vehicle	ACZ	p value
	CV	41.45 ± 4.39	17.10 ± 1.82	<0.001
	PB	5/5	0/5	0.001
Non-poikilocapnic hypoxic gas challenge		Vehicle	ACZ	p value
	CV	39.25 ± 7.90	13.37 ± 3.14	<0.001
	PB	3/5	0/5	0.038

non-poikilocapnic gas challenges. Further, during the first minute after reoxygenation, PB was shown in all vehicle-treated mice in the poikilocapnic hypoxic gas challenge and in 3 of the 5 vehicle-treated mice with non-poikilocapnic hypoxic gas challenge. ACZ completely eliminated PB in the setting of both of the gas challenges (Table 1).

4 Discussion

The present study showed that ACZ did improve the stability of post-hypoxic ventilatory behavior as evidenced by the absence of PB and a reduced coefficient of variation, despite producing PHFD. Therefore, the hypothesis that ACZ would improve PB by producing STP is rejected.

After exposure to acute hypoxia and upon reoxygenation, resulting respiratory patterns may be classified as STP, which ventilation remains elevated above baseline values or PHFD, which frequency falls below baseline values (Powell *et al*. 1998; Dick *et al*. 2000). In our study, ACZ-treated animals still exhibited PHFD; however, unstable post-hypoxic breathing behavior was improved. ACZ might improve the post-hypoxic PB by another mechanism, such as those determining hypercapnic or/and hypoxic ventilatory responsiveness or/and apneic threshold. At least, in this B6 mouse model, PHFD or STP was not responsible for the post-hypoxic PB. Further studies need to determine the site of action of ACZ and its effect on chemosensitivity and thresholds.

Our theory is that in this model of PB derivation of unstable breathing occurs through pathways to or in the central respiratory controller. Further, we feel that this aberration encourages reentry into apnea and is independent of PHFD. ACZ acts on this pathway to reduce this form of instability.

References

Ahmed, M., Serrette, C., Kryger, M.H. and Anthonisen, N.R. (1994) Ventilatory instability in patients with congestive heart failure and nocturnal Cheyne-Stokes breathing. Sleep 17, 527–534.

Dempsey, J.A., Smith, C.A., Harms, C.A., Chow, C. and K.W. Saupe, K.W. (1996) Sleep-induced breathing instability. University of Wisconsin-Madison Sleep and Respiration Research Group. Sleep 19, 236–247.

Dick, T.E. and Coles, S.K. (2000) Ventrolateral pons mediates short-term depression of respiratory frequency after brief hypoxia. Respir. Physiol. 121, 87–100.

Han, F., Subramanian, S., Dick, T.E., Dreshaj, I.A. and Strohl, K.P. (2001) Ventilatory behavior after hypoxia in C57BL/6J and A/J mice. J. Appl. Physiol. 91, 1962–1970.

Han, F., Subramanian, S., Price, E.R., Nadeau, J. and Strohl, K.P. (2002) Periodic breathing in the mouse. J. Appl. Physiol. 92, 1133–1140.

Javaheri, S. (2006) Acetazolamide improves central sleep apnea in heart failure: a double-blind, prospective study. Am. J. Respir. Crit. Care Med. 173, 234–237.

Leung, R.S. and Bradley, T.D. (2001) Sleep apnea and cardiovascular disease. Am. J. Respir. Crit. Care Med. 164, 2147–2165.

Powell, F.L., Milsom, W.K. and Mitchell, G.S. (1998) Time domains of the hypoxic ventilatory response. Respir. Physiol. 112, 123–134.

Younes, M. (1989) The physiologic basis of central apnea and periodic breathing. Curr. Pulmonol 10, 265–326.

Part III
Respiratory Rhythm Generation

14
Catecholaminergic Modulation of the Respiratory Rhythm Generator in the Isolated Brainstem–Spinal Cord Preparation from Neonatal Rat

Akiko Arata[1] and Morimitsu Fujii[2]

1 Introduction

The hypothesized respiratory rhythm generator is located in the neonatal medulla and consists of pre-inspiratory (Pre-I) neurons in the parafacial respiratory group (pFRG) (Onimaru and Homma 2003) and inspiratory (I) neurons in the pre-Botzinger complex (PBC) (Smith, Ellenberger, Ballanyi, Richter and Feldman 1991). The Pre-I neurons are thought to trigger firing of I neurons (Onimaru, Arata and Homma 1997) which, in turn, send axons to the inspiratory motor neurons in the spinal cord. The respiratory rhythm generator is controlled in part by inputs from the nucleus tractus solitarii (NTS). The NTS is the main relay of the Hering-Breuer reflex. Moreover, the NTS receives direct projections from the cerebral cortex and the limbic system, including the insular cortex. The NTS contains catecholaminergic neurons that project to the respiratory rhythm generator in the rostral ventrolateral medulla (RVLM). In rats, adrenaline-containing neurons of the RVLM, namely the C1 group, are primarily unilaterally innervated by neurons in the NTS. Reis and colleagues suggested that these neurons synapsing in or projecting through the C1 area mediate the baro- and cardiopulmonary mechanoreceptor reflex (Granata, Ruggiero, Park, Joh and Reis 1983). Dopamine antagonist administration *in vivo* attenuated ventilatory responses to hypoxia (Hsiao, Lahiri and Mokashi 1989), and direct dopamine application on the rat medulla–spinal cord preparation depressed respiratory frequency (Fujii, Umezawa and Arata 2004; 2006). Using the isolated medulla–spinal cord preparation and single-cell recordings, we investigated the cellular mechanisms of catecholaminergic respiratory regulation. Our data suggest respiratory depression by catecholamine is mediated primarily by effects on Pre-I neurons.

[1–2]Laboratory for Memory and Learning, RIKEN Brain Science Institute, Wako, Saitama, 351–0198 Japan, ako@brain.riken.jp

M.J. Poulin and R.J.A. Wilson (eds.), *Integration in Respiratory Control: From Genes to Systems*.

2 Experimental Procedures

Neonatal Wistar rats, 0–3 days old, were deeply anesthetized with ether. The cerebrum was quickly removed by transection at the intercollicular level, and then the brainstem and spinal cord were isolated according to the previously described methods (Suzue 1984). Medullary unit activity was recorded extracellularly using a glass electrode that contained 0.5 M sodium acetate. Whole-cell recordings from the respiratory neurons were obtained with the "blind" patch-clamp technique described previously (Smith, Ballanyi and Richter, 1992; Onimaru *et al*. 1997). Recording pipettes were filled with either K-gluconate internal solution consisting of (in mM) 130 K-gluconate, 10 EGTA, 10 HEPES, 1 $CaCl_2$, 1 $MgCl_2$, and 2 Na-ATP, adjusted to pH 7.3 with 1N-KOH, or KCl-nystatin internal solution (for inhibitory synapse analysis) consisting of 140 KCl, 10 EGTA, 10 HEPES, and 100 mg/ml Nystatin.

3 Catecholaminergic Depression of the Respiratory Rhythm

3.1 Modulation of Respiratory Network by Adrenaline

Our previous research showed the modulation of respiratory neurons by adrenaline or noradrenaline (NA) in a newborn rat brainstem–spinal cord preparation (Arata, Onimaru and Homma 1998). Adrenaline or NA caused a dose-dependent depression of the respiratory rhythm. The depressive effect of adrenaline (ED_{50} = 0.5 μM) was stronger than that of NA (ED_{50} = 5 μM). Focusing on the effect of adrenaline, adrenaline depressed the Pre-I neuron rhythm and induced respiratory rhythm suppression. The inhibitory effects of adrenaline on the Pre-I neurons were examined using a K-gluconate electrode (Fig. 1A) and a KCl perforated (KCl–NYS) electrode. Nystatin makes tiny holes so that small ions (Cl^-) can pass from the electrode to the cell. When the KCl–NYS electrode was used to record respiratory neurons, we found continual firing with reversed IPSPs (rIPSPs) comprised of depolarized Cl-currents such as the GABA/glycine-induced currents. Adrenaline increased the number of rIPSPs (Fig. 2B, 2E). The results suggest that the depression of respiratory rhythm under intact network conditions is mediated by the GABAergic system. The rIPSPs induced by adrenaline were blocked by the $GABA_A$-antagonist bicuculline (Fig. 2F, 2G). Phasic excitation, that is I phase-EPSPs or phasic-rIPSPs, remained after bicuculline application. These results suggest that adrenaline induces tonic GABA inhibition in the neonatal respiratory network.

3.2 Modulation of Respiratory Network by Dopamine

Dopamine also depressed the respiratory rhythm by the activation of dopamine D_4 receptors (Fujii, Umezawa and Arata 2004; 2006). We investigated the effect of dopamine on the activity patterns of Pre-I and I neurons of the ventral surface in the

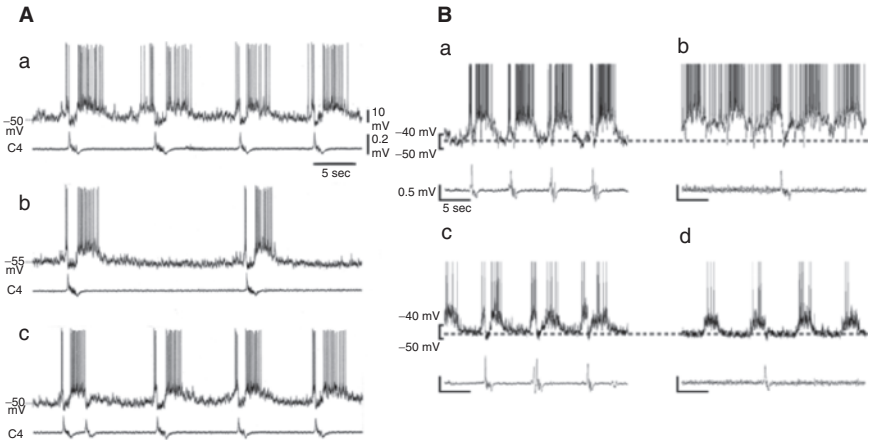

Fig. 1 Effects of adrenaline and dopamine on respiratory rhythm generating neurons. Intracellular recording of Pre-I neurons. In each panel, the upper trance shows a current-clamp recording of a Pre-I neuron. The lower trace shows a simultaneous recording from the C4 root. **A**: Adrenaline-depressed Pre-I neuron; a, control; b, during treatment with 1 mM adrenaline; c, 20 min after wash out. **B**: Dopamine-sensitive (a, b) and insensitive (c, d) Pre-I neurons a and c, control b and d, 5 min after 50 μm dopamine application. Note: only the dopamine-sensitive neuron expressed D4 dopamine receptors

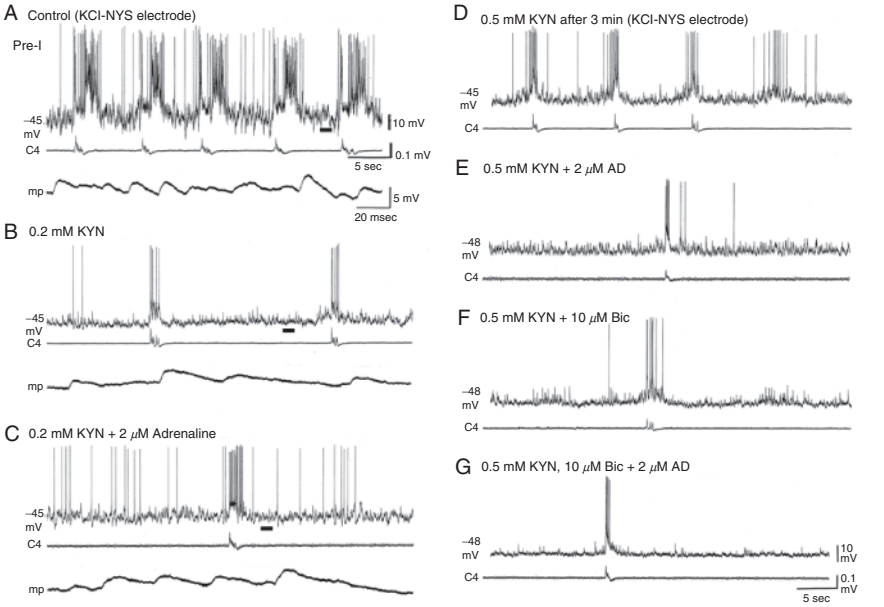

Fig. 2 Modulation of Pre-I neuron by adrenalin. Recording made using KCl–NYS electrodes from 2 cells. (A-C and D-G) are shown. (A-C) After injection of Cl^-, EPSPs and rIPSPs of Pre-I neuron appeared. (A). After application of 0.2 mM kynurenic acid (KYN), EPSPs disappeared. (B). After application of 0.2 mM KYN, rIPSPs frequency was increased by 2 μM adrenaline (C) D-G) Under 0.5 mM KYN, EPSPs disappeared and rIPSPs remained (D). After application of 2 μM adrenaline, tonic rIPSPs appeared (E). After application of GABA-antagonist bicuculline (10 μM Bic) under 0.5 mM KYN, tonic inhibition disappeared, and phasic excitation/rIPSPs remained (F). After application of adrenaline, tonic rIPSPs disappeared (G)

block preparation. In addition to slowing the rhythm (Fig. 1B), dopamine depressed respiratory activity in the Pre-I neurons but not the respiratory activity in I neurons. The dopaminergic suppression of respiratory activity in Pre-I neurons was mimicked by a dopamine D4 receptor agonist, PD168077.

While dopamine, NA and adrenaline depressed respiratory rhythms produced by the block preparation, they enhanced in-phase excitation of I neurons. Unit and patch-clamp recordings demonstrated that dopamine depolarizes the Pre-I neurons (Fig. 1Bb), disperses Pre-I firing, and depresses Pre-I phase PSPs of I neurons.

Immunohistological investigation revealed that approximately 60% of the Pre-I neurons express the dopamine D4 receptors. These results show that dopaminergic depression of the respiratory rhythm is due to dopamine D4 receptor–mediated synchronization of Pre-I neurons that disrupts the normal Pre-I driving of I neurons.

4 Discussion

The depression of respiratory rhythm caused by adrenaline (or NA) is mediated by GABAergic tonic inhibition. This GABAergic inhibition makes the Pre-I neuron activity slow and immediately depresses the respiratory rhythm. In brainstem-spinal cord-lung preparation, depression of the respiratory rhythm caused by lung inflation is mediated by GABAergic/glycinergic inhibition (Murakoshi and Otsuka 1985, Mellen and Feldman 2000). This suggests that adrenaline (or NA) might modulate the lung-inflation reflex and/or an emergency circuit.

In simple neuronal networks, dopaminergic switching of the network dynamics, such as initiation of feeding-like movement in *Aplysia* ganglia (Kabotyanski, Baxter, Cushman and Byrne 2000) and locomotor frequency transition in lamprey spinal cord (Svensson, Woolley, Wikstrom and Grillner 2003) have been reported. The mammalian respiratory rhythm generator also requires state transition between voluntary and involuntary respiration (Mitchell and Berger 1975; Jurgens 2002). The NTS contains a large number of dopaminergic neurons. These neurons might modulate the switching mechanism between voluntary and involuntary respiration such as information from the cerebral cortex to the NTS.

The respiratory depression by catecholamine is mainly mediated by effects on Pre-I neurons; catecholamine also directly influences in-phase excitation of I neurons. We hypothesize that the Pre-I neuron group in the pFRG is the involuntary respiratory rhythm generator and that the I neuron group in PBC is the respiratory pattern generator. Accordingly, the PBC that usually receives signals from the respiratory rhythm generator, sometimes controlled by voluntary movement. Catecholamine might modulate the inspiratory to expiratory phase-switching, and involuntary to voluntary mode-switching.

Acknowledgements We greatly thank Dr. Onimaru and Prof. Homma for their help in starting this project.

References

Arata, A., Onimaru, H. and Homma, I. (1998) The adrenergic modulation of firings of respiratory rhythm generating neurons in medulla-spinal cord preparation from newborn rat. Exp. Brain Res. 119, 399–408.

Fujii, M., Umezawa, K. and Arata, A. (2004) Dopaminergic modulation on respiratory rhythm in rat brainstem-spinal cord preparation. Neurosci. Res. 50, 355–359.

Fujii, M., Umezawa, K. and Arata, A. (2006) Dopamine desynchronizes the pace-making neuronal activity of rat respiratory rhythm generation. Eur. J. Neurosci. 23, 1015–1027.

Granata, A.R., Ruggiero, D.A., Park, D.H., Joh, T.H. and Reis, D.J. (1983) Lesions of epinephrine neurons in the rostral ventrolateral medulla abolish the vasodepressor components of baroreflex and cardiopulmonary reflex. Hypertension 5, V80–84.

Hsiao, C., Lahiri, S. and Mokashi, A. (1989) Peripheral and central dopamine receptors in respiratory control. Respir. Physiol. 76, 327–336.

Jurgens, U. (2002) Neural pathways underlying vocal control. Neurosci. Biobehav. Rev. 26, 235–258.

Kabotyanski, E.A., Baxter, D.A., Cushman, S.J. and Byrne, J.H. (2000) Modulation of fictive feeding by dopamine and serotonin in Aplysia. J. Neurophysiol. 83, 374–392.

Mellen, N.M. and Feldman, J.L. (2000) Phasic lung inflation shortens inspiration and respiratory period in the lung-attached neonate rat brain stem spinal cord. J. Neurophysiol. 83, 3165–3168.

Mitchell, R.A. and Berger, A.J. (1975) Neural regulation of respiration. Am. Rev. Respir. Dis. 111, 206–224.

Murakoshi, T. and Otsuka, M. (1985) Respiratory reflexes in an isolated brainstem-lung preparation of the newborn rat: possible involvement of gamma-aminobutyric acid and glycine. Neurosci. Lett. 62, 63–68.

Onimaru, H., Arata, A. and Homma, I. (1997) Neuronal mechanisms of respiratory rhythm generation: an approach using *in vitro* preparation. Jpn. J. Physiol. 47, 385–403.

Onimaru, H. and Homma, I. (2003) A novel functional neuron group for respiratory rhythm generation in the ventral medulla. J. Neurosci. 23, 1478–1486.

Smith, J.C., Ellenberger, H.H., Ballanyi, K., Richter, D.W. and Feldman, J.L. (1991) Pre-Botzinger complex: a brainstem region that may generate respiratory rhythm in mammals. Science 254, 726–729.

Smith, J.C., Ballanyi, K. and Richter, D.W. (1992) Whole-cell patch-clamp recordings from respiratory neurons in neonatal rat brainstem in vitro. Neurosci. Lett. 134, 153–156.

Suzue, T. (1984) Respiratory rhythm generation in the *in vitro* brainstem-spinal cord preparation of the neonatal rat. J. Physiol. (Lond) 354, 173–183.

Svensson E, Woolley J, Wikstrom M, Grillner S. (2003) Endogenous dopaminergic modulation of the lamprey spinal locomotor network. Brain Res. 970:1–8

15
What Role Do Pacemakers Play in the Generation of Respiratory Rhythm?

Christopher A. Del Negro[1], Ryland W. Pace[2] and John A. Hayes[3]

Abstract The pacemaker hypothesis that specialized neurons with conditional oscillatory- bursting properties are obligatory for respiratory rhythm generation in vitro has gained widespread acceptance, despite lack of direct proof. Here we critique the pacemaker hypothesis and provide an alternative explanation for rhythmogenesis based on emergent network properties. Pacemaker neurons in the preBötC depend on either persistent Na^+ current I_{NaP} or Ca^{2+}-activated nonspecific cationic current (I_{CAN}). Activity in slice preparations and synaptically- isolated pacemaker neurons undergo similar frequency modulation by perturbations including hypoxia and changes in external K_+. These data have been used to argue that pacemaker cells must be rhythmogenic, but may simply reflect the action of these perturbations on intrinsic membrane properties throughout the preBötC and does not constitute proof that pacemakers necessarily drive the rhythm with synaptic coupling in place. Likewise, bath-applied drugs, such as riluzole (RIL) and flufenamic acid (FFA), attenuate I_{NaP} and I_{CAN}, respectively, throughout the slice. Thus, when these drugs stop the rhythm, a widespread depression of excitability is likely the underlying cause, not selective blockade of bursting-pacemaker activity. We propose that rhythmogenesis is an emergent network property, wherein recurrent synaptic excitation initiates a positive feedback cycle among interneurons and that intrinsic currents like I_{CAN} and I_{NaP} promote inspiratory burst generation by augmenting synaptic excitation in the context of network activity. In this *group-pacemaker* framework, individual pacemaker neurons can be embedded but play the same role as every other network constituent.

1 Definition of the Pacemaker Hypothesis

The notion that specialized pacemaker neurons generate the respiratory rhythm is an attractive hypothesis that gained credibility following the demonstration, since repeated many times (Brockhaus and Ballanyi 1998; Feldman and Smith 1989),

[1–3] The College of William and Mary, Department of Applied Science, Williamsburg, Virginia. cadeln@wm.edu

M.J. Poulin and R.J.A. Wilson (eds.), *Integration in Respiratory Control: From Genes to Systems*.

that postsynaptic inhibition was not required to generate respiratory rhythm *in vitro* and, furthermore, after voltage-dependent bursting neurons were identified within the preBötC (Smith, Ellenberger, Ballanyi, Richter and Feldman 1991).

The pacemaker hypothesis stipulates that neurons with conditional bursting properties when synaptically isolated (*i.e*., they oscillate between quiescent phases at baseline membrane potential (V_M) and active phases of rapid spike discharge at depolarized potentials) are obligatory for rhythm generation. Excitatory synaptic interactions have been recognized as important to synchronize pacemaker activity, influence burst duration and frequency, as well as distribute rhythmic activity to a larger population of mundane interneurons dubbed *followers*, which constitutes the neurons without conditional bursting properties (Koshiya and Smith 1999; Smith *et al*. 2000).

Prior to 2001, the ionic mechanism for pacemaker activity was attributed solely to persistent Na^+ current (I_{NaP}), which explained its voltage-dependence, insensitivity to low Ca^{2+} solutions, as well as the subthreshold activation of the burst-generating conductance (Butera *et al*. 1999; Del Negro, Koshiya *et al*. 2002a). However, Thoby-Brisson and Ramirez (2001) identified another type of pacemaker activity that was sensitive to blockade of Ca^{2+} channels with external Cd^{2+}. Subsequent work showed that this bursting mechanism depends on Ca^{2+}-activated nonspecific cationic current (I_{CAN}) (Del Negro *et al*. 2005; Pena *et al*. 2004).

2 Pharmacological Experiments

Pharmacology has been used to bolster support for the pacemaker hypothesis. In the first type of experiment, perturbations that modify burst frequency in synaptically-isolated pacemaker neurons are shown to similarly regulate the frequency of respiratory rhythm in the intact network *in vitro*. For example, changing the external K^+ accelerates pacemaker/slice activity, whereas hypoxia causes biphasic changes in pacemaker/slice rhythms. These data have been considered evidence that pacemaker neurons drive the rhythm of the coupled network and cause the frequency changes observed at the systems level (Del Negro, Johnson, Butera and Smith 2001; Thoby-Brisson and Ramirez 2000). At issue in particular were the voltage dependent I_{NaP} pacemaker neurons: the I_{CAN} pacemaker neurons were precluded by developmental age and the use of low Ca^{2+} solutions (Del Negro *et al*. 2001) or they fell silent in hypoxia (Thoby-Brisson and Ramirez 2000).

This evidence fails to provide a causal link between pacemaker neurons and network activity. An alternative explanation is that the modulation of intrinsic conductances affect baseline V_M in all preBötC neurons, of which pacemakers are a subset, which controls the proximity of baseline V_M and spike threshold. This affects the rate at which recurrent excitation spreads in networks (Darbon *et al*. 2002) and can thus control the interburst interval and respiratory frequency (Kosmidis *et al*. 2004).

In the second type of pharmacological experiment, drugs are used to block either or both I_{NaP} and I_{CAN}, and perturbations of network activity are considered evidence

that either or both types of pacemaker neurons drive the intact system. Since I_{NaP} and I_{CAN} are ubiquitously expressed in preBötC neurons (Del Negro *et al*. 2002a; Pace *et al*. 2007a, 2007b; Ptak *et al*. 2005) this is misleading. Drugs like riluzole (RIL, an I_{NaP} antagonist) and flufenamic acid (FFA, an I_{CAN} antagonist) affect excitability throughout the preBötC, and indeed throughout the entire slice when bath-applied. Separately or in combination, when RIL and FFA stop the rhythm, one cannot conclude that their effects on pacemaker neurons are the cause of rhythm cessation. Pacemaker neurons are a small subset of the entire preBötC: 5–15% dependent on I_{NaP} and 0.6–8% dependent I_{CAN} (Del Negro *et al*. 2005; Pena *et al*. 2004). The actual underlying cause of perturbations to network activity is more likely the modulation of intrinsic conductances throughout the network, which broadly regulates excitability and can stop the network rhythm when excitability is depressed. This explanation is compatible with the observation that rhythmic activity stops in the presence of 10 μM RIL and 100 μM FFA, but can be restarted with substance P (SP, 0.5–2 μM) or AMPA (0.5 μM), agents that boost excitability.

The most reliable pharmacological experiment is one in which drugs are applied at concentrations that attenuate I_{NaP} and I_{CAN}, and have been shown to abolish bursting activity in synaptically-isolated pacemaker neurons, but the respiratory rhythm does not cease. This experiment has been performed using 10 μM RIL and 100 μM FFA, and in natural experiments using only RIL in neonates < P6 where I_{CAN} pacemaker neurons are extraordinarily sparse or nonexistent, even though I_{CAN} itself is widely expressed (Del Negro *et al*. 2005; Pace *et al*. 2007a; Pena *et al*. 2004). In these neonates, the pacemaker set is overwhelmingly I_{NaP}-dependent and bath-applied 10 μM RIL does not modify respiratory frequency, which rules out an obligatory rhythmogenic role for I_{NaP} pacemaker neurons (Del Negro, Morgado-Valle and Feldman 2002b; Pace *et al*. 2007b). Since I_{CAN} pacemaker neurons are ostensibly not present, this seriously challenges the veracity of the pacemaker hypothesis.

The fact that adding FFA to the perfusate stops the rhythm in the presence of RIL helps to elucidate an alternative explanation for rhythmogenesis; it suggests that I_{CAN} may be crucial for promoting inspiratory burst generation *in vitro*. Additionally, since the rhythm restarts in the presence of RIL + FFA after application of excitatory agents that depolarize baseline V_M (Del Negro *et al*. 2005), high levels of cellular excitability appear to be important to maintain rhythmic function. We propose that both I_{CAN} and high baseline cellular excitability are critical aspects of the underlying mechanism for respiratory rhythmogenesis *in vitro*.

3 The Group-Pacemaker Hypothesis

According to the *group-pacemaker hypothesis* (Rekling *et al*. 1996; Rekling and Feldman 1998) rhythmogenesis depends on recurrent excitation among preBötC neurons, a positive feedback process leading to population-level bursts and not requiring specialized pacemakers. In the group pacemaker, a fraction of the neurons are spontaneously active: baseline V_M exceeds spike threshold. These neurons

synaptically excite silent neurons which, in turn, excite additional silent neurons and also feedback and re-excite the already-active neurons. As the positive feedback cycle proceeds, recurrent excitation can also evoke intrinsic cellular currents. Whereas I_{NaP} is voltage dependent, I_{CAN} requires Ca^{2+} influx. We hypothesize that I_{CAN} only fully activates in the context of respiratory network behavior because synaptic excitation initiates second messenger cascades leading to the release intracellular Ca^{2+}, which evokes I_{CAN}. We propose that synaptic glutamate release during recurrent excitation promotes inspiratory burst generation through direct postsynaptic depolarization via AMPA receptors, and additionally via metabotropic receptors that evoke I_{CAN} as described above.

If pharmacology attenuates I_{CAN}, then recurrent excitation can still provide sufficient positive feedback to cause network-wide bursts, as long as neurons remain 'near' to spike threshold. This can be satisfied by boosting excitability with SP or another excitatory agent. I_{NaP} could also be helpful in this regard because of its subthreshold activation properties (Ptak *et al*. 2005).

Therefore, while the group-pacemaker hypothesis depends on recurrent excitation, I_{CAN} putatively augments synaptic input and enhances collective bursts. The group-pacemaker hypothesis is consistent with the experiments described above wherein perturbations that depolarize baseline V_M speed up the rhythm (*e.g*., TRH, SP, elevating K^+) and perturbations that hyperpolarize baseline V_M slow the rhythm or stop it altogether (*e.g*., DAMGO or lowering K^+). Baseline V_M influences rhythmic frequency by controlling the rate of the spread of excitation. Raising neurons closer to threshold accelerates the positive feedback process and speeds the rhythm, whereas hyperpolarizing V_M impedes the process and slows the rhythm. Hyperpolarization can also render network constituents so hyperpolarized as to be ostensibly unexcitable, which stops rhythmogenesis. For example, this is the reason *in vitro* studies are typically performed with elevated K^+ concentrations.

4 Conclusions

We contend that respiratory rhythm generation is an emergent network property. The mechanism we propose normally depends on I_{CAN} *in vitro*, an active membrane property that is only fully available in the context of synaptic excitation. This integration of cellular and synaptic properties in support of rhythmogenesis, which Rekling and Feldman (1998) first dubbed the group-pacemaker hypothesis, is a sensible explanation that is consistent with all the pharmacological experiments to date. Although intrinsic currents like I_{CAN} and I_{NaP} are part of the rhythm-generating mechanism, bursting-pacemaker neurons that depend on these conductances are epiphenomena that do not play a specialized or preeminent role in rhythmogenesis. The pacemaker neurons, in the context of synaptically coupled network, play the same role as other constituent neurons: participate in recurrent excitation and augment synaptic excitation to promote inspiratory bursts.

Acknowledgements Supported by IOB 0616099, HL-40959, the Jeffress Trust (Richmond, Virginia), and the Suzzan Wilson Matthews Research Award (The College of William and Mary).

References

Brockhaus, J. and Ballanyi, K. (1998) Synaptic inhibition in the isolated respiratory network of neonatal rats. Eur. J. Neurosci. 10, 3823–3839.

Butera, R.J., Jr., Rinzel, J. and Smith J.C. (1999) Models of respiratory rhythm generation in the pre-Botzinger complex. I. Bursting pacemaker neurons. J. Neurophysiol. 82, 382–397.

Darbon, P., Scicluna, L., Tscherter, A. and Streit, J. (2002) Mechanisms controlling bursting activity induced by disinhibition in spinal cord networks. Eur. J. Neurosci. 15, 671–683.

Del Negro, C.A., Johnson, S.M., Butera, R.J. and Smith J.C. (2001) Models of respiratory rhythm generation in the pre-Bötzinger complex. III. Experimental tests of model predictions. J. Neurophysiol. 86, 59–74.

Del Negro, C.A., Koshiya, N., Butera, R.J. Jr. and Smith J.C. (2002a) Persistent sodium current, membrane properties and bursting behavior of pre-Botzinger complex inspiratory neurons *in vitro*. J. Neurophysiol. 88, 2242–2250.

Del Negro, C.A., Morgado-Valle, C. and Feldman, J.L. (2002b) Respiratory rhythm: an emergent network property? Neuron 34, 821–830.

Del Negro, C.A., Morgado-Valle, C., Hayes, J.A., Mackay, D.D., Pace, R.W., Crowder, E.A. and Feldman, J.L. (2005) Sodium and calcium dependent pacemaker neurons and respiratory rhythm generation. J. Neurosci. 25, 446–453.

Feldman, J.L. and Smith J.C. (1989) Cellular mechanisms underlying modulation of breathing pattern in mammals. Ann. N.Y. Acad. Sci. 563, 114–130.

Koshiya, N. and Smith, J.C. (1999) Neuronal pacemaker for breathing visualized *in vitro*. Nature 400, 360–363.

Kosmidis, E.K., Pierrefiche, O. and Vibert J.F. (2004) Respiratory-like rhythmic activity can be produced by an excitatory network of non-pacemaker neuron models. J. Neurophysiol. 92, 686–699.

Pace, R.W., MacKay, D.D., Feldman, J.L. and Del Negro, C.A. (2007a) Inspiratory bursts in the preBötzinger complex depend on a calcium-activated nonspecific cationic current linked to glutamate receptors. J. Physiol, in press.

Pace, R.W., MacKay, D.D., Feldman, J.L. and Del Negro, C.A. (2007b) Role of persistent sodium current in mouse preBötzinger complex neurons and respiratory rhythm generation. J. Physiol. 580(2):485–496.

Pena, F., Parkis, M.A., Tryba, A.K. and Ramirez, J.M. (2004) Differential contribution of pacemaker properties to the generation of respiratory rhythms during normoxia and hypoxia. Neuron 43, 105–117.

Ptak, K., Zummo, G.G., Alheid, G.F., Tkatch, T., Surmeier, D.J. and McCrimmon, D.R. (2005) Sodium currents in medullary neurons isolated from the pre-Botzinger complex region. J. Neurosci. 25, 5159–5170.

Rekling, J.C., Champagnat, J. and Denavit-Saubie, M. (1996) Electroresponsive properties and membrane potential trajectories of three types of inspiratory neurons in the newborn mouse brain stem *in vitro*. J. Neurophysiol. 75, 795–810.

Rekling, J.C. and Feldman, J.L. (1998) Prebötzinger complex and pacemaker neurons: hypothesized site and kernel for respiratory rhythm generation. Annu. Rev. Physiol. 60, 385–405.

Smith, J.C., Butera, R.J., Koshiya, N., Del Negro, C., Wilson, C.G. and Johnson, S.M. (2000) Respiratory rhythm generation in neonatal and adult mammals: the hybrid pacemaker-network model. Respir. Physiol. 122, 131–147.

Smith, J.C., Ellenberger, H.H., Ballanyi, K., Richter, D.W. and Feldman, J.L. (1991) Pre-Bötzinger complex: a brainstem region that may generate respiratory rhythm in mammals. Science 254, 726–729.

Thoby-Brisson, M. and Ramirez, J.M. (2001) Identification of two types of inspiratory pacemaker neurons in the isolated respiratory neural network of mice. J. Neurophysiol. 86, 104–112.

Thoby-Brisson, M. and Ramirez, J.M. (2000) Role of inspiratory pacemaker neurons in mediating the hypoxic response of the respiratory network *in vitro*. J. Neurosci. 20, 5858–5866.

16
Pre-Bötzinger Complex Neurokinin-1 Receptor Expressing Neurons in Primary Cell Culture

Shereé M. Johnson

Abstract Phenotypic identification of pre-Bötzinger complex (pre-BötC) neurons is vital to the delineation of endogenous cellular properties involved in respiratory rhythm generation and neuromodulation of breathing. A subpopulation of pre-BötC neurons endowed with intrinsic rhythmicity is proposed as the kernel for inspiratory rhythm generation *in vitro*. In this study, the pre-BötC "island" preparation was excised from medullary slices and reduced to its heterogeneous cellular constituents using primary cell culture techniques. Cultured neurons were labeled with tetramethylrhodamine conjugated to Substance P (TMR-SP) to identify individual NK-1R expressing neurons. Data from this study provide initial evidence that the pre-BötC neurons living in culture remain functionally capable of binding and internalizing the fluorescently-tagged ligand and TMR-SP tagging is a useful experimental tool that reliably identifies the NK-1R phenotype.

1 Introduction

Evidence suggests that specialized neurons within the pre-BötC form an excitatory kernel hypothesized to generate the neural activity for respiration (Rekling and Feldman 1998; Smith, Ellenberger, Ballanyi, Richter and Feldman 1991; Smith, Butera, Koshiya, Del Negro, Wilson and Johnson 2000). This aggregation of synaptically-coupled pacemaker neurons is sufficient for initiating inspiratory-related hypoglossal nerve discharge observed in the medullary slice *in vitro* (Smith *et al*. 1991). Since the rhythmic slice provides greater access to the neurons initiating spontaneous activity, functionally-identified neurons have been studied at the single cell level with multiple approaches including extracellular and intracellular whole cell patch clamp electrophysiology and calcium imaging (Del Negro,

Howard University College of Medicine, Department of Physiology and Biophysics, smjohnson@howard.edu

M.J. Poulin and R.J.A. Wilson (eds.), *Integration in Respiratory Control: From Genes to Systems*.

Johnson, Butera and Smith 2001; Del Negro, Morgado-Valle and Feldman 2002; Koshiya and Smith 1999).

Furthermore, extensive evidence indicates that the expression of NK-1Rs is a trait used to distinguish pre-BötC neurons (Gray, Janczewski, Mellen, McCrimmon and Feldman 2001; Pagliardini *et al*. 2005; Pilowski and Feldman 2001; Stornetta, Rosin, Wang, Sevigny, Weston and Guyenet 2003). Recently, Pagliardini *et al*. (2005) described a precise method for targeting "live" pre-BötC NK-1R expressing neurons with fluorescently conjugated Substance P functioning within rhythmically active slices. The objective of this study was to use the pre-BötC "island" model, which was previously characterized (Fig. 1; Johnson, Koshiya and Smith 2001) to further isolate the heterogeneous cellular constituents comprising the pre-BötC.

2 Isolation of the Pre-Bötzinger Complex Rhythmogenic Kernel

Spontaneously active *in vitro* preparations capturing the pre-BötC have progressively and systematically reduced the respiratory network to its most rudimentary form (slice to island). The central hypothesis for these previous investigations is that rhythm emanating from the pre-BötC network is due to endogenous bursting produced by pacemaker neurons within the network. We reduced the thin slice to the pre-BötC "island" preparation to further establish that the pre-BötC is the source of neural activity initiating rhythm in the slice. The spontaneous bursting activity produced by the island closely resembles that of the thin slice model and supports the hypothesis that a rhythmogenic kernel is responsible for inspiratory bursting under *in vitro* conditions (Johnson *et al*. 2001; Fig. 1). In this study, the island was reduced to its heterogeneous cellular phenotypes using primary cell culture techniques previously described by Wang and Richerson (1998). Pre-BötC islands were bilaterally excised from P0–P3 neonatal rat pups, enzymatically digested in papain solution, triturated in Minimal Essential Medium, plated onto poly-L-ornithine coated glass coverslips and maintained in an incubator for periods ≥ 8 weeks.

3 NK-1R Expressing Neurons Identified in Culture with TMR-SP

Data from this first series of experiments provide an initial evaluation of TMR-SP labeling of neurons (~ 4 weeks in culture) from the pre-BötC (Fig. 2). The fluorescent tag provides a clear outline of neuronal profiles and with a high degree of selectivity. This method identifies the subpopulation of cells with NK-1Rs within heterogeneous cultures obtained from the pre-BötC island (Fig. 3). Cultured TMR-SP positive neurons were characterized by cell bodies ~ 10–20 μm in diameter, dendritic

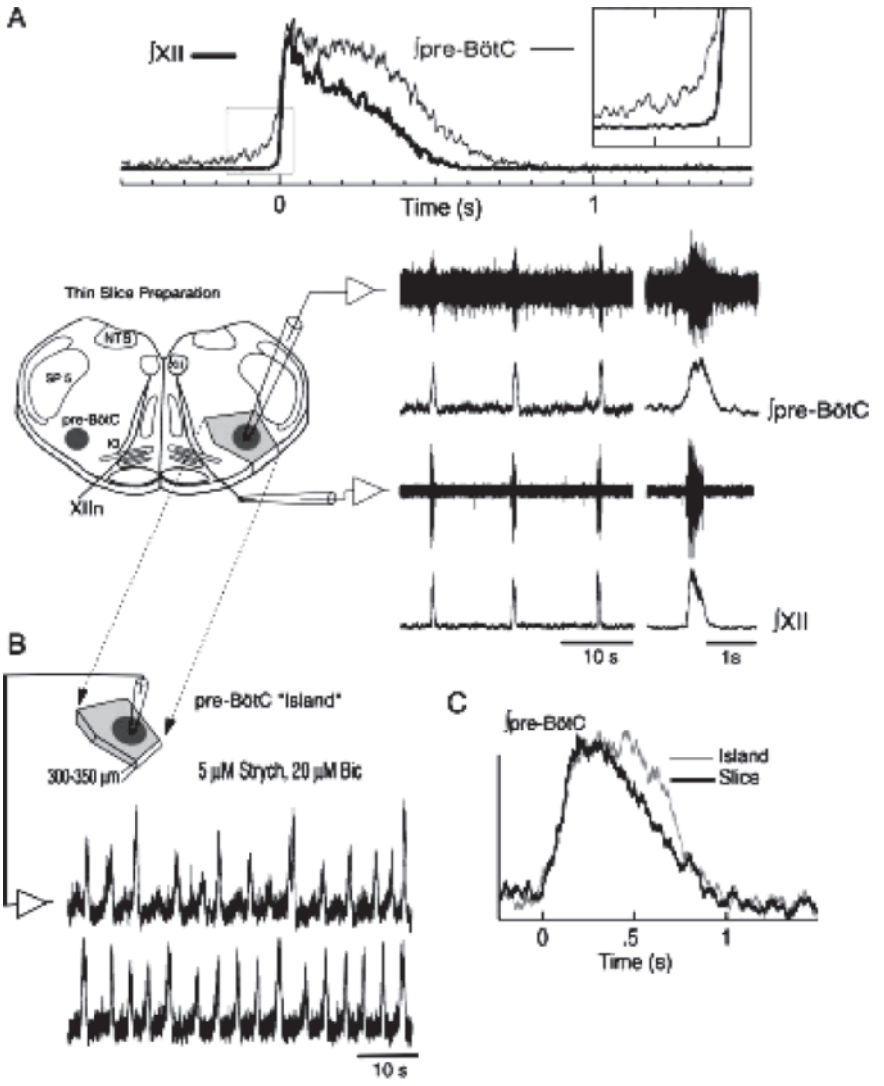

Fig. 1 The spontaneously active pre-BötC "island" preparation was excised from a thin medullary slice to further isolate the pacemaker kernel. (Graphics obtained from the *Journal of Neurophysiology* and used with permission from the American Physiological Society.)

branching and long neuronal processes. Evidence provided in this study indicates that NK-1R expressing neurons of pre-BötC origin, most likely including pacemakers with voltage dependent bursting, can be maintained under primary cell culture conditions. These data further suggest that the pre-BötC neurons living in culture remain functionally capable of binding and internalizing the TMR-SP fluorescently- tagged ligand and that the technique is a reliable method for identifying

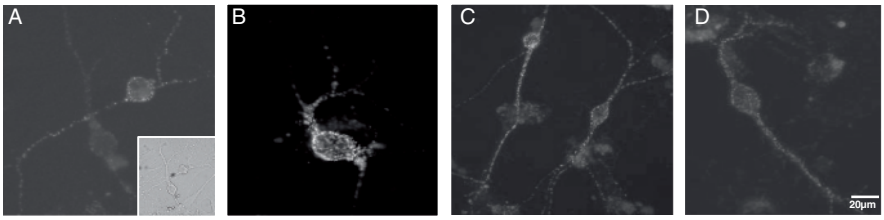

Fig. 2 Fluorescent photomicrographs depict images of cultured pre-BötC neurons (~ 4 weeks in culture) expressing NK-1Rs (A-D). Inset in (A) shows bright field image of the neuronal morphology. The internalization of TMR-SP fluorescent tag produced a punctate profile of living neurons with functional NK-1R receptor systems that optimized visibility of morphological characteristics of individual neurons. Some neurons appeared to express a greater density of NK-1Rs on the soma (B, appearing as the shiny granular particles), while other cells appeared to have receptors that were more evenly distributed on cell bodies and dendritic processes. TMR-SP positive neurons were characterized by cell bodies ~ 10–20 μm in diameter, dendritic branching and long neuronal processes

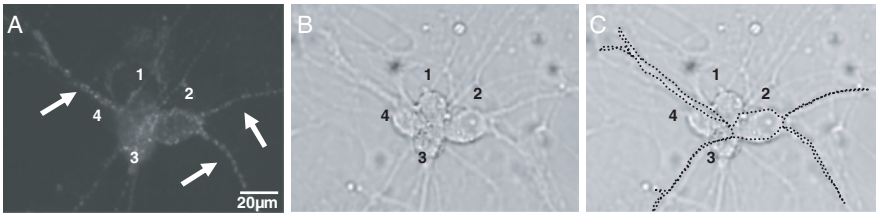

Fig. 3 Fluorescent micrograph depicts TMR-SP labeled neurons and dendritic processes (A, arrowheads). Neurons (1–4) were confirmed with bright field (B). Cell 2 was identified as the TMR-SP positive neuron; punctate labeling outlined the soma with at least 2–3 distinct neuronal processes (arrowheads), while cells 1, 3 and 4 were not as clearly defined. The black dotted line in (C) is a free-hand line tracing of NK-1Rs outlining the anatomical profile of neuron 2. Multiple processes in the immediate vicinity of the TMR-SP positive neuron are visible with bright field; however, they appear unlabeled under fluorescent imaging

the NK-1R phenotype. Therefore, TMR-SP positive neurons in culture will serve as a useful model for studying the electrophysiological properties of individual pre-BötC neurons.

4 Summary and Conclusion

The proposed kernel for respiratory rhythm generation has been systematically reduced to its cellular constituents, from the slice and island preparations to individual neurons in primary cell culture. The hypothesis is that a fraction of TMR-SP positive neurons will display voltage-dependent bursting to further support their

hypothesized role as the pacemakers for breathing *in vitro*. The TMR-SP tag will ultimately function as a useful experimental tool for providing optimal visualization of "live" pre-BötC neurons expressing NK-1Rs. Furthermore, this technique will enhance targeting of the NK-1R phenotype for single cell analysis of intrinsic electrophysiological properties involved in the cellular mechanisms associated with neurogenesis and modulation of breathing. Future studies combining the TMR-SP technique with immunohistochemistry will further characterize the phenotypic traits of TMR-SP positive neurons. The electrophysiological studies including patch clamp recordings and calcium imaging of cultured cells will further elucidate the role of NK-1R expressing neurons in the regulation of breathing at the level of the cell single.

Acknowledgements The author would like to thank Drs. W. Wang and G.B. Richerson for providing training in cell culture techniques at Yale University. Research was funded by NS 47422 to SMJ and supported in part by NS39407.

References

Del Negro, C.A., Johnson, S.M., Butera, R.J. and Smith, J.C. (2001) Models of respiratory rhythm generation in the pre-Botzinger complex. III. Experimental tests of model predictions. J. Neurophysiol. 86, 59–74.

Gray, P.A., Janczewski, W.A., Mellen, N., McCrimmon, D.R., Feldman, J.L. (2001) Normal breathing requires pre-Bötzinger complex neurokinin-1 receptor expressing neurons. Nat. Neurosci. 4, 927–930.

Guyenet, P.G., Sevigny, C.P., Weston, M.C. and Stornetta, R.L. (2002) Neurokinin-1 receptor-expressing cells of the ventral respiratory group are functionally heterogeneous and predominantly glutamatergic. J. Neurosci. 22, 3806–3816.

Johnson, S.M., Koshiya, N. and Smith, J.C. (2001) Isolation of the kernel for respiratory rhythm generation in a novel preparation: the pre-Bötzinger complex 'island.' J. Neurophysiol. 85, 1772–1776.

Koshiya, N. and Smith, J.C. (1999) Neuronal pacemaker for breathing visualized *in vitro*. Nature 400, 360–363.

Pagliardini, S., Adachi, T., Ren, J., Funk, G. and Greer, J. (2005) Fluorescent tagging of rhythmically active neurons within the pre-Bötzinger complex of rat medullary slice preparations. J. Neurosci. 25(10), 2591–2596.

Rekling, J.C. and Feldman, J.L. (1998) Pre-Bötzinger complex and pacemaker neurons: hypothesized site and kernel for respiratory rhythm generation. Annu. Rev. Physiol. 60, 385–405.

Smith, J.C., Ellenberger, H.H., Ballanyi, K., Richter, W. and Feldman, J.L. (1991) Pre-Bötzinger complex: a brainstem region that may generate respiratory rhythm in mammals. Science 54, 726–729.

Smith, J.C., Butera, R.J., Koshiya, N., Del Negro, C.A., Wilson, C.G. and Johnson, S.M. (2000) Respiratory rhythm generation in neonatal and adult mammals: the hybrid pace-maker-network model. Respir. Physiol. 122, 131–147.

Stornetta, R.I., Rosin, D.I., Wang, H., Sevigny, C.P., Weston, M.C. and Guyenet, P.G. (2003) group of glutamatergic interneurons expressing high levels of both neurokinin-1 receptors and somatostatin identifies the region of the pre-Botzinger complex. J. Comp. Neurol. 455, 499–512.

Wang, W., Pizzonia, J.H. and Richerson, G.B. (1998) Chemosensitivity of rat medullary raphe neurons in primary tissue culture. J. Physiol. 511, 433–450.

17
Belt-and-Suspenders as a Biological Design Principle

Nicholas M. Mellen

Abstract Recent studies have shown both the pFRG and the preBötC are sufficient to generate respiratory rhythm, and are hypothesized to do so via distinct mechanisms (Onimaru and Homma 2003; Mellen, Janczewski, Bocchiaro and Feldman 2003). The coexistence of mechanistically distinct, functionally matching networks (defined as degeneracy, Edelman and Gally 2001) is a ubiquitous feature of motor networks in both invertebrates (Selverston and Miller 1980) and vertebrates (DiDomenico, Nissanov and Eaton 1988). In almost all cases, a consensus exists about which subsystem is the "primary" rhythm generator, yet consistently, the effect of modulators on the isolated primary rhythm generator is qualitatively different than their effect on the more intact network (Ayali and Harris-Warrick 1999) and, in the intact animal, all rhythmogenic networks are active during motor pattern generation. Thus, at best, ascribing primacy to a particular network has weak support (since the other networks can produce qualitatively similar patterns; Prinz, Bucher and Marder 2004) and little explanatory power (since effects of modulatory inputs on the isolated "primary" rhythm generator do not persist in more intact networks). The ubiquity of degenerate networks for motor pattern generation suggests that a more useful question is why such an organization exists. We propose that degeneracy is ubiquitous because it reduces the phenotype's sensitivity to genetic mutation and environmental perturbation, and broadens the adaptiveness of motor patterns.

In the last five years, our understanding of how respiratory rhythm is generated has been in flux. Accumulating evidence has established that both the pFRG and the preBötC are sufficient to generate respiratory rhythm (Mellen, Janczewski *et al*. 2003; Onimaru and Homma 2003; Onimaru, Kumagawa *et al*. 2006) and, within the preBötC, multiple mechanistically distinct rhythmogenic mechanisms have been proposed (Del Negro, Morgado-Valle *et al*. 2002; Pena, Parkis *et al*. 2004). In light of these recent findings, a debate about which of these rhythmogenic mechanisms is primary has emerged (Feldman and Janczewski 2006; Onimaru and Homma 2006).

Kosair Children's Hospital Research Institute, University of Louisville, 570 S. Preston Street, Baxter Building 1, Suite 304, Louisville, KY 40202, USA, nicholas.mellen@louisville.edu

M.J. Poulin and R.J.A. Wilson (eds.), *Integration in Respiratory Control: From Genes to Systems*.

This debate has emerged because multiple sites, albeit under rather special conditions, are sufficient to generate respiratory rhythm. Thus, the strong claim that one region or another is both sufficient and necessary has already been ruled out. Weaker claims about the primacy of one region over another are in large part based on the interpretation of lesion studies, which have been carried out using a number of techniques, with ambiguous results.

Lesion studies that generate equivocal results may indicate the existence of functionally equivalent, mechanistically distinct networks subserving the same behavior, which has been termed degeneracy (Edelman and Gally 2001). While the focus here is on functionally overlapping respiratory rhythm generating networks, degeneracy is apparent across levels of biological organization, including the overlapping contribution of multiple genes to a phenotypic feature. An example of this is the nested expression of *HOX* genes controlling rhombomeric specification in vertebrate hindbrain: aside from rhombomere 2, no *HOX* gene is uniquely associated with one rhombomere (Kiecker and Lumsden 2005).

The recent discovery of quantal slowing in both rats (Mellen, Janczewski *et al*. 2003) and bullfrogs (Vasilakos, Wilson *et al*. 2005) lends support to the hypothesis that in both species, despite important differences in respiratory mechanics and physiology, dual oscillators exist. Because the rhombomeric organization of hindbrain is the common scaffolding along which these dual rhythmogenic networks are built, it is possible to establish homologies between respiratory networks in both species. In adult frogs, rhombomeric organization is preserved (Straka, Baker *et al*. 2002) thus, based on its anatomical location, the rostral lung oscillator in frogs is derived from rhombomere 4, while the more caudal buccal oscillator is derived from rhombomeres 7–8. In the rat, rhombomeric structure is less evident in the brainstem at birth; thus, to establish mappings from rhombomere to respiratory network, null mutations were used. In order to selectively ablate neurons descending from rhombomere 4, *Hoxa1*$^{-/-}$ (del Toro, Borday *et al*. 2001) and *Krox20*$^{-/-}$ (Chatonnet, del Toro *et al*. 2002) mutants were developed. These animals died shortly after birth but could be rescued if treated with the μ-opiate receptor antagonist naloxone, consistent with the presence of a normally functioning, but depressed preBötC. Based on these observations, it has been proposed that the pFRG is derived from rhombomeres 3 and 4 (Chatonnet, Borday *et al*. 2006).

Although both the pFRG in rat and the lung rhythm generator in frog lie rostrally, and the preBötC in rat and the buccal rhythm generator lie caudally, the homology between the pFRG and the lung rhythm generator is counterintuitive. The phase of firing of the buccal rhythm generator matches the pre-I neuron phase of firing in the rat pFRG (Wilson, Vasilakos *et al*. 2006), and both buccal and pFRG networks are opiate-insensitive (Vasilakos, Wilson *et al*. 2005). Thus, based on their pharmacological profile, and pattern of activity, networks derived from rhombomeres 3–4 in rats are analogous to networks in frog that descend from rhombomeres 7–8. Similarly, the inspiratory phase of firing and opiate sensitivity of lung rhythm generators in frog and the preBötC in rat suggest that networks derived from rhombomeres 3–4 in frog are functionally analogous to networks likely derived from rhombomeres 6–8 in rat (Chatonnet, Borday *et al*. 2006). If this analysis is

correct, then it appears that in the evolution from anuran to mammal, rostral and caudal respiratory networks swapped pattern of activity and pharmacological profile. Thus, the functional organization of frog respiratory networks was not preserved in mammals, but *recapitulated*, since the rhombomeres of origin of analogous networks in frog and rat are different. The existence of two functionally distinct respiratory networks might explain how such a profound reconfiguration could take place: as long as one network could ensure respiratory patency, the other could undergo cycles of mutation and selection. Thus, degeneracy creates conditions under which networks subserving essential homeostatic function can evolve.

As has been pointed out elsewhere (Viemari, Burnet *et al*. 2003), the existence of functionally similar, mechanistically distinct respiratory rhythm generating networks in ventrolateral medulla also may ensure maintenance of respiratory patency in the perinatal period. During this period, the role of Cl-mediated conductances change continuously in the perinatal period, as a function of changing levels of Cl^- cotransporters (Ren and Greer 2006) and, later, due to changes in glycine receptor structure (Becker, Hoch *et al*. 1988), which are reflected in network-level changes in the role of fast synaptic inhibition in respiratory rhythm generation (Paton and Richter 1995). Likewise in the preBötC at birth, I_{NaP}-mediated bursting mechanisms dominate, while after P6, Ca^{++}-dependent bursters emerge (Pena, Parkis *et al*. 2004). Although developmental changes and network connectivity within the pFRG have been less well described, the role of endogenous bursters appears more pronounced (Onimaru, Arata *et al*. 1989), and these bursters are Ca^{++}-dependent (Onimaru, Arata *et al*. 1997). Because of the differences in rhythmogenic mechanism between pFRG and preBötC, developmental changes are likely to affect these networks differently. This would explain why, despite ongoing changes in cellular and synaptic properties during the first weeks of life, respiratory frequency increases only slightly *in vivo*, while *in vitro* it remains unchanged (Viemari, Burnet *et al*. 2003).

On both phylogenetic and ontogenetic timescales, degeneracy may create conditions under which physiological function can persist even as the mechanisms that give rise to it undergo change. As has been proposed in its original formulation (Edelman and Gally 2001), degeneracy is ubiquitous across levels of description. Together, these properties tend to undermine efforts to experimentally or conceptually isolate one subsystem in a degenerate network. In the matter at hand, even if one were to decide that either the preBötC or the pFRG were the primary rhythm generator, the debate would then shift to what the primary rhythmogenic mechanism is within each region. This debate has already begun with respect to the preBötC, where endogenous bursters (Butera, Rinzel *et al*. 1999; Butera, Rinzel *et al*. 1999) or network properties (Del Negro, Morgado-Valle *et al*. 2002) are being proposed as competing rather than complementary mechanisms. In focusing on the primacy of one mechanism over another, the computational richness of degeneracy that others have begun to explore (Leonardo 2005) is ignored. In the case of breathing, the overlaying of spatially and/or mechanistically distinct rhythmogenic networks, differentially targeted by afferent inputs (Mellen, Roham *et al*. 2004) and neuromodulators (Takeda, Eriksson *et al*. 2001), may provide greater adaptiveness and

robustness to a degenerate network than would be found in any of its constituents. Thus, while it is necessary and important to characterize individual rhythmogenic mechanisms, privileging one over the others may lead us to ignore the richness that arises from their interaction.

References

Becker, C.M., Hoch, W. *et al*. (1988) Glycine receptor heterogeneity in rat spinal cord during postnatal development. The EMBO Journal 7(12), 3717–3726.

Butera, R.J., Jr., Rinzel, J. *et al*. (1999) Models of respiratory rhythm generation in the pre-Botzinger complex. I. Bursting pacemaker neurons. J. Neurophysiol. 82(1), 382–397.

Butera, R.J., Jr., Rinzel, J. *et al*. (1999) Models of respiratory rhythm generation in the pre-Botzinger complex. II. Populations of coupled pacemaker neurons. J. Neurophysiol. 82(1), 398–415.

Chatonnet, F., Borday, C. *et al*. (2006) Ontogeny of central rhythm generation in chicks and rodents. Respir. Physiol. Neurobiol. 154(1–2), 37–46.

Chatonnet, F., del Toro, E.D. *et al*. (2002) Different respiratory control systems are affected in homozygous and heterozygous kreisler mutant mice. Eur. J. Neurosci. 15(4), 684–692.

Del Negro, C.A., Morgado-Valle, C. *et al*. (2002) Respiratory rhythm: an emergent network property? Neuron. 34(5), 821–830.

del Toro, E.D., Borday, V. *et al*. (2001) Generation of a novel functional neuronal circuit in Hoxa1 mutant mice. J. Neurosci. 21(15), 5637–5642.

Edelman, G.M. and Gally, J.A. (2001) Degeneracy and complexity in biological systems. Proc. Natl. Acad. Sci. USA 98(24), 13763–13768.

Feldman, J.L. and Janczewski, W.A. (2006) Point:Counterpoint: The parafacial respiratory group (pFRG)/pre-Botzinger complex (preBotC) is the primary site of respiratory rhythm generation in the mammal. Counterpoint: the preBotC is the primary site of respiratory rhythm generation in the mammal. J. Appl. Physiol. 100(6), 2096–2097 (discussion 2097–2099, 2103–2108).

Kiecker, C. and Lumsden, A. (2005) Compartments and their boundaries in vertebrate brain development. Nat. Rev. Neurosci. 6(7), 553–564.

Leonardo, A. (2005) Degenerate coding in neural systems. J. Comp. Physiol. A Neuroethol. Sens. Neural. Behav. Physiol. 191(11), 995–1010.

Mellen, N.M., Janczewski, W.A. *et al*. (2003) Opioid-induced quantal slowing reveals dual networks for respiratory rhythm generation. Neuron 37(5), 821–826.

Mellen, N.M., Roham, M. *et al*. (2004) Afferent modulation of neonatal rat respiratory rhythm *in vitro*: cellular and synaptic mechanisms. J. Physiol. 556(Pt. 3), 859–874.

Onimaru, H., Arata, A. *et al*. (1989) Firing properties of respiratory rhythm generating neurons in the absence of synaptic transmission in rat medulla *in vitro*. Experimental Brain Research 76(3), 530–536.

Onimaru, H., Arata, A. *et al*. (1997) Neuronal mechanisms of respiratory rhythm generation: an approach using *in vitro* preparation. Jpn. J. Physiol. 47(5), 385–403.

Onimaru, H. and Homma, I. (2003). A novel functional neuron group for respiratory rhythm generation in the ventral medulla. J. Neurosci. 23(4), 1478–1486.

Onimaru, H. and Homma, I. (2006) Point:Counterpoint: The parafacial respiratory group (pFRG)/pre-Botzinger complex (preBotC) is the primary site of respiratory rhythm generation in the mammal. Point: the PFRG is the primary site of respiratory rhythm generation in the mammal. J. Appl. Physiol. 100(6), 2094–2095.

Onimaru, H., Kumagawa, Y. *et al*. (2006) Respiration-related rhythmic activity in the rostral medulla of newborn rats. J. Neurophysiol. 96(1), 55–61.

Paton, J.F. and Richter, D.W. (1995) Role of fast inhibitory synaptic mechanisms in respiratory rhythm generation in the maturing mouse. J. Physiol. 484 (Pt. 2), 505–521.

Pena, F., Parkis, M.A. *et al*. (2004) Differential contribution of pacemaker properties to the generation of respiratory rhythms during normoxia and hypoxia. Neuron 43(1), 105–117.

Ren, J. and Greer, J.J. (2006) Modulation of respiratory rhythmogenesis by chloride-mediated conductances during the perinatal period. J. Neurosci. 26(14), 3721–3730.

Straka, H., Baker, R. *et al*. (2002) The frog as a unique vertebrate model for studying the rhombomeric organization of functionally identified hindbrain neurons. Brain Res. Bull. 57(3–4), 301–305.

Takeda, S., Eriksson, L.I. *et al*. (2001) Opioid action on respiratory neuron activity of the isolated respiratory network in newborn rats. Anesthesiology 95(3), 740–749.

Vasilakos, K., Wilson, R.J. *et al*. (2005) Ancient gill and lung oscillators may generate the respiratory rhythm of frogs and rats. J. Neurobiol. 62(3), 369–385.

Viemari, J.C., Burnet, H. *et al*. (2003) Perinatal maturation of the mouse respiratory rhythm-generator: *in vivo* and *in vitro* studies. Eur. J. Neurosci. 17(6), 1233–1244.

Wilson, R.J., Vasilakos, K. *et al*. (2006) Phylogeny of vertebrate respiratory rhythm generators: The oscillator homology hypothesis. Respir. Physiol. Neurobiol. 154(1–2), 47–60.

18
Two Modes of Respiratory Rhythm Generation in the Newborn Rat Brainstem-Spinal Cord Preparation

Hiroshi Onimaru[1] and Ikuo Homma[2]

Abstract Two respiration-related rhythm generators, the pre-Bötzinger complex inspiratory and the parafacial pre-inspiratory rhythm generators, have been identified in the medulla of rodents that produce intrinsic periodic bursts. Although both generators can be independently active under specific conditions, they interact as a coupled oscillator system to regulate the respiratory rhythm. Here, we summarize different mechanisms of modulation of the respiratory rhythm in the brainstem-spinal cord preparation of newborn rats and discuss factors determining rhythm generator dominance. We show two different modes of respiratory rhythm generation in the brainstem-spinal cord preparation that depends on the background stimulation level.

1 Introduction

Two respiration-related rhythm generators have been identified in the medulla of rodents that produce intrinsic periodic burst activity (Janczewski and Feldman 2006; Onimaru, Kumagawa and Homma 2006). One is an inspiratory (Insp) neuronal network, which is localized predominantly in the pre-Bötzinger complex (PBC) of the ventrolateral medulla (Smith, Ellenberger, Ballanyi, Richter and Feldman 1991). The other is a pre-inspiratory (Pre-I) neuronal network, which generates activity prior to Insp bursts and typically also during the post-inspiratory period. The Pre-I neuronal network includes the parafacial respiratory group (pFRG) in the rostral ventrolateral medulla (Onimaru and Homma 2003). The pFRG is located lateral, ventral, medial, and caudal to the facial nucleus (Fig. 1). The rostral and medial portion of the pFRG may overlap with the retrotrapezoid nucleus (RTN) (Smith, Morrison, Ellenberger, Otto and Feldman 1989), which plays an important role in central chemoreception (Nattie 2001). The major neuron population of the pFRG appears to be localized lateral to the RTN, although the precise localization remains to be elucidated.

[1–2]Showa University School of Medicine, Department of Physiology, oni@med.showa-u.ac.jp ihomma@med.showa-u.ac.jp

M.J. Poulin and R.J.A. Wilson (eds.), *Integration in Respiratory Control: From Genes to Systems*.

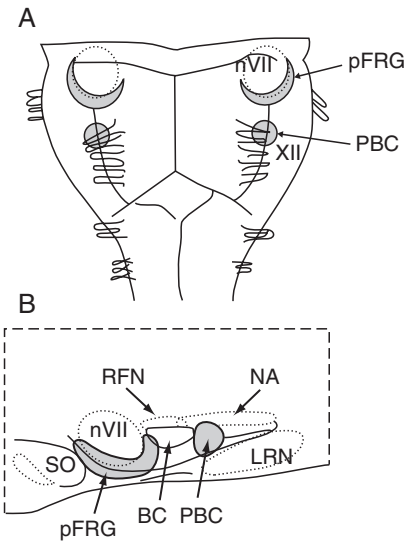

Fig. 1 (A) Approximate area of para-facial respiratory group (pFRG) and pre-Bötzinger complex (PBC) in a ventral view of the medulla. (B) Location of pFRG and PBC in a sagittal view compared with schematic drawing of the ventral medulla nuclei (modified from Smith *et al*. 1991). BC, Bötzinger complex; NA, nucleus ambiguus; LRN, lateral reticular nucleus; nVII, facial nucleus; RFN, retrofacial nucleus; SO, superior olive. Note that these areas do not mean localization of pre-inspiratory and inspiratory neurons, because they overlap to a certain extent in the rostro-caudal column of ventral medulla

The caudal portion of the pFRG overlaps with the most rostral portion of the ventral respiratory group (Bötzinger complex). The pFRG-Pre-I neurons, including those of the caudal part, may receive tonic drive from central chemoreceptors and are also intrinsically chemosensitive (Kawai, Onimaru and Homma 2006).

Although both generators can be independently active under specific conditions, several lines of evidence indicate that pFRG-Pre-I activity triggers the induction of inspiratory bursts and determines the frequency of inspiratory output in the brainstem-spinal cord preparation of newborn rats, in which intrinsic burst generation by the PBC is masked (Onimaru and Homma 2006a). Under more general conditions, however, it is not clear what factors determine primary rhythm generator dominance. Here, we summarize different mechanisms of modulation of respiratory rhythm in the brainstem-spinal cord preparation of newborn rats.

2 Properties of the Two Rhythm Generators

Previous studies have indicated that the pFRG-Pre-I rhythm generator and the PBC-Insp rhythm generator possess different sensitivities to neuromodulators. Therefore, different neuronal mechanisms may be involved in respiratory rhythm modulation.

2.1 Inhibitory Modulation

At least three mechanisms may underlie pharmacologically-induced decreases in the frequency of inspiratory output activity of the respiratory network in the

brainstem-spinal cord preparation (Ballanyi, Onimaru and Homma 1999), as summarized recently (Onimaru and Homma 2006a). These include the following: (1) A decrease in the rate of Pre-I neuron bursts induced by gamma aminobutyric acid directly results in a frequency decrease (Ballanyi *et al*. 1999); (2) A decrease in the intraburst firing frequency of Pre-I neurons induced by dopamine results in decreased respiratory frequency via failure to trigger inspiratory burst generation (Fujii, Umezawa and Arata 2006); (3) Direct (postsynaptic) or indirect (presynaptic) inhibition of inspiratory burst generation by opiates in the absence of an inhibitory effect on Pre-I neurons decreases the frequency of the final inspiratory output (Takeda, Eriksson, Yamamoto, Joensen, Onimaru and Lindahl 2001; Mellen, Janczewski, Bocchiaro and Feldman 2003).

2.2 Excitatory Modulation

The PBC-Insp and pFRG-Pre-I rhythm generators may possess different sensitivities to excitatory substances such as K^+, CO_2, excitatory amino acids and substance P. It has been reported that increased external [K^+] induces an increase in the rate of the fourth cervical ventral root (C4) inspiratory activity (Okada, Kuwana, Kawai, Muckenhoff and Scheid 2005). However, bursting of Pre-I neurons can be disturbed by increased [K^+] (Mellen *et al*. 2003). In addition, burst generation of putative Pre-I neurons in blocks of rostral medulla is strongly disturbed by high [K^+] (Onimaru *et al*. 2006). Therefore, we studied the effect of alterations in [K^+] on Pre-I neurons and C4 activity in the brainstem-spinal cord preparation of newborn rats (Suzue 1984). We recorded membrane potentials of Pre-I or Insp neurons in the medulla and also analyzed the activity of these neurons by optical recording of preparations stained with voltage-sensitive dye (Onimaru and Homma 2006b). Optical and electrophysiological recordings showed that pFRG-Pre-I bursts precede Insp bursts under normal and low [K^+] conditions. Addition of 6 or 8 mM K^+ to the standard solution containing 3 or 6 mM K^+ induced an initial decrease of the C4 burst rate and subsequent high-frequency C4 activity of short burst duration, whereas Pre-I neurons were depolarized and their ability to generate burst was disturbed. In the presence of high [K^+], optical recordings detected only PBC-Insp burst activity, in the absence of pFRG burst activity. These results suggest that the pFRG-Pre-I rhythm generator triggers Insp burst generation under normal or low [K^+] conditions, whereas the PBC-Insp rhythm generator produces rhythmic bursts independently of pFRG activity under high [K^+] condition.

3 Factors Determining Rhythm Generator Dominance

Excitatory or inhibitory substances that affect the cell excitability of rhythm generators can modulate the intrinsic rhythm of the two generators. To refer to the general effects of these substances on rhythm generation, we propose the term

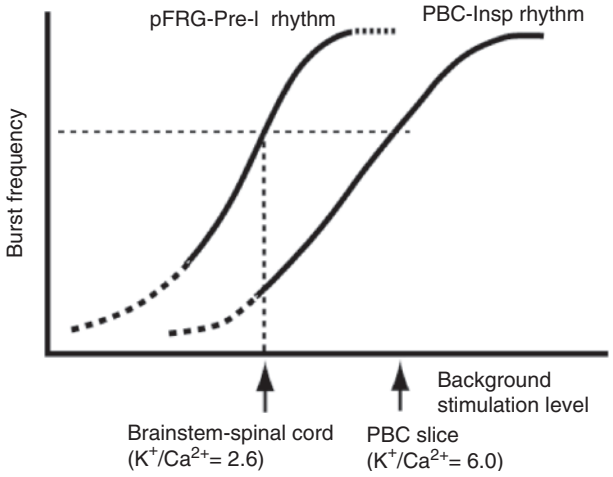

Fig. 2 Putative concentration-response curve of burst frequency in relation to background stimulation level. The stimulation level in the standard solution of the brainstem-spinal cord preparation is denoted by the dotted straight line. In the intact preparation, this Pre-I rhythm determines the rate of inspiratory activity as the final output. In the pre-Bötzinger complex (PBC) slice preparation, increased stimulation level is required to maintain similar inspiratory output frequency

"background stimulation level." This refers to a factor determining the level of excitation (*e.g.*, membrane potential, excitatory synaptic inputs) of rhythm-generating neurons. A representative factor is $[K^+]$ (more likely $[K^+]/[Ca^{2+}]$), although extremely low $[K^+]$ may cause other effects on cell excitability linked to Na/K ATPase activity or other mechanisms. We hypothesize that rhythm generator dominance in determining the basic respiratory rhythm depends on the background stimulation level. Putative concentration-response curves for the pFRG-Pre-I and PBC-Insp rhythm generators are shown in Fig. 2. At low background stimulation levels, the pFRG rhythm generator is more active than the PBC rhythm generator and entrains the activity of the PBC rhythm generator. At high background stimulation levels, the PBC rhythm generator is intrinsically active and determines output frequency.

4 Conclusion

We have discussed two different modes of respiratory rhythm generation in the brainstem-spinal cord preparation of newborn rats that depend on the background stimulation level. These rhythm generators may function *in vivo*; the background stimulation level may differ depending on conditions such as arousal level, anesthesia and afferent inputs (*e.g.*, vagal afferents). The neuronal mechanisms of respiratory rhythm generation (*i.e.*, rhythm generator dominance in the determination of output frequency) *in vivo* and *in vitro* may differ in response to various treatments.

Acknowledgements This study was supported in part by Grants for International Exchange from The Promotion and Mutual Aid Corporation for Private Schools of Japan.

References

Ballanyi, K., Onimaru, H. and Homma, I. (1999) Respiratory network function in the isolated-brainstem-spinal cord of newborn rats. Prog. Neurobiol. 59, 583–634.

Fujii, M., Umezawa, K. and Arata, A. (2006) Dopamine desynchronizes the pace-making neuronal activity of rat respiratory rhythm generation. Eur. J. Neurosci. 23, 1015–1027.

Janczewski, W.A. and Feldman, J.L. (2006) Distinct rhythm generators for inspiration and expiration in the juvenile rat. J. Physiol. 570, 407–420.

Kawai, A., Onimaru, H. and Homma, I. (2006) Mechanisms of CO2/H+ chemoreception by respiratory rhythm generator neurons in the medulla from newborn rats *in vitro*. J. Physiol. 572, 525–537.

Mellen, N.M., Janczewski, W.A., Bocchiaro, C.M. and Feldman, J.L. (2003) Opioid-induced quantal slowing reveals dual networks for respiratory rhythm generation. Neuron 37, 821–826.

Nattie, E.E. (2001) Central chemosensitivity, sleep and wakefulness. Respir. Physiol. 129, 257–268.

Okada, Y., Kuwana, S., Kawai, A., Muckenhoff, K. and Scheid, P. (2005) Significance of extracellular potassium in central respiratory control studied in the isolated brainstem-spinal cord preparation of the neonatal rat. Respir. Physiol. Neurobiol. 146, 21–32.

Onimaru, H. and Homma, I. (2003) A novel functional neuron group for respiratory rhythm generation in the ventral medulla. J. Neurosci. 23, 1478–1486.

Onimaru, H. and Homma, I. (2006a) Point:Counterpoint: The parafacial respiratory group (pFRG)/pre-Botzinger complex (preBotC) is the primary site of respiratory rhythm generation in the mammal. Point: the PFRG is the primary site of respiratory rhythm generation in the mammal. J. Appl. Physiol. 100, 2094–2095.

Onimaru, H. and Homma, I. (2006b) Neuronal mechanisms of respiratory rhythm modulationinduced by external K^+ concentration change in the newborn rat brainstem-spinal cord preparation. Neurosci. Res. 55, s129.

Onimaru, H., Kumagawa, Y. and Homma, I. (2006) Respiration-related rhythmic activity in the rostral medulla of newborn rats. J. Neurophysiol. 96, 55–61.

Smith, J.C., Ellenberger, H.H., Ballanyi, K., Richter, D.W. and Feldman, J.L. (1991) Pre-Botzinger complex: a brainstem region that may generate respiratory rhythm in mammals. Science 254, 726–729.

Smith, J.C., Morrison, D.E., Ellenberger, H.H., Otto, M.R. and Feldman, J.L. (1989) Brain-stem projections to the major respiratory neuron populations in the medulla of the cat. J. Comp. Neurol. 281, 69–96.

Suzue, T. (1984) Respiratory rhythm generation in the *in vitro* brain stem-spinal cord preparation of the neonatal rat. J. Physiol. 354, 173–183.

Takeda, S., Eriksson, L.I., Yamamoto, Y., Joensen, H., Onimaru, H. and Lindahl, S.G. (2001) Opioid action on respiratory neuron activity of the isolated respiratory network in newborn rats. Anesthesiology 95, 740–749.

19
Possible Roles of the Weakly Inward Rectifying K^+ Channel Kir4.1 (KCNJ10) in the Pre-Bötzinger Complex

Nestoras Papadopoulos[1], Stefan M. Winter[1], Kai Härtel[1], Melanie Kaiser[2], Clemens Neusch[2] and Swen Hülsmann[1]

Abstract Rhythmic activity of respiratory neurons is dependent on the clearance of neurotransmitter by astrocytes. Astrocytes should also be involved in the permanent and rapid clearance of extracellular ions. We analyzed the expression of the weakly inwardly rectifying K^+ channel Kir4.1 (KCNJ10) in the respiratory network and studied the possible functions for neuronal activity in the pre-Bötzinger complex.

1 Introduction

Synaptic transmission in the respiratory network is dependent on the glial capacity to buffer neurotransmitters (Gomeza *et al*. 2003). Glial Kir (inwardly-rectifying K^+ channels) channels have been shown to regulate K^+ that is released during neuronal activity (for review see Kofuji and Newman 2004). In the respiratory network, the pre-Bötzinger complex (PreBötC) forms an important kernel for generating ongoing rhythmic activity (Smith *et al*. 1991), which is adjusted by a neuronal network within the brainstem (Richter and Spyer 2001). K^+ buffering by astrocytes seems to be a key factor in protecting the fine-balanced rhythmic activity. One possible candidate gene that could serve spatial K^+ buffering in brainstem astrocytes is the weakly inwardly rectifying K^+ channel subunit Kir4.1 (KCNJ10). In the CNS, Kir4.1 channels appear to be expressed predominantly (Takumi *et al*. 1995) but not exclusively (Bredt *et al*. 1995) in glial cells. Kir4.1 expression has also been reported in neurons of the brainstem at the mRNA level (Wu *et al*. 2004). We sought to determine the specific expression of the Kir4.1 channel subunit in astrocytes of the ventral respiratory group (VRG) including the pre-Bötzinger complex and studied its potential roles for respiratory network function. We took advantage of a mouse line with specific ablation of the Kir4.1 gene expression (Kofuji *et al*. 2000).

[1] Department of Neuro- and Sensory Physiology, Georg-August-University Göttingen, 37073 Göttingen, Germany, shuelsm2@uni-goettingen.de

[2] Department of Neurology, Georg-August-University Göttingen, 37075 Göttingen, Germany

M.J. Poulin and R.J.A. Wilson (eds.), *Integration in Respiratory Control: From Genes to Systems*. © Springer 2008

For the purpose of visual identification of astrocytes in the pre-Bötzinger region, we generated double transgenic mice by interbreeding Kir4.1 mice with transgenic animals expressing the fluorescent protein EGFP under the astrocyte-specific human GFAP promoter (Nolte *et al*. 2001).

2 Methods

Double transgenic mice were generated by interbreeding of transgenic mice expressing EGFP under the human GFAP promoter TgN(hGFAP-EGFP) and mice with heterozygous Kir4.1 subunit gene ablation. Immunohistochemistry and fluorescence was performed as described earlier (Neusch *et al*. 2006; Neusch *et al*. 2001). Rhythmic slice preparation and whole cell recordings were described earlier (Neusch *et al*. 2006). Whole-body plethysmography (refer to Gomeza *et al*. 2003) was performed in animals from P0–P11. Data are given as mean ± SEM.

3 Results

Using double transgenic mice with astroglial-specific EGFP expression in astrocytes (Fig. 1A), we determined Kir4.1 protein expression within the VRG. At P11, Kir4.1 channels were detected, among other brainstem nuclei, in the VRG (Fig. 1A, 1B). Analysis of Kir4.1 immunofluorescence revealed that Kir4.1 is expressed on astrocytic processes including those engulfing capillaries and small vessels (Fig. 1 E, 1F). Kir4.1 labeling in the VRG was also found in some neuronal cells (not shown) (Wu *et al*. 2004; Neusch *et al*. 2006) and in white matter areas as previously described for the spinal cord (Neusch *et al*. 2001).

We additionally analyzed electrophysiological properties of astrocytes in brainstem slices of WT versus Kir4.1–/– mice. Astrocytes were identified by means of their transgenic EGFP expression. Only astrocytes expressing a high fluorescence intensity (Grass *et al*. 2004) were whole-cell voltage clamped, and current-voltage (I-V) relations for these cells were measured at test potentials of 10 mV increments over a voltage range from −150 mV to 60 mV. Kir4.1–/– astrocytes exhibited a prominently depolarized resting membrane potential of –49.2 ± 1.7 mV (n = 39) as compared to WT astrocytes (–72.2 mV ± 2.5 mV; n = 17, mean ± SEM; Fig. 1D). These changes went along with an increase of the membrane resistance and a virtual loss of K^+ induced inward currents. We next wanted to analyze if a failure of the respiratory network is the underlying cause of death Kir4.1–/– mice that is observed around postnatal day 10 to 14. During the first postnatal week, WT mice and Kir4.1 –/– mice did not differ significantly in breathing frequency. However, in older Kir4.1 –/– animals (P6–P11), breathing frequency did not increase to physiological levels as was observed for wild type mice (5.1 ± 0.3 Hz, n = 9) but remained on a significantly lower level (3.2 ± 0.3 Hz, n = 14). Obviously, the

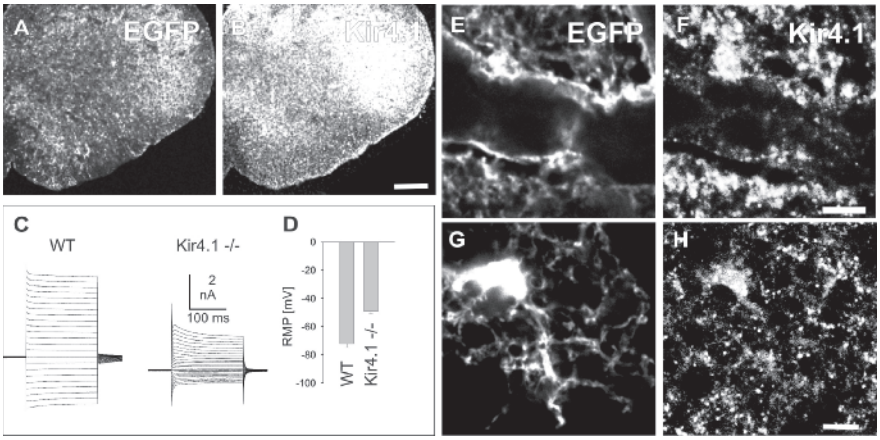

Fig. 1 Expression of Kir4.1 in astrocytes of the VRG. (A, B) Overview of EGFP expression (A) and Kir4.1 immunostaining (B). (C) Superimposed whole-cell currents derived from a step protocol recorded for a WT and a Kir4.1–/– astrocyte (potentials ranging from –150 to +60 mV in 10 mV increments). (D) WT and Kir4.1–/– astrocyte resting membrane potential (RMP). (E-H) Details of Kir4.1 expression on astrocytes. (E, F) Kir4.1 expression around a small vessel. (G, H) Kir4.1 expression of astrocytic processes. Bars, 250 µm (A, B), 5 µm (E-H)

maturation of breathing behavior is disturbed in mice lacking the Kir4.1 channel subunit. However, this change coincided with decreased body weight and dehydrated appearance, making it unlikely that the change of breathing rate is the only cause of death. Additionally, we were unable to detect a difference in respiratory burst frequency in rhythmic slice preparations containing the pre-Bötzinger complex (not shown). On the other hand, histological changes were detected, which might be related to breathing disturbances. In haematoxilin eosin (HE) stainings the gross architecture of the VRG was affected by the Kir4.1 gene ablation. We observed various degrees of cell loss in the VRG, occurring from the second postnatal week on. (Fig. 2 E-H).

To test for the putative role of the Kir4.1 channel subunit in pH/CO_2-regulated neuronal activity, we tested whether the pH/CO_2-dependent modulation of respiratory activity in the pre-Bötzinger complex is negatively affected by the loss of Kir4.1. In a preliminary set of experiments using the rhythmic medullary slice preparation, we increased the extracellular CO_2 from 5% (plus 95% O_2) to 15% (plus 85% O_2) and measured the response of the network activity. The respiratory burst frequency of both WT and Kir4.1–/– slice was increased to 132 ± 15 % in WT mice (n = 3 slices) and 179 ± 20 % in Kir4.1–/– slice (n = 6), indicating that the loss of Kir4.1 does not diminish chemosensitive properties of respiratory neurons in the PBC. This finding is in line with our immunohistochemical data showing that the Kir4.1 channel subunit is predominantly expressed in non-neuronal cells.

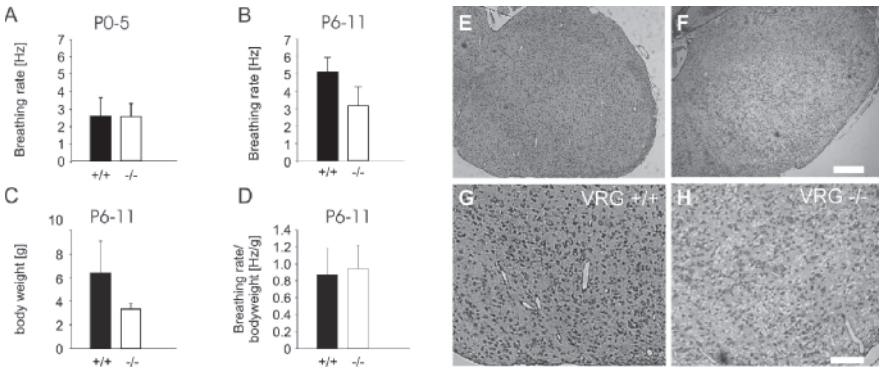

Fig. 2 (A-D) Breathing rate in WT and Kir4.1–/– mice. (E-H) Hematoxylin-eosin staining of brainstem sections. Overview (E, F) and detailed demonstration of the VRG (G, H). Transverse section of the brainstem of a control mouse at P9 (E, G). In Kir4.1–/– mice (F, H) vacuoles are seen (H). Note that the VRG is affected in the Kir4.1–/– mouse. Bars, 250µm (E, F), 100µm (G, H)

4 Discussion

Buffering of extracellular K^+ is one of the basic functions of astrocytes. Its relevance has been demonstrated for a variety of CNS regions. In this study, we show that one candidate for K^+ buffering, the Kir4.1 channel subunit, is up-regulated in the VRG during postnatal maturation coinciding with the developmental stabilization of neuronal respiratory activity. We demonstrate that Kir4.1 channels contribute most of the Kir current in astrocytes, indicating that Kir4.1 is a major molecular substrate for astroglial K^+ uptake (Neusch *et al*. 2006). Although the loss of Kir4.1 dramatically changes electrophysiological properties of astrocytes, the rhythmic activity of pre-Bötzinger complex slices is not significantly altered. This might be because activity-dependent extracellular K^+ increases are additionally controlled by Na^+/K^+ pumps or other K^+ channels (Neusch *et al*. 2006). The immunohistochemical data show that the expression of Kir4.1 in astrocytes allows the redistribution of K^+ from active neurons to blood vessels, as suggested for the siphoning mechanism in the retina. In situations of increased or persistent activity of Na^+/K^+ pumps reversal of K^+ fluxes into the extracellular space might occur via Kir4.1 channels (compare also D'Ambrosio *et al*. 2002).

In Kir4.1–/– mice, additional problems may arise from the fact that Kir4.1 can be also expressed in oligodendrocytes (Neusch et al. 2001). During the first postnatal week of spinal cord development, Kir4.1 also forms a major K+ conductance in oligodendrocytes and a lack of Kir4.1 was detrimental for postnatal myelination (Neusch *et al*. 2001). As is obvious from Fig. 2, similar findings are observed in the brainstem of the Kir4.1–/– mice, providing an additional pathological feature in the mosaic phenotype of the Kir4.1–/– mice. We have no evidence that inactivation of Kir4.1 channel impairs central chemosensitivity in VRG neurons and

therefore we believe that Kir4.1/Kir5.1 heteromeric channels, which exhibit a high pH/CO2-sensitivity at physiological pH-ranges in vitro and which have been postulated as a substrate for central chemosensitivityn (Wu *et al*. 2004), are not the major factors in pH/CO2-regulation of respiratory network activity.

References

Gomeza, J. *et al*. (2003) Inactivation of the glycine transporter 1 gene discloses vital role of glial glycine uptake in glycinergic inhibition. Neuron 40(4), 785–796.

Kofuji, P. and Newman, E.A. (2004) Potassium buffering in the central nervous system. Neuroscience 129(4), 1045–1056.

Smith, J.C. *et al*. (1991) Pre-Botzinger complex: a brainstem region that may generate respiratory rhythm in mammals. Science 254(5032), 726–729.

Richter, D.W. and Spyer, K.M. (2001) Studying rhythmogenesis of breathing: comparison of *in vivo* and *in vitro* models. Trends Neurosci. 24(8), 464–472.

Takumi, T. *et al*. (1995) A novel ATP-dependent inward rectifier potassium channel expressed predominantly in glial cells. J. Biol. Chem. 270(27), 16339–16346.

Bredt, D.S. *et al*. (1995) Cloning and expression of two brain-specific inwardly rectifying potassium channels. Proc. Natl. Acad. Sci. USA 92(15), 6753–6757.

Wu, J. *et al*. (2004) Expression and coexpression of CO_2-sensitive Kir channels in brainstem neurons of rats. J. Membr. Biol. 197(3), 179–191.

Kofuji, P. *et al*. (2000) Genetic inactivation of an inwardly rectifying potassium channel (Kir4.1 subunit) in mice: phenotypic impact in retina. J. Neurosci. 20(15), 5733–5740.

Nolte, C. *et al*. (2001) GFAP promoter-controlled EGFP-expressing transgenic mice: a tool to visualize astrocytes and astrogliosis in living brain tissue. Glia 33(1), 72–86.

Neusch, C. *et al*. (2006) Lack of the Kir4.1 channel subunit abolishes K+ buffering properties of astrocytes in the ventral respiratory group: impact on extracellular K+ regulation. J. Neurophysiol. 95(3), 1843–1852.

Neusch, C. *et al*. (2001) Kir4.1 potassium channel subunit is crucial for oligodendrocyte development and *in vivo* myelination. J. Neurosci. 21(15), 5429–5438.

Grass, D. *et al*. (2004) Diversity of functional astroglial properties in the respiratory network. J. Neurosci. 24(6), 1358–1365.

D'Ambrosio, R., Gordon, D.S. and Winn, H.R. (2002) Differential role of KIR channel and Na(+)/K(+)-pump in the regulation of extracellular K(+) in rat hippocampus. J. Neurophysiol. 87(1), 87–102.

20
Contribution of Pacemaker Neurons to Respiratory Rhythms Generation *in vitro*

Fernando Peña

Abstract Neurons with pacemaker properties have been described in several neural networks. Nonlinearity of their bursting activity might enable them to facilitate onset of excitatory states or to synchronize neuronal ensembles. However, whether such neurons are essential for generating a network activity pattern remains mostly unknown. For the mammalian respiratory network, located in the preBötzinger complex (PBC), two types of pacemaker neurons have been described. Bursting properties of one type of pacemakers rely on the riluzole-sensitive persistent sodium current, whereas bursting mechanisms of a second type are sensitive to Cd^{2+} and flufenamic acid, a calcium-dependent nonspecific cationic current blocker. The role of pacemakers in the generation of respiratory rhythms *in vitro* is state dependent. Under control conditions, the respiratory network generates fictive eupneic activity; this activity depends on both riluzole-sensitive and flufenamic acid-sensitive pacemakers. During hypoxia, fictive eupneic activity is supplanted by the neural correlate of gasping and only riluzole-sensitive pacemaker neurons appear to be necessary for this rhythm. Thus, at least two types of pacemaker bursting mechanisms are present in the PBC and underlie fictive eupnea, whereas only one burst mechanism seems to be critical for gasping generation *in vitro*.

1 Introduction

Rhythmic network activity emerges from the combination of synaptic interactions and intrinsic cellular properties (Peña, Parkis, Tryba and Ramirez 2004; Cunningham, Whittington, Bibbig, Roopun, LeBeau, Vogt, Monyer, Buhl and Traub 2004; Yuste, MacLean, Smith and Lansner 2005; Peña and Ramirez 2005; Peña and García 2006). Regardless of the old dilemma about the relative contribution of intrinsic and synaptic properties to circuit activity, today there is increasing evidence that supports the participation of pacemakers, defined as neurons with the intrinsic ability to generate bursts of action potentials, in the generation of network rhythmic

Departamento de Farmacobiología, Cinvestav, Sede-Sur, jfpena@cinvestav.mx

M.J. Poulin and R.J.A. Wilson (eds.), *Integration in Respiratory Control: From Genes to Systems*.

activity by several networks throughout the brain (Llinas 1988; Stewart and Fox 1990; Leresche, Lightowler, Soltesz, Jassik-Gerschenfeld and Crunelli 1991; Wang 2002; Cunningham *et al*. 2004; Peña *et al*. 2004; Ramirez, Tryba and Peña 2004; Sipilä, Huttu, Soltesz, Voipio and Kaila 2005). As we will review next, pacemaker neurons may be involved in the generation of a vital function such as breathing as well.

2 Pre-Bötzinger Pacemaker Neurons and Respiratory Rhythms Generation

A key role for respiratory rhythm generation has been assigned to a group of neurons in the pre-Bötzinger complex (PBC), which contain a heterogeneous population of respiratory neurons, some of them with pacemaker properties considered important for rhythmogenesis (Smith, Ellenberger, Ballanyi, Richter and Feldman 1991; Reckling and Feldman 1998; Peña *et al*. 2004). When the PBC is isolated in a thick slice preparation (500–700 μM) and recorded in normoxic conditions, it continues to generate the neural correlate of two respiratory rhythms observed *in vivo*: fictive eupneic activity and fictive sighs. If this preparation is challenged with hypoxia, eupnea and sigh rhythms are supplanted by another rhythm called fictive gasping (Lieske, Thoby-Brisson, Telgkamp and Ramirez 2000). It has been proposed that the PBC is a multifunctional neural network, able to produce multiple rhythmic activities by reconfiguration of network properties (Lieske *et al*. 2000). Today the evidence points towards the hypothesis that respiratory rhythm emerges from the coupling of synaptic and intrinsic membrane properties that require (Reckling and Feldman 1998; Peña and Ramirez 2002; 2004; Peña *et al*. 2004; Tryba, Peña and Ramirez 2006), or do not require (Del Negro, Morgado-Valle, Hayes, Mackay, Pace, Crowder and Feldman 2005) pacemaker neurons.

Based on their intrinsic properties and their ability to burst in synaptic isolation, we can distinguish two major types of respiratory neurons: pacemaker and non-pacemaker neurons (Thoby-Brisson and Ramirez 2001; Peña *et al*. 2004). An initial pharmacological characterization showed that there are several types of respiratory pacemakers in the PBC (Thoby-Brisson and Ramirez 2001; Peña *et al*. 2004; Del Negro *et al*. 2005). Despite the fact that all of them are sensitive to tetrodotoxin (TTX) (Thoby-Brisson and Ramirez 2001), two groups were identified based on their sensitivity to the general calcium channel blocker Cd^{2+}. One group of pacemakers failed to continue bursting in presence of Cd^{2+}, whereas another group continued bursting in the same conditions. Then pacemaker neurons were identified as Type II and Type I, respectively (Thoby-Brisson and Ramirez 2001). In general, type I pacemakers produce bursts of shorter duration and smaller amplitude than type II pacemakers (Thoby-Brisson and Ramirez 2001; Peña and Ramirez 2002; 2004; Peña *et al*. 2004). Whereas type I pacemakers are present during all postnatal development, it seems like type II pacemakers are scarce at very early ages (P0-P5) and increase its presence afterwards (Peña *et al*. 2004; Del Negro *et al*., 2005).

Further pharmacological characterization revealed that most type I (or Cd^{2+}-insensitive) pacemakers rely on the activity of a persistent Na^+ current and that bursting activity of most of them might be abolished by the persistent Na^+ current blocker riluzole (Peña *et al*. 2004; Del Negro *et al*. 2005; Tryba *et al*. 2006). It is important to mention that around 25 % of type I (or Cd^{2+}-insensitive) pacemaker neurons were not sensitive to riluzole (Peña *et al*. 2004). On the other hand, type II pacemakers (which are both TTX and Cd^{2+}-sensitive) seem to rely on a Ca^{2+}-activated unspecific cationic current (ICAN) (Peña *et al*. 2004; Del Negro *et al*. 2005; Tryba *et al*. 2006). This is supported by the fact that around 90% of these pacemakers were blocked by the ICAN blocker flufenamic acid (FFA) (Peña *et al*. 2004). Remarkably, none of the type I pacemakers are affected by FFA and none type II pacemakers are affected by riluzole, allowing the use of such channel blockers to diminish the activity of specific populations of respiratory pacemakers without affecting other groups of neurons within the respiratory network (Peña *et al*. 2004; Peña and Aguileta, 2007).

The evidence has shown that in normoxic conditions, riluzole, at the concentration that blocks most of type I pacemakers, affects but does not abolish generation of fictive eupnea (Peña *et al*. 2004). Certainly, riluzole abolishes generation of fictive sighs (Peña *et al*. 2004). A similar effect was observed when FFA was applied at the concentration that blocks most of type II pacemakers (elimination of sighs but maintenance of fictive eupnea generation, Peña *et al*. 2004). However, when both drugs are applied, no rhythmic population activity is recorded in the PBC (Peña *et al*. 2004; Del Negro *et al*. 2005). Taken together, the evidence suggests that eupneic-like activity produced by the PBC *in vitro* can be maintained if one population of pacemakers is blocked either with riluzole or with FFA, but when most type I and type II pacemakers are blocked with both drugs, the PBC is not able to produce any population rhythmic activity whatsoever.

Another seems to be the scenery during gasping generation. As previously mentioned, the PBC undergoes a reconfiguration process during hypoxia to generate gasping (Lieske *et al*. 2000). Reconfiguration includes a differential effect of hypoxia on pacemaker neurons. Type II (or Cd^{2+}-sensitive) pacemakers cease to produce rhythmic bursting activity in hypoxic conditions, whereas a major subset of type I (or Cd^{2+}-insensitive) pacemakers maintain their bursting activity in hypoxia (Thoby-Brisson and Ramirez 2000; Peña *et al*. 2004; Tryba *et al*. 2006). This evidence suggests that type I (or Cd^{2+}-insensitive) pacemakers may play a major role in the generation of gasping in hypoxia (Thoby-Brisson and Ramirez 2000; Peña *et al*. 2004; Tryba *et al*. 2006). Consistent with this idea, we showed that riluzole, but not FFA, specifically blocks gasping generation (Peña *et al*. 2004). Our conclusion that riluzole-sensitive pacemaker activity is necessary for gasping generation, but not eupnea, has been recently corroborated in the *in situ* preparation as well as *in vivo* (Paton, Abdala, Koizumi, Smith and St-John 2006; St. John, Waki, Dutschmann and Paton 2006; Peña and Aguileta, 2007). This leads to some important conclusions: First, type I (or Cd^{2+}-insensitive) pacemakers cannot be considered as the principal drivers of the more complex respiratory network operating during normoxia, but they become the sole drivers of gasping. Second,

hypoxia renders the respiratory network more vulnerable to the blockade of a single ionic mechanism: namely, the persistent Na^+ current (Peña and Ramirez 2002; Tryba *et al*. 2006). Gasping is an important autoresuscitation mechanism that seems to fail in victims of sudden infant death syndrome (SIDS, Poets, Meny, Chobanian and Bonofiglo 1999; Sridhar, Thach, Kelly, Henslee and 2003). Consistent with a change in configuration of the respiratory network, SIDS victims breath normally during normoxia but do not gasp effectively when exposed to hypoxic conditions (Poets *et al*., 1999; Sridhar *et al*. 2003). The journey to understand the basic mechanisms involved in respiratory rhythm generation is at the beginning. This challenge is complicated by the fact that pacemaker neurons in the PBC constitute a highly heterogeneous population. This issue must be taken into account if we want to understand this circuit; it is important never to forget that such diversity is there and might contribute rhythm generation.

Acknowledgement This work was supported by Conacyt-42870, México.

References

Cunningham, M.O., Whittington, M.A., Bibbig, A., Roopun, A., LeBeau, F.E., Vogt, A., Monyer, H., Buhl, E.H. and Traub, R.D. (2004) A role for fast rhythmic bursting neurons in cortical gamma oscillations *in vitro*. Proc. Natl. Acad. Sci. USA 101, 7152–7157.

Del Negro, C.A., Morgado-Valle, C., Hayes, J.A., Mackay, D.D., Pace, R.W., Crowder, E.A. and Feldman J.L. (2005) Sodium and calcium current-mediated pacemaker neurons and respiratory rhythm generation. J. Neurosci. 25, 446–453.

Leresche, N., Lightowler, S., Soltesz, I., Jassik-Gerschenfeld, D. and Crunelli V. Low-frequency oscillatory activities intrinsic to rat and cat thalamocortical cells. J. Physiol. 441, 155–174.

Lieske, S.P., Thoby-Brisson, M., Telgkamp, P. and Ramirez, J.M. (2000) Reconfiguration of the neural network controlling multiple breathing patterns: eupnea, sighs and gasps. Nat. Neurosci. 3, 600–607.

Llinas, R.R. (1988) The intrinsic electrophysiological properties of mammalian neurons: insights into central nervous system function. Science 242, 1654–1664.

Paton, J.F., Abdala, A.P.L., Koizumi, H., Smith, J.C. and St-John, W. (2006) Respiratory rhythm generation during gasping depends on persistent sodium current. Nature Neurosci. 9, 311–313.

Peña, F. and Ramirez, J.M. (2002) Endogenous activation of serotonin-2A receptors is required for respiratory rhythm generation *in vitro*. J. Neurosci. 22, 11055–11064.

Peña, F. and Ramirez, J.M. (2004) Substance P-mediated modulation of pacemaker properties in the mammalian respiratory network. J. Neurosci. 24, 7549–7556.

Peña, F., Parkis, M.A., Tryba, A.K. and Ramirez, J.M. (2004) Differential contribution of pacemaker properties to the generation of respiratory rhythms during normoxia and hypoxia. Neuron 43, 105–117.

Peña, F. and Ramirez, J.M. (2005) Hypoxia-induced changes in neuronal network properties. Mol. Neurobiol. 32, 251–283.

Peña, F. and García, O. (2006) Breathing generation and potential pharmacotherapeutic approaches to central respiratory disorders. Curr. Med. Chem. 13, 2681–2693.

Peña, F. and Aguileta, M.A. (2007) Effects of riluzole and flufenamic acid on eupnea and gasping of neonatal mice *in vivo*. Neurosci. Lett.415, 288–293

Poets, C.F., Meny, R.G., Chobanian, M.R. and Bonofiglo, R.E. (1999) Gasping and other cardiorespiratory patterns during sudden infant deaths. Pediatr. Res. 45, 350–354.

Ramirez, J.M., Tryba, A.K. and Peña, F. (2004) Pacemaker neurons and neuronal networks: an integrative view. Curr. Opin. Neurobiol. 14, 665–674.
Rekling, J.C. and Feldman, J.L. (1998) PreBotzinger complex and pacemaker neurons: hypothesized site and kernel for respiratory rhythm generation. Annu. Rev. Physiol. 60, 385–405.
Sipila, S.T., Huttu, K., Soltesz, I., Voipio, J. and Kaila, K. (2005) Depolarizing GABA acts on intrinsically bursting pyramidal neurons to drive giant depolarizing potentials in the immature hippocampus. J. Neurosci. 25, 5280–5289.
Smith, J.C., Ellenberger, H.H., Ballanyi, K., Richter, D.W. and Feldman, J.L. (1991) Pre-Botzinger complex: a brainstem region that may generate respiratory rhythm in mammals. Science 254, 726–729.
Sridhar, R., Thach, B.T., Kelly, D.H. and Henslee, J.A. (2003) Characterization of successful and failed autoresuscitation in human infants, including those dying of SIDS. Pediatr. Pulmonol. 36, 113–122.
St-John, W.M., Waki, H., Dutschmann, M. and Paton, J.F. (2006) Maintenance of eupnea of in situ and *in vivo* rats following riluzole: A blocker of persistent sodium channels. Respir. Physiol. Neurobiol., in press.
Stewart, M. and Fox, S.E. (1990) Do septal neurons pace the hippocampal theta rhythm? Trends Neurosci. 13, 163–168.
Thoby-Brisson, M. and Ramirez, J.M. (2000) Role of inspiratory pacemaker neurons in mediating the hypoxic response of the respiratory network *in vitro*. J. Neurosci. 20, 5858–5866.
Thoby-Brisson, M. and Ramirez, J.M. (2001) Identification of two types of inspiratory pacemaker neurons in the isolated respiratory neural network of mice. J. Neurophysiol. 86, 104–112.
Tryba, A.K., Peña, F. and Ramirez, J.M. (2006) Gasping activity *in vitro*: a rhythmic behavior dependent on 5HT2A receptors. J. Neurosci. 26, 2623–2634.
Wang, X.J. (2002) Pacemaker neurons for the theta rhythm and their synchronization in the septohippocampal reciprocal loop. J. Neurophysiol. 87, 889–900.
Yuste, R., MacLean, J.N., Smith, J. and Lansner, A. (2005) The cortex as a central pattern generator. Nat. Rev. Neurosci. 6, 477–483.

21
Emergent Bursting in Small Networks of Model Conditional Pacemakers in the pre-Bötzinger Complex

Jonathan E. Rubin

Abstract This paper summarizes some lessons learned from the computational study of bursting oscillations in small networks of model pre-Bötzinger complex (pBC) neurons. Dynamical systems analysis explains the mechanisms through which synaptic coupling enhances the dynamic range of bursting and predicts the existence of multiple forms of busting and tonic spiking solutions. This analysis also demonstrates that intrinsically bursting cells are not required for network bursting and suggests possible roles for cells with different intrinsic behaviors in enhancing the robustness of bursting.

1 Introduction

While a diversity of dynamic behaviors is observed across different isolated pBC cells, excitatory synaptic coupling promotes synchronized bursting oscillations, consisting of alternating *active phases* of repetitive spiking and *silent phases* of recovery without spikes, in pBC slice preparations. Simulations in networks of model pBC cells show that the dynamic range of bursting is further enhanced by heterogeneity (Butera, Rinzel and Smith 1999b). The focus of this work is on the dynamical mechanisms, based on the interaction of intrinsic cellular properties and synaptic dynamics, that explain these observations. The results presented here (see also Butera, Rubin, Terman and Smith 2005) also include a novel classification of bursting and spiking activity patterns that emerge from the study of coupled pairs of model pBC cells. Further, the analysis shows that intrinsically bursting cells are not required for network bursting and characterizes how cells that are intrinsically quiescent or tonically active contribute to bursting in a heterogeneous pBC network.

University of Pittsburgh, Department of Mathematics, rubin@math.pitt.edu

M.J. Poulin and R.J.A. Wilson (eds.), *Integration in Respiratory Control: From Genes to Systems*.

2 Model and Dynamical Systems Analysis

Consider the following model (Model I of Butera, Rinzel, and Smith 1999a):

$$v' = -I_{NaP}-I_{Na}-I_K-I_L-I_{tonic\text{-}e}-I_{syn\text{-}e}-I_{app} \quad (1)$$

$$n'=(n_\infty(v)-n)/\tau_n(v) \quad (2)$$

$$h'=(h_\infty(v)-h)/\tau_h(v), \quad (3)$$

where $I_{Na}=g_{Na}m_\infty(v)(1-n)(v-E_{Na})$, $I_K=g_K n^4(v-E_K)$, $I_{NaP}=g_{Na}m_{\infty P}(v)h(v-E_{Na})$, $I_L=g_L(v-E_L)$, with $x_\infty(v)=(1+\exp((v-\theta_x)/d_x)^{-1}$ and $\tau_x(v)=\tau_x/(\cosh((v-\theta_x)/(2d_x)))$ for $x \in \{h,m,m_p,n\}$. Eqs. 1-3 represent the dynamics of a single pBC cell with a persistent sodium current I_{NaP}. The external input currents in the model consist of an applied stimulus I_{app}, a background excitatory tonic drive $I_{tonic\text{-}e} = g_{tonic\text{-}e}(v-E_{syn})$, and an excitatory synaptic input $I_{syn\text{-}e}=g_{syn\text{-}e}\Sigma s_j(v-E_{syn})$, with summation over the synaptic conductances s_j associated with presynaptic cells. A complete list of model equations and parameters are specified in the papers of Butera et al. (Butera *et al*. 1999a; Butera *et al*. 1999b).

To analyze the above model, note that $\tau_h(v)$ is large, and thus the inactivation *h* of I_{NaP} evolves much slower than the other variables in the model. This observation suggests the utility of a *fast-slow decomposition* (Rinzel 1987). In this approach, for a single cell, the *fast subsystem* is formed from the (*v,n*) equations of the model, with the *slow variable h* taken as a constant parameter. The structure of the important dynamic states of the fast subsystem is mapped out over a range of *h* values; that is, the *bifurcation diagram* of the fast subsystem, with bifurcation parameter *h*, is generated. This process yields the diagrams shown in Fig. 1.

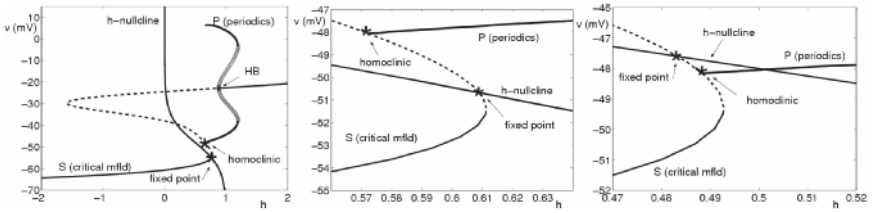

Fig. 1 Bifurcation diagrams from a fast-slow decomposition of Eqs. 1–3 for different values of $g_{tonic\text{-}e}$. Left: Solid curves denote stable features, the dashed curve consists of unstable fixed points, and the broad curve emanating from a Hopf bifurcation (HB) shows the maximum and minimum *v* along an unstable family of periodics. The stable family P of periodics terminates in a homoclinic orbit, with a homoclinic point on an unstable part of the fixed point curve S. Finally, the *h*-nullcline, along which *h'*= 0, is shown, and a stable fixed point for the full system (Eqs. 1–3), corresponding to quiescence, occurs where this nullcline intersects a stable part of S. Left panel used with permission from J. Best *et al*. (2005), SIAM J. Appl. Dyn. Syst. 4, 1107–1139. Middle: A zoomed view for larger $g_{tonic\text{-}e}$ shows that the fixed point has moved to an unstable part of S, yet lies below the homoclinic point. Thus, the full system is predicted to show bursting oscillations. Right: For still larger $g_{tonic\text{-}e}$, the fixed point lies above the homoclinic point. Thus, the full system is predicted to show tonic spiking

Next, the slow dynamics of *h,* as given in Eq. 3, is used to sweep the fast subsystem through the relevant dynamic states, which generates a prediction for the dynamics of the full model (Eqs. 1–3). The Butera model is a *square-wave burster* (Rinzel 1987), with activity onset promoted by the deinactivation of the inward current I_{NaP} and with gradual repolarization via the inactivation of I_{NaP}. Similar bursting can be achieved by other combinations of currents that result in an analogous bifurcation structure.

3 How Synaptic Coupling Promotes Bursting

An isolated pBC cell may be predominantly quiescent, rhythmically active or bursting, or tonically spiking. Increasing $g_{tonic\text{-}e}$ can switch the Butera *et al*. (1999a) model across these states. Interestingly, even though the synaptic coupling between pBC cells is also excitatory, introducing synaptic coupling between two tonically active pBC cells can switch them back to burst mode. More generally, as $g_{syn\text{-}e}$ is raised from zero, the range of $g_{tonic\text{-}e}$ over which pBC cells burst initially expands and then contracts. Moreover, changes in $g_{tonic\text{-}e}$ and $g_{syn\text{-}e}$ induce complex variations in burst characteristics (Butera *et al*. 1999b).

The key to these results is the observation that both $g_{tonic\text{-}e}$ and $g_{syn\text{-}e}$ affect the bifurcation structure of the pBC cell's fast subsystem (Best *et al*. 2005). Consideration of a single self-coupled cell gives a first approximation to the effect of $g_{syn\text{-}e}$. Note from Fig. 1 that the fast-slow decomposition predicts a transition from bursting to tonic spiking when the fixed point of the full system intersects the homoclinic point of the fast subsystem. Increasing $g_{tonic\text{-}e}$ promotes spiking by moving the fixed point to smaller *h* values, such that it may overtake the homoclinic point (Fig. 2). Increasing $g_{syn\text{-}e}$, however, pushes the homoclinic point to smaller *h* values, such that a larger $g_{tonic\text{-}e}$ is needed to attain the bursting-to-spiking transition (Fig. 2; Best *et al*. 2005).

These findings can also be cast in terms of I_{NaP}. Specifically, an elevated $g_{tonic\text{-}e}$ allows the cell to spike with lower I_{NaP} availability and to reach lower voltages on each spike, such that the deinactivation of I_{NaP} on each spike downstroke can balance out its inactivation on each spike upstroke, promoting tonic spiking. Excitatory synaptic coupling also allows for spiking with lower I_{NaP}. However, the synaptic input curtails the downstroke of each spike, such that a net inactivation of I_{NaP} still occurs on each spike and eventually spiking terminates.

An additional broadening of the burst region as $g_{syn\text{-}e}$ increases results from the fact that synaptic coupling induces spike asynchrony within the synchronized active phases of bursting pairs of coupled pBC cells. Spike asynchrony implies that while both cells are in the active phase, a cell receives strongest synaptic input during the downstroke of its spike. This input mitigates the downstroke, which prevents deinactivation of I_{NaP}, such that the cell is prevented from becoming tonically active.

A full analysis of the coupled cell pair requires treatment of a system of two slow variables and is given elsewhere (Best *et al*. 2005; see also Butera *et al*. 2005).

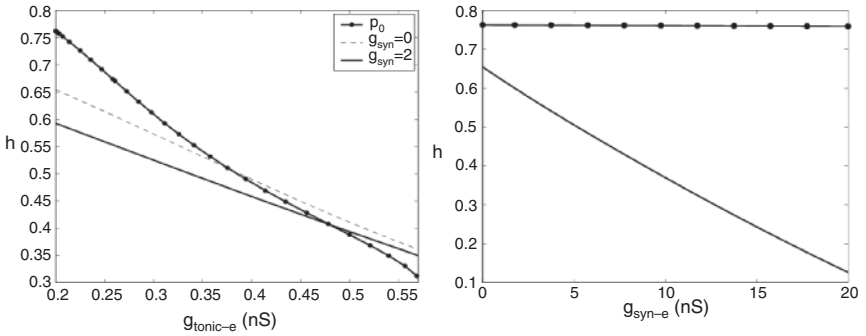

Fig. 2 The parameters $g_{tonic\text{-}e}$, $g_{syn\text{-}e}$ have different effects on the fast subsystem bifurcation structure. Left: As $g_{tonic\text{-}e}$ increases, both the curve of fixed points (p_0; solid dotted curve) and the curve of homoclinic points (solid or dashed) move to smaller *h*, but the fixed points overtake the homoclinic points. Left panel used with permission from J. Best *et al.* (2005), SIAM J. Appl. Dyn. Syst. 4, 1107–1139. Right: As $g_{syn\text{-}e}$ increases, only the homoclinic points (solid) move to smaller *h*, while the fixed points (solid dotted) remain unchanged

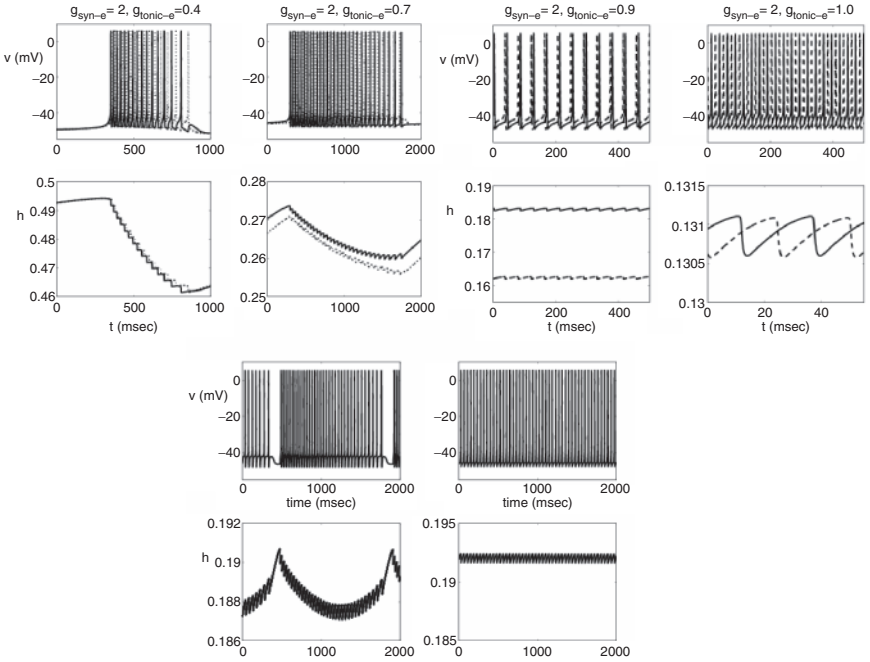

Fig. 3 Different solutions arising for a pair of synaptically coupled model pBC cells, each governed by Eqs. 1–3. For each solution, the top panel shows *v* versus time for both cells, while the bottom shows *h* versus time for both cells. Top row, from left to right: symmetric bursting, asymmetric bursting, asymmetric spiking, symmetric spiking (all in a pair of identical cells). Bottom row: bursting and tonic spiking. The botom two columns were generated with the same parameter values but different initial conditions, using a non-identical pair of cells (one cell shown)

One outcome of this analysis was the discovery of four different modes of activity in the coupled pBC network, namely two types of bursting (symmetric and asymmetric) and two types of spiking (symmetric and asymmetric), with corresponding differences in burst characteristics. Examples of each pattern are shown in Fig. 3. The nomenclature refers to the behavior of the slow variables h_1,h_2; in the symmetric case, h_1 and h_2 follow identical but phase-shifted time courses in the active phase, as seen in Fig. 3. The dynamical systems analysis also explains why different burst characteristics are associated with symmetric versus asymmetric bursts. The bottom line from this analysis is that the presence of synaptic coupling in networks of pBC cells can introduce a subtle variation in the availability of I_{NaP} across cells, even when the parameter values used for the cells are identical.

4 Synaptic Coupling in a Heterogeneous Network

With mild heterogeneity between the cells, the qualitative finding that different types of bursting and spiking solutions exist at different points in ($g_{tonic\text{-}e}$, $g_{syn\text{-}e}$) parameter space persists. One interesting new result is the existence of a parameter regime for which there is bistability between a bursting and a tonic spiking solution, with initial conditions picking which is observed (Fig. 3).

If enough heterogeneity is introduced, the cells may behave qualitatively differently from each other in the absence of coupling. What activity patterns emerge when such cells are synaptically coupled? The discussion in Section 3 shows that synaptic coupling does not necessarily yield a network behavior that averages the cells' intrinsic behaviors. In recent work, I derived sufficient conditions for network bursting to arise when a quiescent (Q) and a tonically active (T) pBC cell are coupled with synaptic excitation (Rubin 2006). First, the input from the T cell to the Q cell must be strong enough to recruit the Q cell into the active phase yet not strong enough to prevent the Q cell from exiting the active phase after a period of spiking. How strong an input is required depends on the rate of deinactivation of I_{NaP} for the Q cell (see below). Second, the synaptic input from the Q cell to the T cell will inactivate the I_{NaP} of the T cell, relative to its resting level in the absence of coupling. The most subtle point in the analysis is that *bursting requires the resulting additional inactivation to be sufficient such that, once the Q cell enters the silent phase and the synaptic input to the T cell wears off, the T cell cannot continue spiking and therefore falls silent as well*. This outcome requires a sufficiently rapid decay of synaptic input, in addition to sufficient inactivation of I_{NaP}. Finally, note that the T cell will eventually return to the active phase and re-excite the Q cell. The duration of the T cell silent phase sets the time available for the deinactivation of the Q cell's I_{NaP} before synaptic input arrives and therefore determines, for a given strength of synaptic coupling, how fast a deinactivation is required for the Q cell to be activated again, maintaining the bursting oscillation.

This analysis (Rubin 2006) shows why intrinsically bursting cells are not needed for bursting in a heterogeneous network of synaptically coupled pBC cells. Like the

other results discussed here, this finding carries over qualitatively to other models of the same burst class. Clearly, the biological relevance of this work will be enhanced by its extension to larger networks of cells, which is in progress (see also Rubin and Terman 2002). However, the results of this analysis already suggest some principles that likely apply to synchronized bursting in a heterogeneous pBC population. In particular, intrinsically tonic cells within the network will enhance the robustness of bursting by preventing the network from falling completely silent, as long as these cells can induce a sufficiently strong synaptic excitation to recruit the other cells in the network. At the same time, robust bursting will require the presence of sufficiently many non-tonic cells such that when these cells enter the silent phase, the resulting withdrawal of excitation from the tonic cells will cause them to fall silent as well. Of course, the emergent activity patterns within a larger pBC network will depend on its synaptic connectivity architecture, which remains for future experimental elucidation. In the meantime, computational simulations and mathematical analysis represent powerful tools for exploring activity under a variety of network architectures and intrinsic activity pattern distributions.

Acknowledgements This work was partially supported by the National Science Foundation Grant No. DMS-0414023. I thank J. Best, A. Borisyuk, E. Manica, D. Terman and M. Wechselberger for collaborating on some of the results discussed here, as well as Jeff Smith and Christopher Del Negro for stimulating discussions.

References

Best, J., Borisyuk, A., Rubin, J., Terman, D. and Wechselberger, M. (2005) The dynamic range of bursting in a model respiratory pacemaker network. SIAM J. Appl. Dyn. Syst. 4, 1107–1139.

Butera, R.J., Rinzel, J. and Smith, J.C. (1999a) Models of respiratory rhythm generation in the pre-Bötzinger complex: I. Bursting pacemaker neurons. J. Neurophysiol. 81, 382–397.

Butera, R.J., Rinzel, J. and Smith, J.C. (1999b) Models of respiratory rhythm generation in the pre-Bötzinger complex: II. Populations of coupled pacemakers. J. Neurophysiol. 81, 398–415.

Butera, R., Rubin, J., Terman, D. and Smith, J. (2005) Oscillatory bursting mechanisms in respiratory pacemaker neurons and networks. In: S. Coombes and P.C. Bressloff (Eds.), *Bursting: The Genesis of Rhythm in the Nervous System*. World Scientific, Singapore, pp. 303–346.

Rinzel, J. (1987) A formal classification of bursting mechanisms in excitable systems. In: A.M. Gleason (Ed.), *Proceedings of the International Congress of Mathematics*. AMS, Providence, pp. 1578–1593.

Rubin, J. and Terman, D. (2002) Synchronized bursts and loss of synchrony among heterogeneous conditional oscillators. SIAM J. Appl. Dyn. Syst. 1, 146–174.

Rubin, J. (2006) Bursting induced by excitatory synaptic coupling in nonidentical conditional relaxation oscillators or square-wave bursters. Phys. Rev. E 74, 021917.

Part IV
Genes and Development

22
Brain Nuclei Controlling the Spinal Respiratory Motoneurons in the Newborn Mouse

Michelle Bévengut[1], Patrice Coulon[2] and Gérard Hilaire[3]

Abstract A retrograde and transneuronal infection with rabies virus was performed in mouse neonates to locate the central nervous structures involved in the motor command of the spinal respiratory motoneurons and to discriminate the location and hierarchical organization of the neurons in and between these infected central nervous structures.

1 Introduction

Breathing is a rhythmic motor behavior which rhythm and motor patterns are highly adaptable to meet short- and long-term physiological changes throughout life. In rodents, breathing rhythm and pattern are generated by a neuronal network located within the brainstem in the form of a bilateral pair of ventrolateral respiratory columns (VRC) (Rekling and Feldman 1998; Ballanyi, Onimaru and Homma 1999; Hilaire and Duron 1999; Feldman, Mitchell, and Nattie 2003). The VRC comprises rostro-caudally a succession of functionally distinct although anatomically overlapping areas (Alheid, Gray, Jiang, Feldman, and McCrimmon 2002) of which two are implicated in rhythm generation, the preBötzinger complex (Smith, Ellenberger, Ballanyi, Richter, and Feldman 1991) and the paraFacial Respiratory Group (Onimaru and Homma 2003) as, respectively, inspiratory and expiratory generators (Feldman and Del Negro 2006). In addition, other discrete brain nuclei implicated in neuromodulation and sensory integration which regulate breathing (Dutschmann, Mörschel, Kron, and Herbert 2004; Hilaire, Viemari, Coulon, Simonneau, and Bévengut 2004; Song and Poon 2004) belong to the respiratory network.

Today, information about the network building blocks and the neuron connectivity in and between building blocks can be obtained using the retrograde transneuronal

[1] CNRS-Groupe d'Étude des Réseaux Moteurs, bevengut@marseille.inserm.fr

[2] pcoulon@marseille.inserm.fr

[3] hilaire@marseille.inserm.fr

M.J. Poulin and R.J.A. Wilson (eds.), *Integration in Respiratory Control: From Genes to Systems*.

transfer and self-replication properties of neurotropic viruses such as pseudorabies (PRV; Card 2001) and rabies viruses (RAB; Ugolini 1995; Kelly and Strick 2000). Respiratory network tracing with PRV have been done in adult rats (Dobbins and Feldman 1994) and ferrets (Yates, Smail, Stocker and Card 1999).

Using RAB, a neuroanatomical study was performed in mouse neonates (C3H/HeJ strain) to locate the central nervous structures involved in the motor command of the spinal respiratory motoneurons and to discriminate the hierarchical organization of the neurons in and between these structures.

2 Methods

Unilateral injections (1 µl containing 2.5×10^7 plaque forming units) of the Challenge Virus Standard fixed strain of RAB were made into either the diaphragm and the intercostal muscles (referred as diaphragm injections) or the intercostal muscles alone of cold-anesthetized (3 min at −80°C) one-day-old mouse neonates.

The animals were anesthetized and sacrificed every 6 hours starting at 24 hr post-injection (hpi). Immunohistochemical detection was performed using a monoclonal antibody raised against the phosphoprotein constitutive of the viral nucleocapsid on 70 µm-thick serial sections of paraformaldehyde-fixed brains and spinal cords. In some animals, double immunostaining of RAB-infected and serotonergic- or catecholaminergic-positive neurons have also been performed.

3 Results

After either diaphragm or intercostal injections, the RAB infection progressed within the CNS as survival time increased. The timing and pattern of infected nervous structures were similar for both types of RAB injections and reproducible for each survival time, although the number of infected neurons in each structure was variable.

Spinal respiratory motoneurons within the ventral horn of the spinal cord were the first and only infected neurons between 24–30 hr post-injection (hpi; Fig. 1A). Within the central nervous system, premotoneurons (first-order interneurons) were infected between 32–36 hpi, whereas second-, third- and fourth-order interneurons were seen at 42, 48, and 54 hpi, respectively.

3.1 Infected Interneurons in the Spinal Cord and Brainstem

First-order interneurons (*i.e.*, premotoneurons), which directly control the spinal respiratory motoneurons, were infected at 36 hpi within the spinal cord and the brainstem. The spinal premotoneurons were bilaterally localized within the ventro-medial

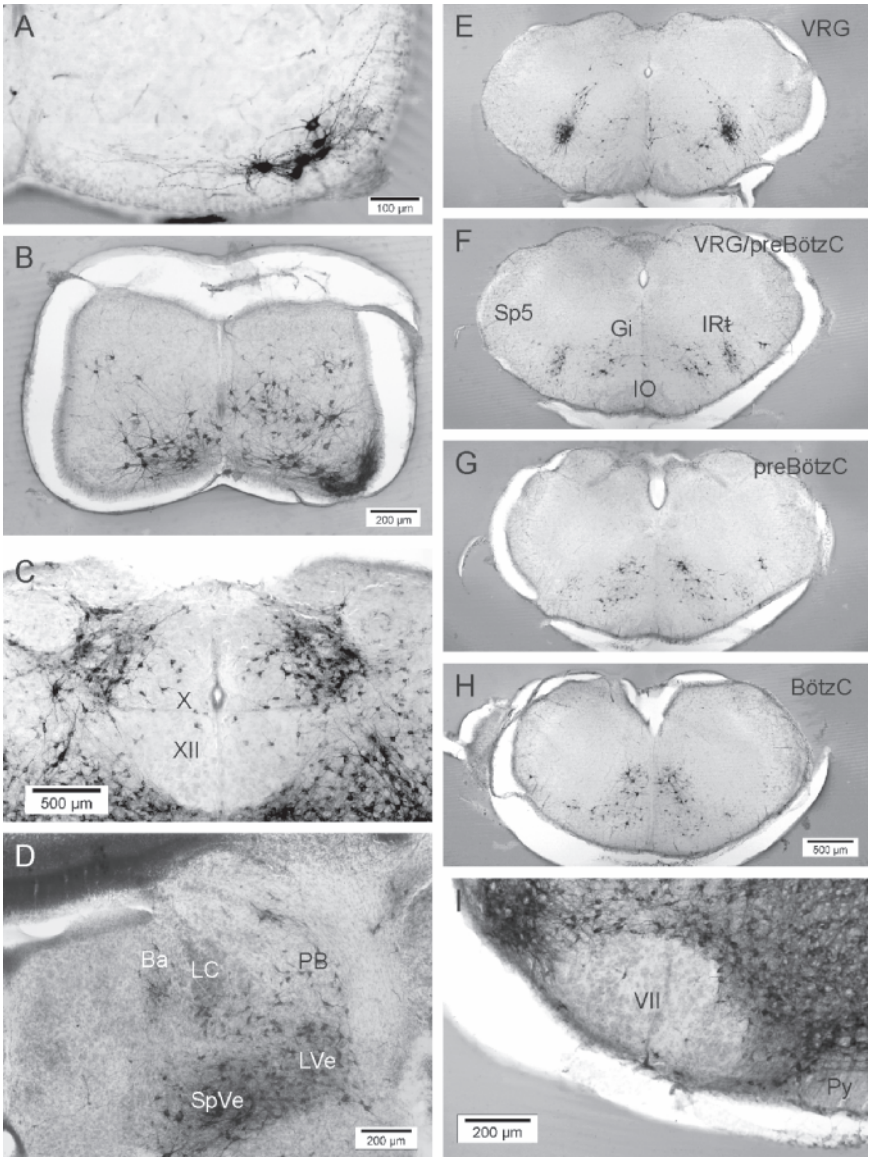

Fig. 1 Rabies-infected neurons in the mouse neonate. In the spinal cord, phrenic motoneurons are infected at 24 hpi (A) and at 42 hpi along with interneurons (B). At 42 hpi, VRC neurons are infected in IRt (VRG, preBötzC, BötzC) in the medulla (from caudal to rostral, E to H). At 48 hpi, neurons are infected in nTS (C), in the caudal pons in Ba, LC, PB, and Ve nuclei (D), and under the facial nucleus (I). The injection side is on the right of the figures

gray matter in laminae VIII. The brainstem premotoneurons were found (1) within the medulla bilaterally in the intermediate reticular (IRt) nucleus (ventral respiratory group, VRG, and Bötzinger complex, BötzC), in the medial reticular (Gi) nucleus with an ipsilateral predominance, and ipsilaterally in the raphe obscurus (RO) and (2) within the pons, ispilaterally in both medial reticular (PnC) and vestibular (lateral, LVe, and spinal, SpVe) nuclei.

Second-order interneurons were bilaterally labeled at 42 hpi in the spinal cord (Fig. 1B), and in the brainstem (Fig. 1E-H) in IRt (VRG, BötzC, and pre-Bötzinger complex, preBötzC), medial (Gi, GiV, GiA, PnC, and PnO), and lateral reticular (PCRt and MLRt, with an ispi- and contralateral predominance respectively) nuclei, caudal raphe nuclei (RO and raphe pallidus, RPa), vestibular nuclei (LVe, SpVe, SuVe, and caudal MVe), and subcoeruleus (SubC), and ipsilaterally, in the nucleus of the tractus solitarius (nTS) and para-Olivary nucleus (PO).

Third-order interneurons were bilaterally infected at 48 hpi in the nTS (Fig. 1C), PO and parapyramidal (PPy), A5, trigeminal and peri-trigeminal areas, raphe magnus (RMg), dorsal raphe nuclei, locus coeruleus (LC), Barrington (Ba), some para-brachial nuclei (PB; Fig. 1D), and in most of the 42 hpi infected nuclei. Under the facial nuclei in the medullary ventral surface, some scattered and small neurons were infected, which may belong to the paraFacial Respiratory Group (pFRG; Fig.1I).

At 54 hpi, new-infected neurons appeared in the already labeled PB subnuclei and scattered ones in an area, which may be part of the rostral Kölliker-Füse (KF).

3.2 Infected Interneurons in the Midbrain and Forebrain

Within the midbrain, only the contralateral ventrolateral red nucleus (RN) was infected at 42 hpi. At 48 hpi, bilaterally-infected neurons were present in the RN, ventrolateral tegmental area, lateral lemniscus, deep mesencephalic nuclei, and peria-queductal gray areas; the first forebrain neurons were infected in zona incerta. At 54 hpi, in midbrain-infected nuclei the number of labeled neurons increased, and neurons were infected in thalamic (prerubral and anterior pretectal areas, parafascicular nucleus, zona incerta, and the fields of Forel), hypothalamic (dorsomedial, lateral, posterior, and paraventricular areas), and amygdaloid nuclei as well as in somatosensory and motor cortices.

4 Conclusions

This study shows that the ventral respiratory column in the brainstem of the mouse neonate comprises the nuclei usually described in adult rats (Dobbins and Feldman 1994; Alheid *et al*. 2002) although few infected neurons were found in an area which may be the pFRG. Outside the VRC, premotoneurons are located in Gi, RO,

and vestibular nuclei (Yates, Billig, Cotter, Mori and Card 2002). This study does not argue, as in adult animals, for a direct control of the respiratory spinal motoneurons by the nTS, and of both the respiratory spinal motoneurons and bulbospinal interneurons by the PB/KF. Thus in mouse neonates, these two structures may be sensory integrative relays to respiratory propriobulbar interneurons (Herbert, Moga, and Saper 1990; Dutschmann *et al*. 2004).

Within the ventral medullary surface, the putative chemosensitive neurons were infected for different hpi, thus suggesting that the infected ipsilateral PO neurons project to premotoneurons, whereas the infected ones in the PPy and contralateral PO project to propriobulbar interneurons.

This study also shows that serotonergic (in caudal and pontine raphé), catecholaminergic (in SubC, A5, and LC; Hilaire and Duron 1999; Hilaire *et al*. 2004), trigeminal, and some suprapontine neurons can already regulate breathing at birth.

References

Alheid, G.F., Gray, P.A., Jiang, M.C., Feldman, J.L. and McCrimmon, D.R. (2002) Parvalbumin in respiratory neurons of the ventrolateral medulla of the adult rat. J. Neurocytol. 31, 693–717.

Ballanyi, K., Onimaru, H. and Homma, I. (1999) Respiratory network function in the isolated brainstem-spinal cord of newbon rats. Prog. Neurobiol. 59, 583–634.

Card, J.-P. (2001) Pseudorabies virus neuroinvasiveness: a window into the functional organization of the brain. Adv. Virus Res. 56, 39–71.

Dobbins, E.G. and Feldman, J.L. (1994) Brainstem network controlling descending drive to phrenic motoneurons in rat. J. Comp. Neurol. 347, 64–86.

Dutschmann, M., Mörschel, M., Kron, M. and Herbert, H. (2004) Development of adaptative behaviour of the respiratory network: implications for the pontine Kölliker-Fuse nucleus. Resp. Physiol. Neurobiol. 143, 155–165.

Feldman, J.L. and Del Negro, C.A. (2006) Looking for inspiration: new perspectives on respiratory rhythm. Nature Rev. Neurosci. 7, 232–242.

Feldman, J.L., Mitchell, G.S. and Nattie, E.E. (2003) Breathing: rhythmicity, plasticity, chemosensitivity. Ann. Rev. Neurosci. 26, 239–266.

Herbert, H., Moga, M. M. and Saper, C. B. (1990) Connections of the parabrachial nucleus with the nucleus of the solitary tract and the medullary reticular formation in the rat. J. Comp. Neurol. 293, 540–580.

Hilaire, G. and Duron, B. (1999) Maturation of the respiratory system. Physiol. Rev. 79, 325–360.

Hilaire, G., Viemari, J.-C., Coulon, P., Simonneau, M. and Bévengut, M. (2004) Modulation of the respiratory rhythm generator by the pontine noradrenergic A5 and A6 groups in rodents. Resp. Physiol. Neurobiol. 143, 187–197.

Kelly, R.B. and Strick, P.L. (2000) Rabies as a transneuronal tracer of circuits in the central nervous system. J. Neurosci. Meth. 103, 63–71.

Omimaru, H. and Homma, I. (2003) A novel functional neuron group for respiratory rhythm generation in the ventral medulla. J. Neurosci. 23, 1478–1486.

Rekling, J.C. and Feldman, J.L. (1998) PreBötzinger complex and pacemaker neurons: hypothesized site and kernel for respiratory rhythm generation. Ann. Rev. Physiol. 60, 385–405.

Smith, J.C., Ellenberger, H.H., Ballanyi, K., Richter, D.W. and Feldman, J.L. (1991) Pre-Botzinger complex: a brainstem region that may generate respiratory rhythm in mammals. Science 254, 726–729.

Song, G. and Poon, C.-S. (2004) Functional and structural models of pontine modulation of mechanoreceptor and chemoreceptor reflexes. Resp. Physiol. Neurobiol. 143, 280–292.

Ugolini, G. (1995) Specificity of rabies virus as a transneuronal tracer of motor networks: transfer from hypoglossal motoneurons to connected second-order and higher order central nervous system cell groups. J. Comp. Neurol. 356, 457–480.

Yates, B.J., Billig, I., Cotter, L.A., Mori, R.L. and Card, J.-P. (2002) Role of the vestibular system in regulating respiratory muscle activity during movement. Clin. Exp. Pharmacol. Physiol. 29, 112–117.

Yates, B.J, Smail, J.A., Stocker, S.D. and Card, J.-P. (1999) Transneuronal tracing of neural pathways controlling activity of diaphragm motoneurons in the ferret. Neurosci. 4, 1501–1513.

23
Superoxide Dismutase-1 Influences the Timing and Post-hypoxic Stability of Neonatal Breathing

Kevin J. Cummings[1], Dan Kalf[1], Sherry Moore[1], B. Joan Miller[2], Frank R. Jirik[2] and Richard J.A. Wilson[1]

Abstract Reactive oxygen species (ROS) likely play a role in the hypoxic ventilatory response. We determined whether hypoxic responses were influenced by alterations in cellular redox status induced by reductions in superoxide dismutase-1 (SOD-1) activity, a cytosolic anti-oxidant enzyme. Using whole-body, continuous-flow plethysmography, we compared ventilatory responses to moderate hypoxia (10% inspired O_2) of *Sod1*$^{+/+}$, $^{+/-}$ and $^{-/-}$ postnatal day 4 (P4) littermates. *Sod1*$^{+/-}$ neonates exhibited a consistently lower breathing frequency than their wild-type littermates, regardless of inspired O_2 level. While SOD-1 deficiency had no effect on the magnitude of the ventilatory response during hypoxia, it did compromise stability of breathing in the post-hypoxic period. Our results suggest SOD-1 stimulates ventilation and helps stabilize breathing after a hypoxic perturbation.

1 Introduction

The hypoxic ventilatory response, originates within carotid body glomus cells. While hypoxic activation of glomus cells involves K^+ channel closure, Ca^{2+} mobilization and neurotransmitter release, the molecules involved in the initial sensing of hypoxia are unresolved. Candidate molecules include proteins associated with (a) membrane-bound K^+ channels (*e.g*., haemoxygenase-2), (b) Ca^{2+} release from intracellular stores (*e.g.,* AMP-kinase) and/or (c) production of reactive oxygen species (ROS) (Kemp 2006). Proteins associated with production of mitochondrial-derived ROS are particularly compelling candidates: ROS are proportional to available oxygen and mitochondrial ROS links O_2-sensing with hypoxia-dependent metabolic changes. The role of ROS in hypoxia sensing remains controversial. Mice lacking NADPH oxidase, an enzyme that produces superoxide anion (O_2-) in proportion to available O_2, demonstrate normal whole-animal and glomus cell responses to hypoxia (Roy *et al*. 2000). However, reduction in NADPH oxidase activity leads to enhanced

[1]Department of Physiology and Biophysics, Hotchkiss Brain Institute, University of Calgary, Calgary, Alberta, Canada T2N 4N1, wilsonr@ucalgary.ca

[2]Department of Biochemistry and Molecular Biology, Hotchkiss Brain Institute, University of Calgary, Calgary, Alberta, Canada T2N 4N1, wilsonr@ucalgary.ca

M.J. Poulin and R.J.A. Wilson (eds.), *Integration in Respiratory Control: From Genes to Systems*.

K^+ channel activity in glomus cells, membrane repolarization and reduced carotid sinus activity (He *et al*. 2005).

Superoxide dismutase-1 is a copper/zinc dependent cytosolic enzyme responsible for the conversion of superoxide anion into hydrogen peroxide (H_2O_2) and O_2. SOD-1 is critical for maintaining the redox status of cells: mice deficient in SOD-1, although normal during development, display cytoplasmic oxidative damage in adulthood (Elchuri *et al*. 2005).

Here, we addressed the possibility that SOD-1 has a role in whole-animal ventilatory responses to moderate hypoxia. Our results suggest that the neonatal response to hypoxia is not dependent on SOD-1 activity *per se*; however, *Sod1* gene deficiency appears to lead to hypoxia-related disruptions in ventilatory stability.

2 Methods

Respiration was assessed in non-anaesthetized *Sod1*$^{+/+}$, $^{+/-}$ and $^{-/-}$ P4 littermate pups (on a C57BL/6 background) using continuous-flow, unrestrained, whole-body plethysmography. The *Sod1* knockout strain was kindly provided by R.W. Scott (Cephalon Inc.). The plethysmography was modified from that described in a previous study (Cummings *et al*. 2004), such that the inlet and outlet gas was regulated using computer-controlled mass-flow controllers programmed to clamp chamber pressure at exactly 1 atm. A thermocouple and heat lamp were used to hold the ambient temperature in the chamber within the thermoneutral range (33 ± 0.5 °C). Pups were subjected to the following protocol: 15 min calm-down, 5 min baseline (room air), 5 min hypoxia (10% O_2–90% N_2), and 15 min washout (room air) period. Data from minutes 3–5 of baseline, minutes 2–3 and 4–5 of treatment and minutes 2–3 and 14–15 of washout were analyzed offline using semi-automated analysis software (written by RJAW). Breathing parameters studied were rate (breaths min-1), inspiratory time (T_I), expiratory time (T_E) and standard deviation of the period (period variability, *SDP*). We integrated the area under the inspiratory pressure curve to obtain an index of V_T (iV_T), as described previously (Cummings *et al*. 2004). An index of minute ventilation, iV_E, was calculated (rate × iV_T). Experiments and analysis of breathing were completed before genotyping, ensuring both were performed blind. A two-factor, repeated-measures ANOVA was used to assess the effects of genotype, treatment (hypoxia) and the interaction between genotype and treatment on breathing parameters.

3 Results

Hypoxic ventilatory responses from Sod1+/+ (n = 24), +/– (n = 30), and –/– (n = 4) neonatal mice are summarized in Fig. 1.

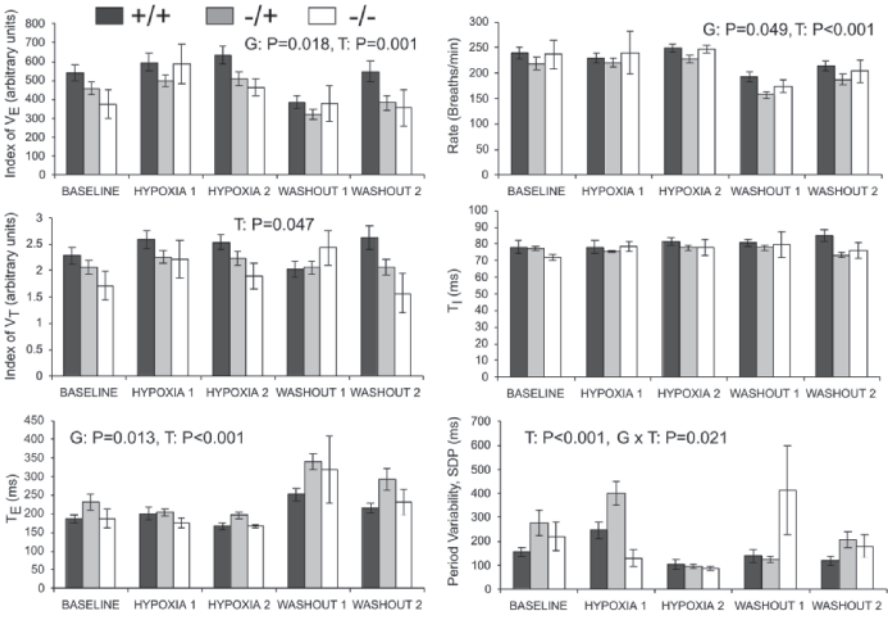

Fig. 1 Effect of hypoxia (10% O_2) and *Sod1* genotype on neonatal breathing. G: genotype; T: treatment; G × T: genotype-treatment interaction

3.1 Effect of Treatment on Ventilation Across Genotypes

Overall, iV_E differed significantly during the course of the protocol (overall treatment effect on iV_E: $p = 0.001$), mainly owing to changes in rate (overall treatment effect on rate: $p < 0.001$). During hypoxia, iV_T increased (Tukey *post hoc*, *TPH*, comparing iV_T during room air with 2nd and 3rd min of hypoxia: $p = 0.024$); however, iV_E during hypoxia was not significantly different than that during room air (TPH comparing iV_E during baseline with 2nd and 3rd min of hypoxia, $p = 0.089$; TPH comparing baseline with 4th and 5th min of hypoxia, $p = 0.269$). Despite the minimal increase in iV_E with hypoxia, a significant hypopnea occurred upon returning to normoxia (*TPH* comparing iV_E in last 2 min of hypoxia with min 4–5 of washout: $p < 0.001$). This effect appears to be due entirely to a post-hypoxic increase in T_E and subsequent reduction in rate (TPH comparing rate in last 2 min of hypoxia with min 4–5 of washout: $p < 0.001$). Breathing variability differed significantly over the course of the protocol (overall treatment effect on SDP: $p < 0.001$); compared to baseline, variability generally decreased towards the end of hypoxic exposure. Taken together, these results indicate that ventilation in these animals is only modestly influenced by hypoxia, with slightly increased frequency and decreased variability.

3.2 *Effect of Sod1 Genotype on Ventilation*

Genotype had a significant effect on iV_E over the course of the protocol, being lower in *Sod1*$^{+/-}$ animals compared to wild-type littermates, regardless of whether animals were subjected to normoxia or hypoxia (overall genotype effect: $p = 0.018$; TPH comparing *Sod1*$^{+/+}$ with $^{+/-}$ genotypes: $p = 0.016$). The effect of genotype on iV_E was mediated by a reduction in rate resulting from an increase in expiratory time (overall genotype effect on rate: $p = 0.049$; TPH comparing *Sod1*$^{+/+}$ and $^{+/-}$ rates: $p = 0.042$; overall effect of genotype on T_E: $p = 0.013$). Genotypic differences in iV_T were less apparent (TPH comparing *Sod1*$^{+/+}$ and $^{+/-}$: $p = 0.01$; overall genotype effect on iV_T: $p = 0.118$). There was a genotype-specific effect on variability after returning to normoxia from hypoxia: *Sod1*$^{+/-}$ animals had increased variability compared to wild-type littermates (overall interaction between genotype and treatment on SDP: $p = 0.021$; TPH comparing SDP during 4th and 5th min of hypoxia with end of washout: *Sod1*$^{+/+}$ $p = 0.664$; *Sod1*$^{+/-}$ $p < 0.001$). The genotypic effect on breathing variability was dependent on previous exposure to hypoxia as evidenced by the fact that genotypes had similar variability during the baseline period (TPH comparing *Sod1*$^{+/+}$ with *Sod1*$^{+/-}$ during baseline breathing: $p = 0.122$). Thus, SOD-1 deficiency appears to mainly influence respiratory timing and post-hypoxic ventilatory stability.

4 Discussion

Sod1$^{+/-}$ neonates appeared to have compromised ventilation throughout the protocol, an effect attributable to a reduced frequency and increased expiratory time. In addition, the transition from hypoxia to normoxia appears to have a more pronounced effect on the variability of breathing in *Sod1*$^{+/-}$ neonates compared to wild-type littermates. These results suggest that SOD-1 might be an important regulator of breathing, presumably by reducing the concentration of intracellular ROS.

4.1 *Effects of Hypoxia on Neonatal Ventilation*

In the current study, wild type neonatal mice had a negligible ventilatory response to hypoxia despite a robust post-hypoxic frequency decline mediated by an increased T_E. A negligible ventilatory response to hypoxia has been observed by others (Bissonnette and Knopp 2001), but contrasts the findings of our previous study that used a similar technique to measure the hypoxic response of a mixed SvJ-Bl/6 line of neonatal mice (Cummings *et al*. 2004). Our data thus corroborate previous reports, that the magnitude of the ventilatory response to hypoxia in the neonate appears to be heavily influenced by strain (Tankersley *et al*. 1994).

4.2 Role of SOD-1 in the Control of Breathing

The most straightforward explanation of our results is that the increase in ROS occurring with SOD-1 deficiency might lead to an increased capacity for glomus cell repolarization, as has been previously described (He *et al*. 2000). This would likely result in reduction in CSN activity, a reduced level of tonic inputs into the respiratory controller and hypoventilation. We cannot exclude an alternate possibility that SOD-1 reduces ventilation indirectly through metabolism as neither O_2 consumption nor CO_2 production was measured. However, we note complete SOD-1 deficiency does not appear to affect growth or overall development (Elchuri *et al*. 2005). Despite having a significant reduction in baseline ventilation, 24 partial SOD-1 deficient mice had a mean hypoxic ventilatory response not significantly different from 30 of their wild type-littermates. In our data set of 58 animals, only four were found to have a complete SOD-1 deficiency when we un-blinded. Therefore, we cannot completely rule out the possibility that the neonatal hypoxic ventilatory response is dependent on at least partial SOD-1 activity. If ROS contribute to the hypoxic ventilatory response, our results suggest other anti-oxidant systems must compensate when SOD-1 activity is reduced. Proteins that might contribute to this redundancy include mitochondrial superoxide dismutase-2 (SOD-2), NADPH-oxidase or glutathione reductase.

Despite a lack of an effect of SOD-1 deficiency on ventilation during hypoxia, the enzyme appears to be important for the maintenance of breathing stability in the post-hypoxic period. In regard to possible sites of SOD-1's action, it is interesting to note that breath-to-breath variability has been shown to be greatly influenced by carotid body inputs (Brown *et al*. 1993). During re-oxygenation, abnormal fluxes of ROS within SOD-1 deficient glomus cells might act to inhibit and/or destabilize respiration. Alternatively, higher breathing variability with SOD-1 deficiency might be explained by changes in the degree of hypometabolism induced by the prolonged hypoxic exposure. Further experiments are required to address these possibilities.

In summary, we have demonstrated that SOD-1 has a role in both the timing of respiratory activity during normal breathing in the neonate as well as in the post-hypoxic stability of breathing. Whether SOD-1 acts at the level of the carotid body or influences the metabolic response to hypoxia remains unknown.

Acknowledgement The authors are grateful for support from AHFMR, CRC, CIHR and the HSFC.

References

Bissonnette, J.M. and S.J. Knopp, S.J. (2001) Developmental changes in the hypoxic ventil-atory response in C57BL/6 mice. Respir. Physiol. 128(2), 179–186.

Brown, D.R. *et al*. (1993) Breathing periodicity in intact and carotid body-denervated ponies during normoxia and chronic hypoxia. J. Appl. Physiol. **7**4(3), 1073–1082.

Cummings, K.J., *et al*. (2004) Sudden neonatal death in PACAP-deficient mice is associated with reduced respiratory chemoresponse and susceptibility to apnoea. J. Physiol. 555(Pt. 1), 15–26.
Elchuri, S., *et al*. (2005) CuZnSOD deficiency leads to persistent and widespread oxidative damage and hepatocarcinogenesis later in life. Oncogene 24(3), 367–380.
He, L., *et al*. (2005) Effect of p47phox gene deletion on ROS production and oxygen sensing in mouse carotid body chemoreceptor cells. Am. J. Physiol. Lung Cell Mol. Physiol. 289(6), L916–L924.
Kemp, P.J. (2006) Detecting acute changes in oxygen: will the real sensor please stand up? Exp. Physiol. 91(5), 829–834.
Roy, A. *et al*. (2000) Mice lacking in gp91 phox subunit of NAD(P)H oxidase showed glomus cell $[Ca^{2+}]_i$ and respiratory responses to hypoxia. Brain Res. 872 (1–2), 188–193.
Tankersley, C.G. *et al*. (1994) Differential control of ventilation among inbred strains of mice. Am. J. Physiol. 267(5 Pt. 2), R1371–R1377.

24
Neurodevelopmental Abnormalities in the Brainstem of Prenatal Mice Lacking the Prader-Willi Syndrome Gene Necdin

Silvia Pagliardini[1], Jun Ren[1], Rachel Wevrick[2] and John J. Greer[1,3]

1 Introduction

Necdin (*Ndn*) is one of the paternally-expressed genes located on chromosome 15q11–q13, which is deleted in Prader-Willi Syndrome (PWS). Typical symptoms of this neurodevelopmental disorder are represented by hypotonia, failure to thrive, hyperphagia leading to severe obesity, somatosensory deficits, behavioral problems and mild-to-moderate mental retardation (Goldstone 2004). Further, PWS is associated with respiratory instability in the newborn period, associated with sleep apneas and blunted chemosensitivity (Nixon and Brouilette 2002).

Different strains of Necdin deficient mice have been generated with variable defects resembling the PWS phenotype. Two strains demonstrated variable penetrance of neonatal lethality caused by severe hypoventilation (Gerard, Hernandez, Wevrick and Stewart 1999; Muscatelli, Abrous, Massacrier, Boccaccio, Moal, Cau and Cremer 2000). We previously demonstrated that in Ndn^{tm2Stw} mice the source of respiratory dysfunction was traced to abnormal neuronal activity within the preBötzinger Complex (preBötC), a key medullary structure responsible for inspiratory rhythm generation (Ren, Lee, Pagliardini, Gerard, Stewart, Greer and Wevrick, 2003).

In this study, we further examined the medulla to determine if there are anatomical defects within the preBötC or synaptic inputs that regulate respiratory rhythmogenesis. We also conducted *in vitro* studies to determine if the unstable respiratory rhythm in Ndn^{tm2Stw} mice could be normalized by exogenous application of different neuromodulators. These results are part of a more extensive study on the developmental abnormalities of medulla and spinal cord in Ndn^{tm2Stw} mice (Pagliardini, Ren, Wevrick and Greer 2005).

[1] Department of Physiology and [2]Department of Medical Genetics, University of Alberta, 513 HMRC, Edmonton, AB T6G 2S2 Canada,[3] john.greer@ualberta.ca

M.J. Poulin and R.J.A. Wilson (eds.), *Integration in Respiratory Control: From Genes to Systems*.

2 Results and Discussion

We initially investigated the cytoarchitectural and anatomical properties of the developing medulla by means of a combination of anatomical markers. An analysis of the medullary cytoarchitecture by means of neurofilament (NF) immunolabeling showed three major defects: (1) a general axonal defasciculation of longitudinally- and commissurally-oriented axons (Fig.1A-B); (2) the presence of dystrophic axons within the cuneate/gracile nuclei and fascicles, (Fig. 1C-D); and (3) a reduction in the cross-sectional size of the motoneuronal pools of the dorsal motor nucleus of the vagus nerve, the hypoglossal and ambiguus nuclei (20 ± 4.5 SD%, 66.6 ± 6.6% and 32 ± 3.3% and in comparison to wild-type, Wt, animals).

We previously showed that the lethal hypoventilation present in *Ndn*^{tm2Stw} mice was due to abnormal neuronal activity within the preBötC, a major site of inspiratory rhythmogenesis within the medulla (Ren *et al*. 2003). We therefore aimed to identify preBötC neurons in the medulla of *Ndn*^{tm2Stw} mice. Neurokinin 1 receptor (NK1R) expression has been used as a marker for preBötC in both adult and perinatal animals (Gray, Rekling, Bocchiaro and Feldman, 1999; Pagliardini, Ren and Greer, 2003). Immunolabeling for NK1R showed that in *Ndn*^{tm2Stw} mice there was a reduction in size and extension of the nucleus ambiguous, as previously described, but the cluster of neurons ventral to the nucleus ambiguus, the putative location of preBötC, appeared normal (Fig. 2A-B). Another marker for preBötC neurons is somatostatin (SST, Stornetta, Rosin, Wang, Sevigny, Weston and Guyenet, 2003). SST expression was similar in both Wt and *Ndn*^{tm2Stw} mice in the preBötC (Fig. 2C-D). Thus, collectively, based on the current criteria for immunohistochemical classification of the preBötC area, there were no obvious anatomical abnormalities within this critical site for inspiratory rhythmogenesis in *Ndn*^{tm2Stw} mice.

We then examined the organization of synaptic inputs from neuromodulatory systems that project to the preBötC and regulate inspiratory rhythmogenesis. Immunolabeling for substance P (SubP) and serotonin (5HT) within the ventrolateral medulla of Wt animals showed presence of fine immunopositive fibers (Fig. 2E), with

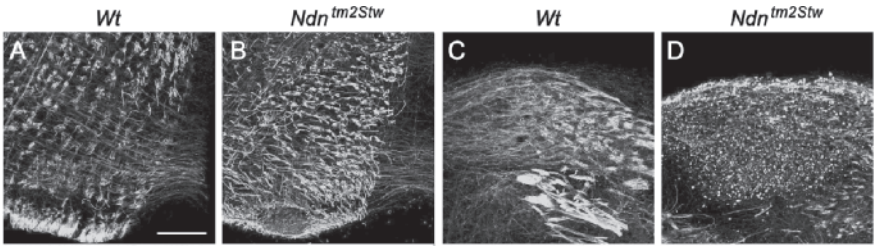

Fig. 1 Cytoarchitectonical abnormalities in *Ndn*^{tm2Stw} mice. NF expression in the medulla of wild-type (A, C) and mutant (B, D) at E18. (A, B) Details of axonal tracts in the ventromedial medulla. Note the reduced size and axonal defasciculation of axonal bundles through the ventral medulla in *Ndn*^{tm2Stw} mice. (C, D) Details of axonal tract in the cuneate nucleus. Note the presence of dystrophic structures in *Ndn*^{tm2Stw} mice. Calibration bar, 100 µm

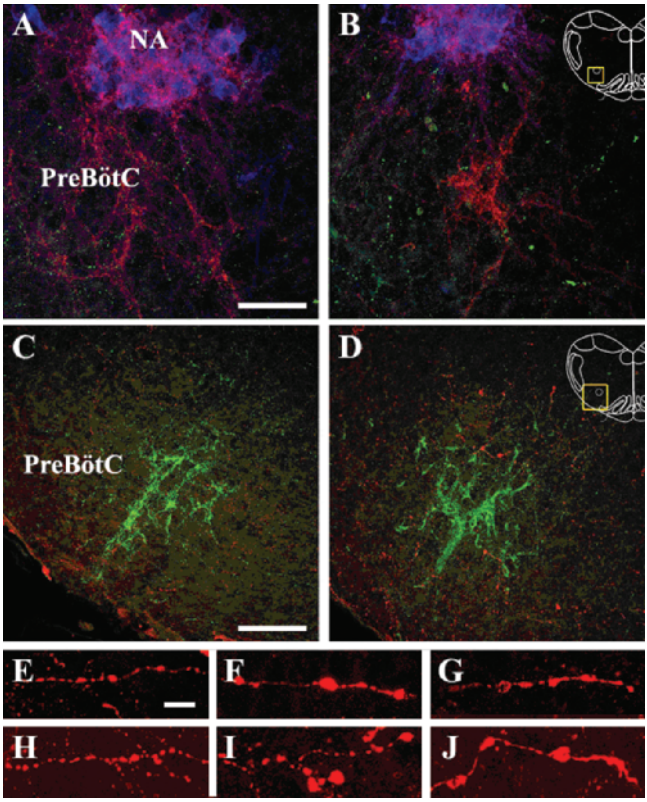

Fig. 2 Expression of NK1R, ChAT, SubP, SST and 5HT in the ventral medulla of wild-type (A, C, E, H) and *Ndn*^{tm2Stw} mice (B, D, F, G, I, J) at E18. (A, B) Transverse sections immunoreacted for ChAT (blue), NK1R (red) and SubP (green) show the reduced extension of the nucleus ambiguus in *Ndn*^{tm2Stw} mice and normal preBötC. (C, D) SST (green) immunoreactivity identifies the region of preBötC in both wild-type and *Ndn*^{tm2Stw} mice. SubP immunoreactive fibers in the medulla (C-G, red) are abnormally distributed and enlarged in *Ndn*^{tm2Stw} mice. Similar defects in 5HT immunoreactive fibers (H-J). Cal bars, A-B, 50 µm; C-D, 100 µm; E-J, 10 µm (see Color Plates)

several synaptic boutons in the preBötC areas. In *Ndn*^{tm2Stw} mice, SubP^{+} and 5HT^{+} fibers were present, but they were enlarged and irregularly oriented within the ventrolateral medulla (Fig. 2E-J). In order to better characterize the abnormalities in the morphology of SubP and 5HT fibers, we measured the cross-sectional area of varicosities. The average area in Wt animals at E18 was 1.57 ± 0.9 µm^2 for 5HT^{+} and 2.64 ± 0.15 µm^2 for SubP^{+} fibers. In *Ndn*^{tm2Stw} mice, the cross-sectional area was significantly increased to 3.14 ± 0.14 µm^2 for 5HT^{+} and 3.28 ± 0.32 µm^2 for SubP^{+} fibers. Our results suggest the presence of major defects in axonal tracts of the medulla, some of which provide neuromodulatory inputs that regulate respiratory rhythmogenesis in the preBötC.

We then performed electrophysiological recordings from brainstem-spinal cordpreparations with the diaphragm attached. The respiratory rhythm generated by *in vitro* preparations isolated from *Ndn*^{tm2Stw} mice was unstable, with prominent

bouts of respiratory depression and apneas during which the inspiratory frequency was typically less than one per minute. The bouts of suppressed respiratory rhythmic discharge (lasting 16 ± 7 min, n = 13) were interspersed with periods of inspiratory motor bursts close to frequencies observed in Wt preparations (lasting 7.5 ± 3.4 min, n = 13).

We tested the hypothesis that the respiratory rhythm could be normalized in the presence of endogenously applied neurotransmitter agonists (SubP and TRH) known to excite preBötC neurons. As shown in Fig. 3, addition of SubP and TRH significantly increased the frequency of discharge and the incidence of apneas diminished. However, fluctuations in respiratory frequency between slow and fast arations had similar modulatory effects (data not shown). Thus, we conclude that addition of neuromodulatory drive to the preBötC could alleviate the long periods of slow respiratory rhythms and apnea; however, the overall respiratory rhythm instability persisted.

Consistent with the proposed role of necdin in axonal growth and elongation (Lee, Walker, Karten, Kuny, Tennese, O'Neill and Wevrick 2005), we identified several defects in the medulla of *Ndn*^{tm2Stw} mice. Among these defects, defasciculation and irregular projections of axonal tracts, and a major defect in the cytoarchitecture of the cuneate/gracile nuclei were the main abnormalities in these animals. In order to explain the respiratory abnormalities observed in *Ndn*^{tm2Stw} mice, we analyzed in detail the region of the ventrolateral medulla. Our anatomical study of the preBötC did not show any gross abnormality. Rather, we observed clear abnormalities in the surrounding medullary structures that provide conditioning drive to respiratory rhythmogenic neurons. In particular, abnormal morphology of SubP$^+$ and 5HT$^+$ fibers suggests that the absence of necdin alters development of axonal tracts that regulate preBötC function.

Brainstem-spinal cord preparation from *Ndn*^{tm2Stw} mice showed irregular respiratory rhythmic activity associated with several periods of apneas and respiratory depression. Our results suggest that endogenous application of SubP and TRH overcame much of the deficit, but a defect in the preBötC function *per se* remains and it is responsible for respiratory irregularities even in presence of SubP and TRH.

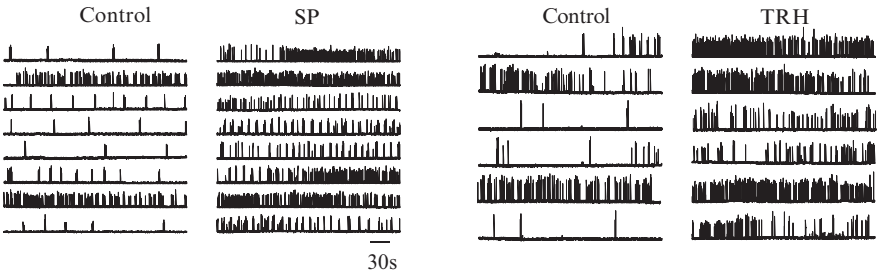

Fig. 3 Effects of excitatory neuromodulators (Substance P, left panel; TRH right panel) on respiratory rhythm generated by *Ndn*^{tm2Stw} mouse brainstem-spinal cord preparation with the diaphragm attached. Trace on the left of each panel represents diaphragm EMG activity before bath application of drugs and trace on the right shows activity in presence of either Substance P (1 μM) or TRH (1 μM)

3 Conclusions

Our results suggest that in *Ndn*^{tm2Stw} mice, abnormalities in the neuromodulatory drive to the preBötC may contribute to respiratory dysfunction. These abnormalities are part of a more widespread deficit in the extension, arborisation and fasciculation of axons during early stages of CNS development that may account for respiratory, sensory, motor and behavioral problems associated with PWS (Pagliardini *et al*. 2005; Lee *et al*. 2005).

Acknowledgements Work funded by the Canadian Institutes of Health (CIHR). JR and SP received studentships from the Alberta Heritage Foundation for Medical Research (AHFMR) and CIHR. RW is an AHFMR Senior Scholar and JJG is an AHFMR Scientist.

References

Gerard, M., Hernandez, L., Wevrick, R. and Stewart, C. (1999) Disruption of the mouse necdin gene results in early postnatal lethality: a model for neonatal distress in Prader-Willi syndrome. Nat. Genet. 23, 199–202.

Goldstone, A.P. (2004) Prader-Willi syndrome advances in genetics, pathophysiology and treatment. Trends Endocrinol. Metab. 15(1), 12–20.

Gray, P.A., Rekling, J.C., Bocchiaro, C.M. and Feldman, J.L. (1999) Modulation of respiratory frequency by peptidergic input to rhythmogenic neurons in the preBotzinger complex. Science 286(5444), 1566–1568.

Lee, S., Walker, C.L., Karten, B., Kuny, S.L., Tennese, A.A., O'Neill, M.A. and Wevrick, R. (2005) Essential role for the Prader-Willi syndrome protein necdin in axonal outgrowth. Hum. Mol. Genet. 14(5), 627–637.

Muscatelli, F., Abrous, D.N., Massacrier, A., Boccaccio, I., Moal, M.L., Cau, P. and Cremer, H. (2000) Disruption of the mouse necdin gene results in hypothalamic and behavioral alterations reminiscent of the human Prader-Willi syndrome. Hum. Mol. Genet. 9, 3101–3110.

Nixon, G.M. and Brouillette, R.T. (2002) Sleep and breathing in Prader-Willi syndrome. Pediatr. Pulmonol. 34, 209–217.

Pagliardini, S., Ren, J. and Greer, J.J. (2003) Ontogeny of the pre-Botzinger complex in perinatal rats. J. Neurosci. 23(29), 9575–9584.

Pagliardini, S., Ren, J., Wevrick, R.and Greer, J.J. (2005) Developmental abnormalities of neuronal structure and function in prenatal mice lacking the Prader-Willi syndrome gene necdin. Am. J. Pathol. 167(1), 175–91.

Ren, J., Lee, S., Pagliardini, S., Gerard, C.L., Stewart, C.L., Greer, J.J. and Wevrick, R. (2003) Absence of Ndn, encoding the Prader-Willi syndrome-deleted gene necdin, results in congenital deficiency of central respiratory drive in neonatal mice. J. Neurosci. 23(5), 1569–1573.

Stornetta, R.L., Rosin, D.L., Wang, H., Sevigny, C.P., Weston, M.C. and Guyenet, P.G. (2003). A group of glutamatergic interneurons expressing high levels of both neurokinin-1 receptors and somatostatin identifies the region of the pre-Botzinger complex. J. Comp. Neurol. 20, 455(4), 499–512.

25
Consequences of Prenatal Exposure to Diazepam on the Respiratory Parameters, Respiratory Network Activity and Gene Expression of α1 and α2 Subunits of $GABA_A$ Receptor in Newborn Rat

Nathalie Picard[1], Stéphanie Guenin[1], Yolande Perrin[2], Gérard Hilaire[3] and Nicole Larnicol[4]

Abstract Diazepam (DZP) enhances GABA action at $GABA_A$ receptor. Chronic prenatal administration of DZP delays the appearance of neonatal reflexes. We examined whether maternal intake of DZP might affect respiratory control system in newborn rats (0–3 day-old). This study was conducted on unrestrained animals and medulla-spinal cord preparations. In addition, the level of expression of the genes encoding for the α1 and α2 subunits of the $GABA_A$ receptor was assessed by quantitative real-time RT-PCR. In rats exposed to DZP, the respiratory frequency was significantly lower and the tidal volume higher than in controls with no significant alteration of the minute ventilation. The recovery from moderate hypoxia was delayed compared to controls. The respiratory-like frequency of medullary spinal cord preparation from DZP-exposed neonates was higher than in the control group. Acute applications of DZP (1 μM) to these preparations increased respiratory-like frequency in both groups, but this facilitation was attenuated following prenatal DZP exposure. The present data indicate that prenatal exposure to DZP alters both eupneic breathing and the respiratory response to hypoxia. These effects might partly be ascribed to the down-regulation of the expression of genes encoding $GABA_A$ receptor subunits. On the other hand, the effects of DZP exposure on reduced preparations suggested changes in the $GABA_A$ receptor efficiency and/or disruption of the normal development of the medullary respiratory network.

1 Introduction

Diazepam (DZP), a benzodiazepine with a broad therapeutic range, potentiates the inhibitory effect of GABA by binding to a site coupled to the $GABA_A$ receptor. The GABAergic system plays a critical role in patterning respiratory neuron activity

[1] Université de Picardie Jules Verne, Amiens, France, picard@marseille.inserm.fr

[2] UTC, CNRS UMR6022, Compiègne, France, yolande.perrin@utc.fr

[3] CNRS FRE2722, GERM, Marseille, France, hilaire@marseille.inserm.fr

[4] CNRS UMR6150, Labo Neurophysiologie Cellulaire, Marseille, France, larnicol@marseille.inserm.fr

M.J. Poulin and R.J.A. Wilson (eds.), *Integration in Respiratory Control: From Genes to Systems*. © Springer 2008

in vivo and *in vitro* (Richter, Ballanyi and Schwarzacher 1992; Brockhaus and Ballanyi 1998). Prenatal exposure to DZP may affect the development of benzodiazepine binding sites, with persisting effects on motor behaviors and learning capacity. DZP delayed the appearance of neonatal reflexes considered as an index of brain maturation, suggesting that diazepam may affect embryological mechanisms responsible for correct development (Nicosia, Giardina, Di Leo, Medico, Mazzola, Genazzani and Drago 2003). The present study in the rat examined whether the respiratory control system might be affected at birth by maternal intake of DZP within therapeutic ranges. To assess the effects of prenatal DZP exposure on ventilation, respiratory parameters were recorded by plethysmography at P0–P3 in normoxia and in moderate hypoxia, which triggers functional adaptation to chemoreceptor stimulation. *In vitro* recordings of medullary-spinal cord preparations were performed to determine the influence of prenatal DZP on respiratory network activity. In addition, the expression of the genes encoding for the $\alpha 1$ and $\alpha 2$ subunits of $GABA_A$ receptor (both containing the benzodiazepine binding site) was monitored by real time RT-PCR at birth in the medulla and the pons, both regions crucial for respiratory control.

2 Materials and Methods

The experimental protocols were carried out in newborn Sprague-Dawley rats. Treated dams had free access to DZP (Roche®) diluted in drinking tap water (0.001%) from the mating day on, to mimic the common situation in humans. Their daily DZP consumption was 2 mg/kg. Changes in respiratory parameters *in vivo* and *in vitro* were assessed using non-parametric statistics (Wilcoxon-matched paired and Mann-Whitney tests).

Ventilation was measured at P0–P3 according to Bartlett and Tenney (1970). Breathing frequency (fR) and tidal volume (Vt) were calculated over 75 min. Separate groups were used for measurements in normoxia and hypoxia (22% and 11% O_2 in N_2, respectively). Basal ventilation (V_E) was assessed prior to the hypoxic challenge (45 min). Rectal temperature was measured as an index of body temperature in separate rats.

En bloc preparations of medulla-spinal cord were performed at P0–P2 according to standard procedures (Brockhaus *et al.* 1998). The frequency of the respiratory-like activity (Rf) recorded from the C4 ventral root was averaged from 10 min recordings together with the amplitude of the integrated burst ($\int$C4). The acute effects of superfused DZP (1 µM, 10 min) were monitored every minute.

Real time RT-PCR was achieved on pooled tissue samples of the medulla and the pons from 3 P0 pups from 3 litters. Real-time PCR was performed according to Gutierrez, Conejero, Castelain, Guenin, Verdeil, Thomasset and Van Wuytswinkel (2006). The primers were: Fw: TTTGGAGTGACGACCG, Rv: CTAATCAGAGCCGAGAA α 1 subunit); Fw: TG GTGCTGGCTAACAT, Rv: GTCCTGGTCTAAGACGAT(α 2 subunit); Fw: CTTAGA GGGACAAGTGGCG, Rv GGACATCTAAGGGCATCACA (18SRNA, used as the housekeeping reference gene).

3 Effects of DZP Exposure on Body Temperature and Ventilation

In controls, rectal temperature was higher in normoxia (36.1 ± 0.3°C) than in hypoxia (34.7 ± 0.2°C; $p \leq 0.002$). Following prenatal exposure to DZP, temperature (35.0 ± 0.2°C) was lower than in controls in normoxia ($p < 0.004$), but it was not significantly affected by hypoxia (35.6 ± 0.2°C). These values were taken into account for the calculation of Vt in the different groups.

In normoxia, DZP-exposure decreased fR (112 ± 4 vs. 122 ± 4 breaths/min; $p \leq 0.024$) and increased Vt above control values (142 ± 7 vs. 107 ± 6 µl; $p \leq 0.001$), but not V_E (1.8 ± 0.1 vs. 1.7 ± 0.1 $l.kg^{-1} \bullet min^{-1}$).

In hypoxia, controls typically displayed an immediate increase in V_E followed by a secondary fall below normoxic values with a significant drop of fR. Respiratory parameters returned to prehypoxic values within 15 minutes under normoxia. The pattern of the ventilatory response to hypoxia was not markedly altered by prenatal exposure to DZP, except that the secondary decrease in fR was reduced and the decrease in Vt augmented, compared to controls ($p < 0.05$). Moreover, neither fR nor Vt did return to prehypoxic values at the end of the recovery period (Fig. 1).

4 Effects of DZP Exposure on Respiratory Network Activity

Basal Rf-like was higher in medulla-spinal cord preparations following prenatal DZP than in controls (12.3 ± 0.8 vs. 10.1 ± 0.6 bursts/min, $p \leq 0.04$). DZP superfused on control medullary-spinal cord preparation produced an immediate increase in Rf-like and a decrease in ∫C4 that plateaued after 3 minutes (158 ± 18 and 85 ± 4% of basal value for Rf-like and ∫C4; $p < 0.05$) (Fig. 2). In the DZP-exposed group, this acute effect of DZP was delayed and attenuated (122 ± 3% and 94 ± 2% for Rf-like and ∫C4).

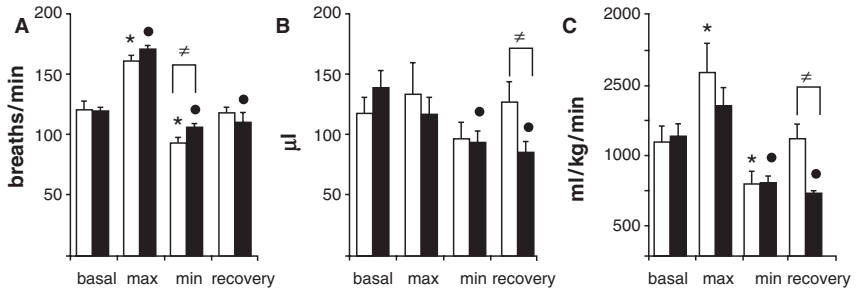

Fig. 1 Effect of prenatal DZP on hypoxic ventilation. Mean values ± SEM of fR (A), Vt (B) and V_E (C) before hypoxia (basal), at peak hyperventilation (max) and secondary decline (min). ❑: control, ❑: exposed; *,● : different from basal values, ≠: different between groups

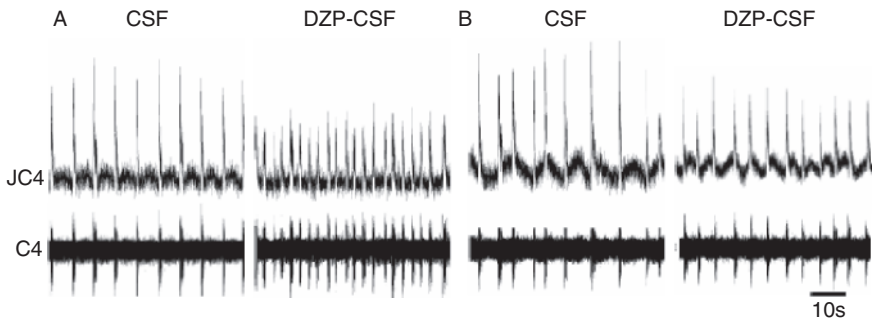

Fig. 2 C4 activity in control (A) and DZP-exposed (B) medullary-spinal cord preparations in aCSF and 10 min after the onset of superfusion of DZP-CSF (1 μM). C4, C4 raw activity; ∫C4, integrated C4 burst activity

5 Effects of DZP Exposure on $GABA_A$ Receptor Subunit Expression

The specificity of real-time PCR products for 18SRNA, α1 and α2 subunits of $GABA_A$ receptor was confirmed by melting curve analysis and gel electrophoresis. Each measurement was achieved in duplicate. DZP-exposure dramatically depressed the expression of genes encoding the two subunits α1 and α2 of the $GABA_A$ receptor in the pons (3% and 6% of control levels). In contrast, the expression of these genes tended to augment in the medulla (111% and 131% of control levels).

6 Conclusion

Our results showed for the first time that chronic exposure to DZP *in utero* at doses within the therapeutic range may affect the expression of homeostatic functions at birth. The effect of DZP on central temperature and V_E of newborn rats in normoxia suggests that DZP may alter the development of thermal and breathing control mechanisms. Moreover, the finding that DZP exposure mostly affects the secondary and recovery phases of the ventilatory response to hypoxia suggests interaction with central mechanisms triggered to adapt metabolism in situation of lack of O_2. Electrophysiological data support the idea that DZP may act on the central respiratory network activity. Surprisingly, bath application of DZP led to an increase in respiratory-like frequency whereas DZP is known to potentiate the inhibitory effect of GABA. This could be explained by the action of GABA in immature neurons that leads to depolarization and even provide most excitatory drive when excitatory glutamatergic synapses are quiescent or less efficient (Ben-Ari, Rovira, Gaiarsa, Corradetti, Robain and Cherubini 1990).

Reasonably, the effects of DZP prenatal exposure on neonatal breathing *in vivo* may partly depend on transcriptional events such as the down-regulation of α 1 and α 2 subunits of the $GABA_A$ receptor in the pons, as this could influence the efficiency of GABAergic control of major cell groups involved in respiratory phase transition and in the plasticity of the breathing pattern to environmental changes (Dutschmann and Herbert 2006). Nevertheless, the apparent desensitization to the acute effects of DZP of medullary-spinal cord preparations from newborn rats prenatally exposed to DZP cannot be explained by similar modifications of gene expression. Alternatively, prenatal DZP might induce functional uncoupling of the $GABA_A$-Benzodiazepine receptor complex, as previously shown in cortical neurons (Hu and Ticku 1994). Moreover, indirect consequences of prenatal DZP on the development of the respiratory network and/or of neuromodulator systems engaged in its control should not be excluded (Kellogg, Kenjarski, Pleger and Frye 2006).

The present investigation indicates that chronic exposure to DZP during pregnancy may alter physiological function in newborn and in particular the capacity of newborns to overcome hypoxic injury and to recover normal VE after hypoxia. Further studies are needed to determine whether chronic DZP acts at post-transcriptional level on location, number or affinity of the subunits α1 and α2 of $GABA_A$ receptor.

References

Bartlett, D., Jr. and Tenney, S.M. (1970) Control of breathing in experimental anemia. Respir. Physiol. 10(3), 384–395.

Ben-Ari, Y., Rovira, C., Gaiarsa, J.L., Corradetti, R., Robain, O. and Cherubini, E. (1990) GABAergic mechanisms in the CA3 hippocampal region during early postnatal life. Prog. Brain. Res. 83, 313–321.

Brockhaus, J. and Ballanyi, K. (1998) Synaptic inhibition in the isolated respiratory network of neonatal rats. Eur. J. Neurosci. 10, 3823–3839.

Dutschmann, M. and Herbert, H. (2006) The Kölliker-Fuse nucleus gates the postinspiratory phase of the respiratory cycle to control inspiratory off-switch and upper airway resistance in rat. Eur. J. Neurosci. 24, 1071–1084.

Gutierrez , L., Conejero, G., Castelain, M., Guenin, S., Verdeil, J.L., Thomasset, B. and Van Wuytswinkel, O. (2006) Identification of new gene expression regulators specifically expressed during plant seed maturation. J. Exp. Bot. 57, 1919–1932.

Hu, X.J. and Ticku, M.K. (1994) Chronic flurazepam treatment produces decreased efficacy of the benzodiazepine ligands and pentobarbital with gamma-aminobutyric acidA receptors in cortical neurons. J. Pharmacol. Exp. Ther. 270, 485–490.

Kellogg, C.K., Kenjarski, T.P., Pleger, G.L. and Frye, C.A. (2006) Region-, age-, and sex-specific effects of fetal diazepam exposure on the postnatal development of neurosteroids. Brain. Res. 5, 115–125.

Nicosia, A., Giardina, L., Di Leo, F., Medico, M., Mazzola, C., Genazzani, A.A. and Drago, F. (2003) Long-lasting behavioral changes induced by pre- or neonatal exposure to diazepam in rats. Eur. J. Pharmacol. 23, 103–109.

Richter, D.W., Ballanyi, K. and Schwarzacher, S. (1992) Mechanisms of respiratory rhythm generation. Curr. Opin. Neurobiol. 2, 788–93.

26
Modulation of Perinatal Respiratory Rhythm by $GABA_A$- and Glycine Receptor-mediated Chloride Conductances

Jun Ren[1] and John J. Greer[2]

1 Introduction

Previous studies demonstrated that chloride-mediated conductances via GABA and glycine strongly modulate neonatal respiratory rhythmogenesis. However, contradictory results were reported (Brockhaus and Ballanyi 1998; Ritter and Zhang 2000). Specifically, whether $GABA_A$- and glycine receptor-mediated actions are depolarizing/hyperpolarizing resulting in stimulation/depression of respiratory frequency in neonates was unclear. Further, the prenatal period had not been studied. Thus, we systematically investigated the actions of chloride-mediated conductances on respiratory rhythmogenesis in perinatal rats from the time of inception of fetal inspiratory drive through to the newborn period (Ren and Greer 2006).

2 Results and Discussion

2.1 Dependence of Chloride-mediated Conductances on $[K^+]_o$

Our initial observation that muscimol, glycine, and taurine caused contrasting changes in respiratory frequency between neonatal brainstem–spinal cord (inhibition in 3 mM $[K^+]_o$) and medullary slice (excitation in 9 mM $[K^+]_o$) preparations was unexpected. Subsequent experimentation demonstrated that the apparent discrepancy could be accounted for by different levels of $[K^+]_o$ in the media used to bathe the two types of *in vitro* preparations (Fig. 1). Gramicidin-perforated-patch recordings (with an intact $[Cl^-]_i$) of respiratory neurons within the region of the preBötC, a putative center for inspiratory rhythmogenesis were performed. Perforated-patch recordings from inspiratory (Fig. 2) and expiratory neurons demonstrated that increasing $[K^+]_o$ from 3 to 9 mM results in an ~ 8 mV depolarization of V_{rest} and a

[1–2]Department of Physiology, Centre for Neuroscience, University of Alberta, Edmonton, Alberta, Canada T6G 2S2, john.greer@ualberta.ca

M.J. Poulin and R.J.A. Wilson (eds.), *Integration in Respiratory Control: From Genes to Systems*. © Springer 2008

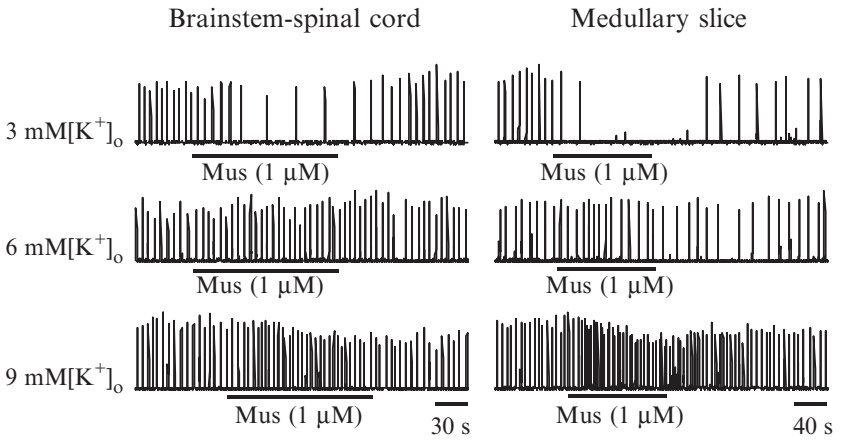

Fig. 1 $[K^+]_o$ dependency of responses to chloride-mediated conductances. Muscimol caused a decrease, no effect, or an increase in respiratory frequency when the P2 brainstem–spinal cord or medullary slice preparations were superfused with 3, 6, or 9 mM $[K^+]_o$ solution, respectively

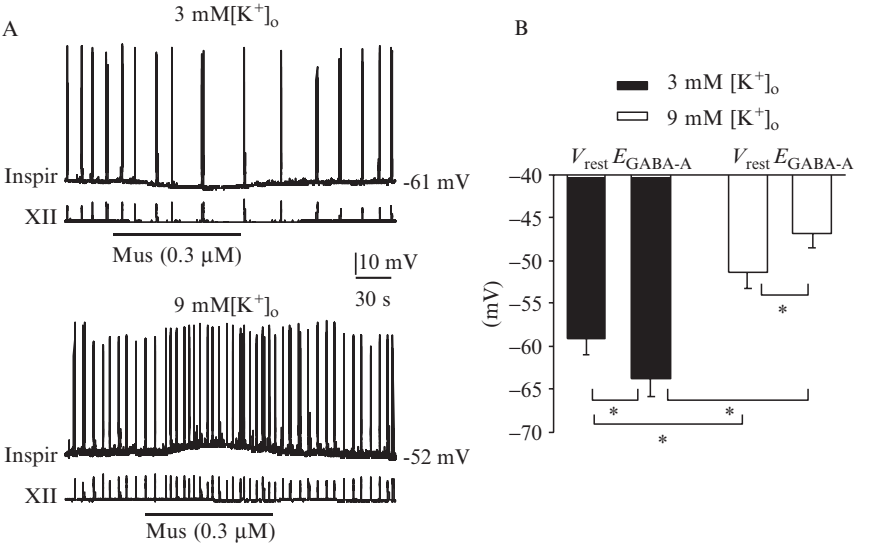

Fig. 2 Influence of $[K^+]_o$ on V_{rest} and $E_{GABA\text{-}A}$ from inspiratory neurons of neonatal medullary slices with perforated-patch recordings. (A) In 3 mM $[K^+]_o$, V_{rest} of the neuron was −61 mV, and muscimol application caused a membrane hyperpolarization and decrease in respiratory frequency. When perfused with 9 mM $[K^+]_o$, V_{rest} was −52 mV, and muscimol caused a membrane depolarization and increase in respiratory frequency. (B) Summary of V_{rest} and $E_{GABA\text{-}A.}$ *$p < 0.05$, significant difference between two groups

15–20 mV depolarization (P0–P4) of the reversal potential for chloride-mediated conductances (E_{Cl}).

Thus, elevating the $[K^+]_o$ to 9 mM in either type of postnatal *in vitro* preparation caused an efflux rather than an influx of Cl^- seen with 3 mM $[K^+]_o$ in response to $GABA_A$ or glycine receptor agonists. These data explain the inconsistencies from past studies from studies using *in vitro* preparations bathed in either 3 or 9 mM $[K^+]_o$

2.2 Dependence of Cl^--mediated Conductances on Perinatal Age

Data from this study demonstrate that agonists to $GABA_A$ and glycine receptors lead to a depolarization of inspiratory neurons and an increase in respiratory frequency at the inception of fetal respiratory drive at E17 (Fig. 3). The switch from excitatory to inhibitory actions of chloride-mediated conductances is at ~ E19. By birth, activation of $GABA_A$ or glycine receptors results in a hyperpolarization of

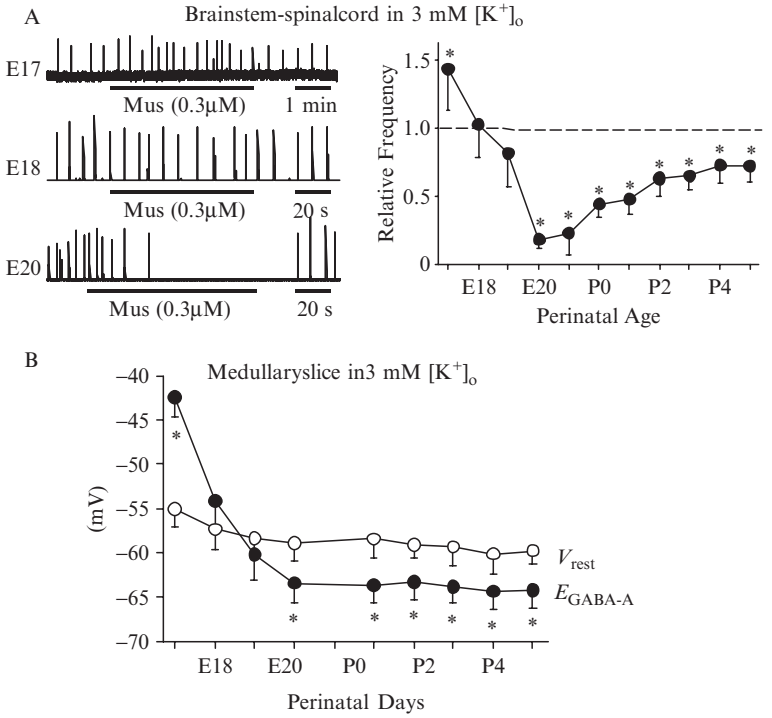

Fig. 3 Age-dependent changes in the effects of chloride-mediated conductances in 3 mM $[K^+]_o$. (A) The transition from an excitatory to inhibitory action occurred at approximately E19. (B) Summary of V_{rest} and $E_{GABA\text{-}A}$ for inspiratory neurons with perforated-patch recordings

respiratory neurons and depression of respiratory frequency *in vitro* under typical physiological levels of $[K^+]_o$.

Functionally, the depolarization of respiratory neurons at early stages of development will remove NMDA voltage-dependent Mg^{2+} block and thus enhance glutamate-mediated depolarization and rise of $[Ca^{2+}]_i$. In turn, elevated $[Ca^{2+}]_i$ regulates neurite outgrowth, gene expression, transmitter release and local receptor protein aggregation (Ben Ari, Khazipo, Leinekugel, Caillard and Gaiarsa 1997). Later in gestation and in the newborn period, elevated levels of GABA, glycine or taurine (*e.g.*, in response to hypoxia) within the preBötC will result in a suppression of respiratory frequency.

2.3 Dependence of Cl^--mediated Conductances on Chloride Cotransporter Function

Early in fetal development, the NKCC1 cotransporter is expressed at relatively high levels, and thus there is an elevated intracellular $[Cl^-]$ relative to mature neurons (Kaila 1994). The increased expression of the KCC2 cotransporter with perinatal age leads to the extrusion of Cl^- from the cytoplasm and establishment of a chloride equilibrium potential (E_{Cl-}) that is hyperpolarized from V_{rest} (Rivera, Voipio, Payne, Ruusuvuori, Lahtinen, Lamsa, Pirvola, Saarma and Kaila 1999). Perturbation of NKCC1 function with $[Na^+]_o$-free solution and bumetanide shifted E_{Cl-} to hyperpolarized values in pre-E18 (Ren and Greer 2006). The shift in E_{Cl-} was sufficient to reverse the normal muscimol-induced increase in respiratory frequency. Perturbations of KCC2 function with furosemide had no significant effect pre-E18. These data are consistent with the dominance of NKCC1 function that results in E_{Cl-} at values less negative than V_{rest}. In contrast, KCC2 inhibitor furosemide blocked the muscimol-induced inhibitory actions and shifted E_{Cl-} to depolarizing values in neonatal *in vitro* preparations perfused with 3 mM $[K^+]_o$ solution. Block of NKCC1 function had no significant effect. Thus, the function of KCC2 extrusion of Cl^- dominated control of E_{Cl-} postnatally. Furthermore, perturbation of KCC2 function with furosemide blocked the muscimol-induced excitatory actions and shifted E_{Cl-} to hyperpolarizing values in preparations perfused with 9 mM $[K^+]_o$ solution (Ren and Greer 2006). These data indicate that changes in KCC2 function in elevated $[K^+]_o$ were responsible for a significant component of the differential responses to chloride-mediated conductances observed in bathing mediums with different $[K^+]_o$. As demonstrated in neocortical pyramidal neurons, there is a > 15 mV depolarization of the E_{Cl-} with a change from 3.5 to 10 mM $[K^+]_o$ (DeFazio, Keros, Quick and Hablitz 2000). These results confirmed the previous observation that KCC2 could extrude or accumulate Cl^- depending on $[K^+]_o$ (Payne 1997).

3 Conclusions

The action of chloride-mediated conductances shifted from depolarizing/excitation to hyperpolarizing/inhibition of respiratory rhythm occurs at ~ E19, which is developmentally regulated by the ontogenesis of chloride cotransporters (NKCC1 and KCC2).

References

Ben Ari, Y., Khazipo, V, Leinekugel, X., Caillard, O. and Gaiarsa, J.L. (1997) $GABA_A$, NMDA and AMPA receptors: developmentally regulated menage a trois. Trends Neurosci. 20, 523–529.

Brockhaus, J. and Ballanyi, K. (1998) Synaptic inhibition in the isolated respiratory network of neonatal rats. Eur. J. Neurosci. 10, 3823–3839.

DeFazio, R.A., Keros, S., Quick, M.W. and Hablitz, J.J. (2000) Potassium-coupled chloride cotransport controls intracellular chloride in rat neocortical pyramidal neurons. J. Neurosci. 20, 8069–8076.

Kaila, K. (1994) Ionic basis of $GABA_A$ receptor channel function in the nervous system. Prog. Neurobiol. 42, 489–537.

Payne, J.A. (1997) Functional characterization of the neuronal-specific K-Cl cotransporter: implications for $[K^+]_o$ regulation. Am. J. Physiol. 273, C1516–C1525.

Ren, J. and Greer, J.J. (2006) Modulation of respiratory rhythmogenesis by chloride mediated conductances during the perinatal period. J. Neurosci. 26, 3721–3730.

Ritter, B. and Zhang, W. (2000) Early postnatal maturation of $GABA_A$-mediated inhibition in the brainstem respiratory rhythm-generating network of the mouse. Eur. J. Neurosci. 12, 2975–2984.

Rivera, C., Voipio, J., Payne, J.A., Ruusuvuori, E., Lahtinen, H., Lamsa, K., Pirvola, U., Saarma, M. and Kaila, K. (1999) The K^+/Cl^- cotransporter KCC2 tenders GABA hyperpolarizing during neuronal maturation. Nature 397, 251–255.

27
Laryngeal Stimulation by an Acid Solution in the Pre-term Lamb

Marie St-hilaire[1], Nathalie Samson[2], Charles Duvareille[3] and Jean-Paul Praud[4]

Abstract In a mature organism, the contact between various liquids and the laryngeal mucosa triggers lower airway protective responses (cough, swallowing, arousal). These laryngeal chemoreflexes (LCR) are essential for preventing aspiration. In contrast, previous studies showed that LCR are responsible for apnea and bradycardia in the neonatal mammal. Consequently, LCR, especially when triggered by acid gastrolaryngeal reflux, are deemed responsible for some apneas of prematurity and many life-threatening events of infancy and, probably, for some cases of sudden infant death syndrome. Recently, we have revisited LCR in full-term lambs during quiet sleep. Our results showed that the LCR triggered by HCl (pH 2), mimicking the acid component of an acid gastro-oesophageal reflux, were consistently like the mature LCR reported in adult mammals, without significant apneas and bradycardias (St-Hilaire 2005). These results prompted us to question whether premature birth alters LCR. Results show that LCR triggered in pre-term lambs by both saline and HCl are much more marked and clinically relevant than the ones observed in full-term lambs. Indeed, life-threatening responses to HCl, including repetitive apneas for more than 90 seconds, severe desaturation and bradycardia, were observed in 2 lambs at postnatal day 7 (D7). In addition, LCR were significantly blunted at D14. In conclusion, HCl can trigger potentially dangerous LCR in pre-term lambs at D7, suggesting that LCR in response to acid gastrolaryngeal refluxes are likely involved in some apnea/bradycardia/desaturation in pre-term infants, before they reach a post-conceptional age equivalent to full gestation.

1 Introduction

The laryngeal chemoreflexes (LCR) are triggered by contact between various liquids and receptors of the laryngeal mucosa in mammals. In a mature organism, liquids trigger highly protective reflexes to prevent subglottal aspiration, including cough,

[1–4]University of Sherbrooke, Departments of Pediatrics and Physiology, jean-paul.praud@usherbrooke.ca

M.J. Poulin and R.J.A. Wilson (eds.), *Integration in Respiratory Control: From Genes to Systems*. © Springer 2008

swallowing and arousal. However, in the neonatal period, previous studies have suggested that laryngeal stimulation induces a very different LCR, which are dominated by a vagal component and include laryngospasm, central or mixed/obstructive apneas, oxygen desaturation and bradycardia (Thach 2001). Clinical evidence strongly suggests LCR's can be triggered by acid gastrolaryngeal reflux and are responsible for some apneas of prematurity and many apparent-life threatening events of infancy, and probably some cases of sudden infant death syndrome (Page and Jeffery 2000; Thach 2001; Wetmore 1993). Although numerous studies have previously assessed LCR in response to various liquids in newborns mammals, most were performed in anesthetized or sedated animals, and/or were aimed at stimulating the subglottal (tracheal) area, and/or suffered from a lack of standardization and/or have been limited to only one aspect of the LCR. Our laboratory recently engaged in a research program on LCR using the newborn (full-term and pre-term) ovine model, with the objective of performing studies more relevant to clinical conditions.

3 Laryngeal Chemoreflexes in the Full-term Lamb

In a recent study, we assessed the various aspects of the LCR induced by various solutions including acid solutions (HCl and citric acid, pH 2), distilled water and saline in full-term lambs (St-Hilaire, Nsegbe, Gagnon-Gervais, Samson, Moreau-Bussière, Fortier and Praud 2005). This study was performed in highly standardized conditions, including control of state of alertness, avoidance of anesthesia or sedation, reproducibility of liquid injection (transcutaneous chronic catheter surgically implanted just above the glottis) and exhaustive analysis of the various components of the LCR. Our results revealed that in non-sedated, full-term lambs during quiet sleep, the cardiorespiratory components of the LCR were identical after instillation of distilled water or acid solutions and consistently very mild, *i.e.*, with a clinically non-significant decrease in heart rate or respiratory rate (Fig. 1, bottom traces, term lamb). In addition, saline injection virtually induced no responses. In summary, full-term lambs appear to have mature LCR resembling the ones reported in adult mammals.

Interestingly, results of this study reflected clinical observations in healthy term infants. Indeed, while all infants present acid gastropharyngeal refluxes (Lopez-Alonso, Jose-Moya, Antonio Cabo, Ribas, Del Carmen Macias, Silny and Silfrim 2006), only a minority suffers from apparent life-threatening events related to LCR. In addition, clinical observations suggest that the development of life-threatening LCR is linked to some abnormal conditions, such as pre-term birth.

4 Laryngeal Chemoreflexes in the Pre-term Lamb

A recently completed study by our group aimed at assessing the LCR in pre-term lambs born at 132 days of gestation (term = 147 days), using the same design as in the previous study in term lambs. Specific objectives of the study included the

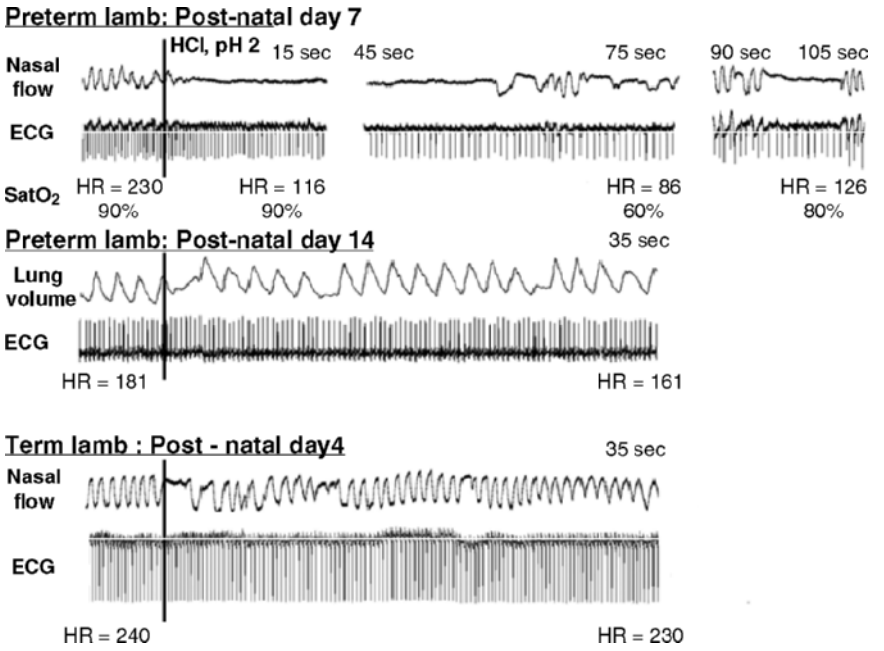

Fig. 1 Laryngeal chemoreflexes in pre-term lamb and term lamb. Laryngeal chemoreflexes in response to instillation of 0.5 ml hydrochloric acid on laryngeal mucosa in a pre-term lamb at post-natal day 7 and 14 and in a term lamb at post-natal day 4 during quiet sleep. Nasal flow, inspiration upward; ECG: electrocardiogram; lung volume: sum signal of the respiratory inductance plethysmograph (inspiration upward); HR: heart rate (beats/min). $SatO_2$: oxygen hemoglobin saturation measured by pulse oximetry

assessment of the effect of both premature birth and post-natal maturation. Six pre-term lambs were born by cesarean section. Laryngeal stimulations were induced by distilled water, saline and HCl (pH 2) at post-natal day 7 (D7) and post-natal day 14 (D14). At D7, all liquids induced clinically significant apneas, bradycardia and desaturation. Potentially life-threatening LCR, characterized by apneas and bradycardia longer than 20 s and severe desaturation (Fig. 1, top traces, pre-term lamb at day 7) were induced in 2 of the 6 lambs following water and/or HCl injection. Result of this study confirmed that exaggerated LCR can be elicited in pre-term lambs, as compared to term lambs. While the exact causes of exaggerated LCR are still unknown, immaturity of the cardio-respiratory "controllers" in the brainstem, increased laryngeal receptor sensitivity and/or subglottal aspiration with stimulation of tracheal receptors may be involved to explain the difference with full-term lambs. Interestingly, even saline injection elicited significant cardiorespiratory responses in some pre-term lambs, showing that pre-term birth is responsible for laryngeal hyperreflectivity to all studied liquids. In addition, at D14, the exaggerated cardiorespiratory responses observed in pre-term lambs were significantly blunted, with no life-threatening

responses observed at this age. Overall, the LCR observed at D14 in pre-term lambs were grossly identical to the LCR observed in term lambs at D4 (Fig. 1, middle traces, pre-term lamb at day 14) (St-Hilaire *et al*. 2005).

Clinical experience and a few studies in pre-term human infants strongly suggest LCR contribute to the cause of apneas of prematurity (Thach 2005). Our results in pre-term lambs clearly show that contact of an acid solution at pH 2 with the laryngeal mucosa (surrogate for the acid component of an acid gastrolaryngeal reflux) can trigger life-threatening reflexes mimicking apneas/bradycardias of prematurity observed in pre-term human infants. In addition, the significant cardio-respiratory reflexes elicited by saline, which has been compared to airway secretions (Pickens, Schefft and Thach 1988), suggest that upper airway secretion/saliva can also be responsible for some apnea/bradycardia in pre-term infants. Finally, post-natal maturation of the LCR, such as the one observed from D7 to D14 in pre-term lambs, is likely involved in the post-natal disappearance of apneas/bradycardias of prematurity, when the infants reach a post-conceptional age equivalent to full-term gestation.

5 Conclusion

In conclusion, our results show that pre-term birth favors the development of life-threatening LCR in lambs. In addition, postnatal maturation blunts these severe LCR. Our results strongly suggest that the LCR is involved in the apneic/bradycardic events observed in premature human infants

Acknowledgements The authors gratefully acknowledge the expert technical assistance of Jean-Philippe Gagné. Marie St Hilaire is a scholar of the Canadian Institutes for Health Research. Jean-Paul Praud is a national scholar of the Fonds de la recherche en santé du Québec. The study was supported by grants from the Canadian Institutes for Health Research (NRF 15558) and the Quebec Foundation for Research into Children's Diseases.

References

Lopez-Alonso, M., Jose-Moya, M., Antonio Cabo, J., Ribas, J., Del Carmen Macias, M., Silny, J. and Silfrim, D. (2006) Twenty-four hour esophageal impedance-pH monitoring in healthy pre-term neonates: rate and characteristics of acid, weakly acidic and weakly alkaline gastro-esophageal reflux. Pediatrics 118, 299–307.

Page, M. and Jeffery, H. (2000) The role of gastro-oesophageal reflux in the aetiology of SIDS. Early Hum. Dev. 59, 127–149.

Pickens, D.L., Schefft, G., and Thach, B.T. (1988) Prolonged apnea associated with upper airway protective reflexes in apnea of prematurity. Am. Rev. Respir. Dis. 137, 113–118.

St-hilaire, M., Nsegbe, E., Gagnon-Gervais, K., Samson, N., Moreau-Bussière, F., Fortier, P.H. and Praud, J.P. (2005) Laryngeal chemoreflexes induced by acid, water, and saline in non-sedated newborn lambs during quiet sleep. J. Appl. Physiol. 98, 2197–2203.

Thach, B.T. (2001) Maturation and transformation of reflexes that protect the laryngeal airway from liquid aspiration from fetal to adult life. Am. J. Med. 111, 69S–77S.
Thach, B.T. (2005) The role of respiratory control disorders in SIDS. Respir. Physiol. Neurobiol. 149, 343–353.
Wetmore, R.F. (1993) Effects of acid on the larynx of the maturing rabbit and their possible significance to the sudden infant death syndrome. Laryngoscope 103, 1242–1254.

28
Necdin Gene, Respiratory Disturbances and Prader-Willi Syndrome

Sébastien Zanella[1], Magali Barthelemy[1], Françoise Muscatelli[2] and Gérard Hilaire[1]

Abstract Prader-Willi Syndrome (PWS) is a complex neurogenetic disease with various symptoms, including breathing deficits and possible alteration of serotonin (5HT) metabolism. As PWS results from the absence of paternal expression of several imprinted genes among which *NECDIN (Ndn)*, we examined whether *Ndn* deficiency in mice induced breathing and 5HT deficits. *In vivo*, *Ndn*-deficient mice (*Ndn*−/−) had irregular breathing, severe apneas and blunted respiratory response to hypoxia. *In vitro*, medullary preparations from *Ndn*−/− neonates produced a respiratory-like rhythm that was highly irregular, frequently interrupted and abnormally regulated by central hypoxia. In wild type (wt) and *Ndn*−/− neonates, immunohistofluorescence and biochemistry revealed that medullary 5HT neurons expressed *Ndn* in wt and that the medulla contained abnormally high levels of 5HT in *Ndn*−/−. Thus, our preliminary results fully confirm a primary role of *Ndn* in PWS, revealing that *Ndn*-deficiency in mice induces respiratory and 5HT alterations reminiscent of PWS.

1 Introduction

Prader Willi Syndrome (PWS) is a complex neurogenetic disorder, with various symptoms including hypotonia, failure-to-thrive, obesity and behavioral alterations (Goldstone 2004). PWS is also associated to breathing deficits such as rhythm instability, severe sleep apneas and blunted responses to hypoxia and hypercapnia that might be a common cause of death in PWS (Nixon and Brouillette 2002). In addition, PWS patients may have an altered 5HT metabolism

[1] CNRS, UMR 6153, 280 boulevard Sainte Marguerite, 13009 Marseille France, hilaire@marseille.inserm.fr

[2] CNRS, UMR 6216, Institut Biologie du Développement de Marseille, Luminy, 13288 Marseille CEDEX9, France

M.J. Poulin and R.J.A. Wilson (eds.), *Integration in Respiratory Control: From Genes to Systems*. © Springer 2008

(Akefeldt, Ekman, Gillberg, and Mansson 1998) since their cerebrospinal fluid contains abnormal concentrations of the 5HT metabolite 5-hydroxyindoleacetic acid (5HIAA).

PWS results from the absence of paternal expression of several imprinted genes of the 15q11–q13 region, among which *NECDIN (Ndn)*. *Ndn*-deficient mice (*Ndn−/−*) have been created and might be a suitable model for PWS since they show neonatal lethality of variable penetrance, hypotonia, failure-to-thrive and adult behavioral alterations reminiscent of PWS (Muscatelli, Abrous, Massacrier, Boccaccio, Le Moal, Cau, and Cremer 2000). Although *Ndn−/−* fetuses have an altered maturation of the respiratory network (Pagliardini, Ren, Wevrick, Greer 2005; Ren, Lee, Pagliardini, Gerard, Stewart, Greer, and Wevrick 2003) and abnormal morphology of maturing bioaminergic neurons (Lee, Walker, Karten, Kuny, Tennese, O'Neill, and Wevrick 2005), little is known about the respiratory and 5HT systems of *Ndn−/−* that survived after birth. Here, we examined whether surviving *Ndn−/−* had respiratory and 5HT deficits. Our preliminary results show breathing instability, severe apneas, altered respiratory regulations and altered 5HT system in *Ndn−/−*, arguing for a primary role of *Ndn* in PWS breathing deficits.

2 Methods

The experimental procedures were carried out in keeping with the European guidelines (Council Directive 86/6009/EEC) in mice at postnatal day 2 (P2) and 30 (P30). Breeding, genotyping and methods have been described in detail elsewhere (Viemari, Roux, Tryba, Saywell, Burnet, Pena, Zanella, Bevengut, Barthelemy-Requin, Herzing, Moncla, Mancini, Ramirez, Villard, and Hilaire 2005; Muscatelli *et al*. 2000). Breathing of unanesthetized, unrestrained P2 and P30 mice were recorded using a constant air flow, whole-body flow plethysmograph to measure mean respiratory frequency, total respiratory cycle duration (T_{TOT}), tidal volume (V_T), minute ventilation (V_E), coefficient of variability of cycle duration (CVd), irregularity score (IS) and number of apneas ($T_{TOT} > 2$ sec) during quiet periods. To check the V_E response to hypoxia in P30 mice, V_E was first measured under air; then air was replaced by hypoxic mixture (10% O2–90% N2) for 5 min and V_E was measured during the last 2 min of hypoxia. In P2 mice, the respiratory-like activity produced by the isolated respiratory rhythm generator (RRG) was recorded in '*en bloc*' medullary preparations (Zanella, Roux, Viemari and Hilaire 2006) to measure frequency, CVd, IS and number of cycle > 10 s. High Performance Liquid Chromatography (HPLC) coupled with electrochemical detection was used to measure the 5HT and 5HIAA concentrations in the medulla and immunohistofluorescence to detect 5HT- and *Ndn*-expressing neurons. Data were analyzed using SigmaStat software.

3 Results

3.1 *Ndn* Deficiency Induces Respiratory Deficits in Mice

In P2 and P30 mice, plethysmography did not reveal significant differences in mean T_{TOT}, V_T and V_E between wt and *Ndn*–/–. However, breathing was highly irregular in *Ndn*–/– when compared to wt (Fig. 1A), with mean CVd and IS 2–3 times larger in *Ndn*–/–. Most *Ndn*–/– had frequent, long lasting apneas at P2 and P30 (about 165 and 105 apneas > 2 s per hour, respectively).

Submitting P30 mice to hypoxia significantly increased V_E in both genotypes but the mean V_E increase was significantly weaker in *Ndn*–/– than in wt by 40%.

3.2 *Breathing Deficits of Ndn–/– Neonates are Central from Origin*

To examine whether *Ndn*–/– breathing deficits originated from central or peripheral alterations, we analyzed the respiratory-like activity produced by the isolated RRG in '*en bloc*' medullary preparations (n = 7 wt and 8 *Ndn*–/–, P2). Although the *in vitro* phrenic bursts had similar shape and mean frequency, the phrenic cycle duration was highly variable in *Ndn*–/– (Fig. 1B) with large CVd and IS. Respiratory arrests (> 10 s) were 3 times more frequent in *Ndn*–/– (52 ± 7 /hr) than wt (16 ± 3 /hr).

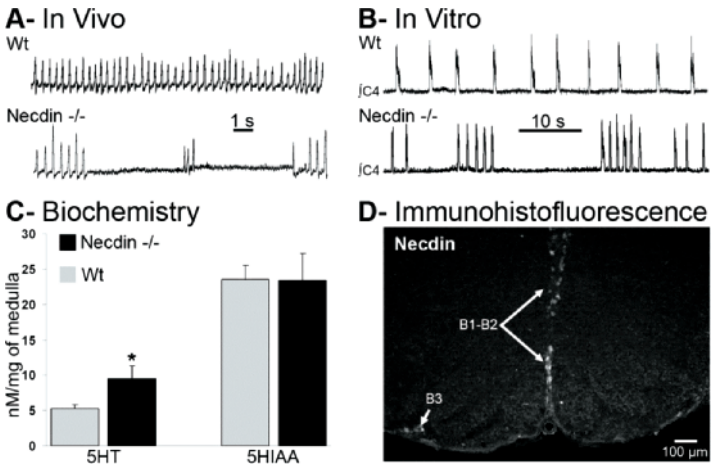

Fig. 1 Respiratory and 5HT deficits of Ndn–/– at P2. (A) Plethysmographic recordings of breathing showed severe apneas in Ndn–/–. (B) Recordings of integrated phrenic bursts produced in medullary preparations showed long-lasting respiratory arrests in Ndn–/–. (C) Mean concentrations of 5HT and 5HIAA in the medulla of wt and Ndn–/– (*, $p < 0.05$). (D) In wt neonates, Ndn is expressed in raphe (B1, B2) and lateral B3 areas (arrows)

Thereafter, we examined the RRG response to central hypoxia. In wt, consistently with previous results (Viemari, Burnet, Bevengut and Hilaire 2003), 5 min applications of non-oxygenated aCSF depressed the respiratory-like frequency to 50% of the control value for 2–3 min, then the frequency slightly increased but remained significantly depressed until the end of the 5-min challenge. Resuming the control conditions restored the normal frequency in about 5 min. In *Ndn*−/−, similar applications of non-oxygenated aCSF also depressed the frequency but the time course of the effect was slower, the mean depression weaker and the recovery period longer.

3.3 Ndn Deficiency Alters 5HT System in Neonatal Mice

As the 5HT metabolism may be altered in PWS, we examined the 5HT system in the medulla of *Ndn*−/− and wt neonates. First, HPLC revealed that the mean 5HT concentration was significantly larger by about 50% in *Ndn*−/− while the 5HIAA concentration was not altered (n = 14 *Ndn*−/− and 9 wt, Fig. 1C). Second, number of 5HT neurons was normal in *Ndn*−/− compared to wt (850 neurons). Third, immunolabeling revealed a high density of *Ndn*-positive neurons in the raphe (B1, B2) and B3 areas (Fig. 1D) but almost no *Ndn*-positive neurons in the ventral respiratory-related areas.

4 Discussion

To secure life at birth, the neonatal RRG must be able to elaborate a central respiratory drive and to adequately adapt it to environmental and behavioral changes. Here we show that *Ndn*-deficiency does not disable the neonatal RRG to function but disables it to generate a stable respiratory drive and to correctly respond to hypoxia.

As PWS patients, surviving *Ndn*−/− had irregular breathing and severe apneas that exist at birth and are central from origin since they occur *in vitro*. Our neonatal results suggest that *Ndn*-deficiency alters RRG maturation, in agreement with fetal results (Pagliardini *et al*. 2005; Ren *et al*. 2003): at gestational day 18, the respiratory-like activity of *Ndn*−/− preparations is highly variable and could stop for several tens of min in some preparations. We never observed such long-lasting arrests, probably because fetuses with such deficits could not have survived until P2. As PWS patients, *Ndn*−/− have blunted respiratory response to hypoxia both *in vivo* and *in vitro. In vivo*, blood hypoxia activates carotid body receptors that, in turn, activate the RRG. If the RRG activation cannot compensate the peripheral hypoxia, a central hypoxia develops that slows down the respiratory rhythm, especially in neonates (Viemari *et al*. 2003). In *Ndn*−/−, a central deficit exists since the RRG depression during central hypoxia is weak and long to recover. Thus, the neonatal

RRG of *Ndn*−/− is not well adapted to respond to hypoxic events that are common during neonatal life, especially in these mutants, and this may contribute to their neonatal lethality.

As PWS patients, *Ndn*−/− have 5HT alterations, suggestive of an altered 5HT metabolism. This is fully supported by our HPLC data, the expression of *Ndn* in 5HT areas of wt neonates (present results) and the abnormal 5HT profiles reported in *Ndn*−/− fetuses (Lee *et al*. 2005). The 5HT phenotype develops soon during gestation, under the control of several key genes (Cheng, Chen, Luo, Tan, Qiu, Johnson and Ma 2003) but *Ndn* might also contribute to 5HT network development. *Ndn*-deficiency might result in aberrant projections of 5HT neurons, outside and inside the raphe, with possible alterations of 5HT autoreceptors regulation and 5HT metabolism. As the 5HT system plays a crucial role in CNS development (Gaspar, Cases, and Maroteaux 2003) and modulates numerous functions, an altered 5HT metabolism may contribute to some of the symptoms of *Ndn*−/− as well as PWS patients. In wt neonates, *Ndn* is expressed within the 5HT areas but not the respiratory-related areas of the ventrolateral medulla. As already suggested in fetuses (Ren *et al*. 2003), *Ndn*−/− respiratory deficits are unlikely to result from a direct alteration of the RRG but may originate from alterations of its regulatory inputs. Our results in *Ndn*−/− are consistent with those gained in Tg8 transgenic mice where inactivation of the gene encoding MAOA, the degradation enzyme for 5HT, increases perinatal 5HT levels and results in RRG instability (Bou-Flores, Lajard, Monteau, De Maeyer, Seif, Lanoir and Hilaire 2000) and depressed responses to hypoxia (Burnet, Bevengut, Chakri, Bou-Flores, Coulon, Gaytan, Pasaro and Hilaire 2001).

To conclude, our preliminary results reveal that *Ndn* plays a primary role in PWS breathing deficits since *Ndn*-deficiency in mice induces 5HT and respiratory deficits reminiscent of PWS, suggesting a causal relationship between excess of 5HT and alteration of RRG perinatal maturation and function.

References

Akefeldt, A., Ekman, R., Gillberg, C. and Mansson, J.E. (1998) Cerebrospinal fluid monoamines in Prader-Willi syndrome. Biol. Psychiatry 44, 1321–1328.

Bou-Flores, C., Lajard, A.M., Monteau, R., De Maeyer, E., Seif, I., Lanoir, J. and Hilaire, G. (2000) Abnormal phrenic motoneuron activity and morphology in neonatal monoamine oxidase A-deficient transgenic mice: possible role of a serotonin excess. J. Neurosci. 20, 4646–4656.

Burnet, H., Bevengut, M., Chakri, F., Bou-Flores, C., Coulon, P., Gaytan, S., Pasaro, R. and Hilaire, G. (2001) Altered respiratory activity and respiratory regulations in adult monoamine oxidase A-deficient mice. J. Neurosci. 21, 5212–5221.

Cheng, L., Chen, C.L., Luo, P., Tan, M., Qiu, M., Johnson, R. and Ma, Q. (2003) Lmx1b, Pet-1, and Nkx2.2 coordinately specify serotonergic neurotransmitter phenotype. J. Neurosci. 23, 9961–9967.

Gaspar, P., Cases, O. and Maroteaux, L. (2003) The developmental role of serotonin: news from mouse molecular genetics. Nat. Rev. Neurosci. 4, 1002–1012.

Goldstone, A.P. (2004) Prader-Willi syndrome: advances in genetics, pathophysiology and treatment. Trends Endocrinol. Metab. 15, 12–20.

Lee, S., Walker, C.L., Karten, B., Kuny, S.L., Tennese, A.A., O'Neill, M.A. and Wevrick, R. (2005) Essential role for the Prader-Willi syndrome protein necdin in axonal outgrowth. Hum. Mol. Genet. 14, 627–637.

Muscatelli, F., Abrous, D.N., Massacrier, A., Boccaccio, I., Le Moal, M., Cau, P. and Cremer, H. (2000) Disruption of the mouse Necdin gene results in hypothalamic and behavioral alterations reminiscent of the human Prader-Willi syndrome. Hum. Mol. Genet. 9, 3101–3110.

Nixon, G.M. and Brouillette, R.T. (2002) Sleep and breathing in Prader-Willi syndrome. Pediatr. Pulmonol. 34, 209–217.

Pagliardini, S., Ren, J., Wevrick, R. and Greer, J.J. (2005) Developmental abnormalities of neuronal structure and function in prenatal mice lacking the Prader-Willi syndrome gene necdin. Am. J. Pathol. 167, 175–191.

Ren, J., Lee, S., Pagliardini, S., Gerard, M., Stewart, C.L., Greer, J.J. and Wevrick, R. (2003) Absence of Ndn, encoding the Prader-Willi syndrome-deleted gene necdin, results in congenital deficiency of central respiratory drive in neonatal mice. J. Neurosci. 23, 1569–1573.

Viemari, J.C., Roux, J.C., Tryba, A.K., Saywell, V., Burnet, H., Pena, F., Zanella, S., Bevengut, M., Barthelemy-Requin, M., Herzing, L.B., Moncla, A., Mancini, J., Ramirez, J.M., Villard, L. and Hilaire, G. (2005) Mecp2 deficiency disrupts norepinephrine and respiratory systems in mice. J. Neurosci. 25, 11521–11530.

Viemari, J.C., Burnet, H., Bevengut, M. and Hilaire, G. (2003) Perinatal maturation of the mouse respiratory rhythm-generator: *in vivo* and *in vitro* studies. Eur. J. Neurosci. 17, 1233–1244.

Zanella, S., Roux, J.C., Viemari, J.C. and Hilaire, G. (2006) Possible modulation of the mouse respiratory rhythm generator by A1/C1 neurones. Respir. Physiol. Neurobiol. 153, 126–138.

Part V
Models of Gas Exchange

29
Quantitative Analysis of the Oxygen Transfer in the Human Acinus

Marcel Filoche[1,2], André A. Moreira[3], José S. Andrade Jr.[1,3] and Bernard Sapoval[1,2]

Abstract The gas transport in the acinus is limited at rest by the finite oxygen diffusivity. Although the simplest steady-state model of diffusion permits understanding a number of observations, it fails to quantitatively fit the value of the absolute flux of oxygen at rest and exercise. In this paper, we show that the binding of oxygen to hemoglobin modifies these values only slightly. In contrast, the dynamics of breathing have a strong effect and allow recovery to known experimental values for oxygen transfer.

1 Diffusion Screening: Quantitative Problems

Gas transport into the human acinus, which is the gas exchange unit of the pulmonary system, is realized first by convection then by diffusion. The transition between both transport modes is rather sharp and occurs at rest around the 18th generation of branching, around the 21st at exercise. Oxygen molecules diffuse in the alveolar gas and eventually reach the alveolar membrane where they are transferred into the blood. Conversely, carbon dioxide is extracted from the venous blood and brought back by diffusion up to the transition region between diffusion and convection.

Inside the region of the acinus where transport is mostly diffusive, physiological parameters, geometrical characteristics and transport coefficients interplay in a complex way. For some values of these parameters, the system may exhibit "screening effects." Screening occurs when it is easier for oxygen molecules to cross the alveolar membrane near the entrance of the diffusion cells than to diffuse down to the more distal regions of the acinus. The mechanism of this phenomenon is sketched elsewhere in this volume (see chapter by Sapoval and Filoche). Although this

[1] Physique de la Matière Condensée, Ecole Polytechnique, CNRS, 91128 Palaiseau, France, marcel.filoche@polytechnique.edu

[2] Ecole Normale Supérieure, C.N.R.S., Centre de Mathématiques et de leurs Applications, 94140, Cachan, France

[3] Departamento de Física, Universidade Federal do Ceará, 60451-970 Fortaleza, Ceará, Brazil.

M.J. Poulin and R.J.A. Wilson (eds.), *Integration in Respiratory Control: From Genes to Systems*.

notion of screening is now well documented (Sapoval, Filoche and Weibel 2002; Felici, Filoche, Straus, Similovski and Sapoval 2005), the mathematical derivation of the steady-state oxygen flux failed to provide a correct order of magnitude. This was mentioned in Sapoval *et al*. (2002), where it was suggested that the discrepancy could be due to the role of oxygen binding by hemoglobin and to the dynamics of the breathing cycle. These are the questions to be discussed below.

The existence of screening effects can be summarized into one number η ($0 \leq \eta \leq 1$) called the efficiency. It is the ratio of the actual flux divided by the flux for an infinite gas diffusivity. It measures the equivalent fraction of the acinus surface that can be considered as "active." The total flux of oxygen in this model can be written as:

$$Flux = S_{\text{lung}} \times W \times \eta \times (P_{\text{entrance}} - P_{\text{blood}}) \tag{1}$$

S_{lung} being the developed acinar surface in the lung, P_{entrance} the partial pressure of oxygen at the entrance of the acinus, and P_{blood} the partial pressure of oxygen in the venous blood. Now this expression predicts, with an efficiency of order 30% at rest, a total flux of oxygen 8 to 10 times larger than the measured value. The aim of this paper is to investigate the influence of two effects that have been left out of the initial model, namely the resistance due to the oxygen trapping by hemoglobin, and the dynamic effects due to the oscillatory ventilation of the lung.

2 Role of Oxygen Binding by Hemoglobin

A possible explanation for the discrepancy between the value of the absolute flux of oxygen measured at rest and the one computed in the model may lie in the oversimplified representation of the gas transfer through the alveolar membrane into the blood. To check the role of the binding, we modify the model to take into account the oxygen trapping by hemoglobin.

The flux density of oxygen from the air to the blood plasma, through the alveolar membrane, is equal to $W\,(P_{O2,\,\text{alv.}} - P_{O2,\,\text{plasma}})$, W being the membrane permeability. But this quantity must also be equal to the flux of oxygen carried away in the arterial blood, both in the plasma and in the hemoglobin. This leads to the following equation:

$$W\,(P_{O2,\,\text{alv.}} - P_{O2,\,\text{plasma}}) = 4\,Z_0\,V_{\text{b}}\,[f(P_{O2,\,\text{plasma}}) - f_0] + \sigma\,P_{O2,\,\text{plasma}}\,V_{\text{b}} \tag{2}$$

where Z_0 is the concentration of hemoglobin in the blood, V_{b} the speed of the blood, σ the solubility of oxygen in blood, f_0 is the fraction of oxyhemoglobin in the venous blood and $f(P)$ represents the fraction of oxyhemoglobin in equilibrium with a given partial pressure P of oxygen in the blood. The function f is given by the Hill's formula (Keener and Sneyd 1998).

Equation 2 permits us to compute $P_{O2,\,\text{plasma}}$ from $P_{O2,\,\text{alv.,}}$ and thus to express the boundary condition on the alveolar membrane in the same way as in the linear

model. The only modification is that the length $\Lambda = D/W$ (Sapoval *et al*. 2002) is now replaced by a pressure-dependent length $\Lambda(P)$, which gives a non-linear boundary condition. This new length is equal to Λ for low partial pressures but increases as the hemoglobin becomes saturated with oxygen. This leads to a decrease of the "effective" permeability of the alveolar membrane and thus a reduction of the screening effect.

The change in screening has been studied on 2D numerical simulations (Felici 2003). These simulations (Fig. 1) have been carried out in finite elements on a Kitaoka's model acinus (Kitoaka, Tamura and Takaki 2000). Although one can clearly see a reduction of the screening effect on the distribution of oxygen into the acinus, screening is still present. As a matter of fact, the acinus efficiency goes from 25% in the linear model to only 30% in the non-linear model. As a consequence, even if the binding of the oxygen by hemoglobin represents an additional resistance that reduces the value of the total flux of oxygen, it cannot explain alone the order of magnitude discrepancy in experimental data.

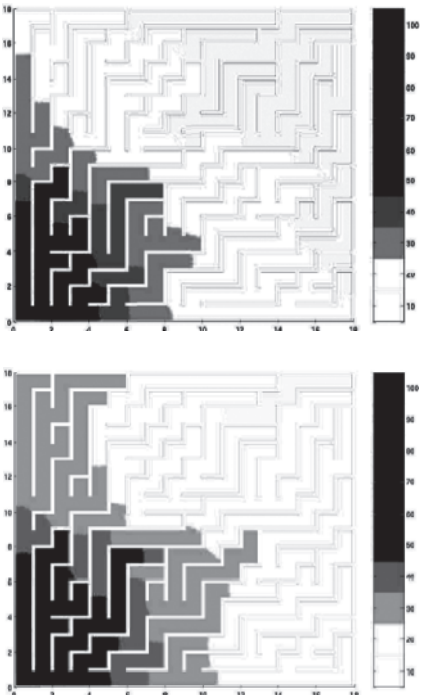

Fig. 1 Distributions of partial pressure of oxygen in the acinus. These simulations have been carried out in a 2D Kitaoka's model geometry of the acinus. The entrance of the acinus is located in the bottom left corner. On the left, the linear model: the blood is considered as an oxygen sink. On the right, the non-linear model: one takes into account the binding of oxygen by hemoglobin. This binding tends to slow the transfer of oxygen when the partial pressure of oxygen is high, thus reducing the screening effects

3 The Role of the Respiratory Cycle

During the breathing cycle, the entrance air velocity varies periodically. So the transition region between diffusion and convection moves accordingly to this variation, and the picture of a static diffusion cell does not hold anymore. In order to study the influence of the breathing cycle on the oxygen transfer in the acinus, we have performed time-dependent simulations.

In these simulations, the air velocity in the acinus is a periodic function of time and depends, at each section of the acinus, on the generation of the particular branch considered. The flux of air at the beginning of any given branch is whatever is necessary to inflate the branch and the part of the acinus located below this branch. For the transport of oxygen, we take a quasi-static approach: at any time, the oxygen distribution (or partial pressure) in the acinus is assumed to be identical to the steady-state distribution obtained for the current entrance velocity of air. To obtain the total flux of air flowing through the system, one only has to integrate the instantaneous flux over a breathing cycle. With this model, one can now compute the acinus efficiency as a function of the breathing frequency.

In order to test the influence of the dynamics, simulations were carried out on a simplified geometry of the acinus. In this geometry, the branching are symmetrical, and each branch has a length of 0.7 mm and an equivalent radius of 0.25 mm. The breathing cycle was assumed to be sinusoidal with a period of 5 seconds.

On the left of Fig. 2, one can see the steady-state flux of oxygen transferred to the blood at each generation of the acinus, for different values of the acinus entrance velocity. Although the partial pressure of oxygen is higher at the entrance of the acinus, the transferred flux is larger in the more distal regions due to the distribution of alveolar surface. On the right of Fig. 2 is represented the evolution of the volume of oxygen in the acinus at various times of the breathing cycle. One can note that during the cycle, the amount of oxygen in the acinus strongly vary, even near the entrance of the acinus.

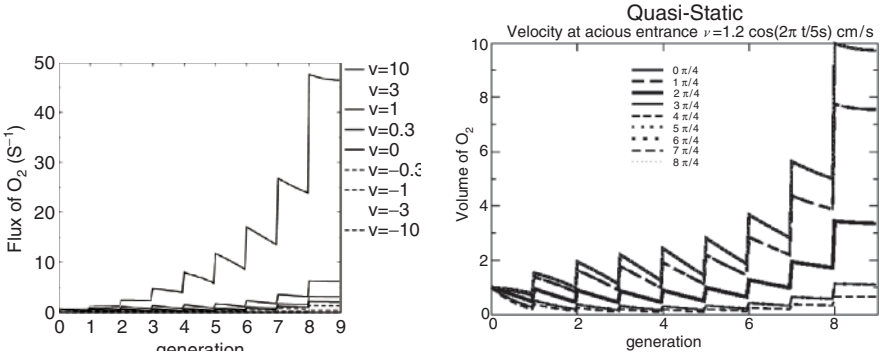

Fig. 2 Left: Flux of oxygen through the alveolar membrane, at each generation of the acinus, for various entrance velocities. Right: Volume of oxygen in the acinus at various times of the breathing cycle (period = 5 s). The interval between two successive times is 1/8 of a period

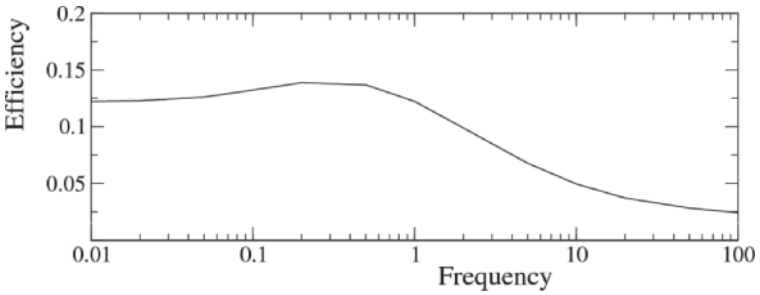

Fig. 3 Acinus efficiency at exercise as a function of the breathing frequency

From these data, an "effective" acinus efficiency has been computed: it is defined as the ratio of the actual flux of oxygen flowing through the acinus over the maximal flux if the acinus was working continuously with the maximum air velocity at the entrance and without diffusion limitation (Fig. 3). One can see that at exercise, the efficiency is now 13% up to a frequency of around 1Hz. This efficiency is 8 to 10 times less than the one obtained in the stationary model. Preliminary results show that at rest, the efficiency is now around 2% to 3%. A complete description of this type of computation will be published in a future paper (Moreira, Filoche, Andrade and Sapoval, unpublished data).

Replacing this computed efficiency in Eq. 1, one obtains a value of the total flux of oxygen in agreement with the experimental data.

4 Conclusion

Although the steady-state linear model of oxygen diffusion is in agreement both qualitatively and quantitatively with many physiological observations, the total flux of oxygen computed in this model does not match the physiological data. The binding of oxygen by hemoglobin slightly modifies the efficiency but not enough to explain the discrepancy. On the other hand, a complete calculation, which takes into account not only the binding effects but, first of all, the dynamics of ventilation would allow recovery of a realistic value for the oxygen flux.

Acknowledgements The authors gratefully acknowledge enlightening discussions with Prof. E.R. Weibel. We wish to acknowledge ANR for financial support (Project ANR No. 0003205).

References

Felici, M. (2003) Physique du transport diffusif de l'oxygène dans le poumon humain, PhD Thesis, Ecole Polytechnique.

Felici, M., Filoche, M., Straus C., Similovski T. and Sapoval B. (2005) Diffusional screening in real 3D human acini – a theoretical study. Resp. Phys. Neurob. 145 (2–3), 279–293 and references therein.

Keener, J. and Sneyd, J. (1998) *Mathematical Physiology*. J.E. Marsden, L. Sirovich and S. Wiggins (Eds.), Springer-Verlag, New York.

Kitaoka, H., Tamura, S. and Takaki, R. (2000) A three-dimensional model of the human pulmonary acinus, J. Appl. Physiol. 88, 2260–2268.

Sapoval, B., Filoche M. and Weibel, E.R. (2002) Smaller is better-but not too small: a physical scale for the design of the mammalian pulmonary acinus. Proc. Nat. Acad. Sci. 99, 10411–10416 and references therein.

30
Role of Diffusion Screening in Pulmonary Diseases

Bernard Sapoval[1,2] and Marcel Filoche[1,2]

Abstract It has been shown recently that the acinus is only partially efficient in normal conditions. This is due to a "screening effect" governed by the relative values of the oxygen diffusivity and the membrane resistance as well as design and size of the acinus. These effects depend on the fraction of the acinus in which gas transport is governed by diffusion, then on the location of the convection-diffusion transition. It is shown that these screening effects gives to respiration at rest a partial protection against several types of pulmonary diseases. This is true for mild emphysema, mild asthma or COPD and mild edema. In contrast, under exercise respiration, the acinus is totally efficient and the protective effects linked to the existence of screening do not exist anymore.

1 Diffusion Screening and Respiration

In order to exchange oxygen and carbon dioxide, blood and air are brought into close contact over a large surface area. In the mammalian lung, the gas exchange occurs in the most peripheral generations of the branched airway tree that form the acini (Weibel 1984; Weibel, Sapoval and Filoche 2005). Beyond the convection-diffusion transition, oxygen diffuses in a quasi-static gas and then eventually crosses the capillary membrane to be finally bound by hemoglobin. The efficiency of the acinus considered as a gas exchanger is then a crucial issue for respiration. A simple discussion of the process can be made by comparing the conductance to reach the surface by diffusion with the permeation conductance to cross the complex acinus surface. The parameters involved in these processes are the oxygen diffusivity, D, and the membrane permeability, W. Consider a part of the acinus surface of area A and diameter L (diameter of the smallest sphere surrounding this part). The conductance to reach the

[1] Ecole Polytechnique, C.N.R.S., Laboratoire de Physique de la Matière Condensée, 91128 Palaiseau, France, bernard.sapoval@polytechnique.edu

[2] Ecole Normale Supérieure, C.N.R.S., Centre de Mathématiques et de leurs Applications, 94140, Cachan, France

M.J. Poulin and R.J.A. Wilson (eds.), *Integration in Respiratory Control: From Genes to Systems*.

surface is of order $Y_{reach} \sim DL$ whereas the conductance to cross is $Y_{cross} = WA$. If the conductance to reach is larger than the conductance to cross ($Y_{reach} > Y_{cross}$), the surface works uniformly. But for a large enough system, the surface increases more rapidly than the diameter and one can have a situation where $Y_{reach} < Y_{cross}$. In that case, diffusion in the volume is a limiting step and the less accessible regions will receive little flux. In the language of physics theses regions are "screened". The transition between the screened and unscreened regimes is obtained when $Y_{reach} \sim Y_{cross}$, or equivalently $D/W \sim A/L$. The ratio $A/L = L_p$ is roughly the length of a planar cut of the surface, which is defined as the "perimeter" of the surface. The length $\Lambda = D/W$ is called the unscreened perimeter length because a part of the surface that has its A/L value smaller than Λ will work uniformly.

For the normal values $D(O_2)$ and $W(O_2)$ in human healthy lungs, $\Lambda(O_2)$ is 28 cm and the morphometrical data gives $L_p \sim 30$ cm for the 1/8 acinus (Weibel *et al*. 2005). The fact that the *purely physico-chemical* length Λ is comparable to the *purely morphological* perimeters of the acini of several mammals gives clear evidence that screening should play a role in mammalian respiration (Sapoval 1984; Sapoval *et al*. 2002). The role of screening in human respiration is now well documented (Felici, Filoche, Straus, Similovski and Sapoval 2005). Note that if the acini were too large, a major part of their surface would be inactive. This is the physical reason why the lungs have to be divided into a large number of small acini.

2 How to Compute the Global Gas Flux in the Acinus

Neglecting the oxygen trapping resistance and dynamical effects to be discussed in by Filoche, Sapoval, Moreira and Andrade in this volume, the flux can be written within constants as:

$$\text{Flux} = (\text{Acinus surface } S)(\text{Permeability } W)(\text{Acinus efficiency } \eta)\,(\text{Entrance to blood pressure drop } P) \quad (1)$$

The acinus efficiency η ($\eta \leq 1$) is the ratio of the real flux divided by the flux for infinite gas diffusivity. It measures the equivalent fraction of the acinus surface that can be considered as "active" although this picture is partly misleading as the gas pressures are functions of space and different regions of the acinus contribute.

It is the influence of all these factors that determine respiration and it is their perturbation by pulmonary diseases that modifies the gas exchanges. These factors are not independent as, for instance, a change in permeability (by pulmonary edema) modifies the unscreened perimeter length Λ and consequently the acinus efficiency. There is also an extra variable, which does not appear directly in the above product: it is the air velocity at the acinus entry that we call U. A change in U will induce a change in the convection-diffusion transition and a modification of the size of the zone where diffusion governs the gas transport as shown in Fig. 1.

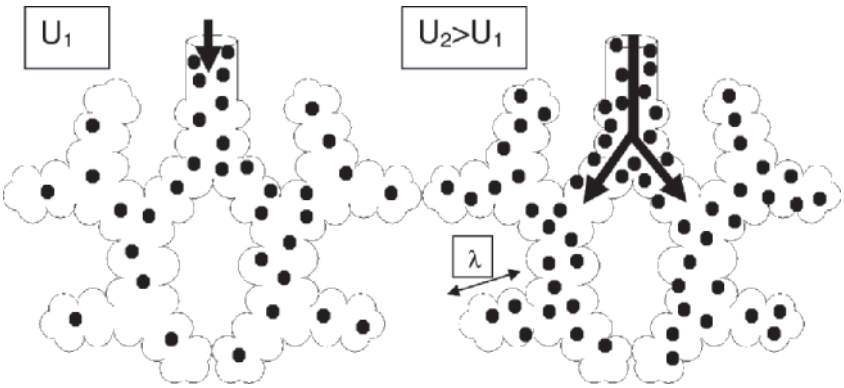

Fig. 1 Schematized representation of diffusion screening and its dependence on the convection-diffusion transition represented by the arrowhead. The dots represent oxygen molecules. For small entrance velocity, the transition is close to the acinus entry and a non-uniform oxygen partial pressure may exist in the deeper regions. For a larger entrance velocity, the transition is deeper and the zones in which a partial pressure gradient may exist are smaller to the point that they may work in a quasi-uniform manner

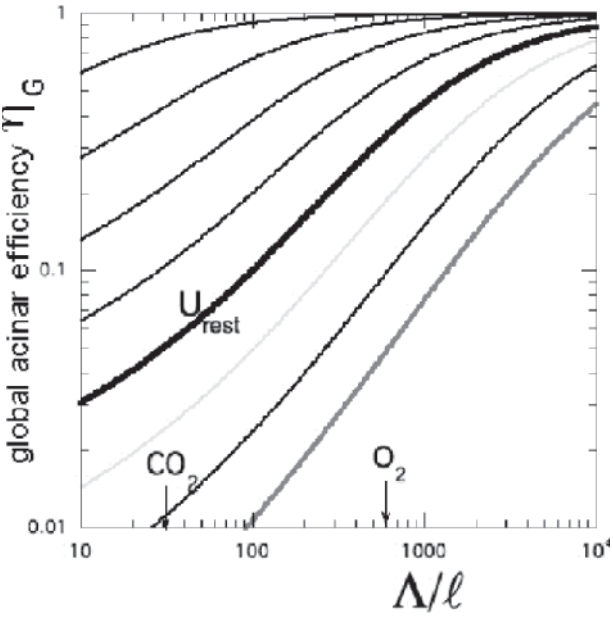

Fig. 2 Global acinar efficiency as a function of the screening length Λ for various air velocities at the acinus entrance. The unit length λ is equal to twice the alveoli diameter. The various curves correspond to entrance velocities increasing from $U_{rest}/8$ by factors 2 up to 16 U_{rest}. At rest velocity, the global efficiency is found to be equal to 0.32 for oxygen

For a given gas velocity U at the acinus entrance, one may define the bronchial tree bifurcation $Z(U)$ below which the corresponding subacini work under diffusion limited conditions, while the part of the acinus with $Z \leq Z(U)$ will work under the entrance partial pressure. To find $Z(U)$, one introduces an "acinus Peclet number" $P(Z)$, which compares the flow velocity at Z with the mean diffusion velocity to reach, from Z, the deeper regions of the acinus. At any branching Z, the distance to cross to the end of the sacs is of order $(Z_{max} - Z)\lambda$ where λ is the mean length of an acinar duct (Fig. 1).

The "acinus Peclet number" $P(Z)$ is defined as $P(Z) = U(Z)(Z_{max} - Z)\lambda / D_{O2,air}$ where the flow velocity $U(Z)$ at stage Z is found from the airway morphometry (Weibel 1984; Weibel *et al*. 2005). Depending on whether $P(Z)$ is larger or smaller than 1 the transport is due to convection or to diffusion. The screening effects in each subacinus can be computed analytically (Grebenkov, Filoche and Sapoval 2005). The global (unscreened + screened) flux can then be obtained together with the global acinus efficiency for different velocities at the acinus entrance. The results are shown in Fig. 2. Details will be published separately. One observes that for the normal healthy lung the efficiency is about 30% at rest and about 90% at exercise where the entrance velocity is around 10 times the rest velocity.

3 Impact of Screening in Pulmonary Diseases

3.1 Asthma or COPD

In the case of severe asthma or COPD, the entrance velocity decrease and the efficiency decreases rapidly as shown in Fig. 2. On the other hand, for mild forms, if one assumes that *the gas flux is kept constant* (because muscular effort keeps the acinus inflation constant), although the diameters of the last bronchioles are reduced, the air velocity at the acinus entrance is *increased*. In that case, the diffusion source for oxygen enters more deeply into the acinus and the diffusion cell is smaller. This increases the diffusion efficiency and globally the oxygen uptake may remain approximately constant. Screening can then be seen as giving some natural protection against mild COPD. This could explain why COPD may remain silent: the patient can compensate the increase of the airway resistance by a stronger inspiratory effort. The same facts should apply to mild asthma.

3.2 Emphysema

In the frame of our model, mild emphysema can be modeled here as a loss of acinar surface. In the context of screening, it implies that the smaller surface works in a

more uniform manner by increasing the efficiency. In consequence, the two factors that determine the flux change in opposite sense. The very existence of screening gives to respiration a protection against mild emphysema, which can remain asymptomatic. Of course, at exercise when the entire surface is working, the loss of exchange surface decreases the gas flux accordingly.

3.3 Pulmonary Edema

In pulmonary edema the alveolar membrane permeability decreases. The permeability deterioration has two opposite effects: it decreases directly the flux (Eq. 1), but at the same time, the increase in Λ tends to increase the efficiency, at least at rest. The combined effect of these factors for oxygen is shown in Fig. 3 where the global flux is given as a function of the ratio of the deteriorated membrane resistance to its value for the healthy case. One observes that at rest, the diminution of the oxygen flux due to the resistance increase is much slower than at exercise. For a doubling of the membrane resistance, the oxygen flux is only decreased by 20% while at exercise (where screening effects are small), the flux decreases by a factor 2. This means that screening creates to some extent a protective effect for respiration. At the same time, it also means that mild edema may remain asymptomatic.

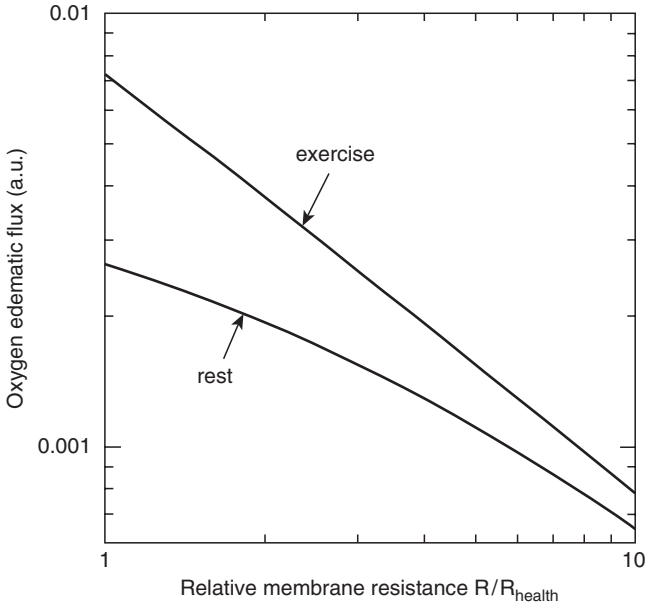

Fig. 3 Dependence of the net oxygen flux on an increase of the membrane resistance due to edema. The effect is very different at rest and exercise where the screening effects are small

Let us mention that if one attributes the resistance increase to the growth of a water film over the lung surface of order of $100\,m^2$, the quantity of water that would produce a decrease of the oxygen flux by 2 is about $300–400\,cm^3$, a value consistent with clinical observations.

4 Conclusion

In summary, we have shown that the existence of diffusion screening which limit the gas flow at rest provides the human respiration with a natural, physical protection against mild aspects of several pulmonary diseases. The general qualitative statement arising form this fact is that many of these diseases may remain asymptomatic.

Acknowledgements The authors gratefully acknowledge enlightening discussions with E.R. Weibel and the use of data from D. Grebenkov and financial support from A.N.R.

References

Felici, M., Filoche, M., Straus C., Similovski T. and Sapoval B. (2005) Diffusion screening in real 3D human acini – a theoretical study. Resp. Phys. Neurob. 145(2–3), 279–293 and references therein.

Grebenkov, D., Filoche, M. and Sapoval, B. (2005) Diffusion-reaction in branched structures: theory and application to the lung. Phys. Rev. Lett. 94, 050602.

Sapoval, B. (1994) Transfer to and across irregular membranes modeled by fractal geometry. In: T.F. Nonnenmacher, G.A. Losa, E.R. Weibel (Eds.), *Fractals in Biology and Medicine*. Birkhäuser-Verlag, Bâle.

Sapoval B., Filoche, M. and Weibel, E.R. (2002) Smaller is better but not too small: a physical scale for the design of the mammalian pulmonary acinus. Proc. Natl. Acad. Sci. 99, 10411–10416 and references therein.

Weibel, E.R. (1984). *The Pathway for Oxygen*. Harvard University Press, Cambridge, MA.

Weibel, E.R., Sapoval B. and Filoche M. (2005) Design of peripheral airways for efficient gas exchange. Resp. Phys. and Neur. 148, 3–21.

31
A dp/dt Method to Assess Dynamic Properties of Lung Mechanoreceptors

C.E. Schweitzer[1, 2], J.L. Johnson[2], C.A. Escudero[2], S.G. Vincent[2] and J.T. Fisher[2]

Abstract The activity of airway slowly adapting mechanoreceptors (SARs) reflects the presence of both a static and dynamic component. The dynamic response is typically assessed by the adaptation index; however, this is an indirect reflection of the more appropriate physiological stimulus, the rate of change of inflation pressure (dp/dt). We describe a method in which measurement of receptor discharge exceeding the SAR static response is used to measure dynamic discharge and dynamic sensitivity of lung mechanoreceptors. Repeat inflations with varying dp/dt illustrate the method for a SAR in which the dynamic sensitivity is inversely related to dp/dt and the initial "onset" discharge is highly dp/dt sensitive. The method may provide new insight into the classification and behaviour of lung mechanoreceptors.

1 Introduction

Airway slowly adapting mechanoreceptors (SARs) possess a static and dynamic mechanosensitivity that is linked to lung volume and rate of inflation respectively (Sant'Ambrogio 1982; Fisher *et al*. 2003; Yu 2005). The actual mechano-stimulus is better reflected by transpulmonary pressure (Ptp) and its rate of change (dp/dt). In contrast, rapidly adapting receptors (RARs) respond to inflation and/or deflation and provide dynamic feedback related to Ptp (Sant'Ambrogio 1982).

Identification of receptors as either SARs or RARs includes an assessment of the pattern of action potential (AP) discharge and the dynamic response as reflected by the adaptation index (AI) (for review see Sant'Ambrogio 1982; Fisher and Sant'Ambrogio 1982; Yu 2005).

[1] Present address: Laboratoire de Physiologie, Faculté de Médecine, Université Henri Poincaré, 9 Av. de la Forêt de Haye, Vandoeuvre les Nancy, 54505 France, cyril.schweitzer@medecine.uhp-nancy.fr

[2] Department of Physiology, Medicine & Pediatrics, Queen's University, Kingston K7L 3N6 Canada, fisherjt@post.queensu.ca

M.J. Poulin and R.J.A. Wilson (eds.), *Integration in Respiratory Control: From Genes to Systems*.

AI is defined as:

$$AI = [(Fp - Fss) \cdot Fp^{-1}] \cdot 100\% \quad (1)$$

where Fp is the peak discharge frequency of the receptor during inflation and Fss is the steady state adapted discharge, usually at 2–3 seconds after reaching a target pressure or volume. SARs typically display an AI of less than 50%, whereas RARs have an AI > 70% (Widdicombe 1954; Sant'Ambrogio 1982; Yu 2005), although exceptions do exist (Tsubone 1986; Yu 2000; Yu 2005).

AI has been used as a surrogate for dynamic responsiveness (Bartlett and St. John 1979; Sant'Ambrogio *et al*. 1983) and AI is inversely related to the time required to reach a target inflation pressure for SARs (Sant'Ambrogio *et al*. 1983). Others have used changes in flow to assess dynamic discharge (Pack *et al*. 1986), although it is well appreciated that dp/dt or the change in tension (dT/dt) at the receptor site is the physiological signal transduced by the receptor (Bartlett *et al*. 1976; Mortola and Mortola 1980). AI remains widely used (for review see Yu 2005), although modern data acquisition systems provide the capability to measure both receptor discharge and dp/dt. We reasoned that relating receptor activity directly to dp/dt would provide insight into receptor behaviour and may result in a more precise appreciation of subcategories of SARs and RARs (Yu 2005). We describe a technique to assess airway mechanoreceptor sensitivity that relates action potential discharge to static and dynamic pressure (dp/dt) stimuli provided during inflations of varying speed.

2 Methods and Results

The dynamic response of a receptor is assessed by connecting the lung to a constant pressure source and relating receptor activity to the dp/dt achieved by altering the target pressure or inserting resistors in the inflation line (present examples) (Bartlett and St. John 1979; Sant'Ambrogio *et al*. 1983). The difference between recorded discharge frequency and the static discharge represents the receptor activity related to the dynamic signal. The static sensitivity of the receptor (imp • s^{-1} • cmH_2O^{-1}) equals the ratio of the Fss and the achieved target pressure (cmH_2O). The static sensitivity and the instantaneous values of Ptp during inflation are used to calculate the instantaneous static discharge that is present for the receptor during inflation. The difference between the recorded discharge frequency and the static values represents the additional receptor discharge related to the dynamic signal or dynamic discharge frequency.

We calculated the dp/dt associated with the inflation from the pressure waveform between a threshold of 0.5 cm H_2O and the pressure value at 80% of the achieved static pressure. The value of the initial pressure threshold can be varied depending on the presence or absence of positive end-expiratory pressure (PEEP). Although one can measure dp/dt on an instantaneous basis, the above-mentioned approach avoids the artefacts associated with slow changes in dp/dt seen at the start of inflation and the decrementing pattern of dp/dt present at the end of inflation.

2.1 Indices of Dynamic Responsiveness

The dynamic sensitivity of SARs (imps • cmH_2O^{-1}) is obtained from the ratio of the average dynamic discharge frequency (imps • s^{-1}) and the dp/dt (cmH_2O • s^{-1}). Dynamic sensitivity can also be expressed as a percentage of the static adapted discharge value (% • s • cmH_2O^{-1}). The latter would be appropriate for comparisons between species with different static receptor sensitivities (Farber *et al*. 1983) or for use in the newborn, where static discharge is decreased (for review see Fisher *et al*. 2003).

Additional information related to dp/dt can also be obtained from the measurement of the latency to the first action potential (onset latency) and the receptor onset discharge frequency calculated from the first pair of AP's.

2.2 Demonstration of the Method for a Slowly Adapting Receptor

Figure 1 displays the results for a typical neonatal canine SAR during inflations to 10 cm H_2O and 20 cm H_2O at 4 different rates of inflation. A digital acquisition system (CED, Spike II) was used to acquire and analyze the inflation pressure waveform, receptor AP and the instantaneous AP discharge frequency. The dynamic discharge frequency (impulses • s^{-1}) increased as the rate of inflation increased for inflations to low or high lung volumes (Fig. 1, Left Panel). Although the mean dynamic discharge increased as dp/dt rose, the magnitude of the change was not proportional to that seen for dp/dt. Thus, the dynamic sensitivity of the SAR (impulses • cmH_2O^{-1}) decreased as the rate of inflation increased (Fig. 1, Right Panel).

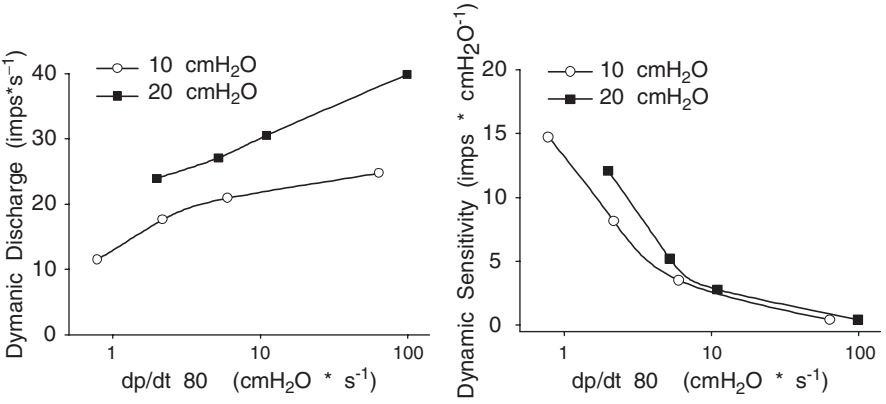

Fig. 1 Dynamic discharge vs. dp/dt 80 (Left Panel). Dynamic discharge represents the mean receptor discharge frequency (imps • s^{-1}) above the theoretical static value. Dynamic discharge for a typical neonatal SAR increased with the speed of inflation (dp/dt) to 10 and 20 cm H_2O. Dynamic sensitivity vs. dp/dt 80 (Right Panel). Dynamic sensitivity (imps • cmH_2O^{-1}) was derived from the ratio of the dynamic discharge (left panel) to dp/dt. Dynamic sensitivity decreased as speed of inflation (dp/dt) increased for inflations to 10 or 20 cm H_2O

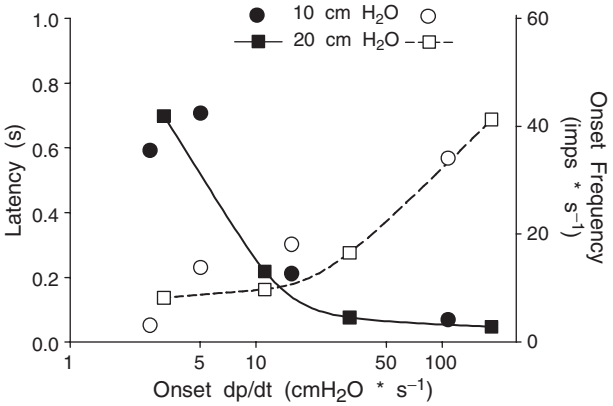

Fig. 2 Latency (s; Left Y-axis, filled symbols) and Onset Frequency (imps • s^{-1}; Right Y-axis, open symbols) for a typical neonatal SAR during inflations of increasing dp/dt. The latency to discharge was inversely related to dp/dt, while onset frequency was positively related to dp/dt

Figure 2 (left axis) illustrates the impact of dp/dt on the latency to receptor discharge from the initiation of inflation, as well as on the onset discharge frequency (right axis). Both variables provide insight into the nature of receptor dynamic signaling to the medulla.

3 Discussion

The mechanical stimulus to airway afferents is likely related to wall or circumferential tension (Bartlett *et al*. 1976; Mortola and Mortola 1980). Although direct measurement of DT/dt is not available during ventilation of the lung, measurement of the dynamic signaling of dp/dt provides a reasonable estimate of the stimulus applied to the receptor ending (Bartlett *et al*. 1976; Mortola and Mortola 1980). Indeed, the use of dp/dt to assess dynamic sensitivity should provide a more robust evaluation of airway mechanoreceptor properties than AI.

The calculation of the magnitude of the dynamic discharge relies on the assumption that static receptor discharge is linearly related to transmural pressure. This assumption can be tested experimentally by measuring the receptor response to different static inflation pressures. If an alinear relationship is present, an appropriate polynomial model of the static response can be employed. Although we presented an example of a receptor that was inactive prior to inflation, the calculations can also be applied to "tonic" receptors that discharge at end-expiration by measuring the increase in activity above the basal frequency. Lastly, the pressure threshold from which dp/dt measurements are initiated (*i.e*., 0.5 cm H_2O) can be adjusted to accommodate inflations performed from pre-existing values of PEEP, as could the 80% target pressure.

The computational ability of modern data acquisition systems led to our development of a new method to assess the dynamic sensitivity of lung mechanoreceptors related to dp/dt. Quantitative assessment of the dynamic sensitivity of slowly and rapidly adapting receptors to dp/dt should yield new insights into the characterization and identification of different categories of myelinated vagal afferents (Tsubone 1986; Yu 2000).

Acknowledgements Supported by grants from the Canadian Institutes of Health Research and the Ontario Thoracic Society to JTF. CES was the recipient of a post-doctoral fellowship from Société des Eaux d'Evian and the Canadian Foundation for Sudden Infant Deaths.

References

Bartlett, D., Jr., Sant'Ambrogio, G. and Wise, J.C.M. (1976) Transduction properties of tracheal stretch receptors. J. Physiol. (Lond.) 258, 421–432.

Bartlett, D., Jr. and St.John, W.M. (1979) Adaptation of pulmonary stretch receptors in different mammalian species. Respiration Physiology 37, 303–312.

Farber, J.P., Fisher, J.T., and Sant'Ambrogio, G. (1983) Distribution and discharge properties of airway receptors in the opossum, *Dedelphis marsupialis*. Am. J. Physiol. 245, R209–R214.

Fisher, J.T., Schweitzer, C.E., Weichselbaum, M. and Sparrow, M.P. (2003) Ontogeny of upper and lower airway innervation. In: O.P. Mathew (Ed.) *Respiratory Control and Disorders in the Newborn*, Marcel Dekker, Inc., New York, pp. 39–81.

Mortola, J.P. and Mortola, S.A. (1980) Tracheal slowly adapting stretch receptors: theoretical models. J. Theor. Biol. 83, 313–320.

Pack, A.I., Ogilvie, M.D., Davies, R.O. and Galante, R.J. (1986) Responses of pulmonary stretch receptors during ramp inflations of the lung. J. Appl. Physiol. 61, 344–352.

Sant'Ambrogio, F.B., Fisher, J.T. and Sant'Ambrogio, G. (1983) Adaptation of airway stretch receptors in newborn and adult dogs. Respiration Physiology 52, 361–369.

Sant'Ambrogio, G. (1982) Information arising from the tracheobronchial tree in mammals. Physiol.Rev. 62, 531–539.

Tsubone, H. (1986) Characteristics of vagal afferent activity in rats: three types of pulmonary receptors responding to collapse, inflation, and deflation of the lung. Exp. Neurol. 92, 541–552.

Widdicombe, J.G. (1954) Receptors in the trachea and bronchi of the cat. J. Physiol. 123, 71–104.

Yu, J. (2000) Spectrum of myelinated pulmonary afferents. Am. J. Physiol. Regul. Integr. Comp. Physiol. 279, R2142–R2148.

Yu, J. (2005). Airway mechanosensors. Respir. Physiol. Neurobiol. 148, 217–243.

32
Pulmonary Gas Exchange in Anatomically-Based Models of the Lung

Annalisa Swan[1], Peter Hunter[2] and Merryn Tawhai[3]

Abstract Pulmonary gas exchange can be investigated at different scales of interest. Our approach is to couple models of gas exchange to anatomically-detailed models of the airway and pulmonary vascular trees. We are linking a hierarchy of models from the capillary segment up to the whole lung, so that a change in the detailed small-scale behaviour has a flow-on effect to function at a larger scale. The anatomically-based models will be used to understand how regional perturbations to the structure or function of the airway and vascular trees and the state of health of the functional tissue affect gas exchange. We are interested in the degree to which the system can be perturbed before it is detected by standard laboratory measures.

1 Introduction

Pulmonary gas exchange has been studied extensively using computational models. Most modelling approaches investigate the behaviour of the whole pulmonary system in response to different inputs. These often take the form of "lumped compartment" models (*e.g.*, Liu, Niranjan, Clark, San, Zwischenberger and Bidani 1998) or "feedback systems" models that usually couple lumped blood and alveolar compartments incorporating lung, heart and tissue interactions. A few authors model gas exchange in anatomically-based geometries (*e.g.*, Felici, Filoche, Straus, Similowski and Sapoval 2005); however, none consider capillary network geometry. In this study, we incorporate gas exchange into detailed models of the airway and vascular trees. These models couple finite deformation elasticity to air and blood flow in order to predict regional inspired gas and perfusion and provide parameters for simulating gas exchange. We are linking together a hierarchy of models from the capillary segment up to whole lung. Outputs will be regional gas partial pressures in the blood and

[1] University of Auckland, Bioengineering Institute, a.swan@auckland.ac.nz

[2] University of Auckland, Bioengineering Institute, p.hunter@auckland.ac.nz

[3] University of Auckland, Bioengineering Institute, m.tawhai@auckland.ac.nz

M.J. Poulin and R.J.A. Wilson (eds.), *Integration in Respiratory Control: From Genes to Systems*.

airways. The motivation for this study is to answer the question: how much regional variation can occur before standard laboratory measures identify the disorder?

2 Current Work: Gas Exchange at the Capillary Scale

Each alveolus in the lung is surrounded by a dense mesh of capillaries that carry blood across the air-blood membrane. In this network, each capillary segment can be considered to be a gas exchange "unit." A model of gas exchange in a single segment is developed so that it can be integrated into a capillary network at the next level.

In the Burrowes microcirculation model (Burrowes, Tawhai and Hunter 2003), the dense capillary network on the surface of an alveolar sac is created using a Voronoi meshing technique. Capillary segments are modelled as 1D elements, and finite element methods are used to solve the pressure-flow relationship and describe blood cell transit through the network. Initially, we use this microcirculation model to solve the blood flow, hematocrit and dimensions for each capillary segment. These solutions are then used as input parameters in the gas exchange model.

There are many mathematical descriptions of pulmonary gas exchange in the literature. We base our work on the mathematical model of Ben-Tal (2006), which is a system of ordinary differential equations, which describe interactions between O_2 and CO_2 concentrations in the pulmonary blood and alveolar air. These are solved for a single capillary segment to find the partial pressures of O_2 (PO_2) and CO_2 (PCO_2) in the blood. The gas exchange model is a quasi-steady state. That is, we are taking a snapshot of the partial pressure distributions in a capillary for a given steady flow.

Assumptions in our model are: (1) blood entering the capillary network has the same composition as mixed venous blood entering the lung; (2) alveolar air partial pressures are constant; (3) the blood flow is constant through the capillary; (4) the interaction of other respiratory gases, such as nitrogen, is negligible. When applying the equations of Ben-Tal (2006) at the capillary level, the diffusive conductance (diffusing capacity) is calculated for each capillary segment. We use equations from Roughton and Forster (1957) and Holland, van Hezewijk and Zubzanda (1977) for the diffusive conductance and rate of O_2 binding to blood, respectively. Estimates of diffusive conductance for each capillary are uncertain because there is debate surrounding the values of parameters in these equations (Weibel 1997). Its importance needs to be investigated further.

3 Current Work: Gas Exchange at the Alveolar Sac Scale

Our alveolar sac model comprises 19 individual alveoli (Fig. 1a). Based on morphological data (Weibel 1963), Burrowes *et al*. (2003) estimated approximately four inlet arterioles and five outlet venules for a single alveolar sac.

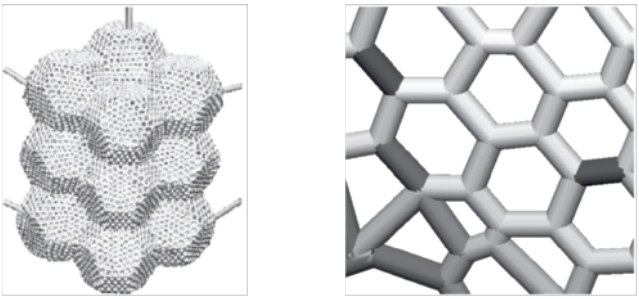

(a) (b)

Fig. 1 (a) Geometry of the capillary mesh that surrounds an alveolar sac (Burrowes *et al*. 2003). (b) PO_2 solution shown in a close-up view of the capillary mesh. Dark grey indicates segments with high blood PO_2

Partial pressure distributions for O_2 and CO_2 are found by iteratively solving the gas exchange ODEs for each capillary segment. A segment cannot be evaluated until all preceding segments that supply blood to that segment are solved. Once the partial pressures of the incoming blood are known, the partial pressures at the opposing end (node) of the segment can be solved. Figure 1b shows the detail of the capillary network, which is predominantly hexagonal. In segments with low flow rates, blood becomes more oxygenated because it spends longer in that segment (higher PO_2 is indicated by dark grey segments).

In order to find the PO_2 at the start node for a given segment, we need to know the end PO_2 for each of the preceding segments. If two or more segments converge at a junction, these segments will have differing flow rates, end PO_2, hemoglobin contents and hemoglobin saturations.

To calculate the PO_2 in the mixed blood just past the junction, we must compare the equilibration time for the reaction between oxygen and hemoglobin with the transit time of blood through the capillary segment. Most mathematical models of pulmonary gas exchange assume instantaneous equilibration because the reaction time is much less than the transit time of blood through the lung. However, these times are similar at the capillary scale.

If we assume that O_2-Hb reaction is instantaneous, then the combined blood will be in equilibrium. Conversely, if we assume a very long equilibration time, then the PO_2 of the mixed blood will simply be the flow-weighted average of the PO_2 of the preceding segments. Comparing both extremes of the reaction time (instantaneous equilibration and no equilibration), we found that the average end PO_2 for an alveolar sac changes by 1.2%, showing little difference in applying either assumption.

The model produces results that are compatible with the scarce experimental evidence in the literature for capillary blood partial pressures, which gives us confidence in the model. It is known that a single red blood cell will traverse about two

or three alveoli en route from pulmonary artery to pulmonary vein (West 2000), and that blood PO_2 is equilibrated by about one third of the distance along the capillary bed in a healthy lung. The model predicts that the blood PO_2 is in equilibrium with the alveolar PO_2 after traversing one alveolus. It is probable that the current model predicts the blood to equilibrate too rapidly because the partial pressures in the alveolar air are held constant, so these do not decrease as the oxygen moves across the membrane into the blood. Varying alveolar air partial pressures will be incorporated into the model at a later stage.

During moderate exercise, the blood flow rate increases by 4–5 times the resting rate. Although the blood spends less time in the pulmonary capillary bed during exercise, the blood PO_2 fully equilibrates by the time it leaves the lung (Poole and Musch 2000). To simulate this condition, the boundary conditions for an alveolar sac are set to resting values. In order to simulate the conditions of exercise, the PO_2 distributions are solved for an increased inlet flow boundary condition. Recruitment of other regions of the lung is ignored.

While the blood PO_2 distributions for the normal flow and the increased flow scenarios differ noticeably, outlet PO_2 values are very similar. Figure 2 shows the distributions for the different flow scenarios: many more capillary segments have a high blood PO_2 for a resting flow rate. Table 1 shows that the average PO_2 at the outlet vessels is only 3% below the alveolar air PO_2 (alveolar PO_2 is set to 97.5 mmHg) for a flow rate of five times the resting rate. This result gives confidence in the gas exchange model: under "exercise" conditions, the blood still equilibrates with the alveolar partial pressures.

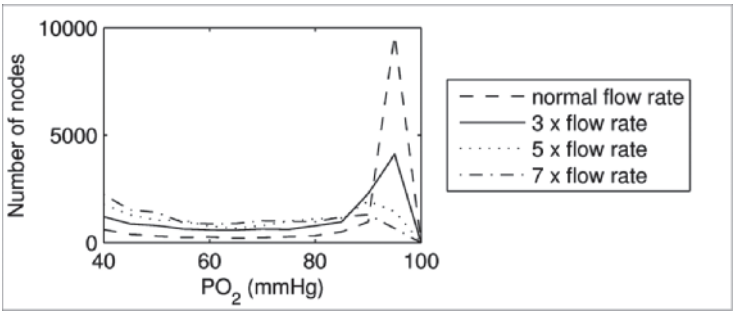

Fig. 2 PO_2 distributions in the alveolar sac capillary mesh for different inlet blood flows

Table 1 Average outlet PO_2 for different flow scenarios

Flow scenario	Total flow into network	Average outlet PO_2	Reduction from alveolar PO_2
normal	0.00616 mm^3/s	97.492 mmHg	0.008 %
3 × flow rate	0.01847 mm^3/s	96.413 mmHg	1.115 %
5 × flow rate	0.03078 mm^3/s	94.458 mmHg	3.120 %

4 Future Directions

We will develop a lumped alveolar sac model that does not contain capillary network detail. Regional gas distributions in the acinus will provide inputs into the lumped alveolar sac models, enabling investigation of regional gas exchange in the acinus.

A model of ventilation distribution coupled to soft tissue mechanics, predicting airflow in the conducting airways, will provide 'air-side' boundary conditions (Hedges, Hunter and Tawhai 2006). Similarly, a model for perfusion of the arterial and venous trees coupled to soft issue mechanics will provide 'blood-side' boundary conditions. Regional gas exchange will be investigated by setting different air-side and blood-side boundary conditions to correspond to different postures, magnitudes of gravity, exercise or disease.

Acknowledgements We acknowledge Dr. Alona Ben-Tal from Massey University and Dr. Kelly Burrowes from the University of Oxford for their ready explanations and invaluable input.

References

Ben-Tal, A. (2006) Simplified models for gas exchange in the human lungs. Journal of Theoretical Biology 238(2), 474–495.

Burrowes, K.S., Tawhai, M.H and Hunter, P.J. (2003) Modeling RBC and neutrophil distribution through an anatomically based pulmonary capillary network. Annals of Biomedical Engineering 32(4), 585–595.

Felici, M., Filoche, M., Straus, C., Similowski, T. and Sapoval, B. (2005) Diffusional screening in real 3D human acini–a theoretical study. Respiratory Physiology and Neurobiology 145(2–3), 279–293.

Hedges, K.L., Hunter, P.J. and Tawhai, M.H. (2006) Image-based computational model of a breathing lung. Proceedings of the American Thoracic Society (PATS), abstract, [Online], 3, A876. Available: http://www.abstracts2view.com/ats06/sessionindex.php [7 September 2006].

Holland, R.A.B., van Hezewijk, W. and Zubzanda, J. (1977) Velocity of oxygen uptake by partly saturated adult and fetal human red cells. Respiration Physiology 29(3), 303–314.

Liu, C.H., Niranjan, S.C., Clark, J.W., Jr., San, K.Y., Zwischenberger, J.B. and Bidani, A. (1998) Airway mechanics, gas exchange, and blood flow in a nonlinear model of the normal human lung. Journal of Applied Physiology 84(4), 1447–1469.

Poole, D.C and Musch, T.I. (2000) Pulmonary and Peripheral Gas Exchange During Exercise. In: J. Roca, R. Rodriguez-Roisin and P.D. Wagner (Eds.), *Pulmonary and Peripheral Gas Exchange in Health and Disease*. Marcel Dekker, Inc., New York, pp. 469–523.

Roughton, F.J.W. and Forster, R.E. (1957) Relative importance of diffusion and chemical reaction rates in determining rate of exchange of gases in the human lung, with special reference to true diffusing capacity of pulmonary membrane and volume of blood in the lung capillaries. Journal of Applied Physiology 11, 290–302.

Tawhai, M.H. and Hunter, P.J. (2001) Characterising respiratory airway gas mixing using a lumped parameter model of the pulmonary acinus. Respiration Physiology 127(2–3), 241–248.

Weibel, E.R. (1963) *Morphometry of the Human Lung*. Springer-Verlag, Berlin.

Weibel, E.R (1997) Design and morphometry of the pulmonary gas exchanger. In: R.G. Crystal, J.B. West, E.R. Weibel, and P.J. Barnes (Eds.), *The Lung; Scientific Foundations (2nd edition)*. Lippincott-Raven Publishers, Philadelphia, pp. 1147–1157.

West, J.B. (2000) *Respiratory Physiology: The Essentials (6th edition)*. Lippincott Williams & Wilkins, Philadelphia, PA.

33
Multi-scale Models of the Lung Airways and Vascular System

Merryn H. Tawhai[1] and Kelly S. Burrowes[2]

Abstract Medical imaging now enables measurement of the lung *in vivo* at controlled volumes, prompting the development of increasingly sophisticated models of the geometry of the lung, from the largest airways and vessels to the alveolar tissue and capillary bed. We have developed methods for deriving subject-specific models of the airway and pulmonary vascular trees and have developed methods to represent the structure of alveolated parenchymal tissue and the segmented alveolo-capillary network. These multi-scale models have geometry that is consistent with published lung morphometry and have defined relationships with one another. The models can therefore be readily exploited to couple multiple processes at the same physical scale (*e.g.*, tissue mechanics and blood flow), or to couple over multiple scales (*e.g.*, Newtonian flow in the large elastic blood vessels, and two-phase fluid transit in the microcirculation). We have studied function in the peripheral pulmonary system (alveolated airways and accompanying arterial and venous vessels) using a multi-scale approach that integrates detailed structure at this level of interest with estimates of air, blood and tissue pressures from functional models in the larger airways and vessels and simulations of soft tissue deformation of the whole lung. This approach allows us to study how ventilation of the acinus, mixing of inert gases and perfusion of the capillary bed varies with gravity, location in the lung and posture. An extension of the multi-scale models is incorporation of respiratory gas exchange, which can also be considered at several scales of interest.

1 Introduction

Alteration of the normal structure or function of the lung ultimately results in an impairment of gas exchange, and we can consider mechanisms that affect this at several scales of interest. For example, at the organ level we may consider the effect of gravity or lung orientation on deformation of the lung tissue and how this changes

[1] University of Auckland, Bioengineering Institute, m.tawhai@auckland.ac.nz

[2] University of Auckland, Bioengineering Institute, k.burrowes@auckland.ac.nz

M.J. Poulin and R.J.A. Wilson (eds.), *Integration in Respiratory Control: From Genes to Systems*.

when material properties are altered by disease (Tawhai, Nash and Hoffman 2005); in the conducting airways we may consider the consequence of airway constriction, investigating the redistribution of flow (Tgavalekos, Tawhai, Harris, Venegas and Lutchen 2005); one mechanism of interest at the level of the pulmonary acinus is the effect of 'diffusional screening' on gas exchange (Felici, Filoche, Straus, Similowski and Sapoval 2005); and in the alveolo-capillary bed we may be interested in preferential pathways for blood cell transit (Burrowes, Tawhai and Hunter 2004).

At any level, assumptions must be made about the conditions under which the system operates. For example, for blood transport in the capillary, the inlet arteriole and outlet venule blood pressures must be specified, as well as the expanding forces acting on the alveolar septa that modify the 'height' of the capillary (Huang, Doerschuk and Kamm 2001). We can scale physiological measurements or estimates at the organ level to obtain the necessary parameters, or we can use a multi-scale approach to estimate a range of functional parameters based on a detailed model at another scale of interest. In the case of capillary flow, this may be simulation of flow through the arterial and venous trees and continuum mechanics theory to estimate tissue-expanding forces.

The advantages of estimating parameters based on physiological measurements are simplicity, clarity and consistency with previous studies but not necessarily accuracy: scaling (*e.g*,. blood pressure to the level of the arteriole requires major assumptions). Using multi-scale models is a more involved approach that may be criticised for its apparent complexity. However, when the links between each model scale are made clear, it is straightforward to specify a range of parameters that may be important, and we can investigate how an alteration in structure and/or function at one scale affects function at another scale.

Multi-detector row computed tomography (MDCT) imaging of the air-filled lung tissue provides high resolution data from which subject-specific interdependent models of lung geometry can be constructed as computational domains through which a set of governing equations will be solved to simulate and understand function. By developing models on a subject-specific basis, the resulting computational meshes have spatially consistent relationships. The process of coupling functional models within the systems is therefore far more straightforward than for models developed independently from different data sets.

2 Air Flow in the Conducting Airways

Air flow can be examined in detail by solving the continuity and Navier-Stokes equations in airway-like geometries to predict 3D patterns of flow and pressure. A major limitation is that the analysis is computationally expensive and hence generally limited to a small number of airways. A flow model that either reduces the equations to a 1D form or assumes Poiseulle flow is not as accurate as the 3D solution but is far less expensive. A 1D system of equations can be solved in an entire conducting airway tree domain to predict whole lung ventilation distribution, hence providing

boundary conditions (BCs) for flow and gas content into the acinus. By using spatially-distributed anatomically/imaging-based airway geometry, predictions of ventilation distribution can be compared against functional imaging.

Tawhai, Hunter, Tschirren, Reinhardt, McLennan and Hoffman (2004) detail a method to derive subject-specific models of the lung, lobe and airway tree from MDCT imaging. The lung and/or lobe boundary is segmented and used to define a finite element (FE) volume mesh for each individual lobe or lung. The airway centrelines are located and the diameters are measured from the MDCT images. The airway data is interpreted into a FE line mesh (1D) for the uppermost bronchial airways with an associated 'field' that records the airway diameter. A volume-filling branching (VFB) algorithm initiates at the end of the airway centrelines defined from imaging and bifurcates to fill the FE volume mesh. Comparison with morphometric studies has confirmed that the algorithm creates trees with average geometry that is representative of our current state of knowledge of the bronchial airway tree.

An advantage of using a 1D model in an anatomically-based tree is that deformation of the 'host' tissue can be used to set BCs for flow through the tree (Hedges, Hunter and Tawhai 2006). Air flow is driven by expansion and recoil of the parenchyma and is modified by airway calibre. Because regional distribution of air is influenced by gravity, posture and material properties, Hedges *et al*. (2006) use a finite deformation non-linear elasticity with sliding contact BCs to predict lung volume change and drive regional flow for different magnitudes and orientation of gravity. Using this iterative method we can examine the relationship between surface pressure, tissue stress, and regional ventilation.

3 The Pulmonary Acinus

The parenchymal (alveolar) tissue has previously been modelled as a 3D space-filling structure for studying micro-mechanics and deriving effective continuum material properties for the parenchyma (Denny and Schroter 2006) and as a space-filling base structure for modelling the pulmonary microcirculation (Burrowes *et al*. 2004). In these examples, the alveoli are multi-faceted and space filling and have shapes that are consistent with real alveoli.

Paiva and co-investigators have used a 1D modelling approach to reduce the complexity of the space-filling alveolar tissue to a tractable model for simulating gas mixing (*e.g*., Verbanck and Paiva 1990; Dutrieue, van Holsbeeck, Verbanck and Paiva 2000). The respiratory airway models have airspace dimensions based upon anatomical data, and they incorporate the alveolar volume as an annulus around each duct. While the multi-branching model has generally been used to understand mixing of inert gases, it is also applicable to predicting distributed concentration of respiratory gases; however, an additional set of equations must be incorporated to account for transfer with the blood. This type of model is sufficient to understand distribution within an average acinus, but to see how exchange is influenced by regional conditions the model must be exposed to appropriate BCs for local ventilation and perfusion, both of which result from coupled functions.

4 The Pulmonary Capillaries

Burrowes *et al*. (2004) isolated a single alveolar sac comprising 19 alveoli around a central duct to use as a scaffold for creating an alveolo-capillary network. The method creates a continuous segmented network using a 2D Delaunay/Voronoi meshing method. The method was designed to ensure that there is a single layer of capillaries between adjacent alveoli that open to the same alveolar duct. The segmented model was used to investigate regional capillary transport in an upright human lung, with function based on the model of Huang *et al*. (2001). The model predicts the distribution of hematocrit and flow rate (including preferential pathways) for a given set of pleural and blood pressures.

5 Perfusion of the Pulmonary Arterial Tree

Burrowes *et al*. (2005b) examined blood flow in an anatomically-based model of the pulmonary arterial tree (Burrowes *et al*. 2005a) when vessels were exposed to an idealized linear pleural pressure gradient of 0.25 cmH_2O/cm of cranio-caudal lung 'height'. Significant heterogeneity was predicted in blood flow entering the capillary bed in any iso-gravitational plane of the upright lung. Burrowes and Tawhai (2005c) compared flow in zero G (no pleural pressure gradient) and normal G in anatomically-based and symmetric branching (with spatial distribution) models. In both cases, the effect of gravity was similar, reducing flow in the non-dependent regions and increasing flow in the dependent regions. An interesting finding was that the branching geometry of the anatomically-based model was sufficient to cause a decrease in flow in the most dependent region (equivalent to West's zone 4) in isolation from any effect of tissue compression.

Burrowes and Tawhai (2006) have advanced this model to calculate the pressures acting on the arterial tree from solution of finite elasticity for a lung at total lung capacity and functional residual capacity, upright, prone and supine. The variation in peripheral flows within any iso-gravitational plane that is inherent in the anatomically-based branching models provides a range of flow conditions under which gas exchange could be estimated, and the coupled mechanics approach provides a distribution of regional tissue expansion in hand with regional estimates of arteriole flow.

6 Multi-scale Boundary Conditions for Gas Exchange

We do not seek to develop a new system of equations to describe the exchange of gases; we aim to develop a multi-scale framework that links several coupled structural and functional systems to provide realistic BCs within which any established model for gas exchange can operate. The multi-scale modelling framework is far from complete: methods have been developed for deriving anatomically-based geometric

models of the lung lobes, pulmonary airways, vascular trees, parenchymal tissue and alveolo-capillary bed; specific function has been simulated within each system independently, and model coupling has been achieved for soft tissue mechanics and airflow or perfusion of the large vessels.

Further detail on linking to models of gas exchange can be found in the article by Swan, Hunter, and Tawhai (2006) in this issue.

References

Burrowes, K.S., Tawhai, M.H. and Hunter, P.J. (2004) Modeling RBC and neutrophil distribution through an anatomically based pulmonary capillary network. Ann. Biomed. Eng. 32, 585–595.

Burrowes, K.S., Hunter, P.J. and Tawhai, M.H. (2005a) Anatomically-based finite element models of the human pulmonary arterial and venous trees including supernumerary vessels. J. Appl. Physiol. 99, 731–738.

Burrowes, K.S., Hunter, P.J. and Tawhai, M.H. (2005b) Evaluation of pulmonary arterial flow heterogeneity via an image-based computational model. Acad. Radiol. 12, 1464–1474.

Burrowes, K.S. and Tawhai, M.H. (2005c) Computational predictions of pulmonary blood flow gradients: Gravity versus structure. Resp. Physiol. Neurobiol., in press. doi:10.1016/j.resp.2005.11.007:2005.

Burrowes, K.S. and Tawhai, M.H. (2006) Evaluation of the effect of lung deformation on pulmonary blood flow distributions via a computational model of coupled mechanics-flow. Proc. Am. Thorac. Soc. 3 (Abstracts Issue, ATS 2006), A705.

Denny, E. and Schroter, R.C. (2006) A model of non-uniform lung parenchyma distortion. J. Biomech. 39, 652–663.

Dutrieue, B., van Holsbeeck, F., Verbanck, S. and Paiva, M. (2000) A human acinar structure for simulation of realistic alveolar plateau slopes. J. Appl. Physiol. 89, 1859–1867.

Felici, M., Filoche, M., Straus, C., Similowski, T. and Sapoval, B. (2005) Diffusional screening in real 3D human acini - a theoretical study. Resp. Physiol. Neurobiol. 145, 279–293.

Hedges, K.L., Hunter, P.J. and Tawhai, M.H. (2006) Image-based computational model of a breathing lung. Proc. Am. Thorac. Soc. 3 (Abstracts Issue, ATS 2006), A876.

Huang, Y., Doerschuk, C.M. and Kamm, R.D. (2001) Computational modeling of RBC and neutrophil transit through the pulmonary capillaries. J. Appl. Physiol. 90, 545–564.

Tawhai, M.H., Hunter, P.J., Tschirren, J., Reinhardt, J.M., McLennan, G. and Hoffman, E.A. (2004) CT-based geometry analysis and finite element models of the human and ovine bronchial tree. J. Appl. Physiol. 97, 2310–2321.

Tawhai, M.H., Nash, M.P. and Hoffman, E.A. (2006) An imaging-based computational approach to model ventilation distribution and soft tissue deformation in the ovine lung. Acad. Radiol. 13, 113–120.

Tgavalekos, N., Tawhai, M.H., Harris, R.S., Venegas, J. and Lutchen, K.R. (2005) Identifying airways responsible for heterogeneous ventilation and mechanical dysfunction in asthma: An image-functional modeling approach. J. Appl. Physiol. 99, 2388–2397.

Swan, A., Hunter, P.J. and Tawhai, M.H. (2006) Pulmonary gas exchange in anatomically-based models of the lung, submitted.

Verbanck, S. and Paiva, M. (1990) Model simulations of gas mixing and ventilation distribution in the human lung. J. Appl. Physiol. 69, 2269–2279.

34
Modeling Structure-Function Interdependence of Pulmonary Gas Exchange

Ewald R. Weibel

Abstract Modeling functional processes, such as gas exchange, that occur deep in the lung far from where one can directly observe, depends on knowledge about the precise and quantitative design of the structure of the gas exchanger. This is the case as well for the actual arrangement of alveoli and blood capillaries at the gas exchange surface as for the disposition of gas exchange units with respect to the airway and vascular trees. The serial arrangement of alveoli and their perfusion as parallel units have important consequences for gas exchange.

1 Modeling the Structural Basis of Lung Function

To a physiologist, the lung looks like a black box: what happens at the site critical for gas exchange, where air in alveoli and blood in capillaries meet, cannot be observed, it must be deduced from indirect measurements. In order to develop a clear understanding of what can happen, it is helpful to resort to models that attempt a theoretical formulation of the various interacting processes in such a way that the predictions can be tested by experiment. Two basic types of such models are to be discussed in the following chapters of this volume: (1) models attempting an in silico reconstruction of lung structure, from the airways and blood vessels to the gas exchange region (Tawhai, this volume); (2) physico-mathematical models of the processes occurring as a precondition for gas exchange (Sapoval and Filoche, this volume).

A primary condition for the validity of such models is that they faithfully reflect the structural design of the pulmonary gas exchanger, both in terms of its topology and of its quantitative aspects. Such information has been assembled over the past decades by using various morphometric techniques and using electron and light microscopy as well as macroscopic methods (Weibel 1963; 2000). Recently, it has also become possible to obtain such information *in vivo* by high resolution computed tomography (Tawhai, Hunter, Tschirren, Reinhardt, McLennan and Hoffman 2004). This chapter presents the essentials of the morphometric basis of the pulmonary

University of Berne, Institute of Anatomy, weibel@ana.unibe.ch

M.J. Poulin and R.J.A. Wilson (eds.), *Integration in Respiratory Control: From Genes to Systems*. © Springer 2008

gas exchanger and its topology as a backdrop to the following attempts at modeling the structure and the functional processes of gas exchange.

2 The Structure of the Pulmonary Gas Exchanger

The lung's main function is to transfer O_2 to the erythrocytes of the blood and to eliminate CO_2. To this end, air and blood must be brought into intimate contact. Airways and blood vessels are designed as trees that branch in concert to reach into all corners of the lung parenchyma. Here they converge in a foam-like structure: the airways form tightly packed alveoli (Fig. 1a) in whose walls or septa the blood spreads out in a dense capillary network fed by pulmonary arteries and drained by the pulmonary veins (Fig. 1b). Electron micrographs of alveolar walls show that the capillary blood occupies half the volume of the alveolar septa with a very thin tissue barrier separating air and blood (Fig. 1c and 1d). This establishes good conditions for gas exchange that is favored by a large surface of contact across a thin barrier.

3 A Model for Pulmonary Gas Exchange

Oxygen flow from air to blood is driven by the difference between alveolar and mean capillary O_2 partial pressure, $PA_{O2} — Pc_{O2}$, as the functional parameter, and the lung's O_2 conductance, called the pulmonary diffusing capacity DL_{O2}:

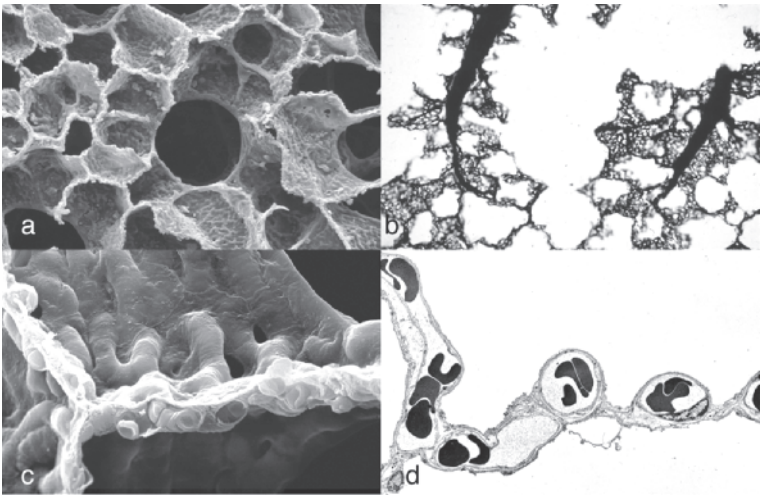

Fig. 1 Fine structure of the pulmonary gas exchanger. (a) Tightly packed alveoli surround alveolar ducts; (b) A dense network of blood capillaries forms in the alveolar septa, fed by the end-branches of pulmonary arteries and drained by veins; (c) Human alveolar septum in scanning electron micrograph; and (d) The tissue barrier separating air and blood is very thin

$$\dot{V}_{O2} = (PA_{O2} - Pc_{O2}) \cdot DL_{O2}$$

DL_{O2} is largely determined by design parameters: the gas exchange surface, the thickness of the barrier and capillary blood volume. A model for calculating DL_{O2} on the basis of morphometric data breaks the diffusion path into two sequential steps, where the first step, Db_{O_2}, is diffusion across a barrier composed of the tissue sheet and the blood plasma (Fig. 1d), and the second step, De_{O_2}, comprises the diffusion of oxygen into the red blood cells and the binding to the hemoglobin molecules. The two serial conductances are added as reciprocals, *i.e.,* as resistances, to yield the total pulmonary diffusing capacity DL_{O_2}:

$$DL_{O_2} = [Db_{O_2}^{-1} + De_{O_2}^{-1}]^{-1}$$

where

$$Db_{O_2} = K_{O_2} \cdot (S(a) + S(c))/2 \cdot \tau_{hb}$$
$$De_{O_2} = \theta_{O_2} \cdot V(c)$$

We notice that four morphometric parameters enter this system of equations, namely the alveolar and capillary surface areas *S(a)* und *S(c)*, the capillary volume *V(c)* and the harmonic mean thickness of the barrier between air and erythrocytes, τ_{hb}. The barrier conductance is further determined by Krogh's diffusion coefficient K_{O2}. The erythrocyte conductance is determined by the rate of O_2 binding to hemoglobin θ_{O_2}, which depends on the O_2-hemoglobin reaction kinetics and on the capillary hematocrit which, in fact, is also a morphometric parameter. As K_{O_2} and θ_{O_2} are known constants the estimation of the morphometric parameters will then allow an estimation of DL_{O_2}.

This can be illustrated on the example of the human lung for which good morphometric data exist (Gehr, Bachofen and Weibel 1978; Weibel, Federspiel, Fryder-Doffey, Hsia, König, Stalder-Navarro and Vock 1993). It is found that the alveolar surface area is on the order of 130 m^2, that of the capillary bed about 10% less, the capillary volume amounts to no more than 200 ml and the harmonic mean barrier thickness measures 1.1 µm. This results in an estimated theoretical diffusing capacity of 158 ml $O_2 \cdot min^{-1} \cdot mmHg^{-1}$. This means that for a P_{O2} difference of 1 mmHg the pulmonary gas exchanger can transfer 158 ml O_2 from the air to the erythrocytes; to achieve an O_2 uptake of 4 L•min^{-1}, as required by a human running at $\dot{V}_{O_2}$max, an alveolar-capillary P_{O_2} difference of 30 mmHg would be needed.

If the lung were designed efficiently, *i.e.,* without excess capacity, we would predict that DL_{O2} is fully exploited at $\dot{V}_{O_2}$max, the limiting value of O_2 uptake elicited by running very hard. This prediction is only partly supported by experimental evidence. It has been estimated that the physiological diffusing capacity of a normal human is about 100 ml $O_2 \cdot min^{-1} \cdot mmHg^{-1}$. It thus appears that the lung is designed with an excess diffusing capacity of 30%; this can be interpreted as a "safety factor" in several respects: (1) athletes can increase their oxygen consumption by about 30%, but evidence shows that the lung of a grown-up human cannot increase the size of its gas exchange apparatus to any appreciable degree, so that it must be assumed that athletes can train up to their existing DL_{O_2}, which would then be a limiting factor for aerobic

exercise; (2) the alveolar P_{O_2} as the driving force for oxygen uptake is affected by the P_{O2} in ambient air which can be reduced, *e.g.,* at high altitude. It is interesting that normal humans can maintain their arterial O_2 saturation while working at high altitude, thus presumably exploiting their somewhat excessive DL_{O2}, whereas athletes cannot: their diffusing capacity becomes the limiting factor for oxygen uptake.

4 Critique of the Model

Another possibility is that DL_{O2} is only apparently excessive because our model does not adequately consider the design complexity of the gas exchanger in relation to physiological constraints. Fig. 2 shows that alveoli form as side-chambers on the last eight generations, on average, of the 23-generations airway tree of the human lung. The complex of airways that emanate from a transitional bronchiole (Fig. 2b) thus form a ventilation unit called the pulmonary acinus. In contrast, the pulmonary arteries reach deep into the acinus forming terminal branches at about the level of alveoli (Fig. 1b) so that there are several thousand terminal arterioles within each acinus. As a consequence, alveolar-capillary gas exchange units are arranged all along the acinar pathway (Fig. 3B).

A morphometric analysis of the human pulmonary acinus showed that the acinar airways continue to branch by dichotomy (Haefeli-Bleuer and Weibel 1988). This causes the number of branches to double with each generation so that in the last or 8th generation there are about 256 alveolar sacs, the same number as the sum of the branches in generations 1–7. Since alveoli form as side-chambers of these airways, it is evident that half of all alveoli are located in the last generation. Accordingly, over half the diffusing capacity are contained in the last generation.

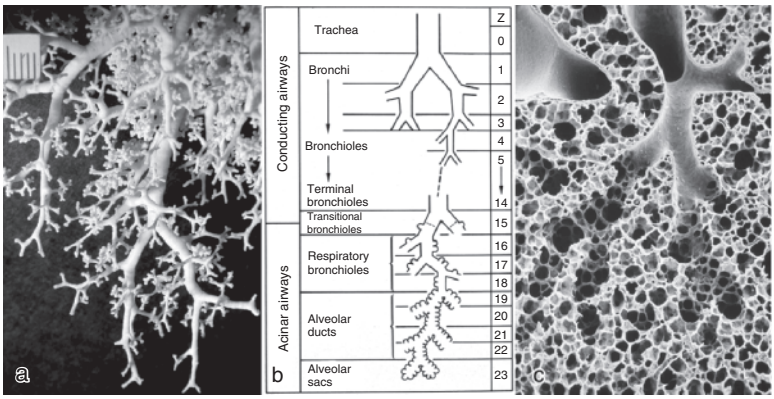

Fig. 2 Design of the airways. The airway tree, shown in a cast in (a) branches by dichotomy with the diameter reduced with each generation by an approximately constant factor. This branching continues as the airways reach into the lung parenchyma where alveoli form as side chambers (c) on the last eight generations of the 23-generation airway tree (b)

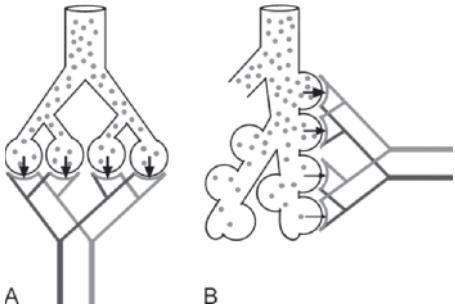

Fig. 3 Models of the relation between the ventilation and perfusion units in the pulmonary acinus. (A) Traditional model with alveoli ventilated and perfused in parallel. (B) Revised model with alveoli ventilated in series but perfused in parallel

This is of high significance for modeling gas exchange because the alveoli in this last generation may be disfavored in terms of O_2 supply by ventilation. On inspiration, the fresh air bolus is brought into the first or central parts of the acinus; from there, O_2 must reach the gas exchange surface by diffusion in the air phase. While diffusing peripherally along the duct system, O_2 molecules are exposed to alveoli with their absorbing surface, eager to load O_2 onto blood (Fig. 3B). So, some O_2 will be absorbed along the way, a process called screening (Sapoval, Filoche and Weibel 2002). This will reduce the prevailing alveolar P_{O2} in the major part of the gas exchanger and thus reduce the efficiency of gas exchange.

5 Conclusions

In order to understand what happens inside the "black box" of the pulmonary gas exchanger, it is not sufficient to describe the effect of structural design by a bulk parameter such as DL_{O2}, estimated on the basis of morphometric data relating to the whole lung. New approaches are needed in order to assess, in addition, the effect of higher order structural design features, such as the hierarchical branching pattern, on gas exchange. Here the detailed *in silico* modeling efforts, as discussed in the following by M. Tawhai, combined with the advanced physico-mathematical analysis, as presented by B. Sapoval and M. Filoche, will be of great value in advancing a deeper understanding of the processes allowing and constraining gas exchange.

References

Gehr, P., Bachofen, M. and Weibel, E.R. (1978) The normal human lung: ultrastructure and morphometric estimation of diffusion capacity. Respir. Physiol. 32, 121–140.

Haefeli-Bleuer, B. and Weibel, E.R. (1988) Morphometry of the human pulmonary acinus. Anat. Rec. 220, 401–414.

Sapoval, B., Filoche, M. and Weibel, E.R. (2002) Smaller is better – but not too small: A physical scale for the design of the mammalian pulmonary acinus. PNAS 99, 10411–10416.

Tawhai, M.H., Hunter, P., Tschirren, J., Reinhardt, J., McLennan, G. and Hoffman, E.A. (2004) CT-based geometry analysis and finite element models of the human and ovine bronchial tree. J. Appl. Physiol. 97, 2310–2321.

Weibel, E.R. (1963) *Morphometry of the Human Lung*. Springer Verlag and Academic Press, Heidelberg-New York.

Weibel, E.R. (2000) *Symmorphosis: On Form and Function in Shaping Life*. Harvard University Press, Cambridge, MA.

Weibel, E.R., Federspiel, W.J., Fryder-Doffey, F., Hsia, C.C.W., König, M., Stalder-Navarro, V. and Vock R. (1993) Morphometric model for pulmonary diffusing capacity. I. Membrane diffusing capacity. Respir. Physiol. 93, 125–149.

Part VI
Plasticity and Adaptation

35
Ventilatory Control during Intermittent High-Intensity Exercise in Humans

Andrew J. Cathcart[1], Anthony P. Turner[2], Christopher Butterworth[3], Matthew Parker[4], John Wilson[5] and Susan A. Ward[6]

Abstract Intermittent supra-maximal cycling of varying work: recovery durations was used to explore the kinetics of respiratory compensation for the metabolic acidosis of high-intensity exercise (> lactate threshold, θ_L). For a 10:20 s duty-cycle, blood [lactate] ($[L^-]$) was not increased, and there was no evidence of respiratory compensation (RC); *i.e*, no increase in the ventilation ($\dot{V}_E$)-CO_2 output ($\dot{V}_{CO2}$) slope, nor fall in end-tidal PCO_2 ($PETCO_2$). For longer duty-cycles, $[L^-]$ was elevated, stabilizing (30 s:60 s exercise) or rising progressively (60 s:120 s, 90 s:180 s exercise). In addition, $\dot{V}_{CO2}$ and $\dot{V}_E$ now oscillated with WR, with evidence of delayed RC (progressive increase in $\dot{V}_E - \dot{V}_{CO2}$ slope; decrease in $PETCO_2$) being more marked with longer duty-cycles. These results, which extend earlier findings with supra- θ_L step and ramp exercise, are not consistent with an appreciable contribution to RC from zero-order central command or peripheral neurogenesis. The reasons for the slow RC kinetics are unclear, but may reflect in part the H^+-signal transduction properties of carotid chemoreceptors.

1 Introduction

For sub-θ_L steady-state work rates (WRs), $\dot{V}_E$ is closely matched to $\dot{V}_{CO2}$ with regulation of arterial PCO_2 ($PaCO_2$) and pH (pHa) (and PO_2) at or close to resting levels. However, $PaCO_2$ is transiently elevated early in the on-transient, reflecting a

[1] University of Glasgow, Institute of Biomedical & Life Sciences, A.Cathcart@bio.gla.ac.uk

[2] University of Edinburgh, Department of Physical Education, tony.turner@ed.ac.uk

[3] University of Glasgow, Institute of Biomedical & Life Sciences

[4] English Institute of Sport, Manchester, Matthew.Parker@eis2win.co.uk

[5] University of Glasgow, Institute of Biomedical & Life Sciences, John.Wilson@bio.gla.ac.uk

[6] University of Leeds, Institute of Membrane & Systems Biology, s.a.ward@leeds.ac.uk

M.J. Poulin and R.J.A. Wilson (eds.), *Integration in Respiratory Control: From Genes to Systems*.

slightly longer $\dot{V}_E$ time constant (τ) relative to $\tau\ \dot{V}_{CO2}$ (reviewed in Whipp and Ward 1991). Above θ_L, $\dot{V}_E$ control is complicated by the requirements to (a) clear the supplemental CO_2 load resulting from the rate of [bicarbonate] ($[HCO_3^-]$) decrease, and (b) effect respiratory compensation (RC) for the metabolic (lactic) acidosis (*i.e.*, hypocapnia from $\dot{V}_E$ increasing disproportionally to $\dot{V}_{CO2}$ - compensatory hyperventilation) to constrain the pHa fall (reviewed in Wasserman and Casaburi 1991; Whipp and Ward 1991). The carotid body (CB) chemoreceptors (CRs) have been implicated in RC mediation, given its absence in bilateral CB resection patients (Wasserman *et al*. 1975) and its modulation by manipulation of CB sensitivity in normal subjects (Rausch *et al*. 1991). However, RC kinetics appear to be surprisingly slow, as evidenced by (a) a transient 3–4 torr $PaCO_2$ increase during supra-θ_L step WR on-transients (Rausch *et al*. 1991) and (b) a delayed fall in $PaCO_2$ above θ_L for rapid ramp exercise (isocapnic buffering) with the slope of the corresponding $\dot{V}_E - \dot{V}_{CO2}$ relationship not being discernibly different from below θ_L (reviewed in Whipp and Ward 1991). We chose to explore RC kinetics further, using a supra-maximal intermittent exercise paradigm that dissociates the energetic requirements for the task from the resulting degree of metabolic-acidaemic stress: low work:recovery (W:R) frequencies result in a sustained elevation of blood [lactate] ($[L^-]$), while high frequencies can be performed with no discernible $[L^-]$ increase (Åstrand *et al*. 1960).

2 Methods

Six males performed cycle-ergometry: (a) a ramp test (15W/min) to the tolerable limit (t_{LIM}) for measurement of peak O_2 uptake ($\dot{V}_{O2}$ peak: 3.71 ± 0.47 l/min), peak WR (WRpeak: 315 ± 1 W) and estimation of θ_L (2.05 ± 0.55 l/min); and (b) four intermittent tests, with WR being switched, from a 20W baseline, between 120% WRpeak and 20W with a 1:2 W:R duty-cycle (Åstrand *et al*. 1960) (10 s:20 s, 30 s:60 s, 60 s:120 s, 90 s:180 s) for 30 min or to t_{LIM} (whichever was sooner). Volume (turbine) and gas concentrations (mass spectrometry) were measured for breath-by-breath determination of ventilatory and gas exchange variables. $[L^-]$ was measured from finger-tip samples at selected end-work and end-recovery points.

3 Results

$\dot{V}_{O2}$, $\dot{V}_{CO2}$ and $\dot{V}_E$ oscillated in response to the intermittent WR for all but the shortest duty-cycle (10:20 s), being more prominent the longer the duty-cycle. Formal frequency-domain characterization of response kinetics was not undertaken, as we were reluctant to make any assumptions *a priori* about model structure (*i.e.*, first-order vs. higher-order models incorporating elements related to the $\dot{V}_{O2}$ slow component, CO_2 buffering of metabolic H^+, and compensatory hyperventilation).

3.1 90:180s Duty-Cycle (Fig. 1, far left)

The 90:180 s blood [L^-] response was reminiscent of the "very-heavy intensity" domain for step exercise (Whipp 1996), increasing progressively with time to a value of 9.4 ± 0.8 mM at t_{LIM} which was reached after only 9.1 ± 4.2 min. The peaks of the $\dot{V}O_2$ oscillation quickly attained maximal values, and the corresponding nadirs did not fully recover to 20W baseline values. In contrast, the peaks of the $\dot{V}CO_2$ oscillation showed an initial overshoot which declined over the subsequent cycles, consistent with an early additional contribution from HCO_3^--buffering of metabolic H^+ (reviewed in Whipp and Ward 1991) at a time when [L^-] and (presumably) [H^+] were increasing most rapidly (Turner *et al*. 2006). The $\dot{V}E$ oscillation showed an opposing tendency, becoming more rather than less prominent over successive cycles. $PETCO_2$ thus fell progressively with time, with a superimposed WR-related oscillation such that $PETCO_2$ was high when $\dot{V}E$ and $\dot{V}CO_2$ were increasing. This developing RC was evident in a systematically increasing slope of the $\dot{V}E - \dot{V}CO_2$ relationship for successive W:R duty cycle (*see arrow*), relative to that of the first cycle whose slope (solid line) was not significantly different from that for sub- θ_L step exercise.

3.2 60:120s Duty-Cycle (Fig. 1, centre left)

[L^-] increased more slowly than for 90:180 s exercise, attaining a value of 9.1 ± 2.4 mM at 30 min. Responses were similar to those for the 90:180 tests but less striking, consistent with the less marked metabolic-acidaemic stress. RC was again delayed (no increase in $\dot{V}E - \dot{V}CO_2$ slope for the first duty-cycle (solid line)), with a subsequent progressive steepening during the test (*see arrow*). However, despite the longer test duration, RC was less marked than for 90:180s exercise: the $\dot{V}E - \dot{V}CO_2$ slope at the end of the test being less steep and the $PETCO_2$ decline less marked.

3.3 30:60s Duty-Cycle (Fig. 1, centre right)

The [L^-] increase was less marked than for the longer duty-cycles, stabilising after ~ 10 min at a value of 4.9 ± 1.1 mM for the remainder of the 30-min period, characteristic of the "heavy-intensity" domain for step exercise (Whipp 1996). The $\dot{V}O_2$ oscillations were less prominent (with peaks just > θ_L), and the $\dot{V}CO_2$ oscillations now showed little early overshooting. RC was also less prominent and still delayed.

3.4 10:20s Duty-Cycle (Fig. 1, far right)

Apart from a small early transient increase, 10:20 s [L^-] values remained at baseline (0.9 ± 0.7 mM); *i.e.,* characteristic of "moderate-intensity" step exercise

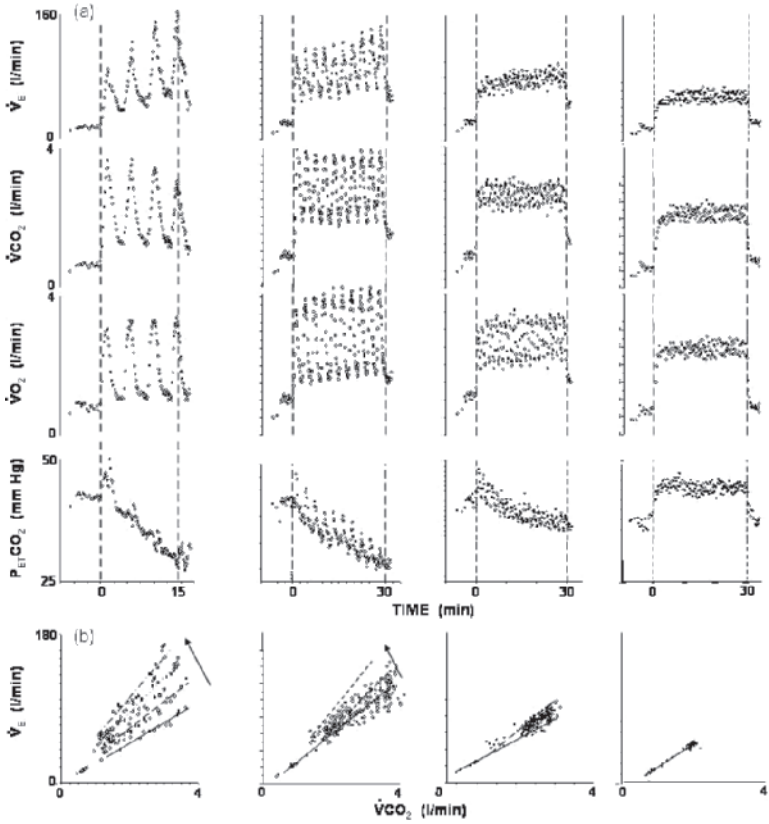

Fig. 1 Representative $\dot{V}E$, $\dot{V}CO2$, $\dot{V}O2$ and $PETCO_2$ responses (a) and $\dot{V}E - \dot{V}CO2$ relationships for successive W:R cycles (*arrow*) with superimposed linear regressions, (b) for (left-right) 90:180s (subj. 2), 60:120s (subj. 1), 30:60s (subj. 1) and 10:20s (subj. 3) W:R duty-cycles

(Whipp 1996). The $\dot{V}O2$ response stabilized within ~3 min (just < θL), and $\dot{V}CO2$ and $\dot{V}E$ within ~ 5–6 min, also reminiscent of moderate exercise (*e.g.,* Whipp and Ward 1991). However, in contrast to the longer duty-cycles, averaging successive breath-by-breath duty-cycle profiles to yield a single ensemble-averaged duty-cycle revealed no discernible oscillations in $\dot{V}O2$, $\dot{V}CO2$ or $\dot{V}E$. Also, $\dot{V}E - \dot{V}CO2$ slope was unaffected, and $PETCO_2$ was not decreased.

4 Discussion

That the $\dot{V}E$ response to intermittent supra-maximal exercise was highly dissociated from WR and therefore, inferentially, from both central command and peripheral neural drive from the exercising limbs does not support a significant role for these

feedforward drives (c.f. Waldrop *et al*. 1996), unless in the seemingly unlikely event that they manifest kinetics similar to those of $\dot{V}CO2$ and RC (c.f. Whipp and Ward 1991). In contrast, despite the supra-maximal WRs, $\dot{V}E$ was clearly not dissociated from the pulmonary CO_2 clearance requirement, whether simply from metabolic sources (*i.e.,* 10:20s exercise) or also from HCO_3^--buffering (30:60s, 60:120s, 90:180s exercise). Thus, even at supra-maximal WRs, it is as if the $\dot{V}E$ control system is somehow "aware" of the component of metabolic CO_2 production that is not expressed at the lungs but rather is stored in the high-capacitance (predominantly exercising-muscle) CO_2 stores. This stored component hence imposes no demand for an hyperpnoeic component to effect $PaCO_2$ regulation. However, the precise mechanisms involved in this apparently CO_2-linked control of $\dot{V}E$ remain conjectural.

The demonstration that RC was evident only for those duty-cycles that elicited a sustained metabolic acidosis, and was more striking the greater the acidosis (90:180s > 60:120s > 30:60s), argues for &Vdot;E responding to the metabolic-acidaemic stress (and/or its sequellae) with little regard to the WR *per se*. The delayed nature of the RC is consistent with earlier observations from supra- θL step (Rausch *et al*. 1991) and rapid-ramp (reviewed in Whipp and Ward 1991) exercise. RC has been proposed to be mediated largely by stimuli such as $[H^+]$, $[K^+]$, catecholamines, increased body temperature, adenosine and osmolarity (reviewed in Wasserman and Casaburi, 1991; Whipp and Ward, 1991; Kaufman and Forster 1996), although it is unclear why the apparent recruitment of such drives should be relatively slow. It has been suggested that this may reflect some time- or amplitude-related "threshold" for CBCR excitation (Whipp and Ward 1991), possibly at the level of an H^+-sensitive Type I voltage-sensitive tandem-P-domain K^+ (TASK-I) channel (Buckler *et al*. 2000) and involving slow intracellular pH response kinetics (Buckler *et al*. 1991).

References

Åstrand, I., Åstrand, P.-O., Christensen, E.H. and Hedman, R. (1960) Myohaemoglobin as an oxygen-store in man. Acta Physiol. Scand. 48, 454–460.

Buckler, K.J., Williams, B.A. and Honore, E. (2000) An oxygen, acid and anaesthetic sensitive TASK-like background potassium channel in rat arterial chemoreceptor cells. J. Physiol. 525, 135–142.

Buckler, K.J., Vaughan-Jones, R.D., Peers, C., Lagadicgossmann, D. and Nye, P.C.G. (1991) Effects of extracellular pH, PCO_2 and HCO_3^- on intracellular pH in isolated type-I cells of the neonatal rat carotid body. J. Physiol. 444, 703–721.

Kaufman, M. P. and Forster, H.V. (1996) Reflexes controlling circulatory, ventilatory and airway responses to exercise. In: L.B. Rowell and J.T. Shepherd (Eds.), *Handbook of Physiology, Section 12: Exercise: Regulation and Integration of Multiple Systems*. Oxford University Press, New York, pp. 381–447.

Rausch, S.M., Whipp, B.J., Wasserman, K. and Huszczuk, A. (1991) Role of the carotid bodies in the respiratory compensation for the metabolic acidosis of exercise in humans. J. Physiol. 444, 567–578.

Turner, A.P., Cathcart, A.J., Parker, M.E., Butterworth, C., Wilson, J. and Ward, S.A. (2006) Oxygen uptake and muscle desaturation profiles during intermittent cycling in humans. Med. Sci. Sports Exerc. 38, 492–503.

Waldrop, T.G., Eldridge, F.L., Iwamoto, G.A. and Mitchell, J.H. (1996) Central neural control of respiration and circulation during exercise. In: L.B. Rowell and J.T. Shepherd (Eds.), *Handbook of Physiology, Section 12: Exercise: Regulation and Integration of Multiple Systems*. Oxford University Press, New York, pp. 333–380.

Ward, S.A. (2003) Models of ventilatory control during exercise: peripheral chemoreflex considerations. Int. J. Computer Sci. 2, 52–65.

Wasserman, K. and Casaburi, R. (1991) Acid-base regulation during exercise in humans. In: B.J. Whipp and K. Wasserman (Eds.), *Pulmonary Physiology and Pathophysiology of Exercise*. Dekker, New York, pp. 405–448.

Wasserman, K., Whipp, B.J., Koyal, S.N. and Cleary, M.G. (1975) Effect of carotid body resection on ventilatory and acid-base control during exercise. J. Appl. Physiol. 39, 354–358.

Whipp, B.J. (1996) Domains of aerobic function and their limiting parameters. In: J.M. Steinacker and S.A. Ward (Eds.), *The Physiology and Pathophysiology of Exercise Tolerance*. Plenum, New York, pp. 83–89.

Whipp, B.J. and Ward, S.A (1991) The coupling of ventilation to pulmonary gas exchange during exercise. In: B.J. Whipp and K. Wasserman (Eds.), *Pulmonary Physiology and Pathophysiology of Exercise*. Dekker, New York, pp. 271–307.

36
Exercise-induced Respiratory Muscle Work: Effects on Blood Flow, Fatigue and Performance

J.A. Dempsey[1], J.D. Miller[2], L. Romer[3], M. Amann[4] and C.A. Smith[5]

In healthy subjects, heavy intensity endurance exercise places substantial demands on the respiratory muscles as breathing frequency, ventilation and the work of breathing rise over time. In the highly trained subject working at high absolute work rates, the ventilatory demand often causes varying degrees of expiratory flow limitation, sometimes accompanied by lung hyperinflation and, therefore, increased elastic work of breathing. Time-dependant increases in effort perceptions for both dyspnea and limb discomfort accompany these increased ventilatory demands. Similar responses to endurance exercise but at much lower exercise intensities also occur in patients with COPD and CHF. Note that these responses significantly influence exercise performance times in both health and disease. This effect was demonstrated by the marked reductions in the rate of rise of effort perceptions and the enhanced exercise performance times elicited by unloading the respiratory muscles using pressure support ventilation or proportional assist mechanical ventilation. In healthy fit subjects, unloading the inspiratory work of breathing by about one half increased performance by an average of 14% (Harms *et al*. 2000), and in CHF and COPD patients performance time more than doubled with respiratory muscle unloading (O'Donnell *et al*. 2001). Why are effort perceptions of limb discomfort markedly reduced and exercise performance increased when the respiratory muscles are unloaded? Our hypothesis is shown in Fig. 1.

We propose that this effect of respiratory muscle work and intrathoracic pressure development on performance and effort perception begins with the substantial amount of work and metabolic cost incurred by the respiratory muscles during sustained high intensity exercise. Thus, 10–15% of the total $\dot{V}O_2$ and cardiac output are estimated to be directed to the respiratory muscles in near maximum exercise (Dempsey *et al*. 2006). The substantial force development and high velocity of shortening required during prolonged exercise, combined with the need to compete with limb muscles for the available cardiac output, causes significant diaphragm and expiratory muscle fatigue during heavy intensity exercise. The exercise-induced diaphragm fatigue is prevented by unloading the respiratory muscles via mechanical ventilation.

[1–5] University of Wisconsin – Madison, John Rankin Laboratory of Pulmonary Medicine, jdempsey@wisc.edu

M.J. Poulin and R.J.A. Wilson (eds.), *Integration in Respiratory Control: From Genes to Systems*.

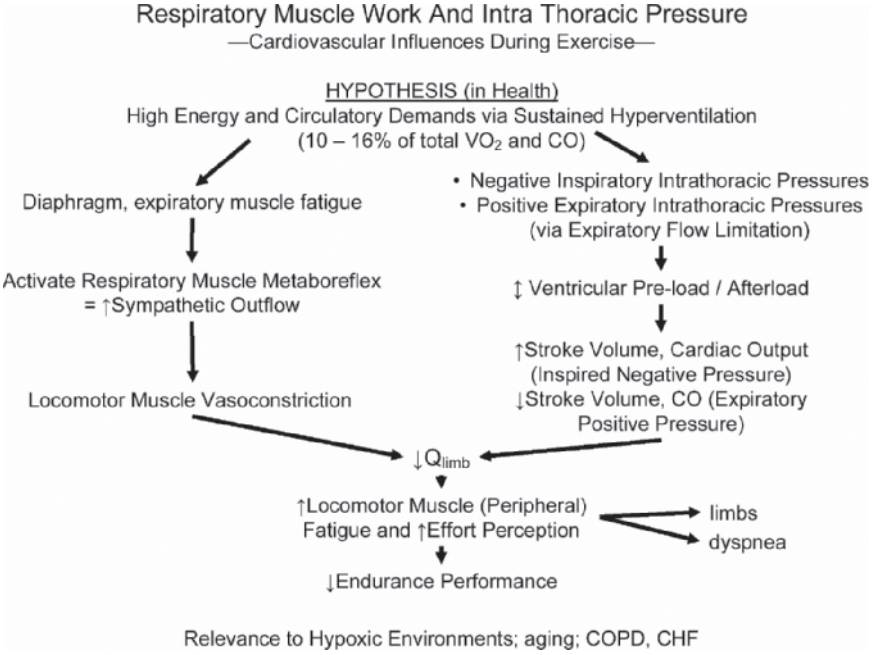

Fig. 1 Hypothesis: ventilatory requirements during sustained, high intensity exercise in healthy subjects leads to diaphragm fatigue and eventually to compromised limb blood flow and fatigue. In addition, inspiratory and expiratory swings in intra-thoracic pressure affect ventricular function (see text). The estimate of the fraction of the cardiac output (and VO_2) devoted to the respiratory muscles during exercise at peak work rate is derived from measurements of muscle blood flow via microspheres in ponies, from the oxygen cost of respiratory muscle work in humans and from the reductions in VO_2 and CO observed during respiratory muscle unloading in highly fit humans at maximal exercise (Dempsey *et al*. 2006)

The major consequences of this respiratory muscle fatigue are cardiovascular in nature. Recordings of electrical activity from metaboreflex receptors in the diaphragm in anesthetized rats show increased activity when the diaphragm is fatigued (via phrenic nerve stimulation) (Hill *et al*. 2000). Furthermore, measurements of muscle sympathetic nerve activity and vascular conductance in the resting limb muscle, and blood flow and vascular conductance in exercising humans and dogs (Dempsey *et al*. 2006), show that a supra-spinal metabo-reflex may be activated from the diaphragm via fatiguing contractions and metabolite accumulation, which cause vasoconstriction and reduced oxygen transport to the exercising limbs.

How might these reflex effects on limb blood flow affect performance? We think the critical effect here is on peripheral limb fatigue, because of the following lines of evidence. First, evidence from isolated contracting muscles shows that even very small reductions in blood flow diminish muscle force production. Second, in humans we used supra-maximal magnetic stimulation of the femoral nerve to quantify force output of the quadriceps before, and immediately following exercise, and

showed that sustained high intensity exercise to exhaustion caused 35–40% reductions in force output. With respiratory muscle unloading during exercise (compared to control conditions at the same power output and exercise duration), this exercise-induced peripheral muscle fatigue was reduced by 30–35% (Romer *et al*. 2006). So, exercise performance and the work of breathing are, at least in part, causally linked via the effects of respiratory muscle work on peripheral fatigue. In turn, this local fatigue effect is likely due to the compromised limb blood flow (see above). In addition, there are likely important feedback effects from peripheral fatigue development (of both respiratory and limb locomotor muscles) on the brain's perception of effort of both dyspnea and limb discomfort. In turn, the exacerbation of effort perception would be expected to precipitate a reduction in central motor output or so-called "central" fatigue.

In health, we emphasize that these effects of respiratory muscle work on peripheral fatigue of both respiratory and limb muscles and on performance likely only occur with high intensity sustained exercise. However, there are conditions in which we would expect the work of breathing to exert an even greater effect on peripheral fatigue and exercise performance. For example, when healthy subjects exercise in the hypoxia of high altitudes, there are marked effects on the work of breathing and on diaphragm fatigue. When the respiratory muscles were unloaded in these conditions (using mechanical ventilation), limb fatigue was reduced to a much greater extent than when unloading was carried out during exercise of similar intensity and duration in a normoxic environment (Amann, unpublished data). Although not directly tested as yet, indirect evidence to date also suggests that the work of breathing during even sub-maximal exercise would be a major determinant of limb blood flow, peripheral muscle fatigue and, therefore, exercise performance in patients with COPD and CHF (Stark-Leyva *et al*. 2004). These patients have the combined problem of a relatively low oxidative capacity of their limb locomotor muscles, together with hyperventilation and high levels of ventilatory work and expiratory flow limitation during exercise. In addition to these extra loads on the respiratory muscles, CHF patients have a limited cardiac output which would compromise blood flow to the diaphragm and possibly elicit respiratory muscle fatigue even during submaximal exercise.

Finally, it is important to emphasize that, in addition to the influence of the work, metabolic and blood flow requirements of the respiratory muscles during exercise, there are also cardiovascular effects resulting from large swings in intra-thoracic pressure that commonly occur in heavy exercise. Using continuous vascular flow probe measurements of cardiac output and limb blood flow in the exercising dog, we have recently observed that the normal negative intra-pleural pressure generated during inspiration is a significant determinant of stroke volume and cardiac output. That is, reducing these negative pressure swings during inspiration (using pressure support ventilation) was shown to *reduce* stroke volume in a healthy animal during mild intensity exercise, but *increased* stroke volume in the animal with CHF (Miller *et al*. 2006). This sharp contrast between healthy and CHF animals reflects the importance of intra-thoracic pressures on ventricular pre-load in health and on ventricular after-load in CHF. On the other hand, when intrathoracic pressure on

expiration is experimentally increased in order to minimize the effects of expiratory flow limitation during exercise, the stroke volume and cardiac output are reduced in both CHF and COPD (Miller *et al*. 2006). These cardiovascular effects of inspiratory and expiratory intrathoracic pressure in the exercising dog have also been reported in healthy humans during exercise (Stark-Leyva, Beck and Johnson 2004; Dempsey, Romer, Rodman, Miller and Smith 2006).

In summary, it is important to emphasize that, in health, over a wide range of exercise intensities the ventilatory responses are highly efficient, vitally important to homeostasis of systemic gas transport and contribute little to the limitation of exercise performance. However, in high intensity, sustained exercise in normoxia and in hypoxic environments in health, or in COPD and CHF patients during even submaximal exercise, the cardiovascular effects of the ventilatory response are substantial. Under these conditions, the work and metabolic requirements of the respiratory muscles and the exaggerated intra-thoracic pressures on inspiration and expiration now become significant determinants of cardiac output, limb blood flow, peripheral and central fatigue and ultimately exercise performance.

Acknowledgement Supported by NHLBI and the American Heart Association.

References

Dempsey, J.A., Romer, L., Rodman, J., Miller, J. and Smith, C. (2006) Consequences of exercise-induced respiratory muscle work. Respir. Physiol. Neurobiol. 151, 242–250.

Harms, C.A., Wetter, T.J., St Croix, C.M., Pegelow, D.F. and Dempsey, J.A. (2000) Effects of respiratory muscle work on exercise performance. J. Appl. Physiol. 89, 131–138.

Hill, J.M. (2000) Discharge of group IV phrenic afferent fibers increases during diaphragmatic fatigue. Brain Res. 856, 240–244.

Miller, J.D., Smith, C.A., Hemaur, S.J. and Dempsey, J.A. (2007) The effects of inspiratory intrathoracic pressure production on the cardiovascular response to submaximal exercise in health and chronic heart failure. Am. J. Physiol. Heart Circ. Physiol., Jan. 292 (1), H580–592.

Miller, J.D., Hemaur, S.J., Smith, C.A., Stickland M.K. and Dempsey, J.A. (2006) Expiratory threshold loading impairs cardiovascular function in health and chronic heart failure during submaximal exercise. J. Appl. Physiol. 101, 213–227.

O'Donnell, D.E., Revill, S.M. and Webb, K.A. (2001) Dynamic hyperinflation and exercise intolerance in chronic obstructive pulmonary disease. Am. J. Respir. Crit. Care Med. 164, 770–777.

Romer, L.M., Lovering, H.C., Haverkamp, A.T., Pegelow, D.F. and Dempsey, J.A. (2006) Effect of inspiratory muscle work on peripheral fatigue of locomotor muscles in healthy humans. J. Physiol. 271, 425–439.

Simon, M., LeBlanc, P., Jobin, J., Desmeules, M., Sullivan, M.J. and Maltais, F. (2001) Limitation of lower limb $\dot{V}O_2$ during cycling exercise in COPD patients. J. Appl. Physiol. 90, 1013–1019.

Stark-Leyva, K.N., Beck, K.C. and Johnson, B.D. (2004) Influence of expiratory loading and hyperinflation on cardiac output during exercise. J. Appl. Physiol. 96, 1920–1927.

37
Phase Relations Between Rhythmical Movements and Breathing in Wind Instrument Players

Dietrich Ebert[1] and Wieland Kaerger[2]

1 Introduction

In humans, the coupling of breathing and limb movements during a lot of different activities has been reported. Relations between particular phases of rhythmical forearm movements and breathing have been measured and may be called coordination in the sense of von Holst (Holst 1939). This coordination occurred in healthy persons in restricted entrainment bands to some degree at different rates. A small percentage of "good" coordinators revealing a high level of fixed-phase relations within a movement rate range was distinguished from the majority of "poor" coordinators showing only a small percentage of fixed phase relations (Ebert *et al*. 2000). The reason for this difference has not yet been established. In both a group of untrained subjects (controls) and a group of well-trained pianists with a high level of sensorimotor capability, a similar distribution of many poor and few good coordinators has been described (Ebert *et al*. 2002). In these investigations it was striking that good coordinators were more experienced in controlling their breathing voluntarily, for instance by practicing singing or yoga breathing. The present study has been carried out to prove the hypothesis that the degree of coordination (coupling strength) may depend on the effect of training on the breathing motor apparatus.

2 Methods

As subjects who are experienced in controlling their breathing motor system voluntarily, 14 well-trained healthy wind instrument players (group a) were observed in the performance of two tasks. In tracking task I, this group was compared with a control group of 15 untrained healthy age and sex matched subjects (group b).

[1] Dept. of Neurology, University of Duesseldorf, Germany; dietrichebert@gmx.de

[2] Carl-Ludwig-Institute of Physiology, University of Leipzig, Germany

M.J. Poulin and R.J.A. Wilson (eds.), *Integration in Respiratory Control: From Genes to Systems*. © Springer 2008

Task I: For this task, as in previous investigations (Ebert *et al*. 2000), the same paradigm of testing sinusoidal tracking movements of the forearm was chosen. While subjects were sitting in a chair watching a sinusoidal moving signal on a screen, they had to perform simple flexion and extension movements with left and right forearm measured by means of a goniometer and displayed also to cover the target signal as precise as possible, a pursuit tracking task. The tracking rate was varied systematically in a frequency range between 0.2 and 0.5 Hz (the 1:1 entrainment band found in previous investigations) in steps of 0.1 Hz. Breathing was recorded simultaneously by means of a pneumotachograph.

Task II: In addition to task I, the musicians were also asked to play an easy and rhythmically simple piano piece (their accompanying education at the musical college). A preludium by J.S. Bach (from "Kleine Präludien und Fughetten," Nr. 2) was chosen since all subjects were capable of playing this piano piece. It had to be performed on a digital piano in three different tempi while breathing was simultaneously recorded by means of a pneumotachograph.

The frequency of stable-phase relations was calculated by counting phase intervals between particular breathing and movement phases. For calculation of coordination frequency, a weak criterion (fluctuations allowed within a confident interval of 25% of the movement cycle duration) and a strong criterion (10%) were used. Only the results using the strong criterion are demonstrated (see details in Ebert *et al*. 2000).

3 Results

Task I: A high and stable coordination frequency in a rate ratio of 1:1 has been detected between breathing and forearm movements in group a, similar to that of the good coordinators described previously. The coordination frequencies of group a differed from those of group b significantly ($p < 0.05$, see Fig.1). Slight differences between the single subjects of group a seem to be related to the type of instrument they played. So it was possible to distinguish in turn within group a between good and poor coordinators, but the group of good coordinators was much larger than in previous investigations mentioned above. The highest level of coordination frequencies was found in the brass players and the highest level inside this group in trombone-players (see Table 1).

Task II: During piano playing, rather low levels of coordination between breathing and musical meter were found (see Table 1). Still, coordination frequency in this group was higher than that of a group of pianists described previously (Ebert *et al*. 2002) and it increased in some individuals when playing the same piece faster.

Mean breathing rates: In all individuals, mean breathing rates during movements were significantly higher than breathing rates at rest ($p < 0.01$). Both breathing rates at rest and breathing rates during movements at all tracking rates were significantly lower in the wind players (Fig. 2). A slight increase of breathing rates correlated to increasing tracking rate ($r = 0.94$ for the right forearm, $r = 0.97$ for the left forearm) as well as to increasing tempi in piano playing ($r = 0.99$).

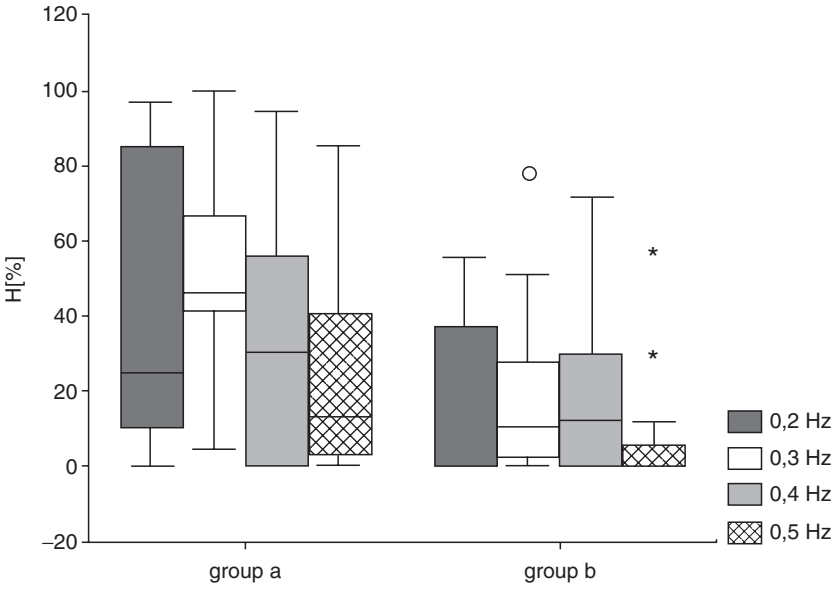

Fig. 1 Box-plots for comparison of coordination frequency (H) of group a (left part) at the four tracking rates within the 1:1 entrainment band tested with that of group b (right side) under the same condition. The differences for all four frequencies between the groups were significant ($p < 0.05$)

Table 1 List of the wind instrument players (group a), their demographical dates and their primary instruments. Subjects are listed in the sequence of the total sum of their coordination frequencies in task 1, summarized over all tracking rates tested and for both arms together using the 10%-criterion (strong) for calculation of coordination frequency (H). In the last row, the total sum of coordination frequencies H [%] of group a in task 2 while playing piano is displayed, summarized over all three tempi (without the values of subject 1 and 15 who could not take part in task 2, subject 12 had to be cancelled for both tasks)

subject	age	sex	Handedness	instrument	task 1 H[%]	task 2 H[%]
13	48	m	R	trombone	691,3	39,2
6	22	f	R	trombone	642,2	18,3
14	24	m	R	trombone	487,1	32,1
4	21	m	R	trumpet	402,2	90,7
7	23	m	R	French horn	362	6,7
8	24	m	R	trombone	317	6,7
5	20	f	R	French horn	307,8	54,3
2	17	w	R	voice	163	20
1	24	m	R	clarinet	157,3	
10	19	f	R	tuba	138	76,1
9	40	f	R	flute	127,5	64,8
3	14	w	R	clarinet	91,3	19,8
15	39	f	both	clarinet	76,4	
11	38	m	both	voice	52	13,8

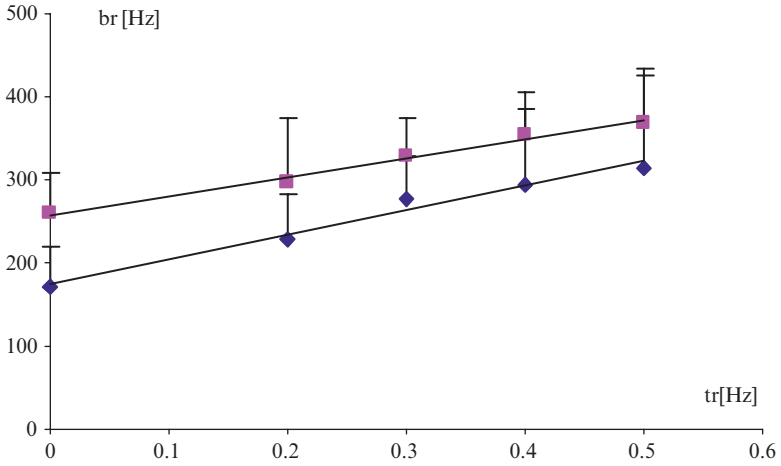

Fig. 2 Mean breathing rates (br) at rest (at tr = 0) and during tracking movements of different tracking rates (tr) of both groups (group a: lower trace, group b: upper trace) in task 1. Regression lines are drawn, for correlation coefficients see text. The difference between the groups in all cases was highly significant ($p < 0.01$) (see Color Plates)

4 Discussion

Players of wind instruments have a significantly higher coordination frequency between breathing and rhythmical movement than people who are not breath-trained. These findings support the hypothesis that the degree of coordination between breathing and other rhythmical motor activities depends on the level of training of the breathing motor system required by playing wind instruments and by singing. Wind players and singers have to control their breathing apparatus in two directions: (1) the exact timing for rhythmical sound production and (2) the strength of expiration to form the volume. In addition, wind instrument players also pay close attention to coordination between movements of extremities and breathing because during voluntarily controlled breathing they have to close holes in the flute, push valves in clarinet, trumpet or French horn or to move the slide of the trombone. The largest amount of coordination in task I was found in trombone players, which may be caused by the special training of coordination between forearm movement and breathing, whereas the others rely more heavily on their fingers to play their instrument. On the other hand, entrainment of breathing by listening to music without movements (Harrer and Harrer 1977) and coordination during poor imagination of rhythmical movements (Decety, Jeannerod, Durozard and Baverel 1995) have been reported.

In terms of the traditional theory of coordination during coordinated activity between breathing and rhythmical voluntary movements, the rhythm of breathing (attracted rhythm) follows the movement rhythm (attractive rhythm), forced by the target rhythm in the tracking task. Playing wind instruments leads to a frequent

voluntary control (central nervous "overwriting") of the normally involuntarily controlled breathing rhythm. This, obviously, seems to amplify the "magnetic effect" (Holst 1939) on the attracted breathing rhythm, which is driven by the voluntary arm movement during tracking.

In terms of the theory of coupled oscillators (Kelso 1995), it means that the coupling strength of the attracted oscillator (breathing) increases by training the attracted oscillator. Training means that the repeated voluntary use probably structures the neuronal network for breathing control.

References

Decety, J., Jeannerod, M., Durozard, D. and Baverel, G. (1993) Central activation of autonomic effectors during mental simulation of motor activities in man. J. Physiol. 461, 549–563.

Ebert, D., Raßler, B. and Hefter, H. (2000) Coordination between breathing and forearm movements during sinusoidal tracking. Eur. J. Appl. Physiol. 81, 288–296.

Ebert, D., Hefter, H., Binkofski, F. and Freund, H.-J. (2002) Coordination between breathing and mental grouping of pianistic finger movements. Perceptual and Motor Skills 95, 339–353.

Harrer, G. and Harrer, H. (1977) Music, Emotion and autonomic function. In: M. Crichley and R.A. Henson (Eds.), *Music and the Brain,* Heinemann Med. Books Lim., London.

Holst, E. von (1939) Die relative Koordination als Phänomen und als Methode zentralnervöser Funktionsanalyse. Erg. Physiol. 42, 228–306.

Kelso, J. (1995) Dynamic Patterns. The Self-organization of Brain and Behaviour. MIT, Cambridge.

Rassler, B., Ebert, D., Waurick, S. and Junghans, R. (1996) Coordination between breathing and finger tracking in man. J. Mot. Behav. 28, 48–56.

38
The Effect of Two Different Intermittent Hypoxia Protocols on Ventilatory Responses to Hypoxia and Carbon Dioxide at Rest

Michael Koehle[1], William Sheel[2], William Milsom[3] and Donald McKenzie[4]

Abstract Intermittent hypoxia (IH) consists of bouts of hypoxic exposure interspersed with normoxic intervals. The optimal IH regime for increasing the ventilatory response in humans is unknown, although in animals there is evidence that multiple short duration bouts of intermittent hypoxia (SDIH) provoke larger changes in chemosensitivity than longer duration bouts of intermittent hypoxia (LDIH). The purpose of this study was to compare responses to both hypercapnia and hypoxia between the two protocols. Methods: In a randomised crossover design, 10 healthy males underwent two 7-day poikilocapnic IH protocols. The LDIH protocol consisted of daily 60-minute exposures to normobaric 12% O_2 (balance N2). The SDIH protocol comprised twelve 5-minute bouts of normobaric 12% O_2, separated by 5-minute bouts of room air daily. We measured the isocapnic acute hypoxic ventilatory response (HVR), hypercapnic ventilatory response (HCVR) and CO_2 threshold and sensitivity by the modified Read rebreathing technique. Pre-testing was performed immediately prior to intermittent hypoxic training. Follow-up testing occurred on the first day following IH and at 7 days after completion of IH. HVR testing was also performed on every day of the IH protocol prior to the hypoxic exposure. Results: Following each 7-day IH protocol, mean HVR was significantly ($p < 0.05$) increased by 67% and 49% (for LDIH and SDIH, respectively). One week post IH, HVR values were not different from pre-values. HCVR was increased significantly by the LDIH protocol by 44.1% ($p < 0.01$) and remained elevated by 41.5% at 7 days post ($p < 0.01$). The changes following the SDIH protocol were smaller (20.7% and 13.5%, at 1 and 7 days post IH, respectively) and not significant. The HCVR remained elevated 7 days following IH (26.7%, $p < 0.01$). In both the hyperoxic and hypoxic modified rebreathing tests, the CO_2 sensitivity was unchanged by either intervention. In hypoxia, the CO_2 threshold was significantly reduced following both protocols ($p < 0.05$). LDIH

[1] University of British Columbia, Faculty of Medicine, michael.koehle@gmail.com

[2] University of British Columbia, School of Human Kinetics, bsheel@interchange.ubc.ca

[3] University of British Columbia, Department of Zoology, milsom@zoology.ubc.ca

[4] University of British Columbia, School of Human Kinetics and Faculty of Medicine, kari@interchange.ubc.ca

M.J. Poulin and R.J.A. Wilson (eds.), *Integration in Respiratory Control: From Genes to Systems*.

reduced the threshold by 1.60 mmHg, whereas following SDIH it was reduced by 1.98 mmHg. Under hyperoxic conditions, LDIH reduced the CO_2 threshold by 2.06 mmHg, and SDIH caused a reduction of 2.53 mmHg. There were no significant differences between the two IH protocols for any of the above measures. A 7-day intermittent hypoxic protocol consisting of daily 60-minute exposures to normobaric poikilocapnic hypoxia caused increases in HVR and HCVR. This protocol caused a left-shift in the CO_2 threshold but no change in CO_2 sensitivity by the modified rebreathing protocol. Neither protocol proved superior in effecting these changes in the resting control of breathing.

1 Introduction

Intermittent hypoxia (IH) has been shown to affect the hypoxic ventilatory response (HVR) at rest in humans (Foster, McKenzie, Milsom and Sheel 2005; Katayama, Sato, Matsuo, Hotta, Sun, Ishida, Iwasaki and Miyamura 2005). The effects of intermittent hypoxia on the response to carbon dioxide are less clear. Investigators have looked at hypercapnic ventilatory response (HCVR) by single breath (Katayama, Sato, Morotome, Shima, Ishida, Mori and Miyamura 2001; Katayama, Sato, Shima, Qiu, Ishida, Mori and Miyamura 2002) and rebreathing techniques (Katayama *et al*. 2001; Foster *et al*. 2005) or have used the modified Read rebreathing method (Mahamed and Duffin 2001; Mateika, Mendello, Obeid and Badr 2004). The results of this research have been inconsistent. As the varying studies used differing IH protocols, it is difficult to compare the results to understand their respective meaning. To do so, these measurements must all be done in the same subjects undergoing the same IH protocols. Furthermore, the optimal IH protocol for augmenting ventilatory responses is unknown. In humans, most studies have focused on single, longer daily exposures to hypoxia (Long Duration Intermittent Hypoxia [LDIH]), whereas there has been some work in animals demonstrating that multiple brief bouts of hypoxia have a more profound effect on ventilatory control (Short Duration Intermittent Hypoxia [SDIH]) (Peng and Prabhakar 2004). The purpose of the present study was to compare SDIH and LDIH and their effects on the control of breathing in humans using a variety of measurements of chemoresponse.

2 Methods

A randomised crossover design was used such that each subject underwent two intermittent hypoxia protocols. Normobaric hypoxia (F_IO_2 = 12%) was administered by mask over 7 consecutive days in either one continuous exposure of 60 minutes duration (LDIH) or in twelve 5-minute bouts interrupted by 5-minute bouts of normoxia for a total of 60 minutes of hypoxic exposure (SDIH). A washout

period of at least two weeks (14–94 days) was used. HVR, HCVR and CO_2 sensitivity and threshold by the modified Read rebreathe method were the measured outcomes. Each measure was assessed prior to the first IH exposure, on the first day following the final exposure and one week following the final exposure. HVR was also assessed daily, prior to each IH exposure. The methodology for HVR measurement followed a protocol previously used in the laboratory and is described in detail elsewhere (Koehle, Foster, McKenzie and Sheel 2005). Briefly, the HVR measurement followed a normobaric, isocapnic, progressive hypoxia model. Subjects rested in the supine position while breathing room air via a non-rebreathing mask. Nitrogen was gradually added to the inspired side, while isocapnia was maintained with the addition of CO_2. Ventilation was then plotted against saturation with the absolute value of the slope used to represent HVR. The measurement of HCVR was based on the method used by Katayama *et al*. (2001) using a rebreathing paradigm. Subjects breathed through a mouthpiece attached to a rebreathing valve. Subjects were asked to take three large breaths and, following maximal exhalation, they were switched from breathing room air to the rebreathing bag containing 7% CO_2, balance O_2. Minute ventilation was plotted against end-tidal CO_2 partial pressure ($PETCO_2$), the slope representing the CO_2 sensitivity. The modified Read rebreathing protocol used in this study was based on that described by Duffin *et al*. (2001). During the test, oxygen pressure was maintained at either $PETO_2$ = 50 mmHg (hypoxia) or $PETO_2$ = 150 mmHg (hyperoxia). Subjects hyperventilated room air for 5 minutes before the test to reduce their $PETO_2$ to subthreshold values. The test started when subjects were switched to the rebreathing bag. Data was analysed using a two-way repeated measures ANOVA.

3 Results

Mean age was 26.0 (± 6.7) years, and mean maximal oxygen consumption was 58.2 (± 3.9) mL•kg-1•min-1. Results are displayed in Fig. 1. Mean baseline HVR for both protocols was 0.47 (± 0.23) L•min-1•%SaO2-1. After the 7-day IH protocols, HVR was increased by 93% (± 120) and 65% (± 74) (for LDIH and SDIH, respectively). HVR remained significantly elevated one week following IH. There were no significant differences in HVR between the two protocols. IH significantly increased HCVR by 42.9% (± 63.4) ($p < 0.01$). This value remained elevated by 38.1% (± 70.9) at 7 days following IH ($p < 0.01$). When analysed by protocol, HCVR was increased significantly by the LDIH protocol by 56.1% (± 71.6) ($p < 0.01$) and remained elevated by 54.4% (± 94.0) at 7 days post ($p < 0.01$). The changes following the SDIH protocol were smaller at 29.7% (± 54.6) and 21.9% (± 34.4), at 1 and 7 days following IH, respectively. The increases following SDIH were not significant. CO_2 sensitivity was unchanged by IH. In both hyperoxia and hypoxia, the CO_2 threshold was significantly reduced following both protocols. In hypoxia, LDIH reduced the threshold by 1.60

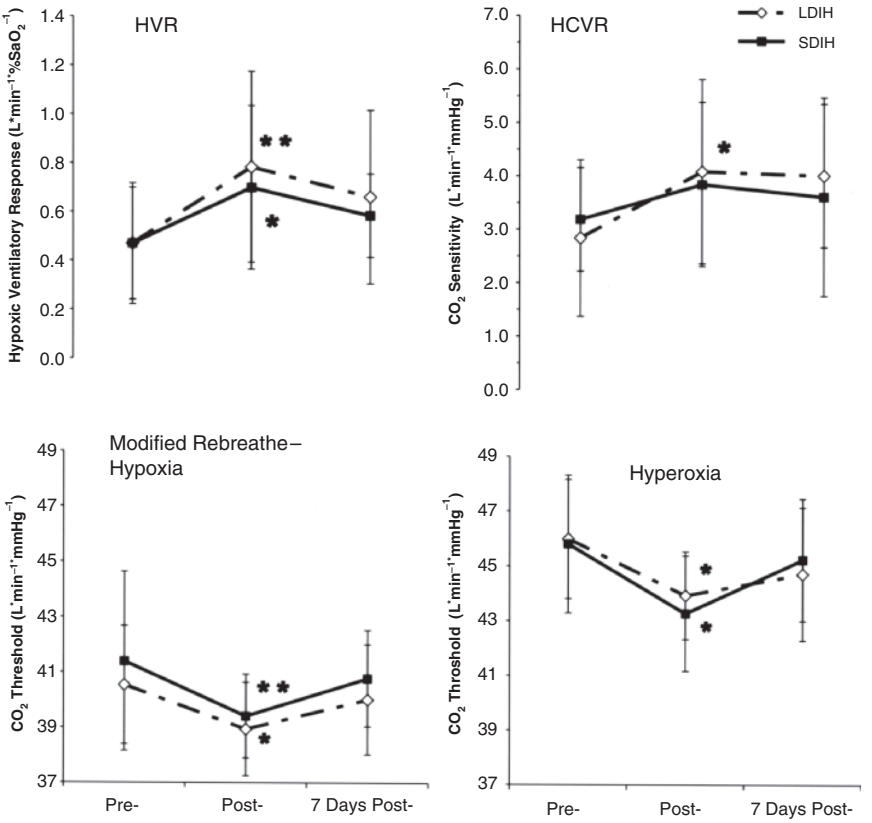

Fig. 1 Effects of IH on ventilatory chemoresponse. Error bars denote standard deviations. Significance: * - $p < 0.05$; ** - $p < 0.01$

(± 0.98) mmHg, whereas following SDIH it was reduced by 1.98 (± 2.60) mmHg. Under hyperoxic conditions, LDIH reduced the CO_2 threshold by 2.06 (± 2.33) mmHg, and SDIH caused a reduction of 2.53 (± 1.36) mmHg. At 7 days following the IH, these values were not significantly lower than baseline. When HVR, measured prior to the first performed protocol, was compared with the values from the modified rebreathing technique, no significant correlations were found for CO_2 threshold ($r = -0.499$ and -0.625, for hypoxic and hyperoxic conditions, respectively) or sensitivity ($r = 0.137$ and 0.233). Secondly, when the change in HVR was compared with the change in CO_2 threshold by the modified rebreathing technique, no significant correlations were found ($r = -0.058$ and 0.091). When HCVR was compared with CO_2 sensitivity by the modified rebreathing method (in hyperoxia), there was no significant relationship ($p = 0.532$).

4 Discussion

Ten subjects underwent two 7-day intermittent hypoxic protocols. HVR and HCVR were increased, while CO_2 threshold was decreased by the IH in both protocols. The increased HVR following a 7-day IH protocol was consistent with comparable previous studies (Katayama *et al*. 2002; Foster *et al*. 2005). The increase in CO_2 sensitivity by HCVR concurs with previous poikilocapnic studies where the daily dose is 8–9 hours (Ainslie, Kolb, Ide and Poulin 2003; Katayama *et al*. 2005) while conflicting with studies where the daily dose is shorter (~ 1 hour) (Katayama *et al*. 2001).

The decrease in CO_2 threshold by the modified rebreathing protocol in both hypoxia and hyperoxia is a unique finding. Mahamed and Duffin (2001) showed a decrease in the CO_2 threshold in the hypoxic test but not the hyperoxic test following a 14-day IH protocol of 20-minute daily exposures. The decreased threshold in the hyperoxic test could be related either to longer daily doses of hypoxia or the poikilocapnia of the present study. As with the Mahamed and Duffin study, no changes in CO_2 sensitivity were observed via the modified rebreathing method. There was no relationship between the CO_2 sensitivities measured by the two different protocols, indicating that HCVR and sensitivity by the modified rebreathing method are not equivalent measures. The prior hyperventilation may introduce other stimuli (behavioural, neural or humoral) to the ventilatory response that are not present during the standard HCVR. Secondly, the CO_2 sensitivity during the HCVR is measured at a higher $PETCO_2$ than during the modified rebreathing method. If such a relationship were not truly linear, one would expect differing results.

In conclusion, IH caused temporary increases in HVR and HCVR and decreases in CO_2 threshold; the modified rebreathing and HCVR methods of measuring CO_2 sensitivity provide differing outcomes, and SDIH was not significantly more efficacious than LDIH for increasing resting chemoresponse in humans.

Acknowledgements Funded by CFI, NSERC, Michael Smith Foundation for Health Research, the Wilderness Medical Society and BC Sports Medicine Research Foundation.

References

Ainslie, P.N., Kolb, J.C., Ide, K. and Poulin, M.J. (2003) Effects of five nights of normobaric hypoxia on the ventilatory responses to acute hypoxia and hypercapnia. Respir. Physiol. Neurobiol. 138, 193–204.

Duffin, J., Mohan, R.M., Vasiliou, P., Stephenson, R. and Mahamed, S. (2000) A model of the chemoreflex control of breathing in humans: model parameters measurement. Respir. Physiol. 120, 13–26.

Foster, G.E., McKenzie, D.C., Milsom, W.K. and Sheel, A.W. (2005) Effects of two protocols of intermittent hypoxia on human ventilatory, cardiovascular and cerebral responses to hypoxia. J. Physiol. 567, 689–699.

Katayama, K., Sato, K., Matsuo, H., Hotta, N., Sun, Z., Ishida, K., Iwasaki, K. and Miyamura, M. (2005) Changes in ventilatory responses to hypercapnia and hypoxia after intermittent hypoxia in humans. Respir. Physiol. Neurobiol. 146, 55–65.

Katayama, K., Sato, Y., Morotome, Y., Shima, N., Ishida, K., Mori, S. and Miyamura, M. (2001) Intermittent hypoxia increases ventilation and SaO_2 during hypoxic exercise and hypoxic chemosensitivity. J. Appl. Physiol. 90, 1431–1440.

Katayama, K., Sato, Y., Shima, N., Qiu, J.C., Ishida, K., Mori, S. and Miyamura, M. (2002) Enhanced chemosensitivity after intermittent hypoxic exposure does not affect exercise ventilation at sea level. Eur. J. Appl. Physiol. 87, 187–191.

Koehle, M.S., Foster, G.E., McKenzie, D.C. and Sheel, A.W. (2005) Repeated measurement of hypoxic ventilatory response as an intermittent hypoxic stimulus. Respir. Physiol. Neurobiol. 145, 33–39.

Mahamed, S. and Duffin, J. (2001) Repeated hypoxic exposures change respiratory chemoreflex control in humans. J. Physiol. 534, 595–603.

Mateika, J.H., Mendello, C., Obeid, D. and Badr, M.S. (2004) Peripheral chemoreflex responsiveness is increased at elevated levels of carbon dioxide after episodic hypoxia in awake humans. J. Appl. Physiol. 96, 1197–1205.

Peng, Y.J. and Prabhakar, N.R. (2004) Effect of two paradigms of chronic intermittent hypoxia on carotid body sensory activity. J. Appl. Physiol. 96, 1236–1242.

39
Respiratory Long-Term Facilitation: Too Much or Too Little of a Good Thing?

Safraaz Mahamed[1] and Gordon S. Mitchell[2]

Abstract Respiratory long-term facilitation (LTF), a prolonged augmentation of respiratory motor output, is induced by intermittent hypoxia in anesthetized or sleeping rats (and humans in limited conditions). Whether such augmentation in the controller response is of physiological benefit in terms of ventilatory stability remains uncertain; its impact on ventilatory stability will be determined to some extent by its effects on CO_2 chemoreflex loop gain. We used integrated nerve responses in a rat model of LTF to assess chemoreflex parameters related to breathing stability. In this model, LTF decreases chemoreflex threshold but increases chemoreflex gain. Whereas a decreased chemoreflex threshold would promote ventilatory stability, increased chemoreflex gain represents a destabilizing influence. Based on these considerations alone, the impact of respiratory LTF on respiratory stability remains unclear.

1 Introduction

To understand the ultimate consequence of respiratory LTF on breathing stability, the relative contributions of stabilizing and destabilizing influences must be assessed. For example, the effects of LTF on overall loop gain in conditions such as obstructive sleep apnea (OSA) might help to determine if LTF may compensate for, or contribute to, the repetitive apneas that characterize OSA.

In a feedback controller, factors promoting stability are: a large set-point to threshold difference, a relatively low controller gain and a low plant gain (Khoo 2000). In the traditional feedback control arrangement, the forward part of the loop is described by a hyperbolic function relating alveolar ventilation to arterial or alveolar carbon dioxide pressure. The feedback part of the loop has been described as the sum of two functions: (1) a carbon dioxide-independent drive to breathing (establishing the ventilatory threshold), and (2) a near linear relationship between

[1] University of Wisconsin Madison, Department of Comparative Biosciences, safraaz.mahamed@gmail.com

[2] University of Wisconsin Madison, Department of Comparative Biosciences, mitchell@svm.vetmed.wisc.edu

M.J. Poulin and R.J.A. Wilson (eds.), *Integration in Respiratory Control: From Genes to Systems*.

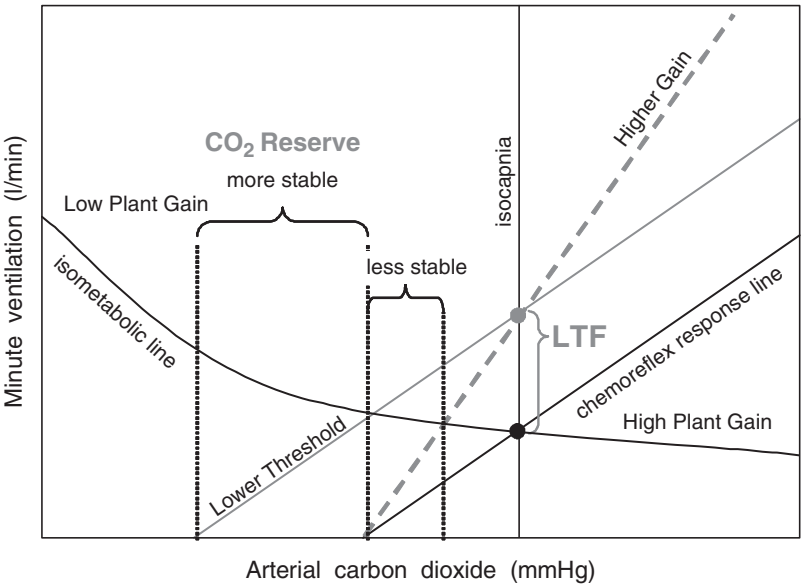

Fig. 1 Schematic representation of respiratory control and the possible impact of LTF. Solid black lines represent the plant behavior (isometabolic line) and chemoreflex feedback. The black, filled circle represents the predicted equilibrium point (eupneic CO_2). Two potential changes due to LTF are shown as gray lines passing through the gray, filled circle. The grey solid line depicts the effect of lowered CO_2 threshold while the dashed gray line depicts increased chemoreflex sensitivity. Stability is represented by the magnitude of the distance along the CO_2 axis representing the difference between the interception of the gray lines with the isometabolic line and the interception of the gray lines with the CO_2 axis (apneic threshold). This difference is labeled as the CO_2 reserve

carbon dioxide pressure and chemoreflex drive, thereby increasing alveolar ventilation above that threshold. Thus, controller threshold, controller gain and their mathematical intercept with the plant equation define the loop gain (Mahamed, Ali, Ho, Wang and Duffin 2001). CO_2 reserve is a measure of the propensity for stable breathing defined here as the gap between eupneic and apneic $P_{ET}CO_2$ (Dempsey 2005). A schematic example is shown in Fig. 1 demonstrating how changes in CO_2 threshold or sensitivity alter the CO_2 reserve.

In this report we provide preliminary evidence from a rat model of respiratory LTF, demonstrating the potential for both stabilizing and destabilizing influences to the chemoreflex feedback control of breathing.

2 Methods

All experiments were performed on male Sprague-Dawley rats (Harlan colony 217) aged 3–4.5 months. All protocols conformed to the requirements of the Institutional Animal Care and Use Committee at the University of Wisconsin, Madison.

2.1 Surgical Preparation and Protocol

Surgical procedures have been described elsewhere (Fuller, Bach, Baker, Kinkead and Mitchell 2000) and are described briefly here. Rats are induced with isoflurane (2.5–3.5% in 50% O_2). They are bilaterally vagotomized, tracheotomized and pump ventilated. The tail vein and femoral artery are catheterized for fluid infusion and blood sampling, respectively. The left phrenic nerve was isolated with a dorsal approach, cut distally, desheathed and submerged in mineral oil. The rats were then converted from isoflurane (2.0–3.5%) to urethane (1.6–1.8 g/kg) and paralyzed with pancuronium bromide (2.5 mg/Kg) via an *i.v.* dose over a period of 15–25 minutes. Throughout the experiment, the rats received a 2–4 mL/h fluid infusion of 11:1 lactated ringers solution and bicarbonate to maintain fluid and acid-base balance.

LTF was induced by performing 6 consecutive, 25-second ventilator apneas with five-minute intervals. The resulting LTF in the integrated phrenic nerve amplitude was ~ 53% (change, % baseline) 60 min post-apneas (Mahamed and Mitchell 2006). Before and after the apnea-induced LTF protocol, the CO_2 recruitment threshold was determined and the baseline nerve activity was established at 2 mmHg CO_2 above the recruitment threshold. The integrated phrenic amplitude during baseline conditions was used to approximate the CO_2 chemoreflex sensitivity before and after the induction of LTF (amplitude post-LTF at 2 mmHg CO_2 above new recruitment threshold). These values were compared for statistical significance ($p < 0.05$) using ANOVA.

3 Results

Baseline motor output increased and recruitment threshold decreased significantly after LTF induction compared to control experiments (Table 1).

4 Discussion

Our results demonstrate a significant decrease in recruitment threshold (~ 4 mmHg) and a significant increase in basal phrenic drive (~ 28% over baseline). The two have opposite predicted effects on breathing stability with the former expected to

Table 1 Recruitment Threshold and Phrenic Nerve Amplitude Results

	Control (n = 6)		LTF(n = 9)	
	Pre	Post	Pre	Post
Recruitment Threshold	43.2	42.2	44.8	40.6*
mean (SEM) mmHg	(0.9)	(0.9)	(0.8)	(1.2)
Change in Baseline		6.7		28.2*†
mean (SEM) % of Pre		(1.5)		(9.5)

(* indicates significant difference from Pre, $p < 0.05$; † indicates significant difference from Time Control experiment, $p < 0.05$)

improve ventilatory stability and the latter tending to destabilize the system. A decrease in the recruitment threshold modestly increases the CO_2 reserve but also shifts the system along the isometabolic hyperbola toward an area of lower plant gain (see Fig. 1, gray line). Thus, a lowered recruitment threshold tends to lower the loop gain compared to an animal that has not undergone LTF. On the other hand, the apparent increase in CO_2-chemoreflex sensitivity attributable to LTF (see Fig. 1, gray dashed line) would tend to reduce the CO_2 reserve and destabilize breathing. Our results indicate that a mix of decreased threshold and increased sensitivity contribute to the expression of LTF and may represent "offsetting" influences on the stability of breathing. The net influence on breathing stability will depend on the quantitative contributions of these changes in the context of the animal (*e.g.*, arousal state, etc.). One recent investigation suggests that the induction of LTF decreases the variability of expiratory time in both spontaneously breathing, anesthetized cats and in normal human subjects (Morris and Gozal 2004). Thus, there is some hint that the stabilizing influences predominate, at least in the experimental conditions utilized by these investigators. Another critical determinant of stability, particularly in obstructive sleep apnea, is upper airway caliber. Facilitation tends to manifest as increased upper airway activity in awake humans (Harris, Balasubramaniam, Badr and Mateika 2006). Thus, LTF can also mitigate instability via mechanisms independent of its effect on the threshold/gain properties of the control system.

Whereas the impact of LTF on ventilatory stability remains uncertain in the context of sleep apnea at this time, our results do suggest that LTF has the potential for both stabilizing and destabilizing influences on breathing and that these issues warrant further investigation.

Acknowledgement Research supported by NIH HL 89209 and SM is supported by CIHR (Canada).

References

Dempsey, J.A. (2005) Crossing the apneic threshold: causes and consequences. Exp. Physiol. 90(1), 13–24.

Fuller, D.D., Bach, K.B., Baker, T.L., Kinkead, R. and Mitchell, G.S. (2000) Long-term facilitation of phrenic motor output. Respir. Physiol. 121(2–3), 135–146.

Harris, D.P., Balasubramaniam, A., Badr, M.S. and Mateika, J.H. (2006) Long-term facilitation of ventilation and genioglossus muscle activity is evident in the presence of elevated levels of carbon dioxide in awake humans. Am. J. Physiol. Regul. Integr. Comp. Physiol. 291(4), R1111–1119.

Khoo, M.C. (2000) Determinants of ventilatory instability and variability. Respir. Physiol. 122(2–3), 167–182.

Mahamed, S., Ali, A.F., Ho, D., Wang, B. and Duffin, J. (2001) The contribution of chemoreflex drives to resting breathing in man. Exp. Physiol. 86(1), 109–116.

Mahamed, S. and Mitchell, G.S. (2006) Does simulated apnea elicit respiratory long-term facilitation? 2006 Experimental Biology meeting abstracts [url not currently available]. *The FASEB Journal* 20, Abstract #231.3.

Morris, K.F. and Gozal, D. (2004) Persistant respiratory changes following intermittent hypoxic stimulation in cats and human beings. Respir. Physiol. Neurobiol. 140(1), 1–8.

40
Contribution of Endothelin-1 and Endothelin A and B Receptors to the Enhanced Carotid Body Chemosensory Responses Induced by Chronic Intermittent Hypoxia

Sergio Rey[1,2], Rodrigo Del Rio[1] and Rodrigo Iturriaga[1]

1 Introduction

Chronic intermittent hypoxia (CIH), a characteristic of obstructive sleep apnea (OSA), has been linked to hypertension and an increased cardiovascular risk (Quan and Gersh 2004). Patients with recently diagnosed OSA show potentiated ventilatory and cardiovascular responses to acute hypoxia, attributed to an enhanced carotid body (CB) reactivity to hypoxia (Narkiewicz *et al*. 1998). Similarly, animals exposed to CIH show enhanced ventilatory (Reeves *et al*. 2003; Rey *et al*. 2004) and cardiovascular (Fletcher 2001) responses to hypoxia. Moreover, Peng *et al*. (2001) found that basal CB discharges and chemosensory responses to acute hypoxia were larger in rats exposed to a CIH pattern consisting of short cyclic hypoxic episodes followed by normoxia, applied for 8 hours during 10 days. Using a similar protocol, we found that cats exposed to cyclic hypoxia followed by normoxia during 8 hours for 4 days showed enhanced CB chemosensory and ventilatory responses to acute hypoxia (Rey *et al*. 2004). Since the CB is a highly vascularized organ, it is possible that factors produced by the endothelium may control the CB vascular tone by modulating the PO_2 tissue level. In fact, endothelium-derived reactive oxygen species have been implicated as mediators of the CIH-induced potentiation of hypoxic CB chemoreception (Peng and Prabhakar 2003). Interestingly, endothelin-1 (ET-1), a potent **vasoactive** excitatory modulator of CB chemoreception (Rey *et al*. 2006) and the endothelin receptor type-A (ET_A-R) are both upregulated in sustained chronic hypoxia (Chen *et al*. 2002a; Chen *et al*. 2002b). However, it is not known whether CIH increases the ET-1 expression in the CB, and if ET-1 contributes to the enhanced CB hypoxic response induced by CIH. Thus, we studied the role played by ET-1 and its receptors in the CIH-induced potentiation of CB hypoxic chemosensory responses.

[1] Laboratorio de Neurobiología, Facultad de Ciencias Biológicas.

[2] Departamento de Nefrología, Facultad de Medicina, P. Universidad Católica de Chile, Santiago, Chile, riturriaga@bio.puc.cl.

M.J. Poulin and R.J.A. Wilson (eds.), *Integration in Respiratory Control: From Genes to Systems*.

2 Methods

Male adult cats were exposed to hypoxic episodes (PO_2 ~ 75 Torr) of 2 min duration, repeated 10 times during 8 hours for 4 days as previously described (Rey *et al*. 2004). Control cats were kept in normoxia and sham-CIH cats were exposed to simulated air-to-air changes. Experiments were approved by the Ethical Committee of the Facultad de Ciencias Biológicas, P. Universidad Católica de Chile. The carotid chemosensory discharge was recorded *in situ* as previously described (Rey *et al*. 2004). We studied the effects of CIH on ET-1 levels within the CB with immunohistochemistry (Rey *et al*. 2006) and plasma ET-1 levels with an enzyme immunoabsorbent assay. The ET_A-R and endothelin receptor type-B (ET_B-R) expression in the CB was assessed using Western blots of control and CIH-exposed CB homogenates electrophoresed by SDS-PAGE (10%). In addition, the localization of ET_A-R and ET_B-R in the CB was studied with immunohistochemistry. We quantified the immunostaining extension and intensity in the photomicrographs with a color deconvolution algorithm (Ruifrok and Johnston 2001). Tissue sections for immunohistochemistry and nitrocellulose membranes for Western blot were incubated for 18 hours at 4°C with rabbit anti-ET_A-R (AER-001, Alomone Labs, Israel) or rabbit anti-ET_B-R (AER-002, Alomone Labs, Israel). We used a monoclonal mouse anti-β-actin antibody (A5441, Sigma-Aldrich, USA) to confirm equal protein loading in gels. Using an *in vitro* perfused preparation of the CB (Iturriaga *et al*. 1991), we assessed the effects of exogenous ET-1 and 50 μM bosentan, a non-selective endothelin A and B receptor ($ET_{A/B}$-R) antagonist, on chemosensory discharges during normoxia and hypoxia.

3 Results

We did not find differences in the chemosensory responses to acute hypoxia of sham-CIH cats, compared to control animals. However, chemosensory responses to acute hypoxia were enhanced in the CIH-treated cats as is shown in Fig. 1.

Positive immunoreactive ET-1 (ET-ir) signal was mainly present in the perilobular areas around the glomus cells, but ET-ir was also detected in glomus cells. The ET-ir positive area and signal intensity were not statistically different between control and sham-CIH CBs. However, in the CIH-treated CBs, both ET-ir positive area and signal intensity increased by ~ 10-fold ($p < 0.01$), in equivalent sectional areas.

CIH increased the ET_B-R expression in the CB (1.6-fold by immunohistochemistry, $p < 0.01$, and 2.1-fold by Western Blot, $p < 0.05$; Fig. 2), while ET_A-R levels remained unchanged. CIH did not change the ET-1 plasma levels (0.44 ± 0.04 fmol/ml *vs*. 0.40 ± 0.04 fmol/ml, respectively in 7 control and 9 CIH-treated CBs). The detection level of the assay was 0.12 fmol/ml.

Application of ET-1 (0.01–1 μg) to control and CIH-treated CBs *in vitro* produced long-lasting dose-dependent increases in chemosensory discharges (Fig. 3A). Doses of 0.5–1 μg of ET-1 produced maximal chemosensory excitation, which lasted ~ 45 min.

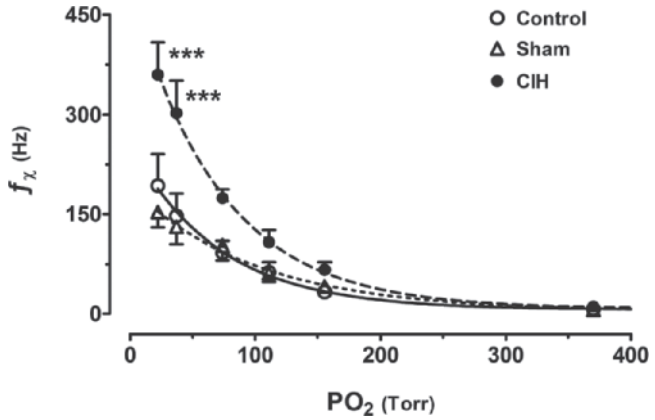

Fig. 1 Frequency of chemosensory discharges (f_χ) recorded at several PO_2 levels in 4 CIH (filled dots), 6 sham-CIH (triangles) and 6 control cats (empty dots). *** $p < 0.001$ CIH *vs*. control and sham-CIH. Two-way ANOVA and *post hoc* Bonferroni test

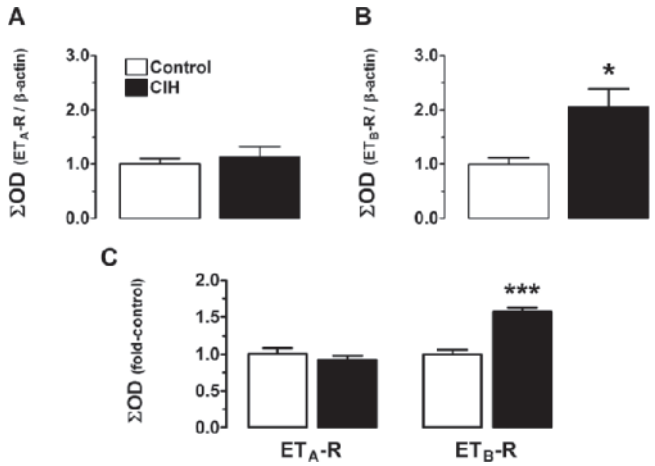

Fig. 2 Expression of endothelin receptors in the CIH-exposed CB (n = 4). (A-B) Densitometric analysis of Western blots for ET_A-R (A) and ET_B-R (B). (C) Intensity of immunohistochemical staining for ET_A-R and ET_B-R. *, $p < 0.05$; ***, $p < 0.001$ Control *vs*. CIH, Mann-Whitney test

The chemoexcitatory response induced by ET-1 was abolished by perfusion with *Tyrode* containing 50 µM bosentan. To study the tonic effect of ET-1 on the CIH-induced potentiation of CB chemoreception to hypoxia, control and CIH-treated CBs were perfused with normoxic Tyrode containing 50 µM bosentan. Perfusion with bosentan reduced baseline CB discharges. The inhibitory effect of bosentan was more pronounced in the CIH-treated CBs (Fig. 3B). The chemosensory response induced by 2 min perfusion of Tyrode equilibrated in mild and severe hypoxia was reduced by bosentan only in the CIH-treated CB (Fig. 3C). In contrast, bosentan did not modify the CB chemosensory response to hypoxia in the control CB (Fig. 3C).

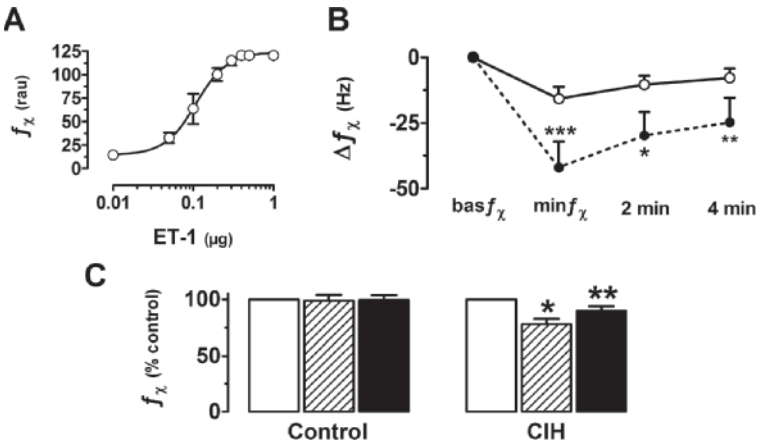

Fig. 3 (A) Dose-response curve for ET-1 in the control CB *in vitro* (n = 6). (B) Effect of 50 µM bosentan on baseline chemosensory discharges (empty dots, control; filled dots, CIH-treated CBs). (C) Effect of bosentan on chemosensory responses to acute mild (PO_2 ~ 70 Torr, shaded bar) and severe (PO_2 ~ 30 Torr, filled bar) hypoxia (n = 9). Responses are expressed as percentages of the hypoxic responses without bosentan (empty bar). *, $p < 0.05$; **, $p < 0.01$; ***, $p < 0.001$. Friedman test and Conover *post hoc* comparisons (*vs*. controls)

4 Discussion

Present results indicate that a local increase of ET-1 in the CB may contribute to the enhanced chemosensory responses induced by CIH predominantly through a vasomotor mechanism. CIH also induces an early increase in ET_B-R expression. Since ET_B-R activation increases NO synthesis (Hirata *et al*. 1993) and inhibits the release of ATP in other tissues (Gardner *et al*. 2005), it is possible that ET_B-R upregulation may contribute to compensate the increased CB activity induced by CIH.

Thus, CIH-induced ET-1 upregulation in the CB may contribute to potentiate the ventilatory and cardiovascular responses to hypoxia, observed in animals exposed to CIH (Fletcher 2001; Reeves *et al*. 2003; Rey *et al*. 2004) and in OSA patients (Narkiewicz *et al*. 1998).

Acknowledgement Supported by FONDECYT 1030330.

References

Chen, J., He, L., Dinger, B., Stensaas, L. and Fidone, S. (2002a) Role of endothelin and endothelin A-type receptor in adaptation of the carotid body to chronic hypoxia. Am. J. Physiol. Lung. Cell. Mol. Physiol. 282, L1314–1323.

Chen, Y., Tipoe, G.L., Liong, E., Leung, S., Lam, S.Y., Iwase, R., Tjong, Y.W. and Fung, M.L. (2002b) Chronic hypoxia enhances endothelin-1-induced intracellular calcium elevation in rat carotid body chemoreceptors and up-regulates ET_A receptor expression. Pflügers Arch. 443, 565–573.

Fletcher, E.C. (2001) Physiological consequences of intermittent hypoxia: systemic blood pressure. J. Appl. Physiol. 90, 1600–1605.

Gardner, A., Westfall, T C. and Macarthur, H. (2005) Endothelin (ET)-1-induced inhibition of ATP release from PC-12 cells is mediated by the ET_B receptor: differential response to ET-1 on ATP, neuropeptide Y and dopamine levels. J. Pharmacol. Exp. Ther. 313, 1109–1117.

Hirata, Y., Emori, T., Eguchi, S., Kanno, K., Imai, T., Ohta, K. and Marumo, F. (1993) Endothelin receptor subtype B mediates synthesis of nitric oxide by cultured bovine endothelial cells. J. Clin. Invest. 91, 1367–1373.

Iturriaga, R., Rumsey, W.L., Mokashi, A., Spergel, D., Wilson, D.F. and Lahiri, S. (1991) *In vitro* perfused-superfused cat carotid body for physiological and pharmacological studies. J. Appl. Physiol. 70, 1393–1400.

Narkiewicz, K., van de Borne, P.J., Montano, N., Dyken, M.E., Phillips, B.G. and Somers, V.K. (1998) Contribution of tonic chemoreflex activation to sympathetic activity and blood pressure in patients with obstructive sleep apnea. Circulation 97, 943–945.

Peng, Y.J., Kline, D.D, Dick, T.E. and Prabhakar, N.R. (2001) Chronic intermittent hypoxia enhances carotid body chemoreceptor responses to low oxygen. Adv. Exp. Med. Biol. 499, 33–38.

Peng, Y.J. and Prabhakar, N.R. (2003) Reactive oxygen species in the plasticity of respiratory behavior elicited by chronic intermittent hypoxia. J. Appl. Physiol. 94, 2342–2349.

Quan, S.F. and Gersh, B.J. (2004) Cardiovascular consequences of sleep-disordered breathing: past, present and future: report of a workshop from the National Center on Sleep Disorders Research and the National Heart, Lung, and Blood Institute. Circulation 109, 951–957.

Reeves, S.R., Gozal, E., Guo, S.Z., Sachleben, L.R., Jr., Brittian, K.R., Lipton, A.J. and Gozal, D. (2003) Effect of long-term intermittent and sustained hypoxia on hypoxic ventilatory and metabolic responses in the adult rat. J. Appl. Physiol. 95, 1767–1774.

Rey, S., Del Rio, R., Alcayaga, J. and Iturriaga, R. (2004) Chronic intermittent hypoxia enhances cat chemosensory and ventilatory responses to hypoxia. J. Physiol. 560, 577–586.

Rey, S., Del Rio, R., Alcayaga, J. and Iturriaga, R. (2006) Endothelins in the cat petrosal ganglion and carotid body: effects and immunolocalization. Brain Res. 1069, 154–158.

Ruifrok, A.C. and Johnston, D.A. (2001) Quantification of histochemical staining by color deconvolution. Anal. Quant. Cytol. Histol. 23, 291–299.

41
Intermittent Hypoxia Induces Respiratory Long-Term Facilitation in Postnatal Rats

Arash Tadjalli[1], James Duffin[2] and John Peever[1, 2]

1 Introduction

One form of central respiratory neuroplasticity is long-term facilitation (LTF), a long-lasting increase in breathing that arises following acute exposure to intermittent, but not continuous, hypoxia (Baker and Mitchell 2000). Respiratory LTF is a serotonin-dependent (Baker-Herman and Mitchell 2002) type of plasticity and is characterized by a persistent augmentation in respiratory frequency and/or inspiratory amplitude, with the cardinal feature being that breathing outlasts (> 1 h) the initial hypoxic stimuli. LTF and its underlying mechanisms have been documented in a variety of model systems including freely-behaving rodents, anaesthetized cats and rodents as well as in the isolated respiratory network *in vitro* (Baker-Herman and Mitchell 2002; Cao, Zwillich, Berthon-Jones and Sullivan 1992; Kline, Overholt and Prabhakar 2002; Olson, Bohne, Dwinell, Podolsky, Vidruk, Fuller, Powell and Mitchel 2001; Blitz and Ramirez 2002).

Age, gender and genetics markedly influence LTF (Fuller, Bach, Baker, Kinkead and Mitchell 2000; Zabka, Behan and Mitchell 2001a). Despite the fact that the respiratory control system undergoes intense maturational changes during postnatal development (Bavis 2005; Gozal and Gozal 2001), LTF and its underlying mechanisms have not been studied during this critical period. The aim of this investigation was to determine whether intermittent hypoxia evokes respiratory LTF in the postnatal respiratory system. Understanding LTF during postnatal development is important because it could play a central role in maintaining ventilatory drive during this pivotal time in CNS development.

[1] University of Toronto, Department of Cell and Systems Biology

[2] University of Toronto, Department of Physiology tadjallia@zoo.utoronto.ca, j.duffin@utoronto.ca, john.peever@utoronto.ca

M.J. Poulin and R.J.A. Wilson (eds.), *Integration in Respiratory Control: From Genes to Systems*.

2 Methods

Experiments were performed on 15–25 day-old male Sprague-Dawley rats. All experiments were pre-approved by the University of Toronto.

The in situ working heart-brainstem preparation was used as a model system to study respiratory LTF (Paton 1996). This preparation is arterially perfused with an artificial blood substitute (ACSF) that allows the oxygenation of the respiratory network in its original intact position so that it generates a normal breathing rhythm. All experimental procedures were carried out as previously described by Paton (1996). Left or the right phrenic nerve activity served as an index of respiratory motor output. Once nerve recordings were established, the in situ preparation was left to stabilize for 45–60 minutes before performing the following experimental protocols.

Intermittent Hypoxia: This protocol was designed to determine whether intermittent hypoxia would evoke respiratory LTF. Phrenic motor output was recorded under baseline conditions (95% O_2 / 5% CO_2) for 45–60 minutes; then the preparation was exposed to three 5-minute episodes of hypoxia (10% O_2 / 5% CO_2 / 85% N_2) that alternated with 5-minute periods of baseline conditions (95% O_2 / 5% CO_2). Following exposure to intermittent hypoxia, baseline conditions were reinstated and phrenic motor output was recorded for another 60 minutes.

The frequency and amplitude of integrated phrenic nerve discharge were analyzed in 60 s time bins under baseline conditions and at 60 min following intermittent hypoxia. Values are expressed as percent changes relative to baseline levels. Statistical differences were determined using paired t-test, and were considered significant when $p < 0.05$ (SigmaStat, Jandel Scientific). Data are expressed as means ± standard errors (mean ± SE) and asterisks (*) indicate statistical significance compared to baseline.

3 Results

Control: To demonstrate that the *in situ* working heart-brainstem preparation generates a stable respiratory pattern during the experimental period, we monitored phrenic nerve burst frequency and amplitude for 150 minutes. This is the total time required to complete an intermittent hypoxia protocol (see methods above). We found that all preparations exhibited a eupneic respiratory motor pattern, with both phrenic burst frequency and amplitude remaining stable over the 150-minute recording period. At the beginning ($t = 0$), phrenic burst frequency and amplitude were: 23 ± 1 bursts/minute (b/min) and 5.3 ± 1.1 arbitrary units (a.u.), respectively; at the end ($t = 150$ minutes), these values were: 22 ± 2 b/min and 4.4 ± 1.1 a.u., respectively ($n = 9$; paired t-tests: frequency ($p = 0.66$) and amplitude ($p = 0.29$)). These results demonstrate that preparations generated a stable breathing rhythm.

Intermittent Hypoxia: Each hypoxic episode (5 minutes of 10% O_2) caused a significant decline in both phrenic nerve discharge frequency and amplitude, which persisted during the 5-minute hypoxic episode. This type of response is consistent with the hypoxic ventilatory response of intact postnatal rats of similar age (Mortola 1999). At the end of the third hypoxic episode, phrenic nerve burst frequency and amplitude returned to baseline values; however, unlike phrenic nerve amplitude, which remained within baseline levels, frequency of phrenic nerve discharge progressively increased during the following 60-minute period (Fig. 1). After intermittent hypoxia, phrenic discharge frequency increased by 40 ± 3.3% above pre-hypoxia baseline levels (n = 8; 24 ± 2 (baseline) versus 33 ± 3 bursts/min at 60 minutes post-hypoxia; paired t-test; p = 0.007). Intermittent hypoxic exposures had no significant effect on burst amplitude, despite a trend for reduced inspiratory amplitude post-hypoxia (n = 8; 3.3 ± 0.5 (baseline) versus 2.9 ± 0.5 a.u. (post-hypoxia); paired t-test; p = 0.06). These results demonstrate that intermittent hypoxic induces long-lasting effects on respiratory frequency, but not inspiratory amplitude, in postnatal rats.

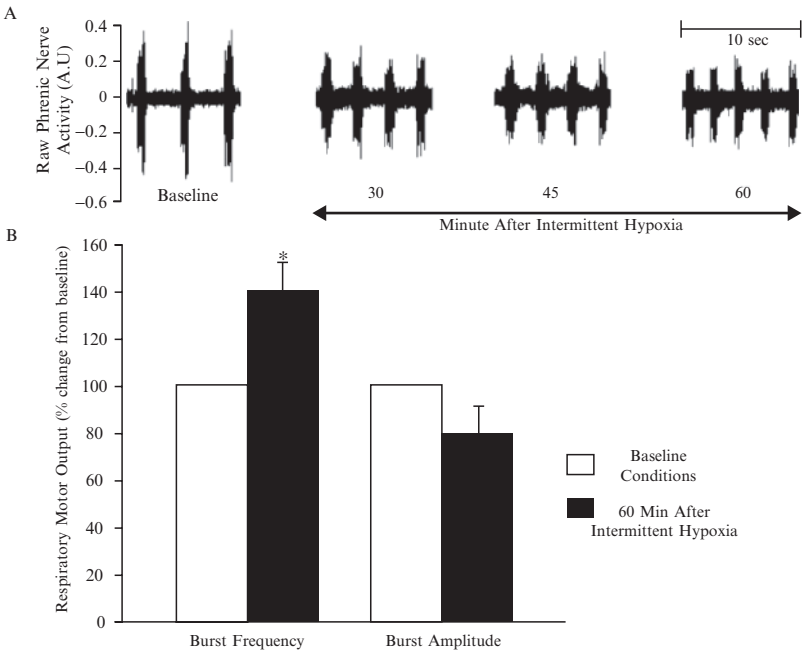

Fig. 1 Phrenic nerve inspiratory activity depicting respiratory frequency and amplitude in response to three episodes of intermittent hypoxia. (A) Raw phrenic nerve activity during baseline conditions, and at 30, 45 and 60 minutes after three 5-min episodes of intermittent hypoxia (10% O_2 / 5% CO_2 / 85% N_2). (B) Respiratory frequency was significantly increased at 60 minutes following intermittent hypoxia compared to baseline values (n = 8; paired t-test; $p < 0.05$). There was a non-significant decline in respiratory burst amplitude compared to baseline levels (n = 8; paired t-test; $p > 0.05$). Data represents mean ± SEM. * denotes a significant difference compared to baseline levels

4 Discussion

We demonstrate that LTF of breathing is evoked by repeated hypoxic exposures in 15–25 day-old rats. Time control experiments confirmed that breathing remained stable across the experimental period and that neither respiratory frequency nor inspiratory amplitude varied with time. Accordingly, respiratory changes following hypoxia are the result of the intermittent stimuli rather than time-dependent changes in respiratory stability. Further, hypoxia-induced LTF was not due to changes in arterial gas concentrations because they were clamped at baseline conditions (95% O_2 and 5% CO_2) throughout the post-hypoxic period.

This study is the first to demonstrate respiratory LTF in the *in situ* working heart-brainstem preparation. Results demonstrate that intermittent hypoxia induces a form of LTF that is similar to that observed in adult mammals (Kline *et al*. 2002; McGuire, Zhang, White and Ling 2004; Olson *et al*. 2001). Results also show that respiratory motor output remains stable over the experimental period. This model has not been used to study the *long-term* effects of hypoxia-induced respiratory neuroplasticity. Accordingly, we propose that the *in situ* working heart-brainstem preparation is a useful model system for studying the biochemical mechanisms of respiratory LTF during early postnatal development.

Previous studies report LTF as an increase in respiratory frequency and/or inspiratory amplitude (Baker and Mitchell 2000; Cao *et al*. 1992; McKay, Janczewski and Feldman 2004). In the unanaesthetized respiratory network of the *in situ* working heart-brainstem model system, we found that LTF was exclusively manifested as an increase in respiratory frequency with no contribution of phrenic nerve inspiratory burst amplitude. This observation is in keeping with studies in unanaesthetised and behaving adult rats, mice and ducks, which report that intermittent hypoxia induces a persistent increase in respiratory frequency with minimal or no change in either tidal volume or inspiratory amplitude (Cao *et al*. 1992; Kline *et al*. 2002; McGuire *et al*. 2004; Olson *et al*. 2001). Similarly, in the isolated respiratory network *in vitro*, Blitz and Ramirez report that intermittent anoxia only evokes frequency LTF with no effect on inspiratory amplitude (Blitz and Ramirez 2002).

Age has powerful affects on CNS plasticity and in particular respiratory LTF. For example, LTF is less pronounced in old (1-year) male rats compared with young (3–4 month-old) ones (Zabka *et al*. 2001). Although the effects of postnatal development on respiratory control mechanisms have been well studied, there has been little focus on early development and LTF, despite the fact that intermittent hypoxia evokes unique forms of respiratory plasticity in newborn rodents and that such changes persist into adulthood (Gozal and Gozal 2001). Therefore, it is also possible that development may affect both the expression and mechanisms that mediate LTF.

Since hypoxia-induced LTF in adults requires serotonin, we hypothesize similar mechanisms in neonatal rats. However, since serotonin projections and receptor expression levels vary as a function of age (Talley, Sadr and Bayliss 1997), this could

affect how LTF is expressed across development. We propose that intermittent hypoxia leads to frequency LTF in postnatal rats because it activates and triggers the medullary raphe nucleus to increase the release of serotonin onto the respiratory network (*e.g.*, pre-Bötzinger complex), which leads to enhanced respiratory frequency. Our observation of frequency LTF is consistent with results from Blitz and Ramirez (2003) who demonstrate that intermittent anoxia evokes frequency LTF (with no change in inspiratory amplitude) in the isolated respiratory network *in vitro*. The lack of effect on inspiratory amplitude could be due to either developmental age or experimental conditions (*e.g.*, lack of anaesthesia).

The study of LTF in development is important because it may function to augment ventilatory drive during vulnerable periods such as sleep, a time in which children with abnormal serotonin systems (Paterson, Trachtenberg, Thompson, Belliveau, Beggs, Darnall, Chadwick, Krous and Kinney 2006) die from sudden infant death syndrome (SIDS). Understanding LTF and its mechanisms may therefore lead to an improved understanding of the fundamental mechanisms that act to combat SIDS and maintain ventilation in instances of life-threatening hypoxia.

Acknowledgements We thank NSERC, CIHR and the Parker B. Francis Family Foundation for supporting this study.

References

Baker, T.L. and Mitchell, G.S. (2000) Episodic but not continuous hypoxia elicits long-term facilitation of phrenic motor output in rats. J. Physiol. 529 Pt. 1, 215–219.

Baker-Herman, T.L. and Mitchell, G.S. (2002) Phrenic long-term facilitation requires spinal serotonin receptor activation and protein synthesis. J. Neurosci. 22, 6239–6246.

Bavis, R.W. (2005) Developmental plasticity of the hypoxic ventilatory response after perinatal hyperoxia and hypoxia. Respir. Physiol. Neurobiol. 149, 287–299.

Blitz, D.M. and Ramirez, J.M. (2002) Long-term modulation of respiratory network activity following anoxia *in vitro*. J. Neurophysiol. 87, 2964–2971.

Cao, K.Y., Zwillich, C.W., Berthon-Jones, M. and Sullivan, C.E. (1992) Increased normoxic ventilation induced by repetitive hypoxia in conscious dogs. J. Appl. Physiol. 73, 2083–2088.

Fuller, D.D., Bach, K.B., Baker, T.L., Kinkead, R. and Mitchell, G.S. (2000) Long-term facilitation of phrenic motor output. Respir. Physiol. 121, 135–146.

Gozal, E. and Gozal, D. (2001) Respiratory plasticity following intermittent hypoxia: developmental interactions. J. Appl. Physiol. 90, 1995–1999.

Kline, D.D., Overholt, J.L. and Prabhakar, N.R. (2002) Mutant mice deficient in NOS-1 exhibit attenuated long-term facilitation and short-term potentiation in breathing. J. Physiol. 539, 309–315.

McGuire, M., Zhang, Y., White, D.P. and Ling, L. (2004) Serotonin receptor subtypes required for ventilatory long-term facilitation and its enhancement after chronic intermittent hypoxia in awake rats. Am. J. Physiol. Regul. Integr. Comp. Physiol. 286, R334–R341.

McKay, L.C., Janczewski, W.A. and Feldman, J.L. (2004) Episodic hypoxia evokes long-term facilitation of genioglossus muscle activity in neonatal rats. J. Physiol. 557, 13–18.

Mortola, J.P. (1999) How newborn mammals cope with hypoxia. Respir. Physiol. 116, 95–103.

Olson, E.B., Jr., Bohne, C.J., Dwinell, M.R., Podolsky, A., Vidruk, E.H., Fuller, D.D., Powell, F.L. and Mitchel, G.S. (2001) Ventilatory long-term facilitation in unanesthetized rats. J. Appl. Physiol. 91, 709–716.

Paterson, D.S., Trachtenberg, F.L., Thompson, E.G., Belliveau, R.A., Beggs, A.H., Darnall, R., Chadwick, A.E., Krous, H.F. and Kinney, H.C. (2006) Multiple serotonergic brainstem abnormalities in sudden infant death syndrome. JAMA 296, 2124–2132.

Paton, J.F. (1996) A working heart-brainstem preparation of the mouse. J. Neurosci. Methods 65, 63–68.

Talley, E.M., Sadr, N.N. and Bayliss, D.A. (1997) Postnatal development of serotonergic innervation, 5-HT1A receptor expression, and 5-HT responses in rat motoneurons. J. Neurosci. 17, 4473–4485.

Zabka, A.G., Behan, M. and Mitchell, G.S. (2001a) Long-term facilitation of respiratory motor output decreases with age in male rats. J. Physiol. 531, 509–514.

42
Respiratory Control, Respiratory Sensations and Cycling Endurance After Respiratory Muscle Endurance Training

Samuel Verges[1], Urs Kruttli[2], Bernhard Stahl[3], Ralf Frigg[4] and Christina M. Spengler[5]

Abstract Respiratory muscle endurance training (RMET) was shown to increase endurance performance in healthy subjects. Reduced adverse respiratory sensations might contribute to this improvement. In the present study, we aimed to assess the relationship between changes in respiratory sensations and changes in ventilation and endurance performance after RMET. Fourteen healthy subjects completed either forty 15-min RMETs (n = 8) or did no training (control, n = 6). Respiratory endurance increased significantly after RMET while breathlessness and respiratory exertion were significantly reduced. Cycling endurance did not change while average ventilation was increased and perception of respiratory exertion was reduced. We conclude that (1) RMET reduces adverse respiratory sensations during isolated and exercise-induced hyperpnea even in the face of increased respiratory drive, and (2) the reduction in adverse respiratory sensations after RMET does not *per se* cause an increase in endurance performance. Whether the reduced perception of adverse respiratory sensations during exercise after RMET might be the cause of the increased respiratory drive remains to be clarified.

1 Introduction

Several well-controlled studies showed that respiratory muscle training can improve endurance performance in healthy subjects (for review see Sheel 2002). However, the underlying mechanisms are still unclear. One potential mechanism might be a reduction in the perception of adverse respiratory sensations being responsible, at least in part, for the improved exercise performance (Sheel 2002).

A reduction in perceived adverse respiratory sensations might, in turn, be responsible for a phenomenon observed by our group (Boutellier, Buchel, Kundert and Spengler 1992; Kohl, Koller, Brandenberger, Cardenas and Boutellier 1997) and others (Reed and Coates 2001), *i.e.*, subjects hyperventilating and cycling for

[1–5] Exercise Physiology, Institute for Human Movement Sciences, ETH Zurich, and Institute of Physiology and Center for Integrative Human Physiology (ZIHP), University of Zurich, Switzerland, spengler@physiol.uzh.ch

M.J. Poulin and R.J.A. Wilson (eds.), *Integration in Respiratory Control: From Genes to Systems*. © Springer 2008

a reduced duration at identical workloads after respiratory muscle endurance training (RMET). Therefore, we aimed to clarify whether increased adverse respiratory sensations might be responsible for the reduced cycling endurance in those subjects who hyperventilated, whether a reduction in the perception of adverse respiratory sensations might be associated with an increase in ventilation after RMET or with increased cycling endurance.

We hypothesized that RMET would decrease the perception of breathlessness and respiratory exertion during isolated and exercise-induced hyperpnea independent of the level of ventilation and that it would increase cycling endurance.

2 Methods

2.1 Subjects

Fourteen healthy, moderately trained men were assigned to two groups (RMET, n = 8, 28 ± 4 yrs, 183 ± 4 cm and 74 ± 7 kg; Control, n = 6, 29 ± 5 yrs, 176 ± 6 cm and 70 ± 8 kg). Subjects were requested to keep their physical training constant and to log their physical activities, which were checked regularly to ensure compliance. Subjects gave written informed consent, and the study was app roved by the local ethics committee.

2.2 Protocol

First (in week 0), lung function was measured and an incremental cycling test was performed to exhaustion to determine peak oxygen consumption ($\dot{V}O2_{peak}$) and maximal work capacity ($\dot{W}_{max}$). Also, subjects were familiarized with the different devices and measurements.

Then, the RMET-group started the 8-week training period (weeks 1–8), performing 15 min of normocapnic hyperpnea (= RMET; see McMahon, Boutellier, Smith and Spengler 2002) daily (days 1–5 of each week), while the control group did no training. Minute ventilation was set at 60% MVV and subjects were instructed to increase breathing frequency linearly to reach 100% MVV in the last RMET session. They reported to the laboratory for a weekly, supervised training.

Subjects reported to the laboratory on day 1 of weeks 1–5 (before the RMET of the day) to assess: (i) respiratory sensations during resistive breathing (5 × 6 levels, *i.e.*, holes with IDs of 1–6 mm, random order), (ii) maximal in- and expiratory pressures, (iii) respiratory endurance at ~ 70% MVV and, after a 1-hr break, (iv) constant-load cycling endurance at 85% $\dot{W}_{max}$.

On day 1 of week 9 (*i.e.*, immediately following the end of the RMET/control period), resistive breathing, maximal pressures, respiratory endurance and, after a 1-hr break, constant-load cycling endurance were assessed again. Two days later, lung function and incremental cycling performance were measured.

2.3 Data Analysis

Lung function, $\dot{V}O2_{peak}$ and $\dot{W}_{max}$ were compared using the Wilcoxon Sign Rank Test. Maximal pressures, respiratory exertion during resistive breathing, variables assessed during respiratory endurance and constant-load cycling tests were compared using the Friedman analysis of variance with the Wilcoxon test for *post hoc* analyses. All results are means ± SD and $p < 0.05$ was considered to be statistically significant.

3 Results

Lung function and respiratory exertion during resistive breathing did not change in either group. $\dot{V}O2_{peak}$ decreased slightly in the RMET (4548 ± 529 vs. 4440 ± 593 ml•min^{-1}, $p = 0.036$) and control group (4239 ± 639 vs. 4062 ± 761 ml•min^{-1}, $p = 0.046$), the changes not being different between groups. $\dot{W}_{max}$ did not change in either group (see Tables 1 and 2).

4 Discussion

The present study showed that 15 min of RMET performed 5x/wk over 8 weeks significantly decreased the perception of adverse respiratory sensations both during isolated and exercise-induced hyperpnea. This change was present despite relative hyperventilation during cycling but it did not translate into improved endurance.

Despite a large improvement in respiratory endurance, cycling endurance did not change significantly after RMET in contrast to most of the previous investigations (Boutellier *et al*. 1992; Boutellier and Piwko 1992; Spengler, Roos, Laube and Boutellier 1999; McMahon *et al*. 2002; Stuessi, Spengler, Knopfli-Lenzin, Markov

Table 1 Variables assessed during respiratory endurance tests during (weeks 2 and 5) and after (week 9) the RMET/control period

Respiratory Endurance	RMET group (n = 8)			Control group (n = 6)		
	Week 2	Week 5	Week 9	Week 2	Week 5	Week 9
Time (min)	18.8 (12.8)	50.3 (13.7)*§	51.0 (12.3)*§	12.2 (6.3)	23.4 (15.0)	19.5 (15.0)
BR (points)	2.3 (2.6)	0.9 (1.6)*	0.8 (1.4)*§	3.6 (2.6)	2.0 (1.9)	2.7 (2.5)
RE (points)	7.0 (1.4)	4.2 (1.7)*	3.6 (1.7)*	6.0 (1.7)	4.5 (1.6)	5.1 (2.6)
HR (beats•min^{-1})	117 (14)	102 (16)*	101 (11)*	101 (24)	94 (15)	95 (15)
[La] (mmol•l^{-1})	2.6 (0.6)	2.4 (0.5)*	2.2 (0.6)*+§	2.2 (0.5)	2.1 (0.7)	2.3 (0.6)

Values are means (SD) of average values corresponding to the duration of the shortest of the 3 tests; values are presented for week 2 as the test in week 1 lasted for only 2 min; RMET, respiratory muscle endurance training; BR, breathlessness; RE, respiratory exertion; HR, heart rate; [La], blood lactate concentration; * different from week 2; + different from week 5; § difference to week 2 larger than control.

Table 2 Variables assessed during exhaustive constant-load cycling tests before (week 1), during (week 5) and after (week 9) the RMET/control period

	RMET group (n = 8)			Control group (n = 6)		
Cycling Endurance	Week 1	Week 5	Week 9	Week 1	Week 5	Week 9
Time (min)	16.4 (1.9)	17.0 (2.7)	16.4 (3.1)	19.2 (3.4)	16.5 (5.1)	17.9 (12.5)
$\dot{V}E(l.min^{-1})$	103.7 (18.1)	113.9 (20.5)*§	118.3 (19.8)*§	96.0 (14.0)	96.0 (14.5)	96.3 (14.5)
V_T (l)	3.2 (0.5)	3.2 (0.5)	3.3 (0.5)	2.9 (0.4)	2.8 (0.4)	2.8 (0.4)
f_B (cycles•min^{-1})	32.6 (7.0)	35.2 (6.7)*	35.9 (5.7)*	33.8 (4.9)	34.5 (6.2)	34.5 (2.7)
$\dot{V}o2(ml•min^{-1})$	3627 (469)	3776 (513)*§	3787 (453)*§	3398 (621)	3330 (606)	3387 (615)
$\dot{V}co2(ml.min^{-1})$	3819 (507)	3949 (542)*	3929 (459)	3536 (629)	3440 (620)	3542 (654)
PET,CO_2 (mmHg)	41.5 (4.7)	39.3 (4.5)*	38.6 (3.8)*§	41.3 (2.9)	40.5 (4.6)	40.3 (2.7)
BR (points)	2.0 (2.0)	1.2 (1.5)	0.9 (1.2)	3.2 (2.2)	2.9 (2.3)	3.0 (2.3)
RE (points)	6.0 (0.8)	5.5 (0.9)	4.5 (0.8)*§	5.4 (1.0)	4.8 (1.4)	5.5 (1.9)
LE (points)	6.8 (0.8)	6.6 (0.6)	6.0 (0.9)	6.2 (1.8)	6.1 (1.7)	6.1 (2.3)
HR (beats•min^{-1})	168 (12)	167 (13)	170 (11)	157 (12)	152 (14)	159 (11)
[La] (mmol•l^{-1})	7.3 (0.8)	8.1 (1.5)	8.0 (1.6)	5.1 (0.9)	5.1 (1.6)	5.2 (1.4)

Values are means (SD) of average values corresponding to the duration of the shortest of the 3 tests; $\dot{V}_E$, minute ventilation; V_T, tidal volume; f_B, breathing frequency; $\dot{V}O2$, oxygen consumption; $\dot{V}CO2$, carbon dioxide production; PET, CO_2, end-tidal CO_2 partial pressure; LE, leg exertion; for other abbreviations see Table 1.
* different from week 1; § difference to week 1 larger than control.

and Boutellier 2001; Markov, Spengler, Knopfli-Lenzin, Stuessi and Boutellier 2001; Holm, Sattler and Fregosi 2004). Subjects hyperventilated during exercise similar to the subjects tested by Kohl *et al*. (1997). Their and our observations suggest that an increase in ventilation after RMET may in fact impede its potential benefit on exercise performance (Boutellier *et al*. 1992; Kohl *et al*. 1997).

With an increase in ventilation, one would expect an increase in adverse respiratory sensations, which could, in turn, impair exercise performance (Mador and Acevedo 1991). In the present study, however, perception of adverse respiratory sensations was decreased after RMET (*i.e*., unlikely to be responsible for the lacking improvement in cycling endurance). Instead, the increase in respiratory work may have impaired cycling performance after RMET, possibly by enhancing the competition for blood flow between respiratory and limb locomotor muscles (Dempsey, Romer, Rodman, Miler and Smith 2006), this factor being more important than the better subjective feeling. The increased ventilation during exercise could possibly be explained by the reduction in adverse respiratory sensations after RMET in that the respiratory controller "aimed" to achieve the same respiratory sensation as previously associated with this particular exercise load.

Changes in respiratory sensations were shown to correspond to the force generated by the respiratory muscles relative to their maximal force (Killian, Bucens and Campbell 1982; Redline, Gottfried and Altose 1991). In the present study, however, maximal in- and expiratory force did not increase significantly after RMET, which likely explains that perception of respiratory exertion did not change during resistive breathing. Thus, the level of perceived respiratory exertion during hyperpnea does not seem to be determined by the force generated relative to the maximal force but other mechanisms are likely involved (*e.g*., a decrease in respiratory muscle fatigue) (Verges, Lenherr, Haner, Schulz and Spengler 2006).

Acknowledgements Financial support was provided by the Swiss National Science Foundation (grant no. 3100A0-103716). Samuel Vergès was supported by the AGIR, France.

References

Boutellier, U., Buchel, R., Kundert, A. and Spengler, C. (1992) The respiratory system as an exercise limiting factor in normal trained subjects. Eur. J. Appl. Physiol. 65, 347–353.

Boutellier, U. and Piwko, P. (1992) The respiratory system as an exercise limiting factor in normal sedentary subjects. Eur. J. Appl. Physiol. 64, 145–152.

Dempsey, J.A., Romer, L., Rodman, J., Miller, J. and Smith, C. (2006) Consequences of exercise-induced respiratory muscle work. Respir. Physiol. Neurobiol. 151, 242–250.

Killian, K.J., Bucens, D.D. and Campbell, E.J. (1982) Effect of breathing patterns on the perceived magnitude of added loads to breathing. J. Appl. Physiol. 52, 578–584.

Kohl, J., Koller, E.A., Brandenberger, M., Cardenas, M. and Boutellier, U. (1997) Effect of exercise-induced hyperventilation on airway resistance and cycling endurance. Eur. J. Appl. Physiol. 75, 305–311.

Mador, M.J. and Acevedo, F.A. (1991) Effect of respiratory muscle fatigue on subsequent exercise performance. J. Appl. Physiol. 70, 2059–2065.

Markov, G., Spengler, C.M., Knopfli-Lenzin, C., Stuessi, C. and Boutellier, U. (2001) Respiratory muscle training increases cycling endurance without affecting cardiovascular responses to exercise. Eur. J. Appl. Physiol. 85, 233–239.

McMahon, M.E., Boutellier, U., Smith, R.M. and Spengler, C.M. (2002) Hyperpnea training attenuates peripheral chemosensitivity and improves cycling endurance. J. Exp. Biol. 205, 3937–3943.

Redline, S., Gottfried, S.B. and Altose, M.D. (1991) Effects of changes in inspiratory muscle strength on the sensation of respiratory force. J. Appl. Physiol. 70, 240–245.

Reed, J.W. and Coates, J.C. (2001) Induction of long-term modulation of the exercise ventilatory response in man. Adv. Exp. Med. Biol. 499, 221–224.

Sheel, A.W. (2002) Respiratory muscle training in healthy individuals: physiological rationale and implications for exercise performance. Sports Med. 32, 567–581.

Spengler, C.M., Roos, M., Laube, S.M. and Boutellier, U. (1999) Decreased exercise blood lactate concentrations after respiratory endurance training in humans. Eur. J. Appl. Physiol. 79, 299–305.

Stuessi, C., Spengler, C.M., Knopfli-Lenzin, C., Markov, G. and Boutellier, U. (2001) Respiratory muscle endurance training in humans increases cycling endurance without affecting blood gas concentrations. Eur. J. Appl. Physiol. 84, 582–586.

Verges, S., Lenherr, O., Haner, A.C., Schulz, C., Spengler, C.M. (2007) Increased fatigue resistance of respiratory muscles during exercise after respiratory muscle endurance training. Am. J. Physiol. Regul. Integr. Comp. Physiol., 292, R1246–R1253.

43
Non-dimensional Quantification of the Interactions Between Hypoxia, Hypercapnia and Exercise on Ventilation in Humans

H.E. Wood[1], M. Fatemian[2] and P.A. Robbins[3]

Abstract The purpose of this study was to develop a non-dimensional approach towards the description of interaction between the three respiratory stimuli of hypoxia, hypercapnia and exercise and to use this approach to quantify the relative strengths of their interactions. Only a part of the study related to the overall interaction of the three stimuli is presented here. Nine volunteers took part in the study and their ventilatory responses to hypoxia were measured under four different conditions of rest-eucapnia, rest-hypercapnia, exercise-eucapnia and exercise-hypercapnia. Non-dimensional linear functions of hypercapnia (x), hypoxia (y) and exercise (z) were defined such that a value of one would double the resting ventilation. Non-dimensional ventilation v was derived as: $v(x,y,z) = 1 + x + y + z + g_1xy + g_2xz + g_3yz + g_4xyz$, where g_1, g_2, g_3 and g_4 provide non-dimensional measures of the strength of stimulus interaction. These interactions were calculated from the parameters obtained by fitting simple respiratory models to the data. The values for g_1, g_3 and g_4 were significantly different from zero ($p < 0.05$, t-test). An intriguing result of this study is the overall negative interaction of the three stimuli, which may suggest that the linear, stimulus-response models commonly used to describe respiratory data may not be adequate for describing these complex interactions.

1 Introduction

Ventilation is increased upon stimulation by hypoxia, hypercapnia and exercise. It is well known that hypoxia and hypercapnia (Nielsen and Smith 1952) and also hypoxia and exercise (Asmussen and Neilsen 1946) interact in their effects on ventilation, but there are conflicting results regarding the interaction between hypercapnia and exercise (Poon and Greene 1985). However, there are very few reports in the literature of the combined effects of hypercapnia, hypoxia and exercise on ventilation.

[1–3] University of Oxford, Department of Physiology, Anatomy and Genetics, peter.robbins@physiol.ox.ac.uk

M.J. Poulin and R.J.A. Wilson (eds.), *Integration in Respiratory Control: From Genes to Systems*.

In order to quantify the degree of interaction between the stimuli, a model of the most general form of stimulus interaction that can occur if the ventilatory responses to hypercapnia, hypoxia (*i.e.*, desaturation) and exercise are all linear was developed. Based on this model, a non-dimensional ventilation equation containing all the interaction terms was derived to quantify the strength of stimulus interactions via the non-dimensional parameters of the model.

2 Methods

Nine volunteers (8 males, 1 female) aged between 19 and 25 yr took part in the study. All were healthy non-smokers with no history of respiratory or cardiovascular disease. The study was approved by the Central Oxford Research Ethics Committee and informed written consent was obtained from all volunteers.

2.1 Protocols

Four protocols were employed for the part of the study presented in this chapter. Ventilatory response to acute hypoxia was measured under the conditions of:

(1) Rest-eucapnia; subject was at rest, the end-tidal P_{CO_2} ($P_{ET_{CO_2}}$) was held at 1.5 Torr above subject's air-breathing value at rest, and the end-tidal oxygen ($P_{ET_{O_2}}$) was varied between 100 and 50 Torr (in a square wave pattern).
(2) Rest-hypercapnia; subject was at rest, $P_{ET_{CO_2}}$ was held at 8 Torr above subject's air-breathing value at rest and $P_{ET_{O_2}}$ was varied between 100 and 50 Torr.
(3) Exercise-eucapnia; subject was cycling at a constant work rate of 30% of his/her maximal work rate, $P_{ET_{CO_2}}$ was held at 1.5 Torr above subject's air-breathing value at this work rate and $P_{ET_{O_2}}$ was cycled between 100 and 57 Torr.
(4) Exercise-hypercapnia, subject was cycling at a constant work rate of 30% of his/her maximal work rate, $P_{ET_{CO_2}}$ was held at 8 Torr above subject's air-breathing value at this work rate and $P_{ET_{O_2}}$ was cycled between 100 and 57 Torr.

2.2 Experimental Technique

The gas controls were carried out using a dynamic end-tidal forcing (DEF) system. The volunteer was seated in an upright position in a chair for the measurements at rest and on a cycle ergometer for those during exercise and breathed through a mouthpiece with the nose occluded by a clip. Respiratory volumes were measured using a turbine volume-measuring device fixed in series with the mouthpiece; flows and timing information were recorded using a pneumotachograph. Gas was sampled continuously from this dead space, close to the mouth, and analyzed for P_{O_2} and P_{CO_2} by a mass spectrometer. During the experiment, actual $P_{ET_{O_2}}$ and $P_{ET_{CO_2}}$

values were compared with the desired values, and a new inspired gas mixture was calculated by using an integral-proportional feedback scheme (Robbins, Swanson and Howson 1982) and delivered via mouth piece assembly.

3.3 Data Analysis

It can be shown that where linear responses to hypercapnia, hypoxia (*i.e.*, desaturation) and exercise exist, the most general form of stimulus interaction that can occur can be expressed as:

$$v(x,y,z) = 1 + x + y + z + g_1xy + g_2xz + g_3yz + g_4xyz$$

where, x,y,z are defined as the non-dimensional stimulus functions for hypercapnia, hypoxia, and exercise, respectively. $v(x,y,z)$ is the non-dimensional ventilation (expressed in multiples of the unstimulated ventilation) and g_1, g_2, g_3 and g_4 provide non-dimensional measures of the strength of stimulus interaction. Parameters related to the effect of each stimulus on the ventilation were obtained by fitting simple ventilatory models to the ventilation data and these parameter values were used in turn, to calculate g_1, g_2, g_3 and g_4. Statistical analysis was performed to determine the significant changes in the strength of stimulus interactions.

4 Results

Figure 1 is an example of the breath-by-breath ventilatory data and model fits for one subject and all protocols. The parameters of these model fits were used to calculate the strength of stimuli interactions, averaged for all subjects.

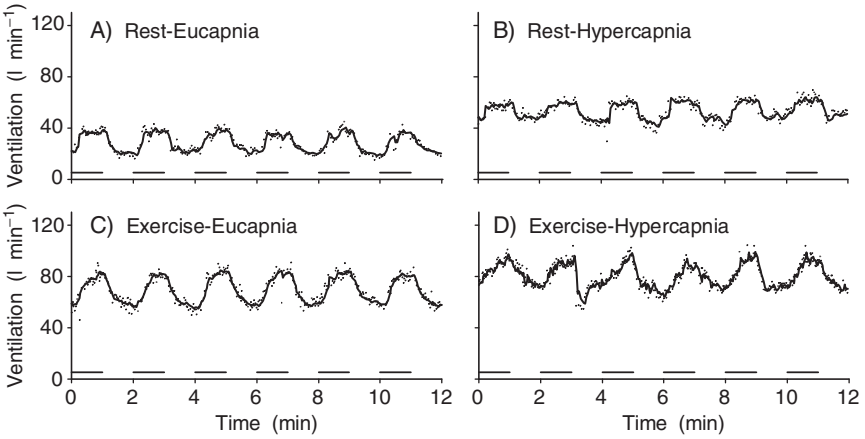

Fig. 1 Breath-by-breath ventilation data (dots) and respiratory model fits (lines) for one subject. Hypoxia periods are indicated by horizontal bars

The numerical values calculated for the non-dimensional parameters (mean ± SD) were: $g_1 = 0.37 \pm 0.39$; $g_2 = -0.07 \pm 0.82$; $g_3 = 1.19 \pm 0.65$; and $g_4 = -0.76 \pm 0.95$. The values for g1, g3 and g4 were significantly different from zero ($p < 0.05$, t-test), but that for g_2 was not significantly different from zero (t-test).

5 Conclusions

A significant negative interactive effect on ventilation was detected for the overall interaction of hypercapnia, hypoxia and exercise. This suggests that some saturation mechanism may be present which, for example, could reside within the peripheral chemoreceptors, within the brainstem or within the peripheral/mechanical motor output of the respiratory centres. This result also may suggest that the linear, stimulus-response models commonly used to describe respiratory data may not be adequate for describing these complex interactions.

Acknowledgement This study was funded by the Wellcome Trust.

References

Asmussen, E. and Neilsen, M. (1946). Studies on the regulation of respiration in heavy work. Acta. Physiol. Scand. 12, 171–188.

Nielsen, M. and Smith, H. (1952). Studies on the regulation of respiration in acute hypoxia: with an appendix on respiratory control during prolonged hypoxia. Acta. Physiol. Scand. 24, 293–313.

Poon, C-S. and Greene, J.G. (1985). Control of exercise hyperpnea during hypercapnia in humans. J. Appl. Physiol. 59, 792–797.

Robbins, P.A., Swanson, G.D. and Howson, M.G. (1982). A prediction-correction scheme for forcing alveolar gases along certain time courses. J. Appl. Physiol. 52, 1353–1357.

44
Elevated Body Temperature Exaggerates Laryngeal Chemoreflex Apnea in Decerebrate Piglets

Luxi Xia[1], Tracey Damon[2], J.C. Leiter[3] and Donald Bartlett, Jr.[4]

Abstract We investigated the interaction between body temperature and the duration of the laryngeal chemoreflex (LCR) in decerebrate piglets. Elevating body temperature by ~ 2°C prolongs the duration of the LCR and the length of apnea associated with the reflex. This thermal prolongation seems to arise within the nucleus of the solitary tract in the brainstem, and we believe the thermal effect is mediated by enhanced GABAergic neurotransmission.

1 Epidemiology and Pathogenesis of Sudden Infant Death Syndrome

The Sudden Infant Death Syndrome (SIDS) is, by definition, a rare event occurring only once in the life of each of its victims and not at all in the lives of other infants. Such a rare, but devastating event may occur through a confluence of other, less rare events which, by themselves, do not have lethal consequences. Thus, death may result from a "perfect storm" of events that almost never occur together but, when they do, are overwhelming, or perhaps a less than perfect storm but in an abnormal infant. This concept has led investigators to search for developmental abnormalities in SIDS victims and for environmental stressors that are particularly disruptive in infancy.

SIDS has been epidemiologically linked to a number of risk factors. The most important known risk factors are maternal cigarette smoking (Mitchell *et al*. 1993) and the prone sleeping position (Paris *et al*. 2001). SIDS is also associated with postnatal heat stress. Many reports indicate that death frequently occurs in overheated rooms, with excessive bundling or wrapping of the infant (Fleming *et al*. 1990; Iyasu *et al*. 2002), who occasionally is found covered with sweat (Kleeman *et al*. 1996). As emphasized by Guntheroth and Spiers (2001), the demonstrated danger of the prone sleeping position may relate more to heat stress than to asphyxia. Prone infants lose heat more slowly than supine infants do, both from the body surface and via the respiratory tract (Bolton *et al*. 1996).

[1–4] Dartmouth Medical School, Department of Physiology, james.c.leiter@dartmouth.edu

M.J. Poulin and R.J.A. Wilson (eds.), *Integration in Respiratory Control: From Genes to Systems*. © Springer 2008

1.1 The Laryngeal Chemoreflex and SIDS

The laryngeal chemoreflex (LCR) is prominent in newborn animals and human infants, and it has long been suspected as a cause of some cases of SIDS (Downing and Lee 1975). The LCR is elicited by fluid in the airway (Downing and Lee 1975; Boggs and Bartlett 1982), and the central afferent projections travel in the superior laryngeal nerve (SLN) and terminate in the nucleus of the solitary tract (NTS). Once stimulated, the reflex response consists of apnea, respiratory disruption, coughing, swallowing, bradycardia and redistribution of blood flow (Harding *et al*. 1975). Haraguchi *et al*. (1983) found that the latency and threshold of laryngeal closure induced by electrical stimulation of the SLN, which mimics aspects of the LCR, was reduced when the body temperature of puppies was elevated. The thermal enhancement of the reflex waned as the puppies aged and was absent in animals 12 weeks of age and older. Given the importance of temperature and the LCR in the epidemiology and putative pathogenesis of SIDS, we conducted a series of studies to test the hypothesis that hyperthermia increases the severity of the apnea and respiratory disruption associated with the LCR.

2 Methods of Studying Decerebrate Piglets

We studied piglets aged 3–16 days with body weights ranging from 1.5 to 5.5 Kg. Animals were anesthetized, decerebrated and paralyzed as described previously (Curran *et al*. 2005). Integrated phrenic nerve activity, phrenic frequency, body temperature, end-tidal CO_2 and blood pressure were recorded on a computer for later analysis. The LCR was stimulated by infusing 0.1 ml of distilled water during inspiration through a tube inserted into one nostril with its tip located just rostral to the larynx. We defined the duration of the LCR as the period of respiratory instability from the beginning of the breath during which water was injected into larynx to the onset of at least five regular breaths. Apnea was defined as a cessation of breathing greater than the duration of the two breaths preceding the breath during which the LCR was elicited.

3 Elevated Temperature Increases the Duration of the LCR

In our first study, we raised the temperature of the entire piglet using a servo-controlled heating pad. We found that elevating body temperature ~ 2.4°C prolonged the LCR ~ 8-fold (Curran *et al*. 2005). When body temperature was restored to the control level, both apnea and LCR duration also returned to control values.

We subsequently determined that the response of water receptors in the larynx to elevated body temperature was not affected by temperature changes from 37.7 ±

0.3°C to 40.6 ± 0.2°C (Xia *et al*. 2005). Thus, the thermal prolongation of the LCR seemed to arise from elevation of the brain temperature.

3.1 Elevating the Temperature of the NTS Prolongs the LCR

To determine the location within the central nervous system that mediates the effect of elevated temperature on the LCR, we used a thermode to heat small volumes of the brainstem (Xia *et al*. 2006). Elevating the temperature of the NTS prolonged the LCR significantly, but elevating the temperature of the caudal raphé did not alter the LCR. Thermal prolongation of the LCR seems, therefore, to arise from a specific site in and around the NTS. Our thermode heated a relatively large volume of tissue, and we could not isolate the temperature effect to specific regions within the NTS.

3.2 GABA May Mediate the Thermal Prolongation of the LCR

We started a series of studies to determine whether GABAergic mechanisms may mediate the enhanced respiratory inhibition following stimulation of the LCR at elevated body temperatures. The effect of elevating body temperature on the LCR is shown in the top two panels of Fig. 1, and the effect of infusing bicuculline, a $GABA_A$ receptor antagonist, is shown in the lowest panel. Note that the thermal prolongation of the LCR previously evident in this animal was markedly diminished by infusion of bicuculline.

4 Discussion

Elevated body temperature prolongs the LCR, and this thermal prolongation is mediated by elevating the temperature of the brainstem in and adjacent to the NTS. Elevated temperature seems to enhance GABAergic neurotransmission and, in this way, enhances the respiratory inhibition associated with the LCR. The effect of temperature may depend on neurons that receive laryngeal afferent information in the NTS, but there are thermo-sensitive neurons in and around the NTS (Inoue and Murakami 1976), which may also be involved. Although the thermal effects seem to originate in the NTS, the enhanced effects of GABA may be manifest outside of the NTS, particularly since GABA seems to mediate respiratory inhibition during the LCR and other inhibitory reflexes through neuronal interactions in the ventral respiratory group (VRG) and ventral medulla (van der Velde *et al*. 2003; Ezure and Tanaka 2004). Thus, thermo-sensitive neurons in the region of the NTS may augment the inhibition of VRG neurons elicited during the LCR by interacting with either of those neurons that receive laryngeal afferent information in the NTS or directly with respiratory related neurons in the DRG and ventral medulla.

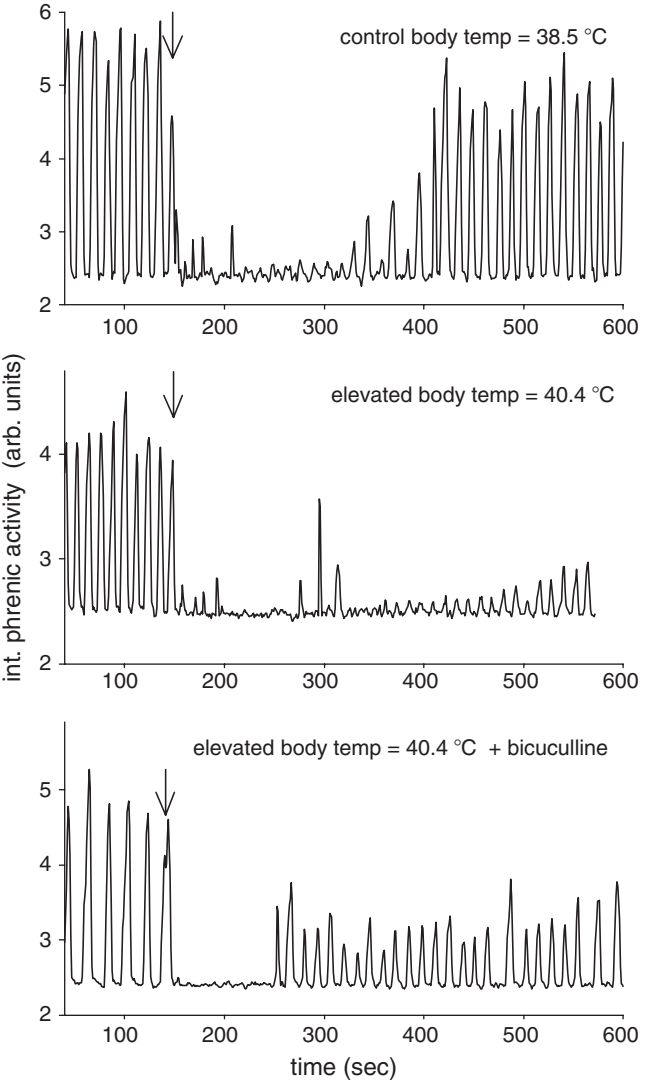

Fig. 1 Three examples of the LCR at different body temperatures (arrows indicate the time of laryngeal injection). In the final example, the LCR was stimulated ~ 40 minutes after 0.3 mg/kg bicuculline was given intravenously. Note that bicuculline, which blocks $GABA_A$ receptors, markedly reduced the thermal prolongation of the LCR apparent in the middle panel

This series of studies is highly relevant to SIDS and highly relevant to prone sleeping. Elevated body temperature is a well-recognized risk factor for SIDS, and prone sleeping reduces the capacity of infants to lose heat. Moreover, our studies demonstrate that hyperthermia may potentiate an inhibitory reflex that is frequently activated in infants. In those infants with underlying developmental abnormalities that delay or prevent excitatory respiratory reflexes or arousals, the combination of

elevated body temperature and the LCR may produce prolonged apnea and may begin the process that results in the sudden unexpected death of an infant.

The effects of bicuculline on laryngeal apnea and muscimol on the LCR (Abu-Shaweesh *et al*. 2001; van der Velde *et al*. 2003) suggest to us that the prolongation of the LCR reflects enhanced GABAergic inhibition of respiratory activity. Although GABA receptor alterations are not among the neurotransmitter receptors abnormalities identified in babies who died of SIDS, enhanced inhibitory activity associated with GABAergic neurotransmission may increase respiratory instability or apnea in infants with the neurotransmitter defects that have been described in babies who died of SIDS.

References

Abu-Shaweesh, J.M., Dreshaj, I.A., Haxhiu, M.A. and Martin, R.J. (2001) Central GABAergic mechanisms are involved in apnea induced by SLN stimulation in piglets. J. Appl. Physiol. 90, 1570–1576.

Boggs, D.F. and Bartlett, D., Jr. (1982) Chemical specificity of a laryngeal apneic reflex in puppies. J. Appl. Physiol. 53, 455–462.

Bolton, D.P.G., Nelson, E.A.S., Taylor, B.J. and Weatherall, I.L. (1996) Thermal balance in infants. J. Appl. Physiol. 80, 2234–2242.

Curran, A.K., Xia, L., Leiter, J.C. and Bartlett, D., Jr. (2005) Elevated body temperature enhances the laryngeal chemoreflex in decerebrate piglets. J. Appl. Physiol. 98, 780–786.

Downing, S.E. and Lee, J.C. (1975) Laryngeal chemosensitivity: A possible mechanism of sudden infant death. Pediatrics 55, 640–649.

Ezure, K. and Tanaka, I. (2004) GABA, in some cases together with glycine, is used as the inhibitory transmitter by pump cells in the Hering-Breuer reflex pathway of the rat. Neuroscience 127, 409–417.

Fleming, P.J., Gilbert, R., Azaz, Y., Berry, P.J., Rudd, P.T., Stewart, A.J. and Hall, E. (1990) Interaction between bedding and sleeping position in the SIDS: a population based case-control study. BMJ 301, 85–89.

Guntheroth, W.G. and Spiers, P.S. (2001) Thermal stress in Sudden Infant Death: Is there an ambiguity with the rebreathing hypothesis? Pediatrics 107, 693–698.

Haraguchi, S., Fung, R.Q. and Sasaki, R. (1983) Effect of hyperthermia on the laryngeal closure reflex. Implications in the sudden infant death syndrome. Ann. Otol. Rhinol. Laryngol. 92, 24–28.

Harding, R., Johnson, P. and Johnston, B.E. (1975) Cardiovascular changes in new-born lambs during apnoea induced by stimulation of laryngeal receptors with water. J. Physiol. (Lond.) 256, 35P–37P.

Inoue, S. and Murakami, N. (1976) Unit responses in the medulla oblongata of rabbit to changes in local and cutaneous temperature. J. Physiol. 259, 339–356.

Iyasu, S., Randall, L.L., Welty, T.K., Hsia, J., Kinney, H.C., Mandell, F., McClain, M., Randall, B., Habbe, D., Wilson, H. *et al*. (2002) Risk factors for sudden infant death syndrome among northern plains Indians. JAMA 288, 2717–2723.

Kleeman, W.J., Schlaud, M., Poets, C.F., Rothämel, T. and Tröger, H.D. (1996) Hyperthermia in sudden infant death. Int. J. Legal Med. 109, 139–142.

Mitchell, E.A., Ford, R.P.K., Stewart, A.K., Taylor, B.J., Becroft, D.M.O., Thompson, J.M.D., Scragg, R., Hassall, M.B., Barry, D.M.J., Allen, E.M. *et al*. (1993) Smoking and the Sudden Infant Death Syndrome. Pediatrics 91, 893–896.

Paris, C.A., Remler, R. and Daling, J.R. (2001) Risk factors for sudden infant death syndrome: Changes associated with sleep position recommendations. J. Pediatr. 139, 771–777.

van der Velde, L., Curran, A., Filiano, J.J., Darnall, R.A., Bartlett, D., Jr. and Leiter, J.C. (2003) Prolongation of the laryngeal chemoreflex prolongation after inhibition of the rostroventral medulla: A role in SIDS? J. Appl. Physiol. 94, 1883–1895.

Xia, L., Leiter, J.C. and Bartlett, D., Jr. (2005) Laryngeal water receptors are insensitive to body temperature in neonatal piglets. Respir. Physiol. Neurobiol. 150, 82–86.

Xia, L., Damon, T.A., Leiter, J.C. and Bartlett, D., Jr. (2006) Focal warming of the nucleus of the solitary tract prolongs the laryngeal chemoreflex in decerebrate piglets. J. Appl. Physiol. 102, 54–62.

Part VII
Neuromodulation

45
Effects of Systemic Administration of Mirtazapine on Respiratory Muscle Activity in Sleeping Rats

Y.-L. Chou[1], J.T. Stanley[2], K.Vujisic[1], R.B. Berry[2], P.W. Davenport[1], J.J. Anderson[3] and L.F. Hayward[1]

Abstract Mirtazapine (MIRT) is an antidepressant with mixed noradrenergic and serotonergic effects in central nervous system. The present study was undertaken to assess whether MIRT can stimulate genioglossus muscle (GG) activity in the conscious, behaving rat. Nine male rats were chronically instrumented with GG and neck muscle EMG electrodes. EEG electrodes were implanted to acquire sleep stage. Results demonstrated a dose-dependent effect of MIRT on GG activity during sleep, although no changes reached statistical significance. Low dose MIRT (0.1 mg/kg) showed a slight increase in GG phasic activity. In contrast, higher doses of MIRT (0.5–1.0 mg/kg) tended to decrease GG activity relative to vehicle, in addition to decreasing total sleep time.

1 Introduction

Alpha-adrenergic-agonists have been shown to increase GG activity. Mirtazapine (MIRT) is a mixed noradrenergic and serotonergic antidepressant with 5-HT1 receptor agonist, as well as 5-HT2 and 5-HT3 receptor antagonist effects in the central nervous system (Devance, 1998). In contrast to sleep disruption associated with serotonin reuptake inhibitors (SSRIs), MIRT has been shown to produce increased sleep efficiency and augmented slow wave sleep (Devance, 1998; Ruigt, Kemp, Groenhout, and Kamphuisen, 1990). In rodents, Carley & Radulovacki (1999) found that MIRT decreased central apnea during both non-rapid eye movement (NREM) and rapid eye movement (REM) sleep. Previously we demonstrated that low-dose (0.5 mg/kg) MIRT increased GG activity in the anesthetized, vagotomized rat (Berry, Koch, and Hayward, 2005). The present study was undertaken to assess whether systemic administration of MIRT can also stimulate GG activity in the conscious, behaving rat.

[1] University of Florida, Department of Physiological Sciences, yangling@ufl.edu

[2] Malcom Randall VAMC/University of Florida College of Medicine, sleep_doc@msn.com

[3] Cypress Bioscience, janderson@CypressBio.com

M.J. Poulin and R.J.A. Wilson (eds.), *Integration in Respiratory Control: From Genes to Systems*.

2 Method

2.1 General Preparation

Experiments were performed on 9 male 350–450 g Sprague-Dawley rats (Charles River). All rats were chronically instrumented under isoflurane anesthesia with EEG electrodes and insulated EMG electrode wires in the GG and neck and allowed a week of recovery. On the day of the experiment, one hour following the beginning of data collection (09:00 to 13:00), all rats received a single intraperitoneal (*i.p.*) injection. Experimental trials of MIRT (0.1, 0.5 and 1.0 mg/kg) and vehicle were randomly scheduled with a 2-day inter-trial interval. The EEG signals were amplified and filtered between 0.3–100 Hz. Neck and GG EMGs were amplified and filtered between 100–1000 Hz.

2.2 Data Analysis

Data were analyzed off-line (Grass Review software). Within trials, the sleep-wake cycle was determined by analysis of the EEG signal, neck EMG and video images for every consecutive 30 s epoch by an experimenter blinded to the treatment given the animal. Sleep-wake stages were identified by visual inspection and were classified by standard characteristics into four stages, active wake (AW), quite wake (QW), NREM, and REM. After sleep/wake staging, the magnitude of neck and GG rectified and integrated EMG were quantified for each sleep-wake cycle from one 30 s epoch within each consecutive 4-min. interval. To assess the relationship between MIRT and vehicle within in each sleep/wake stage over time, the averaged neck and GG EMG were expressed as a percentage of the maximum EMG levels observed during AW in the 1st hr of each trial. Significant changes in GG and neck EMG muscle activity during the total recording time within each vigilance state were identified using an analysis of variance for repeated measures followed by post hoc comparison to control (Statview). An alpha-level of $p < 0.05$ was considered as statistical significance.

3 Results and Discussions

3.1 Sleep-Wake Cycle

Nine male rats of mean weight 368±8 g were studied. Following injection, MIRT had a dose dependent effect on sleep time, including an overall reduction in the total amount of sleep (NREM+REM) over the 3 hrs measured post-injection. This decrease in total sleep time however was only significantly different from vehicle at the highest dose of MIRT (1.0 mg/kg).

The effect of 1.0 mg/kg MIRT on total sleep time included a significant reduction in NREM activity compared to vehicle during each hour following injection

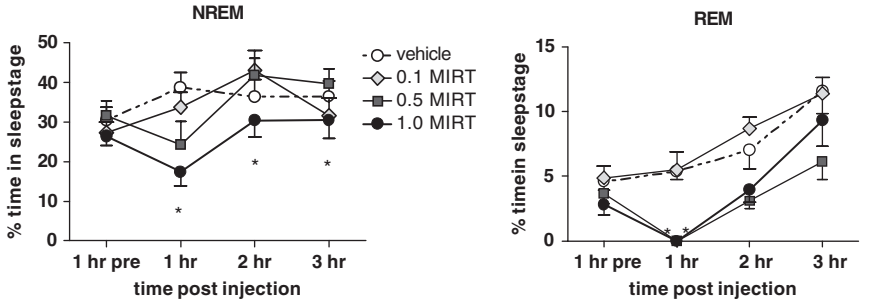

Fig. 1 NREM activity was significantly reduced during each hour following administration of 1.0 mg/kg MIRT and there was no REM activity during the first hour following either 0.5 mg/kg or 1.0 mg/kg MIRT injection (n=9).* represents a significant difference from vehicle

(Fig.1). Additionally, REM activity was completely suppressed during the 1st hour post-injection. There was also a reduction in both NREM and REM activity during the 1st hour following administration of 0.5 mg/kg MIRT, but only the reduction in REM activity was significant from vehicle. Systemic administration of 0.1 mg/kg MIRT had no effect on sleep structure compared to vehicle.

3.2 Genioglossus and Neck Muscle Activities

Before drug injection, neck muscle activity demonstrated a significant reduction across sleep/wake states (30 ± 3% AW max, QW; 15 ± 2%, NREM; 6 ± 1%, REM). MIRT administration did not significantly change neck muscle activity levels compared to pre-injection levels in any sleep/wake state (data not shown).

During the pre-injection period GG muscle activity also showed a significant reduction in levels from QW to NREM (16±2% vs. 10±3% AW max, respectively). GG activity levels during REM however were variable (14±3% AW max), and as a result, were not significantly different from either QW or NREM levels during the pre-injection period.

MIRT administration did not significantly change GG muscle activity compared to vehicle at any dose during NREM or REM (Fig. 2). There was however a trend for 1.0 mg/kg MIRT to decrease GG activity during NREM. Additionally, 1.0 and 0.5 mg/kg MIRT showed a trend to decrease GG activity during REM in the second hour (−8 ± 3% for 1.0 mg/kg). In contrast, 0.1 mg/kg tended to increase GG activity modestly in NREM and REM.

4 Discussion

Results from the present study support a dose-dependent effect of MIRT in which the lowest dose (0.1 mg/kg) showed very modest benefit to upper airway tone and did not alter sleep structure. In contrast, at the higher doses (0.5 and 1.0 mg/kg), MIRT administration tended to decrease GG activity relative to vehicle, particularly

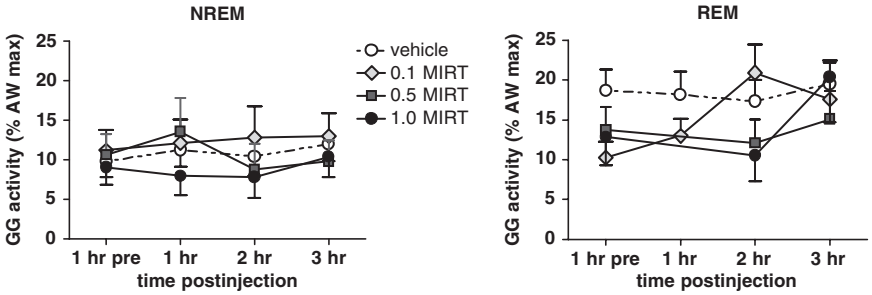

Fig. 2 The average change in genioglossus (GG) EMG activity (as %AW max) plotted over time following 0.1, 0.5, 1.0 mg/kg MIRT versus vehicle (n=9). Systemic MIRT did not significantly change GG activities at any time point; however 1.0 mg/kg MIRT tended to depress GG activity during NREM and REM during the first 2 hours following treatment

during REM. The highest dose of MIRT also induced a significant reduction in REM activity within the 1st hr following administration and NREM activity during the 3 hrs following administration. Augmentation of GG muscle activity at lower doses and inhibition of activity by a high dose of MIRT has been reported previously in anesthetized, vagotomized rats (Berry *et al*., 2005). The same general phenomenon was shown in the present study with conscious moving rat (intact vagal nerve), but the effects in the conscious animal were considerably weaker. This suggests the presence of vagal inputs may suppress the facilitatory effect of MIRT on GG activity. Indeed, Sood and colleagues (Sood, Morrison, Liu, and Horner, 2005) have demonstrated that the facilitatory effects of endogenous 5-HT on GG activity are only observed following vagotomy in the anesthetized animal. This suggests that previous results regarding the role of 5-HT in the modulation of GG activity from vagotomized animals may not apply to naturally sleeping animals. Furthermore, 5-HT2 receptor blockers have been shown to decrease GG activity (Fenik and Veasey, 2003); however, 5-HT3 blocker has been shown to increase GG activity at higher doses. Thus, the net effect of MIRT on GG activity may depend on the relative importance of its different actions on these receptor subtypes in an intact, normally behaving system and these might vary with the doses presented.

Acknowledgement Cypress Bioscience (RBB) and NIH HL-076518 (LFH).

References

Berry, R.B., Koch, G.L. and Hayward, L.F. (2005) Low-dose mirtazapine increases genioglossus activity in the anesthetized rat. Sleep. 28, 78–84.

Carley, D.W. and Radulovacki, M. (1999) Mirtazapine, a mixed-profile serotonin agonist/antagonist, suppresses sleep apnea in the rat. Am. J. Respir. Crit. Care Med. 160, 1824–1829.

Devance, C.L. (1998) Differential pharmacology of newer antidepressants. J. Clin. Psychiatry. 59 Suppl. 20, 85–93.

Fenik, P. and Veasey, S.C. (2003) Pharmacological characterization of serotonergic receptor activity in the hypoglossal nucleus. Am. J. Respir. Crit. Care Med. 167, 563–569.
Ruigt, G.S., Kemp, B., Groenhout, C.M., and Kamphuisen, H.A. (1990) Effect of the antidepressant Org 3770 on human sleep. Eur. J. Clin. Pharmacol. 38, 551–554.
Sood, S., Morrison, J.L., Liu, H. and Horner, R.L. (2005) Role of endogenous serotonin in modulating genioglossus muscle activity in awake and sleeping rats. Am. J. Respir. Crit. Care Med. 172, 1338–1347.

46
Control of Genioglossus Muscle by Sleep State-Dependent Neuromodulators

Richard L. Horner

Abstract Pharyngeal muscle tone decreases in sleep and this predisposes some individuals to obstructive sleep apnea. This review summarizes the control of the genioglossus muscle by sleep-state dependent neuromodulators at the hypoglossal motor nucleus, the source of motor output to the genioglossus muscle of the tongue. Knowledge of such mechanisms is relevant to identifying and developing new strategies to augment pharyngeal muscle activity in sleep, potentially as treatments for obstructive sleep apnea.

1 Sleep and Pharyngeal Muscle Tone

Obstructive sleep apnea (OSA) is characterized by repeated episodes of upper airway collapse during sleep resulting in interruption of airflow despite persisting, but futile, respiratory efforts. Such abnormal breathing effects produce repetitive episodes of asphyxia leading to sleep disturbance. Suppression of pharyngeal muscle activity in sleep is critical to OSA by producing a narrower airspace that is more vulnerable to collapse on inspiration (Horner 1996). The genioglossus (GG) muscle of the tongue is an important pharyngeal muscle which, in conjunction with other muscles, contributes to airway patency by enlarging and stiffening the pharyngeal airspace.

In wakefulness, there is respiratory modulation of GG activity superimposed on a background of tonic activation. Tonic activity is important in setting baseline airway size and stiffness, with the respiratory activation counteracting the collapsing pressures generated during inspiration. In non-rapid-eye-movement (non-REM) sleep, there is suppression of GG activity, mainly in the tonic component, but in REM sleep there are periods of major suppression of pharyngeal muscle activity resulting in episodes of atonia which renders the upper airspace particularly vulnerable to collapse (Horner 1996). Several discrete neuronal systems in the

University of Toronto, Departments of Medicine and Physiology, richard.horner@utoronto.ca

M.J. Poulin and R.J.A. Wilson (eds.), *Integration in Respiratory Control: From Genes to Systems*.

brainstem contribute to the control and maintenance of sleep-wake states and are also positioned to influence respiratory muscle activity via their anatomical projections to respiratory neurons and motoneurons (Horner 2001). We have developed an animal model for manipulation of neurotransmission at the hypoglossal motor nucleus in the medulla of freely behaving rats (Jelev, Sood, Liu, Nolan and Horner 2001) to determine for the first time those mechanisms modulating motor outflow to GG muscle across natural sleep-wake states. Some recent key findings from such studies are summarized below.

2 GG Activation in Wakefulness and Reduced Activity in Sleep

The activity of brainstem serotonin (5-hydroxytryptamine, 5-HT) and noradrenergic neurons is highest in wakefulness, reduced in non-REM sleep and minimal in REM sleep (Horner 1996; Kubin, Davies and Pack 1998). Hypoglossal motor neurons receive excitatory 5-HT and noradrenergic inputs, with the former from medullary raphe neurons also containing co-released thyrotropin releasing hormone and Substance P that are also excitatory. Based on this circuitry, withdrawal of these excitatory inputs in sleep, especially REM sleep, was thought to contribute to decreased GG activity but this had not been tested in natural sleep.

From studies in reduced preparations, withdrawal of 5-HT was long hypothesized to be the main mechanism underlying decreased GG activity in sleep, especially REM sleep (Kubin *et al*. 1998). We showed for the first time *in vivo*, however, that despite robust GG activation with delivery of 5-HT to the hypoglossal motor nucleus in conscious rats (Jelev *et al*. 2001), endogenous 5-HT plays a minimal role in the normal modulation of GG activity (Sood, Morrison, Liu and Horner 2005). Inhibition of serotonergic medullary raphe neurons, the source of 5-HT inputs to the hypoglossal motor nucleus, confirmed this result (Sood, Raddatz, Liu, Liu and Horner 2006). We also showed that the potential role of 5-HT in modulating GG activity was over-emphasized from previous studies in reduced preparations, including our own experiments that used the same methodology as our subsequent studies in conscious animals (Sood, Liu, Liu, Nolan and Horner 2003). This overestimation of the normal physiological role of 5-HT in pharyngeal motor control was likely because of the use of vagotomy in those previous studies using reduced preparations, a procedure which augments the role of 5-HT at the hypoglossal motor nucleus (Sood *et al*. 2005; Sood *et al*. 2006). These results emphasize the importance of studies in intact preparations to determine mechanisms of respiratory motor control, as procedures such as de-afferentation can alter the neurochemical environment and normal physiological processes.

In contrast to 5-HT, however, we identified a functional endogenous noradrenergic drive to respiratory motoneurons that contributes to both the respiratory-related and tonic components of GG muscle activation in wakefulness, and the residual respiratory-related GG activity that persists in non-REM sleep (Chan, Steenland,

Liu and Horner 2006). However, the noradrenergic contribution to GG motor tone was minimal in REM sleep explaining, at least in part, the decreased GG activity encountered in this state (Chan *et al*. 2006). This result is significant because since the first clinical description of OSA more than 35 years ago, this is the first identification of a neural drive contributing to the activity in natural sleep of a muscle that is central to this disorder.

3 GG Motor Suppression in REM sleep

Decreased 5-HT and noradrenergic activity in sleep withdraws inhibition of pontine cholinergic neurons and their subsequent activation increases acetylcholine release into the pontine reticular formation to trigger REM sleep (Kubin *et al*. 1998). Application of a cholinergic agonist (*e.g*., carbachol) by microinjection into this region is used to mimic this process and elicit REM-like neural events in anesthetized or decerebrate animals, *i.e*., the carbachol model of REM sleep (Kubin *et al*. 1998). However, carbachol does not produce the whole range of electrocortical and respiratory events that characterize natural REM sleep and the general applicability of this model is debated.

Studies in the carbachol model of REM sleep provide evidence that spinal motoneurons are inhibited by glycine and γ-amino-butyric acid-A (GABAA) receptor mechanisms (Chase and Morales 2000). REM sleep is also characterized by periods of major suppression of GG activity that occurs even with strong respiratory stimulation. Whether inhibitory glycine and GABAA receptor mechanisms contribute to this GG suppression in REM sleep was controversial with conflicting data from the carbachol model. We showed that although glycine and GABAA receptor mechanisms are functional at the hypoglossal motor nucleus *in vivo* and across sleep-wake states, they contribute minimally to the major suppression of GG activity in REM sleep (Morrison, Sood, Liu, Park, Nolan and Horner 2003a; 2003b) and other mechanisms are more importantly involved. Reduced α1 adrenergic receptor excitation contributes to this decreased GG activity in REM sleep (Fenik, Davies and Kubin 2005; Chan *et al*. 2006). However, loss of excitation is not the sole explanation for the decreased activity because REM sleep processes can also largely overcome the otherwise robust GG activation produced by application of 5-HT (Jelev *et al*. 2001) or the α1 receptor agonist phenylephrine (Chan *et al*. 2006) to the hypoglossal motor nucleus.

Cholinergic neurons are retrogradely labeled following injection of fluorescent tracers into the trigeminal, facial and hypoglossal motor nuclei. We characterized cholinergic influences at the hypoglossal motor nucleus *in vivo* and showed in anesthetized rats that cholinergic stimulation led to net decreases in respiratory-related GG activity, with muscarinic receptor-mediated suppression predominating over nicotinic excitation (Liu, Sood, Liu and Horner 2005). Although REM sleep is a cholinergic event, it remains to be determined if modulation of central cholinergic activity importantly contributes to changes in GG activity across sleep-wake states.

Overall, characterization of cholinergic influences on motor output to pharyngeal muscles is clinically relevant because modulation of central cholinergic activity has been attempted as a pharmacological treatment for OSA despite no knowledge of the sites and mode of action of the cholinergic agents being tested.

4 Modulation of Responses to Excitatory Inputs

All previous studies in animals and humans aiming to increase pharyngeal muscle activity in sleep have targeted receptors on pharyngeal motoneurons via manipulation of extracellular neurotransmitters. However, *in vitro* experiments show that respiratory motoneuron excitability is dynamically modulated by a variety of intracellular signaling molecules that are amenable to manipulation (Feldman, Neverova and Saywell 2005), and modulation of intracellular targets down-stream from surface receptors may offer new and alternative approaches to develop pharmacological strategies for OSA. We examined the effects on respiratory muscle activity of manipulating intracellular signaling molecules at respiratory motoneurons in freely behaving animals *in vivo*, and we also determined the effects of prevailing sleep-wake states on those responses (Aoki, Liu, Downey, Mitchell and Horner 2006). In that study, we showed that modulation of the cyclic adenosine-3'-5'-monophosphate (cAMP)-protein kinase A pathway at the hypoglossal motor nucleus led to increases in GG activity in wakefulness and non-REM sleep but not REM sleep (Aoki *et al*. 2006). This result further emphasizes the consistent finding that REM sleep recruits powerful mechanisms that can overcome excitatory stimuli and powerfully suppress GG activity but also emphasized that responses observed *in vitro* are not intractable but are importantly modified by interactions with other state-dependent systems that are normally engaged in the intact organism *in vivo*.

We also demonstrated a new mechanism in respiratory motor control by which cyclic guanosine-3'-5'-monophosphate (cGMP) at the hypoglossal motor nucleus abolished the normally potent excitatory responses to locally applied 5-HT and phenylephrine while the ionotropic responses to the non-N-methyl-d-aspartate (non-NMDA) glutamate receptor agonist (S)-2-amino-3-(3-hydroxy-5-phenyl-4-isoxazolyl) propionic acid (AMPA) were preserved (Aoki *et al*. 2006). Given that this effect of cGMP mimics the effects of natural REM sleep on responses to 5-HT and phenylephrine (Jelev *et al*. 2001; Chan *et al*. 2006), the data suggested that recruitment of the nitric oxide (NO)-cGMP pathways in REM sleep may contribute to the major suppression of GG muscle activity and reduced responses to excitatory monoaminergic inputs. Increased cGMP in REM sleep would also explain why muscle twitches are preserved in REM sleep (Jelev *et al*. 2001; Chan *et al*. 2006) because these excitatory events are produced by non-NMDA receptor mechanisms, and responses to non-NMDA receptor stimulation with AMPA were unaffected by cGMP (Aoki *et al*. 2006). Characterizing the mechanisms underlying the lack of excitatory responses to applied monoamines (*e.g*., 5-HT) are also clinically relevant because although pharmacological strategies aiming to increase 5-HT at

pharyngeal motoneurons have some beneficial effects in OSA patients, any benefit is largely confined to non-REM sleep with minimal effects observed in REM sleep (Horner 2001).

5 Summary

There have been several previous attempts in humans to increase pharyngeal muscle tone and alleviate OSA by neurochemical approaches, with a resurgence of interest in these approaches as knowledge of the neural systems modulating upper airway muscle activity increases. To date, however, these clinical studies have met with only limited success, in large part because the basic mechanisms underlying suppression of pharyngeal muscle activity in natural sleep, and the neurotransmitters and receptor subtypes involved, had not been determined. Once these neural systems and receptors have been identified, however, and their relative importance determined, it is expected that more rational and systematic approaches can be devised for pharmacological interventions to increase pharyngeal muscle tone in sleep. Indeed, as in other disciplines, an effective route for overcoming the many obstacles in this field will likely be forthcoming only after the basic physiological experiments guide the clinical and therapeutic approaches and problems of targeted delivery are addressed.

References

Aoki, C.R., Liu, H., Downey, G.P., Mitchell, J. and Horner, R.L. (2006) Cyclic nucleotides modulate genioglossus and hypoglossal responses to excitatory inputs in rats. Am. J. Respir. Crit. Care Med. 173, 555–565.

Chan, E., Steenland, H.W., Liu, H. and Horner, R.L. (2006) Endogenous excitatory drive modulating respiratory muscle activity across sleep-wake states. Am. J. Respir. Crit. Care Med. [E-pub ahead of print].

Chase, M.H. and Morales, F.R. (2000) Control of motoneurons during sleep. In: M.H. Kryger, T. Roth and W.C. Dement (Eds.), *Principles and Practice of Sleep Medicine*. W.B. Saunders, Philadelphia, pp. 155–168.

Feldman, J.L., Neverova, N.V. and Saywell, S.A. (2005) Modulation of hypoglossal motoneuron excitability by intracellular signal transduction cascades. Resp. Physiol. Neurobiol. 147, 131–143.

Fenik, V.B., Davies, R.O. and Kubin, L. (2005) REM sleep-like atonia of hypoglossal (XII) motoneurons is caused by loss of noradrenergic and serotonergic inputs. Am. J. Respir. Crit. Care Med. 172, 1322–1330.

Horner, R. L. (1996) Motor control of the pharyngeal musculature and implications for the pathogenesis of obstructive sleep apnea. Sleep 19, 827–853.

Horner, R. L. (2001) The neuropharmacology of upper airway motor control in the awake and asleep states: implications for obstructive sleep apnoea. Resp. Res. 2, 286–294.

Jelev, A., Sood, S., Liu, H., Nolan, P. and Horner, R.L. (2001) Microdialysis perfusion of 5-HT into hypoglossal motor nucleus differentially modulates genioglossus activity across natural sleep-wake states in rats. J. Physiol. 532, 467–481.

Kubin, L., Davies, R.O. and Pack, L. (1998) Control of upper airway motoneurons during REM sleep. News Physiol. Sci. 13, 637–656.

Liu, X., Sood, S., Liu, H. and Horner, R.L. (2005) Opposing muscarinic and nicotinic modulation of hypoglossal motor output to genioglossus muscle in rats *in vivo*. J. Physiol. 565, 965–980.

Morrison, J.L., Sood, S., Liu, H., Park, E., Nolan, P. and Horner, R.L. (2003a) GABA-A receptor antagonism at the hypoglossal motor nucleus increases genioglossus muscle activity in NREM but not REM sleep. J. Physiol. 548, 569–583.

Morrison, J.L., Sood, S., Liu, H., Park, E., Nolan, P. and Horner, R.L. (2003b) Role of inhibitory amino acids in control of hypoglossal motor outflow to genioglossus muscle in naturally sleeping rats. J. Physiol. 552, 975–991.

Sood, S., Liu, X., Liu, H., Nolan, P. and Horner, R.L. (2003) 5-HT at hypoglossal motor nucleus and respiratory control of genioglossus muscle in anesthetized rats. Resp. Physiol. Neurobiol. 138, 205–221.

Sood, S., Morrison, J.L., Liu, H. and Horner, R.L. (2005) Role of endogenous serotonin in modulating genioglossus muscle activity in awake and sleeping rats. Am. J. Respir. Crit. Care Med. 172, 1338–1347.

Sood, S., Raddatz, E., Liu, X., Liu, H. and Horner, R.L. (2006) Inhibition of serotonergic medullary raphe obscurus neurons suppresses genioglossus and diaphragm activities in anesthetized but not conscious rats. J. Appl. Physiol. 100, 1807–1821.

47
Significance of Multiple Neurochemicals that Regulate Respiration

Paul M. Pilowsky[1], Qi-Jian Sun[2], Tina Lonergan[3], John M. Makeham[4], Maryam Seyedabadi[5], Todd A. Verner[6] and Ann K. Goodchild[7]

Abstract Current efforts to characterize the neuronal mechanisms that underlie automatic breathing generally adopt a 'minimalist' approach. In this review, we survey three of the many neurochemicals that are known to be present in raphe neurons and may be involved in respiration. Specifically, we ask the question, 'Is the minimalist approach consistent with the large number of neuronal types and neurochemicals found in respiratory centres?'

1 Defining an 'Adequate' Respiratory Circuit

Certain aspects of respiratory rhythmogenesis can be replicated by computational modeling and simulation in which the component neurons are modeled with currents such as the persistent sodium and delayed rectifier potassium currents (Rybak, Shevtsova, St-John, Paton and Pierrefiche 2003). These modeling approaches are extremely valuable because they suggest the minimum necessary requirements for generation of an 'adequate' respiratory behaviour.

However, there are many different types of respiratory behaviour that range in type from very steady and apparently ordered to seemingly chaotic. The time domain parameters of many of these states remain unknown while in others, such as sleep, they have been characterised (Li and Nattie 2006). All of the different behaviours require different modes of interplay between central command and peripheral adaptive reflexes. How does the central nervous system generate an adequate range of different frequency and amplitude responses in respiration? Even if one ignores higher centres, this is a very difficult question.

Interestingly, in addition to the small number of elements that may be essential to elaborate a minimal form of respiration with little variation in activity, a large number of other neurochemicals and neurotransmitter systems are now reported

[1–7] Australian School of Advanced Medicine, Macquarie Unviersity, paul.pilowsky@mq.edu.au

M.J. Poulin and R.J.A. Wilson (eds.), *Integration in Respiratory Control: From Genes to Systems*. © Springer 2008

to be present in and around the cell groups that are responsible for the initiation and elaboration of respiratory activity, its rhythmic activity (both intrinsically and in response to external influences), its amplitude modulation and its transmission, at appropriately timed intervals to motoneurons that are normally active during quiet breathing and to those that develop a 'respiratory activity' during special circumstances.

Here we briefly survey some of the neurochemical features of the respiratory centers in the ventral medulla that have emerged over the past 5 to 10 years.

2.1 Serotonin (5-hydroxytryptamine, 5HT)

5HT-synthesising neurons are located in the caudal brainstem and have influence throughout the neuraxis. They act on at least 14 different receptors (all except one of which are G-protein coupled receptors).

A role for 5HT in ventilation is indicated from a large number of anatomical (Steinbusch 1984) and physiological studies (Holtman, Dick and Berger 1986) (Holtman and King 1994; Schwarzacher, Pestean, Gunther and Ballanyi 2002). 5HT is present in varicosities that surround identified respiratory neurons including laryngeal motoneurons (Sun, Berkowitz, Goodchild and Pilowsky 2002), dorsal respiratory group neurons (Voss, de Castro, Lipski, Pilowsky and Jiang 1990) and phrenic motoneurons (Pilowsky, de Castro, Llewellyn-Smith, Lipski and Voss 1990; Voss *et al*. 1990) and causes depolarization of neurons that fire in synchrony with the phrenic or hypoglossal nerve (Schwarzacher *et al*. 2002).

A recent series of experiments from Mitchell's laboratory implicates 5HT, amongst other factors (such as brain derived neurotrophic factor), in a novel form of motor plasticity termed 'long-term facilitation' that can be induced by intermittent hypoxia (Mitchell, Baker, Nanda, Fuller, Zabka, Hodgeman, Bavis, Mack and Olson 2001) *in vivo* and *in vitro* (Lovett-Barr, Mitchell, Satriotomo and Johnson 2006).

How important is 5HT in normal respiration? Evidence is emerging that 5HT, and or 5HT-ergic neurons, may be essential. In cat, activation of raphe nuclei can block respiration (Lalley, Benacka, Bischoff and Richter 1997). In rat, activation of sites within the raphe nuclei at the level of the caudal pole of facial nuclei can lead to prolonged apnoea (Verner, Goodchild and Pilowsky 2004). The effects on respiration that follow activation of neurons in the raphe nuclei can be attenuated by administration of methysergide, a 'broad-spectrum' 5HT antagonist (Cao, Matsuyama, Fujito and Aoki 2006). More recently, it was found that in slice preparations in neonatal mice, 5HT2a receptors are crucial for the elaboration of gasping activity as monitored from population recordings of the ventral respiratory group (Tryba, Pena and Ramirez 2006). Pharmacological blockade of 5HT2a receptors prevented gasping activity (Tryba *et al*. 2006). Activation of 5HT1a receptors following stimulation of the raphe is also reported to inhibit phrenic nerve discharge (Lalley *et al*. 1997).

There is now strong evidence that 5HT may be important in central chemosensory function. Richerson's group suggested that a proportion of the medially placed 5HT neuronal population are likely to be part of the physiologically adequate central chemosensory neuronal cell group (Richerson, Wang, Hodges, Dohle and Diez-Sampedro 2005). On the other hand, Guyenet's group identified a non-5HT population of neurons in the ventrolaterally situated retrotrapezoid nucleus that may also have properties of central chemosensory neurons in that, amongst other things, they respond appropriately to changes in pH in the physiological range (Guyenet, Stornetta, Bayliss and Mulkey 2005).

2.2 Substance P

Nattie and colleagues suggest that a non-5HT cell group that expresses the neurokinin-1 receptor is important as a central chemosensor (Nattie, Li, Richerson and Lappi 2004). Although the data from the Guyenet and Richerson groups reveals cells that are chemosensory in the physiological range, the extent to which they are crucial for central chemosensation remains to be determined. It may be that chemosensation is a highly distributed central phenomenon that is not solely the responsibility of one cell group at all times. Our data, in which we activated the peripheral chemoreflex with brief hypoxia and found attenuation of the sympathetic chemoreflex when the substance P antagonist WIN 51708 was injected into the rostral ventrolateral medulla (RVLM) (Makeham, Goodchild and Pilowsky 2005), could be seen as supporting the findings of Richerson's group to the extent that the same cells might mediate both the central and peripheral chemoreflex. However, 5HT neurons are not the sole source of brain substance P, and even a large proportion of adrenaline synthesizing neurons in the C1 cell group are now known to express the preprotachykinin gene (Li, Goodchild, Seyedabadi and Pilowsky 2005).

Like 5HT, substance P is also localized to terminals in nuclei with respiratory functions such as the hypoglossal (Gatti, Llewellyn-Smith, Sun, Chalmers and Pilowsky 1999), laryngeal (Holtman, Jr. 1988) and phrenic motoneurons (Holtman, Norman, Skirboll, Dretchen, Cuello, Visser, Hökfelt and Gillis 1984).

Substance P acts on excitatory GPCR receptors (neurokinin 1, 2 and 3). Feldman's group found that neurons in the rhythmogenic preBötzinger region express the neurokinin 1 receptor and that application of substance P-saporin, a toxin that binds specifically to NK receptors and becomes internalized resulting in cell death, causes a severe progressive ataxic breathing pattern (McKay, Janczewski and Feldman 2005). In these experiments, the NK receptors are used as a doorway for the toxin, but the physiological role of substance P in breathing remains unclear. The recent development of labeling NK receptor positive neurons with tetramethylrhodamine conjugated to substance P provides a novel way to identify preBötzinger complex neurons (Pagliardini, Adachi, Ren, Funk and Greer 2005).

2.3 Opioids

Opioids are a rather unusual neurotransmitter system in respiration. Countless studies have shown that administration of delta and mu-opioid agonists will potently depress respiration in almost any system in which they are tested (Ballanyi, Lalley, Hoch and Richter 1997; Lalley 2003; Lonergan, Goodchild, Christie and Pilowsky 2003a, 2003b). Paradoxically, antagonism with naloxone has no effect in the absence of narcotics (Janczewski and Feldman 2006).

3 Conclusion

Many different neurotransmitters and neurochemicals play a role in central respiratory circuits including 5HT, substance P and opioids. It may be that an approach that is less, rather than more, 'minimalist' is required to understand the physiology of respiration.

Acknowledgements Work in the authors' laboratory is supported by the NHMRC of Australia (211196, 211023), the North Shore Heart Research Foundation (6-05/06), the NSCCHS (2006:03) and the Garnett Passe and Rodney Williams Memorial Foundation.

References

Ballanyi, K., Lalley, P.M., Hoch, B. and Richter, D.W. (1997) cAMP-dependent reversal of opioid- and prostaglandin-mediated depression of the isolated respiratory network in newborn rats. J. Physiol. (Lond.) 504, 127–134.

Cao, Y., Matsuyama, K., Fujito, Y. and Aoki, M. (2006) Involvement of medullary GABAergic and serotonergic raphe neurons in respiratory control: Electrophysiological and immunohistochemical studies in rats. Neurosci. Res. 56(3), 322–331.

Gatti, P.J., Llewellyn-Smith, I.J., Sun, Q.J., Chalmers, J. and Pilowsky, P.M. (1999) Substance P-immunoreactive boutons closely appose inspiratory protruder hypoglossal motoneurons in the cat. Brain Res. 834, 155–159.

Guyenet, P.G., Stornetta, R.L., Bayliss, D.A. and Mulkey, D.K. (2005) Retrotrapezoid nucleus: a litmus test for the identification of central chemoreceptors. Exp. Physiol. 90, 247–253.

Holtman, J.R., Dick, T.E. and Berger, A.J. (1986) Involvement of serotonin in the excitation of phrenic motoneurons evoked by stimulation of the raphe obscurus. J. Neurosci. 6, 1185–1193.

Holtman, J.R., Jr. and King, K.A. (1994) Effect of activation of 5-HT1A receptors at the ventral medulla on phrenic nerve activity. Eur. J. Pharmacol. 253, 307–310.

Holtman, J.R., Norman, W.P., Skirboll, L., Dretchen, K.L., Cuello, C., Visser, T.J., Hökfelt, T. and Gillis, R.A. (1984) Evidence for 5-hydroxytryptamine, substance P and thyrotropin-releasing hormone in neurons innervating the phrenic motor nucleus. J. Neurosci. 4, 1064–1071.

Holtman J.R., Jr. (1988) Immunohistochemical localization of serotonin- and substance P-containing fibers around respiratory muscle motoneurons in the nucleus ambiguus of the cat. Neuroscience 26, 169–178.

Janczewski, W.A. and Feldman, J.L. (2006) Distinct rhythm generators for inspiration and expiration in the juvenile rat. J. Physiol. (Lond.) 570, 407–420.

Lalley, P.M. (2003) Mu-opioid receptor agonist effects on medullary respiratory neurons in the cat: evidence for involvement in certain types of ventilatory disturbances. Am. J. Physiol. 285, R1287–R1304.

Lalley, P.M., Benacka, R., Bischoff, A.M. and Richter, D.W. (1997) Nucleus raphe obscurus evokes 5-HT-1A receptor-mediated modulation of respiratory neurons. Brain Res. 747, 156–159.

Li, A. and Nattie, E. (2006) Catecholamine neurones in rats modulate sleep, breathing, central chemoreception and breathing variability. J. Physiol. (Lond.) 570, 385–96.

Li, Q., Goodchild, A.K., Seyedabadi, M. and Pilowsky, P.M. (2005) Pre-protachykinin A mRNA is colocalized with tyrosine hydroxylase-immunoreactivity in bulbospinal neurons. Neuroscience 136, 205–216.

Lonergan, T., Goodchild, A.K., Christie, M.J. and Pilowsky, P.M. (2003a) Mu opioid receptors in rat ventral medulla: effects of endomorphin-1 on phrenic nerve activity. Respir. Physiol. Neurobiol. 138, 165–178.

Lonergan, T., Goodchild, A.K., Christie, M.J. and Pilowsky, P.M. (2003b) Presynaptic delta opioid receptors differentially modulate rhythm and pattern generation in the ventral respiratory group of the rat. Neuroscience 121, 959–973.

Lovett-Barr, M.R., Mitchell, G.S., Satriotomo, I. and Johnson, S.M. (2006) Serotonin-induced *in vitro* long-term facilitation exhibits differential pattern sensitivity in cervical and thoracic inspiratory motor output. Neuroscience 142, 885–892.

Makeham, J.M., Goodchild, A.K. and Pilowsky, P.M. (2005) NK1 receptor activation in rat rostral ventrolateral medulla selectively attenuates somato-sympathetic reflex while antagonism attenuates sympathetic chemoreflex. Am. J. Physiol. 288, R1707–R1715.

McKay, L.C., Janczewski, W.A. and Feldman, J.L. (2005) Sleep-disordered breathing after targeted ablation of preBotzinger complex neurons. Nat. Neurosci. 8, 1142–1144.

Mitchell, G.S., Baker, T.L., Nanda, S.A., Fuller, D.D., Zabka, A.G., Hodgeman, B.A., Bavis, R.W., Mack, K.J. and Olson, E.B., Jr. (2001) Invited review: Intermittent hypoxia and respiratory plasticity. J. Appl. Physiol. 90, 2466–2475.

Nattie, E.E., Li, A., Richerson, G. and Lappi, D.A. (2004) Medullary serotonergic neurones and adjacent neurones that express neurokinin-1 receptors are both involved in chemoreception *in vivo*. J. Physiol. (Lond.) 556, 235–253.

Pagliardini, S., Adachi, T., Ren, J., Funk, G.D. and Greer, J.J. (2005) Fluorescent tagging of rhythmically active respiratory neurons within the pre-Botzinger complex of rat medullary slice preparations. J. Neurosci. 25, 2591–2596.

Pilowsky, P.M., de Castro, D., Llewellyn-Smith, I.J., Lipski, J. and Voss, M.D. (1990) Serotonin immunoreactive boutons make synpases with feline phrenic motoneurons. J. Neurosci. 10, 1091–1098.

Richerson, G.B., Wang, W., Hodges, M.R., Dohle, C.I. and Diez-Sampedro, A. (2005) Homing in on the specific phenotype(s) of central respiratory chemoreceptors. Exp. Physiol. 90, 259–266.

Rybak, I.A., Shevtsova, N.A., St-John, W.M., Paton, J.F. and Pierrefiche, O. (2003) Endogenous rhythm generation in the pre-Botzinger complex and ionic currents: modelling and *in vitro* studies. Eur. J. Neurosci. 18, 239–257.

Schwarzacher, S.W., Pestean, A., Gunther, S. and Ballanyi, K. (2002) Serotonergic modulation of respiratory motoneurons and interneurons in brainstem slices of perinatal rats. Neuroscience 115, 1247–1259.

Steinbusch, H.W.M. (1984) Serotonin-immunoreactive neurons and their projections in the CNS. In: A. Björklund, T. Hökfelt and M. J. Kuhar (Eds.), *Handbook of Chemical Neuroanatomy,* Elsevier Science, pp. 68–125.

Sun, Q.J., Berkowitz, R.G., Goodchild, A.K. and Pilowsky, P.M. (2002) Serotonin inputs to inspiratory laryngeal motoneurons in the rat. J. Comp. Neurol. 451, 91–98.

Tryba, A.K., Pena, F. and Ramirez, J.M. (2006) Gasping activity *in vitro*: a rhythm dependent on 5-HT2A receptors. J. Neurosci. 26, 2623–2634.

Verner, T.A., Goodchild, A.K. and Pilowsky, P.M. (2004) A mapping study of cardiorespiratory responses to chemical stimulation of the midline medulla oblongata in ventilated and freely breathing rats. Am. J. Physiol. 287, R411–R421.

Voss, M.D., de Castro, D., Lipski, J., Pilowsky, P.M. and Jiang, C. (1990) Serotonin immunoreactive boutons form close appositions with respiratory neurons of the dorsal respiratory group in the cat. J. Comp. Neurol. 295, 208–218.

48
Disinhibition of the Dorsomedial Hypothalamus Increases the Frequency of Augmented Breaths in the Anesthetized Rat

C.R. Reynolds[1], K.Vujisic[2], P.W. Davenport[3] and L.F. Hayward[4]

Abstract The present study was undertaken to identify if activation of the dorsomedial hypothalamus (DMH) elicits augmented breaths (ABs). DMH disinhibition in urethane anesthetized rats produced both an increase in baseline respiratory rate (RR) and an increase in the number of ABs. The increase in RR was associated with a decrease in both the time of inspiration (T_i) and expiration (T_e) and the peak change in RR was observed 5 min post DMH activation. In contrast, the increase in ABs was greatest during the first 1.25 min, and both T_is of the ABs did not change significantly from pre-injection values. The T_e of the ABs did decrease but remained significantly greater than the T_e of the normal breath during DMH disinhibition. Our results support the hypothesis that the central neural pathway involved in the maintenance of normal respiratory pattern may be distinct from pathways involved in the generation of ABs.

1 Introduction

Previous observations from our laboratory demonstrated that stimulation of the periaqueductal grey (PAG) evoked a significant increase in ventilation that induced an increased production of augmented breaths (ABs) (Shahan, Zhang, and Davenport 2004). Much investigation has been done using peripheral stimuli, such as arterial chemoreceptor activation, to elicit an AB. However, our previous work in the PAG suggests that ABs can be evoked through a central mechanism as well (Shahan *et al*. 2004). Since disinhibition of the dorsomedial hypothalamus (DMH) produces a similar increase in respiratory rate (RR) to that observed during PAG stimulation, the present study was undertaken to test the hypothesis that disinhibition of the DMH would also increase the frequency of ABs and the increase in ABs would be coupled to the change in RR.

[1–4] University of Florida, Department of Physiological Sciences, reynoldsc@mail.vetmed.ufl.edu

M.J. Poulin and R.J.A. Wilson (eds.), *Integration in Respiratory Control: From Genes to Systems*. © Springer 2008

2 Method

2.1 General Preparation

The experiments were performed on nine urethane anesthetized male Sprague Dawley rats (397 ± 15 g). All animals were spontaneously breathing room air mixed with 100% oxygen throughout the experiment. A craniotomy was preformed to expose the area overlaying the DMH (3.2 mm caudal, 0.4 mm lateral to bregma). After stabilization, animals either received a single unilateral microinjection of bicuculline (BIC: 2–3 mM), a $GABA_A$ receptor antagonist, or served as controls and received a single microinjection of artificial cerebrospinal fluid (aCSF: 45 nL) in the DMH. Arterial pressure and diaphragm EMG (dEMG) data were collected for 10 min before and 30 min following microinjection.

2.2 Data Analysis

All data were analyzed off-line. Time point zero was defined as the time of DMH microinjection. Prior to and beginning 5 min following central microinjection, respiratory data were averaged within successive 5 min blocks. During the first 5 min following microinjection, when RR showed the greatest change, data were averaged within 1.25 and 2.5 min blocks. Figure 1 illustrates an AB and all breathing parameters measured. The time of inspiration (T_i) was set as the time from initiation of increasing dEMG amplitude to the peak of that inspiratory effort. The time of expiration (T_e) was defined as the peak of the inspiratory effort to the start of the next inspiration (or next T_i). Frequency of breathing was determined by the inverse of the sum of T_i and T_e. The frequency of ABs was determined by counting the number of occurrences and dividing by the total elapsed time in minutes. An AB was defined by criteria (Fig.1) set by Cherniack, Euler, Glogowska and Homma (1981). A paired t-test was used to determine significance between frequencies of augmented breaths and respiration rate within groups. Statistical significance was corrected with a Bonferroni adjustment, which resulted in a p-value of 0.006. A one-way ANOVA was used to measure significance within groups for timing values. Statistical significance was considered $p \leq 0.05$.

3 Results

3.1 Respiratory Rate

Disinhibition of the DMH (n = 6) induced a rapid increase in baseline RR. The mean latency to the onset of the BIC response was 20 ± 5 seconds. The onset of the response was defined as a 20% increase above baseline RR. The RR increase

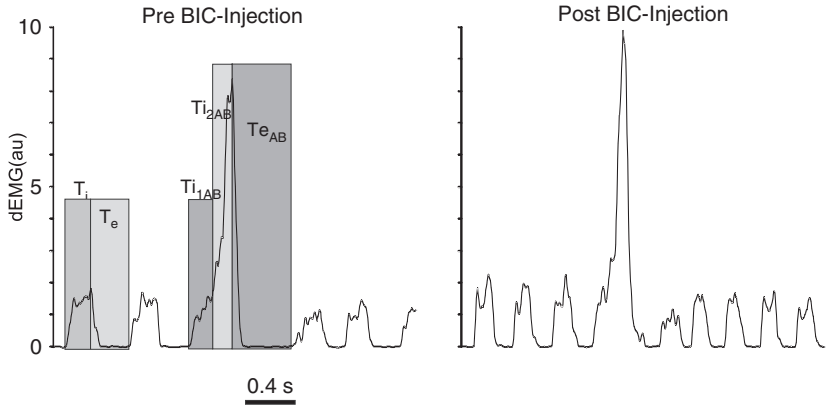

Fig. 1 Representative tracing of an augmented breath (AB) before (left panel) and during DMH disinhibition (right panel). Shaded boxes indicate time periods used for the measurement of respiratory parameters: (T_i: duration of inspiration; T_e: duration of expiration; Ti_{1AB}: duration of the first inspiratory effort during an AB; Ti_{2AB}: duration of the second inspiratory effort during an AB; Te_{AB}: duration of expiration during an AB)

following BIC was significantly different from pre-injection values at 1.25 min post-injection (Fig. 2A) and the peak increase in RR occurred at 5 min post-injection (98 ± 4 bpm vs 210 ± 19 bpm; BIC pre-injection vs BIC post-injection). RR remained elevated compared to pre-injection values until 20 min post-injection and by 25 min RR had returned to pre-injection values (Fig. 2A). aCSF microinjection into the DMH did not induce any significant change in breathing pattern at any time point. The increased RR observed following disinhibition of the DMH was mediated by a significant decrease in both T_i and T_e. Both parameters were significantly shorter in duration at 1.25 min post-injection compared to pre-injection (Fig. 2B). The greatest decrease in T_i and T_e was observed at 5 min post-injection, respectively. By 20 min post-injection, T_i was not significantly different from pre-injection. In contrast, by 25 min, T_e remained significantly shorter than pre-injection values.

Disinhibition of the DMH also induced a significant increase in the frequency of ABs. Relative to pre-injection, AB frequency increased immediately following BIC-injection and was significantly different from pre-injection within the first time block measured. The number of ABs reached a maximum at the second time point, but was not significant from pre-injection. From time point 1.25 to 25 min, the number of AB declined steadily. aCSF-injected animals showed no significant change in frequency of ABs at any time point post-injection.

Evaluation of breath timing within the ABs post BIC injection demonstrated that the first two phases of the ABs, Ti_{1AB} and Ti_{2AB}, did not significantly change over time compared to pre-injection, despite a significant reduction in the duration of the normal breath's T_i (Fig. 2C). In contrast, the third phase of the ABs, Te_{AB}, decreased following DMH stimulation, becoming significantly shorter in duration at the first time period and showed the greatest change at 5 min (0.813 ± 0.07 s *vs*. 0.322 ± 0.05 s; pre-injection

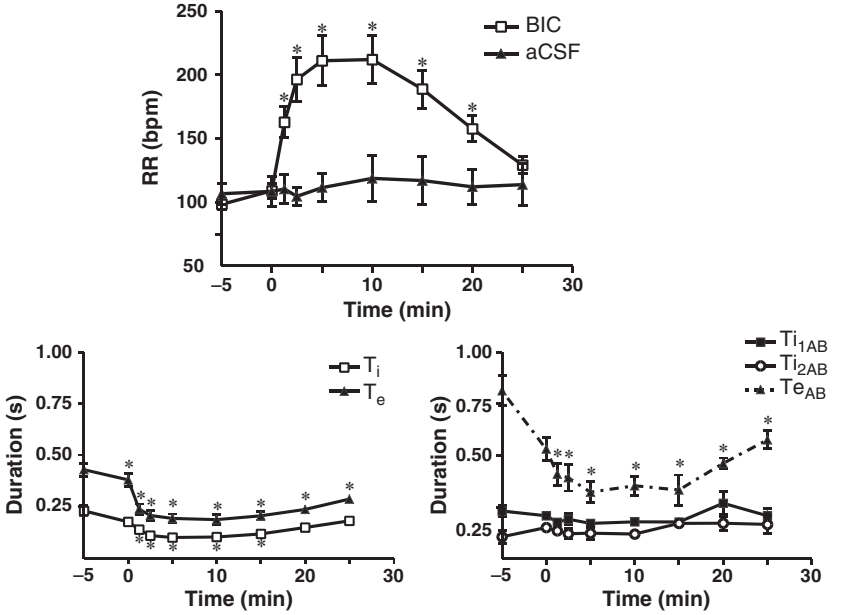

Fig. 2 Changes in breathing timing following DMH disinhibition. (A) Respiratory response to bicuculline (BIC) or aCSF microinjection into the DMH. (B) Normal breath inspiration (T_i) and expiration (T_e) timing over time after BIC-microinjections. (C) AB inspiration (Ti_{1AB} and Ti_{2AB}) and expiration (Te_{AB}) timing over time after BIC-microinjections. DMH injection occurred at time zero. * denotes significant differences from pre-injection values

vs post-injection 5 min). Unlike the T_e of the normal breaths, Te_{AB} returned to a pre-injection duration by 20 min post-injection (Fig. 2C).

4 Discussion

The present results support the hypothesis that disinhibition of the DMH produces an increased frequency of ABs. We observed that the increase in RR was associated with a decrease in T_i and T_e of normal breaths; however, neither the Ti_{1AB} nor the Ti_{2AB} of the ABs was changed significantly during DMH activation. In contrast, the change in Te_{AB} during DMH stimulation paralleled the changes in duration of the T_e of the normal breaths but the Te_{AB} had a faster time course for recovery. Furthermore, the peak increase in RR was not directly coupled to the peak frequency of ABs, which occurred earlier. Our observations support previous studies, which have suggested that the neural circuitry governing the timing of an AB may be separate from that used to generate a normal breath (Orem and Trotter 1993). Our results also support previous work (Hodges, Forster, Papanek, Dwinell and Hogan 2002) suggesting that the majority of the central neural drive involved in the production of

ABs may be recruited prior to the onset of an AB since Ti_{IAB} did not show changes as T_i did. At present the neural circuitry involved in the production of ABs following stimulation of the DMH remains to be defined.

Acknowledgement NIH grant HL-076518 (LFH).

References

Cherniack, N.S., von Euler, C., Glogowska, M. and Homma, I. (1981) Characteristics and rate of occurrence of spontaneous and provoked augmented breaths. Act. Physiol. Scand. 111, 349–360.

Hodges, W.R., Forster, H.V., Papanek, P.E., Dwinell, M.R. and Hogan, G.E. (2002) Ventilatory phenotypes among four strains of adult rats. J. Appl. Physiol. 93, 974–983.

Orem, J. and Trotter, R.H. (1993) Medullary respiratory neuronal activity during augmented-breaths in intact unanesthetized cats. J. Appl. Physiol. 74, 761–769.

Shahan, C.P., Zhang, W. and Davenport P.W., (2004) Dorsal periaqueductal gray (dPAG) neural activation increases respiratory activity and the incidence of augmented breaths. Annual Meeting of the Society for Neuroscience, San Diego, CA.

49
Major Components of Endogenous Neurotransmission Underlying the Discharge Activity of Hypoglossal Motoneurons *in vivo*

Edward J. Zuperku[1,2], Ivo F. Brandes[1], Astrid G. Stucke[1], Antonio Sanchez[1], Francis A. Hopp[2] and Eckehard A. Stuth[1]

Abstract Multibarrel micropipettes were used to simultaneously record unit activity and apply antagonists on individual inspiratory hypoglossal motoneurons (IHMNs) to determine the endogenous activation levels of NMDA, non-NMDA, $GABA_A$ and serotonin receptors responsible for the IHMN spontaneous discharge patterns in decerebrate dogs. IHMN activity is highly dependent on glutamatergic phasic and tonic drives, which are differentially mediated by the receptor subtypes. Endogenous serotonin significantly amplifies IHMN activity, while GABAergic gain modulation acts to attenuate activity. Thus, alterations in the neurotransmission of any of these systems could markedly alter neuronal output to target muscles.

1 Introduction

Hypoglossal motoneurons innervate all tongue muscles, including the genioglossal muscle, the main protruder of the tongue, and thus contribute significantly to the maintenance of upper airway patency during inspiration. Partial or complete loss of inspiratory hypoglossal motoneuron (IHMN) activity during sleep, during various stages of anesthesia or during postanesthetic recovery can lead to upper airway obstruction resulting in hypoxia.

A variety of neurotransmitters and modulators have been proposed to generate and control the spontaneous discharge patterns of IHMNs. Respiratory-related phasic glutamatergic drive may arise from presynaptic neurons located in medullary reticular formation and regions of the pontine Kölliker-Fuse and intertrigeminal nuclei (Peever, Shen and Duffin 2002; Gestreau, Dutschmann, Obled and Bianchi 2005). Serotonergic and peptidergic raphe neurons project to hypoglossal motoneurons as well as noradrenergic neurons that originate from the locus subceruleus. Evidence from *in vitro* and *in vivo* studies suggest that both GABA and glycine inhibit hypoglossal motoneurons.

[1] Medical College of Wisconsin, Anesthesiology Department, ezuperku@mcw.edu

[2] Zablocki VA Medical Center, Milwaukee, WI 53066

M.J. Poulin and R.J.A. Wilson (eds.), *Integration in Respiratory Control: From Genes to Systems*.

At the cellular level, however, the major factors that contribute to generation and control of IHMN spontaneous activity in vivo, which may be targets for drug-induced depression, are incompletely understood. Accordingly, we have investigated the role of glutamatergic, serotonergic, and GABAergic endogenous inputs to the IHMNs in terms of the relative magnitude of their contribution to the baseline discharge pattern in a decerebate canine model.

2 Methods

These studies were approved by the local Animal Care Committee and conformed to standards set forth by the National Institutes of Health. Under isoflurane anesthesia (1.3–1.8 MAC), mechanically ventilated dogs were vagotomized and decerebrated and then studied during moderate hypercapnic hyperoxia in the absence of anesthesia. Neurograms (moving time-averages) were obtained from isolated desheathed hypoglossal and phrenic nerves. For neuronal recording, an occipital craniotomy was performed to expose the dorsal surface of the medulla. Multibarrel micropipettes were used to simultaneously record unit activity from single IHMNs before and during pressure ejection of the following selective antagonists: 2-amino-5-phosphonovalerate (AP5, 500 µM; NMDA), 2,3-dihydroxy-6-nitro-7-sulfamoyl-benzo(f)quinoxaline (NBQX, 250 µM; non-NMDA), 500 µM ketanserin (5-HT_{2A}), and 200 µM bicuculline ($GABA_A$). Online spike-triggered averaging was used to confirm that the recorded action potentials originated from a hypoglossal motoneuron. A series of repeated ejections, "picospritzes," was used to provide a quasi-continuous ejection or dose rate to obtain steady-state dose-response data. Dose-dependent effects were studied by progressive step increases in picoejection rate. The dose rate (volume/time) was measured via height changes of the meniscus in the pipette barrel with a reticule-equipped microscope. Each neuron was exposed to only one of the antagonists. Antagonist-induced changes in discharge frequency (F_n) patterns were analyzed using cycle-triggered histograms from which peak and time-averaged F_n values were obtained. In addition, the relationship between the control and drug-altered discharge patterns in terms of gain (slope) and offset (y-intercept) was determined via linear regression of plots of F_n patterns during antagonist application vs. control condition (F_{DRUG} vs. F_{CON} plots). Data are presented as mean and SE.

3 Results

The IHMNs were recorded in a region from 0.25 mm caudal to 2.0 mm rostral to obex, at a mean depth of 2.75 mm (SD 1.11), and centered 1.16 mm (SD 0.31) lateral from the midline. IHMNs displayed phasic activity throughout the whole or the later part of the I-phase.

A typical protocol of the effects of picoejection of AP5 on an IHMN is shown in Fig. 1. Progressive step increases in ejection rate produced a graded reduction in F_n. The ejection rate was increased until a maximum effect was observed. Recovery times varied from 25–45 minutes. Analysis of CTH data for the neuron of Fig. 1 shows that the antagonism of NMDA receptors produced a parallel downward shift of the F_n pattern (Fig. 2A). Linear regression analysis of the plots of the F_n patterns with AP5 (F_{AP5}) versus the control F_n pattern (F_{CON}) have a slope of ~1 with dose-dependent decreases in the y-intercept indicative of a reduction in tonic glutamater-gic input (Fig. 2A, lower). The data from 26 IHMNs indicates that block of NMDA receptors produced mainly a parallel downward shift in discharge patterns with a 51 ± 2.9% decrease in peak F_n (n = 25). The slope of the relationship between F_n patterns was reduced by 21 ± 6% with a 16.3 ± 3.2 Hz decrease in the y-intercept (Fig. 3).

Block of the non-NMDA receptors with NBQX often resulted in a decrease in the slope of the F_n patterns indicative of a block phasic glutamatergic input (*e.g.*, Fig. 2B). For some IHMNs, this was also combined with a downward shift in the pattern, suggesting a block of tonic input also. At maximum effective dose rates, NBQX decreased peak F_n by 60 ± 3.3%, slope by 54 ± 2%, and y-intercept by 4.5 ± 1.4 Hz (Fig. 3). The NBQX-induced decrease in slope was significantly greater than that due to AP5, while the y-intercept was significantly less (Fig. 3).

The block of $GABA_A$ receptors with bicuculline produced a proportional increase in the F_n pattern of IHMNs (*e.g.*, Fig 2C). The mean response data from 3 IHMNs are shown in Fig. 3. Block of 5-HT_{2A} receptors with ketanserin (*e.g.*, Fig. 2D) decreased the slope of the F_{5HT} vs. F_{CON} plots by 63 ± 5% and peak F_n by 68 ± 3% (n = 21; Fig. 3).

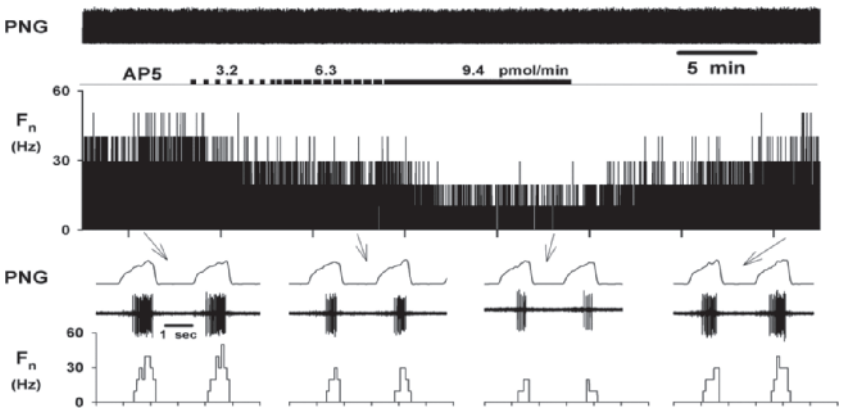

Fig. 1 Upper: Example protocol showing the effects of picoejection of AP5 on an IHMN. Progressive step increases in ejection rate produced a graded reduction in discharge frequency F_n (rate-meter recording). Ejection rate was increased until a maximum effect was obtained. Lower: time expanded views including unit activity. PNG: phrenic neurogram

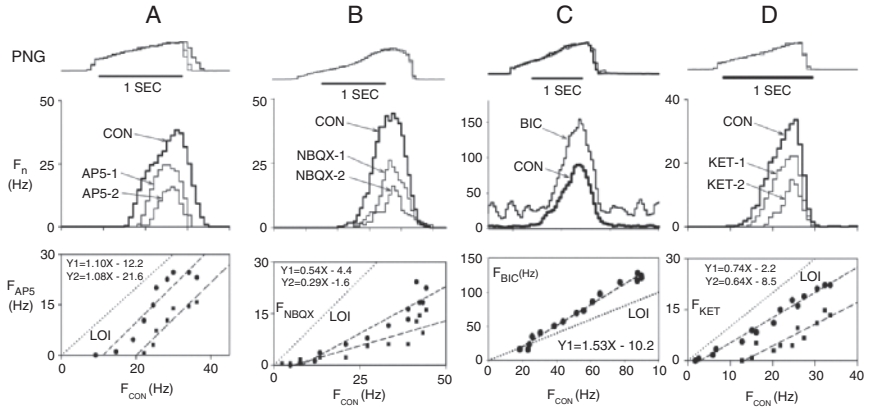

Fig. 2 Examples of antagonist effects on IHMN discharge frequency (F_n) patterns. (A) AP5 produced a downward parallel shift of the F_n pattern. F_{AP5} vs. F_{CON} plot slopes are ~1.0 (neuron of Fig. 1). AP5-1: 6.3 pmol/min; AP5-2: 9.4 pmol/min. (B) NBQX produced a dose-dependent reduction in the ramp slope of F_n patterns. NBQX-1: 0.45 pmol/min.; NBQX-2: 0.75 pmol/min. (C) BIC at the maximum effective dose-rate (4.22 pmol/min) increased the slope of the ramp pattern. The F_{BIC} vs. F_{CON} plot slope is 1.53. (D) Ketanserin dose rate dependently reduced the F_n pattern. F_{KET} vs. F_{CON} plots are linear with a decreased slope and y-intercept. KET-1: 0.45 pmol/min; KET-2: 0.90 pmol/min. 11–18 cycles/cycle-triggered histogram. LOI: line of identity. Linear regression equations Y = slope X + y-intercept are shown. PNG: ensemble average of phrenic activity

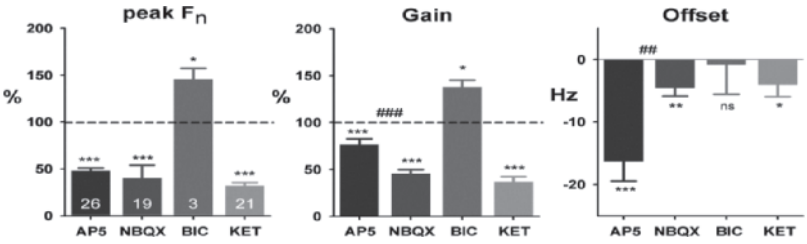

Fig. 3 Summary data for peak F_n, Gain and Offset (slope and y-intercept of the F_{DRUG} vs. F_{CON} plots) in terms of mean and SE relative to control conditions at maximum effective dose rate for each antagonist. Number of neurons is shown in bars. Block of NMDA, AMPA, and 5-HT_{2A} receptors produced a significant decrease in peak F_n and gain (*** $p < 0.001$), while block of $GABA_A$ receptors produced a significant increase in both peak F_n and Gain (* $p < 0.05$). NBQX reduced the gain more than AP5 (0.46 ± 0.04 vs. 0.77 ± 0.06; ### $p < 0.0001$), while AP5 increased the offset more than NBQX (-16.3 ± 3.2 vs. -4.5 ± 1.4 Hz; ##: $p < 0.001$)

4 Discussion

Taken together, these results indicate that in vivo IHMN discharge patterns are primarily dependent on endogenous glutamatergic excitation. NMDA receptors appear to mediate most of the tonic excitatory drive as well as some of the phasic drive, whereas the non-NMDA receptors primarily mediate phasic drive (Fig. 4). In

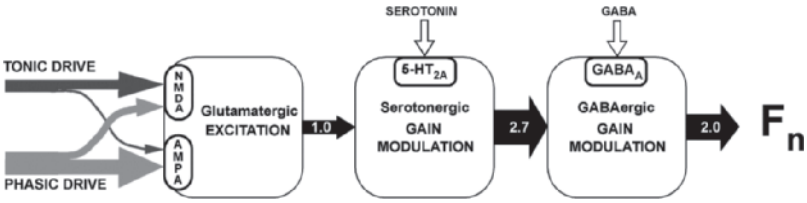

Fig. 4 Hypothetical model of possible contributions of endogenous neurotransmitter/ modulator levels to the spontaneous IHMN discharge patterns in the decerebrate canine. Only those systems studied are shown, and others may be contributory. Thicknesses of arrows suggest estimated contributions derived from pooled data. Index of phasic drive based on ratio of %Δ slope to %Δ peak Fn. Index of tonic drive: 1 - index of phasic drive. Output of Excitation block was set to 1.0. Serotonin gain: 100/KET gain (100/37 = 2.70). GABAergic gain: 100/138 = 0.725. Final output: 1×2.7×0.725 = 2.0

addition, the IHMN discharge patterns are strongly modulated by serotonergic inputs via 5-HT2A receptors (Brandes, Zuperku, Stucke, Jakovcevic, Hopp and Stuth 2006) and by GABAAergic gain modulation (Zuperku and McCrimmon 2002) with these two forms of modulation acting in opposite directions (Fig. 4).

These findings from single IHMNs in the decerebrate dog model are consistent with the findings based on hypoglossal nerve activity responses to antagonists injected or dialyzed in the hypoglossal motor nucleus in anesthetized rats (Fenik, Davies and Kubin 2005) or during non-REM natural sleep (Morrison, Sood, Liu, Park, Nolan and Horner 2003; Sood, Morrison, Liu and Horner 2005).

Acknowledgements The authors thank Jack Tomlinson for outstanding surgical and technical assistance. Supported by NIH R01 GM-059234 (EAS) and VA Medical Research Funds (EJZ).

References

Brandes, I.F., Zuperku, E.J., Stucke, A.G., Jakovcevic, D., Hopp, F.A. and Stuth, E.A. (2006) Serotonergic modulation of inspiratory hypoglossal motoneurons in decerebrate dogs. J. Neurophysiol. 95, 3449–3459.

Fenik, V.B., Davies, R.O. and Kubin, L. (2005) Noradrenergic, serotonergic and GABAergic antagonists injected together into the XII nucleus abolish the REM sleep-like depression of hypoglossal motoneuronal activity. J. Sleep Res. 14, 419–429.

Gestreau, C., Dutschmann, M., Obled, S. and Bianchi, A.L. (2005) Activation of XII motoneurons and premotor neurons during various oropharyngeal behaviors. Respir. Physiol. Neurobiol. 147, 159–176.

Morrison, J.L., Sood, S., Liu, H., Park, E., Nolan, P. and Horner, R.L. (2003) $GABA_A$ receptor antagonism at the hypoglossal motor nucleus increases genioglossus muscle activity in NREM but not REM sleep. J. Physiol. 548, 569–583.

Peever, J.H., Shen, L. and Duffin, J. (2002) Respiratory pre-motor control of hypoglossal motoneurons in the rat. Neuroscience 110, 711–722.

Sood, S., Morrison, J.L., Liu, H. and Horner, R.L. (2005) Role of endogenous serotonin in modulating genioglossus muscle activity in awake and sleeping rats. Am. J. Respir. Crit. Care Med. 172, 1338–1347.

Zuperku, E.J. and McCrimmon, D.R. (2002) Gain modulation of respiratory neurons. Respir. Physiol. Neurobiol. 131, 121–133.

Part VIII
Comparative Aspects

50
Control of Ventilation in Diving Birds

Patrick J. Butler[1] and Lewis G. Halsey[2]

Abstract Studies on diving ducks indicate that the carotid bodies affect dive duration when the birds are hypoxic before a dive but not when they are hypercapnic. When close to their critical concentrations (beyond which the ducks will not dive), both oxygen and carbon dioxide reduce dive duration but hypercapnia has a much larger influence than hypoxia on surface duration. Also, excessive removal of carbon dioxide before a dive may be as important a factor in preparing for that dive as the replacement of the oxygen used during the previous dive. This observation is compatible with a physiological model of the control of diving behaviour in the Weddell seal which emphasises the significance of the level of carbon dioxide in the blood perfusing the brain.

1 Background

When diving, aquatic birds cease ventilating and rely entirely on the oxygen stored within their bodies to fuel aerobic metabolism. For this reason, the majority of models on diving behaviour of birds have focused on the management of the oxygen stored in their bodies (Halsey, Reed, Woakes and Butler 2003). Clearly, other factors such as food density, rate of food ingestion and giving up times when pursuing mobile prey, will all exert an influence on dive duration (Butler 2004; Halsey and Butler 2006).

In some species of birds, such as the ducks, which dive relatively shallowly, all dives seem to be terminated well before their usable oxygen stores are exhausted, whereas in others, such as the penguins, which dive much more deeply, a reasonably large proportion of their dives seem to last close to the point when all of the usable oxygen is exhausted (Butler 2004; Knower Stockard, Heil, Meir, Sato, Ponganis and Ponganis 2005). This raises the question as to what effect the partial pressures of oxygen, and indeed of carbon dioxide, have on the duration aquatic birds remain

[1–2] School of Biosciences, University of Birmingham, Birmingham, B15 2TT, United Kingdom, p.j.butler@bham.ac.uk; l.g.halsey@bham.ac.uk

M.J. Poulin and R.J.A. Wilson (eds.), *Integration in Respiratory Control: From Genes to Systems*.

submerged and subsequently remain at the surface. While most of the relevant experiments have been performed on ducks, the data they have provided do give us some insight into the possible influence of the respiratory gases on the diving behaviour of aquatic birds in general.

2 The Role of the Carotid Body Chemoreceptors

The increase in ventilation in response to hypoxia in tufted and domesticated ducks, *Aythya fuligula* and *Anas platyrhynchos*, respectively, is abolished or dramatically reduced after bilateral denervation of the carotid body chemoreceptors (Jones and Purves 1970; Butler and Woakes 1982). Tufted ducks can dive, on average, for durations in excess of 30 s (Butler and Stephenson 1988) and have sufficient useable oxygen stored in their bodies to enable them to remain submerged and fully aerobic for up to 50 s (Woakes and Butler 1983). However, the carotid bodies appear to influence the duration of much shorter dives (Butler and Woakes 1982; Butler and Stephenson 1988). For example, in the experiments of Butler and Woakes (1982), sham-operated ducks diving to a maximum depth of 2.7 m on an outside pond remained submerged, on average, for 18.0 ± 0.3 s, whereas ducks with denervated carotid bodies dived for a significantly longer period of 22.3 ± 0.5 s. Also, the longest dive performed by the two groups was 30 s and 40 s, respectively. Thus, while the ducks dive for longer durations after denervation of their carotid bodies, they still surface well within their aerobic diving capabilities, and this suggests that there may be other physiological mechanisms, beyond the level of oxygen in the blood, involved in determining when a dive is terminated.

Data from ducks diving from hypoxic or hypercapnic gas mixtures indicate that the carotid bodies are responding to the decline in oxygen rather than to the increase in carbon dioxide (Butler and Stephenson 1988). This is not surprising since, unlike the situation with hypoxia, the hyperventilatory response to a step increase in inspired carbon dioxide in domesticated ducks is not abolished after denervation of the carotid bodies (Jones and Purves 1970). In order to manipulate the composition of the gas the diving ducks breathed, Butler and Stephenson (1988) held them in a chamber above an inside tank of water with a depth of 1.7 m. When diving from approximately 10% oxygen and normal levels of carbon dioxide, dive duration of intact ducks was significantly lower than that in ducks diving from air. However, in tufted ducks with denervated carotid bodies, this difference was abolished (Fig. 1A). On the other hand, when the tufted ducks were diving from approximately 5% carbon dioxide and normal levels of oxygen, dive durations of both intact and carotid body denervated ducks were significantly lower than those in air (Fig. 1A). Thus, even with adequate oxygen stores, dive duration was shorter when carbon dioxide was elevated, and the carotid body chemoreceptors were not involved in this response.

The levels of oxygen and carbon dioxide used in the above experiments were close to those beyond which the ducks would not dive (Butler and Stephenson 1988), which were largely between 8–10% for oxygen (lowest 7.5%) and 5.5–6.5%

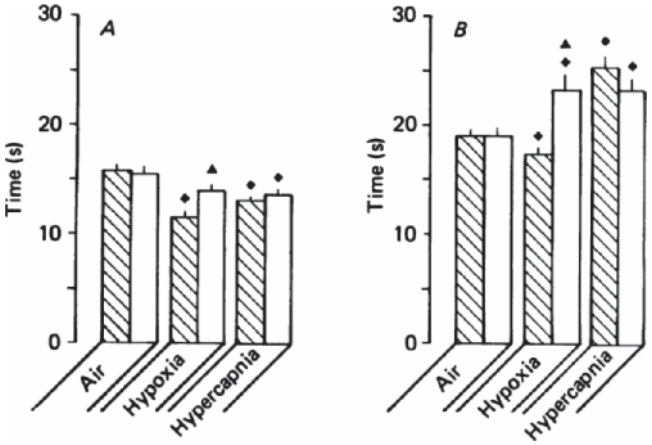

Fig. 1 Effects of various inspired gas mixtures on diving behaviour of control (n = 13, data from intact and sham-operated tufted ducks combined – striped columns) and carotid body denervated ducks (n = 6, open columns). Columns represent mean (± SEM) dive duration (A) and inter-dive surface duration (B). Hypoxia was approximately 10% oxygen with a normal level of carbon dioxide and hypercapnia approximately 5% carbon dioxide with a normal level of oxygen. ◆ represents a significant difference ($p < 0.05$) between the marked value and the respective value in air, while ▲ represents a significant difference between the marked value and the respective value in control ducks (modified from Butler and Stephenson 1988).

for carbon dioxide (highest 7.7%). It is interesting to note that diving activity did not decline gradually to zero as gas concentrations changed, but there was an abrupt cessation of diving activity at the critical gas levels. In tufted ducks, denervation of the carotid bodies had no detectable effect on these critical gas concentrations.

The durations that the birds remained at the surface between dives were significantly lower in intact birds diving from a hypoxic gas mixture compared with when they dived from air, but were significantly longer when they dived from the hypercapnic gas mixture (Fig. 1B). As with dive duration, surface duration was also affected by denervation of the carotid bodies when the birds dived from the hypoxic gas mixture, but not when they dived from the hypercapnic mixture (Fig. 1B). It would appear from Fig. 1 that in tufted ducks at least, hypoxia and hypercapnia close to the critical concentrations of oxygen and carbon dioxide predominantly influence dive duration, whereas the duration of the period spent at the surface is primarily controlled by carbon dioxide (Butler and Stephenson 1988). However, the exact influence of the respiratory gases on diving behaviour may vary between species and can certainly be affected by the diving environment. For example, double-crested cormorants, *Phalacrocorax auritus*, diving into a long, 1 m deep tank for a single piece of food did not change dive duration in response either to breathing a hypoxic or a hypercapnic gas mix (Enstipp, Andrews and Jones 2001). However, in both cases, surface durations were significantly longer than when the cormorants dived to and from air. Possibly, the cormorants adjusted their diving behaviour in response to the levels of oxygen and carbon dioxide only by changing

the duration that they spent at the water surface because there was no reason to remain underwater for longer than necessary to obtain the item of food. Nevertheless, these findings tend to support those for tufted ducks, since for both species, the ratio of dive duration to surface duration decreased when the birds dived from hypoxic or hypercapnic gas mixes.

3 The Role of Carbon Dioxide

There is evidence to suggest that, even when diving from air, the elimination of carbon dioxide may be at least, if not more, important than the replenishment of the oxygen stores between dives (Halsey *et al*. 2003). The increase in respiratory frequency and heart rate that occur during the last few seconds before the start of a dive in tufted ducks (Butler and Woakes 1979) were initially thought to serve mainly to load the oxygen stores as much as possible. However, it is known that human breath-hold divers are able to increase their dive durations by hyperventilating before submersion even though there is very little effect on the oxygen level in arterial blood which is already close to saturation during 'normal' ventilation (Ferringo and Lundgren 1999).

Most diving animals tend to perform a number of dives in fairly quick succession, so it is difficult to separate out what ventilatory behaviour at the surface is recovery from the previous dive and preparation for the next dive. However, there are some data from tufted ducks on the rates of gas exchange just before the first dive of a bout, and these illustrate an interesting phenomenon (Halsey *et al*. 2003). When at rest on the water, rate of oxygen consumption was 0.25 ± 0.01 ml s^{-1} and rate of carbon dioxide production was 0.20 ± 0.01 ml s^{-1}, giving a respiratory exchange ratio of 0.81 ± 0.01. However, during the period of hyperventilation before the first dive of a bout, the rate of carbon dioxide elimination increased more than the rate of oxygen consumption, and respiratory exchange ratio rose to 1.21 (Fig. 2). This suggests that the partial pressure of carbon dioxide in the arterial blood would have been lower than normal and the animals would have been hypocapnic. This interpretation is supported by measurements of the respiratory exchange ratio in Humbolt penguins, *Spheniscus humboldti*, in anticipation of a dive, which at 0.97 is most likely higher than the resting value (Butler and Woakes 1984).

On the basis of these and other data (see Halsey *et al*. 2003 for further details), it is proposed that before every dive, the ducks hyperventilate not only to replace the oxygen that has been used during the previous dive, but also to remove carbon dioxide to the point where they become hypocapnic. It is quite possible, therefore, that when a duck is diving from air, it is the level of carbon dioxide in the blood that is important in signalling when a dive should ultimately be terminated and when the bird should begin to ventilate. This is consistent with a recent model on the cardio-respiratory control of diving in Weddell seals, *Leptonychotes weddellii* (Stephenson 2005). In this model, the hyperventilation at the surface between dives has to be of sufficient duration to reduce the partial pressure of carbon dioxide in

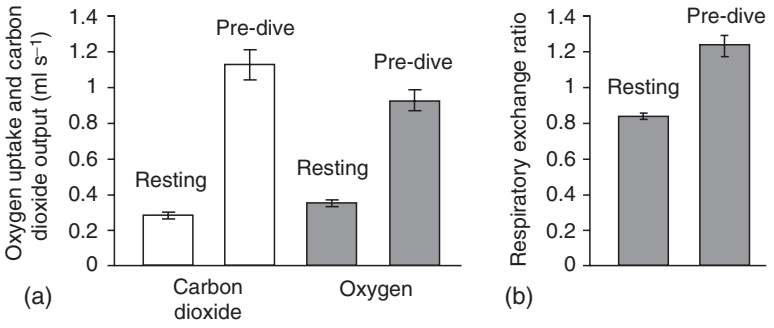

Fig. 2 Mean values (± SEM) for rate of oxygen uptake and carbon dioxide output and respiratory exchange ratio of six tufted ducks at rest on water and during the hyperventilation just before the first dive of a bout of diving (modified from Halsey *et al*. 2003).

the brain tissue (presumably, the central carbon dioxide receptors) below the threshold for the chemical stimulation of respiration, and this requires a reduction in the partial pressure of carbon dioxide in mixed venous blood. It is only when the oxygen stores are close to being exhausted during a dive that the carotid bodies may become important (*cf* Fig. 1a). In other words, dive duration is ultimately determined by the length of time that the central carbon dioxide receptors remain unstimulated.

References

Butler, P.J. (2004) Metabolic regulation in diving birds and mammals. Respir. Physiol. Neurobiol. 141, 297–315.

Butler, P.J. and Stephenson, R. (1988) Chemoreceptor control of heart rate and behaviour during diving in the tufted duck (*Aythya fuligula*). J. Physiol. 397, 63–80.

Butler, P.J. and Woakes, A.J. (1979) Changes in heart rate and respiratory frequency during natural behaviour of ducks, with particular reference to diving. J. Exp. Biol. 79, 283–300.

Butler, P.J. and Woakes, A.J. (1984) Heart rate and aerobic metabolism in Humboldt penguins, *Spheniscus humboldti*, during voluntary dives. J. Exp. Biol. 108, 419–428.

Butler, P.J. and Woakes. A.J. (1982) Control of heart rate by carotid body chemo-receptors during diving in tufted ducks. J. Appl. Physiol. 53, 1405–1410.

Enstipp, M.R., Andrews, R.D. and Jones, D.R. (2001) The effects of depth on the cardiac and behavioural responses of double-crested cormorants (*Phalacrocorax auritus*) during voluntary diving. J. Exp. Biol. 204, 4081–4092.

Ferringo, M. and Lundgren, C.E.G. (1999) Human Breath-Hold Diving. In: C.E.G. Lundgren and J.N. Miller (Eds.), *The Lung at Depth*. Marcel Dekker, New York, pp. 529–589.

Halsey, L.G. and Butler, P.J. (2006) Optimal diving behaviour and respiratory gas exchange in birds. Resp. Physiol. Neurobiol., 154, 268–283.

Halsey, L., Reed, J.Z., Woakes, A.J. and Butler, P.J. (2003) The influence of oxygen and carbon dioxide on diving behaviour of tufted ducks, *Aythya fuligula*. Physiol. Biochem. Zool. 76, 436–446.

Jones, D.R. and Purves, M.J. (1970) The effect of carotid body denervation upon the respiratory response to hypoxia and hypercapnia in the duck. J. Physiol. 211, 295–309.

Knower Stockard, T., Heil, J., Meir, J.U., Ponganis, K.V. and Ponganis, P.J. (2005) Air sac PO_2 and oxygen depletion during dives of emperor penguins. J. Exp. Biol. 208, 2973–2980.
Stephenson, R. (2005) Physiological control of diving behaviour in the Weddell seal *Leptonychotes weddelli*: a model based on cardiorespiratory control theory. J.Exp. Biol. 208, 1971–1991.
Woakes, A.J. and Butler, P.J. (1983) Swimming and diving in tufted ducks, *Aythya fuligula*, with particular reference to heart rate and gas exchange. J. Exp. Biol. 107, 311–329.

51
Evolutionary Trends in Respiratory Mechanisms

William K. Milsom

Abstract As we progress through the vertebrate phyla we see a number of changes in the functional morphology of the respiratory system that offer insights into the physiological systems that control them. We see a switch from a buccal pump powered by branchiomeric and hypobranchial muscles innervated by cranial nerves to a thoraco-abdominal aspiration pump powered by axial muscles innervated by spinal nerves with pre-motor neurons situated in the ventral respiratory column. The initial steps in the evolution of air breathing were a behavioural commitment to surface and changes in valving of the mouth/spiracle/nares and the operculum and glottis (or their equivalents) (*i.e.*, changes in the activation of the muscles dilating and/or constricting various openings). These allowed the production of water breaths versus deflation or inflation of the air-breathing organ. Changes in the respiratory pump muscles evolved later. While highly speculative, it is suggested that these three independent valving circuits may have arisen in association with different pairs of segmental rhythm generators, and that all circuits continue to work together in a coordinated fashion to produce all types of breaths (including eupneic breaths and gasps).

1 Introduction

The evolution of respiratory mechanisms in vertebrates progresses from aquatic ventilation primarily driven by a buccal force pump to aerial ventilation primarily driven by an aspiration or suction pump. Bearing in mind that there are numerous variations in the mechanisms that underlie the operation of these pumps, several general trends can be recognized. The first is a switch in the primary muscle groups associated with these two pumps. The buccal force pump operates with branchiomeric and hypobranchial muscles associated with the buccal and pharyngeal cavities. These muscles are innervated by cranial nerves, specifically the trigeminal, facial and hypoglossal nerves. The aspiration pump is driven primarily by axial muscles associated with the thorax and abdomen and innervated by spinal nerves.

University of British Columbia, Department of Zoology, milsom@zoology.ubc.ca

M.J. Poulin and R.J.A. Wilson (eds.), *Integration in Respiratory Control: From Genes to Systems*.

These nerves receive excitation primarily from pre-motor neurons in the ventral medullary respiratory column. A muscular diaphragm is found only in mammals but is none-the-less of axial origin and innervated by spinal motor neurons. Many ideas have been put forward concerning the origins of aspiration breathing (Brainerd, E.L. 1999; Brainerd and Owerkowicz 2006) and the mammalian diaphragm (Perry, Codd and Klein 2005), which are beyond the scope of this brief review. The focus of this review will be on how changes in respiratory mechanics and behaviour, particularly associated with the advent of air-breathing (via buccal force pump and aspiration suction pump) alter the phase relationships of the various pumps and the implication of this for the evolution of respiratory central rhythm generators.

2 Pulmonary Mechanics, Behaviour and the Phases of the Respiratory Cycle

2.1 Water Breathers

In adult lampreys, branchial muscles surround the branchial basket, which consists of elastic cartilage and contains the gill sacs. Synchronous contraction of these muscles compresses the branchial basket and produces exhalation. As the muscles relax, the spring-like basket expands by passive recoil drawing fresh water back into the sacs. Ventilation is often tidal, in and out through the pharyngeal gill slits. In larval lampreys and in hagfish, ventilation is unidirectional. The branchial muscles contract during exhalation just as in the adults. Unlike in adults, the valves over the gill openings close during branchial expansion so that water is drawn in through the mouth. Larvae also use the velum (a pair of muscular pouches in the pharynx) to push water from the pharynx during exhalation (Fig. 1) (Johansen and Strahn 1963).

In all of the remaining water-breathing vertebrates, both phases of the buccal ventilation cycle are active. While a second pump operates outside the gills to expand and compress the parabranchial or opercular cavity, it is the buccal pump that primarily powers ventilation. Water flow is uni-directional, in through the mouth/ spiracle/nares (depending on species) and out over the gills (Fig. 1) (Shelton 1970).

2.2 Early Air Breathers

The origins of air breathing were initially associated with a behavioural commitment to swim to the surface of the water and changes in valving of the mouth/spiracle/nares and the operculum and glottis (or their equivalents). At least 47 species from 24 genera of bony fish are known to breathe air using a lung or a respiratory gas bladder. These fishes use the same buccal pump that they do for water breathing but devote one full cycle of the pump to each of lung deflation and inflation.

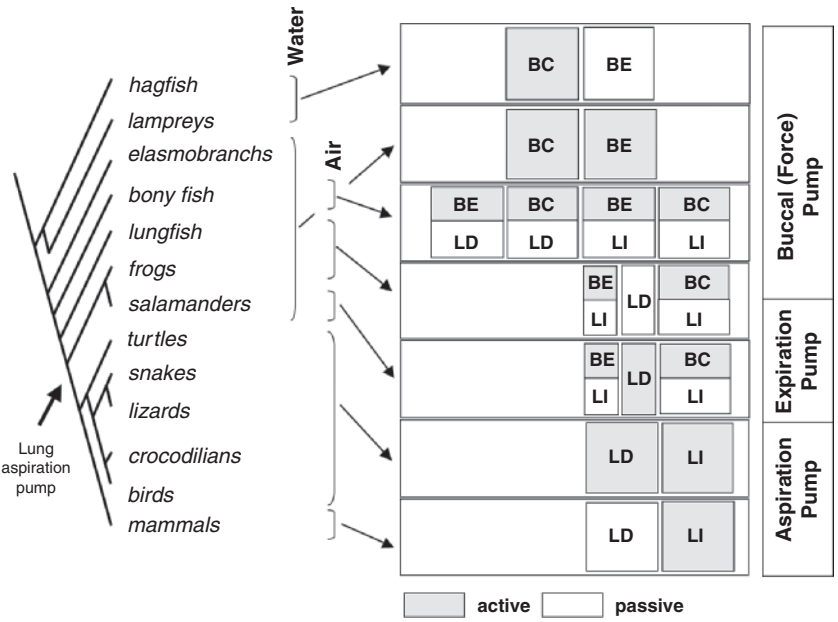

Fig. 1 Dendrogram of various vertebrate groups showing active/passive phases of the buccal/lung ventilation cycles associated with aquatic and aerial respiration. See text for details. (BE = buccal expansion, BC = buccal compression, LD = lung deflation, LI = lung inflation)

The respiratory pause in the lung ventilation cycle is at end-inspiration with the lungs full (Brainerd 1994). What determines whether a cycle of the pump produces a water breath, lung deflation or lung inflation is the valving mechanism that is employed, which orifices are open and which are closed. Without going into detail, the glottis (or sphincter to the air breathing organ) remains closed during a water breath while the glottis remains open but the operculum remains closed during an air breath. Furthermore, the sequence of opening and closing the mouth and glottis are reversed during the buccal expansion and compression phases associated with lung deflation and inflation. The critical point is that three different neural circuits associated with the timing of the opening and closing of the various valves (mouth/spiracle/nares/ operculum/glottis) must exist.

Unlike the bony fishes, in the lungfish and most frogs and toads, both lung deflation and inflation are accommodated within a single buccal pump cycle. Lung deflation is purely passive and occurs during a pause in the buccal cycle (between buccal expansion and compression). Both phases of the buccal cycle are associated with lung inflation; buccal expansion primes the pump by filling the buccal cavity initially and then, following lung deflation, buccal compression is used to force this air into the lung (Vitalis and Shelton 1990). Again, what determines whether a cycle of the pump produces a water breath (in lungfish and anuran larvae; a buccal oscillation in anuran adults), lung deflation or lung inflation is the valving mechanism that is employed. Three neural circuits associated with the timing of the

opening and closing of the various valves (mouth/spiracle/nares/operculum/glottis) must exist here also.

2.3 Active Expiration and the Origins of Aspiration Breathing

Until recently there was no evidence of an intermediate mechanism between the buccal pump of fishes and amphibians and the aspiration pump of reptiles, birds and mammals. It has now been shown, however, that many amphibians use axial muscles for active expiration along with the buccal pump for active inspiration (see Brainerd 1999; Brainerd and Owerkowicz 2006, for reviews). This suggests that aspiration breathing evolved in two steps: (1) from buccal pumping alone to buccal pumping for inspiration and axial muscles for expiration and then (2) to aspiration breathing alone using axial muscles for both expiration and inspiration (Brainerd 1999).

2.4 Aspiration Breathing in "Higher" Vertebrates

Although aspiration breathing consists of both active lung deflation and inflation in reptiles and birds, active deflation is only associated with increased respiratory drive in mammals. Interestingly, in mammals we see a switch in relative contributions of chest wall compliance and air flow resistance to pulmonary work (the former dominates in birds and reptiles, the latter takes on increased importance in mammals), the evolution of a muscular diaphragm and a reduction in the need for active lung deflation as the system returns to functional residual capacity following inhalation.

3 Implications for Central Rhythm Generation

Initially, in water breathing vertebrates, there was one set of pump muscles (those associated with the buccal pump) and one valving mechanism. With the advent of air breathing, multiple valving mechanisms for different behaviours evolved; independent circuits arose for generating a H2O breath (or buccal oscillation), lung deflation, and lung inflation. While highly speculative, it is possible that the three independent valving circuits may have arisen in association with different pairs of segmental rhythm generators in a rostral-caudal arrangement (Fig. 2). The suggestion put forward in Fig. 2 separates the lung oscillator into a deflation and an inflation oscillator associated with the parafacial respiratory group and the PreBötzinger Complex, respectively, in mammals and implies that none of the oscillators arose anew but all are based on reconfiguring pre-existing embryonic segmental rhythm generators.

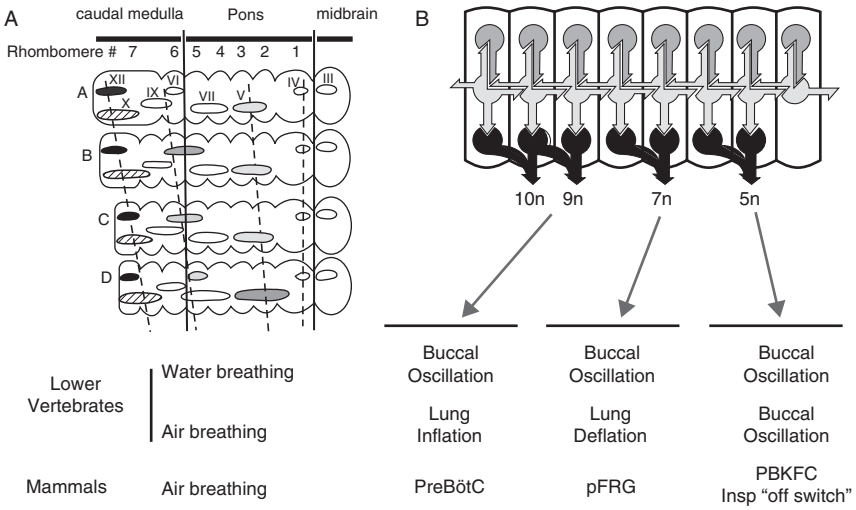

Fig. 2 (A) Hypothetical arrangement of rhythm generators (top), interneurons (middle) and motor neurons (bottom) within the segmented hindbrain of a vertebrate embryo (modified from Champagnat and Fortin 1997). (B) Highly speculative suggestion of the relationship between various segmental rhythm generators in the vertebrate embryo, the respiratory behaviours seen in lower vertebrates, and elements of the respiratory neuraxis in mammals.

Finally, I would suggest that while different segmental oscillators may have taken over primary roles associated with different respiratory behaviours, all oscillators are still entrained and still participate in each respiratory cycle. The production of any lung inflation event (from eupnea to gasping) with all of the nuances in timing and shaping of air flow requires the participation of all sites even though its phenotypic expression (inspiration) must be predominately mediated by the PreBötC.

Acknowledgement This work was supported by the NSERC of Canada.

References

Brainerd, E.L. (1994) The evolution of lung-gill bimodal breathing and the homology of vertebrate respiratory pumps. Am. Zool. 34, 289–299.

Brainerd, E.L. (1999) New perspectives on the evolution of lung ventilation mechanisms in vertebrates. J. Exp. Biol. 4, 11–28.

Brainerd E.L. and Owerkowicz (2006) Respir. Physiol. Neurobiol. www.sciencedirect.com/sciences/journal/15699048)

Champagnat, J. and Fortin, G. (1997) Primordial respiratory-like rhythm generation in the vertebrate embryo. TINS 20, 119–124.

Johansen, K. and Strahn, R. (1963) The respiratory system of *Myxine glutinosa*. In: A. Brodal and R. Fänge (Eds.) *The Biology of Myxine*. Universitetsforlaget, Oslo, pp. 352–371.

Perry, S.F., Codd, J.R. and Klein, W. (2005) Evolutionary biology of aspiration breathing and origin of the mammalian diaphragm. Rev. Mal. Respir. 22, 2S19–2S38.
Shelton, G. (1970) The regulation of breathing. In: *Fish Physiology IV*, pp. 293–359.
Vitalis, T.Z. and Shelton, G. (1990) Breathing in *Rana pipiens*: the mechanism of ventilation. J. Exp. Biol. 154, 537–556.

Part IX
Central Chemosensitivity

52
A Computer Model of Mammalian Central CO_2 Chemoreception

Mykyta Chernov[1], Robert W. Putnam[2] and J.C. Leiter[3]

Abstract We developed a single compartment model of a mammalian CO_2 sensitive neuron and tested the hypothesis that pH-dependent inhibition of multiple potassium channels contributes to CO_2 sensitivity. pH-dependent inhibition of potassium channels by either intracellular or extracellular pH was sufficient to alter neuronal activity, but changes in neither intracellular nor extracellular pH are required to elicit a neuronal response to hypercapnic stimulation.

1 Introduction

We developed a computer model of mammalian central chemoreception and examined the mechanisms whereby neurons translate CO_2 levels into electrical signals based on earlier experimental and computer modeling work with an invertebrate preparation (Chernov *et al*., 2006; Denton *et al*., 2006). Two issues dominate debate about the mechanism of neuronal CO_2 chemosensitivity: whether the principal chemosensory stimulus is extracellular pH (pH_o) or intracellular pH (pH_i), and which potassium channel is the main sensor (Putnam *et al*., 2004). We developed a model that reproduces pH transients similar to those obtained during hypercapnic acidosis and demonstrates the effect of acidosis on potassium channels and electrical activity of a virtual neuron.

2 Methods

We created a single-compartment model of a neuron containing seven mammalian ion channels (a fast sodium channel, I_{Na}, peak conductance = 10 μS; a T-type calcium channel, I_{CA}-0.2 μS; a TASK channel, I_{TASK}-0.004 μS; an A-type channel, I_{KA}-

[1]Dartmouth Medical School, Department of Physiology, mykyta.chernov@dartmouth.edu

[2]Wright State University Boonshoft School of Medicine, Department of Neuroscience, Cell Biology & Physiology, robert.putnam@wright.edu

[3]Dartmouth Medical School, Department of Physiology, james.c.leiter@dartmouth.edu

M.J. Poulin and R.J.A. Wilson (eds.), *Integration in Respiratory Control: From Genes to Systems*.

0.25 μS; an inward rectifier, I_{KIR}-0.2 μS; a delayed rectifier, I_{KDR}-1 μS; and a Ca^{2+}-activated potassium channel, I_{KCa}-0.13 μS) and altered the concentrations of CO_2 and bicarbonate to change pH and determine the cell's electrophysiological behavior. We adapted I_{Na}, I_{Ca}, I_{KA}, I_{KDR} and I_{KCa} currents from Rybak *et al*. (1997). We added an I_{KIR} from a description by Williams *et al*. (1988) and I_{TASK}, a two-pore potassium conductance, adapted from Washburn *et al*. (2002). We incorporated pH-sensitivity into I_{KIR}, I_{KDR}, I_{KCa} and I_{TASK} by multiplying the maximal conductance of each channel by a pH titration curve with a pK_a appropriate for the particular channel. Except for I_{KA}, the channels are sensitive to either pH_o or pH_i. I_{KA}, which has both a pH_o- and a pH_i- dependent inhibition was modeled by two independent titration curves so that the maximal conductance (g*) of I_{KA} equals $g \cdot f(pH_i) \cdot f(pH_o)$. This channel also has a pH_i-dependent time constant of inactivation based on observations by Pandanilam *et al*. (2002) in a K_V 1.4 channel. The pH responses were modeled using the equations derived by Boron and De Weer (1976). We included a chloride-bicarbonate and a sodium-hydrogen exchanger (Leem *et al*., 1999), and we modified the behavior of the exchangers so that they were inhibited by low pH_o, but activated by low pH_i (Ritucci *et al*. 1997; Nottingham *et al*. 2001; Chernov *et al*. 2006). The model was implemented in a Matlab/Simulink programming environment using a variable-step differential equation solver.

3 Results: Patterns of Neuronal Firing

When 250 pA of current were injected, the model exhibited repetitive firing. During simulated hypercapnic acidosis, inhibition of potassium channels resulted in higher firing rates. We examined the effect of pH-dependent inhibition of only one channel at a time, and we studied the effect of pH-dependent inhibition of all channels save one (Table 1). Despite its rather small absolute conductance, approximately half of the increase in firing rate due to hypercapnic acidosis could be attributed to the TASK channel. Inhibition of all potassium channels by pH resulted in an increase in firing from 0.2 to 15 Hz, and inhibition of TASK alone resulted in a frequency of 8.0 Hz. Similarly, when pH inhibition of the TASK channel was removed, but other channels were allowed to be pH-sensitive, the response was blunted by about 50%. The TASK current is a voltage-independent conductance; it is constitutively active and therefore has a major influence on the resting membrane potential.

3.1 Multiple Channels Contribute to the Maximal Response

Although the TASK channel is the major determinant of the model's sensitivity to acidosis, it only accounts for half of the response. Inhibition of any other channels also results in faster firing (Table 1), and the contributions of each channel to the

Table 1 Model frequency responses in hertz when only one channel or all potassium channels save one were inhibited during hypercapnia. The ratio is the relative change during hypercapnia compared to normocapnia

Single channel inhibited	pH sensor location	5% CO_2	10% CO_2	ratio	All channels inhibited except	10% CO_2	ratio
I_{TASK}	outside	0.2	8.0	40	I_{TASK}	6	33
I_{KA}	outside	0.2	1.4	7	I_{KA}	13.8	69
I_{KA}	inside	0.2	1.6	8	I_{KA}	12.4	62
I_{IR}	outside	0.2	1.4	7	I_{IR}	14	70
I_{DR}	outside	0.2	0.6	3	I_{DR}	13.4	67
I_{KCa}	inside	0.2	2.6	13	I_{KCa}	12.4	62
All		0.2	15	75			

overall effect are approximately additive. Thus, chemosensitive cells have a degree of redundancy, and expression of even a few relevant types of potassium channels is sufficient to elicit a response to alterations in pH.

3.2 A Drop in pH_o is a Stronger Stimulus than a Drop in pH_i

We simulated isohydric hypercapnia (a drop in internal pH only) by raising extracellular concentrations of both bicarbonate and CO_2. Extracellular acidification only was achieved by raising the level of CO_2 outside the cell, but renders the membrane impermeable to either CO_2 or bicarbonate at the same time. Either stimulus was sufficient to produce an increase in the firing rate, but the response to extracellular acidification was greater (Fig. 1). The majority of the channels are sensitive to pH_o. During isohydric hypercapnia, the action of the pH-regulating transporters is unmasked and one observes the gradual decrease in the firing rate as the pH_i is brought back towards normal (spike frequency adaptation), as well as a temporary cessation of activity after the stimulus is removed and the cell becomes alkalotic.

4 Discussion

We simulated the electrophysiological properties of chemosensitive neurons. Varying the magnitudes of potassium currents and their kinetics results in quantitative changes in chemosensitivity of the neuron to acidosis, but the cell remains responsive as long as we accept the broad concept that potassium channels are inhibited by pH. The design of the model with respect to pH inhibition is

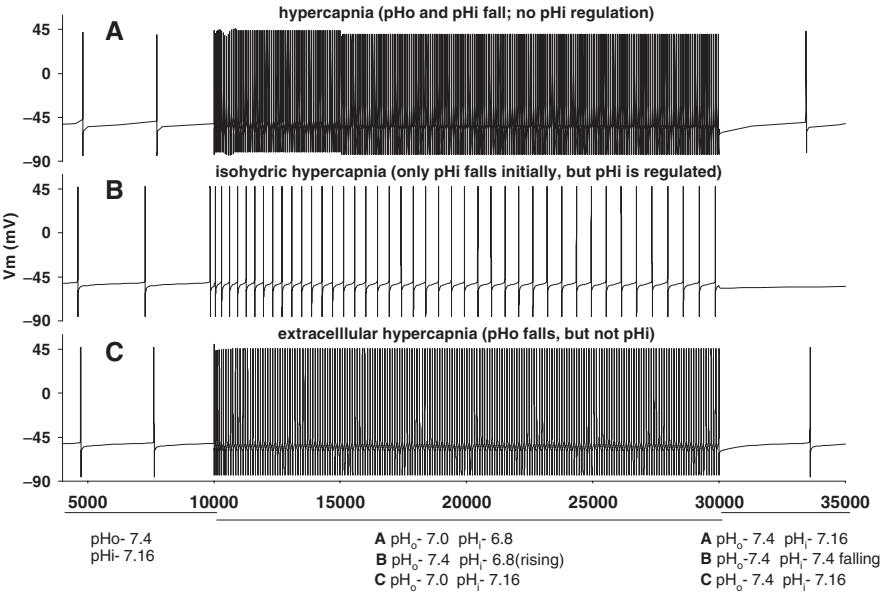

Fig. 1 Model response to three stimuli: the pH values are shown below for each condition. Hypercapnia (combined fall in pH_i and pH_o) has the greatest effect, and isohydric hypercapnia (only pH_i falls) has the least effect. Time is in milliseconds

conservative. The titration curves used have a shallow slope of 1, so that over the 0.2 - 0.4 variation in pH, the maximal conductance varies by 15–20%. This change is enough to increase the firing rate by a factor of 10–75. Most experimenters report 1- to 10-fold increases in rate, which could occur with inhibition of potassium conductances by only a few percent.

If inhibition of potassium channels by pH is as ubiquitous as our work suggests, the question becomes not why some cells alter their firing rate in response to pH, but how do the other neurons maintain a constant firing rate despite being subjected to pH fluctuations?

Our results suggest that either pH_o or pH_i is a sufficient chemosensory stimulus. The maximum effect is obtained during acidification of both pH_i and pH_o although extracellular acidification is a more powerful single stimulus. This occurs because the extracellular fluid is less effectively buffered, and I_{TASK} and the majority of other potassium currents are primarily affected by pH_o. An increase in expression of channels such as I_{KA} and I_{KCa} may render a cell more responsive to intracellular acidification, but changes in pH_i will be attenuated by the intrinsic buffering power and pH regulatory processes that determine pHi, in part.

Although the TASK channel is the principal sensor, other potassium currents make up for half of the total response, suggesting that chemosensitivity is not a property of a single current and may be more common than previously thought. The results of this simulation suggest that cells sense primarily extracellular pH concentrations.

We would like to explore this model in the future by introducing morphologically realistic neurons and distributing the channels heterogeneously within the neuron. It will also be interesting to explore the role that astrocytes might play in modulating neuronal chemosensitivity, both through electrical connections via gap junctions and by modulating the pH of the microenvironment of neighboring neurons.

Acknowledgement This work was supported by NIH grants HL71001 and HL56683.

References

Boron, W.F. and De Weer, P. (1976) Intracellular pH transients in squid giant axons caused by CO_2, NH_3, and metabolic inhibitors. J. Gen. Physiol. 67, 91–112.

Chernov, M.M., Daubenspeck, J.A., Denton, J.S., Pfeiffer, J.R., Putnam, R.W. and Leiter, J.C. (2007) A computational analysis of central CO_2 chemosensitivity in *Helix aspersa*. Am. J. Physiol., 292, C278–291.

Denton, J.S., McCann, F.V. and Leiter, J.C. (2007) CO_2 chemosensitivity in *Helix aspersa*: Three K+ currents mediate pH-sensitive neuronal activity. Am. J. Physiol., 292, C292–304.

Leem, C.H., Lagadic-Gossman, D. and Vaughan-Jones, R.D. (1999) Characterization of intracellular pH regulation in guinea-pig ventricular myocyte. J. Physiol. (Lond.) 517.1, 159–180.

Nottingham, S., Leiter, J.C., Wages, P., Buhay, S. and Erlichman, J.S. (2001) Developmental changes in intracellular pH regulation in medullary neurons of the rat. Am. J. Physiol. 281, R1940–R1951.

Padanilam, B.J., Lu, T., Hoshi, T., Padanilam, B.A., Shibata, E.F. and Lee, H.-C. (2002) Molecular determinants of intracellular pH modulation of human $K_v1.4$ N-type inactivation. Molec. Pharmacol. 62, 127–134.

Putnam, R.W., Filosa, J.A. and Ritucci, N.A. (2004) Cellular mechanisms involved in CO_2 and acid sensing in chemosensitive neurons. Am. J. Physiol. 287, C1493–C1526.

Ritucci, N.A., Dean, J.B. and Putnam, R.W. (1997) Intracellular pH response to hypercapnia in neurons from chemosensitive areas of the medulla. Am. J. Physiol. 273, R433–R441.

Rybak, I., Paton, J.F.R. and Schwaber, J.S. (1997) Modeling neural mechanisms for genesis of respiratory rhythm and pattern. I. Models of respiratory neurons. J. Neurophysiol. 77, 1994–2006.

Washburn, C.P., Sirois, J.E., Talley, E.M., Guyenet, P. and Bayliss, D.A. (2002) Serotonergic raphe neurons express TASK channel transcripts and a TASK-like pH- and halothane-sensitive K^+ conductance. J. Neurosci. 22, 1256–1265.

Williams, J.T., North, R.A. and Tokimasa, T. (1988) Inward rectification of resting and opitate-activated potassium currents in rat locus coeruleus neurons. J. Neurosci. 8, 4299–4306.

53
A Mathematical Model of pH_i Regulation in Central CO_2- Chemoreception

Juan M. Cordovez[1], Chris Clausen[2], Leon C. Moore[3] and Irene C. Solomon[4]

Abstract In CO_2 chemosensitive neurons, an increase in CO_2 (hypercapnia) leads to a maintained reduction in intracellular pH (pH_i) while in non-chemosensitive neurons pH_i recovery is observed. The precise mechanisms for the differential regulation of pH_i recovery between these cell populations remain to be identified; however, studies have begun to explore the role of Na^+/H^+ exchange (NHE). Here, we compare the results of two different formulations of a mathematical model to begin to explore pH_i regulation in central CO_2 chemoreception.

1 Introduction

A decrease in intracellular pH (pH_i) is thought to be the primary stimulus for CO_2 sensing in central CO_2 chemoreceptors. In CO_2 chemosensitive neurons, an increase in CO_2 (hypercapnia) leads to a maintained reduction in pH_i while in non-chemosensitive neurons pH_i recovery is observed (Ritucci, Dean, and Putnam 1997). Regulation of pH_i in most cells is dependent upon the rate of CO_2 hydration, intrinsic buffering capacity, Na^+/H^+ exchange (NHE), and HCO_3^-/Cl^- exchange (AE). Thus, increased levels of CO_2, which lead to the rapid hydration of CO_2 to H^+ and HCO_3^- (catalyzed by carbonic anhydrase, CA), result in a fall in pH_i that is partially offset by intracellular buffering and transmembrane extrusion of H^+. Although the precise mechanism(s) for the differential regulation of pH_i recovery in CO_2 chemosensitive versus non-chemosensitive neurons remains to be identified, numerous *in vitro* studies have begun to evaluate the role of NHE in pH_i regulation in these cell populations. These studies have demonstrated that functional NHE is necessary for pH_i recovery and that impairment of normal NHE activity may be responsible for the lack of pH_i recovery in chemosensitive neurons. An alternate explanation suggests that expression of different NHE isoforms may be responsible for this differential regulation. To begin to evaluate these possibilities, we developed a preliminary

[1–4] State University of New York at Stony Brook, Department of Physiology and Biophysics, jcordove@ic.sunysb.edu

M.J. Poulin and R.J.A. Wilson (eds.), *Integration in Respiratory Control: From Genes to Systems*.

mathematical model to investigate potential mechanisms participating in pH_i regulation in response to simulated hypercapnic acidosis. In that model, we described passive electrolyte transport using Ohm's law. For each ion, current (i) was described by $i = g\ (V_m - E)$, where g is the ionic conductance, V_m is membrane potential, and E is the ion's equilibrium potential.

Two disadvantages to this approach were that ion flow generally does *not* adhere to the linear I/V relation implied by the equation above describing ionic current, and that g is *proportional* to permeability, but it is also a function of V_m as well as the intra- and extracellular ion concentrations. These considerations prompted us to reformulate the model.

In the new formulation of the model fluxes are described by ion permeability (P) *not* conductance, therefore we have a more realistic nonlinear flux relationship. Also, the new model formulation implements a general procedure for computing V_m that is valid irrespective of the mechanism of transport, and it provides a means to simulate experimental situations where concentrations change significantly (*e.g.*, NH_4^+ substitution).

The purpose of the current investigation is to validate the new model formulation by re-assessing pH_i regulation in response to simulated hypercapnic acidosis. The results of the new model formulation are compared to those of our original model.

2 Description of the Models

2.1 Features Common to Both Models

Both the original model formulation and the new model formulation incorporate conservation of mass and electroneutrality constraints, kinetic models of the Na^+/K^+-ATPase, AE (Chang and Fujita 2000), NHE (Weinstein 1995), passive permeation pathways for solute species and H_2O, and hydration/dehydration of CO_2 that is catalyzed by carbonic anhydrase. Cell volume (V) is determined by water flux (J_w):

$$\frac{dV}{dt} = -AJ_w,$$

where A represents the area.

Intracellular solute concentrations are determined by solute (J_i) and water fluxes:

$$\frac{V}{A}\frac{dC}{dt} = C_i^i J_w - J_i$$

(Note. extracellular concentrations C_i^o are constant)

Thus, the models consist of 10 coupled differential equations, one for each of the following variables:

$$V, C^i_{Na^+}, C^i_{K^+}, C^i_{Cl^-}, C^i_{X^-}, C^i_{Y^0}, C^i_{H_t}, C^i_{B_{bicarbonate}}, C^i_{B_{phosphate}}, C^i_{B_{ammonium}}$$

where C_i^i and C_i^o refer to the intra- and extracellular concentrations, respectively, the subscript *i* denotes solute species (Na^+, K^+, etc.), and B refers to the total buffer concentration. The initial conditions are specified, and the above differential equations are integrated numerically as a function of time.

2.2 Additional Features of the Original Model

In the original model formulation, solute species were divided into non-electrolytes and electrolytes, and their fluxes were computed separately. Movement of non-electrolytes was described by simple diffusion: $J_i^{passive} = P_i (C_i^i - C_i^o)$, where P is permeability. Ionic current (i_i) for electrolytes was described by $i_i = g_i (V_m - E_i)$, as defined above, and the flux was given by

$$J_i^{Passive} = \frac{i_i}{z_i F},$$

where z_i denotes valence and F is Faraday's constant. V_m, which results in zero net current flow was defined by

$$V_m = \frac{\left(\sum_i g_i E_i\right) - i_p}{\sum g_i},$$

where i_p is the Na^+-K^+ ATPase sodium pump current according to the cooperativity binding model.

2.3 Additional Features of the New Model Formulation

In the new model formulation, the *passive* flux of solute *i* is given by the Goldman-Hodgkin-Katz (GHK) equation. For a constant electrical field across the membrane,

$$J_i^{Passive} = P_i (C_i^i e^{z_i U} - C_i^o) \frac{z_i U}{e^{z_i U} - 1},$$

where $U = V_m F/RT$; R is the gas constant and T is absolute temperature. It should be noted that when z_i is zero, the GHK equation describes simple diffusion.

For determination of V_m, a thermodynamic constraint on solute flow is that at all times the cell and bathing solution must both remain electrically neutral, namely,

$$\sum_i z_i C_i^i = \sum_i z_i C_i^o = 0 \cdot$$

Net transcellular current i_T (as a function of V_m) is given by

$$i_T(V_m) = F\sum_i z_i J_i ,$$

where J_i is total flux of solute i, irrespective of the actual transport mechanism (*e.g.*, passive, active, exchange, co-transport, etc). Implementation of the electroneutrality constraint is done numerically using a root finding algorithm (*e.g.*, Newton's method) that solves V_m such that $i_T(V_m) = 0$.

3 Validation of the New Model Formulation

Both the original model formulation and the new model formulation were used to assess pH_i regulation in response to simulated hypercapnic acidosis, which was produced by doubling the concentration of CO_2. In these simulations, both model formulations show identical pH_i recovery responses when membrane potential is established based on a "normal" level of $[K^+]_o$ (*i.e.*, 4 mM). In contrast, when the $[K^+]_o$ was increased to 8 mM (*i.e.*, high), the two model formulations exhibited different V_m, which reflects the differences between the linear I/V relationship (original model formulation) and the non-linear I/V relationship introduced by the GHK equation (new model formulation). Under the high $[K^+]_o$ condition, the resting pH_i was slightly elevated when compared to normal $[K^+]_o$ (*i.e.*, 7.35 instead of 7.33); however, both the dynamics and the magnitude of the pH_i responses to hypercapnic acidosis were very similar for both model formulations. An example showing the results of these simulations are provided in Fig. 1.

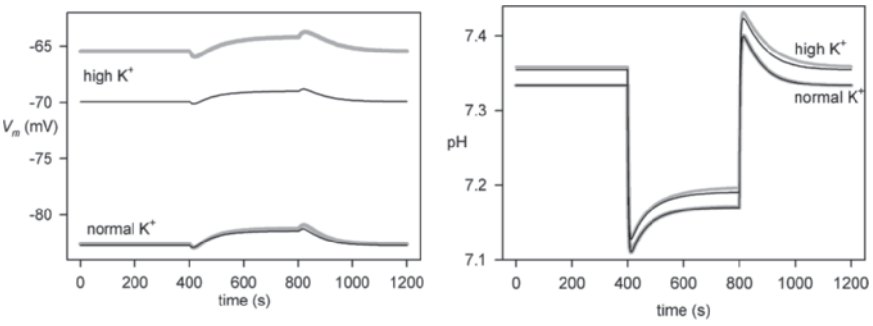

Fig. 1 Comparison of model results for V_m and pH_i responses to hypercapnic acidosis. Simulated hypercapnic acidosis (increased CO_2) was produced from 400–800 s during normal and high $[K^+]_o$. In the original model formulation with a linear I/V relationship (gray), the change in V_m produced by elevated $[K^+]_o$ is ~18 mV as predicted by the Nernst equation. In the new model formulation which implements the GHK equation (black), the change in V_m produced by elevated $[K^+]_o$ is ~13 mV due to the non-linearity of the I/V relationship. Both models, however, exhibit similar pH_i responses to hypercapnic acidosis

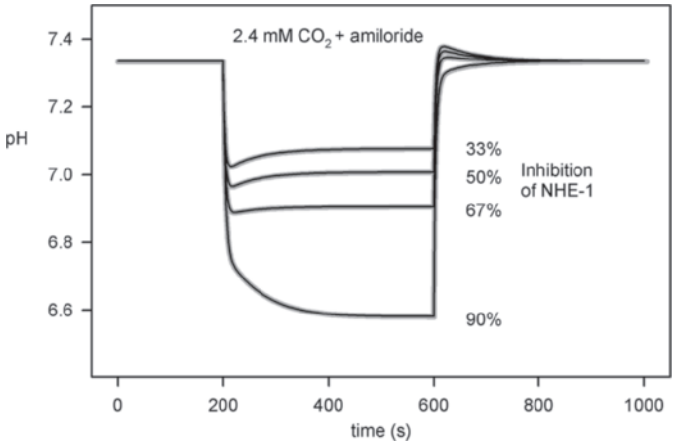

Fig. 2 Comparison of model results for pHi responses to hypercapnic acidosis during blockade of NHE. Both the original model (gray) and the new model formulation (black) show that pHi recovery is impaired in a dose-dependent manner with inhibition of NHE activity

To determine whether functional NHE is necessary for pH_i recovery during hypercapnic acidosis, we examined the effects of inhibition of NHE activity (*i.e.*, simulation of amiloride effects) using both model formulations. Both model formulations demonstrate that pH_i recovery is impaired in a dose-dependent manner with inhibition of NHE activity, supporting a role for NHE in pH_i recovery. However, pH_i recovery is seen during low NHE activity, suggesting that the lack of pH_i recovery in CO_2 chemosensitive cells is not due to impairment of NHE activity. An example showing the results of these simulations is provided in Fig. 2.

4 Summary and Conclusions

Our results indicate that both model formulations are able to reproduce experimental observations of pH_i responses to hypercapnic acidosis, including the dependence on NHE for pH_i recovery. However, in order to simulate common experimental protocols in which V_m is altered (viz., NH_4^+ pre-pulse experiments), we were compelled to revise our original formulation of the model by incorporating the GHK equation. This was necessary because the linear conductance formulation previously used can produce erroneous results when V_m changes substantially (see Fig. 1) owing to a nonlinear I/V relation, coupled with the dependence of conductance on concentration. On the other hand, when species concentrations do not change significantly or changes in V_m are modest, as in simulation of hypercapnia, the two formulations of the model show expected close agreement. Thus with the new formulation, we are now able to investigate a broader range of experimental perturbations.

Additional studies focusing on NHE isoforms, other H^+ extrusion pathways, and the role of the AE need to be explored to identify potential mechanisms mediating the differences in pH_i regulation in CO_2 chemosensitive versus non-chemosensitive neurons.

Acknowledgements This work was initiated as part of a graduate course entitled, Mathematical Modeling of Physiological and Biophysical Systems, which was developed with financial support from a NIH/NIDDK curriculum development grant DK66124. This work was also supported by NIH grant NS045321.

References

Ritucci, N.A.,Chambers-Kersh, L., Dean, J.B. and Putnam R.W. (1998) IntracellularpH regulation from chemosensitive and nonchemosensitive areas of the medulla. Am. J. Physiol. 275 (4 Pt 2), R1152–R1163.

Ritucci, N.A., Dean, J.B. and Putnam R.W. (1997) Intracellular pH response to hypercapnia in neurons from chemosensitive areas of the medulla. Am. J. Physiol. 273 (1 Pt 2), R433–R441.

Chang H. and Fujita T. (2001) A numerical model of acid-base transport in rat distal tubule. Am. J. Physiol. Renal Physiol. 281(2), F222–F243.

Weinstein, A.M. (1995) A kinetically defined Na+/H+ antiporter within a mathematical model of the rat proximal tubule. J. Gen. Physiol. 105(5), 617–641.

54
Plasticity in the Brain: Influence of Bilateral Carotid Body Resection (bCBR) on Central CO_2 Sensitivity

Albert Dahan[1], Elise Sarton[2] and Luc Teppema[3]

Abstract We investigated the effect of bilateral carotid body resection (bCBR) in a patient with bilateral carotid body tumors on central CO_2 sensitivity. We applied multiple square-wave changes in end-tidal CO_2 and measured ventilation before the first surgery and at regular intervals for 3 years after surgery. The data were analyzed using a two-compartment model of the ventilatory control system. bCBR resulted in the loss of the fast response to CO_2, and a sharp reduction in the magnitude of central CO_2 sensitivity (a reduction of about 80% within 3 months after bCBR). Central CO_2 sensitivity gradually increased to pre-operative values within 2 years after surgery. These observations are a strong indication for (1) the existence of a tonic influence from the peripheral chemoreceptors of the carotid bodies on central CO_2 drive; (2) absence of any recovery of the peripheral drive after bCBR; and (3) neural plasticity causing the regeneration of central drive after bCBR.

1 Discovery of the Carotid Bodies

In the first two decades of the 20th century, the Belgian scientist, Corneille Heymans (Ghent: 1892–1962), studied the reflexogenic role of the cardio-aortic and the carotid sinus areas in the regulation of respiration and blood pressure. He injected the highly toxic Na-cyanide into the carotid artery of a dog and, to his surprise, discovered that hyperventilation occurred only when the artery was not stripped of its nerves (denervated). He concluded that a small organ was present in the wall of the carotid artery which senses the chemical content of blood and which carries this information to the brainstem. For his work, and especially his discovery of the carotid body (glomus caroticum), Heymans received the Nobel Prize in Physiology in the same

Leiden University Medical Center, Department of Anesthesiology, 2300 RC Leiden, The Netherlands

[1] a.dahan@lumc.nl

[2] e.y.sarton@lumc.nl

[3] l.j.s.m.teppema@lumc.nl

M.J. Poulin and R.J.A. Wilson (eds.), *Integration in Respiratory Control: From Genes to Systems*.

year that Enrico Fermi received his Nobel Prize in Physics (1938). The carotid body (CB) is strategically situated in the bifurcation of the common carotid artery and contains the peripheral chemoreceptors. The peripheral chemoreceptors sense oxygen, carbon dioxide, pH and glucose in the arterial blood, which will supply the brain.

2 Carotid Body Tumors

Tumors of the carotid bodies are commonly associated with chronic tissue hypoxia from altitude, cyanotic heart disease and chronic pulmonary disease (Dahan, Taschner, Jansen, van der Mey, Teppema and Cornelisse 2004). There is also a hereditary form of CB tumors, which is not related to exposure to chronic hypoxia but is related to a missense mutation in the gene that encodes for succinate dehydrogenase D (SDHD) (Taschner, Jansen, Baysal, Bosch, Rosenberg, Bröcker-Vriends, van der Mey, van Ommen, Cornelisse and Devilee 2001; Dahan *et al*. 2004). SDHD is a small part of cytochrome b588 of the mitochondrial respiratory chain complex II and an essential enzyme in the Krebs tricarboxylic-acid cycle. These carotid body tumors are part of the hereditary paraganglioma type I (PGL1) syndrome. This PGL1 gene is located on the long arm of chromosome 11. In Dutch founder families, a missense mutation (c.274G > T) causing p.Asp92Tyr (replacement of aspartic acid by tyrosine at amino acid position 92) in the SDHD gene product was observed.

The PGL1 syndrome is characterized by slowly-growing tumors derived from paraganglia in the head and neck area. Paraganglia are cell-clusters of neuroectodermal origin that have a close relationship with the autonomic nervous system and have the ability to synthesize catecholamines (*e.g*., dopamine). The most common PGL tumor locations are the carotid bodies and the adrenal medulla. Other paraganglia which may be affected are: the vagal bodies at the nodose ganglion of the vagal nerve, the tympanic bodies at the promontory of the middle ear, the jugular bodies at the jugular foramen, the laryngeal bodies in the larynx, and the aortic bodies in the wall of the ascending aorta and aortic arch.

3 Carotid Body Resection

The fact that patients with carotid body tumors at one time or another require the resection of their tumors gives us the opportunity to study the effect of removal of the CBs on the control of breathing. We followed a group of patients for up to three years after bilateral CB resection. Here we report on the effect of bCBR on the ventilatory response to carbon dioxide in a single patient (patient B, 35 years at his first operation, otherwise in excellent health). Ventilatory responses were obtained prior to his first and second CBR (one carotid body was resected at a time) and at regular intervals for up to 3 years following the last operation. Ventilatory responses were obtained using the ‘dynamic end-tidal forcing’ technique (Dahan,

DeGoede, Berkenbosch and Olievier 1990). We applied a multi-frequency binary sequence (MFBS) in end-tidal PCO_2 (Pedersen, Fatemian and Robbins 1999). A two-compartment model of the ventilatory control system was used to separate the ventilatory response into a fast (peripheral) and a slow (central) component (Dahan et al. 1990).

3.1 Effect of bCBR on Central CO_2 Sensitivity

Patient B had a normal ventilatory response to CO_2 prior to surgery (an indication that the mechanism of CO_2-sensing and communication of carotid body type I cells with the sinus nerve was not affected). His pre-operative values averaged to: central CO_2 sensitivity (Gc) = 9.5 L·min^{-1}·kPa^{-1}, peripheral CO_2 sensitivity (Gp) = 4.2 L·min^{-1}·kPa^{-1}· Removal of the first carotid body resulted in an appreciable reduction of both Gp (2.2 L·min^{-1}·kPa^{-1}) and Gc (5.8 L·min^{-1}·kPa^{-1}). After the final CBR, a

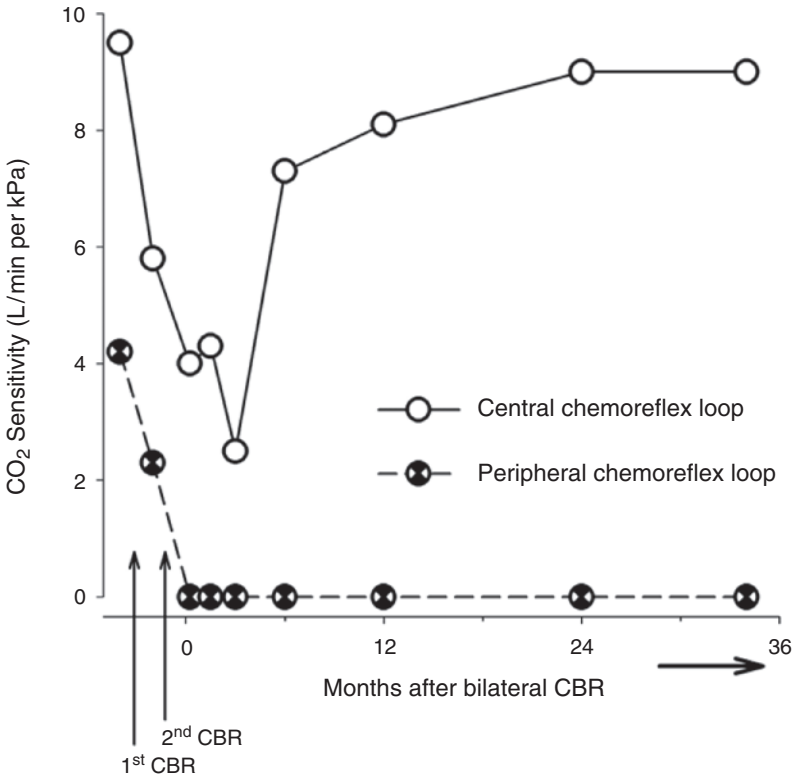

Fig. 1 Influence of bilateral carotid body resection on the outputs of the central and peripheral chemoreflex loops in a single patient. On the *y*-axis the ventilatory CO_2-sensitivity derived from MFBS experiments is shown. CBR is carotid body resection

contribution of the peripheral chemoreceptors was not detectable (*i.e.*, Gp = 0). Gc reduced further to a nadir at 3 months postoperatively (2.4 $L.min^{-1}.kPa^{-1}$; see also Fig. 1). Subsequently, Gc showed a slow increase to preoperative values, which were reached after about 18 to 24 months postoperatively.

4 Discussion

Our findings in this single patient are in full agreement with the data of the other bCBR patients that were studied by us. There are three main findings:

The removal of the carotid bodies results in a sharp decline in central CO_2-sensitivity.

There is a significant and possibly even total recovery of the central CO_2-chemoreflex drive over time (< 3 years).

Absence of any recovery of peripheral CO_2 chemoreflex drive (similar observations were made for the peripheral O_2 chemoreflex drive, data not given).

The observation that central CO_2-sensitivity is reduced after bCBR is not new and can already be found in data from Jay Bellville (Bellville, Whipp, Kaufman, Swanson, Aqleh and Wiberg 1979). He and his group observed a 50% smaller Gc in carotid body resected subjects (their value of Gp was not significantly different from zero; hypoxia did not affect the value of Gp) compared to healthy controls (Bellville *et al*. 1979). Note, however, that Bellville studied asthmatic patients that were resected to get some relief from severe dyspnea. Our patients are without pulmonary and cardiovascular disease. Our data, together with those of Bellville *et al*. (1979) suggest the existence of central-peripheral interaction. However, against a possible interaction is the fact that during hypoxia Gc remains unaffected despite a large increase in Gp (Bellville *et al*. 1979; Dahan *et al*. 1990). Furthermore, reduction of Gp by pharmacological means (such as occurs during inhalation of 100% oxygen, inhalation of low dose halothane or infusion of dopamine) has similarly no effect on Gc (Ward and Bellville 1983; Dahan *et al*. 1990; Dahan, van den Elsen, Berkenbosch, deGoede, Olievier, van Kleef and Bovill 1994). These latter data suggest the absence of central-peripheral interaction but indicate rather that the mere presence of the carotid bodies is required for a normal functioning of the central chemoreflex loop. It may well be that the carotid bodies exert a tonic drive (or tonic facilitation; see also Pan, Forster, Martino, Strecker, Beales, Serra, Lowry, Forster and Forster 1998) on the central chemoreflex loop which is lost upon their resection. This basal drive is more or less constant and is not affected by changes in the output of intact carotid bodies.

The observed return of the central CO_2-drive is a clear evidence for central plasticity within the ventilatory control system. In goats, Pan *et al*. (1998) observed a more rapid return of central CO_2-sensitivity (full return within 15 days) after carotid body denervation (see also Forster 2003). This suggests a difference in the mechanism of central plasticity among species. Taken into account the very fast changes seen in goats, a change or shift in neurotransmitter turnover seems the most

plausible cause for the return of central CO_2-sensitivity. In humans, the very slow return precludes a simple mechanism. Possible mechanism include upregulation of synaptic activity from growth (sprouting) or activation of silent synapses, synaptic remodeling, rerouting of afferent respiratory information, reorganization of respiratory centers, recruitment of different neuronal centers, changes in neuromodulators (see Fuller and Mitchell 2005).

The absence of recovery of the peripheral response to CO_2 and hypoxia upon the resection of both carotid bodies indicates absence of plasticity within the peripheral chemoreflex loop. This contrasts findings is some species (cats, rats) but is in agreement with others (dogs, ponies, goats) (Forster 2003). Apparently, in adult humans, the function of the peripheral chemoreceptors of the carotid bodies is not replaced by other sensors such as possibly present in the aortic bodies or the medulla.

In conclusion, we observed a temporary dysfunction of the central chemoreflex loop upon bilateral resection of the carotid bodies, a demonstration of neural plasticity within the human ventilatory control system.

References

Bellville, J.W., Whipp, B.J., Kaufman, R.D., Swanson, G.D., Kamel, K.A. and Wiberg, D.M. (1979). Central and peripheral chemoreflex loop gain in normal and carotid body-resected subjects. J. Appl. Physiol. 46, 843–853.

Dahan, A., DeGoede, J., Berkenbosch, A. and Olievier, I.C.W. (1990). The influence of the ventilatory response to carbon dioxide in man. J. Physiol. (Lond.) 428, 485–499.

Dahan, A., Taschner, P.E.M., Jansen, J.C., van der Mey, A.G.L., Teppema, L.J. and Cornelisse, C. (2004). Carotid body tumors in humans caused by a mutation in the gene for succinate dehydrogenase D (SDHD). Adv. Exp. Med. Biol. 551, 71–76.

Dahan, A., van den Elsen, M., Berkenbosch, A., DeGoede, J., Olievier, I., van Kleef, J. and Bovill, J. (1994). Effects of subanesthetic halothane on the ventilatory responses to hypercapnia and acute hypoxia in healthy volunteers. Anesthesiology 80, 727–738.

Forster, H.V. (2003). Plasticity in the control of breathing following sensory denervation. J. Appl. Physiol. 94, 784–794.

Fuller, D.D. and Mitchel, G.S. (2005). Respiratory neuroplasticity: respiratory gases, development, and spinal injury. In: D.S. Ward, A. Dahan and L.J. Teppema (Eds.). *Pharmacology and Pathophysiology of the Control of Breathing*. Taylor & Francis, New York, pp. 155–223.

Pan, L.G., Forster, H.V., Martino, P., Strecker, P.J., Beales, J., Serra, A., Lowry, T.F., Forster, M.M. and Forster, A.L. (1998). Important role of the carotid afferents in the control of breathing. J. Appl. Physiol. 85, 1299–1306.

Pedersen, M.E., Fatemian, M. and Robbins, P.A. (1999). Identification of fast and slow ventilatory responses to carbon dioxide under hypoxic and hyperoxic conditions in humans. J. Physiol. (Lond.) 521, 273–287.

Taschner, P.E.M., Jansen, J.C., Baysal, B.E., Bosch, A., Rosenberg, E.H., Bröcker-Vriends, A.H.J.T., van der Mey, A.G.L., van Ommen, G.J., Cornelisse, C.J. and Devilee, P. (2001). Nearly all hereditary paragangliomas in the Netherlands are caused by two founder mutations in the SDHD gene. Genes Chromosomes Cancer 31, 274–281.

Ward, D.S. and Bellville, J.W. (1983). Effect of intravenous dopamine on hypercapnic ventilatory response in humans. J. Appl. Physiol. 55, 1418–1425.

55
Glial Modulation of CO_2 Chemosensory Excitability in the Retrotrapezoid Nucleus of Rodents

Joseph S. Erlichman[1], Robert W. Putnam[2] and J.C. Leiter[3]

Abstract We investigated the possibility that astrocytes modify the extracellular milieu and thereby modify the activity of central CO_2 chemosensory neurons. The ability of astrocytes to modify the extracellular milieu is heterogeneously distributed among chemosensory sites that have, at least nominally, the same function. The differences in astrocytic activity may make some central chemosensory sites better attuned to the local brain tissue environment and other chemosensory sites better suited to integrate chemosensory activity from multiple sites within and outside the central nervous system.

1 Astrocytes and Neurons

It is becoming a truism that astrocytes modify neuronal function. However, actual demonstrations of this 'truism' in intact animals are a rarity (most of the evidence is from cultured cells or brain slices). Many astrocytic functions are relevant to central CO_2 chemosensitivity and may actually modify respiratory behavior in normal freely moving animals. We will focus only on astrocytic pH regulation in this report. Astrocytes express a variety of pH regulatory transport proteins and, to the extent that astrocytes regulate their own intracellular pH (pHi), they create reciprocal changes in pHe in the environment of neurons.

1.1 Central CO_2 Chemosensitivity

The activity of CO_2 chemosensory neurons is stimulated by reductions in pHi (Filosa *et al*. 2002; Wang *et al*. 2002). The most frequently described ionic mechanisms of CO_2 chemosensitivity involve pH-dependent inhibition of potassium

[1] St. Lawrence University, Department of Biology, jerlichman@stlawu.edu

[2] Wright State University Boonshoft School of Medicine, Department of Neuroscience, Cell Biology and Physiology, robert.putnam@wright.edu

[3] Dartmouth Medical School, Department of Physiology, james.c.leiter@dartmouth.edu

M.J. Poulin and R.J.A. Wilson (eds.), *Integration in Respiratory Control: From Genes to Systems*.

channels (Putnam *et al*. 2004); however, these ionic conductances are often modulated by pHe, rather than pHi. If potassium channels with either pHi or pHe sensitivity are present in central CO_2 chemosensory cells, and both types of potassium channels do seem to be present in chemosensory neurons (Putnam *et al*. 2004), the chemosensory neuron can respond to either pHe or pHi or both in combination (Chernov *et al*. 2007).

Neurons in chemosensory regions of the brainstem do not restore pHi effectively during acid stresses in which both pHe and pHi fall (Nishimura *et al*. 1989; Nottingham *et al*. 2001). This is good design for a pHi sensor: it is not logical to have a sensor that alters its stimulus (just as a thermostat with a heater within the thermostat would regulate room temperature poorly). However, this peculiarity of neuronal pH regulation means that chemosensory neurons are dependent on non-neuronal (astrocytic) regulation of pHe during hypercapnic acidosis, and astrocytic activity may actually exacerbate the acidosis.

We have been studying the interactions between astrocytes and neurons in the retrotrapezoid nucleus (RTN) and the nucleus of the solitary tract (NTS) in rats and mice to test the hypothesis that pHi regulation by astrocytes may modify pHe and amplify the chemosensory stimulus of CO_2-sensitive neurons in these regions.

1.2 Astrocytic pH Regulation

Astrocytes express robust pH regulatory processes, and any astrocytic process that regulates pHi will have a reciprocal effect on pHe. Astrocytes express a variety of ion transporters, including Na/H exchange (NHE), sodium-independent chloride-bicarbonate exchange (known as anion exchange; AE), sodium-driven chloride bicarbonate exchange (NDCBE) and electrogenic sodium bicarbonate cotransport (NBCe) (Deitmer and Rose 1996). NBCe activity is associated with astrocytes in the brain (Deitmer and Rose 1996), and the transporter is not active in medullary neurons as far as we have been able to determine. The NBCe in astrocytes transports 2 HCO_3^- and 1 Na^+. Therefore, the astrocytic membrane potential (Vm) affects the rate and direction of transport. Astrocytes are highly permeable to potassium. Increased neuronal activity may elevate extracellular K^+, depolarize astrocytes, enhance the inward movement of HCO_3^- and Na^+ and alkalinize the astrocytes while acidifying pHe. This is called depolarization-induced alkalosis (DIA), and it is one of the mechanisms whereby neuronal activity is coupled to astrocytic function.

2 Results

There is already evidence that astrocytic activity makes a significant contribution to neuronal chemosensory responses in intact animals. Fluorocitrate (FC) is a specific astrocytic toxin that depolarizes astrocytes, increases extracellular potassium

concentrations, and reduces pHe, probably as a result of DIA (Erlichman *et al*. 1998). Microperfusion of FC into the RTN stimulated ventilation in awake animals (Erlichman *et al*. 1998). pH measurements in the RTN confirmed that pHe was lower when FC was present, and the respiratory effects of FC were correlated with the fall in pHe in the region of microperfusion. FC is an ineffective respiratory stimulus when injected into the NTS (Erlichman, unpublished observations) even though injections of acidic stimuli into the same location stimulate ventilation. There are fewer astrocytes in the NTS and, therefore, there is little effect of the FC on pHe in the NTS and little respiratory response after FC treatment in the NTS.

2.1 Heterogeneous Patterns of pHi Regulation Among Astrocytes

In brain slices, NBC was active during normocapnia (pH 7.48, 5% CO_2) in the RTN, but much less active in the NTS (Erlichman *et al*. 2004). Elevating extracellular K^+ substantially depolarized and alkalinized astrocytes in the RTN but not in the NTS. On the other hand, NHE seemed to be more important in the NTS than in the RTN. The nuclei also differ anatomically: the NTS is a compact nucleus with few astrocytes, whereas the RTN is more loosely organized with many astrocytes intercalated between the neurons adjacent to the ventral surface of the medulla. Moreover, elevating the extracellular potassium reduced pHe in the RTN by 0.3 pH units, and this effect was blocked by DIDS, which inhibits NBC. Elevated extracellular potassium had no effect on pHe in the NTS. Therefore, NBCe does not seem to be present or active in astrocytes in the NTS, but it is active in astrocytes in the RTN. Thus, differences in the function of astrocytes in medullary chemosensory areas may affect how pH is regulated locally and may modify ventilatory responses to CO_2.

2.2 Heterogeneous Astrocytic Responses to Hypercapnia

Astrocytes have electrophysiological and pH responses to hypercapnia. For example, Fukuda *et al*. (1978) recorded Vm using sharp electrodes in ‘silent cells’ in brain slices from the ventral medulla (these were probably in the RTN). The electrophysiological properties of these cells indicated that they were astrocytes, and about half of them were depolarized when pHe was reduced (Fukuda and Honda 1976; Fukuda *et al*. 1978). Hypercapnia and the fall in pHe may inhibit potassium channels and depolarize astrocytes. However, we recently studied neurons and astrocytes in the RTN using electrophysiological methods, and the astrocytes that we studied were not depolarized by hypercapnia (Ritucci *et al*. 2005). The brain slices we studied were from younger animals, and the astrocytes demonstrated negligible alkalinization when forcibly depolarized

(no real DIA, unlike astrocytes from older animals). There is an interesting developmental issue lurking here. Astrocytes begin to proliferate about P11 and do not reach maturity for many weeks. In older animals, hypercapnia does depolarize astrocytes (Fukuda and Honda, 1976; Fukuda *et al*. 1978). Therefore, we believe that NBC expression is actually changing as the astrocytes mature, which has interesting implications for the maturation of ventilatory responses to CO_2 (Putnam *et al*. 2005).

We re-examined the effect of hypercapnia on the membrane potential of astrocytes in the RTN. We first identified astrocytes by exposing cells to increased extracellular potassium and demonstrating that DIA was present (pHi rose), and this DIA was inhibited by DIDS. Approximately half of theses astrocytes regulated pHi when they were subsequently exposed to hypercapnia (10% CO_2, pH ~ 7.1). In these cells pHi increased toward the normocapnic control value over the duration of the hypercapnic exposure. In the other astrocytes, pHi fell and remained low for the duration of the hypercapnia. We also used a voltage-sensitive dye (DI-8-ANEPPS) to study changes in membrane potential in astrocytes. Some of the astrocytes were unaffected by hypercapnia; membrane potential changed by 0.2 ± 0.4 mV (n = 20). Other astrocytes were depolarized by 10.7 ± 0.3 mV (n = 23). Thus, there is a significant bimodal distribution ($p < 0.001$) of astrocytes in response to hypercapnia; some cells are depolarized and some cells regulate pHi. We do not yet know whether the astrocytes that are depolarized by CO_2 also regulate pHi, but it is our hypothesis that hypercapnia-mediated depolarization induces DIA, which restores pHi toward normocapnic values and reduces pHe. Any astrocytically-mediated reduction in pHe will enhance the CO_2-related respiratory stimulus for chemosensory neurons.

The difference between the RTN and NTS are even more interesting when one examines the immunohistochemical distribution of NBC. In the RTN, one sees many astrocytes in which NBC is expressed (GFAP+/NBC+). In the NTS, there are fewer astrocytes, and they do not express NBC (GFAP+ cells that are NBC−). The differences in the astrocytic distribution of NBC is exactly what one would predict based on the functional studies described above: subsets of astrocytes in the RTN demonstrate DIA, regulate pHi and are depolarized by hypercapnia, whereas astrocytes in the NTS express little DIA and do not seem to regulate pHi nor depolarize during hypercapnia.

3 Discussion

Astrocytic pHi regulation may amplify the chemosensory stimulus by modifying pHe. This hypothesis adds a new dimension to CO_2 chemosensory function. The foregoing studies are consistent with the hypothesis that heterogeneous astrocytic pH regulatory processes may alter neural processing of chemosensory information in different chemosensory areas even in intact animals; astrocytic function, by altering pHe, really matters at the level of whole animal behavior.

Interestingly, all of these local factors (K+, H+, etc.) are modified by astrocytes in the RTN. Thus, astrocytes in the RTN may play an important role in sensing local levels of circuit activation and seem to have the capacity to modulate local circuits and respond to regional/local metabolic changes. The NTS, on the other hand, deals more with integrating peripheral and central inputs, but is unconcerned with the local brain tissue environment. Thus, these chemoreceptive areas may differ not only in their state dependency but also in the extent to which they serve as local brain tissue chemosensors. Finally, the heterogeneity of acid-base regulation among astrocytes may make the RTN a more sensitive chemosensory site not because the neurons differ (which they may as well), but because the astrocytes in the two regions create different pHe stimuli even when the level of hypercapnia is identical.

Acknowledgement Funded by NIH HL71001.

References

Chernov, M.M., Daubenspeck, J.A., Denton, J.S., Pfeiffer, J.R., Putnam, R.W. and Leiter, J.C. (2007) A computational analysis of central CO_2 chemosensitivity in Helix aspersa. Am. J. Physiol. 292, C278–291.

Deitmer, J.W. and Rose, C.R. (1996) pH regulation and proton signaling by glial cells. Prog. Neurobiol. 48, 73–103.

Erlichman, J.S., Li, A. and Nattie, E.E. (1998) Ventilatory effects of glial dysfunction in a rat brain stem chemoreceptor region. J. Appl. Physiol. 85, 1599–1604.

Erlichman, J.S., Cook, A., Schwab, M.C., Budd, T.W. and Leiter, J.C. (2004) Heterogeneous patterns of pH regulation in glial cells in the dorsal and ventral medulla. Am. J. Physiol. 286, R289–R302.

Filosa, J.A., Dean, J.B. and Putnam, R.W. (2002) Role of intracellular and extracellular pH in the chemosensitive response of rat locus coeruleus neurones. J. Physiol. (Lond) 541.2, 493–509.

Fukuda, Y. and Honda, Y. (1976) pH sensitivity of cells located at the ventrolaeral surface of the cat medulla oblongata *in vitro*. Pflügers Arch. - Eur. J. Physiol. 364, 243–247.

Fukuda, Y., Honda, Y., Schläfke, M.E. and Loeschke, H.H. (1978) Effect of H^+ on the membrane potential of silent cells in the ventral and dorsal surface layers of the rat medulla *in vitro*. Pflugers Arch. 376, 229–235.

Nishimura, M., Johnson, D.C., Hitzig, B.M., Okunieff, P. and Kazemi, H. (1989) Effects of hypercapnia on brain pHi and phosphate metabolite degradation by ^{31}PNMR. J. Appl. Physiol. 66, 2181–2188.

Nottingham, S., Leiter, J.C., Wages, P., Buhay, S. and Erlichman, J.S. (2001) Developmental changes in intracellular pH regulation in medullary neurons of the rat. Am. J. Physiol. 281, R1940–R1951.

Putnam, R.W., Filosa, J.A. and Ritucci, N.A. (2004) Cellular mechanisms involved in CO_2 and acid sensing in chemosensitive neurons. Am. J. Physiol. 287, C1493–C1526.

Putnam, R.W., Conrad, S.C., Gdovin, M.J., Erlichman, J.S. and Leiter, J.C. (2005) Neonatal maturation of the hypercapnic ventilatory response and central neural CO_2 chemosensitivity. Respir. Physiol. Neurobiol. 149, 165–179.

Ritucci, N.A., Erlichman, J.S., Leiter, J.C. and Putnam, R.W. (2005) Response of membrane potential (Vm) and intracellular pH (pHi) to hypercapnia in neurons and astrocytes from rat retrotrapezoid nucleus (RTN). Am. J. Physiol. 289, R851–R861.

Wang, W., Bradley, S.R. and Richerson, G.B. (2002) Quantification of the response of rat medullary raphe neurones to independent changes in pH_o and P_{CO2}. J. Physiol. (Lond) 540.3, 951–970.

56
The Carotid Chemoreceptors are a Major Determinant of Ventilatory CO_2 Sensitivity and of $PaCO_2$ During Eupneic Breathing

Hubert V. Forster[1,3], Paul Martino[1], Matt Hodges[1], Katie Krause[1], Josh Bonis[1], Suzanne Davis[1] and L. Pan[2]

Abstract Both carotid and intracranial chemoreceptors are critical to a normal ventilatory CO_2-H^+ chemosensitivity. At low levels of hypercapnia, the carotid contribution is probably greater than the central contribution but, at high levels, the intracranial chemoreceptors are dominant. The carotid chemoreceptors are also critical to maintaining a stable and normal eupneic $PaCO_2$, but lesion-induced attenuation of intracranial CO_2-H^+ chemosensitivity does not consistently alter eupneic $PaCO_2$. A major unanswered question is why do intracranial chemoreceptors in carotid body denervation (CBD) animals tolerate an acidosis during eupnea which prior to CBD elicits a marked increase in breathing.

For years, views on ventilatory CO_2-H+ chemosensitivity were based primarily on elegant studies in awake goats (Fencl, Miller and Pappenheimer 1966). Under conditions of acute and chronic metabolic and respiratory acidosis and alkalosis, alveolar ventilation was a single function of cerebral interstitial fluid (ISF) [H+]. These data indicated that intracranial chemoreceptors were solely responsible for CO_2-H+ ventilatory responsiveness. Contributing to this view were studies showing only small changes in carotid sinus nerve activity of anesthetized mammals when arterial PCO_2 was altered, suggesting that carotid chemoreceptors contributed minimally to CO_2-H+ ventilatory responsiveness (Lahiri and DeLaney 1975).

However, views on CO_2-H^+ chemosensitivity have changed as a result of recent studies, which utilized different techniques such as transient CO_2 administration (Edelman, Epstein, Lahiri and Cherniack 1973), carotid body denervation (CBD) (Belleville, Whipp, Kaufman, Swanson, Aqleh and Wiberg 1979; Bisgard, Forster, Orr, Buss, Rawlings and Rasmussen 1976; Hodges, Opansky, Qian, Davis, Bonis, Krause, Pan and Forster 2005; Pan, Forster, Martino, Strecker, Beales, Serra, Lowry, Forster and Forster 1998; Rodman, Curran, Henderson, Dempsey and Smith 2001), mathematical modeling (Belleville, *et al*. 1979), and isolated perfusion of carotid and intracranial chemoreceptors (Heeringa, Berkenbosch, de Goede and Olievier 1979;

[1] Medical College of Wisconsin, Physiology, bforster@mcw.edu

[2] Marquette University, Program in Physical Therapy, lawrence.pan@mu.edu

[3] Zablocki VA Affairs Center, bforster@mcw.edu

M.J. Poulin and R.J.A. Wilson (eds.), *Integration in Respiratory Control: From Genes to Systems*. © Springer 2008

Table 1 Intracranial and carotid chemoreceptors contribute to CO_2-H^+ sensitivity

Investigator	Central (%)	Peripheral (%)	Species	Technique
Edelman, *et al*. 1973	66	33	Awake human	Single breath
Heeringa, *et al*. 1979	66	33	Anesthetized cats	Isolated perfusion
Bellville, *et al*. 1979	66	34	Awake human	2 compartment model
Bellville, *et al*. 1979	35	—	CBD human	2 compartment model
Pan, *et al*. 1998	40	60	Awake goat	CBD
Rodman, *et al*. 2001	66	33	Awake dog	CBD
Smith, *et al*. 2006	63	37	Awake dog	Isolated perfusion

Smith, Rodman, Chenuel, Henderson and Dempsey 2006). The consistent finding has been that intracranial chemoreceptors contribute about two-thirds of the CO_2-H^+ ventilatory response while the carotid chemoreceptors contribute one third of the response (Table 1). However, as detailed later, it is likely that near the eupneic $PaCO_2$, the carotid contribution exceeds the intracranial contribution.

The carotid contribution seems large in spite of the small increase in sinus nerve activity during hypercapnia. This apparent discrepancy might be a result of carotid afferents having an effect beyond signaling the hypercapnia to medullary rhythm (RGN) and pattern (PGN) generating neurons. Indeed, studies on anesthetized rats indicate that carotid afferents modulate the activity of chemoreceptor neurons in the retrotrapezoid nucleus (Takakura, Moreira, Colombari, West, Stornetta and Guyenet 2006). Absence of this modulation might explain why in awake goats CBD accentuates the hypopnea induced by cooling the rostral ventrolateral medulla (Pan, Forster, Ohtake, Lowry, Korducki and Forster 1995). Also, carotid modulation of intracranial chemoreceptors may explain why CBD atttenuates the hyperpnea induced by focal acidosis in raphe nuclei (Hodges *et al*. 2005). Accordingly, it appears that carotid afferents affect the activity of intracranial chemoreceptor neurons and/or the response of the RGN and PGN to intracranial chemoreceptor activity.

The carotid CO_2-H^+ chemoreceptors are also determinants of eupneic breathing in the awake state. This conclusion is based on findings that hypocapnia specific to the carotid body reduced breathing (Daristotle, Berssenbrugge, Engwall and Bisgard 1990). Also, studies have found that CBD decreased eupneic breathing resulting in an increased $PaCO_2$ which, in awake dogs, goats and ponies reached 13.0, 13.3 and 18.1 mmHg above control respectively (Bisgard *et al*. 1976; Hodges *et al*. 2005; Pan *et al*. 1998; Rodman *et al*. 2001). This hypercapnia results in at least a 0.03 acidosis in cerebral ISF, which should increase activity of intracranial chemoreceptors (Bisgard *et al*. 1976). Accordingly, these data provide further evidence that absence of carotid chemoreceptor activity reduces sensitivity of intracranial chemoreceptors.

CBD also increases the minute-to-minute variation in eupneic $PaCO_2$ (Klein, Forster, Bisgard, Kaminski, Pan and Hamilton 1982). The increased variation likely

results from the slower response to changes in $PaCO_2$ of intracranial compared to carotid chemoreceptors; thus, after CBD, there is a relative delay in correction of $PaCO_2$ fluctuations resulting in more variability (Smith *et al*. 2006). Accordingly, it has been concluded "that the slower response of the central vs. the carotid chemoreceptors prevents the central chemoreceptors from contributing significantly to ventilatory responses to rapid, transient changes in arterial PCO_2" (Smith *et al*. 2006).

The contribution of the intracranial chemoreceptors to eupneic breathing in the awake state is unclear. Studies have found attenuated CO_2 sensitivity and decreased eupneic breathing after perturbations in the medulla (Forster, Ohtake, Pan, Lowry, Korducki, Aaron and Forster 1995; Gray, Janczewski, Mellen, McCrimmon and Feldman 2001). However, it is likely that these perturbations also affected RGN and PGN neurons; thus, these studies do not provide a clear indication of the contribution of intracranial chemoreceptors to eupneic breathing.

Many studies have found that lesions within known intracranial chemoreceptor areas result in a dissociation between effects on eupneic breathing and CO_2-H^+ ventilatory chemosensitivity. For example, in rats during wakefulness and NREM sleep, neurotoxic destruction of 58% to 79% of NK1R expressing neurons in the ventral medulla reduced CO_2 sensitivity by about 60%, but reduced eupneic breathing only 10% (Nattie and Li, in press). Similarly, in awake goats, lesions in the raphe, RTN, or cerebellar fastigial nucleus (CFN) reduced CO_2 sensitivity by 20% to 50% with no or minimal hypercapnia during eupnea (Forster, Pan, Lowry, Feroah, Gershan, Whaley, Forster and Sprtel 1998; Hodges, Opansky, Qian, Davis, Bonis, Bastasic, Leekley, Pan and Forster 2004; Martino, Davis, Opansky, Krause, Bonis, Pan, Qian and Forster, submitted). This dissociation differs markedly from the effects of CBD, after which there is always a close correspondence between changes in eupneic $PaCO_2$ and CO_2 sensitivity (Pan *et al*. 1998).

Data from lesioning the CFN suggest one contributing factor to the dissociation between eupneic $PaCO_2$ and CO_2-H^+ sensitivity (Martino *et al*., submitted). Specifically, after CFN lesioning, CO_2 sensitivity (pulmonary ventilation, $\dot{V}_1$ /$PaCO_2$) was reduced by a maximum of 43%, and the coefficient of variation (CV), assessed eight to ten times before and after lesioning, increased from 15% to 30%. In contrast, CFN lesioning only increased eupneic $PaCO_2$ by 0.3 ± 0.3 mmHg and the respective CVs were 4.0 ± 0.6 and 3.7 ± 0.4%. When $\dot{V}_1$ at elevated inspired CO_2 was expressed as a percent of the room air $\dot{V}_I$, the absolute values (Fig. 1A) and the CV at 3% and 5% inspired CO_2 did not differ between pre and post CFN lesion studies. However, the values at 7% inspired CO_2 were reduced ($p < 0.05$) by 14% and the CV was increased from 17 to 24% ($p < 0.05$). In contrast, in awake goats after CBD, all values were reduced ($p < 0.05$) after the first minute at 3% inspired CO_2 (Fig. 1B) (Hodges *et al*. 2005). It appears then that the CFN lesions did not affect the carotid contribution to CO_2 sensitivity. This unaltered carotid contribution could then at least partially explain the dissociation of CO_2 sensitivity and eupneic breathing following CFN lesioning. In essence, the tonic carotid input and the rapid response of carotid chemoreceptors to changes in $PaCO_2$ normally maintains a near normal and stable $PaCO_2$ in spite of changes in intracranial CO_2-H^+ chemosensitivity.

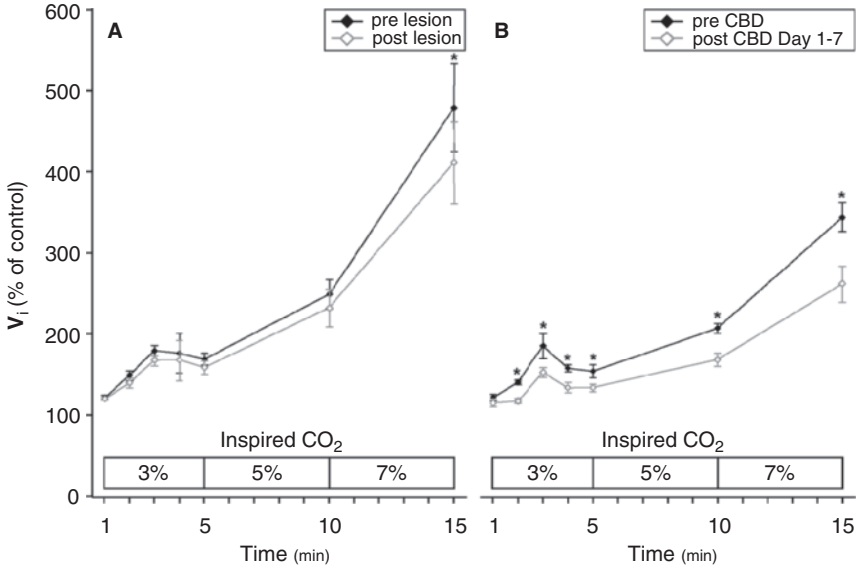

Fig. 1 Lesions within the CFN (n = 9) do not reduce CO_2 sensitivity until inspired CO_2 exceeds 5%, but CBD (n = 8) reduces sensitivity even at 3% inspired CO_2. Asterisks denote significant ($p < 0.05$) differences between pre and post CFN lesioning (A) and CBD (B)

Acknowledgements These studies supported by NHLBI Grant HL-25739 and the Veterans Administration.

References

Belleville, J.W., Whipp, B.J., Kaufman, R.D., Swanson, G.D., Aqleh, K.A. and Wiberg, D.M. (1979) Central and peripheral chemoreflex loop gain in normal and carotid body-resected subjects. J. Appl. Physiol.: Respirat. Environ. Exercise Physiol. 46, 843–853.

Bisgard,G.E., Forster, H.V., Orr, J.A., Buss, D.D., Rawlings, C.A. and Rasmussen, B. (1976) Hypoventilation in ponies after carotid body denervation. J. Appl. Physiol. 40, 184–190.

Daristotle, L., Berssenbrugge, A.D., Engwall, M.J. and Bisgard, G.E. (1990) The effects of carotid body hypocapnia on ventilation in goats. Respir. Physiol. 79, 123–136.

Edelman, N.H., Epstein, P.E., Lahiri, S. and Cherniack, N.S. (1973) Ventilatory responses to transient hypoxia and hypercapnia in man. Respir. Physiol. 17, 302–314.

Fencl, V., Miller, T.B. and Pappenheimer, J.R. (1966) Studies on the respiratory response to disturbances of acid-base balance, with deductions concerning the ionic composition of cerebral interstitial fluid. Am. J. Physiol. 210, 459–472.

Forster, H.V., Pan, L.G., Lowry, T.F., Feroah, T., Gershan, W.M., Whaley, A.A. Forster, M.M. and Sprtel, B. (1998) Breathing of awake goats during prolonged dysfunction of caudal M ventrolateral medullary neurons. J. Appl. Physiol. 84, 129–140.

Forster, H.V., Ohtake, P.J., Pan, L.G., Lowry, T.F., Korducki, M.J., Aaron, E.A. and Forster, A.L. (1995) Effects on breathing of ventrolateral medullary cooling in awake goats. J. Appl. Physiol. 78, 258–265.

Gray, P.A., Janczewski, W.A., Mellen, N., McCrimmon, D.R. and Feldman, J.L. (2001) Normal breathing requires pre-Bötzinger Complex neurokinin-1 receptor-expressing neurons. Nature Neurosci. 4, 927–930.

Heeringa, J., Berkenbosch, A., de Goede, J. C.M. Olievier, C.M. (1979) Relative contribution of central and peripheral chemoreceptors to the ventilatory response to CO_2 during hyperoxia. Respir. Physiol. 37, 365–379.

Hodges, M.R., Opansky, C., Qian, B., Davis, S., Bonis, J., Bastasic, J., Leekley, T., Pan, L.G. and Forster, H.V. (2004) Transient attenuation of CO_2 sensitivity after neurotoxic lesions in the medullary raphe area of awake goats. J. Appl. Physiol. 97, 2236–2247.

Hodges, M.R., Opansky, C., Qian, B., Davis, S., Bonis, J.M., Krause, K., Pan, L.G. and Forster, H.V. (2005) Carotid body denervation alters ventilatory responses to ibotenic acid injections or focal acidosis in the medullary raphe. J. Appl. Physiol. 98, 1234–1242.

Klein, J.P., Forster, H.V., Bisgard, G.E., Kaminski, R.P., Pan, L.G. and Hamilton, L.H. (1982) Ventilatory response to inspired CO_2 in normal and carotid body-denervated ponies. J. Appl. Physiol. 52, 1614–1622.

Lahiri, S. and DeLaney, R.G. (1975) Relationship between carotid chemoreceptor activity and ventilation in the cat. Respir. Physiol. 24, 267–286.

Martino, P.F., Davis, S., Opansky, C., Krause, K., Bonis, J., Pan, L.G., Qian, B., Forster, H.V. The cerebellar fastigial nucleus contributes to CO2-H+ ventilatory sensitivity in awake goats. J. Appl. Physiol., Resp. Physiol. and Neurobiol. in press.

Nattie, E. and Li, A. (2006) Neurokinin-1 receptor expressing neurons in the ventral medulla are essential for normal central and peripheral chemoreception in the conscious rat. J. Appl. Physiol. 101: 1596–1606.

Pan, L.G., Forster, H.V., Martino, P., Strecker, P.J., Beales, J., Serra, A., Lowry, T.F., Forster, M.M. and Forster, A.L. (1998) Important role of carotid afferents in control of breathing. J. Appl. Physiol. 85, 1299–1306.

Pan, L.G., Forster, H.V., Ohtake, P.J., Lowry, T.F., Korducki, M.J. and Forster, A.L. (1995) Effect of carotid chemoreceptor denervation on breathing during ventrolateral medullary cooling in goats. J. Appl. Physiol. 79, 1120–1128.

Rodman, J.R., Curran, A.K., Henderson, K.S., Dempsey, J.A. and Smith, C.A. Carotid body denervation in dogs: eupnea and the ventilatory response to hyperoxic hypercapnia. J. Appl. Physiol. 91, 328–335, 2001.

Smith, C.A., Rodman, J.R., Chenuel, B.J.A., Henderson, K.S. and Dempsey, J.A. (2006) Response time and sensitivity of the ventilatory response to CO_2 in unanesthetized intact dogs: central vs. peripheral chemoreceptors. J. Appl. Physiol. 100, 13–19.

Takakura, A.C.T., Moreira, T.S., Colombari, E., West, G.H., Stornetta, R.L. and Guyenet, P.G. (2006) Peripheral chemoreceptor inputs to retrotrapezoid nucleus (RTN) CO_2-sensitive neurons in rats. J. Physiol. 572, 503–523.

57
The Retrotrapezoid Nucleus and Central Chemoreception

Patrice G. Guyenet[1], Douglas A. Bayliss[2], Daniel K. Mulkey[3], Ruth L. Stornetta[4], Thiago S. Moreira[5] and Ana T. Takakura[6]

Abstract Central respiratory chemoreception (CRC) is the mechanism by which brain pCO_2 regulates breathing. The molecular and cellular basis of CRC is still poorly understood. In this review, we describe the properties of a cluster of pH-responsive neurons located in the retrotrapezoid region of the medulla oblongata and analyze whether these cells qualify as central respiratory chemoreceptors.

1 The Retrotrapezoid Nucleus (RTN)

The RTN was originally defined by Smith *et al*. (1989) as a cluster of cells that innervate more caudal regions of the ventral respiratory column. RTN resides under area M, a highly chemosensitive region of the ventral medullary surface (Loeschcke 1982). Acidification of RTN *in vivo* stimulates breathing, whereas inhibition reduces breathing and central chemoreflexes (Feldman, Mitchell and Nattie 2003; Li and Nattie 2002; Nattie 2001). RTN is also part of a broad superficial medullary region known to express the early gene c-Fos after exposure to hypercapnia (Okada, Chen, Jiang, Kuwana and Eldridge 2002).

2 Properties of RTN Neurons *in vivo*

2.1 Sensitivity to Hypercapnia and Evidence for Intrinsic Sensitivity to CO_2 in vivo

Under anesthesia, RTN neurons are silent at low levels of end-expiratory pCO_2 (arterial pH of 7.5). Their firing rate reaches about 8–12 Hz at 10% end-expiratory pCO_2 (Guyenet, Mulkey, Stornetta and Bayliss 2005; Mulkey, Stornetta, Weston, Simmons, Parker, Bayliss and Guyenet 2004; Takakura, Moreira, Colombari,

[1-6]University of Virginia, Department of Pharmacology, pgg@virginia.edu

M.J. Poulin and R.J.A. Wilson (eds.), *Integration in Respiratory Control: From Genes to Systems*. © Springer 2008

West, Stornetta and Guyenet 2006). Their discharge rate is tonic at low levels of pCO_2 and increasingly respiratory modulated as pCO_2 is raised (Guyenet *et al*. 2005). In vagotomized rats, RTN neurons typically do not display an ON-OFF discharge pattern like classic CPG neurons even at the highest levels of pCO_2 (Guyenet *et al*. 2005). Evidence that the sensitivity of RTN neurons to CO_2 *in vivo* could be intrinsic relies on the observation that ionotropic glutamatergic receptor blockade silences the central respiratory pattern generator (CPG) and blocks synaptic inputs to RTN neurons but does not change their response to hypercapnia (Guyenet *et al*. 2005; Mulkey *et al*. 2004). Additionally, the sensitivity of RTN neurons to hypercapnia is largely unaffected by morphine (Mulkey *et al*. 2004).

2.2 Synaptic Inputs of RTN Neurons

RTN neurons are not just pH/pCO_2 detectors. In vagotomized rats, there is clear evidence that these cells also receive CPG-related inputs. These inputs seem predominantly inhibitory and are most likely responsible for the saturation of the discharge of RTN neurons that is observed at high levels of CO_2 (Guyenet *et al*. 2005). The central respiratory pattern of RTN neurons appears due to inputs from early-I, post-I and E-2 neurons. These inputs recombine in various proportions depending on the particular RTN neuron causing a variety of respiratory patterns (Guyenet *et al*. 2005). RTN neurons are strongly activated by carotid chemoreceptor stimulation via a pathway that may consist of only two neurons (Fig. 1A) (Takakura *et al*. 2006). In other words, the activity of RTN neurons is driven by both CNS extracellular fluid H^+ and by the composition of arterial blood gases as detected by peripheral chemoreceptors. As such, RTN

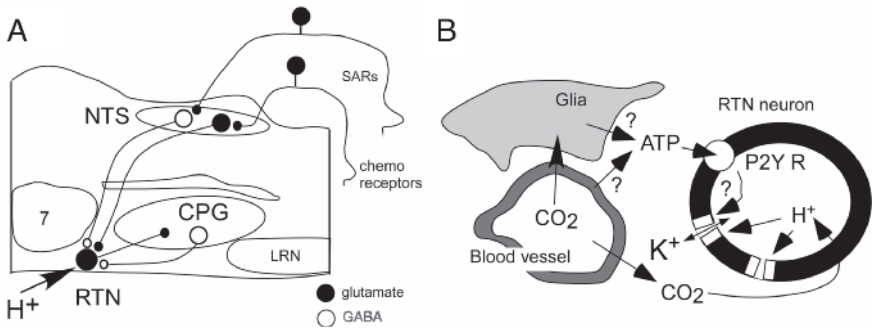

Fig. 1 (A) The RTN and its main putative connections (CPG, central respiratory pattern generator; SARs, slowly-adapting lung receptors). (B) Chemosensitivity of RTN neurons. A direct modulation by pH of a potassium channel is suspected. The contribution of ATP is not observed *in vitro*. The source of ATP (glia or blood vessels) is unidentified

neurons have the properties of a chemosensory integrating center. RTN neurons are also variously inhibited by lung inflation suggesting that they receive polysynaptic inhibitory inputs from slowly-adapting lung receptors (SARs) responsible for the Hering-Breuer reflex (Takakura, Moreira and Guyenet, unpublished results) (Fig. 1A).

The existence of additional inputs to RTN neurons is suggested by the presence of a neurochemically-diverse neuropil in the vicinity of their basal dendrites (PNMT, serotonin, substance P, vesicular glutamate-3 / VGLUT3, etc.) (Rosin, Chang and Guyenet 2006). This preliminary anatomical evidence suggests that RTN neurons could be up-regulated by serotonergic inputs from the raphe and by stress-related systems such as the C1 neurons of the ventrolateral medulla.

2.3 Transmitters, Structure and Anatomical Projections of RTN Neurons

RTN neurons are non-serotonergic and express VGLUT2 suggesting that they release glutamate and are probably excitatory (Mulkey *et al*. 2004). This fact is consistent with prior evidence that the RTN region is a source of excitatory drive to the CPG (Nattie 2006; Takakura *et al*. 2006).

RTN neurons have extensive dendrites within 50 μm of the ventral surface (the marginal layer) (Guyenet *et al*. 2005; Mulkey *et al*. 2004), which should make these cells unusually responsive to drugs or pH changes applied at the ventral medullary surface. Since RTN lies approximately under area M, RTN cells are presumably among the VMS chemoreceptors whose existence was postulated by earlier investigators (Loeschcke 1982; Millhorn and Eldridge 1986).

RTN neurons do not project to the spinal cord but, as a group, they innervate the entire ventrolateral medulla, the dorsolateral pontine regions traditionally associated with cardiorespiratory integration and selected regions of the solitary tract nucleus (Cream, Li and Nattie 2002; Mulkey *et al*. 2004; Rosin *et al*. 2006). The precise targets of RTN neurons within these regions are still unidentified.

RTN neurons express Phox2b, a homeobox transcription factor whose mutation causes most cases of congenital central hypoventilation syndrome (CCHS) (Amiel, Laudier, Attie-Bitach, Trang, de, Gener, Trochet, Etchevers, Ray, Simonneau, Vekemans, Munnich, Gaultier and Lyonnet 2003; Stornetta, Moreira, Takakura, Kang, Chang, West, Brunet, Mulkey, Bayliss and Guyenet 2006). CCHS is a condition in which breathing automaticity is severely depressed due to a profound loss of peripheral and central chemosensory integration (Gaultier, Amiel, Dauger, Trang, Lyonnet, Gallego and Simonneau 2004; Spengler, Gozal and Shea 2001). The presence of Phox2b in RTN neurons suggests that a developmental defect of these neurons could contribute to the reduced central chemoreception in CCHS.

3 Properties of RTN Neurons *in vitro* and Mechanisms of pH Sensitivity

In coronal brain slices (age P7–P12), 40% of RTN neurons are activated by acidification, the rest being insensitive to pH (Mulkey *et al*. 2004). The firing threshold of the chemosensitive neurons *in vitro* is close to pH 7.5 regardless of bath temperature (Guyenet *et al*. 2005) and the cells respond to increases in pCO_2 via changes in extracellular fluid pH (Mulkey *et al*. 2004). The dynamic range of their response to pH is temperature-sensitive (Q_{10} ~ 2.5) reaching a mean of 2.2 Hz per 0.1 pH unit at 37 °C (Guyenet *et al*. 2005). In slices, RTN neurons discharge tonically regardless of the temperature (Guyenet *et al*. 2005). Their pH sensitivity is unaffected by ATP receptor antagonists (P2X and P2Y) or by blockers of glutamate ionotropic receptors, but the cells are excited by the P2Y agonist UTP and respond to application of P2X receptor agonists by an inhibition that is dependent on the release of GABA or glycine (Mulkey, Mistry, Guyenet and Bayliss 2006; Mulkey *et al*. 2004). Under voltage clamp (−60 mV) in the presence of TTX, alkalization causes an outward current and a decrease in input resistance. The pH-induced current has the appearance of a leak potassium current (Mulkey *et al*. 2004), but the responsible potassium channel has not been identified.

In short, the relationship between neuronal discharge rate and extracellular pH in coronal slices is comparable to that observed for RTN neurons recorded in anesthetized rats under conditions of reduced synaptic activity. The pH threshold is very similar in both conditions (~ 7.5) but the dynamic range of the response is somewhat smaller *in vitro* even when the effect of temperature is factored in (average of 2.2 vs. 3.9 Hz per 0.1 pH unit) (Guyenet *et al*. 2005). Further similarities between the cells identified *in vivo* and *in vitro* include the fact that the neurons do not burst in either preparation and are not serotonergic.

4 Conclusions

RTN neurons have the characteristics that one would expect from central chemoreceptors, namely location at the ventral medullary surface (Loeschcke 1982), sensitivity to pH that appears independent of conventional synaptic activity, an excitatory transmitter (glutamate), a pCO_2 threshold below that at which the CPG is activated and projections to the ventral respiratory column, to the NTS and to other essential cardiorespiratory regions of the pons. Finally, these cells express a genetic marker (Phox2b) which, when mutated (CCHS), causes a dramatic and selective loss of central chemosensitivity in man.

The molecular mechanism responsible for the pH sensitivity of RTN neurons is still unknown and does not have to be unique to these neurons. What makes central chemoreceptors unique could simply be the dynamic range of their integrated neuronal response to mild acidification, the effectiveness of the transmitters that

they release and the anatomical selectivity of their connections. RTN neurons appear to fit this concept.

Purinergic transmission is not essential to the pH sensitivity of RTN neurons *in vitro* but these cells are excited by P2Y agonists (Mulkey *et al*. 2006) and ATP is released from the VMS by hypercapnia *in vivo* (Gourine, Llaudet, Dale and Spyer 2005). This CO_2-induced release of ATP could account for the slightly higher dynamic range of the pH-response of RTN neurons *in vivo* than in slices.

References

Amiel, J., Laudier, B., Attie-Bitach, T., Trang, H., de, Pontual, L., Gener, B., Trochet, D., Etchevers, H., Ray, P., Simonneau, M., Vekemans, M., Munnich, A., Gaultier, C. and Lyonnet, S. (2003) Polyalanine expansion and frameshift mutations of the paired-like homeobox gene PHOX2B in congenital central hypoventilation syndrome. Nat. Genet. 33, 459–461.

Cream, C., Li, A. and Nattie, E. (2002) The retrotrapezoid nucleus (RTN): local cytoarchitecture and afferent connections. Respir. Physiolo. Neurobiol. 130, 121–137.

Feldman, J.L., Mitchell, G.S. and Nattie, E.E. (2003) Breathing: rhythmicity, plasticity, chemosensitivity. Annu. Rev. Neurosci. 26, 239–266.

Gaultier, C., Amiel, J., Dauger, S., Trang, H., Lyonnet, S., Gallego, J. and Simonneau, M. (2004) Genetics and early disturbances of breathing control. Pediatr. Res. 55, 729–733.

Gourine, A.V., Llaudet, E., Dale, N. and Spyer, K.M. (2005) ATP is a mediator of chemosensory transduction in the central nervous system. Nature 436, 108–111.

Guyenet, P.G., Mulkey, D.K., Stornetta, R.L. and Bayliss, D.A. (2005) Regulation of ventral surface chemoreceptors by the central respiratory pattern generator. J. Neurosci. 25, 8938–8947.

Li, A. and Nattie, E. (2002) CO_2 dialysis in one chemoreceptor site, the RTN: stimulus intensity and sensitivity in the awake rat. Respir. Physiol. Neurobiol. 133, 11–22.

Loeschcke, H.H. (1982) Central chemosensitivity and the reaction theory. J. Physiol. 332, 1–24.

Millhorn, D.E. and Eldridge, F.L. (1986) Role of ventrolateral medulla in regulation of respiratory and cardiovascular systems. J. Appl. Physiol. 61, 1249–1263.

Mulkey, D.K., Mistry, A.M., Guyenet, P.G. and Bayliss, D.A. (2006) Purinergic P2 receptors modulate excitability but do not mediate pH sensitivity of RTN respiratory chemoreceptors. J. Neurosci. 26, 7230–7233.

Mulkey, D.K., Stornetta, R.L., Weston, M.C., Simmons, J.R., Parker, A., Bayliss, D.A. and Guyenet, P.G. (2004) Respiratory control by ventral surface chemoreceptor neurons in rats. Nat. Neurosci. 7, 1360–1369.

Nattie, E.E. (2001) Chemoreception and tonic drive in the retrotrapezoid nucleus (RTN) region of the awake rat: bicuculline and muscimol dialysis in the RTN. Adv. Exp. Med. Biol. 499, 27–32.

Nattie, E.E. (2006) The retrotrapezoid nucleus and the 'drive' to breathe. J. Physiol. 572, 311.

Okada, Y., Chen, Z., Jiang, W., Kuwana, S. and Eldridge, F.L. (2002) Anatomical arrangement of hypercapnia-activated cells in the superficial ventral medulla of rats. J. Appl. Physiol. 93, 427–439.

Rosin, D.L., Chang, D.A. and Guyenet, P. G. (2006) Afferent and efferent connections of the rat retrotrapezoid nucleus. J. Comp. Neurol., in press.

Smith, J.C., Morrison, D.E., Ellenberger, H.H., Otto, M.R. and Feldman, J.L. (1989) Brainstem projections to the major respiratory neuron populations in the medulla of the cat. J. Comp. Neurol. 281, 69–96.

Spengler, C.M., Gozal, D. and Shea, S.A. (2001) Chemoreceptive mechanisms elucidated by studies of congenital central hypoventilation syndrome. Resp. Physiol. 129, 247–255.

Stornetta, R.L., Moreira, T.S., Takakura, A.C., Kang, B.J., Chang, D.A., West, G. H., Brunet, J.F., Mulkey, D.K., Bayliss, D.A. and Guyenet, P.G. (2006) Selective expression of Phox2b by brainstem neurons involved in chemosensory integration in the adult rat. J. Neurosci. 26, 10305–10314.

Takakura, A.C., Moreira, T.S., Colombari, E., West, G.H., Stornetta, R.L. and Guyenet, P.G. (2006) Peripheral chemoreceptor inputs to retrotrapezoid nucleus (RTN) CO_2-sensitive neurons in rats. J. Physiol. 572, 503–523.

58
The Chemosensitive Response of Neurons from the Locus Coeruleus (LC) to Hypercapnic Acidosis with Clamped Intracellular pH

Lynn K. Hartzler[1], Jay B. Dean[2] and Robert W. Putnam[1]

Abstract Currently, a change in pH_i is believed to be the major signal in the chemosensitive (CS) response of brainstem neurons to hypercapnia; however, multiple factors (*e.g.*, Ca^{2+}, CO_2, pH_i, and pHo) have been suggested to contribute to this increase in firing rate. While there is evidence for a significant role of pH_i in the CS response, we hypothesize that hypercapnic acidosis (HA) can increase firing rate even with no change in pH_i. We tested several methods to clamp pH_i, including high intracellular buffer and the use of rapid diffusion of weak bases or weak acids through the cell membrane. We were able to clamp pH_i during hypercapnic exposure using weak acids. We observed a CS response to HA, with pH_i clamped, indicating that intracellular acidification, while sufficient to increase firing rate, is not required for the response of CS neurons. The CS response to HA without a change in pH_i is most likely due to extracellular acidification and/or increased CO_2 and strongly supports the multiple factors model of chemosensitive signaling.

1 Introduction

We have long known that CO_2 increases ventilation (Haldane and Priestley 1905), but the mechanism(s) of this increase are still debated (Putnam, Filosa and Ritucci 2004). Both peripheral and central chemoreceptors can alter ventilation; however, denervation of peripheral chemoreceptors does not prevent the ventilatory response to CO_2. It appears that CO_2 alone has little effect on the chemosensitive (CS) regions of the brainstem, but changes in pH of the extracellular fluid surrounding the CS neurons of the brainstem elicit a CS response (for review see Loeschcke 1982). Extracellular pH (pH_o) and intracellular pH (pH_i) are normally coupled, and CO_2 can diffuse across the cell membrane causing intracellular acidification. Thus, changes in pH_o often lead to changes in pH_i.

[1] Wright State University Boonshoft School of Medicine, Department of Neuroscience, Cell Biology, and Physiology, lynn.hartzler@wright.edu, robert.putnam@wright.edu

[2] University of South Florida, Department of Molecular Pharmacology and Physiology, jdean@health.usf.edu

M.J. Poulin and R.J.A. Wilson (eds.), *Integration in Respiratory Control: From Genes to Systems*.

In the current study, we sought to develop a technique by which we could alter CO_2 and pH_o, with pH_i clamped, to directly test the hypothesis that a change in pH_i is necessary to elicit a CS response.

2 Materials and Methods

2.1 Solutions

Whole cell patch clamp pipette filling solutions for controls contained in mM: 120 K-gluconate, 0.4 EGTA, 1 $MgCl_2$, 0.3 Na_2-GTP, 2 Na_2-ATP, 10 K-HEPES. For high internally-buffered filling solutions, an additional 90 mM K-HEPES isosmotically replaced K-gluconate. For experiments with diffusion of weak base/acid, 50 mM weak base or weak acid isosmotically replaced K-gluconate. All whole cell patch clamp pipette-filling solutions were adjusted to pH 7.3 (37°C). Extracellular solutions of artificial cerebral spinal fluid (aCSF) contained in mM: 124 NaCl, 26 $NaHCO_3$, 3 KCl, 1.25 NaH_2PO_4, 10 glucose, 1.3 $MgSO_4$, 2.4 $CaCl_2$, pH 7.45 equilibrated with 5% CO_2, balance O_2, or pH 7.15 equilibrated with 15% CO_2, balance O_2 at 37°C. Superfusion solutions of aCSF for weak base diffusion experiments had isosmotic replacement of 17.7 mM of weak base for NaCl with pH 7.45 equilibrated with 5% CO_2, balance O_2, and 49.9 mM weak base for NaCl with pH 7.0 equilibrated with 15% CO_2, balance O_2 at 37°C. Solutions of aCSF for weak acid diffusion experiments had isosmotic replacement of 70.4 mM weak acid for NaCl with pH 7.45 equilibrated with 5% CO_2, balance O_2, or 25 mM weak acid isosmotically replacing NaCl with pH 7.0 equilibrated with 15% CO_2, balance O_2 at 37°C.

2.2 Brain Slices

Brain slices (300 μm) containing neurons from the locus coeruleus were cut from the rostral pontine region of the brainstem of rat pups (post-natal days 1–18). Slices were allowed to recover in aCSF equilibrated with 5% CO_2, balance O_2 at room temperature for at least 1 hour before experimentation.

2.3 Measurement of pH_i

Intracellular pH measurements were made by loading a neuron with the pH-sensitive dye, pyranine, as previously described (Ritucci, Erlichman, Leiter and Putnam 2005). Briefly, 200 μM pyranine was added to the pipette filling solution

and allowed to diffuse into the neuron through a whole cell patch clamp (see Electrophysiological Methods below). Pyranine was excited at 450 and 415 nm wavelengths; emitted fluorescence (at 515 nm) was collected and processed with Metafluor 4.6r5 software (Universal Imaging). Fluorescence ratios (R_{Fl}) were determined from 450/415 wavelengths and normalized to controls (N_{Fl}). pH_i was calculated from a calibration equation: $pH_i = 7.5561 + \log(N_{Fl} - 0.1459)/(2.0798 - N_{Fl})$ (Ritucci, Dean and Putnam 2005).

2.4 Electrophysiological Methods

Electrophysiological recordings were made with pipettes (5 MΩ resistance) pulled from borosilicate glass (TW150–3; World Precision Instruments) using conventional whole cell recording techniques. Recordings were conducted in current-clamp mode, and V_m was measured using a Dagan BVC-700 amplifier and saved to Axoscope software (version 8.0). Firing rates were collected in 10-second bins using a window discriminator/integrator (Winston Electronics) and stored in Axoscope. We expressed the magnitude of the firing rate response as the chemosensitivity index (CI) according to Wang, Pizzonia and Richerson (1998).

3 Results and Discussion

3.1 HEPES-buffered Internal Solution

We isosmotically replaced K-HEPES (100 mM) for K-gluconate in the intracellular filling solution with the intent to increase cellular buffering and reduce changes of pH_i in response to changes of pH_o or CO_2. Exposure to hypercapnic acidosis (HA) elicited an increase in firing rate (CI = 208%), a slight depolarization of V_m, but a decrease in pH_i similar to normal ΔpH_i (Fig. 1). Using HEPES as an internal buffer did not prevent hypercapnia-induced intracellular acidification of LC neurons (Fig. 1). It may be that using 100 mM HEPES altered the viscosity of the pipette filling solution so that it did not diffuse as freely as control solutions, which is consistent with a reduction in the amount of pyranine loaded in the neurons (unpublished observations). Reducing [HEPES] in the filling solution allowed greater loading of pyranine and, presumably, the amount of buffer entering the intracellular space. Loading with 70 or 40 mM HEPES, however, did not prevent acidification. Substituting Trizma® base (Tris[hydroxymethyl]amino-methane) for the HEPES to buffer pH_i similarly did not alter hypercapnia-induced acidification (data not shown). Thus, we were unable to clamp pH_i by adding pH buffer to the pipette filling solution.

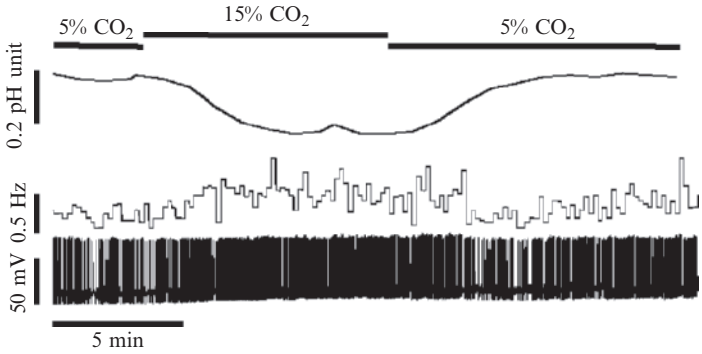

Fig. 1 Effect of HA on pH_i, integrated firing rate, and V_m with 100 mM HEPES buffer in the whole cell patch pipette

3.2 pH_i Clamped by Diffusion of Weak Bases or Acids

The rapid diffusion of a weak base to clamp pH_i was first used in peritoneal macrophages (Grinstein, Romanek and Rotstein 1994). This technique involves loading the neuron with a weak base and altering the concentration of that weak base outside the cell. Because the weak base is permeable across the membrane, altering the external concentration will cause diffusion of the weak base either into or out of the cell. We found that diffusion of weak bases (tetrabutylammonium chloride, tetrapropylammonium hydroxide, dimethylamine hydrochloride, ammonium chloride or ammonium sulfate) clamped pH_i in response to HA, but they all caused irreversible depolarization of V_m. Therefore, weak acids were used in the experiments reported here. The same principle by which weak bases clamp pH_i holds for weak acids.

By loading a neuron with weak acid from the whole cell patch clamp pipette, pH_i can be varied by altering the extracellular concentration of the weak acid ($[A^-]$) according to the equation $pH_i = pH_o + \log([A^-]_i/[A^-]_o)$ (Grinstein *et al*. 1994). Conversely, pH_i can be clamped at a fixed value upon exposure to HA by reducing the extracellular weak acid concentration. Thus, the acidification of the neuron normally seen upon exposure to HA is counterbalanced by weak acid efflux from the neuron.

DMO (5,5-dimethyl-2,4-oxazolidinedione) was loaded into the neuron from the whole cell patch pipette (50 mM) and was added to the superfusate at a concentration to successfully clamp pH_i (changing from initial DMO_o of 70.4 mM to 25 mM) in the face of HA (Fig. 2). We observed that firing rate still increased in response to HA despite the lack of any HA-induced decrease of pH_i (Fig. 2). This is consistent with recent findings using a mathematical model of cellular signaling for mammalian CS neurons (see chapter by Chernov *et al*. in this volume). These data indicate that a decrease in pH_i, while sufficient, is not necessary to elicit a CS response to HA, suggesting that other signals, such as decreased pH_o or increased molecular CO_2, also contribute to the CS response of LC neurons.

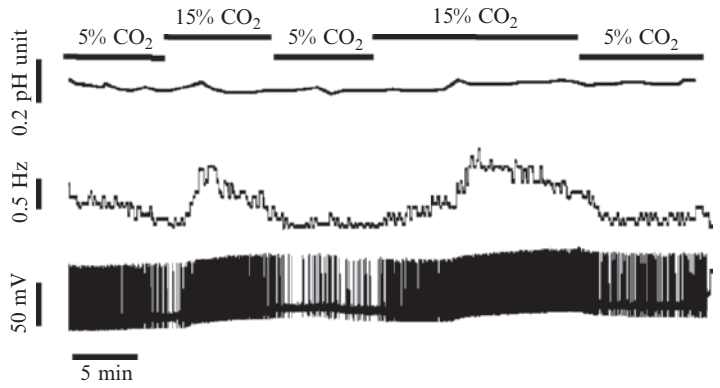

Fig. 2 Effect of HA on pH_i, integrated firing rate and V_m with pH_i clamped by rapid diffusion of DMO

4 Summary

We describe here a practical technique to clamp pH_i in the face of HA that does not disrupt the V_m of excitable cells. These data indicate that while intracellular acidification is a sufficient signal to elicit a chemosensitive response, it is *not necessary*; neurons with pH_i clamped at control levels can still increase firing in the face of HA. We conclude there are multiple factors acting as cell signals in these chemosensitive neurons.

Acknowledgements We would like to thank Phyllis Douglas and Dr. Nick Ritucci for technical assistance and Dr. Paul Martino and Nicole Nichols for helpful comments on this manuscript. This research was supported by NIH grants R01 HL56683 and F32 HL80877.

References

Grinstein, S., Romanek, R. and Rotstein, O.D. (1994) Method for manipulation of cytosolic pH in cells clamped in the whole cell or perforated-patch configurations. Am. J. Physiol. Cell Physiol. 267, C1152–C1159.

Haldane, J.S. and Priestley, J.G. (1905) The regulation of the lung ventilation. J. Physiol., London 32, 225–266.

Loeschcke, H.H. (1982) Central chemosensitivity and the reaction theory. J. Physiol., London 332, 1–24.

Putnam, R.W., Filosa, J.A. and Ritucci, N.A. (2004) Cellular mechanisms involved in CO_2 and acid signaling in chemosensitive neurons. Am. J. Physiol. Cell Physiol. 287, C1493–C1526.

Ritucci, N.A., Dean, J.B. and Putnam, R.W. (2005) Somatic vs. dendritic responses to hypercapnia in chemosensitive locus coeruleus neurons from neonatal rats. Am. J. Physiol. Cell Physiol. 289, C1094–C1104.

Ritucci, N.A., Erlichman, J.S., Leiter, J.C. and Putnam, R.W. (2005) Response of membrane potential and intracellular pH to hypercapnia in neurons and astrocytes from rat retrotrapezoid nucleus. Am. J. Physiol. Regul. Integr. Physiol. 289, R851–R861.

Wang, W., Pizzonia, J.J. and Richerson, G.B. (1998) Chemosensitivity of rat medullary raphe neurons in primary tissue culture. J. Physiol., London 511, 433–450.

59
CO_2-sensitivity of GABAergic Neurons in the Ventral Medullary Surface of GAD67-GFP Knock-in Neonatal Mice

Junya Kuribayashi[1], Shigeki Sakuraba[1], Yuki Hosokawa[1], Eiki Hatori[1], Miki Tsujita[1], Junzo Takeda[1], Yuchio Yanagawa[2,3], Kunihiko Obata[4] and Shun-ichi Kuwana[5]

Abstract We investigated the CO_2 responsiveness of GABAergic neurons in the ventral medullary surface (VMS), a putative chemoreceptive area using a 67-kDa isoform of GABA-synthesizing enzyme (GAD67)-green fluorescence protein (GFP) knock-in neonatal mouse, in which GFP is specifically expressed in GABAergic neurons. The slice was prepared by transversely sectioning at the level of the rostral rootlet of the XII nerve and the rostral end of the inferior olive in mock cerebrospinal fluid (CSF). Each medullary slice was continuously superfused with hypocapnic CSF. GFP-positive neurons in the VMS were selected by using fluorescent optics and their membrane potentials and firing activities were analyzed with a perforated patch recording technique. Thereafter, superfusion was changed from hypocapnic to hypercapnic CSF. In 4 out of 8 GABAergic neurons in the VMS, perfusion with hypercapnic CSF induced more than a 20% decrease in the discharge frequency and hyperpolarized the neurons. The remaining 4 GFP-positive neurons were CO_2-insensitive. GABAergic neurons in the VMS have chemosensitivity. Inhibition of chemosensitive GABAergic neural activity in the VMS may induce increases in respiratory output in response to hypercapnia.

1 Introduction

Central chemosensitive respiratory neurons are thought to be distributed over the ventral medullary surface (VMS) that is bathed in cerebrospinal fluid (CSF). These neurons are stimulated by excess CO_2/H^+ in the CSF and then induce a hyperpneic

[1] Department of Anesthesiology, Keio University School of Medicine, Shinjuku-ku, Tokyo 160-8582, Japan, j_kuriba0416@yahoo.co.jp

[2] Department of Genetic and Behavioral Neuroscience, Gunma University Graduate School of Medicine, Maebashi, Japan

[3] SORST, Japan Science and Technology Corporation, Kawaguchi, Japan

[4] Neural Circuit Mechanisms Research Group, RIKEN Brain Science Institute, Wako, Japan

[5] Department of Physiology, Teikyo University School of Medicine, Tokyo, Japan

M.J. Poulin and R.J.A. Wilson (eds.), *Integration in Respiratory Control: From Genes to Systems*.

and/or tachypneic response (Loeschcke 1982). Although other regions of the brainstem are reported to contain chemosensitive neurons, it is believed that the VMS is particularly significant in mediating CO_2-induced respiratory responses, since neither the pons nor the dorsal medulla is required for these responses (Ballantyne and Scheid 2000). The pattern of distribution and density of CO_2/H^+-sensitive neurons in the VMS is similar to that of neurons containing gamma-aminobutyric acid (GABA) (Miura *et al*. 1998). Moreover, *in vivo* extracellular recordings of VMS neurons in rats have revealed that ionophoretic application of GABA induces complete cessation of the discharge evoked by hypercapnia (Gourine and Spyer 2001). These results lead us to hypothesize that, during hypercapnia, high PCO_2 reduces tonic GABA-mediated inhibition leading to an increase in the activity of respiratory neurons. However, the precise role of GABAergic neurons in the chemosensitivity of neonatal mammals is not well understood.

In the past decade, gene-targeting techniques have been effectively employed in studies of several ontogenetic processes, including those of the respiratory system. We have also studied the role of GABA in respiratory rhythm and pattern generation (Kuwana, Tsunekawa, Yanagawa, Okada, Kuribayashi and Obata 2006). In the present study, we used a 67-kDa isoform of GABA-synthesizing enzyme (GAD67)-green fluorescence protein (GFP) knock-in neonatal mouse, in which GFP is specifically expressed in GABAergic neurons, and investigated the CO_2 responsiveness of GABAergic neurons in the VMS.

2 Methods

2.1 Experimental Animals

We used GAD67-GFP (Δneo) knock-in ($GAD67^{GFP/+}$) mice at 0–4 days of age (Tamamaki, Yanagawa, Tomioka, Miyazaki, Obata and Kaneko 2003). These mice were made by gene targeting of GFP to the locus of the GAD67 gene, so that the expression of GFP is under the control of the endogenous GAD67 promoter. The genotypes of the $GAD67^{GFP/+}$ mice were distinguished by detection through the skull of GFP fluorescence in the brain using a fluorescence microscope. All efforts were made to minimize the number of animals used, and the experimental procedures were performed in accordance with the Guiding Principles for the Care and Use of Animals of the Physiological Society of Japan.

2.2 Medullary Slice Preparation

Medullary slice preparation and perforated patch recording of medullary neurons have been described in detail elsewhere (Kuwana, Okada and Natsui 1998; Okada, Chen, Jiang, Kuwana and Eldridge 2002). Mice (n = 8) were deeply

anesthetized with ether, and the brainstem was isolated in a dissecting chamber that was filled with oxygenated mock CSF. Medullary slice preparations were made using a brain slicer (Microslicer DTK-1000, Dosaka EM, Kyoto, Japan). The medulla was transversely sectioned caudally at the level of the rostral rootlet of the XII nerve. The slice was sectioned at the level of 400 µm rostral to the caudal cut end so that the rostral cut end corresponded to the level of the rostral end of the inferior olive. The ventral surface at this level is known to be a respiratory chemosensitive area (Miura *et al*. 1998). The slice was transferred to a recording chamber and fixed with the rostral side up. The preparation was perfused at 26°C with control mock CSF, which was equilibrated with a gas mixture of 2% CO_2 in O_2 (pH 7.8). The composition of the control mock CSF was as follows (in mM): 126 NaCl, 5 KCl, 1.5 $CaCl_2$, 1.3 $MgSO_4$, 1.25 NaH_2PO_4, 26 $NaHCO_3$ and 30 glucose. After the preparation was perfused for at least 30 minutes with control mock CSF, the perfusate was switched to hypercapnic CSF (8% CO_2 in O_2; pH 7.2).

2.3 Neuronal Recording

The activity of neurons in the superficial (< 300 µm) VMS was recorded intracellularly using a perforated patch technique. A glass pipette was pulled with a horizontal puller (PA-91, Narishige, Tokyo, Japan) to a tip size of approximately 2 µm. Electrode resistance ranged from 12 to 18 MΩ when filled with a solution containing (in mM): 140 K-gluconate, 10 EGTA, 10 HEPES, 1 $CaCl_2$, 1 $MgCl_2$ and nystatin (100 µg/ml). After the GFP-positive neuron in the VMS was selected by using fluorescent optics, the micropipette was attached to it with a manual hydraulic micromanipulator. The membrane potentials were recorded using a single electrode voltage clamp amplifier (CEZ 3100, Nihon Koden, Tokyo, Japan). The signals were recorded on a thermal array recorder and stored on a digital tape for subsequent analysis. Positive DC current was injected into silent neurons to generate spikes. Neurons were identified and classified on the basis of their firing pattern (Wang *et al*. 2002). CO_2-inhibitory neurons exhibited more than a 20% decrease in their discharge frequency after perfusion with hypercapnic CSF, while CO_2-excitable neurons showed more than a 20% increase in discharge frequency after perfusion with hypercapnic CSF. The remaining neurons were classified as CO_2-insensitive neurons.

2.4 Data Analysis

Data are presented as mean ± standard deviation (SD). The significance of the differences in values was evaluated using a paired *t*-test. We considered a difference to be statistically significant when $p < 0.05$.

3 Results

We succeeded in recording neuronal activity in 8 GFP-positive cells in the VMS. Figure 1 shows a representative recording of a CO_2-inhibitory neuron whose discharge frequency was markedly decreased and whose membrane was hyperpolarized by the superfusion with hypercapnic CSF. The electrophysiological properties and locations of these neurons are summarized in Table 1. They were all located at a depth of 178 ± 63 µm below the ventral surface. Four out of 8 GFP-positive neurons in the VMS were CO_2-inhibitory neurons and their membrane potentials ($p < 0.05$) were hyperpolarized. Their input resistance was slightly increased by superfusion of hypercapnic CSF, but this difference was not significant ($p = 0.1$). The remaining 4 GFP-positive neurons were CO_2-insensitive. We did not see any significant differences in the electrophysiological properties of CO_2-insensitive neurons when we compared the values for perfusion with control and with hypercapnic CSF. We could not find any CO_2-excitable neurons.

4 Discussion

We have demonstrated that the CO_2 sensitivity of GABAergic neurons in the VMS is either inhibitory or insensitive. CO_2-inhibitory GABAergic neurons in the present study may contribute to the CO_2 responsiveness of the respiratory neural network.

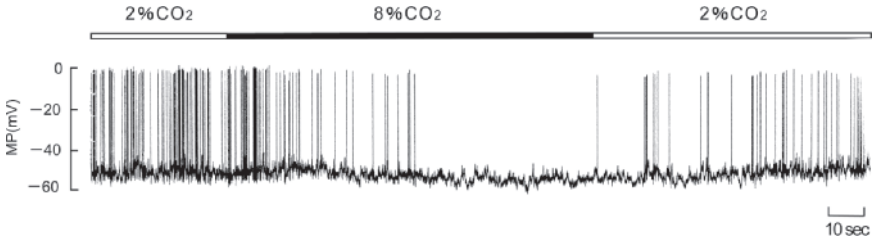

Fig. 1 CO_2-inhibitory response of a GABAergic neuron. This neuron was injected with DC current (20 pA) to generate spikes during perfusion with control CSF (2% CO_2). Discharge frequency was decreased by perfusion with hypercapnic CSF (8% CO_2). MP: membrane potential

Table 1 Membrane potential, input resistance and location of each type of GFP-positive neuron in the VMS

Neuron Type	n	Membrane potential (mV) 2% CO_2	Membrane potential (mV) 8% CO_2	Input resistance (MΩ) 2% CO_2	Input resistance (MΩ) 8% CO_2	Location of neurons Depth from ventral surface (µm)
CO_2-inhibitory	4	−71 ± 19	−76 ± 18**	796 ± 194	968 ± 324*	175 ± 86
CO_2-insensitive	4	−73 ± 16	−73 ± 17	891 ± 276	890 ± 294	183 ± 28

** $P < 0.05$ and * $P = 0.1$ for comparison between 2% and 8% CO2, respectively.

It has been reported that three types of neurons, *i.e*. CO_2-excitable, CO_2-inhibitory and CO_2-insensitive neurons, are located in the VMS (Kawai, Ballantyne, Mückenhoff and Scheid 1996). The CO_2-excitable neurons are considered to be a candidate for respiratory chemoreceptors. However, previous extracellular recordings of VMS neurons *in vivo* have revealed that ionophoretic application of GABA induces complete cessation of discharge evoked by hypercapnia (Gourine *et al*. 2001). Pharmacological studies have shown that application of a GABA receptor agonist attenuates the CO_2-ventilation responsiveness (Kanazawa, Sugama, Okada and Miura 1998). These studies suggest that the GABAergic inhibitory system is involved in respiratory control. Therefore, our observation that the activity of GABAergic neurons was suppressed by CO_2 may support the hypothesis that during hypercapnia, inactivation of these neurons may induce disinhibition of the central respiratory neuronal network that generates respiratory rhythm and pattern.

In summary, GABAergic neurons in the VMS exhibit chemosensitivity. Inhibition of chemosensitive GABAergic neural activity in the VMS may induce an increase in respiratory output in response to hypercapnia.

Acknowledgements This work was supported by a Grant-in-Aid for Scientific Research from the Ministry of Education, Science, Sports and Culture of Japan (J.K.).

References

Ballantyne, D. and Scheid, P. (2000) Mammalian brainstem chemosensitive neurones: linking them to respiration *in vitro*. J. Physiol. 525, 567–577.

Gourine, A.V. and Spyer, K.M. (2001) Chemosensitivity of medullary inspiratory neurones: a role for GABA(A) receptors? Neuroreport 12, 3395–3400.

Kanazawa, M., Sugama, S., Okada, J. and Miura, M. (1998) Pharmacological properties of the CO_2/H^+-sensitive area in the ventral medullary surface assessed by the effects of chemical stimulation on respiration. J. Auton. Nerv. Syst. 6, 24–33.

Kawai, A., Ballantyne, D., Mückenhoff, K. and Scheid, P. (1996) Chemosensitive medullary neurones in the brainstem-spinal cord preparation of the neonatal rat. J. Physiol. 492, 277–292.

Kuwana, S., Okada, Y. and Natsui, T. (1998) Effects of extracellular calcium and magnesium on central respiratory control in the brainstem-spinal cord of neonatal rat. Brain Res. 786, 194–204.

Kuwana, S., Tsunekawa, N., Yanagawa, Y., Okada, Y., Kuribayashi, J. and Obata, K. (2006) Electrophysiological and morphological characteristics of GABAergic respiratory neurons in the mouse pre-Bötzinger complex. Eur. J. Neurosci. 23, 667–674.

Loeschcke, H.H. (1982) Central chemosensitivity and the reaction theory, J. Physiol. 332, 1–24.

Miura, M., Okada, J. and Kanazawa, M. (1998) Topology and immunohistochemistry of proton-sensitive neurons in the ventral medullary surface of rats. Brain Res. 780, 34–45.

Okada, Y., Chen, Z., Jiang, W., Kuwana, S. and Eldridge, F.L. (2002) Anatomical arrangement of hypercapnia-activated cells in the superficial ventral medulla of rats. J. Appl. Physiol., 93, 427–439.

Tamamaki, N., Yanagawa, Y., Tomioka, R., Miyazaki, J., Obata, K. and Kaneko, T. (2003) Green fluorescent protein expression and colocalization with calretinin, parvalbumin, and somatostatin in the GAD-GFP knock-in mouse. J. Comp. Neurol. 467, 60–79.

Wang, W., Bradley, S.R. and Richerson, G.B. (2002) Quantification of the response of rat medullary raphe neurones to independent changes in pHo and $P_{CO2.}$ J. Physiol. 540, 951–970.

60
Multiple Central Chemoreceptor Sites: Cell Types and Function *in vivo*

Gene Nattie[1] and Aihua Li[2]

Abstract Central chemoreception is a distributed property involving many sites and neuronal types. Focal acidosis in conscious or anesthetized animals at many hindbrain sites stimulates breathing. The steady-state CO_2 response in conscious animals is reduced by cell specific lesions of catecholamine, 5HT or neurokinin-1 receptor (NK1R) expressing neurons and by focal inhibition at the retrotrapezoid nucleus (RTN) and medullary raphe (MR). Is the steady-state CO_2 response a physiologically relevant way to study central chemoreception? Central chemoreceptors also: (1) provide a 'tonic drive' to breathe, (2) are modified by and/or modulate other control systems, *e.g.*, temperature and hypoxia, (3) affect breath-to-breath variability, (4) can respond dynamically to few breath changes in CO_2, and (5) interact in complex ways. We contend that central chemoreceptors detect interstitial pH and thus monitor the balance of arterial PCO_2, cerebral blood flow and neuronal/glial metabolism. They affect physiological control systems in many ways, perhaps not all measurable, via the study of the steady-state CO_2 response.

1 Widespread Central Chemoreceptor Sites: Focal Stimulation *in vivo*

Focal, mild acidosis produced by microdialysis of artificial cerebrospinal fluid equilibrated with CO_2 in conscious rats and goats stimulates breathing at many hindbrain locations including the retrotrapezoid nucleus (RTN), the rostral medullary raphe (MR), the caudal nucleus tractus solitarius (NTS) and the fastigial nucleus (FN) of the cerebellum. Focal acidosis under anesthesia has also implicated the locus ceruleus, A5 region and pre-Bötzinger complex (PBC)/rostral ventral respiratory group. Studies in numerous reduced preparations *in vitro* have shown that many types of neurons can respond to CO_2 (see Nattie and Li 2006a and other chapters in this monograph).

[1–2]Department of Physiology, Dartmouth Medical School, Lebanon, NH, USA, Eugene.nattie@dartmouth.edu, Aihua.Li@dartmouth.edu

M.J. Poulin and R.J.A. Wilson (eds.), *Integration in Respiratory Control: From Genes to Systems*.

2 Effects of Site-specific Inhibition or Cell Specific Lesions on the Steady-state CO_2 Response

To examine the physiological importance and role of different central chemoreceptor sites and neuronal types we have used focal microdialysis of neuronal inhibitors and injections of cell specific toxins.

In the RTN, under anesthesia, very small lesions or focal inhibition by muscimol dialysis produce apnea, virtually abolish the CO_2 response and decrease the response to hypoxia. In conscious animals, small lesions or focal inhibition decrease the CO_2 response in wakefulness and sleep. Bilateral lesions of RTN NK1R-expressing neurons produce hypoventilation and a reduced CO_2 response. RTN neurons produce tonic excitation of breathing, participate importantly in central and peripheral chemoreception and appear to be vital in anesthesia (see Nattie and Li, 2006a; 2006b).

In the MR, in conscious rats, a 28% loss of 5HT neurons decreases the steady-state CO_2 response by 20% in NREM sleep and wakefulness. Focal 5HT neuron inhibition by dialysis of 8-OH-DPAT in the rostral medulla decreases the steady-state CO_2 response by ~ 20% in NREM sleep and wakefulness while similar inhibition in the caudal medulla has no effect (Nattie and Li 2006a; Taylor *et al*. 2005a; Li *et al*. 2006). In contrast, in conscious newborn piglets, 60% loss of 5HT neurons has no effect on the steady-state CO_2 response except in male piglets in NREM sleep (Penatti *et al*. 2006), while focal 5HT neuron inhibition by dialysis of 8-OH-DPAT in the rostral medulla decreases the steady-state CO_2 response but in an age dependent manner affecting only piglets older than 8 days (see Nattie and Li 2006a). The chemoreceptor function of 5HT neurons varies by species, age, state, temperature (see below) and gender.

Large lesions of catecholamine (CA) neurons with 84% loss at A6, 78% loss at A5, 60% loss at A1/C1 and 56% loss at A2/C2 result in a ~ 28% reduction in the CO_2 response in wakefulness and NREM sleep (Li and Nattie 2006). CA neurons participate in chemoreception as studied by the steady-state CO_2 response.

We have lesioned NK1R-expressing neurons (1) in the RTN producing a 44% loss associated with a ~ 30% decrease in the CO_2 response in sleep and wakefulness and (2) in the MR producing a 31% loss associated with a 15–21% decrease in the CO_2 response (see Nattie and Li 2006a). Injection of the toxin (substance P-saporin) into the cisterna magna produced a 65% loss in A5, 70% loss in the RTN and 49% loss in the rostral ventral respiratory group with no effects more dorsally (Nattie and Li 2006b). These substantial lesions reduced the steady-state CO_2 response by 65%, a very large effect. Substance P and NK1Rs are importantly involved in the steady-state CO_2 response. Putative chemosensitive neurons (*e.g*., serotonergic and glutamatergic) can contain substance P. We hypothesize that substance P is an important modulator/transmitter of chemosensitive ventral medullary neurons.

3 Is the Steady-State CO_2 Response Physiologically Relevant?

We, like others, have focused our approach to the study of central chemoreception on examination of the steady-state breathing response to inhaled CO_2 usually at 5% or 7% levels. The rationale is that this response yields insight into the sensitivity of central chemoreceptors that is applicable to their physiological functions in normal life. This rationale may not be entirely correct. Certainly few animals are ever naturally exposed to these levels of inspired CO_2. As we learn more about the functions of neurons that are demonstrably chemosensitive, we likely will see that this property, chemosensitivity, has other functional outlets.

3.1 What is the Function of Central Chemoreceptors: Are We Testing Them Appropriately?

We suggest the following additional measures of physiological function for central chemoreceptors.

(1) Central chemoreceptors provide a **'tonic drive'** to breathe. Lesions of NK1R-expressing neurons in the RTN and ventral medulla cause hypoventilation while lesions of 5HT or CA neurons do not. Simultaneous focal inhibition of RTN and caudal MR also causes hypoventilation.

(2) Central chemoreception is **modified** by and/or **modulates** other systems. Large lesions of NK1R-expressing neurons reduce the hypoxic response but with partial recovery in conscious rats. With dialysis of muscimol in the rostral MR the response of ventilation to 7% CO_2 is unaffected by ambient temperature (23 vs. 32°C) but the response of the ratio of ventilation/oxygen consumption is greater at 23°C and there is an excitatory effect of muscimol on the ratio in both temperatures (Taylor *et al*. 2005b). Conversely, the ventilatory response to hypoxia is the same at both temperatures with no effect of muscimol while the ratio of ventilation to oxygen consumption in hypoxia varies with temperature and is increased by muscimol at 32°C but decreased at 23°C.

(3) Central chemoreceptors affect **breath-to-breath variability**. Following CA neuron lesions, breath-to-breath variability, as examined by the Poincare analysis, is unaffected in wakefulness and NREM sleep but is increased significantly in REM sleep (Li and Nattie 2006). After 5HT neuron lesions, we have not observed changes in breath-to-breath variability in wakefulness or NREM sleep but have not examined REM sleep (Li and Nattie, unpublished observations). With lesions of NK1R-expressing neurons there is no effect on variability in wakefulness or NREM sleep but in REM breath-to-breath variability increases as does the coefficient of variability. Both are attributable to periods of rapid frequency (Li and Nattie, unpublished observations).

(4) Central chemoreceptors respond to **few breath changes in CO_2**. Modarreszadeh and Bruce (1992) showed a small but clear ventilatory

response to pseudorandom single breath CO_2 application in hyperoxia to minimize carotid body inputs, which is about 50% of that obtained in air with greater carotid body participation. These results are obtained in a closed-loop control system and the estimated time constant for an abrupt change in CO_2 is 55 s, which is shorter than time constants obtained by open loop application of CO_2 step forcing. Modarreszadeh and Bruce (1992) speculate that central chemoreceptors in a closed-loop control system with feedback controls operative can respond to changes in CO_2 "… that occur on the average over several breaths." The carotid body can provide single breath dynamics; the central chemoreceptors can provide several breath dynamics.

(5) Central chemoreceptor sites **interact in complex ways**. We have placed microdialysis probes simultaneously into the RTN and the MR. Due to space constraints, we were forced to place the MR probe more caudally than in our prior MR single probe experiments (Taylor *et al*. 2005a; Li *et al*. 2006). We found that inhibition of 5HT neurons in the caudal MR alone had no effect on the CO_2 response, a surprising result since similar inhibition more rostrally did decrease the CO_2 response by 22% (Taylor *et al*. 2005b), but did potentiate the effects of RTN inhibition producing hypoventilation and a 51% decrease in the CO_2 response. The MR is heterogeneous in respect to responses to inspired CO_2 and the caudal MR has a powerful modulatory effect on RTN chemoreception.

3.2 What Variables Do Central Chemoreceptors Monitor?

In terms of chemodetection, we favor the hypothesis that central chemoreceptors monitor brain interstitial fluid pH as suggested by the earlier, powerful studies in conscious goats by Fencl, Miller and Pappenheimer (Fencl *et al*. 1966). This interstitial pH value reflects blood PCO_2, cerebral blood flow and neuronal metabolism and thus reflects an integrated estimate of these variables.

4 Conclusions

(1) There are many sites within the hindbrain that respond to focal acidification *in vivo* and many types of neurons that respond to CO_2/pH *in vitro*.
(2) Focal inhibition or cell specific lesion at some of these sites reduces the steady-state response to CO_2 supporting their participation in central chemoreception.
(3) Substance P and NK1R-expressing neurons appear to be very important for steady-state central chemoreception *in vivo*.
(4) The steady-state CO_2 response may not be the single best approach to evaluate the physiological function of central chemoreceptors.

(5) Central chemoreception may reflect a property (CO_2/pH sensitivity) of many types of brainstem neurons that affect a variety of functions. These functions, once understood, may be useful adjuncts in the study of central chemoreception. Examples include: tonic drive, modulation of other control systems, breath-to-breath variability and breathing stability, responses to few breath changes in CO_2 and interactions among sites.
(6) Central chemoreceptors likely monitor brain interstitial pH, which reflects arterial PCO_2, cerebral blood flow and neuronal metabolism.

Acknowledgement Supported by NIH R01 HL 28066 and P01-HD 36379.

References

Fencl, V., Miller, T.B. and Pappenheimer, J.R. (1966) Studies on the respiratory response to disturbances of acid-base balance, with deductions concerning the ionic composition of cerebral interstitial fluid. Am. J. Physiol. 210, 459–472.

Li, A. and Nattie, E.E. (2006) Catecholamine neurons in rats modulate sleep, breathing, central chemoreception and breathing variability. J. Physiol. 570, 385–396.

Li, A., Zhou, S. and Nattie, E. (2006) Simultaneous inhibition of caudal medullary raphe and retrotrapezoid nucleus decreases breathing and the CO_2 response in conscious rats. J. Physiol., July 6. [Epub ahead of print.]

Modarreszadeh, M. and Bruce E.N. (1992) Long-lasting ventilatory response of humans to a single breath of hypercapnia in hyperoxia. J. Appl. Physiol. 72, 242–250.

Nattie, E. and Li, A. (2006a) Central chemoreception 2005: A brief review. Auton. Neurosci.: Basic and Clin. 126–127, 332–338.

Nattie, E. and Li, A. (2006b). Neurokinin-1 receptor expressing neurons in the ventral medulla are essential for normal central and peripheral chemoreception in the conscious rat. J. Appl. Physiol., August 10 [Epub ahead of print].

Penatti, E.M., Berniker, A.V., Kereshi, B., Cafaro, C., Kelly, M. L., Niblock, M.M., Gao, H.G., Kinney, H.C., Li, A. and Nattie, E.E**.** (2006) Ventilatory response to hypercapnia and hypoxia after extensive lesion of medullary serotonergic neurons in newborn conscious piglets. J. Appl. Physiol. 101, 1177–1188.

Taylor, N.C., Li, A. and Nattie, E.E. (2005a) Medullary serotonergic neurons modulate the ventilatory response to hypercapnia, but not hypoxia in conscious rats. J. Physiol. 566.2, 543–557.

Taylor, N.C., Li, A. and Nattie, E.E. (2005b). Ventilatory effects of muscimol microdialysis into the rostral medullary raphe region of conscious rats. Respir. Physiol. Neurobiol., Dec. 7. [Epub ahead of print.]

61
Intrinsic Chemosensitivity of Individual Nucleus Tractus Solitarius (NTS) and Locus Coeruleus (LC) Neurons from Neonatal Rats

Nicole L. Nichols[1], Lynn K. Hartzler[1], Susan C. Conrad[1], Jay B. Dean[2] and Robert W. Putnam[1]

Abstract Chemosensitive (CS) neurons are found in discrete brainstem regions, but whether the CS response of these neurons is due to intrinsic chemosensitivity of individual neurons or is mediated by changes in chemical and/or electrical synaptic input is largely unknown. We studied the effect of synaptic blockade (11.4 mM Mg^{2+}/0.2 mM Ca^{2+}) solution (SNB) and a gap junction uncoupling agent carbenoxolone (CAR—100 μM) on the response of neurons from two CS brainstem regions, the NTS and the LC. In NTS neurons, SNB decreased spontaneous firing rate (FR). We calculated the magnitude of the FR response to hypercapnic acidosis (HA; 15% CO_2) using the Chemosensitivity Index (CI). The percentage of NTS neurons activated and CI were the same in the absence and presence of SNB. Blocking gap junctions with CAR did not significantly alter spontaneous FR. CAR did not alter the CI in NTS neurons and resulted in a small decrease in the percentage of activated neurons, which was most evident in NTS neurons from rats younger than postnatal day 10. In LC neurons, SNB resulted in an increase in spontaneous FR. As with NTS neurons, SNB did not alter the percentage of activated neurons or the CI in LC neurons. CAR resulted in a small increase in spontaneous FR in LC neurons. In contrast, CAR had a marked effect on the response of LC neurons to HA: a reduced percentage of CS LC neurons and decreased CI. In summary, both NTS and LC neurons appear to contain intrinsically CS neurons. CS neurons from the two regions receive different tonic input in slices (excitatory for NTS and inhibitory for LC); however, blocking chemical synaptic input does not affect the CS response in either region. In NTS neurons, gap junction coupling plays a small role in the CS response, but gap junctions play a major role in the chemosensitivity of many LC neurons.

[1] Wright State University Boonshoft School of Medicine, Department of Neuroscience, Cell Biology & Physiology, nichols.36@wright.edu, robert.putnam@wright.edu

[2] University of South Florida, College of Medicine, Department of Molecular Pharmacology and Physiology, jdean@health.usf.edu

M.J. Poulin and R.J.A. Wilson (eds.), *Integration in Respiratory Control: From Genes to Systems*.

1 Introduction

Central CS neurons respond to HA and serve to modulate ventilation. There are multiple CS regions located in the central nervous system which include, but are not limited to, the NTS and the LC. In response to HA, neurons in these areas are activated, which is measured by an increase in neuronal FR. Only 40–50% of NTS neurons are activated by HA (Conrad, Mulkey, Ritucci, Dean and Putnam 2005), whereas > 80% of LC neurons are activated (Filosa, Dean and Putnam 2002; Oyamada, Ballantyne, Mückenhoff and Scheid 1998) by HA. Whether these neurons are activated intrinsically or are dependent on the input of other neurons is not known. Both NTS (Dean, Bayliss, Erickson, Laying and Millhorn 1990) and LC (Ballantyne and Scheid 2000; Oyamada *et al*. 1998) neurons respond to HA even with chemical synaptic transmission blocked by SNB. It is not known what happens to the percentage of neurons that respond or to the CI of neurons in the presence of SNB. In addition, CS NTS and LC neurons are coupled by gap junctions, with LC neurons being most extensively coupled (Ballantyne, Andrzejewski, Mückenhoff and Scheid 2004; Dean, Ballantyne, Cardone, Erlichman and Solomon 2002; Dean, Huang, Erlichman, Southard and Hellard 1997; Dean, Kinkade and Putnam 2001; Huang, Erlichman and Dean 1997; Solomon and Dean 2002). The larger percentage of activated LC neurons may be due to extensive gap junction coupling. The focus of the current study was to determine if neurons from the NTS and LC are intrinsically CS by using SNB and CAR to block chemical and electrical transmission, respectively.

2 Methods

The brainstem from neonatal rats (ages P1–P18) was isolated and 300 µm transverse slices were sectioned using a vibratome. Slices were incubated at room temperature in artificial cerebral spinal fluid (aCSF) equilibrated with 95% O_2 / 5% CO_2. The aCSF contained in mM: 5 KCl, 124 NaCl, 1.3 $MgSO_4$, 26 $NaHCO_3$, 1.24 KH_2PO_4, 10 glucose, and 2.4 $CaCl_2$. Individual slices were placed in a superfusion chamber and immobilized by a nylon grid while being superfused with aCSF equilibrated with 95% O_2 / 5% CO_2 at 37°C. Membrane potential (V_m) of individual neurons from the NTS and LC was measured using the whole cell patch method in current clamp mode using pipettes with 5 MΩ resistance. The intracellular solution contained in mM: 130 K-gluconate, 0.4 EGTA, 1 $MgCl_2$, 0.3 Na_2-GTP, 2 Na_2-ATP, and 10 HEPES. This solution prevents washout of the electrical response to HA (Filosa and Putnam 2003). Once the neuron stabilized (V_m of −45 to −60 mV), recording began. Neurons were then exposed to acute HA (85% O_2 / 15% CO_2) for 4–10 minutes. If a neuron was activated by acute HA, then the hypercapnic exposure was repeated in the presence of either SNB (0.2 mM Ca^{2+}, 11.4 mM Mg^{2+}) or CAR (100 µM) solutions. A neuron was considered activated if the CI value was ≥ 120%, calculated according to Wang, Pizzonia and Richerson (1998). Statistical significance was determined using Student's *t*-tests or χ^2 analyses.

3 Results and Discussion

Between 40–50% of NTS neurons from both neonatal and adult rats are activated by HA (Conrad *et al*. 2005; Dean *et al*. 1990). Further, in neonates (Conrad *et al*. 2005; Huang *et al*. 1997) and adults (Dean *et al*. 1990) NTS neurons are intrinsically CS since SNB reduced the percentage of activated neurons by only a small amount. The current study focused on whether activated neurons are intrinsically CS by blocking both chemical and electrical input. SNB was used to verify that chemical transmission did not play a major role in the CS response of NTS neurons. SNB decreased spontaneous FR from about 1.4 Hz to 0.6 Hz (Fig. 1A). The CI was the same in the absence and presence of SNB (Fig. 1A) with a value of 157 ± 49% and 200 ± 51%, respectively (n = 10). All neurons that were activated by HA in the absence of SNB were also activated in the presence of SNB. Thus, we conclude that the CS response of NTS neurons does not depend on chemical transmission.

Gap junctions are expressed in the NTS and are formed preferentially between CS neurons (Dean *et al*. 1997; Huang *et al*. 1997). To test if electrical transmission is involved in the activation of NTS neurons by HA, CAR was used to block gap junctions. Blocking gap junctions decreased spontaneous FR by about 0.7 Hz (Fig. 1B). CI was unchanged by CAR (Fig. 1B) with a value of 182 ± 17% in the absence of and 171 ± 12% in the presence of CAR. Further, CAR had a small effect on the percentage of NTS neurons activated by HA (27/53 or 51% in the absence and 20/53 or 38% in the presence of CAR), which was most pronounced in neonates aged P1–P10. Thus, we conclude that gap junctions play at most a small role in the hypercapnic activation of NTS neurons.

In LC, the percentage of activated neurons is > 80% (Filosa *et al*. 2002; Oyamada *et al*. 1998). Again, we used SNB (Fig. 2A) and CAR (Fig. 2B) to test whether LC neurons are intrinsically CS. SNB resulted in an increase in spontaneous FR (Fig. 2A) from 1.01 Hz to 2.55 Hz. The CI was not altered in LC neurons activated by HA in the absence (141 ± 6%) or presence (145 ± 13%) of SNB. SNB did not

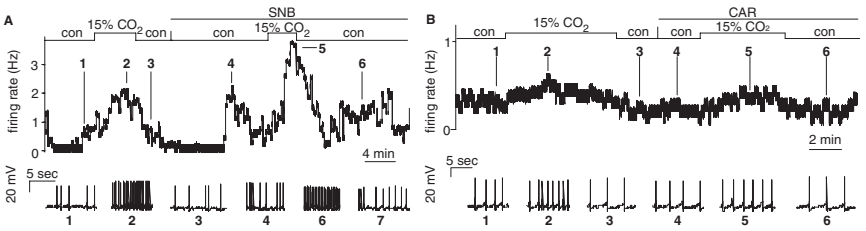

Fig. 1 (A) The response to HA of an NTS neuron exposed to SNB. Top panel: integrated FR of the NTS neuron. SNB caused a decrease in spontaneous FR. Depolarizing current was injected to return FR to near normal values (points 1 and 4 in panel A). Bottom panel: 10 s samples of V_m traces at times indicated. (**B**) The response to HA of an NTS neuron exposed to CAR. Top panel: integrated FR of the NTS neuron. CAR resulted in a slight decrease in spontaneous FR. Bottom panel: 10 s samples of V_m traces at times indicated

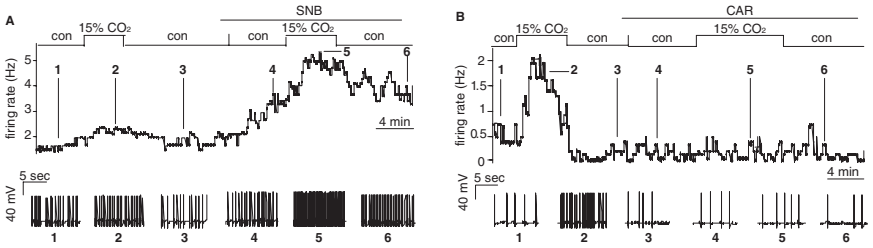

Fig. 2 (A) The response to HA of an LC neuron exposed to SNB. Top panel: integrated FR of the LC neuron. SNB caused an increase in spontaneous FR. Bottom panel: 10 s samples of V_m traces at times indicated. (**B**) The response to HA of an LC neuron exposed to CAR. Top panel: integrated FR of the LC neuron. CAR resulted in no change in spontaneous FR. Bottom panel: 10 s samples of V_m traces at times indicated

alter the percentage of neurons activated by HA, which was 79% (11/14) in the absence and presence of SNB. Thus, the CS response of LC neurons does not depend on synaptic transmission.

CAR resulted in a small increase in spontaneous FR in LC neurons (Fig. 2B), but CAR decreased the CI from 149 ± 8% to 118 ± 3% ($p < 0.01$). The percentage of LC neurons activated by HA in the presence of CAR also decreased from 71% (17/24) in the absence to 42% (10/24) in the presence of CAR ($p < 0.05$). Thus, gap junctions are critical for the CS response of LC neurons from neonates.

In summary, the NTS and LC both contain intrinsically CS neurons. These two regions have neurons that receive different tonic input in slices. NTS neurons receive tonic excitatory input since SNB decreased spontaneous FR, which is in agreement with earlier findings (Dean *et al*. 1997; Huang *et al*. 1997). In contrast, LC neurons receive tonic inhibitory input since SNB increased spontaneous FR. Blocking chemical synaptic input does not affect the CS response in neurons from either region. Furthermore, gap junction coupling is not critical in the CS response of NTS neurons but is critical in the CS response of many LC neurons. The extensive electrical coupling in LC neurons may explain why about 80% of these neurons are activated by HA. It appears that the LC behaves like a syncytium, with intrinsically CS neurons activating neighboring, non-CS neurons in response to HA.

In conclusion, NTS neurons from neonates appear to be intrinsically CS and for the most part do not rely on the input of neighboring neurons. In contrast, LC neurons from neonates may be compensating for a small individual neuronal CS response by acting as a syncytium and activating most neurons in the region via gap junctions.

Acknowledgements We would like to thank Phyllis Douglas for her technical support and Dr. Adrian Corbett for her help with the statistical analyses. This research was supported by the Wright State University Biomedical Sciences Ph.D. program and NIH grants R01 HL56683 and F32 HL80877.

References

Ballantyne, D., Andrzejewski, M., Mückenhoff K. and Scheid, P. (2004) Rhythms, synchrony and electrical coupling in the locus coeruleus. Respir. Physiol. Neurobiol. 143, 199–214.

Ballantyne, D. and Scheid, P. (2000) Mammalian brainstem chemosensitive neurones: linking them to respiration *in vitro*. J. Physiol., London 525, 567–572.

Conrad, S.C., Mulkey, D.K., Ritucci, N.A., Dean, J.B. and Putnam, R.W. (2005) Development of chemosensitivity in neurons from the nucleus tractus solitarius (NTS). FASEB J. 19, A649.

Dean, J.B., Ballantyne, D., Cardone, D.L., Erlichman, J.S. and Solomon, I.C. (2002) Role of gap junctions in CO_2 chemoreception and respiratory control. Am. J. Physiol. Lung Cell Mol. Physiol. 283, L665–L670.

Dean, J.B., Bayliss, D.A., Erickson, J.T., Lawing, W.L. and Milhorn, D.E. (1990) Depolarization and stimulation of neurons in nucleus tractus solitarii by carbon dioxide does not require chemical synaptic input. Neuroscience 36, 207–216.

Dean, J.B., Huang, R.-Q., Erlichman, J.S., Southard, T.L. and Hellard, D.T. (1997) Cell-cell coupling occurs in dorsal medullary neurons after minimizing anatomical-coupling artifacts. Neuroscience 80, 21–40.

Dean, J.B., Kinkade, E.A. and Putnam, R.W. (2001) Cell-cell coupling in CO_2/H^+-excited neurons in brainstem slices. Respir. Physiol. 129, 83–100.

Filosa, J.A., Dean, J.B. and Putnam, R.W. (2002) Role of intracellular and extracellular pH in the chemosensitive response of rat locus coeruleus neurones. J. Physiol., London 541, 493–509.

Filosa, J.A. and Putnam, R.W. (2003) Multiple targets of chemosensitive signaling in locus coeruleus neurons: role of K^+ and Ca^{2+} channels. Am. J. Physiol. Cell Physiol. 284, C145–C155.

Huang, R.-Q., Erlichman, J.S. and Dean, J.B. (1997) Cell-cell coupling between CO_2-excited neurons in the dorsal medulla oblongata. Neuroscience 80, 41–57.

Oyamada, Y., Ballantyne, D., Mückenhoff, K. and Scheid, P. (1998) Respiration-modulated membrane potential and chemosensitivity of locus coeruleus neurones in the *in vitro* brainstem-spinal cord of the neonatal rat. J. Physiol., London 513, 318–398.

Solomon, I.C. and Dean, J.B. (2002) Gap junctions in CO_2-chemoreception and respiratory control. Respir. Physiol. Neurobiol. 131, 155–173.

Wang, W., Pizzonia, J.J. and Richerson, G.B. (1998) Chemosensitivity of rat medullary raphé neurones in primary tissue culture. J. Physiol., London 511, 433–450.

62
Chemosensitive Neuronal Network Organization in the Ventral Medulla Analyzed by Dynamic Voltage-Imaging

Yasumasa Okada[1], Shun-ichi Kuwana[2], Haruko Masumiya[3], Naofumi Kimura[4], Zibin Chen[5] and Yoshitaka Oku[3]

Abstract Central chemosensitivity is critically important to maintain homeostasis. We have successfully applied a voltage-imaging technique to medullary slice and isolated brainstem-spinal cord preparations and analyzed chemosensitive neuronal network organization in the rat ventral medulla. Our results indicate that neurons in the superficial ventral medullary chemosensitive regions and deeply located medullary respiratory neuronal network are interconnected. We propose a neuronal network organization model for central chemoreceptors.

1 Introduction

The ventral medullary surface (VMS) had been considered the main site for central chemoreception (Loeschcke 1982) until it was reported that central chemosensitive sites are widespread in the brainstem (Coates, Li and Nattie 1993). Smith, Morrison, Ellenberger, Otto and Feldman (1989) found a neuronal population near VMS with extensive efferent projections to the ventral respiratory group (VRG) and referred to it as the retrotrapezoid nucleus (RTN), which overlaps with the recently identified parafacial respiratory group (pFRG) (Onimaru and Homma 2003). The group of Rosin *et al*. (2006) identified anatomical connection from VMS marginal glial layer (MGL) and RTN subsurface neurons to preBötzinger Complex and VRG (preBötC/VRG). Functional connection from VMS to the respiratory neuronal network was previously analyzed by electrically stimulating VMS in cats (Loeschcke 1982), and recently in rats by electrical stimulation and microinjection of high CO_2

[1] Keio University Tsukigase Rehabilitation Center, Department of Medicine, yasumasaokada@1979.jukuin.keio.ac.jp

[2] Teikyo University, Department of Physiology, kuwanas@med.teikyo-u.ac.jp

[3] Hyogo College of Medicine, Department of Physiology, masumiya@hyo-med.ac.jp (HM), yoku@hyo-med.ac.jp (YO)

[4] Jikei University School of Medicine, Department of Pharmacology (II), kimura@jikei.ac.jp

[5] GlaxoSmithKline, Department of Biochemical and Analytical Pharmacology, zibin.b.chen@gsk.com

M.J. Poulin and R.J.A. Wilson (eds.), *Integration in Respiratory Control: From Genes to Systems*.

saline into VMS (Okada, Chen, Jiang, Kuwana and Eldridge 2004). Although these studies indicated that chemosensitive neurons near VMS are anatomically and functionally connected to the respiratory neuronal network, precise functional connectivity between VMS and deep medullary respiratory neurons has not been fully elucidated. We intended to analyze the functional organization of the chemosensitive neuronal network in the ventral medulla by dynamic voltage imaging.

2 Methods

Medullary slice and isolated brainstem-spinal cord (*en bloc*) preparations were made from neonatal rats (n = 20, 0–5 days old). To make slice preparations, the rostral medulla (at the level between the IX nerve and the most rostral rootlet of the XII nerve) was transversely sectioned with a slicer (400–600 μm thick) similarly to our spinal cord slice experiments (Fukuda, Okada, Yoshida, Aoyama, Nakamura, Chiba and Toyama 2006). The procedure for obtaining *en bloc* preparations was as described previously (Okada, Mückenhoff and Scheid 1993).

Preparations were stained with a voltage-sensitive dye (di-4-ANEPPS or di-2-ANEPEQ, 0.1–0.2 mg/mL, Invitrogen, Carlsbad, CA) for 30–50 min (Ito, Oyamada, Okada, Hakuno, Aoyama and Yamaguchi 2004; Onimaru *et al*. 2003). They were superfused with a standard superfusate that was equilibrated with 95% O_2 and 5% CO_2 (pH 7.4 at 26°C). In slice preparations, a single-pulse electrical current (amplitude 1.2 mA, duration 80 μs) was applied through a metal microelectrode (tip diameter 1 μm) to various points in subsurface medullary regions, including the raphe pallidus (RP), parapyramidal region (PPY) and RTN and neuronal excitation was evoked. In *en bloc* preparations, inspiratory activity was monitored from C4 ventral roots. Electrical stimulation-induced activity on the transverse plane in slices and spontaneous respiratory activity on VMS in *en bloc* preparations were analyzed using an optical recording system (MiCAM01 or MiCAM Ultima, BrainVision, Tokyo) (Fukuda *et al*. 2006; Okada, Chen, Yoshida, Kuwana, Jiang and Maruiwa 2001a; Onimaru *et al*. 2003). Briefly, preparations were placed under a fluorescent microscope and illuminated with a tungsten-halogen lamp through an excitation filter (λ = 480 ~ 550 nm). Epifluorescence through a barrier filter (λ > 610 nm) was detected with a MiCAM-camera with a frame rate of 2 ms in slices and 20 ms in *en bloc* preparations. In *en bloc* preparations, signals were averaged 30 times triggered by C4 activity in standard and hypercapnic (92% O_2 and 8% CO_2; pH 7.2) superfusates.

3 Results

With electrical stimulation of subsurface ventral medullary regions, especially in RP, PPY and RTN, we observed initial excitation around the tip of a microelectrode. The depolarized region then extended to deeper regions, especially to preBötC/VRG.

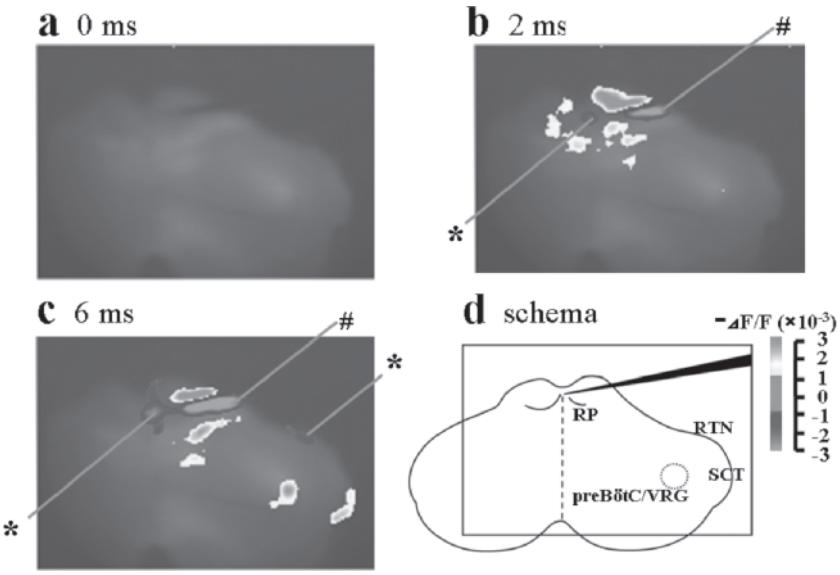

Fig. 1 Electrical stimulation of RP evoked depolarization around the electrode tip in 2 ms after stimulation. In 6 ms preBötC/VRG and SCT were depolarized, and RTN was hyperpolarized. *Hyperpolarized regions. #Artifact by a microelectrode temperature change

We show examples of excitation propagation when RP was stimulated. The initial excitation in RP propagated to preBötC/VRG as well as to a surface portion of the spinocerebellar tract (SCT). Hyperpolarization was detected in RTN (Fig. 1).

In *en bloc* preparations, neuronal activities synchronized with C4 inspiratory output were detected mainly in a columnar region on VMS extending from pFRG/RTN to preBötC/VRG. Various response patterns were found in these regions when superfusate CO_2 fraction was elevated from 5% to 8%. We will report the data obtained in *en bloc* preparations separately (original article in submission).

4 Discussion

In the present study, we applied a voltage-imaging technique to the analysis of neuronal network organization involved in central chemosensitivity. In slice preparations, we visually demonstrated the functional connection from the superficial ventral medullary regions to preBötC/VRG. In *en bloc* preparations, we succeeded to analyze the effects of CO_2 on the spatiotemporal profiles in the respiratory neuronal network. Our results are in agreement with previous anatomical and functional studies that showed connection from the superficial ventral medullary regions to deep respiratory neuronal network. It is interesting to find that RTN is hyperpolarized by electrical stimulation of other superficial medullary

chemosensitive regions. This finding is consistent with the report that RTN neurons receive respiratory synchronous inhibition from deep respiratory neuronal network (Guyenet, Mulkey, Stornetta and Bayliss 2005). We suggest that neurons in pFRG/RTN and preBötC/VRG are bidirectionally connected. These excitatory and inhibitory connections may contribute to the complex feedback control of respiratory chemosensitivity.

We previously proposed that small cells surrounding penetrating ariterioles in MGL are chemoreceptor cell candidates (Okada, Chen, Jiang, Kuwana and Eldridge 2002; Okada, Kuwana, Oyamada and Chen 2006). Based on our previous and present studies, as well as on the reports by others, here we propose a chemosensitive neuronal network model (Fig. 2). Primary chemoreceptor cells are located within thickened portions of MGL often beneath surface vessels and surround entry portions of penetrating arterioles for sensing perivascular CO_2/H+ (Bradley, Pieribone, Wang, Severson, Jacobs and Richerson 2002; Okada *et al*. 2002). Subsurface relay neurons project dendrites to MGL, contact primary chemoreceptor cells and transmit the amplified information to preBötC/VRG (Okada, Chen and Kuwana 2001b). Some of these relay neurons and preBötC/VRG respiratory neurons are intrinsically chemosensitive (Kawai, Ballantyne, Mückenhoff and Scheid 1996; Kawai, Onimaru and Homma 2006; Nattie and Li 1996), although caudal VRG neurons are not chemosensitive (Mitchell and Herbert 1974). We conclude that VMS is the primary site for central chemoreception and that mutually connected superficial ventral medullary and preBötC/VRG neurons compose the chemosensitive neuronal network.

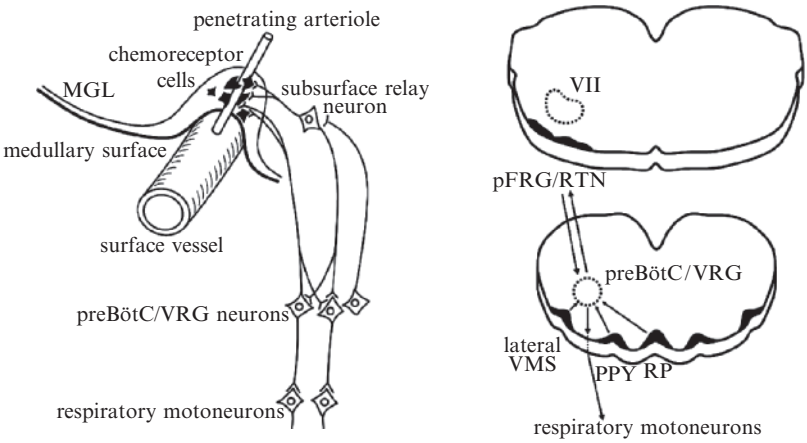

Fig. 2 Chemosensitive neuronal network model. Chemoreceptor cells within MGL beneath a surface vessel surround an entry portion of a penetrating arteriole. Information detected in pFRG/RTN and other superficial medullary regions (*e.g*., lateral VMS, PPY and RP) is transmitted to preBötC/VRG neurons that are bidirectionally connected with pFRG/RTN neurons

References

Bradley, S.R., Pieribone, V.A., Wang, W., Severson, C.A., Jacobs, R.A. and Richerson, G.B. (2002) Chemosensitive serotonergic neurons are closely associated with large medullary arteries. Nat. Neurosci. 5, 401–412.

Coates, E.L., Li, A. and Nattie, E.E. (1993) Widespread sites of brain stem ventilatory chemoreceptors. J. Appl. Physiol. 75, 5–14.

Fukuda, K., Okada, Y., Yoshida, H., Aoyama, R., Nakamura, M., Chiba, K. and Toyama, Y. (2006). Ischemia-induced disturbance of neural network function in the rat spinal cord analyzed by voltage-imaging. Neuroscience 140, 1453–1465.

Guyenet, P.G., Mulkey, D.K., Stornetta, R.L. and Bayliss, D.A. (2005) Regulation of ventral surface chemoreceptors by the central respiratory pattern generator. J. Neurosci. 25, 8938–8947.

Ito, Y., Oyamada, Y., Okada, Y., Hakuno, H., Aoyama, R. and Yamaguchi, K. (2004) Optical mapping of pontine chemosensitive regions of neonatal rat. Neurosci. Lett. 366, 103–106.

Kawai, A., Ballantyne, D., Muckenhoff, K. and Scheid, P. (1996) Chemosensitive medullary neurones in the brainstem–spinal cord preparation of the neonatal rat. J. Physiol. 492, 277–292.

Kawai, A., Onimaru, H. and Homma, I. (2006) Mechanisms of CO2/H^+ chemoreception by respiratory rhythm generator neurons in the medulla from newborn rats *in vitro*. J. Physiol. 572, 525–537.

Loeschcke, H.H. (1982) Central chemosensitivity and the reaction theory. J. Physiol. 332, 1–24.

Mitchell, R.A. and Herbert, D.A. (1974) The effect of carbon dioxide on the membrane potential of medullary respiratory neurons. Brain Res. 75, 345–349.

Nattie, E.E. and Li, A. (1996) Central chemoreception in the region of the ventral respiratory group in the rat. J. Appl. Physiol. 81, 1987–1995.

Okada, Y., Mückenhoff, K. and Scheid, P. (1993) Hypercapnia and medullary neurons in the isolated brain stem-spinal cord of the rat. Respir. Physiol. 93, 327–336.

Okada, Y., Chen, Z., Yoshida, H., Kuwana, S., Jiang, W. and Maruiwa, H. (2001a) Optical recording of the neuronal activity in the brainstem-spinal cord: application of a voltage-sensitive dye. Adv. Exp. Med. Biol. 499, 113–118.

Okada, Y., Chen, Z. and Kuwana, S. (2001b) Cytoarchitecture of central chemoreceptors in the mammalian ventral medulla. Respir. Physiol. 129, 13–23.

Okada, Y., Chen, Z., Jiang, W., Kuwana, S. and Eldridge, F.L. (2002) Anatomical arrangement of hypercapnia-activated cells in the superficial ventral medulla of rats. J. Appl. Physiol. 93, 427–439.

Okada, Y., Chen, Z., Jiang, W., Kuwana, S. and Eldridge, F.L. (2004) Functional connection from the surface chemosensitive region to the respiratory neuronal network in the rat medulla. Adv. Exp. Med. Biol. 551, 45–51.

Okada, Y., Kuwana, S., Oyamada, Y. and Chen, Z. (2006) The cell-vessel architecture model for the central respiratory chemoreceptor. Adv. Exp. Med. Biol. 580, 233–238.

Onimaru, H. and Homma, I. (2003) A novel functional neuron group for respiratory rhythm generation in the ventral medulla. J. Neurosci. 23, 1478–1486.

Rosin, D.L., Chang, D.A. and Guyenet, P.G. (2006) Afferent and efferent connections of the rat retrotrapezoid nucleus. J. Comp. Neurol. 499, 64–89.

Smith, J.C., Morrison, D.E., Ellenberger, H.H., Otto, M.R. and Feldman, J.L. (1989) Brainstem projections to the major respiratory neuron populations in the medulla of the cat. J. Comp. Neurol. 281, 69–96.

Part X
Brainstem Mechanisms Underlying Cardio-Respiratory Control

63
The Effects of a Respiratory Acidosis on Human Heart Rate Variability

S.J. Brown[1] and R. Howden[2]

Abstract Human heart rate variability (HRV) was examined during a mild respiratory acidosis induced by inhalation of a normoxic hypercapnic gas mixture. On two separate occasions, separated by 72 but not more than 120 hr, ECG was recorded from 9 normotensive subjects during supine rest. ECG was recorded for 20 min breathing room air or a 5% CO_2 in normoxic air mixture. Expired V'E, O_2 and CO_2 were measured with breath-by-breath mass spectrometry. HRV spectra were calculated using a Welch averaged periodogram method and banded as Very Low Frequency (VLF: 0 – 0.04 Hz), Low Frequency (LF: 0.04 – 0.15 Hz), and High Frequency (HF: 0.15 – 0.4 Hz). Student paired samples t-tests were used to compare room air (RA) versus inhaled 5% CO_2 in air (5% CO_2) data. All results reported as mean +/– SD. In the HRV time domain, hypercapnic normoxia reduced mean r-r intervals (5% CO_2: 956.1 ± 149.2 *vs*. RA: 1035 ± 146.8 ms, p = 0.022) and median r-r intervals (5% CO_2: 942.6 ± 153.1 *vs*. RA: 1047.8 ± 157.3 ms, p = 0.010), and increased heart rates (5% CO_2: 64.4 ± 12 *vs*. RA: 59.3 ± 10.1 bpm, p = 0.019). In the HRV frequency domain, hypercapnic normoxia increased the high frequency component of HRV (5% CO_2: 9799 ± 7649 *vs*. RA: 4399 ± 3857 ms^2, p = 0.004) and reduced the LF/HF ratio (5% CO_2: 0.243 ± 0.145 *vs*. RA: 0.906 ± 0.672, p = 0.017). An incomplete ventilatory compensation probably accounts for the increased HF contribution. An increased heart rate with a mild respiratory acidosis may be caused by a vasodilator effect of elevated arterial PCO_2, stimulating the increase in heart rate to maintain blood pressure.

1 Introduction

The analysis of human heart rate variability (HRV) potentially identifies the inherent rhythmic fluctuations in efferent and vagal outflow directed at the sinus node. Very low frequencies (VLF) in the range 0 – 0.04 Hz, low frequencies (LF) in the

[1] Massey University, Auckland, NZ, s.j.brown@massey.ac.nz

[2] Laboratory of Respiratory Biology, National Institute of Environmental Health Sciences, Research Triangle Park, North Carolina 27709, USA.

M.J. Poulin and R.J.A. Wilson (eds.), *Integration in Respiratory Control: From Genes to Systems*.

range 0.04 – 0.15 Hz, and higher frequencies (HF) in the range 0.15 – 0.4 Hz are present in the normal human heart rate (Akselrod, Gordon, Madwed, Snidman, Shannon and Cohen 1981; Task Force of the ECS 1996).

Frequency domain analysis of HRV has been used to suggest the cardiac autonomic balance by separating high frequency variation resulting from parasympathetic vagal modulation from low frequency variation, although data confirming the origins of HRV in the VLF, LF, and HF ranges remain equivocal.

The lower frequency component has been attributed to time delays in baroreceptor feedback (Malpas 2002), and it has been shown that an elevated arterial PCO_2 may increase carotid sinus baroreflex sensitivity (Hainsworth, Magregor, Rankin, and Soladoye 1984). The magnitude of the LF component of human muscle sympathetic nerve activity increased with progressive baroreceptor unloading (induced by whole body head-up tilting); however, the LF power in the r-r interval spectra remained unchanged and power in the HF range decreased (Cooke, Hoag, Crossman, Kuusela, Tahvanainen and Eckberg 1999). This suggested that low frequency oscillations in HRV may be independent of baroreceptor activity.

The higher frequency component has been attributed to a respiratory sinus arrhythmia, such that breathing frequencies in the range 12–18 breaths min^{-1} (0.2 – 0.3 Hz) manifest as peaks in the HF range, and if breathing frequency changes to 9 breaths min^{-1} (0.15 Hz), this may start to affect the LF component. However, previous studies (Goupolpoulou, Heffernan, Fernhall, Yates, Baxter-Jones and Unnithan 2006; James, Barnes, Lopes and Wood 2001) during which breathing rate was controlled at 15 and 12 breaths min^{-1}, did not report an increased contribution to the ECG frequency spectra at 0.25 and 0.2 Hz. Similarly, others (Parekh and Lee 2005; Takahashi, Okada, Hayano and Tamura 2002; Uusitalo, Laitinen, Vaisanen, Lansimies and Rauramaa 2004) allowed for spontaneous voluntary ventilation during post-exercise ECG spectral analysis and did not report significant changes in the HRV high frequency component.

The present study examined the autonomic neural control of the heart rate during a mild respiratory acidosis using the HRV technique. The respiratory acidosis was induced by inhalation of a normoxic hypercapnic gas mixture. It was hypothesized that during elevated steady-state ventilation, there would be a reduced variability in the heart rate attributable to an increased high frequency component.

2 Methods

On two separate occasions, separated by 72 but not more than 120 hr, ECG was recorded from nine normotensive subjects during supine rest. Subjects were at least 2 hr post-prandial, did not consume drinks containing caffeine for at least 2 hr before testing, and had not exercised for the preceding 12-hr period. All subjects were asked to maintain their normal dietary habits throughout the study. Subjects' ECG (limb lead 2, PowerLab 8SP, AD Instruments) were recorded with a sampling frequency of 1000 Hz (Chart version 5, AD Instruments) for 20 min during which

they breathed either room air or a 5% CO_2 in normoxic air mixture. Ventilation and expired gas were continuously analysed for O_2 and CO_2 content using breath-by-breath mass spectrometry (Pulmolab EX670, Morgan Medical Ltd, UK).

Heart rate variability was assessed using the final 5 min of the 20-min recording period using commercially-available software (HRV Module for Chart 5, AD Instruments). Intervals between adjacent r waves were detected using a threshold detection of between 0.5 and 1.0 mV, and classified as artifact (less than 5 ms and greater than 2000 ms), ectopic (between 5 ms and 400 ms, and between 1500 ms and 2000 ms), and normal (between 400 ms and 1500 ms). HRV spectra were calculated using a Welch averaged periodogram method and have been banded as Very Low Frequency (VLF: 0 – 0.04 Hz), Low Frequency (LF: 0.04 – 0.15 Hz), and High Frequency (HF: 0.15 – 0.4 Hz).

Student paired samples t-tests were used to compare room air versus inhaled 5% CO_2 in air data, where significance was $p < 0.05$.

3 Results

Pulmonary ventilation increased from 5.5 ± 0.5 L min^{-1} during supine rest to 15.0 ± 0.5 L min^{-1} after 15 min of breathing the 5% CO_2 in normoxic air. The ventilatory response, when averaged for 15 s epochs, was modelled by a 6th order polynomial, returning a coefficient of determination of 0.98. The ventilatory response appeared to have reached a new elevated steady state after 15 min, and during the following 5-min period, the heart rate also demonstrated stationarity.

In the HRV time domain, the hypercapnic normoxia significantly reduced mean r-r intervals (5% CO_2: 956.1 ± 149.2 *vs*. RA: 1035 ± 146.8 ms, $p = 0.022$) and median r-r intervals (5% CO_2: 942.6 ± 153.1 *vs*. RA: 1047.8 ± 157.3 ms, $p = 0.010$), and increased heart rates (5% CO_2: 64.4 ± 12 *vs*. RA: 59.3 ± 10.1 beats min^{-1}, $p = 0.019$).

In the HRV frequency domain, the hypercapnic normoxia significantly increased the high frequency component of HRV (5% CO_2: 9799 ± 7649 *vs*. RA: 4399 ± 3857 ms^2, $p = 0.004$) and reduced the LF/HF ratio (5% CO_2: 0.243 ± 0.145 *vs*. RA: 0.906 ± 0.672, $p = 0.017$).

4 Discussion

The reduced LF/HF ratio with a mild respiratory acidosis can be attributed to an increased high frequency component with no significant change in the low frequency component. Increases in pulmonary ventilation induced by the respiratory acidosis probably account for the increased HF contribution.

In conscious healthy human volunteers, adding CO_2 to the inspiratory gas increased both the HF and LF components of HRV (Poyhonen, Syvaoja,

Hartikainen, Ruokonen and Takala 2004). These authors suggested that cortical modulation of the autonomic nervous system activity by elevated arterial PCO_2 probably caused the changes in HRV. Data from the present study do not indicate changes in the low frequency component of HRV during a mild respiratory acidosis, contrary to the findings of Poyhonen *et al*. (2004). Recording no significant changes in the LF component of HRV with a mild respiratory acidosis may also suggest that elevated arterial PCO_2 may not be influencing baroreceptor sensitivity, as suggested by Hainsworth *et al*. (1984). However, there is some doubt as to the ability of the HRV technique to isolate the influence of baroreceptor feedback on r-r interval variability, and the possibility of an undetermined origin for the VLF and LF frequency components of HRV remains (Cooke *et al*. 1999).

An increased heart rate with a mild respiratory acidosis may be caused by the vasodilatory effect of elevated arterial PCO_2, stimulating the increase in heart rate to maintain blood pressure. Peripheral vasodilation induced by the mild respiratory acidosis would decrease total peripheral resistance, necessitating an increase in cardiac output to maintain mean arterial pressure. An increase in the respiratory pump with elevated minute ventilation may have increased central venous pressure and probably increased stroke volume, thereby limiting the heart rate increase required for blood pressure homeostasis. However, in the present study, the contribution to pulmonary vascular resistance induced by an elevated CO_2 content in the inspiratory gas, and subsequent influences on pulmonary perfusion and arterial pressure within the lung, remain unknown.

References

Akselrod, S., Gordon, D., Madwed, J., Snidman, N., Shannon, D. and Cohen, R. (1981) Power spectrum analysis of heart rate fluctuations: a quantitative probe of beat–to–beat cardiovascular control. Science 213, 220–222.

Cooke, W.H., Hoag, J.B., Crossman, A.A., Kuusela, T.A., Tahvanainen, K.U.O. and Eckberg, D. (1999) Human responses to upright tilt: a window on central autonomic integration. J. Physiol. 517, 617–628.

Goulopoulou, S., Heffernan, K., Fernhall, B., Yates, G., Baxter-Jones, A. and Unnithan, V. (2006) Heart rate variability during recovery from a Wingate test in adolescent males. Med. Sci. Sports Exerc. 38(5), 875–881.

Hainsworth, R., Magregor, K.H., Rankin, A.J. and Soladoye, A.O. (1984) Cardiac inotropic responses from changes in carbon dioxide tension in the cephalic circulation of anaesthetized dogs. J. Physiol. 357, 23–25.

James, D., Barnes, A., Lopes, P. and Wood, P. (2002) Heart rate variability: Response following a single bout of interval training. Int. J. Sports Med. 23, 247–251.

Malpas, S. (2002) Neural influences on cardiovascular variability: possibilities and pitfalls. Am. J. Physiol. 282, H6–H20.

Parekh, A. and Lee, C. (2005) Heart rate variability after isocaloric exercise bouts of different intensities. Med. Sci. Sports Exerc. 37(4), 599–605.

Poyhonen, M., Syvaoja, S., Hartikainen, J., Ruokonen, E. and Takala, J. (2004) The effect of carbon dioxide, respiratory rate and tidal volume on human heart rate variability. Acta Anaesthesiol. Scand. 48(1), 93–101.

Takahashi, T., Okada, A., Hayano, J. and Tamura, T. (2002) Influence of cool-down exercise on autonomic control of heart rate during recovery from dynamic exercise. Frontiers Med. Biol. Eng. 11(4), 249–259.

Taskforce of the European Society of Cardiology and North American Society of Pacing and Electrophysiology (1996) Heart rate variability (standards of measurement, physiological interpretation and clinical use). Circulation 93, 1043–1065.

Uusitalo, A., Laitinen, T., Vaisanen, S., Lansimies, E. and Rauramaa, R. (2004) Physical training and heart rate and blood pressure variability: a 5-yr randomized trial. Am. J. Physiol. – Heart Circ. Physiol. 286, H1821–H1826.

64
Neurokinin-1 Receptor Activation in the Bötzinger Complex Evokes Bradypnea and is Involved in Mediating the Hering-Breuer Reflex

Angelina Y. Fong[1] and Jeffrey T. Potts[2]

Abstract The role of substance P (SP) and its receptor, the neurokinin-1 (NK1R), in the generation of respiratory rhythm has received considerable attention, particularly at the Pre-Bötzinger Complex of the ventral respiratory group (VRG). However, the functional role of SP and NK1R in other VRG regions has not been explored in detail. We review the current literature and describe recent data demonstrating that selective activation of NK1R in the Bötzinger Complex (BötC) of the VRG evoked bradypnea by lengthening expiratory period. In addition, endogenous activation of NK1R in the BötC participates in the expiratory lengthening effect of the Hering-Breuer reflex. These data suggest that NK1R expressing neurons in different subregions of the VRG have functionally diverse roles and provide new insight on the modulatory role of SP on respiratory reflexes.

1 Neurokinin-1 Receptor (NK1R) and Respiratory Control

Breathing is an ongoing activity that must adapt to environmental stimuli and is continually modulated by a host of different afferent inputs. A number of brainstem regions are involved in the control of respiration and are integral to the generation of respiratory rhythm, including the ventral respiratory group (VRG), which is typically divided into four rostrocaudal compartments; Bötzinger complex (BötC), PreBötzinger complex (PreBötC), rostral VRG (rVRG) and caudal VRG (cVRG, (Feldman and McCrimmon 2003). These subregions can be distinguished electrophysiologically (Schwarzacher, Wilhelm, Anders and Richter 1991) and functionally, as chemical activation of these subregions elicit distinct functional responses (Monnier, Alheid and McCrimmon 2003).

A variety of neurotransmitters and neuromodulators participate in the central control of respiration, including the neuropeptide substance P (SP) and its receptor,

[1] University of British Columbia, Department of Zoology and University of Missouri, Dalton Cardiovascular Research Center, fong@zoology.ubc.ca

[2] University of Missouri, Department of Biomedical Science & Dalton Cardiovascular Research Center, pottsjt@missouri.edu

M.J. Poulin and R.J.A. Wilson (eds.), *Integration in Respiratory Control: From Genes to Systems*. © Springer 2008

neurokinin-1 (NK1R). Exogenous SP excites respiratory activity *in vivo* (Hedner, Hedner, Wessberg and Jonason 1984) and *in vitro* (Monteau, Ptak, Broquere and Hilaire 1996; Morgado-Valle and Feldman 2004). NK1R expressing neurons are found throughout the VRG with the greatest concentration in the PreBötC (Guyenet, Sevigny, Weston and Stornetta 2002). Activation of NK1R in the PreBötC by exogenous SP increases respiratory frequency (Gray, Rekling, Bocchiaro and Feldman 1999) and endogenous SP in the PreBötC appears to be essential for the generation of respiratory rhythm (Morgado-Valle and Feldman 2004). In addition, selective ablation of NK1R expressing neurons in the PreBötC disrupts basal respiratory rhythm (Gray, Janczewski, Mellen, McCrimmon and Feldman 2001; Wenninger, Pan, Klum, Leekley, Bastastic, Hodges, Feroah, Davis and Forster 2004). Collectively, these studies demonstrate an important functional role of SP and NK1R expressing neurons in the PreBötC. However, the role of NK1R and SP in other subregions of the VRG, including the BötC remains unclear.

1.1 NK1R in the Bötzinger Complex (BötC)

A number of previous studies demonstrated that NK1R activation in the rostral ventrolateral medulla decreases respiratory frequency (Chen, Hedner and Hedner 1990b; Makeham, Goodchild and Pilowsky 2005). While these studies suggest that NK1R activation in regions around the BötC may slow respiratory rhythm, the large injection volumes used (50–100 nl) in these studies preclude the precise localization of the site of action. Thus, the effect of NK1R activation in the BötC remained unclear.

In a recent study, we examined the effect of NK1R activation using discrete microinjections of a selective NK1R agonist [Sar^{9}-$Met(O_2)^{11}$]-SP (SSP) into the BötC (Fong and Potts 2006). Microinjection sites were electrophysiologically identified expiratory regions and were confirmed functionally using the glutamate receptor agonist DL-homocysteic acid (DLH), as a bradypneic site corresponding to BötC (Fig. 1A, 1B). We showed that small microinjections of SSP (6 pmol in 6 nl) into the BötC evoked bradypnea, mediated exclusively by a 53% lengthening of expiratory duration (T_E) with a 2-fold increase in post-inspiratory period (Post-I) determined by recordings from the cervical vagus nerve (Fig. 1C). No effect was observed on late expiratory or inspiratory times. The effect of NK1R activation was specific to the BötC since SSP microinjection into the adjacent PreBötC evoked tachypnea (Fong & Potts 2006), similar to previous reports using DLH microinjection (Monnier *et al*. 2003; Wang, Germanson and Guyenet 2002). Therefore, these data demonstrate that selective activation of NK1Rs in the BötC excites expiration.

This is the first report to demonstrate that discrete activation of NK1R expressing neurons in the BötC evokes bradypnea. Previously, we demonstrated that picoejection of SSP increased the discharge rate of a subpopulation of expiratory BötC neurons which could be prevented by pretreatment with a selective NK1R antagonist (Fong and Potts 2004). These findings indicate that expiratory BötC neurons, in addition to pre-inspiratory neurons in the PreBötC (Guyenet and Wang

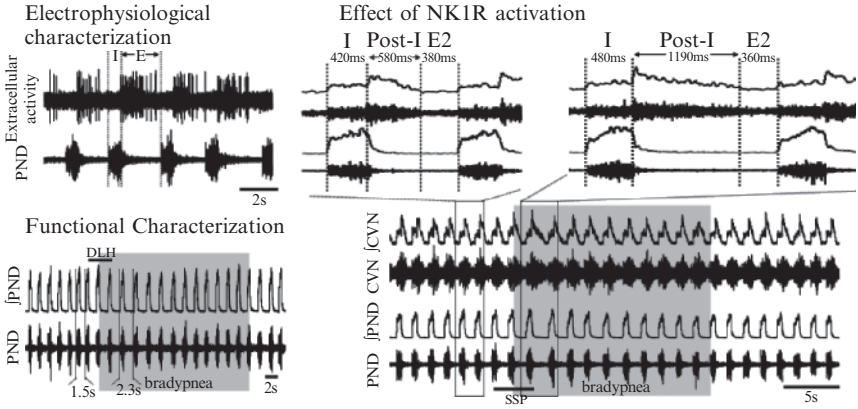

Fig. 1 (A) In an electrophysiologically identified expiratory region, corresponding to the Bötzinger Complex, (B) chemical activation by DLH microinjection (horizontal bar), evoked bradypnea (shaded area) as determined by the time between phrenic nerve discharge (PND). (C) In the same site, microinjection of a selective neurokinin-1 receptor agonist, [Sar^{9}-$Met(O_2)^{11}$]-substance P (SSP, horizontal bar) evoked bradypnea (shaded area) by increasing post-inspiratory period (post-I) with no effect on inspiratory (I) or late expiration (E2) periods, as determined by measurements of the cervical vagus nerve (CVN)

2001), express NK1R and suggest that SP in BötC may function as a timing mechanism in the generation of respiratory rhythm.

2 Functional Role of NK1R in the Bötzinger Complex

Our recent finding that activation of NK1R in BötC excites expiration, likely by direct activation of expiratory neurons raises the question: Under what physiological condition(s) would SP and NK1Rs in the BötC control respiration? In the brainstem, SP and NK1Rs are involved in mediating a range of respiratory reflex responses, including hypoxia, hypercapnia, somatosensory stimulation and lung afferent input, such as the Hering-Breuer (H-B) reflex (Chen, Hedner and Hedner 1990a; Mutoh, Bonham and Joad 2000; Nattie and Li 2002; Potts, Paton, Mitchell, Garry, Kline, Anguelov and Lee 2003). However, there is no direct evidence for the involvement of SP and NK1R expressing neurons in respiratory reflexes at the level of the BötC.

To identify a physiological role for neurokinin signaling in the BötC, we focused on the H-B reflex for several reasons: (1) the BötC is involved in the H-B reflex (Hayashi, Coles and McCrimmon 1996); (2) H-B reflex activation selectively lengthens post-I duration (Hayashi *et al*. 1996); (3) SP mediates the H-B reflex pathway at the level of the NTS (Mutoh *et al*. 2000); and (4) NK1R activation in the BötC mimics H-B reflex activation. Thus, we speculated that NK1R activation in the BötC may be involved in the expiratory lengthening effect of the H-B reflex.

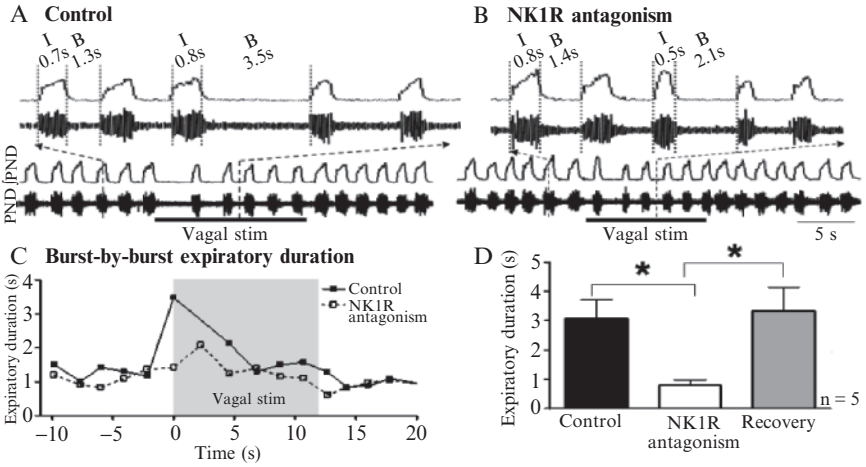

Fig. 2 (A) Electrical stimulation of the vagus nerve reduced phrenic nerve (PND) discharge frequency by extending expiratory (*E*) period; (B) which was reduced following neurokinin-1 receptor (NK1R) antagonism in the Bötzinger complex. Inspiratory period (I) was not altered. (C) Burst-by-burst plot of expiratory duration for the examples illustrated in panels A and B. (D) Group data on the effect of NK1R blockade on extension of expiratory duration produced by the Hering-Breuer Reflex

We hypothesized that the expiratory lengthening component of the H-B reflex required NK1R activation in the BötC (Fong and Potts 2006) and tested this hypothesis by simulating the H-B reflex using unilateral electrical stimulation of the vagus nerve. Vagus nerve stimulation produced a 3-fold increase in T_E (Fig 2A).

Blockade of NK1Rs in the BötC using CP99,994 reduced the vagally mediated extension of T_E by 70% compared to control stimulus (Fig. 2B-2D). This finding indicates that activation of the H-B reflex evokes endogenous release of SP in the BötC that, in turn, activates NK1R expressing neurons to inhibit inspiration. These data provide the first functional evidence demonstrating that SP activation of NK1Rs in the BötC participates in the excitation of expiratory neurons in the H-B reflex.

3 Concluding Remarks

The neuropeptide SP and NK1R activation in the VRG exerts powerful and functionally diverse effects on respiratory rhythm. Our recent data (Fong and Potts 2006) indicates that NK1R expressing neurons in the BötC exert important modulatory effects on respiratory rhythm, in addition to the vital role NK1R expressing neurons play in the PreBötC in generation basal respiratory rhythm generation. Moreover, we have shown that activation of the H-B reflex evokes endogenous SP release in the BötC that is necessary to inhibit inspiration and lengthen expiration.

References

Chen, Z., Hedner, J. and Hedner, T. (1990a) Substance P in the ventrolateral medulla oblongata regulates ventilatory responses. J. Appl. Physiol. 68, 2631–2639.

Chen, Z.B., Hedner, J. and Hedner, T. (1990b) Local effects of substance P on respiratory regulation in the rat medulla oblongata. J. Appl. Physiol. 68, 693–699.

Feldman, J.L. and McCrimmon, D.R. (2003) Neural control of breathing. In: L.R. Squire, F.E. Bloom, S.K. McConnell, J.L. Roberts, N.C. Spitzer and M.J. Zigmond (Ed.), *Fundamental Neuroscience*. Academic Press, New York, pp. 967–990.

Fong, A.Y. and Potts, J.T. (2004) Substance P modulation of ventral respiratory group neurons. FASEB J. (Abstracts) 18, 222.3.

Fong, A.Y. and Potts, J.T. (2006) Neurokinin-1 receptor activation in Botzinger complex evokes bradypnea. J. Physiol. 575, 869–886.

Gray, P.A., Janczewski, W.A., Mellen, N., McCrimmon, D.R. and Feldman, J.L. (2001) Normal breathing requires preBotzinger complex neurokinin-1 receptor-expressing neurons. Nat. Neurosci. 4, 927–930.

Gray, P.A., Rekling, J.C., Bocchiaro, C.M. and Feldman, J.L. (1999) Modulation of respiratory frequency by peptidergic input to rhythmogenic neurons in the preBotzinger complex. Science 286, 1566–1568.

Guyenet, P.G., Sevigny, C.P., Weston, M.C. and Stornetta, R.L. (2002) Neurokinin-1 receptor-expressing cells of the ventral respiratory group are functionally heterogeneous and predominantly glutamatergic. J. Neurosci. 22, 3806–3816.

Guyenet, P.G. and Wang, H. (2001) Pre-Botzinger neurons with preinspiratory discharges *in vivo* express NK1 receptors in the rat. J. Neurophysiol. 86, 438–446.

Hayashi, F., Coles, S.K. and McCrimmon, D.R. (1996) Respiratory neurons mediating the Breuer-Hering reflex prolongation of expiration in rat. J. Neurosci. 16, 6526–6536.

Hedner, J., Hedner, T., Wessberg, P. and Jonason, J. (1984) Interaction of substance P with the respiratory control system in the rat. J. Pharmacol. Exp. Ther. 228, 196–201.

Makeham, J.M., Goodchild, A.K. and Pilowsky, P.M. (2005) NK1 receptor activation in rat rostral ventrolateral medulla selectively attenuates somato-sympathetic reflex while antagonism attenuates sympathetic chemoreflex. Am. J. Physiol. 288, R1707–R1715.

Monnier, A., Alheid, G.F. and McCrimmon, D.R. (2003) Defining ventral medullary respiratory compartments with a glutamate receptor agonist in the rat. J. Physiol. 548, 859–874.

Monteau, R., Ptak, K., Broquere, N. and Hilaire, G. (1996) Tachykinins and central respiratory activity: an *in vitro* study on the newborn rat. Eur. J. Pharmacol. 314, 41–50.

Morgado-Valle, C. and Feldman, J.L. (2004) Depletion of substance P and glutamate by capsaicin blocks respiratory rhythm in neonatal rat *in vitro*. J. Physiol. 555, 783–792.

Mutoh, T., Bonham, A.C. and Joad, J.P. (2000) Substance P in the nucleus of the solitary tract augments bronchopulmonary C fiber reflex output. Am. J. Physiol. 279, R1215–R1223.

Nattie, E.E. and Li, A. (2002) Substance P-saporin lesion of neurons with NK1 receptors in one chemoreceptor site in rats decreases ventilation and chemosensitivity. J. Physiol. 544, 603–616.

Potts, J.T., Paton, J.F., Mitchell, J.H., Garry, M.G., Kline, G., Anguelov, P.T. and Lee, S.M. (2003) Contraction-sensitive skeletal muscle afferents inhibit arterial baroreceptor signalling in the nucleus of the solitary tract: role of intrinsic GABA interneurons. Neuroscience 119, 201–214.

Schwarzacher, S.W., Wilhelm, Z., Anders, K. and Richter, D.W. (1991) The medullary respiratory network in the rat. J. Physiol. 435, 631–644.

Wang, H., Germanson, T.P. and Guyenet, P.G. (2002) Depressor and tachypneic responses to chemical stimulation of the ventral respiratory group are reduced by ablation of neurokinin-1 receptor-expressing neurons. J. Neurosci. 22, 3755–3764.

Wenninger, J.M., Pan, L.G., Klum, L., Leekley, T., Bastastic, J., Hodges, M.R., Feroah, T., Davis, S. and Forster, H.V. (2004) Small reduction of neurokinin-1 receptor-expressing neurons in the pre-Botzinger complex area induces abnormal breathing periods in awake goats. J. Appl. Physiol. 97, 1620–1628.

65
Brainstem Catecholaminergic Neurons Modulate both Respiratory and Cardiovascular Function

Aihua Li[1], Laura Emond[2] and Eugene Nattie[3]

Abstract Catecholamine neurons (CA) located in the brainstem project widely in the forebrain, hindbrain and spinal cord to many regions involved in the control of respiratory and cardiovascular function. For example, A6 noradrenergic neurons provide a tonic excitatory stimulus that maintains breathing frequency while A5 neurons provide an inhibitory influence on both cardiovascular and respiratory function to slow breathing frequency and heart rate. Mice with genetic defects that include CA neurons have abnormal respiration and blood pressure. For example, mice heterozygous for Phox2b with CA neuron defects have sleep-disordered breathing, and DBH knockout mice with absent CA cells centrally and peripherally have hypotension. Our hypothesis is that widespread brainstem CA neuron lesions in adult rats would significantly affect cardiorespiratory functions including breathing, chemoreception, blood pressure and heart rate. We produced the widespread brainstem CA neuron lesion by injecting anti-dopamine-β-hydroxylase-saporin (DBH-SAP) via the 4th ventricle. The lesioned group had a 64–84% loss of A5, A6 and A7 tyrosine hydroxylase immunoreactive (ir) neurons along with 56–64% loss of C1 and C2 phenyl ethanolamine-N methyltransferase (PNMT)-ir neurons over 2–3 weeks. The significant respiratory changes included: (1) a decreased breathing frequency during air and 7% CO_2 breathing in both wakefulness and non-REM (NREM) sleep; (2) a reduced ventilatory response to 7% CO_2 in wakefulness (−28%) and in NREM sleep (−26%); and (3) increased variability of breathing in REM sleep but not in wakefulness or NREM sleep. Significant cardiovascular changes at two weeks included: (1) an increased MAP by 11.7 mmHg in the room air resting condition; (2) an unaffected cardiovascular response to hypercapnia; and (3) a smaller decrease of MAP in response to hypoxia. Conclusions: Central CA neurons have a net excitatory effect on breathing and chemoreception but a net inhibitory effect on blood pressure.

[1–3] Department of Physiology, Dartmouth Medical School, Lebanon, NH, USA, Aihua.Li@dartmouth.edu, Laura.Edmon@dartmouth.edu, Eugene.nattie@dartmouth.edu

M.J. Poulin and R.J.A. Wilson (eds.), *Integration in Respiratory Control: From Genes to Systems*. © Springer 2008

1 Introduction

Catecholamines (CA) are important neurotransmitters in both the central and peripheral nervous systems. In the central nervous system, CA neurons located in the brainstem project widely to forebrain, hindbrain and spinal cord. Norepinephrine (NE) and epinephrine (EPI) not only modulate emotion, anxiety and neuronal excitability but also regulate the control of respiratory and cardiovascular function (Guyenet *et al*. 1993; Li and Nattie 2006; Schreihofer and Guyenet 2000). In the periphery, the sympathetic nervous system exerts widespread control, from cardiovascular regulation to energy balance. The principal neurotransmitter in the sympathetic nervous system is NE. Release of NE from sympathetic nerve terminals constricts arterioles, increases heart rate and contractility and constricts the abdominal vasculature (Carson and Robertson 2002).

Genetic alteration of either the formation of the CA neurons in the brain or of the biosynthesis of noradrenalin (NA) will directly or indirectly affect cardiorespiratory functions. For example, both Rnx- and Phox2a-deficient mice die within 24 hours after birth. Rnx mutants (with no A5, A1/C1 and A2/C2 but intact A6 CA neuron groups) have very high respiratory frequency and variable breath durations, while Phox2a mutants (with no A6 but intact A5, A1/C1 and A2/C2 CA neuron groups) have abnormally low breathing frequency and variable breath durations (Hilaire 2006). Dopamine-β-hydroxylase (DBH) deficient mice with complete lack of NE and EPI exhibit a slow heart rate and severe hypotension similar to DBH deficient patients (Swoap *et al*. 2004). Pharmacological manipulation and lesions of the central CA system can significantly alter cardiovascular and respiratory functions (Li and Nattie 2006; Schreihofer and Guyenet 2000).

We hypothesized that brainstem CA neurons: (1) produce an excitatory drive that affects breathing frequency and its variability, mean arterial blood pressure (MAP) as well as heart rate (HR), predominantly in wakefulness when these neurons are most active, and (2) participate in central chemoreception. To test these hypotheses, we produced widespread brainstem CA neuron lesions without affecting the peripheral CA system by injecting anti-DBH-SAP via the 4th ventricle of rats and measured ventilation, blood pressure and HR during sleep and wakefulness over 14–21 days.

2 Methods

The detailed methods have been described in our previous publication (Li and Nattie 2006). All the experiments were performed in conscious rats with pre-instrumented electroencephalogram (EEG), electromyogram (EMG) electrodes and a telemetry probe either for body temperature (TA-F20, DSI) or for electrocardiogram, arterial blood pressure and body temperature (PhysioTel C50-PXT, DSI). After at least 7 days' recovery from the surgery and baseline measurements, the rats received one microinjection (2.2 µl, 5 µg) of anti-DBH-SAP or IgG-SAP as control into the 4th ventricle of the brainstem. Ventilatory and mean arterial pressure

(MAP) and heart rate (MHR) data were collected before and 14 days after the drug injection. To evaluate the lesion effect, immunohistochemical staining for CA neurons of the brainstem are processed as we described previously. For analysis of physiological responses we used two-way repeated measures ANOVA with the physiological measure, say ventilation, as the repeated measures variable and state (awake, NREM sleep), treatment (IgG-SAP, DBH-SAP) and CO_2 (room air, 3% CO_2, 7% CO_2) as categorical variables.

3 Results

3.1 CA Cell Loss

Both experimental groups (the respiratory studies and the cardiovascular studies) have similar CA cell loss in the same brainstem regions as shown in Fig. 1, with a 64–84% loss of A5, A6 and A7 tyrosine hydroxylase immunoreactive (ir) neurons along with 56–64% loss of C1 and C2 phenyl ethanolamine-N methyltransferase (PNMT)-ir neurons over 2–3 weeks.

3.2 Cardiorespiratory Changes

3.2.1 Cardiorespiratory Changes During Room Air Breathing

There is a significant increase in MAP by 11.7 mmHg and a significant decrease in respiratory frequency in both wakefulness and NREM sleep in the room air breathing two weeks after the lesions. Ventilation and MHR were not significantly altered.

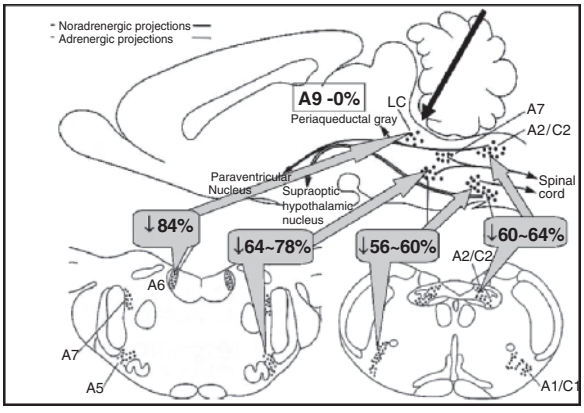

Fig. 1 Figure 1 shows the brainstem CA projections and cell loss at the four major brainstem CA groups after lesion. The arrow indicates the injection site

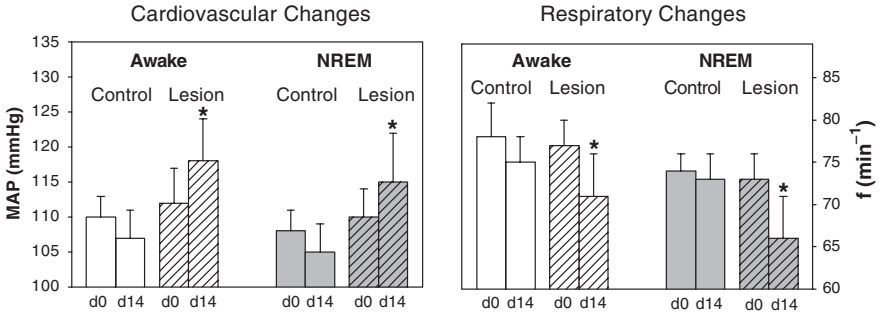

3.2.2 Cardiorespiratory Changes in Response to Hypercapnia

As shown in our previous published data (Li and Nattie 2006), the ventilatory response to 7% CO2 was reduced significantly in wakefulness (−28%) and in NREM sleep (−26%) 14 days after lesion, and the decrease was predominantly due to the respiratory frequency. MAP and MHR changes in response to hypercapnia were unaffected.

3.2.3 Cardiorespiratory Changes in Response to Hypoxia

The decreased response of MAP and MHR in response to hypoxia was lesser two weeks after lesion compared to control during both wakefulness and NREM sleep. These data were significant only when all the awake and NREM data were combined.

3.2.4 The Variability of Breath Duration Increased in REM Sleep But Not in Wakefulness or NREM Sleep after Lesion

To quantify the distribution of each breath, we used the parameters SD1, SD2 and the area of the ellipse that fits the distribution of points in a Poincare plot of breath duration (Li and Nattie 2006). In REM sleep, all parameters showed a significant increase after the lesions compare to baseline before the lesion.

4 Discussion

4.1 Brainstem Specific CA Lesion

Injection of anti-DBH-SAP directly into the 4th ventricle allowed us to effectively eliminate a majority of CA neurons in the brainstem including four major CA groups, A5 and A6 in the pons, and A1/C1 and A2/C2 in the medulla. Our anatomic

results are similar to those in the genetic knock-out mice for CA neurons, but in our experiments the CA neurons were deleted in the adulthood of the normal rat so there is no developmental issue involved. Further, the DBH deficient mice have the abnormalities in both central and peripheral CA system our brainstem CA neuron lesion is unlikely to affect the peripheral CA system.

4.2 Brainstem CA and Respiration

Studies have shown that A6 and A1/C1 provide an excitatory influence on the respiratory rhythm while A5 provides the opposite, an inhibitory influence (Hilaire 2006). The role of A2/C2 is not clear, they may contribute to the rhythm stability (Hilaire 2006); Rnx-, Phox2a- and Phox2b- deficient mice, with severely impaired central CA systems, die before or shortly after birth all with severe respiratory abnormalities including a highly irregular respiratory rhythm (Erickson *et al*. 1996; Hilaire 2006; Ide *et al*. 2005; Shirasawa *et al*. 2000). Our results show that substantial loss of brainstem CA neurons (1) significantly slow the breathing frequency during air and CO_2 breathing in adult rats in both wakefulness and NREM sleep, suggesting that brainstem CA neurons provide a tonic excitatory drive to maintain the normal respiratory frequency in both states in normal conditions; (2) significantly reduce the respiratory response to 7% CO_2 in both wakefulness and NREM sleep, suggesting that brainstem CA neurons are (directly or indirectly) involved in central chemoreception; and (3) significantly increase respiratory variability in REM sleep, not in wakefulness and NREM sleep, suggesting that modulation of respiration by the brainstem CA may be state dependent. Unlike the genetically-altered mice mentioned above, brainstem CA lesions in adult rats are not lethal; the influence of brainstem CA neurons on respiration may be more crucial in the early development stages than in adulthood.

4.3 Brainstem CA Neurons and Cardiovascular Functions

Brainstem CA neurons may affect cardiovascular function at rest and during stress. DBH knock-out mice, with complete central and peripheral absence of NE and EPI, have severe hypotension and slow HR and their MAP and HR response to stresses are blunted. Our brainstem CA lesions, with partial but substantial elimination of the brainstem CA neurons, produce a significant increase in MAP at rest. The changes of MAP and MHR in response to hypercapnia are unaffected, but there is a trend that the decrease of MAP and MHR in response to hypoxia are impaired. The different cardiovascular responses between the DBH deficient mice and our data can be explained at least partially by geographic differences. In rodents, the peripheral sympathetic branches of the autonomic nerve system play a dominant role in the regulation of chronic MAP (Del Bo *et al*. 1985). Our findings are a result

of central CA neuron dysfunction only, as those in the periphery were not altered. Our results also suggest that the central influences on cardiovascular function differ from the pressor modulation induced by peripheral CA neurons.

5 Summary and Significance

We conclude that in conscious rats brainstem CA neurons contribute to the regulation of respiration, including central chemoreception, and of cardiovascular functions, including blood pressure and heart rate. The MAP and MHR response to brainstem specific loss of CA neurons differs from that in DBH KO mice, which have both central and peripheral loss of CA neurons. Central CA neurons have a net excitatory effect on breathing frequency and chemoreception in wakefulness and NREM sleep and a stabilizing effect on breathing in REM but a net inhibitory effect on blood pressure.

Acknowledgement Supported by NIH R01 HL 28066 and P01-HD 36379.

References

Carson, R. and Robertson, D. (2002) Genetic manipulation of noradrenergic neurons. J. Pharmacol. Exp. Ther. 301, 410–417.

Del Bo, A., Le Doux, J. and Resi, D. (1985) Sympathetic nervous system and control of blood pressure during natural behaviour. J. Hypertens. Supp. 3, S105–S106.

Erickson, J., Conover, J., Borday, V., Champagnat, J., Barbacid, M., Yancopoulos, G. and Katz, D. (1996) Mice lacking brain-derived neurotrophic factor exhibit visceral sensory neuron losses distinct from mice lacking NT4 and display a severe developmental deficit in control of breathing. J. Neurosci. 16, 5361–5371.

Guyenet, P., Koshiya, N., Huangfu, D., Verberne, A. and Riley, T. (1993) Central respiratory control of A5 and A6 pontine noradrenergic neurons. Am. J. Physiol. 264, 1035–1044.

Hilaire, G. (2006) Endogenous noradrenaline affects the maturation and function of the respiratory network: possible implication for SIDS. Auton. Neurosci. 126–127, 320–331.

Ide, S., Itoh, M. and Goto, Y. (2005) Defect in normal developmental increase of the brain biogenic amine concentrations in the mecp2-null mouse. Neurosci. Lett. 386, 14–17.

Janssen, B. and Smits, J. (2002) Autonomic control of blood pressure in mice: basic physiology and effects of genetic modification. Am. J. Physiol. Regul. Integr. Comp. Physiol. 282, R1545–1564.

Li, A. and Nattie, E. (2006) Catecholamine neurones in rats modulate sleep, breathing, central chemoreception and breathing variability. J. Physiol. 570, 385–396.

Schreihofer, A. and Guyenet, P. (2000) Sympathetic reflexes after depletion of bulbospinal catecholaminergic neurons with anti-DBH-saporin. Am. J. Physiol. Regul. Integr. Comp. Physiol. 279, R729–R742.

Shirasawa, S., Arata, A., Onimaru, H., Roth, K., Brown, G., Horning, S., Arata, S., Okumura, K., Sasazuki, T. and Korsmeyer, S. (2000) Rnx deficiency results in congenital central hypoventilation. Nat. Genet. 24, 287–290.

Swoap, S., Weinshenker, D., Palmiter, R. and Garber, G. (2004) Dbh(-/-) mice are hypotensive, have altered circadian rhythms and have abnormal responses to dieting and stress. Am. J. Physiol. Regul. Integr. Comp. Physiol. 286, R108–113.

66
Responses of Brainstem Respiratory Neurons to Activation of Midbrain Periaqueductal Gray in the Rat

Hari Subramanian[1], Zheng-Gui Huang[2] and Ron Balnave[3]

1 Introduction

Eupneic breathing has been shown to be affected by output from the midbrain periaqueductal gray matter (PAG) (Huang *et al*. 2000; Hayward *et al*. 2003; Subramanian *et al*. 2007). In the rat, anatomical tracing studies have demonstrated connections between the PAG and other brainstem areas. It is generally accepted that PAG efferents activate descending pathways that originate in the medulla (Holstege 1991b). The aims of our studies were to isolate and record from respiratory cells in the ventral respiratory group (VRG) and the nucleus tractus solitarius (NTS) regions of the rat brainstem and to examine the changes in firing patterns and timing of these cells following excitatory amino acid (EAA) stimulation of the PAG. We also investigated the effect of β-adrenergic blockade in the vlNTS on the PAG induced respiratory patterning.

2 Methods

Sprague-Dawley rats (either sex, 350–450 g) were anaesthetised (pentabarbitol, 70 mg/kg, i.p.). Surgery to remove skull bone enabled access to the PAG and dorsal brainstem. Stereotaxically-guided extracellular electrode recordings were obtained from respiratory-related cells located in r-cVRG or vl and mNTS, obex referenced (Paxinos and Watson 1997). Microinjections of excitatory amino acid (0.2 M DLH) were made into the d, dl, l and vl PAG (30–60 nl), using glass micropipettes and pressure injection, bregma referenced (Paxinos and Watson 1997). Intramuscular stainless steel wire electrodes were used to record diaphragm, external intercostal

[1] UMCG, Center for Uroneurology, University of Groningen, Postbus 196, 9700 AD Groningen, The Netherlands, h.h.subramanian@med.umcg.nl

[2] Department of Pharmacology, Wannan Medical College, Wuhu City, 241001, P.R.China

[3] School of Biomedical Sciences, Faculty of Health Sciences, The University of Sydney, P.O.Box 170, Lidcombe, NSW 2141, Australia

M.J. Poulin and R.J.A. Wilson (eds.), *Integration in Respiratory Control: From Genes to Systems*. © Springer 2008

and abdominal muscle EMGs. Activity of respiratory-related cells was recorded during the activation of the PAG with DLH. Histology confirmed location of electrode tips. Positioning of electrode tip was by anodal lesion in the brainstem and by rhodamine beads, injected with DLH into PAG (Huang *et al*. 2000). Propanolol, a ß-antagonist (150 pmol) was pressure microinjected into vlNTS sites prior to DLH stimulation of the PAG.

3 PAG Stimulation and Respiratory Function

Stimulation of the dPAG led to increases in respiratory frequency (RF), with shortening of both Ti and Te (Fig. 1). DLH microinjections into more lateral and vlPAG resulted in a tachypneic response with dramatic changes to respiratory motor output and huge increases in diaphragm amplitude (Fig. 2). Recruitment of abdominal muscles was seen following PAG stimulation (Fig. 1).

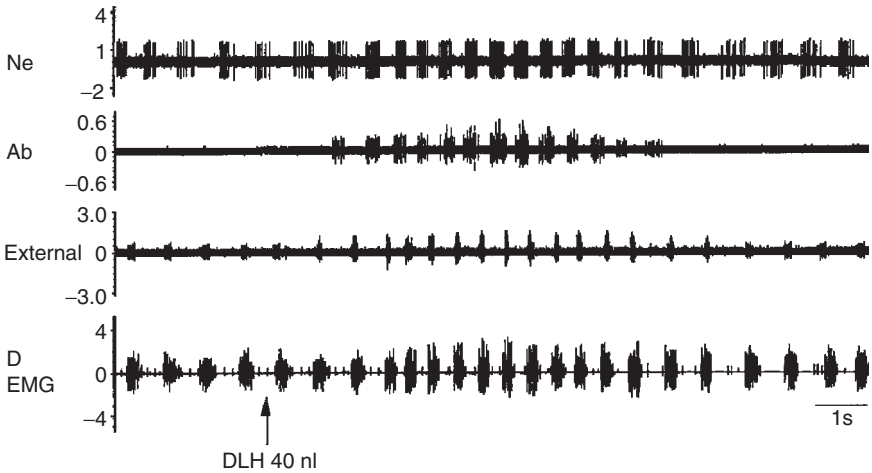

Fig. 1 Effects of DLH 40 nL microinjection into dlPAG on activities of abdominal, ext. intercostals, diaphram EMGs and on the firing of a neuron in r-cVRG. Ne, E-all neuron; ab, abd. muscle EMG; External, ext. intercostals EMG; Demg, diaphragm EMG

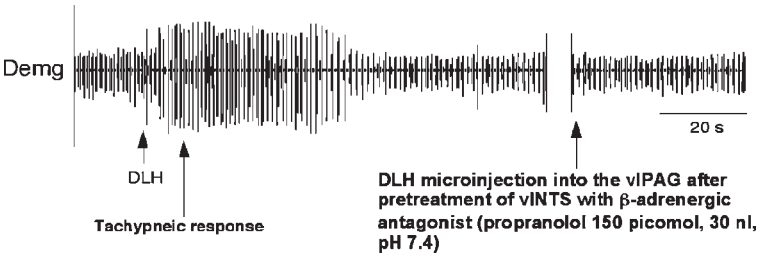

Fig. 2 Effect of stimulation of vlPAG with DLH (30 nl). Demg as before

4 β–adrenergic Blocker into vlNTS

The PAG-induced tachypnea could be blocked by prior microinjection of ß-adrenergic antagonist (propranolol 150 pmol, 30 nl, pH 7.4) into the vlNTS (Subramanian *et al*. 2007); *i.e*., DLH microinjections into vlPAG no longer induced tachypnea (Fig. 2). Propranolol, itself, injected into vlNTS did not significantly alter cardiorespiratory function in the absence of DLH.

5 Brainstem Respiratory Neurons

Six types of respiratory-related cells were stereotaxically isolated and recorded both in the r-cVRG as well as in the NTS. These were classified as early-I, late-I, I-all, early-E, late-E and E-all cells. The time course of their firing was determined by cycle-triggered histograms (CTH); a schematic is shown in Fig. 3. These cells were further sub-classified into decrementing or augmenting depending on their frequency discharge pattern (such as eI-dec, I-all-aug cells).

6 Responses of Respiratory Neurons to PAG Stimulation

All the respiratory cells increased their firing significantly in response to DLH stimulation of the dPAG, the increased frequency due to shortening of both Ti and Te. The relationship of each cell firing to the respiratory cycle was maintained

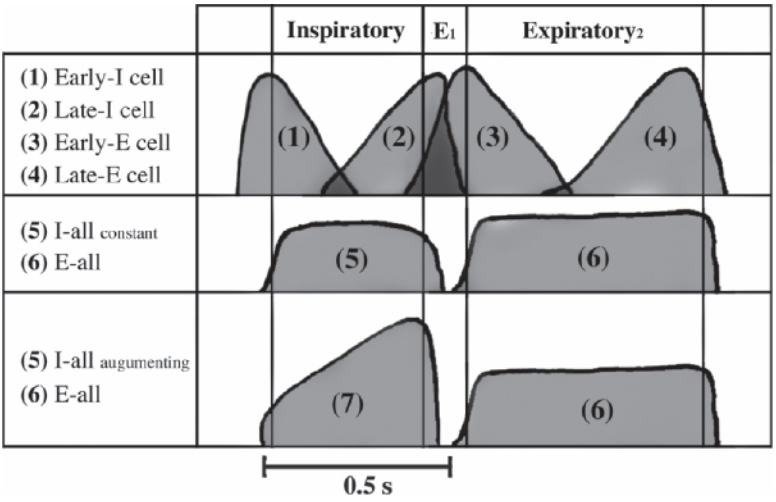

Fig. 3 Cell classification schematic.CTH: 15 ms bins, 30 sweeps

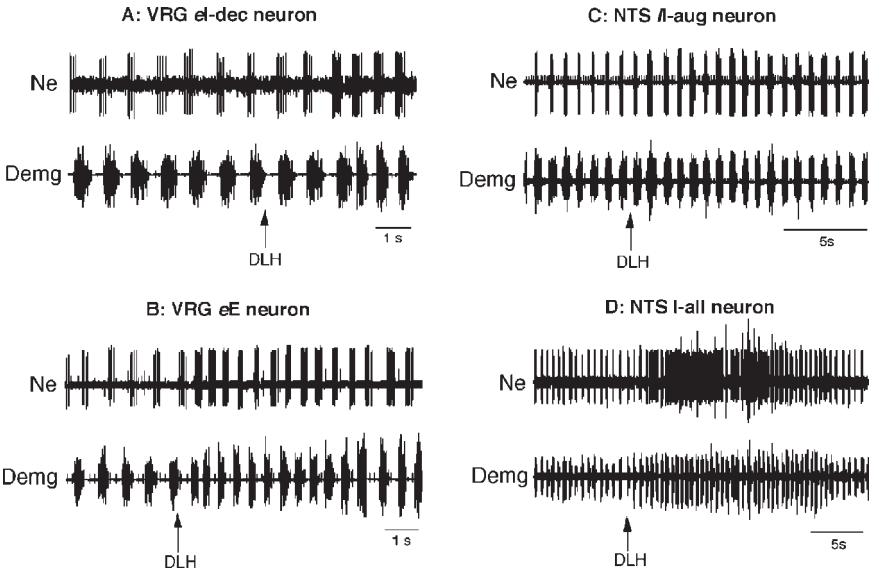

Fig. 4 Effects of DLH (30 nl) stimulation of dPAG on VRG and NTS respiratory neurons. Ne: neuron, Demg: diaphram EMG

except for I-all cells found in the vlNTS, which showed tonic activation occasionally. Figure 4 illustrates the influence of dPAG on some of the cells (representative) found in the r-cVRG and vlNTS regions, respectively.

7 Discussion

Our data suggest the presence of discrete neuronal populations in the PAG (Fig. 5) capable of modulating quiet breathing to hyperpnea with activation of expiratory muscles and tachypnea. The findings demonstrate an electrophysiological link between PAG and VRG and NTS respiratory neurons. Our results imply that VRG and NTS cells also form the relay nuclei through which PAG brings about modulation to eupneic breathing. An important link within this network is the noradrenergic link to the NTS. The finding that inspiratory cells in the VRG and NTS were excited by PAG stimulation suggests that the PAG could be using these cells in shaping the diaphragm EMG as required for different behaviors. A similar proposal could be made for expiratory patterning with the VRG expiratory network participating as the relay circuit. The activation of the abdominal muscles shows that this expiratory relay could be exclusively through the VRG since abdominal premotoneurons are predominantly located in the caudal VRG (Feldman 1986), unlike the inspiratory relay that could also involve the NTS (Subramanian *et al*. 2007) and/or the PBN (Hayward *et al*. 2004) circuits.

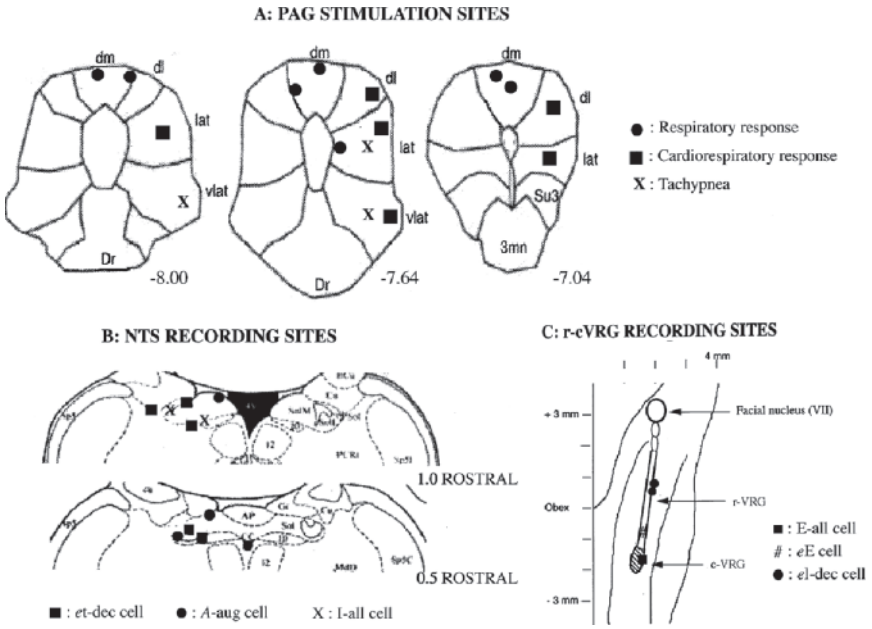

Fig. 5 Representative histology of: (A) location of stimulation sites in PAG; (B) recording sites in the NTS; and (C) stimulation sites in the r-cVRG

References

Feldman, J.L. (1986) Neurophysiology of breathing in mammals. In: *Handbook of Physiology. The Nervous System. Intrinsic Regulatory System in the Brain*. Washington, DC: Am. Physiol. Soc. 4, 463–524.

Hayward, L.F., Swartz, C.L. and Davenport, P.W. (2003) Respiratory response to activation and disinhibition of the dorsal periaqueductal gray in rats. J. Appl. Physiol. 94, 913–922.

Hayward, L.F., Castellanos, M. and Davenport, P. (2004) Parabrachial neurons mediate dorsal periaqueductal gray evoked respiratory responses in the rat. J. Appl. Physiol. 96, 1146–1154.

Holstege, G. (1991b) Descending pathways from the periaqueductal gray and adjacent areas. In: A. Depaulis and R. Bandler (Eds.), *The Midbrain Periaqueductal Gray Matter: Functional Anatomical and Immunohistochemical Organization*. Plenum Press, New York, pp. 239–265.

Huang, Z.G., Subramanian, S.H., Balnave, R.J., Turman, A.B. and Chow, C.M. (2000) Roles of periaqueductal gray and nucleus solitarius in cardiorespiratory function in the rat brainstem. Respiration Physiol. 120, 185–195.

Paxinos, G. and Watson, C. (1997) The rat brain in stereotaxic co-ordinates. San Diego, CA: Academic respiratory groups of neurons in the medulla of the rat. Brain Res. 419, 87–96.

Subramanian H.H., Chow, C.M. and Balnave, R.J. (2007) Identification of different types of respiratory neurons in the dorsal brainstem nucleus tractus solitarius of the rat. Brain Res. 1141, 119–132.

67
Computational Model of TASK Channels and PKC-Pathway Dependent Serotonergic Modulatory Effects in Respiratory-Related Neurons

Tzu-Hsin B. Tsao[1, 2] and Robert J. Butera[1, 2, 3]

Abstract Hypoglossal motoneurons (HMs) receive serotonergic innervations from medullary raphe neurons and produce rhythmic discharge patterns closely associated with respiratory rhythm generated in the pre-Bötzinger complex (pBC). HM activity is subject to modulation by numerous factors including serotonin (5-HT), TRH, norepinephrine (NE), substance P (SP), pH, multiple protein kinases and phosphatases. In this present work, we introduce a computational HM model that facilitates the investigation of how neuromodulatory factors. such as 5-HT and pH, can affect HM activities.

1 Introduction

Respiratory motoneurons receive rhythmic medullary and spinal pre-motoneuronal inputs and transform them into commands for controlling respiratory pump and modulating airway resistance. Respiratory motoneurons are not directly involved in respiratory rhythmogenesis. However, their discharge pattern is an important determinant for alveolar ventilation through convolving with respiratory mechanics. Therefore, changes in respiratory motoneuron excitability are functionally important and failure to regulate this aspect can lead to pathological conditions (Feldman, Neverova and Saywell 2005).

In mammals, hypoglossal motoneurons receive serotonergic innervation from medullary raphe neurons and respond with membrane depolarization, increased excitability and different intracellular calcium dynamics accompanying action potential discharges (Ladewig, Lalley and Keller 2004). The serotonergic modulation of calcium-signaling is mediated by two subtypes of 5-HT receptors, namely, the 5-HT_{1A} and the 5-HT_{2} receptors (Bayliss, Viana, Talley and Berger 1997). Both

[1] Laboratory for Neuroengineering

[2] Wallace H. Coulter GT/Emory Department of Biomedical Engineering, Georgia Institute of Technology, Atlanta, GA, USA. rbutera@gatech.edu

[3] School of Electrical and Computer Engineering, Georgia Institute of Technology, Atlanta, GA, USA.

M.J. Poulin and R.J.A. Wilson (eds.), *Integration in Respiratory Control: From Genes to Systems*. © Springer 2008

receptor subtypes are abundant in neonatal HM and the activation of each contributes differentially to the regulation of intracellular calcium profile. Activation of 5-HT_{1A} reduces current flow through N- and P/Q-type calcium channels and consequently inhibits after-hyperpolarization (AHP) caused by calcium-activated potassium current (Ladewig *et al*. 2004).

On the other hand, the activation of 5-HT_2 receptors affects basal intracellular calcium concentration and has generally been linked to the PKC-pathway leading to calcium release from intracellular stores (Fig. 1). The PKC-pathway involves phospholipase C (PLC)-mediated production of inositol triphosphate (IP_3) that leads to calcium release from intracellular stores and diacylglyceral (DAG) activation of protein kinase C leading to phosphorylation and dephosphorylation of membrane proteins.

Neurotransmitter-induced enhancement of excitability can be mediated by inhibition of a resting K^+ current. TASK-1 channels, TASK-3 channels, as well their heterodimers provide prominent leak K^+ currents and are targets for neurotransmitter modulation in HMs (Berg, Talley, Manger and Bayliss 2004). These pH-sensitive K^+ channels can be fully inhibited by 5-HT, NE and SP and causes depolarization (Talley, Lei, Sirois and Bayliss 2000). Furthermore, it has been shown that 5-HT induced depolarizing current has a pH-sensitive component mediated by the TASK channels.

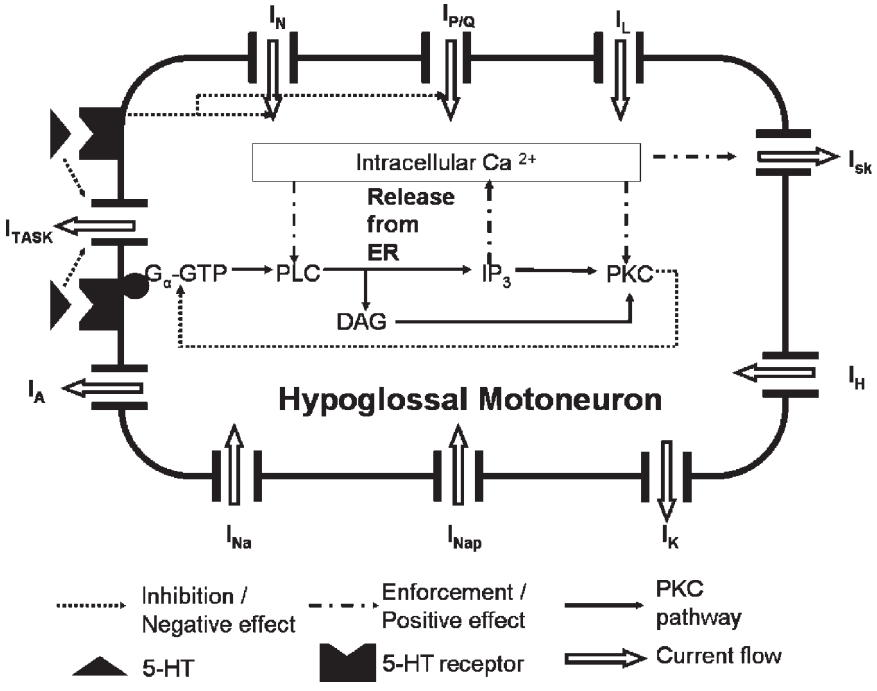

Fig. 1 Graphical representation of our working modified HM model

In the present work, we introduce a computational HM model that includes a TASK channel conductance as well as cellular mechanisms for the protein kinase C (PKC) pathway that allow for the neuromodulatory effect by 5-HT.

2 Results

Our working model qualitatively reproduces features of serotonin-mediated effects on HM excitability. These features include increased membrane excitability, decreased AHP amplitude, elevated basal intracellular calcium concentration ($[Ca^{2+}]_i$) and depressed $[Ca^{2+}]_i$ oscillation amplitude. We started with the HM model of Purvis and Butera (2005). The total TASK-channel conductance of 3.5 nS was adopted from Talley *et al*. (2000). As proposed in Talley *et al*. (2000), TASK channels are considered to be fully inhibited with the application of 5-HT. The mechanisms through which 5-HT receptor activation modulates $[Ca^{2+}]_i$ can be represented by a set of three simultaneous differential equations originally presented in Cutherbertson and Chay (1991) (Eqs. 1–3):

$$d[G-GTP]/dt = r_g - h_g R_{pkc}[G\text{-}GTP] \tag{1}$$

where R_{pkc} is the fraction of activated PKC.

$$d[DAG]/dt = k_d R_{PLC} - hd[DAG] \tag{2}$$

where R_{PLC} is the fraction of activated PLC.

$$d[Ca^{2+}]_i/dt = R_{IP3} - h_c[Ca^{2+}]_i + \tag{3}$$

The preliminary results from our working model are illustrated in Fig. 2 and two scenarios were investigated. Scenario one considered 5-HT modulatory effect on intracellular calcium dynamics and consequently membrane electrodynamics. Results from scenario one are illustrated in panel A1 and A2 of Fig. 2. The second scenario considers the effects of 5-HT on both calcium dynamics and TASK-channel conductance. The resulting intracellular calcium concentration profile and corresponding membrane potential trace are illustrated in panel B1 and B2. Action potentials were evoked via a 600 ms current pulse of 1 nA. Bath application of 5-HT (25 uM) was simulated for 200 ms and is signified by the horizontal bar in Fig. 2.

The simulation results indicate that 5-HT application causes reduced AHP amplitude, which leads to a higher AP firing frequency (Fig. 2A1). The corresponding intracellular calcium profile (Fig. 2A2) demonstrates 5-HT modulatory effects characterized by an elevated basal $[Ca^{2+}]_i$ and a smaller oscillation amplitude. The smaller oscillation amplitude is caused by calcium induced calcium release from the endoplasmic reticulum (Ladewig, Kloppenburg, Lalley, Zipfel and Webb 2003). When the inhibition of 5-HT on TASK-channel conductance is taken into

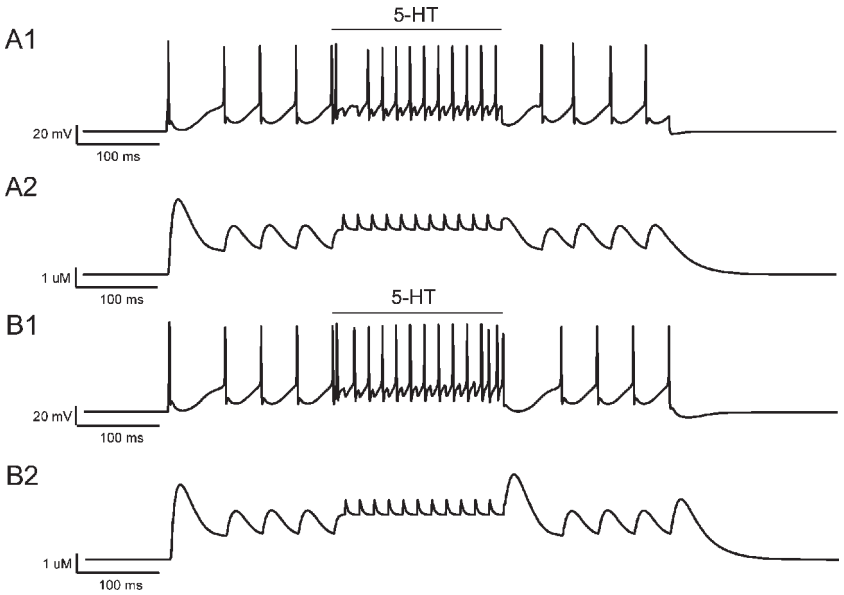

Fig. 2 HM response to current step. Simulation results from considering only the PKC-pathway mediated 5-HT modulations: panel A1 and A2. Results from considering both PKC-pathway and TASK-channel mediated 5-HT modulations: panel B1 and B2. A1: membrane potential. A2: $[Ca^{2+}]$i dynamics. B1: membrane potential. B2: $[Ca^{2+}]$i dynamics

consideration, the simulation results illustrate higher membrane excitability signified by accelerated AP firing frequency while the $[Ca^{2+}]_i$ profile remains unchanged from scenario one (Fig. 2B1, 2B2). The gradual increase in AP firing frequency can be attributed to a decrease in the fast-transient potassium current (I_A, results not shown).

3 Conclusions and Significance

Respiratory motoneuronal excitability is subject to modulation by several transmitters. Some of these modulatory effects, such as those mediated by 5-HT, are highly correlated with sleep-wake states and rhythmic motor activities. Activation of 5-HT receptors have been traditionally linked to the activation of PKC pathway. The PKC pathway can also be activated by mGluRs, which are also abundantly expressed in HMs. It has been proved that the PKC pathway is crucial to the induction of ivLTF in motoneurons and has a significant impact on intracellular calcium dynamics (Feldman *et al*. 2005). The second feature of the PKC pathway renders more investigation because intracellular calcium dynamics have been linked to several physiological and patho-physiological states. The disruption of calcium signaling can have detrimental effects especially in neurons such as HMs that have low

calcium-buffering capacity (Lips and Kellar 1999). In addition to peptidergic and serotonergic modulations, HMs are also subject to modulation by pH values. Variations in pH values are associated with physiological states such as hypoxia. The pH-sensitivity in HM is mediated by TASK channels, which are inhibited in acidic condition and activated in alkaline condition. Excitation caused by TASK-channel inhibition can also be with 5-HT and occur in be parallel with the activation of PKC pathway (Talley *et al*. 2000).

Our new HM model qualitatively reproduces observations of how 5-HT application can alter membrane electrodynamics both directly by inhibiting a "leak" conductance (TASK) and indirectly through the PKC-pathway ($[Ca^{2+}]_i$). This new HM model serves as a first step to modeling how neuromodulators affect respiratory-related activity either directly or via intracellular signaling pathway at a single cell level. Our next step is to modify this preliminary model so that the accelerated AP firing frequency with 5-HT application falls within physiological range. Current implementation of the PKC-pathway can also be improved via differentiating effects mediated by different receptor subtypes. Additional second-messenger pathways mediated by other protein kinases such as protein kinase A (PKA) and protein kinase G (PKG) can also be implemented for further investigation of how each pathway affects HM membrane electrodynamics.

References

Bayliss, D.A., Viana, F., Talley, E.M. and Berger, A.J. (1997) Neuromodulation of hypoglossal motoneurons: cellular and developmental mechanisms. Respir. Physiol. 110, 139–150.

Berg, A.P., Talley, E.M., Manger, J.P. and Bayliss, D.A. (2004) Motoneurons express heteromeric TWIK-related acid-sensitive K+ (TASK) channels containing TASK-1 (KCNK3) and TASK-3 (KCNK9) subunits. J. Neurosci. 24, 6693–6702.

Cuthbertson, K.S. and Chay, T.R. (1991) Modelling receptor-controlled intracellular calcium oscillators. Cell Calcium 12, 97–109.

Feldman, J.L., Neverova, N.V. and Saywell, S.A. (2005) Modulation of hypoglossal motoneuron excitability by intracellular signal transduction cascades. Respir. Physiol. Neurobiol. 147, 131–143.

Ladewig, T., Kloppenburg, P., Lalley, P.M., Zipfel, W.R., Webb, W.W. and Keller, B.U. (2003) Spatial profiles of store-dependent calcium release in motoneurones of the nucleus hypoglossus from newborn mouse. J. Physiol. 547, 775–787.

Ladewig, T., Lalley, P.M. and Keller, B.U. (2004) Serotonergic modulation of intracellular calcium dynamics in neonatal hypoglossal motoneurons from mouse. Brain Res. 1001, 1–12.

Lips, M.B. and Keller, B.U. (1999) Activity-related calcium dynamics in motoneurons of the nucleus hypoglossus from mouse. J. Neurophysiol. 82, 2936–2946.

Purvis, L.K. and Butera, R.J. (2005) Ionic current model of a hypoglossal motoneuron. J. Neurophysiol. 93, 723–733.

Talley, E.M., Lei, Q., Sirois, J.E. and Bayliss, D.A. (2000) TASK-1, a two-pore domain K+ channel, is modulated by multiple neurotransmitters in motoneurons. Neuron 25, 399–410.

68
Modulation of Hering-Breuer Reflex by Ventrolateral Pons

Hui Wang[1], Heng Zhang[1], Gang Song[1,2] and Chi-Sang Poon[2]

Abstract The vagally-mediated Hering-Breuer reflex (HBR) is known to be modulated by the classic pneumotaxic center in the dorsolateral pons. In this work, we investigated whether the HBR was also modulated by the ventrolateral pons (vl-pons). Experiments were performed on urethane anesthetized adult rats. The HBR was elicited by electrical stimulation of the vagus nerve and its strength was compared before and after electrical stimulation or microinjection of MK-801 (non-competitive NMDA receptor antagonist) at the vl-pons. We found that the inspiratory inhibition and expiratory prolongation effects of the HBR were strengthened after electrical stimulation at the vl-pons but were weakened after microinjecting MK-801. Results suggested that the vl-pons could influence the respiratory rhythm by modulating the strength of HBR via NMDA receptor-mediated neurotransmission.

1 Introduction

The classic Hering-Breuer reflex (HBR) consists of expiration lengthening and inspiration shortening upon the activation of slowly-adapting pulmonary stretch receptors. This vagally-mediated reflex is of critical importance in promoting inspiratory-to-expiratory phase switching and preventing apneusis.

Recent studies have shown that the HBR is subject to modification under certain conditions. For example, the inspiratory inhibition and expiratory prolongation of the HBR were significantly attenuated after electrical or chemical stimulation at the serotonergic raphe pallidus (RP), and this effect showed short-term memory (Li *et al*. 2006). In addition, it was reported that the fast component of the adaptation

[1] Shandong University, Laboratory of Respiratory Neurobiology, Institute of Physiology, School of Medicine, Jinan 250012, PR China, wanghui200211742@yahoo.com.cn (Hui Wang), zhheng@sdu.edu.cn (Heng Zhang)

[2] Harvard-MIT Division of Health Sciences and Technology, Massachusetts Institute of Technology, Cambridge, MA 02139, gangsg@mit.edu (Gang Song), cpoon@mit.edu (Chi-Sang Poon)

M.J. Poulin and R.J.A. Wilson (eds.), *Integration in Respiratory Control: From Genes to Systems*.

and post-stimulus rebound of HBR are abolished after bilateral dorsolateral pontine lesions or systemic NMDA receptor blockade with the non-competitive antagonists MK-801 (Siniaia *et al*. 2000).

The ventrolateral pons (vl-pons) is reciprocally connected with the classic pneumotaxic center in the dorsolateral pons (dl-pons) (Song and Poon 2004; Song *et al*. 2006). An area has been identified in the vl-pons of adult rats that modulates respiratory phase durations and consequently, the respiratory frequency (F_R) (Dick and Coles 2000; Jodkowski *et al*. 1994). Specifically, electrical or chemical stimulation at the vl-pons caused strong inspiratory inhibition and expiratory prolongation, while bilateral electrolytic or chemical lesions, or microinjection of muscimol (agonist for $GABA_A$ receptor) into this region, resulted in apneusis in vagotomized rats (Jodkowski *et al*. 1994). Thus, the definition of the classic 'pneumotaxic center' may be extended ventrally to include the vl-pons. The latter may share the same modulatory mechanism as the dl-pons and may interact with it in influencing the respiratory timing (Dick *et al*. 2000). We hypothesized that the vl-pons is also involved in the modulation of HBR. In this study, we tested this hypothesis by comparing the HBR before and after electrical stimulation or microinjection of MK-801 into the vl-pons.

2 Materials and Methods

Experiments were done on 26 adult SD rats of either sex. All animals were anesthetized with urethane (initial dosage of 1.5 g/kg, *i.p*., supplemented periodically at 0.15 g/kg *i.v*.) A tracheostomy was performed and atropine sulphate (0.05 mg/kg *s.c*.) was given to minimize tracheal secretions. Animals were paralyzed with pancuronium bromide and artificially ventilated with medical air. The end-tidal CO_2 was monitored and kept at 5–5.5%. Rectal temperature was kept at 37 ± 0.5°C.

A phrenic nerve was dissected at the C_5 level and mounted on a custom-made bipolar silver wire electrode. Phrenic discharges were recorded and sampled into a computer with Biobench software (NI Corporation, US). Both vagus nerves were isolated and severed at the cervical level. The central end of one vagus was put on a bipolar silver hook electrode for stimulation (20–40 μA, 80 Hz).

Tungsten microelectrode was stereotaxically inserted into the vl-pons (−1.0–1.3 mm from interaural level, 2.2–2.4 mm lateral from midline, and depth at 8.6–9.6 mm from the Lambda surface; Paxinos and Watson 1986) for delivering electrical stimulation (20–40 μA, 80 Hz). MK-801 (Sigma) was dissolved in saline (concentration 0.03 μM/L) and microinjected into vl-pons (0.1–0.3 μl) with a glass micropipette (tip diameter 30 μm) connected to a 1 μl Hamilton microsyringe.

All data were presented as mean ± SD. Student's *t*-test was used to determine the difference. Statistical significance level was set at $p < 0.05$.

3 Results

3.1 HBR Is Enhanced Following Electrical Stimulation at vl-pons

As reported in previous studies, repetitive vagal stimulation caused a typical inhibition of phrenic discharge with shortening of Ti and lengthening of Te. During the ctrHBR, Ti was decreased by 10.02±7.55% ($p < 0.05$), Te prolonged by 34.48±14.5% ($p < 0.01$), and F_R decreased by 24.56 ± 2.73% ($p < 0.01$). Upon cessation of stimulation, the F_R increased briefly by 11.58 ± 2.74% ($p < 0.01$) (Fig. 1B, left panel).

Electrical stimulation at vl-pons caused respiratory inhibition by prolonging expiratory duration and decreasing inspiratory amplitude. During vl-pons stimulation, Te was prolonged by 17.6 ± 11.38% ($p < 0.05$) and t he inspiratory amplitude was decreased by 18.22 ± 9.03% ($p < 0.05$) (Fig. 1A, left panel).

Immediately after vl-pons stimulation (within 5 sec), another vagal stimulation evoked stronger respiratory inhibition of HBR (tHBR) (Fig. 1C, left panel). During the tHBR, the Te of the first 5 respiratory cycles was increased by 42.83 ± 18.01%

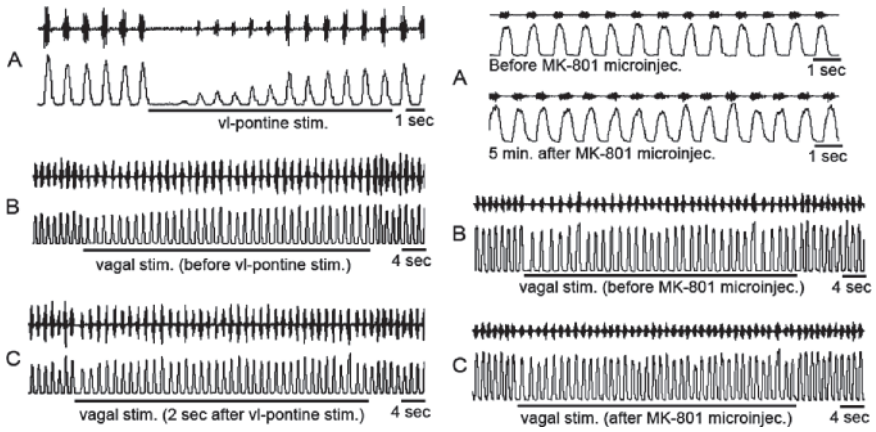

Fig. 1 Left panel: Pre-stimulation of vl-pons strengthened the respiratory inhibition of HBR. (A) Electrical stimulation at the vl-pons caused respiratory inhibition (upper trace, original phrenic discharge; lower trace, integrated phrenic discharge). (B) Repetitive stimulation of vagus nerve (20 μA, 60 s) caused HBR (ctrHB). (C) Immediately after stimulation at the vl-pons, another stimulation at the vagus nerve (with the same intensity as in B) caused stronger respiratory inhibition. Right panel: Microinjection of MK-801 into the vl-pons attenuated the respiratory inhibition of HBR. (A) Microinjecting MK-801 (0.1–0.3 μL) into the vl-pons caused prolongation of inspirtory time, shortening of expiratory time and increased respiratory frequency. (B) Control vagal stimulation (ctrHB) caused inhibition of phrenic discharge and prolongation of expiratory duration. (C) Another vagal stimulation (tHB) after the microinjection of MK-801 caused weaker respiratory inhibition

($p < 0.01$), Ti was attenuated by 11.24 ± 5.55% ($p < 0.05$), and F_R attenuated by 34.62 ± 4.42% ($p < 0.01$). When compared with the ctrHBR, the increase in Te was 23.38 ± 6.78% ($p < 0.01$) larger, and the attenuations of Ti and F_R were respectively 11.3 ± 3.22% ($p < 0.05$) and 40.68 ± 11.27% ($p < 0.01$) more prominent. The post-stimulus rebound of tHBR was 7.16 ± 1.4% ($p < 0.01$), which was weakened by 38.3 ± 5.39% ($p < 0.01$) compared with that of ctrHBR (Fig. 1C, left panel).

3.2 HBR is Weakened after Microinjection of MK-801 at vl-pons

Microinjection of MK-801 into the vl-pons caused prolongation of Ti by 28.46 ± 6.39% ($p < 0.01$) and shortening of Te by 29.8 ± 6.6% ($p < 0.01$). The F_R was increased by 10.57 ± 2.57% ($p < 0.01$) (Fig. 2A, right panel).

After the microinjection of MK-801, another vagal stimulation still evoked HBR (tHBR) (Fig. 2C, right panel) but weaker than the ctrHBR (Fig. 2B, right panel). During the tHBR, Te was increased by 18.51 ± 4.19% ($p < 0.01$), Ti was attenuated by 5.7 ± 2.11% ($p < 0.01$), and F_R was attenuated by 12.4 ± 4.33% ($p < 0.01$). When compared with the ctrHBR, the increase in Te was 46.11 ± 4.27% ($p < 0.01$) smaller, and the attenuations in Ti and F_R were respectively 42.94 ± 8.91% ($p < 0.01$) and 49.41 ± 10.32% ($p < 0.01$) less prominent. The post-stimulus rebound was insignificant (0.16 ± 0.15%, $p > 0.05$) (Fig. 2C, right panel).

In another group of animals, microinjection of ACSF into the vl-pons had no significant effect on phrenic discharge. Subsequent vagal stimulation produced almost identical respiratory response as the first vagal stimulation (data not shown).

4 Discussion

The major finding of this study was that activation of neurons in the vl-pons could modulate the HBR and this modulation might involve NMDA receptor-mediated neurotransmission. The vl-pons is considered as an auxiliary part or a subdivision of "pneumotaxic center", which was first defined by Lumsden eight decades ago (Lumsden 1923). The principal function of the "pneumotaxic center" is to promote the respiratory phase-switching, especially the switching from inspiratory phase to expiratory phase. This function is complementary to the HBR. When both the pneumotaxic center and HBR were disabled, complete failure of phase-switching, *i.e*., apneusis, ensued (Lumsden 1923; Cohen 1971; von Euler 1986).

Recently, studies by our laboratories have shown that the pneumotaxic function and the HBR are fail-safe mechanisms for each other (Siniaia *et al*. 2000). Under normal conditions, the level of activity of each part is counterbalanced by the other. When one of them fails, the other will be enhanced or sensitized to take over the function to maintain respiratory phase-switching. This is evidenced by the finding

that the pneumotaxic center is normally desensitized by the afferents from SAR (Siniaia *et al*. 2000) and that the HBR is significantly enhanced after bilateral lesions of the dorsolateral pons (MacDonald *et al*. 2006).

The present study showed that the HBR is enhanced instead of attenuated following the electrical activation of vl-pons. Apparently, different mechanisms are employed by the dl- and vl- pontine subdivisions in modulating HBR. The chemical phenotypes of neurons in these two subdivisions are also different, with the dl-pontine pneumotaxic neurons possibly being glutamatergic and the vl-pontine (A5) being noradrenergic. The latter has been found to send axonal projections to respiratory related brainstem structures such as NTS, ventrolateral medulla and the dorsolateral pons (Byrum and Guyenet 1987; Smith *et al*. 1989; Nunez-Abades *et al*. 1993). We suggest that the activation of the vl-pontine A5 neurons led to the release of NE at those structures to up-regulate the strength of the HBR. But, the discrete mechanism remains to be clarified.

NMDA receptors are densely expressed in A5 neurons. We found that blocking of this subtype of glutamate receptors in the vl-pons with MK 801 caused Ti prolongation and Te shortening, similar to that produced by local blockade with muscimol (Jodkowski *et al*. 1994). On the other hand, microinjection of glutamate into the A5 decreased respiratory rate and phrenic nerve activity (Dawid-Milner *et al*. 2001). We suggest that the blocking of NMDA receptors decreased the excitability of those A5 neurons, thus partially disabling their pneumotaxic function. This finding also shows that the vl-pons exerted tonic facilitating effect on the HBR through NMDA receptor mediated excitatory afferent inputs.

Acknowledgements This work was supported by National Institutes of Health grants HL067966 and HL072849 and a grant from China Ministry of Education.

References

Byrum, C.E. and Guyenet, P.G. (1987) Afferent and efferent connections of the A5 noradrenergic cell group in the rat. J. Comp. Neurol. 261, 529–542.

Cohen, M.I. (1971) Switching of the respiratory phases and evoked phrenic responses produced by rostral pontine electrical stimulation. J. Physiol. (Lond.) 217, 133–158.

Dawid Milner, M.S., Lara, J.P. and Gonzalez-Baron, S. (2001) Respiratory effects of stimulation of cell bodies of the A5 region in the anaesthetised rat. Pflügers Arch. – Eur. J. Physiol. 441, 434–443.

Dick, T.E. and Coles, S.K. (2000) Ventrolateral pons mediates short-term depression of respiratory frequency after brief hypoxia. Respir. Physiol. 121, 87–100.

Jodkowski, J.S., Coles, S.K. and Dick, T.E. (1994) A 'pneumotaxic centre' in rats. Neurosci. Lett. 172, 67–72.

Lumsden, T. (1923) Observations on the respiratory centres in the cat. J. Physiol. (Lond.) 57, 153–160.

MacDonald, S.M., G. Song and C. Poon (2006) Pontine lesion eliminates adaptation during PEEP evoked Hering-Breuer Reflex. Xth Oxford Conference on Modeling and Control of Breathing. A29. Lake Louise, Alberta, Canada.

Nunez-Abades, P.A., Morillo, A.M. and Pasaro, R. (1993) Brainstem connections of the rat ventral respiratory subgroups: Afferent projections. J. Auton. Nerv. Syst. 42, 99–118.

Paxinos, G. and Watson, C. (1986) *The Rat Brain in Stereotaxic Coordinates*, 2nd edn. Academic Press, New York.

Siniaia, M.S., Young, D.L. and Poon, C.S. (2000) Habituation and desensitization of the Hering-Breuer reflex in rat. J. Physiol. (Lond.) 523(2), 479–491.

Smith, J.C., Morrison, D.E., Ellenberger, H.H., Otto, M.R. and Feldman, J.L. (1989) Brainstem projections to the major respiratory neuron populations in the medulla of the cat. J. Comp. Neurol. 281, 69–96.

Song, G. and Poon, C.S. (2004) Functional and structural models of pontine modulation of mechanoreceptor and chemoreceptor reflexes. Respir. Physiol. Neurobiol. 143(2–3), 281–292.

Song, G., Yu, Y. and Poon, C.S. (2006) Cytoarchitecture of pneumotaxic integration of respiratory and nonrespiratory information in the rat. J. Neurosci. 26(1), 300–310.

Von Euler, C. (1986) Brain stem mechanisms for generation and control of breathing pattern. In: A.P. Fishman, N.S. Cherniack, J.G. Widdicombe and S.R. Geiger (Eds.), *Handbook of Physiology*. Bethesda: American Physiological Society, Vol. II, Sec. 3, pp. 1–67.

Li, Y., Song, G., Ying, Cao, Y., Wang, H., Wang, G., Yu, S. and Zhang, H. (2006) Modulation of the Hering-Breuer reflex by Raphe pallidus in rabbits. Neurosci. Letts. 397, 259–262.

69
Respiratory Network Complexity in Neonatal Rat *in vivo* and *in vitro*

Hui Jing Yu[1], Xinnian Chen[1], Ryan M. Foglyano[2], Christopher G. Wilson[2] and Irene C. Solomon[1]

Abstract Numerous experimental preparations from neonatal rodents have been developed to study mechanisms responsible for respiratory rhythm generation. Amongst them, the *in vivo* anesthetized neonatal rat preparation and the *in vitro* medullary slice preparation from neonatal rat are commonly used. These two preparations not only contain a different extent of the neuroanatomical axis associated with central respiratory control, but they are also studied under markedly different conditions, all of which may affect the complex dynamics underlying the central inspiratory neural network. Here, we evaluated the *approximate entropy* (ApEn) underlying inspiratory motor bursts as an index of inspiratory neural network complexity from each preparation to address this possibility. Our findings suggest that the central inspiratory neural network of the *in vivo* anesthetized neonatal rat exhibits lower complexity (*i.e*., more order) than that observed in the *in vitro* transverse medullary slice preparation, both of which are substantially lower than that observed in more intact *in vitro* (*e.g*., arterially-perfused rat) and mature *in vivo* (*e.g*., anesthetized rat, piglet, cat) preparations. We suggest that additional studies be conducted to identify the precise mechanisms responsible for the differences in central inspiratory neural network complexity between these two neonatal rat preparations.

1 Introduction

Developmental changes in intrinsic membrane properties and synaptic transmission are present within the central respiratory network. To study mechanisms responsible for respiratory rhythm generation, numerous experimental preparations from neonatal rodents (*circa* postnatal (P) day 0–7) have been developed. Amongst them, the *in vivo* anesthetized neonatal rat preparation and the *in vitro* medullary slice preparation from neonatal rat are commonly used. For the *in vivo* anesthetized

[1] State University of New York at Stony Brook, Department of Physiology and Biophysics, hjyu@ic.sunysb.edu

[2] Case Western Reserve University, Department of Pediatrics, cgw5@case.edu

M.J. Poulin and R.J.A. Wilson (eds.), *Integration in Respiratory Control: From Genes to Systems*. © Springer 2008

neonatal rat preparation, inspiratory motor output is generally recorded from the diaphragm (*i.e*., electromyogram (EMG) activity) or from the phrenic or hypoglossal (XII) nerve while the preparation is supplied with a hyperoxic gas mixture (≤ 50% O_2), ventilated or allowed to breathe spontaneously and maintained at a body temperature of ~ 36–37°C. In contrast, for the *in vitro* medullary slice preparation, which is capable of generating spontaneous respiratory rhythm as long as it contains the pre-Bötzinger complex, inspiratory motor output is generally recorded from the XII nerve while the preparation is superfused with an artificial cerebrospinal fluid (aCSF) containing an elevated concentration of KCl (~ 8–9 mM) to enhance excitability and inspiratory drive, and the preparation is maintained at a temperature of ~ 27–30°C. Thus, these two preparations not only contain a different extent of the neuroanatomical axis associated with central respiratory control, but they are also studied under markedly different conditions, all of which may affect the complex dynamics underlying the central inspiratory neural network. The goal of the current investigation was, therefore, to examine the complexity of the central inspiratory neural network from each preparation in an attempt to assess this possibility.

Since the complexity of a signal can be quantified using *approximate entropy* (ApEn), which is a statistical index that measures the regularity (orderliness) in a time series (Pincus 1991; Pincus and Goldberger 1994), we calculated the ApEn of inspiratory motor discharges recorded from both of these *in vivo* and *in vitro* neonatal rat preparations. Higher values of ApEn are associated with irregularity and greater randomness, and thus reflect less system order or higher system complexity. Conversely, lower values of ApEn are associated with a higher degree of regularity and predictability and thus reflect an ordered system or lower system complexity. For our study, we reasoned that since the *in vitro* preparation contains less of the neural axis (*i.e*., fewer neural elements), it would have lower values for ApEn, and therefore exhibit reduced complexity of the central inspiratory neural network as compared to that of the *in vivo* preparation.

2 Methods

To test the above hypothesis, we calculated the ApEn of diaphragm EMG bursts recorded from 11 *in vivo* spontaneously breathing urethane-anesthetized neonatal rats and of XII bursts recorded from 14 *in vitro* transverse medullary slice preparations (400–500 µm thick; superfused with aCSF containing 8 mM KCl) obtained from neonatal rats. All data used for this study were recorded from preparations aged P1–P5, and 20–50 inspiratory bursts were recorded from each preparation. The inspiratory discharge signals were amplified, notch filtered at 60 Hz, filtered to pass frequency between 10 Hz and 1 kHz and recorded on a computer at a sampling rate of ≥ 2 kHz for off-line analyses (MatLab7.0.1). The data were then segmented to obtain to data lengths corresponding to the inspiratory burst. These segmented data were then digitally band-pass filtered (10–50 Hz) using a 6-pole Butterworth filter and re-sampled with a sampling rate of 1 kHz. These filtering parameters were chosen based on previous observations from power spectral analyses showing that

the inspiratory burst dynamics from neonatal mammals are restricted to this range (see review by Funk and Parkis 2002). Further, the 1 kHz down-sampling rate was used to ensure that an adequate number of data points (N) (*i.e.*, ≥ 100 data points, Pincus and Goldberger 1994) would be available for the computation of ApEn for data from both preparations.

Inspiratory burst data were evaluated for temporal (*i.e.*, T_I, T_E, burst frequency) characteristics, and ApEn was calculated as a function of the parameters *m*, the embedding dimension, and *r*, the tolerance (threshold) level. The calculation of ApEn was as follows (Pincus 1991):

$$ApEn(m,r,N) = \phi^m(r) - \phi^{m+1}(r)$$

where

$$\phi^m(r) = \frac{1}{N-m+1}\sum_{i=1}^{N-m+1} \ln(C_r^m(i)) \text{ and } C_r^m(i) = N^m(i)/(N-m+1)$$

$N^m(i)$ = *no. of* $d[X(i), X(j)] \leq r$, where *X(i), X(j)* are vectors defined by *X(i)=[u(i), u(i+1),…, u(i+m−1)]* and *X(j)=[u(j), u(j+1),…, u(j+m−1)]* from the original time series *u(i), u(2),…, u(N)*.

For the determination of *m* and *r*, we followed the recommendations of Pincus and Goldberger (1994). They recommend that $N = 10^m$–30^m and $r = 0.1$–$0.25 \times SD$, so for our analyses, we used $m = 2$ and $r = 0.2 \times SD$. The ApEn of each inspiratory burst was computed as well as the mean (± SE) for all data bursts. The coefficient of variation (CV) was also computed to provide an index of variability in the ApEn measure for each preparation. Temporal data are reported as mean ± SE. Statistical analyses were performed on both the temporal characteristics and ApEn using *Unpaired t-tests*, for which the criterion level was set at $p < 0.05$.

3 Results

In the current investigation, analyses of diaphragm EMG and XII nerve activity recorded from the *in vivo* and *in vitro* neonatal preparations, respectively, revealed differences in the patterning and timing of the inspiratory bursts. An example of inspiratory discharge recorded from each preparation is shown in Fig. 1. In general, inspiratory bursts recorded from the *in vivo* preparation exhibited an augmenting or bell-shaped pattern of discharge while those recorded from the *in vitro* preparation were predominantly decrementing or square-wave. Overall, the *in vivo* preparation exhibited significantly shorter burst durations (T_I) and expiratory pauses (T_E) as compared to the *in vitro* preparation ($p < 0.001$); these differences in timing resulted in significantly higher burst frequencies *in vivo* ($p < 0.001$). Table 1 summarizes these temporal characteristics.

Evaluation of the ApEn values computed for the inspiratory bursts recorded from the *in vivo* and *in vitro* preparations revealed that the two preparations differed

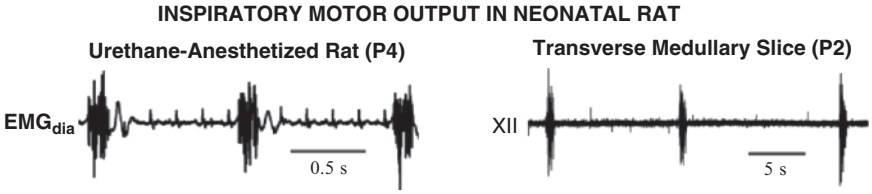

Fig. 1 Example traces of diaphragm EMG activity recorded from an *in vivo* urethane-anesthetized neonatal rat preparation and XII nerve discharge recorded from an *in vitro* transverse medullary slice preparation

Table 1 Summary data (mean ± SE) of the temporal characteristics in inspiratory bursts from neonatal rat in vivo and in vitro. TI, burst duration; TE, duration between bursts

	In Vivo (n = 11)	*In Vitro* (n = 14)
T_I (ms)	100.2 ± 10.0	532.7 ± 46.6
T_E (s)	0.8 ± 0.1	7.3 ± 1.3
Frequency (bpm)	69 ± 4	10 ± 1

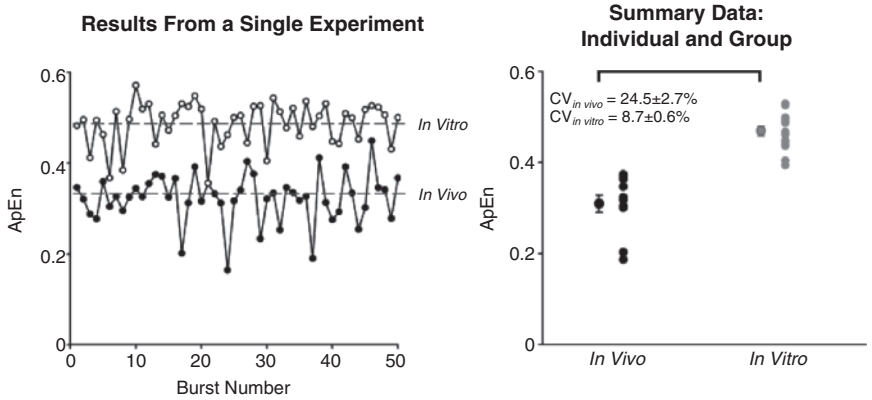

Fig. 2 ApEn of inspiratory motor discharges recorded from the *in vivo* anesthetized neonatal rat preparation and the *in vitro* transverse medullary slice preparation. Results are shown for burst data from a single experiment for each preparation (left panel) and for summary data from individual experiments and ensemble-averaged group data (right panel). $^{*}p \leq 0.001$ for *in vivo* vs. *in vitro* comparison

substantially in inspiratory network complexity. For the *in vivo* preparation, ApEn values were significantly lower than those obtained for the *in vitro* preparation (0.31 ± 0.02 vs. 0.47 ± 0.01, $p < 0.001$), and the ApEn values for the *in vivo* preparation exhibited a higher degree of variability (*i.e.*, larger CV) ($p < 0.001$). An example showing burst-to-burst ApEn values computed for one experiment from each preparation is provided in Fig. 2. Also shown in Fig. 2 is the summary data for the 20–50 bursts recorded from each preparation studied as well as the mean (± SE) group data.

4 Discussion

Our findings demonstrate that T_I and ApEn are significantly lower for the *in vivo* anesthetized neonatal rat preparation than for the *in vitro* transverse medullary slice preparation, although a greater degree of variability (*i.e.*, larger CV) is seen in the *in vivo* data. This difference in ApEn suggests that the central inspiratory neural network of the *in vivo* preparation is more ordered (*i.e.*, less complex) than that of the *in vitro* preparation. Although the precise reason for this difference is unclear, there are a number of possible explanations. For example, the *in vivo* data used for this study were obtained from urethane-anesthetized neonatal rats. Since anesthesia may depress neuronal excitability, fewer neuronal elements could be participating in the expression (complex dynamics) of the inspiratory burst. We do not believe that this is the case because the medullary slice preparation (by definition) contains a reduced extent of the neuroanatomical substrate, yet it exhibits a higher level of complexity. Further, we have found that ApEn values from anesthetized adult mammals are higher than that seen in the anesthetized neonatal rat preparation used in the current study. Another possible explanation may be related to differences in the temperatures of the two preparations. The *in vivo* preparation is maintained at a higher temperature; thus, neuronal excitability could be enhanced leading to increased synchronization of neuronal activity (see Funk and Parkis 2002). Additional studies are needed, however, to support (or refute) this possibility. Alternatively, the difference may be related to the fact that the inspiratory burst from the *in vivo* preparation contains fewer data points (*i.e.*, shorter T_I), which could result in the appearance of reduced system complexity. This explanation, however, is unlikely since the number of data points is taken into consideration in the computation of ApEn, and fewer data points does not directly result in decreased ApEn. Finally, the difference may be related to the fact that for the computation of ApEn we used fixed values for the parameters *m* and *r*, which were assigned according to the recommendations of Pincus and Goldberger (1994) and not specifically determined for the current data sets. As a result, these values may not have been optimal for data from one or both preparations.

Even though differences in inspiratory network complexity were noted between the two neonatal preparations, the ApEn values computed in the current study are markedly lower than those observed in more mature in vitro (e.g., arterially-perfused rat) and in vivo (e.g., anesthetized/decerebrate rat, piglet, cat) preparations. This observation suggests that the inspiratory network of both neonatal preparations is more regular or predictable than that of more mature preparations. Additional studies are needed to identify the precise mechanisms responsible for differences in central inspiratory neural network complexity between the two neonatal rat preparations used in the current study as well as between neonatal and more mature mammalian preparations.

Acknowledgement This work was supported by NIH grants NS045321 and NS049310.

References

Funk, G.D. and Parkis, M.A. (2002) High frequency oscillations in respiratory networks: functionally significant or phenomenological? Respir. Physiol. Neurobiol. 131, 101–120.

Pincus, S.M. (1991) Approximate entropy as a measure of system complexity. Proc. Natl. Acad. Sci. 88, 2297–2301.

Pincus, S.M. and Goldberger, A.L. (1994) Physiological time-series analysis: what does regularity quantify? Am. J. Physiol. 266, H1643–H1656.

Part XI
Multifunctional and Reconfiguring Networks

70
Fast Oscillatory Rhythms in Inspiratory Motor Discharge: A Mathematical Model

Xinnian Chen[1,2], Ki H. Chon[2] and Irene C. Solomon[1]

Abstract In this paper, a mathematic model is applied to characterize spectral activity associated with fast oscillatory rhythms inherent in inspiratory discharges. Based on the estimated parameters, features are extracted to allow the model to discriminate between changes in the location, magnitude, and shape of spectral activities under basal conditions and during pharmacological blockade of gap junctions.

1 Introduction

Fast oscillatory neuronal activity, which may serve as an index for synchronization of neuronal discharges, is a prominent feature observed in many CNS areas, including regions associated with motor control. Power spectral density (PSD) of phrenic nerve discharge has provided insight into the frequency components of fast oscillatory rhythms within the inspiratory phase. Two dominant peaks in the power spectrum, referred to as medium (MFO) and high frequency oscillations (HFO) (Cohen, See, Christakos and Sica 1987; Richardson and Mitchell 1982), have been identified in all adult mammalian species studied thus far, and these two peaks provide an index of inspiratory-phase neuronal synchronization. Changes in spectral power and/or peak frequencies underlying these fast oscillatory rhythms can be modified by different physiological and pathological states (*e.g.*, hypercapnia, hypoxia, maturation, temperature) as well as in response to pharmacological manipulations of the brainstem respiratory neural network (*e.g.*, activation or blockade of receptors/channels). Previous work from our laboratory, for example, has demonstrated that pharmacological blockade of gap junction coupling in an arterially-perfused adult rat preparation elicits not only

[1] SUNY at Stony Brook, Department of Physiology and Biophysics, xinnchen@ic.sunysb.edu

[2] SUNY at Stony Brook, Department of Biomedical Engineering

M.J. Poulin and R.J.A. Wilson (eds.), *Integration in Respiratory Control: From Genes to Systems*.

a decrease in amplitude and an increase in frequency of phrenic bursts but also a reduction in spectral power in both the MFO and HFO ranges, suggesting reconfiguration of the central inspiratory neural network (Solomon, Chon and Rodriguez 2003).

Although the general features (*e.g*., peak frequencies or power) can be extracted from the power spectrum, systematic interpretations about the PSD output are still necessary. In an attempt to better characterize and quantify the spectral features inherent in physiological signals, Knudsen and colleagues have developed a mathematical model (Knudsen, Elmer, Knudsen and Holstein-Rathlou 2004). In their model, they track the frequency changes in renal blood flow between normo- and hyper-tensive rats, and the model has successfully allowed for differentiation between these two conditions. Here, we use a similar approach to gain a better understanding of the spectral dynamics inherent in inspiratory motor discharge. To represent the dynamic features, the model contains 9 parameters, which have been optimized to fit the PSD characteristics inherent in inspiratory motor discharges; the model is implemented using a nonlinear least squares method. This approach allows for quantification of the dominant spectral peaks and power distribution (*i.e*., shape) as well as providing the ability to differentially discriminate between changes in MFO and HFO spectral activities. The results of the model were then compared to the experimental data obtained from an arterially-perfused adult rat preparation under baseline conditions and during blockade of gap junctions.

2 Mathematical Model

To quantify the characteristics associated with the dominant peaks represented in the PSD of each phrenic burst, a second order system was applied (Eq. 1), with the location of the peak being determined by the primary frequency ω_0 and the shape of the peak resulting primarily from the damping coefficient *d*.

Assuming the MFO and HFO are generated and modified by two components in the central respiratory control network that are connected in series, as suggested by the literature (Cohen *et al*. 1987), the overall frequency representation of an inspiratory burst can be suggested by multiplication of the two second-order systems by the overall system gain *k,* as shown in Eq. 2.

$$\mathrm{H(s)} = \frac{\dfrac{s^2}{\omega'^2_0} + \dfrac{2d's}{\omega'_0} + 1}{\dfrac{s^2}{\omega_0^2} + \dfrac{2d \cdot s}{\omega_0} + 1} \tag{1}$$

$$H(\omega) = K \cdot \frac{\frac{\omega^2}{\omega'^2_{MFO}} + \frac{2d'_{MFO}\omega}{\omega'_{MFO}} + 1}{\frac{\omega^2}{\omega^2_{MFO}} + \frac{2d_{MFO}\omega}{\omega_{MFO}} + 1} \cdot \frac{\frac{\omega^2}{\omega'^2_{HFO}} + \frac{2d'_{HFO}\omega}{\omega'_{HFO}} + 1}{\frac{\omega^2}{\omega^2_{HFO}} + \frac{2d_{HFO}\omega}{\omega_{HFO}} + 1} \quad (2)$$

Thus, to represent the frequency content using the above model, 9 parameters were assigned, as vector $\theta = (K\ \omega'_{MFO}\ d'_{MFO}\ \omega'_{MFO}\ d_{MFO}\ \omega'_{HFO}\ d'_{HFO}\ \omega_{HFO}\ d_{HFO})$. Note that the combination of the left and right sides of Eq. 2 is responsible for the generation of the two spectral peaks.

The model parameters are optimized using a nonlinear least squares method. To start the optimization, initial parameter values for ω_{MFO} and ω_{HFO} were set to 50 Hz and 100 Hz, respectively, and were constrained within the range of MFO and HFO values previously defined (Cohen *et al*. 1987; Richardson *et al*. 1982; Solomon *et al*. 2003). Since there is no *a priori* information about the other model parameters, no restrictions were set for these.

2.1 Computer Simulation Data

Data were generated for two simulations using Matlab 6.5. In both simulations, two main peaks were generated, with one peak located at 38 Hz and the other at ~120 Hz. In the second simulation, however, the magnitude of power of the 38 Hz peak and the location and shape of the 120 Hz peak in the PSD were modified in order to further assess the capabilities (*i.e*., adequacy and accuracy) of the 9-parameter model. The PSD and model fitting results from these two simulations are shown in Fig. 1.

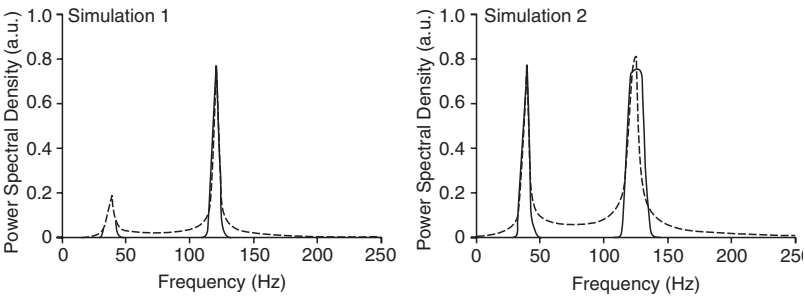

Fig. 1 Example demonstrating the PSD and the fit of the mathematical model to computer simulation data. The mathematical model is able to accurately track spectral activity in both simulations, even though the shape and power distribution were modified in simulation 2. PSD, solid line; mathematical model, dotted line

2.2 Experimental Data

The experimental data used for this study correspond to previously acquired phrenic nerve activity recorded in an arterially-perfused decerebrate adult rat preparation under baseline conditions and during blockade of gap junctions by perfusion with the gap junction blocker carbenoxolone (CBX; 100 μM final concentration) (Solomon *et al*. 2003). Phrenic nerve discharge data under each condition were extracted from the time series trace, and then segmented to obtain to data lengths corresponding to the inspiratory bursts. These phrenic burst data were re-sampled with a sampling rate of 500 Hz (originally sampled at 2 kHz), after digital band-pass filtering from 20–250 Hz using a 6th order Butterworth filter, and power spectral analysis using Welch's periodogram method was performed on individual bursts and as ensemble averages of 10 bursts for each condition. The 9-parameter mathematical model was fit to both individual bursts and ensemble averages.

Examples of phrenic nerve discharge before and during perfusion with CBX, and its corresponding PSD, are shown in Fig. 2. Also shown is the fit of the mathematical model to these spectral data. As described above, perfusion with CBX modifies the amplitude and frequency of phrenic bursts, and markedly reduces the power of the HFO peak (resulting in fairly broad-band HFO activity); the effects

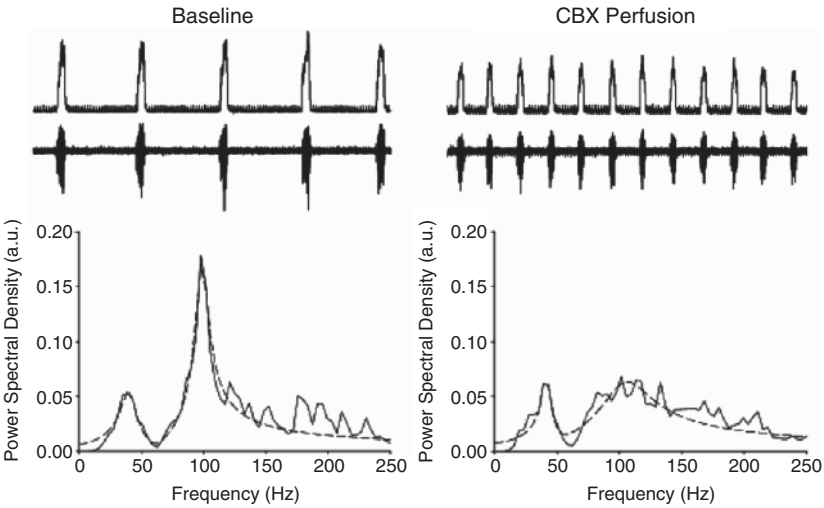

Fig. 2 Example of phrenic nerve discharge and PSD, including the fit of the mathematical model, observed under baseline conditions and during perfusion with CBX. During perfusion with CBX, phrenic burst amplitude and frequency were modified, and HFO power was markedly reduced. Note that the mathematical model fairly accurately fits the experimental data under both conditions. PSD, solid line; mathematical model, dotted line

Table 1 Model Parameter Values: Baseline vs. CBX Perfusion, *p < 0.05

Parameter	Baseline	CBX Perfusion
K	0.0043 ± 0.0004	0.0015 ± 0.0005*
ω_{MFO}	44.26 ± 2.97	34.8 ± 0.42
d_{MFO}	0.199 ± 0.038	0.180 ± 0.027
ω'_{MFO}	146.12 ± 22.33	413.40 ± 202.88
d'_{MFO}	4.392 ± 0.922	2.440 ± 0.646
ω_{HFO}	98.94 ± 6.32	121.32 ± 7.67*
d_{HFO}	0.148 ± 0.044	0.252 ± 0.043*
ω'_{HFO}	0.353 ± 0.036	0.240 ± 0.020*
d'_{HFO}	0.221 ± 0.112	0.806 ± 0.259

on MFO activity were more variable across experiments. Applying the 9-parameter mathematical model to these experimental data reveals that the model fairly accurately tracks the amplitude, shape, and frequencies of MFO and HFO activities under baseline conditions and during perfusion with CBX. Thus, the model was able to capture the dominant changes in spectral activity observed during blockade of gap junctions.

The model parameter values corresponding to baseline conditions and perfusion with CBX are provided in Table 1. The model reveals (1) a significant reduction of system gain k during CBX perfusion (*i.e.*, global reduction in fast oscillatory rhythms), (2) an alteration in the shape and amplitude of HFO activity (indicated by change in d_{HFO}) and (3) no significant differences in the shape and amplitude of MFO activity. In contrast to the experimental data, the model predicts an upward shift in the HFO resonance frequency ω_{HFO} during CBX perfusion; this difference may be due to the loss of a distinct HFO peak in the experimental data.

3 Summary and Conclusion

In this study, we applied a 9-parameter mathematical model to both computer simulation and experimental (inspiratory burst) data, and demonstrated that the model is able to adequately and accurately track induced changes in spectral activity in a manner similar to that identified by PSD analysis (based on 256 parameters). We suggest that the proposed mathematical model provides a promising tool, with greater efficiency of spectral representation, for further examination of spectral dynamics in inspiratory motor discharge, including their modulation under various pathological states and during pharmacological perturbations.

Acknowledgements The authors thank Melissa N. Rodriguez for contributions to the experimental data. This study was supported by the NIH Grants NS045321 and NS049310.

References

Cohen, M.I., See, W.R., Christakos, C.N. and Sica A.L. (1987) High-frequency and medium-frequency components of different inspiratory nerve discharges and their modification by various inputs. Brain Res. 417, 148–152.

Knudsen, T., Elmer, H., Knudsen, M., Holstein-Rathlou, N.H. and Stoustrup J. (2004) Dynamic modeling of renal blood flow in Dahl hypertensive and normotensive rats. IEEE Transactions on Biomedical Engineering 51(5), 689–697.

Richardson, C.A. and Mitchell, R.A. (1982) Power spectral analysis of inspiratory nerve activity in the decerebrate cat. Brain Res. 233, 317–336.

Solomon, I.C., Chon, K.H. and Rodriguez, M.N. (2003) Blockade of brain stem gap junctions increases phrenic bursts frequency and reduces phrenic burst synchronization in adult rat. J. Neurophysiol. 89, 135–149.

71
Burst-to-Burst Variability in Respiratory Timing, Inspiratory-Phase Spectral Activity, and Inspiratory Neural Network Complexity in Urethane-Anesthetized C57BL/6 Mice *in vivo*

Hyun Hye Chun[1] , Evan T. Spiegel[2] and Irene C. Solomon[3]

Abstract Recent work from our laboratory has focused on identifying burst-to-burst variability in temporal and spectral characteristics for 5-minute time series segments of basal inspiratory motor discharges from urethane-anesthetized adult C57BL/6 mice. The current investigation, as the continuation of our previous studies, examined short- and long-term burst-to-burst variability in temporal and spectral components as well as in complexity, which reflects the central respiratory network dynamics. All measures were assessed by quantitative poincaré plot analyses and the determination of the coefficient of variation.

1 Introduction

The primary function of the respiratory system is to maintain arterial blood gases and pH within the normal physiological range. As a result, the neural control of the respiratory system must be dynamic in order to cope with any disturbances that we encounter in our everyday life and under pathological conditions. Previous work from our laboratory using time-frequency (TF) spectral analysis has suggested that the spectral components of basal inspiratory motor output in mice are highly dynamic (O'Neal, Spiegel, Chon and Solomon 2005). In that study, however, relatively short duration time segments (10 s) were evaluated, even though these analyses were made over both short- and long-time scales (*e.g.*, 1–10 min). To gain insight into burst-to-burst variability over a longer duration, Gonsenhauser and colleagues used poincaré plot analysis to examine the burst-to-burst variability in 5-min time series segments recorded from mice; however, their study focused only on variables associated with respiratory timing (Gonsenhauser, Wilson, Han, Strohl and Dick 2004).

Complexity, another characteristic inherent in inspiratory motor discharges can be used as an indication of the central respiratory network dynamics.

[1] Stony Brook University, Graduate Program in Neuroscience, hhchun@ic.sunysb.edu

[2] Stony Brook University, Department of Physiology and Biophysics, evan.spiegel@gmail.com

[3] Stony Brook University, Department of Physiology and Biophysics, Irene.Solomon@stonybrook.edu

M.J. Poulin and R.J.A. Wilson (eds.), *Integration in Respiratory Control: From Genes to Systems*.

Approximate entropy (ApEn) analysis is a statistical index for measuring or quantifying the degree of regularity or predictability in time series of data (Pincus 1991; Pincus and Goldberger 1994). Although this measure provides insight into intra-burst complexity, it provides no information about inter-burst diversity in a series of inspiratory bursts.

Thus, the purpose of the current investigation was to extend our previous observations to examine both short- and long-term burst-to-burst variability concerning temporal and spectral features as well as complexity in basal inspiratory motor output recorded from the diaphragm of urethane-anesthetized adult C57BL/6 mice during a longer period time. In order to accomplish our goal, we used poincaré plot analysis (*a.k.a.*, dynamical systems analysis) of breath n + 1 vs. n on all extracted or computed parameters in 5-minute data segments. We then assessed the data dispersion within the poincaré plots in order to better characterize and quantify the burst-to-burst variability. The coefficient of variation (CV = [SD/mean] 100) was also computed for each parameter to provide additional insight into long-term variability.

2 Methods

All experiments were performed under protocols approved by the Institutional Animal Care and Use Committee at SUNY Stony Brook following the NIH Policy of Humane Care and Use of Laboratory Animals. Experiments were carried out on 7 urethane-anesthetized, spontaneously breathing adult C57BL/6 mice (n = 3 males, n = 4 females, 12–42 weeks old, 20–45 g). All mice were supplied with a mixture of 40% O_2 in a balance of N_2 by a nose cone, and diaphragm electromyogram (EMG) activity was recorded through a small gauge twisted platinum-iridium wire electrode. The signals were amplified (x1k), notch filtered at 60 Hz, filtered to pass frequency between 10 Hz and 1 kHz, and digitized with 2 K sampling rate.

Temporal and spectral features were extracted from 5-minute segments of basal diaphragm EMG activity. Respiratory-related timing components included inspiratory duration (T_I), interburst interval (T_E), breathing frequency and inspiratory duty cycle (T_I/T_{Tot}). Spectral parameters included power of the dominant peaks associated with the medium (MFO; 20–60 Hz), high (HFO; 70–150 Hz), and upper-high frequency oscillations (UHFO; 170–250 Hz), all of which characterize the inherent intra-burst dynamics and were obtained by implementation of FFT-based spectral analyses (Welch's periodigram method) on the inspiratory burst data. ApEn was computed as a function of the parameter *m*, the embedding dimension and *r*, the tolerance (threshold) level. For these analyses, $m = 2$ and $r = 0.2 \times$ SD of the data, in accordance with the recommendations of Pincus and Goldberger (1994).

Poincaré plots (*n+1* vs. *n*; n is burst number) were constructed for all extracted/computed variables. The width and length of the dispersion of data in the poincaré plots is thought to reflect the level of short- and long-term burst-to-burst variability, respectively. SD1 was defined as the standard deviation of the scattered points

perpendicular to the line-of-identity and SD2 as the standard deviation of dispersed points along the line-of-identity. SD1/SD2 ratio and Pearson's correlation coefficients were computed as a quantitative index of poincaré plot topography (Brennan, Palaniswami and Kamen 2001).

3 Results

In this paper, we include data from mice that exhibited breathing frequencies between 155–185 breaths/min, which correspond to the typical range of breathing frequencies noted in our previous study (O'Neal *et al*. 2005). Fig. 1A provides a representative trace from one mouse, illustrating the general pattern of integrated and raw basal diaphragm EMG activity encountered in the current study. The ensemble-averaged power spectrum computed from the diaphragm EMG burst data recorded over the 5-minute time segment in this mouse is shown in Fig. 1B. Dominant peaks in the power spectrum were observed in the MFO, HFO and UHFO ranges, showing a distribution of power consistent with our previous report.

Following extraction of the temporal and spectral parameters of interest and computation of ApEn for each burst, poincaré plots were constructed for assessment of the variability in these measures. Fig. 2 provides an example of these poincaré plots. A tightly-clustered poincaré plot structure is seen for both the temporal features and ApEn; however, the poincaré plot structure is more dispersed for spectral power in all ranges.

Table 1 provides a summary of the values obtained for all of the measured parameters and their computed burst-to-burst variability estimates. Our quantitative analyses confirm that the temporal features, as well as intra-burst complexity, exhibit a small degree of burst-to-burst variability while spectral features show a greater degree of burst-to-burst variability (*e.g*., CV values). Variability estimates

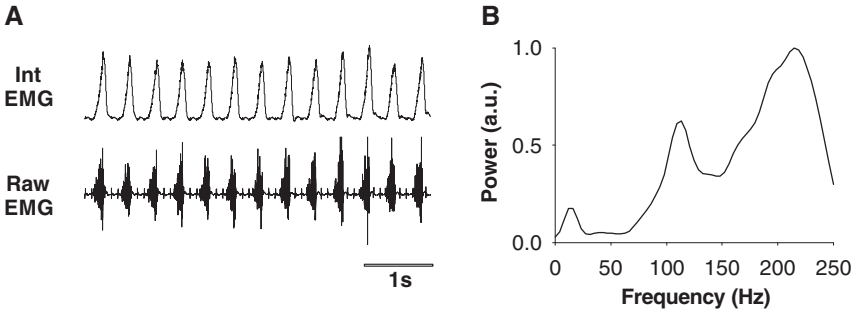

Fig. 1 Examples of diaphragm EMG activity and its corresponding power spectrum from a urethane-anesthetized mouse. (A) Both integrated (upper) and raw (lower) EMG activity are shown. (B) Ensemble-averaged FFT-based power spectrum demonstrates the three prominent peaks corresponding to MFO, HFO and UHFO

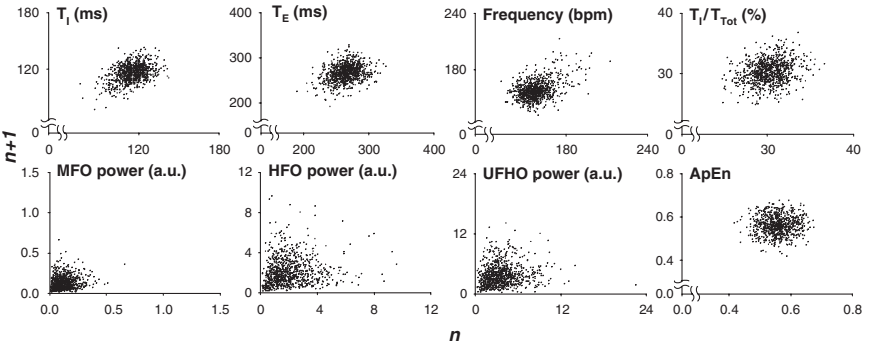

Fig. 2 Poincaré plots for temporal, spectral and complexity components in inspiratory motor output extracted from a representative mouse.

(*e.g*., SD1, SD2, etc.) varied according to the feature of interest, and our analyses suggest that SD1, SD2, and SD1/SD2, but not the Pearson correlation coefficients, may provide adequate information about dispersion for some, but not all, respiratory variables.

4 Discussion

Our findings demonstrate that temporal features and inspiratory network complexity (ApEn) exhibit less burst-to-burst variability than that observed for spectral activity. Differences were noted in the poincaré plot structure for the temporal features and ApEn, which exhibited a tightly clustered geometry, versus spectral activity, which exhibited a more diffuse data distribution. The magnitude of variability in these parameters was also identified by differences in the CV, which was substantially larger for the spectral features.

Amongst the temporal characteristics, T_E appeared to exhibit the greatest degree of variability, with a wider spread of data in the poincaré plot and in the computed SD1 and SD2 (*i.e*., short- and long-term, respectively) variability estimates. It should be noted, however, that the CV for T_E was less than that for T_I, which is consistent with previous observations in the urethane-anesthetized C57BL/6 mouse (Gonsenhauser *et al*. 2004). Our data, however, appear to be more tightly clustered than those of Gonsenhauser and colleagues and our CV values are also smaller. One possible explanation for this difference in burst-to-burst variability may be related to the basal breathing frequencies of the mice used in each study, which were markedly different (*e.g*., 260 ± 43 breaths/min in the study by Gonsenhauser and colleagues; 170 ± 5 breaths/min); however, data from a series of ongoing experiments in our laboratory focusing on the influence of breathing frequency (*i.e*., slow, 120–140 breaths/min; normal, 155–185 breaths/min; fast, 195–250 breaths/min) on burst-to-burst variability suggest that this is not the case.

Table 1 Summary data (mean ± SE) of all variables examined and the various indices of burst-to-burst variability computed for each variable. T_I, inspiratory duration; T_E, duration between bursts; Freq, breathing frequency; MFO, medium frequency oscillation; HFO, high frequency oscillation; UHFO, upper-high frequency oscillations; ApEn, approximate entropy value; CV, coefficient of variation; SD1, short-term burst-to-burst variability; SD2, long-term burst-to-burst variability; SD1/SD2, SD1 to SD2 ratio; Pearson, Pearson's correlation coefficient

	T_I (ms)	T_E (ms)	Frequency (bpm)	MFO	HFO	UHFO	ApEn
Mean ± SE	103.1 ± 4.6	252.9 ± 7.5	170 ± 5	0.19 ± 0.06	1.71 ± 0.37	2.88 ± 0.56	0.56 ± 0.01
CV	6.49 ± 0.48	5.03 ± 0.53	4.07 ± 0.51	65.26 ± 3.13	55.11 ± 1.69	50.93 ± 1.85	8.10 ± 0.17
SD1	5.99 ± 0.55	11.91 ± 1.05	6.36 ± 0.59	0.12 ± 0.02	0.94 ± 0.20	1.43 ± 0.26	0.04 ± 0.001
SD2	7.35 ± 0.73	13.33 ± 1.60	7.29 ± 1.28	0.13 ± 0.02	0.95 ± 0.21	1.45 ± 0.27	0.04 ± 0.001
SD1/SD2	0.83 ± 0.05	0.92 ± 0.06	0.96 ± 0.11	1.00 ± 0.04	1.00 ± 0.02	0.99 ± 0.01	0.98 ± 0.01
Pearson	0.18 ± 0.05	0.10 ± 0.05	0.07 ± 0.11	0.01 ± 0.04	−0.00 ± 0.02	0.01 ± 0.01	0.02 ± 0.01

Although burst-to-burst variability was greater in the spectral characteristics than in the other measured/computed parameters, there did not appear to be differences associated with the different spectral peaks (*i.e.*, MFO, HFO and UHFO). In the current study, however, our analyses were limited to only spectral power. Additional analyses focusing on the burst-to-burst dynamics of the location of spectral peaks within each range as well as the timing (time-varying) features of spectral activity remains to be determined. It also remains to be determined which of the quantitative indices best characterizes the burst-to-burst variability associated with spectral activity as both the variability estimates SD1/SD2 and the Pearson correlation coefficient seem to be inadequate to explain the degree of dispersion in these data. The present study, however, does indicate that quantitative characterization of burst-to-burst variability in conjunction with poincaré plot analyses may provide additional (objective) insight into the dynamic nature of the central respiratory neural controller.

Acknowledgement This research has been supported by NIH grant NS045321.

References

Brennan, M., Palaniswamim, M. and Kamen, K. (2001) Do existing measure of poincare plots geometry reflect nonlinear features of heart rate variability? IEEE Trans. Biomed. Eng. 48(11), 1342–1347.

Gonsenhauser, I., Wilson, C.G., Han, F., Strohl, K.P, and Dick, T.E. (2004) Strain differences in murine ventilatory behavior persist after urethane anesthesia. J. Appl. Physiol. 97(3), 888–894.

O'Neal, M.H. 3rd, Spiegel, E.T., Chon, K.H, and Solomon, I.C. (2005) Time-frequency representation of inspiratory motor output in anesthetized C57BL/6 mice *in vivo*. J. Neurophysiol. 93(3), 1762–1775.

Pincus, S.M. and Goldberger, A.L. (1994) Physiological time-series analysis: what does regularity quantify? Am. J. Physio. 266, H1643–H1656.

Pincus, S.M. (1991) Approximate entropy as a measure of system complexity. Proc. Natl. Acad. Sci. 88, 2297–2301.

Tulppo, M.P., Mäkikallio, T.H., Takala, T.E.S., Seppänen, T. and Huikuri, H.V. (1996) Quantitative beat-to-beat analysis of heart rate dynamics during exercise. Am. J. Physio. 271, H244–H252.

72
Effects of Hypercapnia on Non-nutritive Swallowing in Newborn Lambs

Charles Duvareille[1], Nathalie Samson[1], Marie St-Hilaire[1], Philippe Micheau[2], Véronique Bournival[1] and Jean-Paul Praud[1]

1 Summary

The purpose of this study was to determine the effect of hypercapnia on non-nutritive swallowing (NNS) frequency and on NNS-breathing coordination in newborn lambs. Six lambs were chronically instrumented for recording electroencephalogram, eye movements, diaphragm and thyroarytenoid muscle activity, nasal airflow and electrocardiogram. Each lamb was placed in a Plexiglas chamber and exposed to a hypercapnic gas mixture (21% O_2, 5% CO_2). Polysomnographic recordings were conducted in non-sedated lambs using a custom-designed radiotelemetry system. Results show that hypercapnia increased NNS frequency in all three states of alertness ($p < 0.0001$ to 0.03), through a specific increase in *ie*-type NNS. Causal mechanisms and potential consequences of such observations on aspirations and apneas, as well as on swallowing maturation, will require further studies.

2 Introduction

Breathing and swallowing are two competing functions at the upper airway level (Oommen 2004). As breathing and swallowing cannot occur simultaneously, they must be perfectly coordinated, and a short respiratory pause is observed with laryngeal closure during swallowing. Furthermore, swallowing and respiratory central pattern generators are located in neighboring regions in the brainstem, mainly the nucleus tractus solitarius and nucleus ambiguus (Ertekin and Aydogdu 2003). This neuronal co-localization facilitates both reciprocal inhibition and coordination (Miller and Kiatchoosakun 2004).

[1] Neonatal Respiratory Research Unit, Departments of Pediatrics and Physiology, Université de Sherbrooke, Quebec, Canada, charles.duvareille@usherbrooke.ca

[2] Department of Mechanical Engineering, Université de Sherbrooke, Quebec, Canada

M.J. Poulin and R.J.A. Wilson (eds.), *Integration in Respiratory Control: From Genes to Systems*. © Springer 2008

Studies on breathing-swallowing coordination have led to the description of 4 types of non-nutritive swallowing (NNS). These include the *e*-type NNS (begins and ends in expiration), the *i*-type NNS (begins and ends in inspiration), the *ie*-type NNS (occurs at the transition between inspiration and expiration) and the *ei*-type NNS (occurs at the transition between expiration and inspiration). Relevance for studying the precise NNS-breathing coordination arises from the premise that NNS occurring during inspiration could carry a higher risk of aspiration (Lau, Smith and Schanler 2003), while NNS occurring during expiration may carry a higher risk of apnea.

Following our recent descriptions of NNS-breathing coordination in our term and pre-term ovine newborn models (Reix, Fortier, Niyonsenga, Arsenault, Letourneau and Praud 2003; Reix, Arsenault, Langlois, Niyonsenga and Praud 2004), we elected to study the effect of various conditions on this coordination, such as hypercapnia, a respiratory stress frequently encountered in newborns. The only two previous studies on the effects of hypercapnia on swallowing have yielded contradictory results. Indeed, while no effects were observed in anesthetized adult cats (Nishino, Kohchi, Honda, Shirahata and Yonesawa 1986), a decrease in swallowing was reported in adult humans (Nishino, Hasegawa, Ide and Isono 1998). To our knowledge, there is no available study on the effects of hypercapnia in the neonatal period. The aim of the present study was therefore to investigate the effects of hypercapnia on NNS frequency and NNS-breathing coordination in newborn lambs.

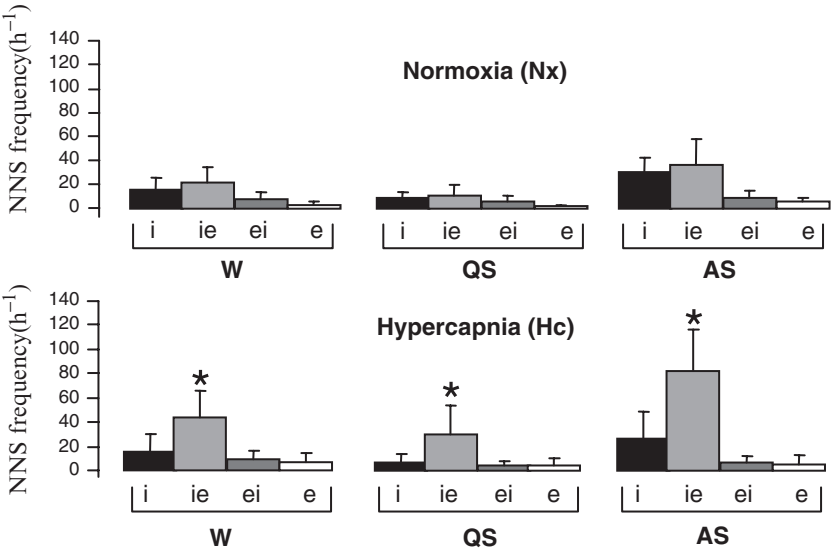

Fig. 1 NNS-breathing coordination during hypercapnia

3 Methods

3.1 Surgical Preparation

Six lambs were chronically instrumented under general anesthesia for recording NNS (laryngeal constrictor EMG), states of alertness (electrocorticogram and eye movements), respiration (diaphragm EMG, respiratory inductance plethysmography, nasal flow, pulse oximetry, end-tidal PCO_2) and electrocardiogram.

3.2 Design of the Study

Non-sedated lambs underwent 2 polysomnographic recordings on 2 different days while in a Plexiglas chamber flushed with air (Nx: normoxia, FiO_2 0.21) or a hypercapnic mixture (Hc: FiO_2 0.21, $FiCO_2$ 0.05, $P_{ET}CO_2 \approx 50$ mmHg) in a random order. A custom-designed radiotelemetry system was used for polysomnography.

4 Results

Hypercapnia (Table 1) led to a significant increase in NNS frequency during the three states of alertness [$p < 0.0001$ to 0.03 *vs*. Nx]. Analysis of NNS-breathing coordination showed that this increase was entirely due to an increase in *ie*-type NNS ($p = 0.0004$ to 0.004 *vs*. Nx). Consequently, irrespective of the state of alertness, the *ie*-type frequency in Hc was greater than *i*-type, *ei*-type and *e*-type frequency altogether ($p < 0.0001$ to 0.01 *vs*. Nx).

Table 1 RR: respiratory rate (h^{-1}); iNNS/eNNS: NNS frequency occurring in inspiration or expiration (h^{-1}); ieNNS/eiNNS: NNS frequency occurring at the transition between inspiration-expiration or expiration-inspiration (h^{-1}). $^{*}p < 0.05$, Nx *vs*. Hc

	Normoxia (Nx)			Hypercapnia (Hc)		
	W	QS	AS	W	QS	AS
RR	63 ± 21	60 ± 22	61 ± 10	90 ± 30*	89 ± 29*	77 ± 17*
NNS freq	57 ± 14	29 ± 9	87 ± 25	82 ± 33*	45 ± 25*	128 ± 48*
iNNS/eNNS	16 ± 10/3 ± 3	9 ± 5/2 ± 1	31 ± 12/6 ± 3	15 ± 15/7 ± 8	7 ± 7/4 ± 6	27 ± 22/5 ± 8
ieNNS/eiNNS	22 ± 13/8 ± 6	11 ± 9/6 ± 6	36 ± 22/9 ± 6	43 ± 22*/9 ± 7	30 ± 24*/4 ± 4	82 ± 35*/7 ± 5

5 Discussion

The present study provides new insight on the differential effect of moderate hypercapnia on non-nutritive swallowing in the neonatal period. Hypercapnia was observed to increase NNS frequency, this increase being specifically due to an increase in *ie*-type NNS, regardless of the state of alertness. To our knowledge, this is the first study to assess the effect of hypercapnia on spontaneous NNS, including on NNS-breathing coordination, in the neonatal period.

Causal mechanisms involved in this increase are still under study. Several hypotheses can be formulated. First, acute hypercapnia may increase saliva secretion, as previously reported in sheep (16% CO_2) (Hoover, Sawyer and Apgar 1971). Secondly, swallowing upper airway receptors could be stimulated by hypercapnia and/or consequent hyperventilation (Nishijima, Tsubone and Atoji 2004). Finally, hypercapnia may have a direct effect on the swallowing centers, which share common medullary locations with respiratory centers (Ertekin *et al*. 2003).

6 Conclusion

Our results suggest that moderate hypercapnia stimulates both respiration and NNS, more specifically *ie*-type NNS. Potential consequences of such observations on swallowing maturation will require further studies.

Acknowledgements The authors would like to gratefully acknowledge the technical assistance of Jean-Philippe Gagné, and M-P Garant for statistical help. The experiments were supported by the Canadian Institutes of Health Research (NRF 15558) and the Quebec Foundation for Research into Children's diseases. Jean-Paul Praud is a national scholar of the *Fonds de la Recherche en Santé du Québec*.

References

Ertekin, C. and Aydogdu, I. (2003) Neurophysiology of swallowing. Clin. Neurophysiol. 114, 2226–2244.

Hoover, W.H., Sawyer, M.S. and Apgar, W.P. (1971) Ovine nutritional responses to elevated ambient carbon dioxide. J. Nutr. 101, 1595–1600.

Lau, C., Smith, E.O. and Schanler, R.J. (2003) Coordination of suck-swallow and swallow respiration in pre-term infants. Acta Paediatr. 92, 721–727.

Miller, M.J. and Kiatchoosakun, P. (2004) Relationship between respiratory control and feeding in the developing infant. Sem. Neonatol. 9, 221–227.

Nishijima, K., Tsubone, H. and Atoji, Y. (2004) Contribution of free nerve endings in the laryngeal epithelium to CO_2 reception in rats. Auton. Neurosci. 110, 81–88.

Nishino, T., Kohchi, T., Honda, Y., Shirahata, M. and Yonesawa, T. (1986) Differences in the effect of hypercapnia on the swallowing reflex in cats. Br. J. Anaesth. 58, 903–908.

Nishino, T., Hasegawa, R., Ide, T. and Isono, S. (1998) Hypercapnia enhances the development of coughing during continuous infusion of water into the pharynx. Am. J. Respir. Crit. Care. Med. 157, 815–821.

Oommen, M.P. (2004) Respiratory control during oral feeding. In : M.P. Oommen MP (Ed.), *Respiratory Control and Disorders in the Newborn. Lung Biology in Health and Disease*, Vol. 173. Marcel Dekker, New York, pp. 373–393.

Reix, P., Fortier, P.H., Niyonsenga, T., Arsenault, J., Letourneau, P. and Praud, J.P. (2003) Non-nutritive swallowing and respiration coordination in full-term newborn lambs. Respir. Physiol. Neurobiol. 134, 209–218.

Reix, P., Arsenault, J., Langlois, C., Niyonsenga, T. and Praud, J.P. (2004) Non-nutritive swallowing and respiration relationships in pre-term lambs. J. Appl. Physiol. 97, 1283–1290.

73
CPAP Inhibits Non-nutritive Swallowing Through Stimulation of Bronchopulmonary Receptors

Nathalie Samson[1], Charles Duvareille[2], Marie St-Hilaire[3], Véronique Clapperton[4] and Jean-Paul Praud[5]

1 Summary

While swallowing and respiratory problems are among the most frequent disorders encountered in neonates, the interrelationships between both functions are not completely understood. This is especially true for non-nutritive swallowing (NNS), which fulfills the important function of clearing upper airways from both local secretions and liquids refluxed from the stomach. Recently, we showed that nasal CPAP inhibits NNS during quiet sleep in the newborn lamb (Samson, St-Hilaire, Nsegbe, Reix, Moreau-Bussière and Praud 2005). The present study was aimed at testing the hypothesis that NNS inhibition is eliminated when CPAP is directly administered through a tracheostomy, thus eliminating reflexes originating from upper airway receptors. Results show that both nasal and tracheal CPAP 6 cm H_2O similarly inhibit total NNS during quiet sleep, thus suggesting that the inhibiting effect of nasal CPAP on NNS is mainly mediated through bronchopulmonary mechanical receptors with minimal participation of the upper airways.

2 Introduction

Swallowing and breathing control mechanisms are intimately related and are competing functions at the upper airways level. A perfect breathing-swallowing coordination is crucial in preventing both lung aspiration and apnea development. This is especially true for NNS, which serves the major function of clearing both the large amount of upper airway secretions produced daily, and gastropharyngeal refluxes particularly frequent in the neonatal period.

[1–5] Neonatal Respiratory Research Unit, Departments of Pediatrics and Physiology, Université de Sherbrooke, Québec, Canada, jean-paul.praud@usherbrooke.ca

M.J. Poulin and R.J.A. Wilson (eds.), *Integration in Respiratory Control: From Genes to Systems*.

Very few data are available on the potential effects of various conditions such as hypoxia, hypercapnia and nasal administration of positive pressure on breathing swallowing coordination. Nasal application of positive pressure, either intermittently (nasal intermittent positive pressure ventilation) or continuously (nasal continuous positive airway pressure = nCPAP), is increasingly used in the neonatal period as treatment for mild respiratory distress syndrome, apneas of prematurity and as a means of reducing the rate of extubation failure following endotracheal mechanical ventilation (Brochard 2003). Limited data from the literature suggest that nCPAP can influence swallowing function. Indeed, nCPAP has been shown to inhibit swallowing in awake human adults (Nishino, Sugimori, Kohchi and Hiraga 1989) and NNS in quiet sleep in the newborn lamb (Samson *et al*. 2005). In comparison, the effects of nasal intermittent positive pressure ventilation on NNS frequency were more variable in the newborn lamb (Samson *et al*. 2005).

Studies are currently ongoing to understand the mechanisms responsible for decreasing NNS frequency in quiet sleep in our lamb model. The present study was aimed at testing the hypothesis that NNS inhibition is eliminated when CPAP is directly administered through a tracheostomy, thus eliminating reflexes originating from upper airway receptors.

3 Methods

3.1 Surgical Preparation

Six full-term lambs were included in this study. At day two of life, surgery was performed under general anesthesia for chronic instrumentation of the lambs:

(1) electrodes were inserted into two glottal constrictor muscles (thyroarytenoid muscles) for electrical activity (EMG) recording, as a surrogate for NNS activity; (2) one electrode was inserted 5 cm distal to the esophageal inlet to record esophageal muscle EMG; (3) two platinum needle-electrodes were inserted into the parietal cortex for electrocorticogram recording and for states of alertness scoring; and (4) an external tracheostomy (= no endotracheal tube) was installed, as previously described (Lemaire, Létourneau, Dorion and Praud 1999).

3.2 Design of the Study

Three polysomnographic recordings of 4 to 6 h were performed in each lamb at postnatal days 4, 5 and 6 between 6:00 a.m. and 12:00 p.m. Each non-sedated lamb was exposed to three different experimental conditions in random order: (1) a control recording during which the lamb breathed through its nasal mask with no CPAP and with the tracheostomy closed; (2) a recording during administration of a CPAP of 6 cmH_2O through the nasal mask, with the tracheostomy closed

(nCPAP); and (3) a recording during administration of a CPAP of 6 cm H_2O through the tracheostomy tube (tCPAP). All recordings were performed using our custom-designed radiotelemetry system. Data from quiet sleep only were analyzed. Frequency of isolated NNS, NNS in bursts (≥ 2 NNS occurring within 4 seconds), and total NNS (isolated NNS + NNS in bursts) were calculated.

4 Results

Results are illustrated in Fig. 1. Compared to control conditions (45 ± 18 h^{-1}), total NNS frequency was significantly decreased by nCPAP 6 (26 ± 12 h^{-1}, $p < 0.0001$) and tCPAP 6 (25 ± 14 h^{-1}, $p = 0.0001$) during quiet sleep. No statistical difference was observed between nCPAP 6 and tCPAP 6 ($p = 1.0$). Identical results were also observed for isolated NNS frequency. However, compared with control conditions (4 ± 4 h^{-1}), only nCPAP 6 (1 ± 1 h^{-1}, $p = 0.001$) inhibited bursts of NNS. No statistical difference was observed between no CPAP and tCPAP 6 ($p = 0.1$) and between nCPAP 6 and tCPAP 6 ($p = 0.4$).In summary, both nasal and tracheal CPAP 6 inhibited total and isolated NNS frequency during quiet sleep. Oppositely, only nasal CPAP 6 inhibited bursts of NNS frequency during quiet sleep.

5 Discussion

Preliminary results from our mechanistic studies show that application of CPAP through a tracheostomy induces a decrease in NNS frequency similar to nasal CPAP, suggesting that the inhibiting effect of nasal CPAP on NNS is mainly mediated through vagal afferent messages originating from bronchopulmonary receptors, likely the slowly adapting receptors. Accordingly, two separate prior studies

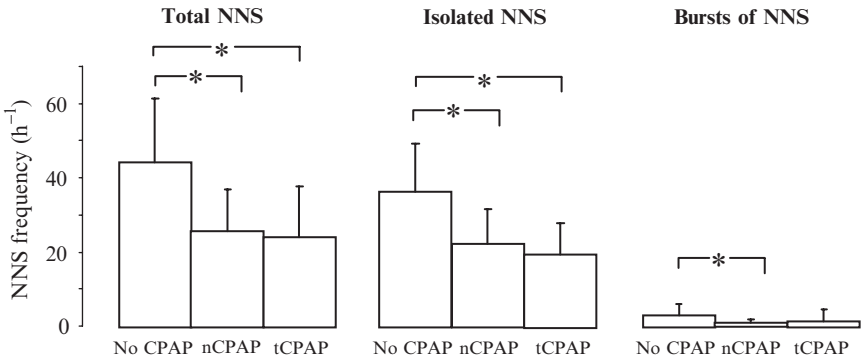

Fig. 1 Relationships between NNS frequency and the different experimental conditions studied during quiet sleep

concluded that stimulation of slowly adapting bronchopulmonary receptors by nasal CPAP inhibits water-induced swallowing in awake adult humans (Kijima, Isono and Nishino 2000; Yamamoto and Nishino 2002). Studies are currently ongoing in our laboratory to further test this hypothesis, comparing the effects of nasal CPAP administration in lambs before and after bilateral thoracic vagotomy, thus eliminating the afferent messages originating from bronchopulmonary receptors. While our results to date strongly suggest an important role for bronchopulmonary receptors, it must be acknowledged that additional mechanisms may also involve a direct effect of CPAP on the upper airways. Thus, CPAP could decrease upper airway secretions or dilate piriform sinuses, which would increase their reservoir capacity for secretions and delay NNS. Alternatively, CPAP may also decrease the sensitivity of upper airway swallowing receptors. Finally, the inhibiting effect of nCPAP on gastropharyngeal refluxes could be involved (Fournier, Kerr, Shoenut and Yaffe 1999).

6 Conclusion

The present mechanistic study reveals that both nasal and tracheal CPAP 6 cm H_2O similarly inhibit total NNS during quiet sleep, thus suggesting that the inhibiting effect of nasal CPAP on NNS is mainly mediated through bronchopulmonary receptors, likely the slowly adapting receptors. Irrespective of the mechanism(s) involved, clinical relevance of these results is intimately related to the importance of NNS for clearing the upper airways from secretions and gastric content frequently regurgitated in the neonatal period. In addition, prolonged application of nCPAP in the immature newborn may lead to a delay in swallowing maturation or even long lasting disturbances in swallowing function. However, this remains to be tested.

Acknowledgements The authors would like to acknowledge Jean-Philippe Gagné for technical support as well as Marie-Pierre Garant for statistical counseling. Nathalie Samson is a recipient of a Canada graduate scholarship award. Jean-Paul Praud is a national scholar of the "Fonds de la recherche en santé du Québec". This work was supported by the Canadian Institutes of Health Research (NRF 15558), and the Quebec Foundation for Research into Children's Diseases.

References

Brochard, L. (2003) Mechanical ventilation: invasive versus noninvasive. Eur. Respir. J. Suppl. 47, 31s–37s.

Fournier, M.R., Kerr, P.D., Shoenut, J.P. and Yaffe, C.S. (1999) Effect of nasal continuous positive airway pressure on esophageal function. J. Otolaryngol. 28, 142–144.

Kijima, M., Isono, S. and Nishino, T. (2000) Modulation of swallowing reflex by lung volume changes. Am. J. Respir. Crit. Care Med. 162, 1855–1858.

Lemaire, D., Létourneau, P., Dorion, D. and Praud, J.P. (1999) Complete glottic closure during central apnea in lambs. J. Otolaryngol. 28, 13–19.

Nishino, T., Sugimori, K., Kolchi, A. and Hiraga, K. (1989) Nasal constant positive airway pressure inhibits the swallowing reflex. Am. Rev. Respir. Dis. 140, 1290–1293.
Samson, N., St-Hilaire, M., Nsegbe, E., Reix, P., Moreau-Bussiere, F., Praud, J.P. (2005) Effect of nasal continuous or intermittent positive pressure on non-nutritive swallowing in newborn lamb. J. Appl. Physiol. 99, 1636–42.
Yamamoto, F., and Nishino, T., (2002) Phasic vagal influence on the rate and timing of reflex swallowing. Am. J. Respir. Crit. Care Med. 165, 1400–3.

74
Glutamatergic Neurotransmission is Not Essential for, but Plays a Modulatory Role in, the Production of Gasping in Arterially-Perfused Adult Rat

Kelly A. Warren[1] and Irene C. Solomon[2]

Abstract Glutamatergic neurotransmission appears to be essential for generation of the eupneic pattern of inspiratory motor discharge as well as the expression of inspiratory-phase synchronization. The role of glutamatergic neurotransmission in the generation of gasping, including its accompanying modulation of spectral activity, is less well understood. The current investigation was, therefore, undertaken to investigate the effects of blockade of ionotropic glutamate receptors on (1) the generation and expression of gasping and (2) the magnitude and timing of spectral activity during gasping using an arterially-perfused decerebrate adult rat preparation. Our findings suggest that glutamatergic neurotransmission is not required for the production of gasping, but it may play a modulatory role in the expression of both the temporal and spectral characteristics of phrenic nerve discharge during gasping.

1 Introduction

Numerous studies have demonstrated a role for glutamatergic neurotransmission in the eupneic pattern of inspiratory motor discharge by showing that blockade of N-methyl-D-aspartate (NMDA) and/or non-NMDA (*i.e.*, ionotropic excitatory amino acid (EAA) receptor subtypes) receptors alters inspiratory burst timing and patterning, both *in vivo* and *in vitro*. These studies have also shown that ionotropic EAA receptor activation is essential for the generation of respiratory rhythm (*i.e.*, breathing) as well as for synchronization amongst subsets of inspiratory-related neurons (*e.g.*, putative rhythmogenic neurons). Recent work from our laboratory, for example, has demonstrated that blockade of ionotropic EAA receptors not only abolishes basal phrenic nerve discharge but also markedly reduces spectral activity (which serves as an index of inspiratory-phase synchronization) in an arterially-perfused adult rat preparation. The role of ionotropic EAA receptor activation in the generation of hypoxia/ischemia-induced gasping, including its accompanying modulation of spectral activity, is less well understood.

[1–2] SUNY at Stony Brook, Department of Physiology and Biophysics, kwarren@ic.sunsyb.edu

M.J. Poulin and R.J.A. Wilson (eds.), *Integration in Respiratory Control: From Genes to Systems*. © Springer 2008

To date, only a limited number of studies have explored a potential role for the activation of ionotropic EAA receptors in the production of gasping (Chae, Melton, Neubauer and Edelman 1993; Gozal and Torres 1997; Solomon 2004). Chae and colleagues (1993), for example, have demonstrated that systemic administration of either NMDA or non-NMDA receptor antagonists is ineffective in altering gasping produced by carbon monoxide in the anesthetized adult cat. Gozal and Torres (1997) also reported a similar finding for gasping produced by anoxia following systemic administration of a NMDA receptor antagonist in 15-day-old rats although in younger animals (*i.e.*, 2- to 10-day-old), a delay in the onset to gasping was noted. In these studies, however, no attempt was made to simultaneously block both ionotropic EAA receptor subtypes. In contrast, recent work from our laboratory in the anesthetized adult cat has shown that simultaneous blockade of ionotropic EAA receptors in the pre-Bötzinger complex (*i.e.*, primary locus of respiratory rhythm generation) eliminates not only eupneic phrenic bursts but also modifies the threshold for elicitation of hypoxia-induced gasps, gasp duration and gasp frequency (Solomon 2004). In this study, however, ionotropic EAA receptor blockade was restricted to only the pre-Bötzinger complex; thus, the potential contribution of ionotropic EAA receptor activation by other regions of the central respiratory network in the production of gasping remain to be investigated.

The current investigation was, therefore, undertaken to investigate the effects of simultaneous blockade of NMDA and non-NMDA receptors using systemic application of antagonists on (1) the generation and expression of gasping and (2) the magnitude and timing of spectral activity during gasping using an arterially-perfused decerebrate adult rat preparation.

2 Experimental Protocol

All experiments were performed under protocols approved by the Institutional Animal Care and Use Committee at SUNY Stony Brook following the NIH Policy of Humane Care and Use of Laboratory Animals. The methods have been previously published and will not be repeated here (Solomon, Chon and Rodriguez 2003).

We examined the temporal and spectral characteristics of phrenic nerve discharge during gasping in both the absence and presence of pharmacological blockade of NMDA and non-NMDA receptors in an arterially-perfused decerebrate adult rat preparation. Simultaneous blockade of both receptor subtypes was accomplished by systemic administration of kynurenic acid (KYN, 1.5–3.0 mM, n = 3) or a cocktail containing the NMDA receptor antagonist AP5 and the non-NMDA receptor antagonist NBQX (20 μM/5 μM, n = 1). Gasping was produced by opening a bypass that redirected the perfusate away from the preparation (*i.e.*, ischemia), and 3–15 gasps were recorded before the bypass was closed to re-establish perfusion. Basal phrenic nerve discharge was recorded for 10 minutes; the preparation was then perfused with the antagonist for at least 15 minutes, after which the bypass was opened. In some experiments, multiple gasping trials were performed. In control experiments (n = 5), similar gasping trials were conducted in the absence of antagonists.

2.1 Data Acquisition and Analysis

Phrenic nerve activity was amplified (×10 K), notch filtered (60 Hz), analog filtered (10 Hz and 1 kHz), and recorded on a computer at a sampling rate of 2 kHz (Chart 5.0, PowerLab, ADInstruments) for offline analyses (MatLab 7.0.1). From the time series trace, phrenic nerve activity corresponding to (1) basal discharge, (2) antagonist-induced discharge and (3) gasping were extracted. For control experiments, only basal discharge and gasping were obtained. For all analyses, these data were segmented to obtain data lengths corresponding to the inspiratory burst. The data were then re-sampled with a sampling rate of 500 Hz, after digital band-pass filtering from 20–250 Hz using a 100th order Hamming window.

Inspiratory burst duration (T_I), the duration between bursts (T_E), and burst frequency were determined under each condition. Time-frequency (TF) spectra were computed using a generalized TFR with the smoothed pseudo Wigner-Ville distribution (SPWD) kernel. A detailed description of the methods and algorithms for these analyses has been previously published (O'Neal, Spiegel, Chon and Solomon 2005).

All data are reported as mean ± SE. TF spectra are presented as ensemble averages. Statistical comparisons were made using a one-way RM ANOVA, followed by Holm-Sidak *post hoc* analyses for all pairwise comparisons.

3 Results

In each of the experiments conducted, blockade of ionotropic EAA receptors by KYN or the AP5/NBQX cocktail markedly altered the timing, patterning and spectral content of phrenic nerve discharge; however, gasping could still be produced in response to opening the bypass. In general, antagonist perfusion was accompanied by an initial prolongation of T_I (from 659 ± 53 ms to 1107 ± 236 ms), a decrease in T_E (from 3.75 ± .53 s to 1.36 ± 0.12 s), a reduction in burst amplitude (by ~ 60%), and a decrease in total spectral power. With continued perfusion, basal phrenic nerve discharge was ultimately eliminated. An example of modulation of these temporal and spectral features in phrenic nerve discharge in response to perfusion with KYN are shown in Figs. 1 and 2, respectively.

3.1 Effects on Gasping

Both in the absence and presence of antagonist, opening the bypass elicited gasping. An example of gasping during antagonist perfusion is shown in Fig. 1. Under control conditions, T_I during gasping was reduced from 654 ± 32 to 489 ± 15 ms ($p < 0.05$) while T_I during gasping with ionotropic EAA blockade was reduced to 409 ± 24 ms ($p < 0.05$ vs. baseline and vs. KYN alone). It should be noted that T_I of gasps during antagonist perfusion was also significantly shorter than T_I of control gasps ($p < 0.05$).

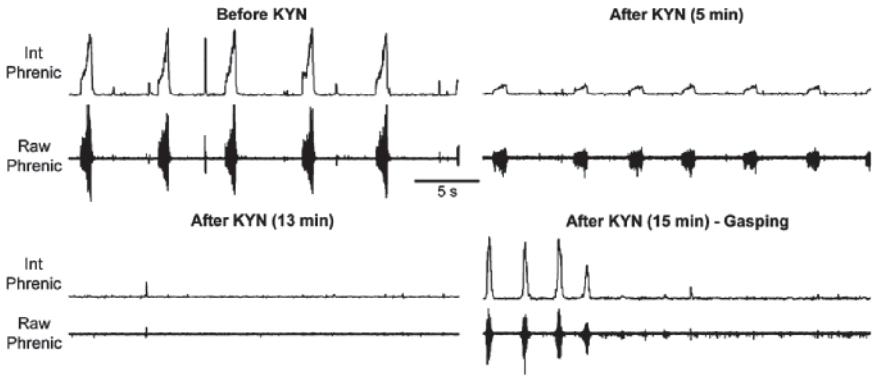

Fig. 1 Example traces of phrenic nerve discharge before and after blockade of ionotropic EAA receptors with KYN. Perfusion with KYN decreases and then abolishes basal phrenic nerve discharge; however, gasping can still be elicited by hypoxia/ischemia

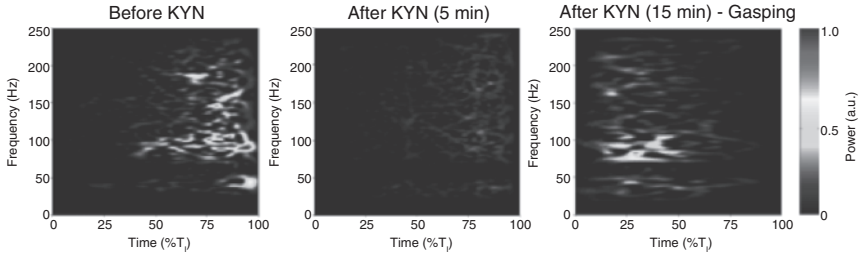

Fig. 2 TF spectra of phrenic nerve discharge before and after blockade of ionotropic EAA receptors with KYN. Perfusion with KYN decreases spectral activity; however, gasping not only recovers spectral power but also shifts spectral activity to an earlier time point in the inspiratory burst

Antagonist perfusion also produced marked changes in spectral activity during gasping. An example of spectral activity during gasping with antagonist perfusion is shown in Fig. 2. As can be seen, although blockade substantially reduced the power of both the MFO and HFO peaks under baseline conditions, power of the HFO peak was partly or completely restored during gasping and power of the MFO peak was enhanced above baseline levels. In addition, similar to the changes in spectral timing observed under control conditions (not shown), spectral activity shifted to an earlier time point in the inspiratory burst during gasping in the presence of antagonist; however, some degree of dysynchronization (*i.e.*, diffuse spectral bursts) was noted.

4 Discussion

Our findings demonstrate that simultaneous blockade of NMDA and non-NMDA receptors, which is capable of eliminating basal phrenic nerve discharge, does not abolish gasping. In addition, the blockade-induced reduction in HFO power is partly or completely recovered during gasping and MFO activity is enhanced.

Our observation that gasping could be elicited following blockade of ionotropic EAA receptors is consistent with those of previous studies that examined the effects of blockade of either NMDA or non-NMDA receptors alone (Chae *et al*. 1993; Gozal and Torres 1997) or simultaneous blockade of these receptors in only the pre-Bötzinger complex (Solomon 2004). In contrast to the results of these studies, however, we found that the magnitude of the reduction in T_I during gasping was greater in the presence of antagonist perfusion than under control conditions.

To our knowledge, these are the first observations regarding changes in spectral activity, including its timing, during eupnea and gasping in the presence of ionotropic EAA receptor blockade. Recent observations in this preparation, however, have shown that during gasping (under control conditions), HFO power is enhanced (St. John and Leiter 2003). Our current findings extend these observations to demonstrate that not only is HFO power enhanced but spectral activity shifts to an earlier part of the inspiratory burst, and that this modulation is also seen during ionotropic EAA receptor blockade. Taken together, these findings suggest that EAA neurotransmission is not required for the production of gasping, but it may play a modulatory role in the expression of both the temporal and spectral characteristics of phrenic nerve discharge during gasping.

Acknowledgements This work was supported by NIH grants NS045321 and NS049310.

References

Chae, L.O., Melton, J.E., Neubauer, J.A. and Edelman, N.H. (1993) Phrenic and sympathetic nerve responses to glutamatergic blockade during normoxia and hypoxia. J. Appl. Physiol. 74, 1954–1963.

Gozal, D. and Torres, J.E. (1997) Maturation of anoxia-induced gasping in the rat: potential role for N-methyl-D-aspartate glutamate receptors. Pediatr. Res. 42, 872–877.

O'Neal, M.H., Spiegel, E.T., Chon, K.H. and Solomon, I.C. (2005) Time-frequency representation of inspiratory motor output in anesthetized C57BL/6 mice *in vivo*. J. Neurophysiol. 93, 1762–1775.

Solomon, I.C. (2004) Ionotropic excitatory amino acid receptors in pre-Bötzinger complex play a modulatory role in hypoxia-induced gasping *in vivo*. J. Appl. Physiol. 96, 1643–1650.

Solomon, I.C., Chon, K.H. and Rodriguez, M.N. (2003) Blockade of brain stem gap junctions increases phrenic burst frequency and reduces phrenic burst synchronization in adult rat. J. Neuorophysiol. 89, 135–149.

St. John, W.M. and Leiter, J.C. (2003) High-frequency oscillations of phrenic activity in eupnea and gasping of *in situ* rat: influence of temperature. Am. J. Physiol. Regul. Integr. Comp. Physiol. 285, R404–R412.

Part XII
Clinical Perspectives: Modeling and Control of Breathing (*i.e.*, Sleep Apnea)

75
Potential Mechanism for Transition Between Acute Hypercapnia During Sleep to Chronic Hypercapnia During Wakefulness in Obstructive Sleep Apnea

Kenneth I. Berger[1], Robert G. Norman[2], Indu Ayappa[3], Beno W. Oppenheimer[4], David M. Rapoport[5] and Roberta M. Goldring[6]

Abstract This paper presents a series of experiments, both in patients and computer models, investigating the transition from acute to chronic hypercapnia in OSA. The data demonstrate that acute hypercapnia during periodic breathing occurs due to either reduction in magnitude of inter-event ventilation and/or reduction in inter-event ventilatory duration relative to duration of the preceding event. The transition between acute hypercapnia during sleep and chronic sustained hypercapnia during wakefulness may be determined by an interaction between respiratory control and renal handling of HCO_3^- .

1 Introduction

Chronic daytime hypercapnia occurs in a subset of patients with obstructive sleep apnea (OSA). The observation that hypercapnia may correct with administration of continuous positive airway pressure supports a role for the apnea phenomenon *per se* in generation of the chronic hypercapnia (Rapoport, Garay, Epstein and Goldring 1986). The observation that most patients with OSA are not hypercapnic suggests that, although respiratory control mechanisms may incite periodic breathing, they remain responsive to the accompanying acute changes in CO_2 balance. Therefore, acute hypercapnia during periodic breathing results from an imbalance between

[1] NYU School of Medicine, Department of Medicine, kenneth.berger@med.nyu.edu

[2] robert.norman@med.nyu.edu

[3] indu.ayappa@med.nyu.edu

[4] beno.oppenheimer@med.nyu.edu

[5] david.rapoport@med.nyu.edu

[6] roberta.goldring@med.nyu.edu

M.J. Poulin and R.J.A. Wilson (eds.), *Integration in Respiratory Control: From Genes to Systems*.

CO_2 loading during respiratory events and the inter-event CO_2 unloading that results from compensatory ventilatory response (Javaheri, Colangelo, Lacey and Gartside 1994).

2 Acute Hypercapnia during Periodic Breathing

Computer simulation revealed that maintenance of eucapnia during periodic breathing required increased post-event ventilation above that required to compensate for apnea (Rapoport, Norman and Goldring 1993). This occurred because periodic breathing produces a temporal dissociation between CO_2 delivery to the lung and ventilatory excretion ('temporal' $\dot{V}\dot{Q}$ mismatch). During apnea/hypopnea there is continued perfusion with limited ventilation, and during inter-event periods ventilation is increased relative to blood flow. As with other causes of $\dot{V}\dot{Q}$ mismatch, CO_2 homeostasis during temporal $\dot{V}\dot{Q}$ mismatch requires that inter-event ventilation be increased above that required for maintenance of steady-state ventilation.

These data were extended to human subjects with OSA utilizing studies of whole body CO_2 balance during periodic breathing (Berger *et al*. 2000). A breath-by-breath method was used to calculate whole body CO_2 balance (Fig. 1). Using this technique, we measured CO_2 balance during periodic breathing and addressed the ventilatory compensation for maintenance of CO_2 homeostasis. The results demonstrated that: (1) periodic breathing provides a mechanism for acute hypercapnia in OSA; (2) acute hypercapnia during periodic breathing occurs despite maintenance of average minute ventilation at the steady-state level, in accord with

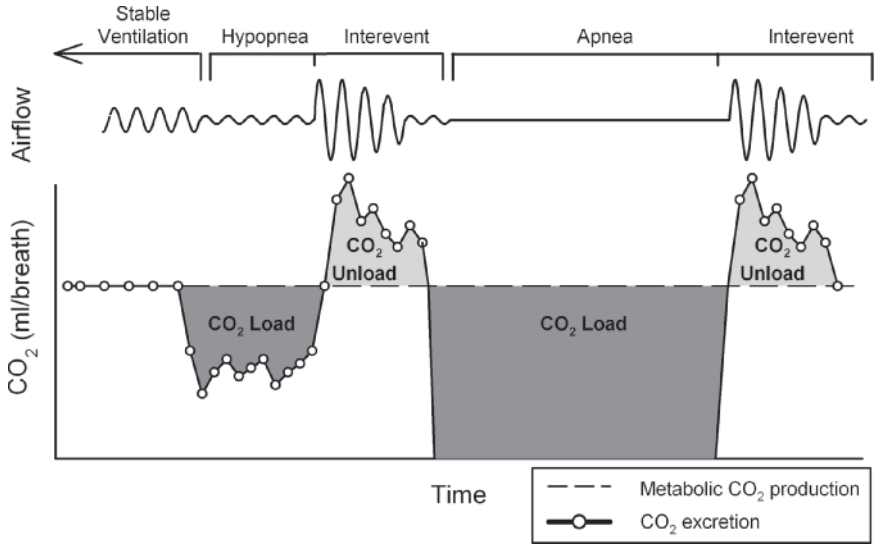

Fig. 1 Calculation of whole body CO_2 balance (Berger, Ayappa, Sorkin, Norman, Rapoport and Goldring 2000)

presence of temporal $\dot{V}\,\dot{Q}$ mismatch; and (3) compensation for CO_2 loading during apnea may be limited by the duration of the inter-event interval and by the magnitude of the inter-event ventilation.

3 Relationship to Chronic Hypercapnia

The above mechanisms were studied in patients with severe OSA and chronic stable hypercapnia. The first study hypothesized that hypercapnic patients will have shorter inter-event duration relative to duration of the preceding event (Ayappa, Berger, Norman, Oppenheimer, Rapoport and Goldring 2002). 18 subjects with severe OSA (waking P_aCO_2 36–62 torr) were studied. There was no relationship between P_aCO_2 and apnea or interapnea duration. However, chronic P_aCO_2 was directly related to apnea/interapnea duration ratio; increasing P_aCO_2 was associated with shortening of interapnea duration relative to duration of the preceding event ($r = 0.47$, $p < 0.05$).

The next study examined the magnitude of post-event ventilation in 14 patients (waking P_aCO_2 42–56 torr) with severe OSA (Berger, Ayappa, Sorkin, Norman, Rapoport and Goldring 2002). The volume of CO_2 loaded during each event and the immediate post-event ventilatory rate (first 10 seconds of inter-event interval) were determined. The post-event ventilation was directly related to the CO_2 loaded during the preceding event in 12 subjects. This slope represents a measure of ventilatory responsiveness, which varied across patients. An inverse relationship was noted between this post-event ventilatory response slope and the awake P_aCO_2 indicating impairment of this mechanism in chronic hypercapnia ($r = 0.90$, $p < 0.05$).

Thus, control of inter-apnea duration relative to duration of the preceding event and control of post-event ventilatory response to the volume of CO_2 loaded are both impaired in patients with OSA and established chronic daytime hypercapnia.

4 Transition Between Acute to Chronic Hypercapnia

Elevated $[HCO_3^-]$ may provide a mechanism for development and perpetuation of the chronic hypercapnic state. Elevated $[HCO_3^-]$ would blunt the change in [H+] for a given change in PCO_2, in accord with the Henderson-Hasselbalch relationship, thereby blunting ventilatory CO_2 drive. This alteration of CO_2 drive has been demonstrated in humans under experimentally altered serum $[HCO_3^-]$ (Goldring, Heinemann and Turino 1975). To investigate this transition, we constructed a novel iterative model of whole body CO_2 kinetics which incorporates respiratory control and renal HCO_3^- kinetics (Norman, Goldring, Clain, Oppenheimer, Charney, Rapoport and Berger 2006). This model allows observation of the transition between acute hypercapnia during periods of sleep containing apneas to chronic sustained hypercapnia during wakefulness, which cannot be accomplished in the clinical setting.

The model was utilized to investigate the role of respiratory-renal interactions in the transition from acute to chronic hypercapnia (Norman *et al*. 2006). Acute hypercapnia during periodic breathing would initiate HCO_3^- retention. Although the magnitude of HCO_3^- retention during a single night is small, the time constant for HCO_3^- excretion is longer than that for PCO_2; therefore, this increase may not be fully excreted before the next period of sleep. Persistence of elevated [HCO_3^-] would blunt CO_2 responsiveness amplifying this mechanism on subsequent nights.

The present model expands a validated model of whole-body CO_2 kinetics (Rapoport *et al*. 1993). A ventilatory controller has been added which responds to deviations in [H^+] from normal using a user-defined ventilatory response slope (Severinghaus 1998; Nattie 1999), entered as the change in ventilation per change in P_aCO_2. The ventilatory response is reexpressed by the model as the change in minute ventilation per change in [H^+], dictating that the ventilatory response to PCO_2 will vary as serum [HCO_3^-] changes. A renal HCO_3^- controller has also been added to simulate metabolic compensation for respiratory-induced changes in P_aCO_2. Time courses for changes in blood [HCO_3^-] replicate published data (Polack, Haynie, Hays and Schwarz 1961; Gledhill, Beirne and Dempsey 1975).

Simulations were run for 20 days. Each day contained 8 hours of simulated sleep containing periodic breathing. Interapnea periods were limited to 2 breaths forcing a 6 torr increase in P_aCO_2 over the 8-hour period. The ensuing 16-hour periods of wakefulness contained regular unconstrained breathing, allowing for CO_2 excretion. P_aCO_2 and blood [HCO_3^-] were recorded at the end of each day. Figure 2 illustrates 4 simulations. When CO_2 response and renal HCO_3^- excretion were normal, P_aCO_2 and HCO_3^- remained unchanged. When a single perturbation was entered, such as reduced CO_2 response or reduced HCO_3^- excretion rate (as in chloride depletion) both P_aCO_2 and [HCO_3^-] increased. Alterations of both parameters

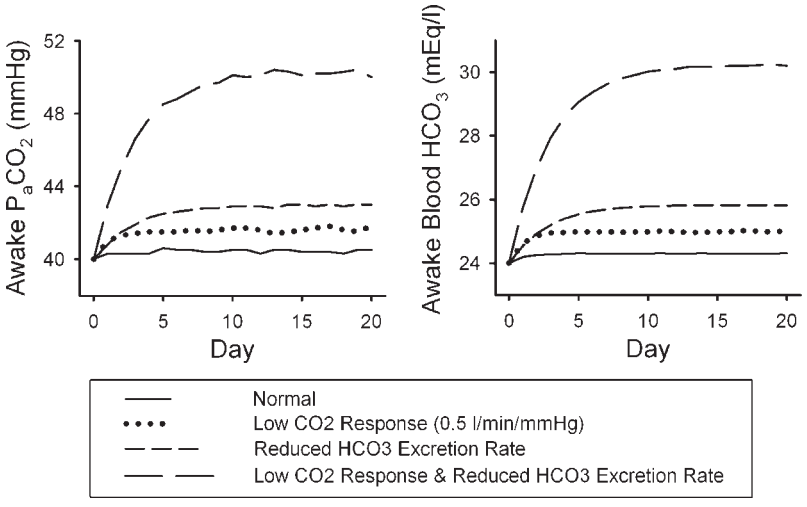

Fig. 2 $PaCO_2$ and HCO_3^- trends from 20-day simulations (Norman *et al*. 2006)

simultaneously resulted in a synergistic effect with greater increase of P_aCO_2 and $[HCO_3^-]$. As $[HCO_3^-]$ increased, there was a progressive blunting of both the awake ventilatory CO_2 response and the post-event ventilatory response to volume of CO_2 loaded during the event.

Thus, acute hypercapnia during periodic breathing can transition into chronic sustained hypercapnia during wakefulness. This transition required persistence of elevated $[HCO_3^-]$ during wakefulness. Persistence of elevated $[HCO_3^-]$ was induced by either alteration of renal HCO_3^- kinetics, reduction of ventilatory drive, or both. Elevated $[HCO_3^-]$ blunted ventilatory CO_2 responsiveness from its initial value yielding higher P_aCO_2 values on awakening, which further reduced HCO_3^- excretion. These respiratory-renal interactions created a cumulative effect over subsequent periods of sleep that eventually resulted in a self-perpetuating state of chronic hypercapnia.

5 Summary

We propose the following mechanism for generation and maintenance of chronic hypercapnia in patients with OSA. An acute respiratory event leads to a transient increase in PCO_2 during the event. If the post-event ventilatory response is adequate in magnitude & duration, patients will remain eucapnic. If the post-event ventilatory response is inadequate, there will be a progressive increase in PCO_2 during the night, which will initiate HCO_3^- retention. Unloading of the accumulated CO_2 and HCO_3^- during wakefulness is dependent upon magnitude of load, the level of CO_2 responsiveness, and the time course for renal HCO_3^- excretion. Persistence of elevated HCO_3^- not only defines the state of chronic hypercapnia, but also provides a mechanism for the development and perpetuation of this state, through blunting of respiratory drive, in accord with the concept of "compromise adaptation" (Tenney 1957).

References

Ayappa, I., Berger, K.I., Norman, R.G., Oppenheimer, B.W., Rapoport, D.M. and Goldring, R.M. (2002) Hypercapnia and ventilatory periodicity in obstructive sleep apnea syndrome. Am. J. Respir. Crit. Care Med. 166, 1112–1115.

Berger, K.I., Ayappa, I., Sorkin, I. B., Norman, R.G., Rapoport, D.M. and Goldring, R.M. (2002) Post-event ventilation as a function of CO_2 load during respiratory events in obstructive sleep apnea. J. Appl. Physiol. 93, 917–924.

Berger, K.I., Ayappa, I., Sorkin, I.B., Norman, R.G., Rapoport, D.M. and Goldring, R.M. (2000) CO_2 homeostasis during periodic breathing in obstructive sleep apnea. J. Appl. Physiol. 88, 257–264.

Gledhill, N., Beirne, G.J. and Dempsey, J.A. (1975) Renal response to short-term hypocapnia in man. Kidney Int. 8, 376–384.

Goldring, R.M., Heinemann, H.O. and Turino, G.M. (1975) Regulation of alveolar ventilation in respiratory failure. Am. J. Med. Sci. 269, 160–170.

Javaheri, S., Colangelo, G., Lacey, W. and Gartside, P.S. (1994) Chronic hypercapnia in obstructive sleep apnea-hypopnea syndrome. Sleep 17, 416–423.

Nattie, E. (1999) CO_2, brainstem chemoreceptors and breathing. Prog. Neurobiol. 59, 299–331.

Norman, R.G., Goldring, R.M., Clain, J.M., Oppenheimer, B.W., Charney, A.N., Rapoport, D.M. and Berger, K.I. (2006) Transition from acute to chronic hypercapnia in patients with periodic breathing: predictions from a computer model. J. Appl. Physiol. 100, 1733–1741.

Polack, A., Haynie, G.D., Hays, R.M. and Schwarz, W.B. (1961) Effects of chronic hypercapnia on electrolytes and acid-base equilibrium. I. Adaptation. J. Clin. Invest. 40, 1223–1237.

Rapoport, D.M., Garay, S.M., Epstein, H. and Goldring, R.M. (1986) Hypercapnia in the obstructive sleep apnea syndrome. A re-evaluation of the "Pickwickian syndrome." Chest 89, 627–635.

Rapoport, D.M., Norman, R.G. and Goldring, R.M. (1993) CO_2 homeostasis during periodic breathing: predictions from a computer model. J. Appl. Physiol. 75, 2302–2309.

Severinghaus, J.W. (1998) Hans Loeschcke, Robert Mitchell and the medullary CO_2 chemoreceptors: a brief historical review. Respir. Physiol. 114, 17–24.

Tenney, S.M. (1957) Respiratory control in chronic pulmonary emphysema: a compromise adaptation. J. Maine Med. Ass. 48, 375.

76
Biochemical Control of Airway Motor Neurons During Rapid Eye Movement Sleep

Patricia L. Brooks[1] and John H. Peever[2]

1 Introduction

Skeletal muscle tone is potently suppressed during rapid eye movement (REM) sleep. It is hypothesized that this suppression is due to the active inhibition of somatic motor neurons. Active inhibition involves an increase in the release of inhibitory neurotransmitters, specifically glycine and γ-aminobutyric acid (GABA), which work to actively suppress motor neuron excitability and hence muscle tone. While there is evidence supporting a role for active inhibition in REM sleep, most of this work derives from single-cell recordings in head-restrained cats or from pharmacological models of REM sleep (*e.g.*, carbachol-induced REM-like sleep) (Chase, Soja and Morales 1989; Chirwa, Stafford-Segert, Soja and Chase 1991; Fenik, Davies and Kubin 2005; Soja, Finch and Chase 1987).

The current study takes a physiologically relevant approach, directly manipulating muscle activity at the level of motor neurons in freely moving, naturally behaving rats. The aim of this study was to determine if there is a role for active inhibition, and specifically glycine, in regulating somatic motor neuron excitability and hence muscle activity in REM sleep. The results reported herein indicate that glycine is not involved in the atonia of REM sleep.

2 Methods

Twelve male Sprague-Dawley rats (350–400 g) were instrumented with electroencephalogram (EEG) and masseter and neck electromyogram (EMG) electrodes to determine sleep state and muscle activity. In addition, a microdialysis probe (34 K Da cut-off; membrane length and diameter: 1 mm by 250 μM; CMA, St. Laurent, QC) was inserted into the trigeminal motor nucleus (9.4 caudal, 1.8 lateral, 8.2 ventral).

[1] University of Toronto, Department of Cell & Systems Biology, patti.brooks@utoronto.ca

[2] University of Toronto, Departments of Cell & Systems Biology and Physiology, john.peever@utoronto.ca

M.J. Poulin and R.J.A. Wilson (eds.), *Integration in Respiratory Control: From Genes to Systems*.

Artificial cerebral spinal fluid (ACSF; 125 mM NaCl, 5 mM KCl, 1.25 mM KH_2PO_4, 24 mM $NaHCO_3$, 2.5 mM $CaCl_2$, 1.25 mM $MgSO_2$, 20 mM D-glucose) followed by 0.1 mM strychnine (glycine receptor antagonist, strychnine hydrochloride, Sigma) dissolved in ACSF were perfused onto trigeminal motor neurons.

EEG and EMG criteria were used to identify episodes of REM sleep under both ACSF (baseline) and strychnine treatments. REM sleep is characterized by periods of tonic and phasic activity. It is the tonic atonia of REM sleep that has been traditionally hypothesized to be controlled by glycine (Chase *et al*. 1989; Chirwa *et al*. 1991; Soja *et al*. 1987; Yamuy, Fung, Xi, Morales and Chase 1999), whereas little focus has been on phasic activity. Thus, to determine the effects of strychnine on both the tonic and phasic portions of REM sleep, all episodes were divided into tonic and phasic activity. To differentiate between tonic and phasic activity, the first 5 s of basal muscle activity during each episode was averaged. Phasic activity was then classified as any activity that was greater than the 99th percentile of this mean basal activity and tonic activity was everything equal to or less than the 99th percentile.

All statistical analyses used Sigmastat (SPSS Inc., Chicago, IL) and applied a critical alpha value of 0.05. Data were tested for normality using the Kolmogorov-Smirnov test. Paired t-tests were used for all comparisons. Data are expressed as mean ± SEM.

3 Results

All microdialysis probes were within or immediately adjacent to the trigeminal motor nucleus (n = 12). This was confirmed in two ways. We first identified probe location by demonstrating that microdialysis of 0.1 mM AMPA onto trigeminal motor neurons caused a specific activation of masseter muscle activity. This procedure was carried out at the end of each experiment and not only verified probe placement but also that the microdialysis probe was functional and that trigeminal motor neurons were viable and able to respond to neurochemical stimuli. Probe place was also confirmed by post-mortem histology. In all animals, probe tract lesions were identified either within or immediately beside the trigeminal motor nucleus (Fig. 1a).

In all rats, masseter EMG activity was potently suppressed in REM sleep (compared to waking levels; n = 12; paired t-test: $p < 0.05$). Since our major experimental goal was to determine a role for glycinergic inhibition in the suppression of masseter muscle activity in REM sleep, we applied 0.1 mM strychnine onto trigeminal motor neurons to block post-synaptic glycine-induced inhibition. Antagonism of glycine receptors had no effect on basal levels of masseter muscle activity in REM sleep; the characteristic periods of muscle atonia and muscle twitches were unperturbed by strychnine application (Fig. 1b, 1c).

No change in muscle activity from ACSF levels was seen in tonic activity (Fig. 1d; $p = 0.68$), however, although not statistically significant, there was a trend towards increased phasic activity (Fig. 1e; $p = 0.06$) after treatment with strychnine. Lack of changes in muscle activity in REM sleep cannot be explained by either

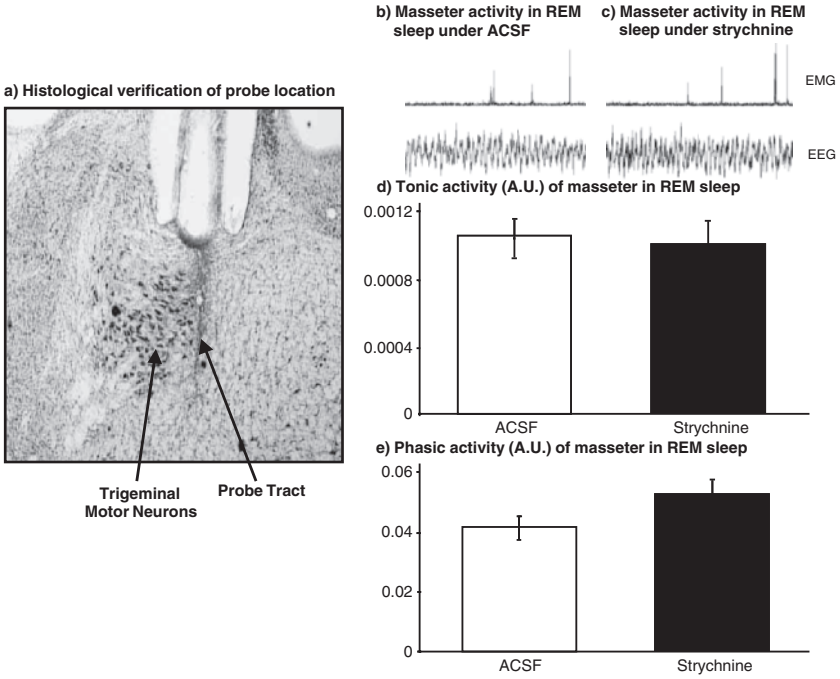

Fig. 1 Panel (a): An example of a lesion site left by a microdialysis probe in the trigeminal motor nucleus. Neutral Red was used for staining. Panels (b, c): Representative traces from one rat showing changes in muscle activity in REM sleep when (b) ACSF or (c) 0.1 mM strychnine was applied onto the trigeminal motor nucleus. EMG of the masseter and EEG recordings are shown. Panels (d, e): Masseter EMG activity (n = 12) for ACSF (white bars) and 0.1 mM strychnine treatment (black bars) during (d) Tonic REM activity and (e) Phasic REM activity. No significant change in muscle activity was found in tonic activity ($p = 0.68$); however, there was a trend for increased phasic activity ($p=0.06$) in REM sleep after glycinergic antagonism. All values are means ± SEM

alterations REM sleep architecture or insufficient glycinergic antagonism because: (1) REM sleep episode duration was unaffected by strychnine application (relative to ACSF; paired t-test, $p = 0.41$); and (2) 0.1 mM strychnine induced a significant increase in muscle activity in NREM sleep ($p < 0.001$; data not shown).

4 Conclusion

Antagonism of glycine receptors had no effect on muscle activity in REM sleep. These findings refute the traditionally accepted hypothesis that glycinergic inhibition of somatic motor neurons is responsible for REM sleep muscle atonia (Nakamura, Goldberg, Chandler and Chase 1978). This indicates that mechanisms

other than glycinergic inhibition are responsible for the suppression of muscle activity in REM sleep.

Although glycinergic inhibition does not mediate muscle atonia during REM sleep, it may have a role in regulating the phasic muscle twitches that characterize this state since twitches were potentiated by strychnine antagonism. This observation is in agreement with that of enhanced phasic genioglossus muscle activity in REM sleep that is seen following strychnine application in the hypoglossal motor nucleus (Morrison, Sood, Liu, Park, Liu, Nolan and Horner 2003). It therefore appears that inhibitory glycinergic inputs function to dampen the muscle twitches during REM sleep. This assertion supports the hypothesis that phasic activity in REM sleep is due to the simultaneous co-activation of excitatory and inhibitory inputs (Chase and Morales 1983). We hypothesize that disruption of normal glycinergic processes during sleep may lead to elevated muscle activity during REM sleep and particularly during phasic REM events. This postulate is supported by the fact that clonazepam, which increases inhibitory neurotransmission, potently suppresses the excessive motor activity that defines REM sleep behaviour disorder (Olson, Boeve and Silber 2000; Schenck and Mahowald 1990), a neurological condition that results from abnormal muscle activity during REM sleep. It also explains how low-doses of strychnine augment palatal activity in sleeping OSA patients (Remmers, Anch, Degroot, Baker and Sauerland 1980). A role for glycinergic processes in REM sleep is also supported by the observation that humans and calves suffering from hyperekplexia, a rare genetic condition in which the alpha-subunit of the glycine receptor is mutated, display excessive myoclonic twitching during sleep (De Groen and Kamphuisen 1978; Gundlach, Dodd, Grabara, Watson, Johnston, Harper, Dennis and Healy 1988).

There is also evidence indicating a role for GABA in the atonia of REM sleep (Fenik *et al*. 2005). While we did not address this issue in the current study, we hypothesize that increased GABA release during tonic REM sleep may explain the persistence of atonia during pharmacological blockade of glycine receptors. This aspect of motor regulation in REM sleep requires investigation.

In conclusion, this study refutes the traditional hypothesis that glycinergic inhibition is responsible for the atonia of REM sleep; however, we demonstrate that glycine plays a role in regulating phasic muscle twitches during this state. Other inhibitory processes must be involved in the control of muscle activity during REM sleep.

Acknowledgements This work was supported by funds from Canadian Institutes of Health Research (CIHR). PLB is the recipient of a PGS Scholarship from Natural Sciences and Engineering Research Council of Canada (NSERC). The authors thank Christian Burgess.

References

Chase, M.H. and Morales, F.R. (1983) Subthreshold excitatory activity and motoneuron discharge during REM periods of active sleep. Science 221, 1195–1198.

Chase, M.H., Soja, P.J. and Morales, F.R. (1989) Evidence that glycine mediates the postsynaptic potentials that inhibit lumbar motoneurons during the atonia of active sleep. J Neurosci. 9, 743–751.

Chirwa, S.S., Stafford-Segert, I., Soja, P.J. and Chase, M.H. (1991) Strychnine antagonizes jaw-closer motoneuron IPSPs induced by reticular stimulation during active sleep. Brain Res. 547, 323–326.

de Groen, J.H. and Kamphuisen, H.A. (1978) Periodic nocturnal myoclonus in a patient with hyperexplexia (startle disease). J. Neurol. Sci. 38, 207–213.

Fenik, V.B., Davies, R.O. and Kubin, L. (2005) Noradrenergic, serotonergic and GABAergic antagonists injected together into the XII nucleus abolish the REM sleep-like depression of hypoglossal motoneuronal activity. J. Sleep Res. 14, 419–429.

Gundlach, A.L., Dodd, P.R., Grabara, C.S., Watson, W.E., Johnston, G.A., Harper, P.A., Dennis, J.A. and Healy, P.J. (1988) Deficit of spinal cord glycine/strychnine receptors in inherited myoclonus of Poll Hereford calves. Science 241, 1807–1810.

Morrison, J.L., Sood, S., Liu, H., Park, E., Liu, X., Nolan, P. and Horner, R.L. (2003) Role of inhibitory amino acids in control of hypoglossal motor outflow to genioglossus muscle in naturally sleeping rats. J. Physiol. 552, 975–991.

Nakamura, Y., Goldberg, L.J., Chandler, S.H. and Chase, M.H. (1978) Intracellular analysis of trigeminal motoneuron activity during sleep in the cat. Science 199, 204–207.

Olson, E.J., Boeve, B.F. and Silber, M.H. (2000) Rapid eye movement sleep behaviour disorder: demographic, clinical and laboratory findings in 93 cases. Brain 123 (Pt. 2), 331–339.

Remmers, J.E., Anch, A.M., deGroot, W.J., Baker, J.P., Jr. and Sauerland, E.K. (1980) Oropharyngeal muscle tone in obstructive sleep apnea before and after strychnine. Sleep 3, 447–453.

Schenck, C.H. and Mahowald, M.W. (1990) A polysomnographic, neurologic, psychiatric and clinical outcome report on 70 consecutive cases with REM sleep behavior disorder (RBD): sustained clonazepam efficacy in 89.5% of 57 treated patients. Clev. Clin. J. Med. 57, Suppl. 10–24.

Soja, P.J., Finch, D.M. and Chase, M.H. (1987) Effect of inhibitory amino acid antagonists on masseteric reflex suppression during active sleep. Exp. Neurol. 96, 178–193.

77
Prediction of Periodic Breathing at Altitude

Keith Burgess [1,2,3], Katie Burgess[2], Prajan Subedi[4], Phil Ainslie[5], Zbigniew Topor[5] and William Whitelaw[6]

1 Background

Periodic breathing at high altitude has been known to occur for perhaps hundreds of years, but was first described in the medical literature by Mosso in 1898 (Mosso 1898). Lahiri *et al*. (1983) published an examination of the relationship between ventilatory response to hypoxia measured at high altitude (5,300 m) and prevalence of periodic breathing during sleep at that altitude in a group of acclimatized mountaineers and high altitude sherpas as part of the American Medical Expedition to Mount Everest (Lahiri, Maret and Sherpa 1983). They showed a strong correlation between high ventilatory response to hypoxaemia at altitude in awake subjects who were acclimatized for a month and the prevalence of central sleep apnea. When we studied the relationship between ventilatory response to hypoxia and hypercapnia at sea level, and the subsequent prevalence of periodic breathing at high altitude, we found no such relationship (Burgess 2001; Burgess Johnson and Edwards 2004), probably because ventilatory responses change due to acclimatization.

These studies were undertaken to investigate the possible relationship between ventilatory response and periodic breathing during sleep, in a group of normal volunteers, at a low altitude and high altitude. Although there are too few subjects to generate a new model after the style of Topor *et al*. (2004), we hoped there would be sufficient data to test his current model.

[1] University of Sydney, Dept. of Medicine, kburgess@nsccahs.health.nsw.gov.au

[2] Peninsula Private Sleep Laboratory, kburgess@nsccahs.health.nsw.gov.au

[3] Manly Hospital, Dept. of Critical Care, kburgess@nsccahs.health.nsw.gov.au

[4] Institute of Medicine and Patan Hospital

[5] University of Calgary, Department of Physiology and Biophysics

[6] University of Calgary, Department of Pulmonary Medicine, wwhitela@ucalgary.ca

M.J. Poulin and R.J.A. Wilson (eds.), *Integration in Respiratory Control: From Genes to Systems*.

2 Methods

The studies were approved by the Human Research and Ethics Committee of the University of Calgary, the Northern Sydney Area Health Service and the Nepal Health Medical Research Council. Each subject gave informed written consent.

Five healthy individuals [aged 32 ± 10 (mean ± SD) years; body mass index 22.8 ± 1.6 $kg.m^2$] were studied. Subjects were studied within 48 hr of arrival in Kathmandu from sea level abode. Subjects then flew to Lukla and hiked initially to Mount Everest Basecamp at 5,340 m over 6 days. They remained at Basecamp for 4 days and then descended over 2 days to Kunde, where the repeat experiments were conducted over the succeeding 3 days. The repeat experiments were initially intended for Mount Everest Basecamp, however the ventilatory response equipment would not function at that altitude. Subjects were studied in the afternoon fasting, having avoided alcohol and caffeine for at least 18 hr prior to the test. They then underwent ventilatory response testing in the awake sitting position. Subjects wore eyeshades and headphones playing relaxing music of their choice, to minimise distraction during the ventilatory response testing. Two runs were performed of each of the hypoxic and hypercapnic ventilatory tests. In addition, subjects also underwent arterial blood gas collection after 10 minutes rest in the sitting position at each altitude. Finally each subject underwent 13-channel polysomnography during overnight sleep.

The ventilatory responses were tested using combined rebreathing techniques developed by Duffin and McEvoy (1988). In the hypercapnic ventilatory responses, subjects rebreathed a mixture of 7% CO_2 in 93% oxygen from an 8 litre reservoir bag, after hyperventilating down to a end tidal CO_2 of approximately 17 mmHg for 5 min. Ventilation was measured by a turbine system, and end tidal CO_2 was measured by a portable high-speed infrared CO_2 analyser (Jaeger Oxycon mobile system, Rietzens, Keizer and Kuipers 2000).

The hypoxic ventilatory responses were measured using the same system, except that subjects rebreathed from an 8 litre bag containing 4 litres of 9% oxygen in 7% CO_2, with the balance nitrogen (Duffin *et al.* 1988). Supplemental oxygen was added to the bag to try to maintain an end tidal oxygen between 45 and 55 mmHg (SaO_2, 80–90%). The results of the two separate runs are shown in Table 3.

The arterial blood gas samples were analysed using an i-STAT machine (Jacobs, Vadasdi, Sarkozi and Colman 1993; Sediame, Zerah-Lancer, d'Ortho Arnet and Harf 1999) that was electronically calibrated before each blood gas analysis. The blood gases were collected either in the afternoon before the sleep study or the following morning.

The sleep studies were performed using the Compumedics PS2 portable polysomnogram equipment (Compumedics, Melbourne, Australia), (Burgess, Cooper, Rice, Wong, Kinsman and Hahn 2006). The recorded data included: EKG, 2 channels EEG, 2 channels EOG, leg movement, oxygen saturation, nasal flow by pressure transducer attached to nasal cannulae, thoracic and abdomen effort by piezo-electric band system, snoring, body position and lights on/off.

The results were tested for normality. In those results where the results appeared to be normally distributed, paired t-tests were used for comparison between the two altitudes (Bland 1996; Lang and Secic 1997). In those results where the data appeared not to be normally distributed, the Wilcoxin sign rank test (Aabel for the Macintosh, Gigawiz Ltd. Co., USA) was used. In the HVR runs, data points where the SaO_2 was < 80% or > 90% were excluded. The intersection of the regression lines was determined in an interactive process that maximised the r values for the intersecting linear regression lines.

3 Results

Results are represented in Tables 1 to 5.

Table 1 ABG Data

	1,400 m					3,840 m				
SUB	pH	$PaCO_2$	PaO_2	HCO_3	BE	pH	$PaCO_2$	PaO_2	HCO_3	BE
01	7.38	37.5	76	22.2	–3	7.456	26.2	50	18.5	–5
02	7.393	36	74	22	–3	7.459	28.1	58	19.9	–4
03	7.472	36.2	75	26.5	+3	7.439	29.7	56	20.1	–4
04	7.468	31.9	78	23.1	–1	7.440	27.3	55	18.5	–6
08	7.416	35.9	69	23.1	–1	7.453	28	53	19.6	–4
Mean ± SD	7.426	35.5	74	23.4	–1	7.449	27.9	54	17.1	–5
	0.042	2.1	3	1.8	2	.009	1.3	3	5.5	1

Statistical comparison between low and high altitude. pH: p = .36 $PaCO_2$: p = 0.002; PaO_2: p = 0.001; HCO_3: p = 0.005; BE: p = 0.029 (Paired t-test)

Table 2 Key Sleep Variable Data

	1,400 m					3,840 m				
SUBJ	AI	OAHI	CAHI	Min Sat%	Mean Sat%	AI	OAHI	CAHI	Min Sat%	Mean Sat%
01	7.0	1.4	0	85	93	9.2	0.3	22.4	77	86
02	7.4	6.6	0	89	95	13.7	0	50.7	83	91
03	8.4	0	0	93	96	8.5	2.3	48	79	86
04	6.7	0	0	90	95	8.7	0	1.2	84	89
08	9.7	0	0	90	95	9.9	0	2.0	82	86
Mean ± SD	7.8	1.6	0	89	91	10.0	0.5	24.9	81	88
	1.2	2.0	0	3	1	2.1	1.0	23.9	3	2

AI = Arousal Index; OAHI = Obstructive Apnea – Hypopnea Index; CAHI = Central Apnea – Hypopnea Index; Min Sat = Minimum Saturation; Mean Sat = Mean Saturation; NS = Not Significant. Results of comparison between low and high altitude by paired t-test:- AI = NS OAHI = NS CAHI = p = 0.08 Min Sat = p = 0.005 Mean Sat = p = 0.003

Table 3 Sleep Architecture Data

SUBJ	1,400 m				3,840 m			
	1	2	3&4	REM	1	2	3&4	REM
01	3.9	55.9	20.4	19.8	5	60.4	12	22.7
02	3.8	47.7	18.4	30	11.7	60.9	10.5	16.9
03	2.9	50.1	24.5	19.3	2	46.9	15.6	35.4
04	1.3	54.2	39.6	4.9	1.8	66.1	22.5	9.5
08	3.2	43.4	30.8	22.5	7.6%	60.6%	9.8%	22
Mean ± SD	3.0	50.3	26.7	19.3	5.6	59.0	14.1	21.3
	1.0	5.0	8.6	9.1	4.2	7.2	5.2	9.5

Results of statistical comparison between low and high altitude (paired t-test)
Stage 1: NS Stage 2: $p = 0.07$ Stages 3&4: $p = 0.009$ REM: NS

Table 4 Ventilatory Response Data

	1,400 m		3,840 m	
SUBJECT	HVR	HCVR	HVR	HCVR
01	5.1	8.1	5.8	26.9
	4.1	8.7	4.1	29.6
02	0.5	1.4	2.1	1.9
	0.7	2.1	2.7	1.9
03	0.4	10.8	3.2	6.6
	0.4	6.8	5.1	7.8
04		2.1		8.6
	0.5	1.2	3.7	8.3
08	0.7	0.8	0.8	1.5
		1.3	0.9	2.1
Mean	1.6	4.3	3.2*	9.5+
SD	1.9	3.8	1.7	10.3

The ventilatory response data shown here are the values of the slopes of the linear portions of the relationships between ventilation and end tidal PCO_2. * $p = 0.02$ high altitude compared to low altitude.+ $p < 0.05$ high altitude compared to low altitude (Wilcoxin sign rank test).

Table 5 Regressions of VRs Against CSA Index at 3,840 m

HVR at 1,400 m Vs. CSAI at 3,840 m	r = −0.26
HVR at 3,840 m Vs. CSAI at 3,840 m	r = 0.29
HCVR at 1,400 m Vs. CSAI at 3,840 m	r = 0.43
HCVR at 3,840 m Vs. CSAI at 3,840 m	r = −0.09
Delta HVR Vs. CSAI at 3,840 m	r = 0.42
Delta HCVR Vs. CSAI at 3,840 m	r = −0.32

Results of linear regressions of VR data shown in Table 4 against CSA Index of the same subjects at 3,840 m.

4 Conclusion

These are pilot data, with too few subjects to allow us to draw convincing conclusions. However, we can say that ventilatory responses do increase with acclimatization to altitude. The trends in change in the ventilatory response at altitude and the development of CSA suggest that it is the change in hypoxic ventilatory response moving to high altitude that is more important in the development of central sleep apnea, than the hypercapnic ventilatory response. Indeed, the general pattern suggests that (and this fits with Topor's model) it is the disproportionate increase in one ventilatory response relative to the other ventilatory response, that predicts or predisposes to the development of CSA at high altitude.

Acknowledgements The authors wish to gratefully acknowledge the following: Leanne Taylor for assistance during the experiments, Compumedics (Melbourne, Australia) for the loan of PS2 equipment. Peninsula Health Care P/L (Sydney) and Professor John Remmers (University of Calgary) for financial support. Ms. P. Saye (Peninsula Private Sleep Laboratory, Sydney) for scoring all Sleep Studies. Ms. S. Coulson for preparing and formatting the manuscript.

References

Bland, M. (1996) *An Introduction to Medical Statistics*, 2nd Edit. Oxford Univ. Press. Oxford.

Burgess, K.R. (2001) Central sleep apnea and left ventricular failure. PhD Thesis University of Sydney.

Burgess, K.R., Johnson, P.L. and Edwards, N. (2004) Central and obstructive sleep apnea during ascent to high altitude. Respirology 9(2), 222–229.

Burgess, K.R., Cooper, J., Rice, A, Wong, K., Kinsman, T. and Hahn A. (2006) Effect of simulated altitude during sleep on moderate severity obstructive sleep apnea. Respirology 11, 62–69.

Duffin, J. and McAvoy, G.V. (1988) The peripheral-chemoreceptor threshold to carbon dioxide in man. J. Physiol. (London) 406, 15–26.

Jacobs, E., Vadasdi, E., Sarkozi, L. and Colman N. (1993) Analytical evaluation of i-Stat™ bedside blood gas analyser and use by non-laboratory health-care professionals. Clin. Chem. 39, 1069–1074.

Lahiri, S., Maret, K. and Sherpa, M.G. (1983) Dependence of high altitude sleep apnea on ventilatory sensitivity to hypoxia. Respir. Physiol. 52, 281–301.

Lang, T. and Secic, M. (1997) How to report statistics in medicine. Am. College Physicians. Phil. Mosso, A. (1898) *A Life of Man on the High Alps*. London: T. Fisher, Unwin.

Rietzens, G.J.W.M., Keizer, H.A. and Kuipers H. (July 2000) Validation of oxygen PO_2 measurements. Jaeger Info. Magazine.

Sediame, S., Zerah-Lancer, F., d'Ortho, M.P., Arnet, S. and Harf A. (1999) Accuracy of the i-Stat™ bedside blood gas analysers. Eur. Respir. J. 14, 214–217.

Topor, Z.L., Vasilakos, K. and Remmers, J.E. (2004) Stability analysis of the respiratory control system during sleep. Adv. Exp. Med. Biol. 551, 203–209.

78
A Negative Interaction Between Central and Peripheral Respiratory Chemoreceptors May Underlie Sleep-Induced Respiratory Instability: A Novel Hypothesis

Trevor A. Day[1] and Richard J.A. Wilson[2]

Abstract Central (brainstem) and peripheral (carotid body) respiratory chemoreflexes act in concert to modulate breathing during sleep, maintaining blood gases (PCO_2 and PO_2) within narrow limits. Increases in both central and peripheral chemoreflex gain have been reported in clinical populations that experience central sleep apnoea and likely underlie the pathophysiology of this disorder. However, how central-peripheral chemoreceptor interaction affects the apparent gain of each chemoreflex is controversial. Data from our laboratory demonstrate that there is a negative interaction between central and peripheral chemoreceptors in the rat, such that brainstem hypocapnia augments peripheral chemoreflex gain in response to both carotid body PCO_2 and PO_2. We note that a negative interaction may also occur in humans, especially relevant in those experiencing chronic hypocapnia. Interestingly, chronic hypocapnia occurs in populations prone to central sleep apnea, such as congestive heart failure (CHF) patients and individuals sleeping at high altitude. These observations lead us to propose the novel hypothesis that a negative interaction between chemoreceptors results in an augmented peripheral chemoreceptor gain when the central chemoreceptors are hypocapnic, thereby contributing directly to breathing instability during sleep.

1 Introduction

Normal breathing maintains the pressure of arterial oxygen (PaO_2) and carbon dioxide ($PaCO_2$) within narrow limits. The respiratory chemical control system maintains these blood gasses through two negative feedback loops with different temporal dynamics (Topor, Vasilakos and Remmers 2004): (1) slow central (brainstem) chemoreceptors, which monitor brain tissue pH/CO_2 (Nattie 2000) and (2) fast peripheral (carotid body) chemoreceptors, which sense $PaCO_2$ in a PaO_2-dependent manner (Lahiri and DeLaney 1975). The importance of these respiratory chemoreceptors is particularly apparent during sleep (Skatrud and Dempsey 1983).

[1] University of Calgary, Physiology and Biophysics, taday@ucalgary.ca

[2] University of Calgary, Physiology and Biophysics, wilsonr@ucalgary.ca

M.J. Poulin and R.J.A. Wilson (eds.), *Integration in Respiratory Control: From Genes to Systems*. © Springer 2008

Sleep apnoea likely affects between 5–20% of the North American population (Young, Peppard and Gottlieb 2002). Interestingly, approximately 50% of congestive heart failure (CHF) patients have central sleep apnoea (CSA; Topor, Johannson, Kasprzyk and Remmers 2001) as do most individuals sleeping at high altitude. The hallmark of CSA is a ventilatory overshoot in response to an apnoeic-induced hypoxic episode. Sustained oscillations result, with alternating apnoeas and hyperpnoeas with a period of approximately 50–70 seconds in the setting of CHF (*i.e*., Cheyne-Stokes respiration) or 20–30 seconds in the setting of high altitude (Topor *et al*. 2004).

Topor *et al*. (2001) found that CHF patients exhibiting CSA had significantly higher central chemoreflex gain in response to inspired hypercapnia. However, increased peripheral chemoreflex gain has also been reported in CSA patients (Solin, Roebuck, Johns, Walters and Naughton 2000; Xie, Rutherford, Rankin, Wong and Bradley 1995). Further, recent modeling work suggests that peripheral chemoreceptor activation can modulate the period of CSA (Topor, Vasilakos, Younes and Remmers 2006). In support of this, most individuals sleeping at high altitude experience CSA with a period of ~ 20 seconds (Berssenbrugge, Dempsey, Iber, Skatrud and Wilson 1983). Because of the shorter period associated with CSA at high altitude and the fact that hypoxia is sensed primarily by the carotid bodies, periodic breathing in this population is likely due in part to increased peripheral chemoreflex gain (Lahiri, Maret and Sherpa 1983).

To investigate the interaction between chemoreceptors, we developed a decerebrate, vagotomized, arterially-perfused rat preparation, whereby the central and peripheral chemoreceptors are perfused independently with defined medium containing precisely controlled gas concentrations (Day and Wilson 2005). Using this preparation, we demonstrated that phrenic responses to a single step of carotid body hypoxia elicited a larger ventilatory response when the brainstem was 25 Torr PCO_2 compared to when the brainstem was 50 Torr PCO_2. This finding indicates a negative interaction exists between chemoreceptors, at least for a single step of carotid body hypoxia (Day and Wilson 2006). Preliminary data from our laboratory suggest that this negative interaction exists for both carotid body PCO_2 and PO_2 perturbations above and below eupnoeic levels (manuscript in preparation). This interaction manifests in an increased peripheral chemoreflex gain when the central chemoreceptors are hypocapnic.

A consistent observation in CHF patients and high altitude populations is hyperpnoea-induced arterial hypocapnia. Thus, we advance the novel hypothesis that a negative interaction between central and peripheral chemoreceptors may underlie the observation of increased peripheral chemoreflex gain in populations experiencing chronic hypocapnia. Therefore, a negative interaction may contribute directly to the pathophysiology of CSA in the settings of CHF and high altitude.

2 Discussion

In the respiratory chemical control system, chemoreceptor-mediated ventilatory responses counter-act blood gas perturbations, thereby maintaining homeostasis through central and peripheral negative feedback loops. However, increases in

central and peripheral chemoreflex gain have been implicated in periodic breathing during sleep through the destabilizing influence of inappropriately large ventilatory overshoots in response to an apnoeic event (Solin *et al*. 2000; Topor *et al*. 2001 and 2004). Why some individuals have higher central and/or peripheral chemoreflex gains than others is currently unknown.

Data from our laboratory suggest that there is a negative interaction between central and peripheral chemoreceptors, such that central hypocapnia augments peripheral chemoreflex gain in response to carotid body perturbations. For the negative interaction to be most efficacious in increasing peripheral gain, the central chemoreceptor must be hypocapnic when the peripheral chemoreceptors are stimulated (*i.e*., hypercapnic and/or hypoxic).

The central chemoreflex has a delayed onset and a longer time constant in response to blood gas perturbations compared to the peripheral chemoreflex (Pedersen, Fatemian and Robbins 1999; Smith, Rodman, Chenuel, Henderson and Dempsey 2006). Owing to this difference in the response dynamics of chemoreflexes to blood gas perturbations, a mismatch in the stimuli at the two sites may occur. Thus, transient swings in blood gases resulting from an apnoeic event may be sufficient to stimulate the carotid bodies without significantly affecting the activity of the central chemoreceptors.

We propose that the negative interaction between chemoreceptors may influence the gain of the peripheral chemoreflex, contributing to periodicity due to the mismatch in chemo-stimuli between the central and peripheral compartments. Further, we propose that the negative interaction is particularly detrimental in individuals that are chronically hypocapnic. Under chronic conditions, the negative interaction may render the peripheral chemo-response magnitude inappropriately large, initiating oscillations by driving the $PaCO_2$ below the apnoeic threshold.

An important caveat regarding the clinical applicability of this "negative interaction hypothesis" in producing periodic breathing lies in the degree of blood, cerebral spinal fluid (CSF) and brain parenchyma pH adaptation in individuals that experience chronic hypocapnia. It is still controversial as to what the proximal stimulus is for central chemoreceptors: molecular CO_2 or $[H^+]$. Although both CHF patients and high altitude travelers have sustained hyperpnoea-induced hypocapnia, renal compensation will reduce the blood, CSF and brain parenchyma bicarbonate level over time, effectively inducing a compensatory metabolic acidosis.

In support of the possibility that a compensatory metabolic acidosis may impact the negative interaction between chemoreceptors, individuals sleeping at high altitude experience a paradoxical reduction in CSA as they acclimatize (Goldenberg, Richalet, Onnen and Antezana 1992; Przybylowski, Ashirbaev, Le Roux and Zielinski 2003; Weil 1985). Acclimatization is a myriad of mechanisms including (a) an increase in carotid body sensitivity to hypoxia (which would potentially exacerbate ventilatory instability) and (b) renal compensation of blood, CSF and brain parenchyma pH from metabolic acidosis. We propose that any detrimental effect of increased carotid body sensitivity on breathing stability is more than offset by the compensatory metabolic acidosis. The metabolic acidosis returns brainstem pH toward normal values, thereby mitigating the augmenting effect of the negative chemoreceptor interaction on peripheral chemoreflex gain. The result is the paradoxical reduction of CSA observed during acclimatization.

Many studies have demonstrated that the compensatory metabolic acidosis in CSF pH in response to sustained hypocapnia remains incomplete (Dempsey, Forster, Gledhill and doPico 1975; Orr, Bisgard, Forster, Buss, Dempsey and Will 1975; Forster, Dempsey and Chosy 1975). This suggests that a negative interaction between chemoreceptors may still serve to increase the peripheral chemoreflex gain in populations that are chronically hypocapnic. Thus, in clinical populations, the effect of a negative interaction between chemoreceptors on the magnitude of peripheral chemoreflex gain and its subsequent contribution to ventilatory instability during sleep is likely dependent upon the completeness of pH adaptation of brainstem parenchyma in response to sustained hypocapnia.

Acknowledgements We gratefully acknowledge: (a) salary support for RJAW from the AHFMR and the CIHR/Rx&D Focus on Stroke Partnership Award in Health Research Program (sponsored jointly by HSF, Canadian Stroke Network, CIHR and AstraZeneca) (b) salary support for TAD from a CIHR Doctoral Award and (c) operating grants from the following Canadian funding agencies: AHFMR, CIHR, and NSERC.

References

Berssenbrugge, A., Dempsey, J., Iber, C., Skatrud, J. and Wilson, P. (1983) Mechanisms of hypoxia-induced periodic breathing during sleep in humans. J. Physiol. 343, 507–526.

Day, T.A. and Wilson, R.J. (2005) Specific carotid body chemo-stimulation is sufficient to elicit phrenic post-stimulus frequency decline in a novel *in situ* dual perfused rat preparation. Am. J. Physiol. Regul. Integr. Comp. Physiol. 289, R532–R544.

Day, T.A. and Wilson, R.J. (2006) Brainstem PCO_2 modulates phrenic responses to specific carotid body hypoxia in an *in situ* dual perfused rat preparation. J. Physiol. Nov 2; [Epub ahead of print].

Dempsey, J.A., Forster, H.V., Gledhill, N. and doPico, G.A. (1975) Effects of moderate hypoxemia and hypocapnia on CSF $[H^+]$ and ventilation in man. J. Appl. Physiol. 38(4), 665–74.

Dempsey, J.A. and Skatrud, J.B. (1986) A sleep-induced apnoeic threshold and its consequences. Am. Rev. Respir. Dis. 133, 1163–1170.

Forster, H.V., Dempsey, J.A. and Chosy, L.W. (1975) Incomplete compensation of CSF $[H^+]$ on man during acclimatization to high altitude (48300 M). J. Appl. Physiol. 38(6), 1067–1072.

Goldenberg, F., Richalet, J.P., Onnen, I. and Antezana, A.M. (1992) Sleep apneas and high altitude newcomers. Int. Sports Med. 13(1), S34–S36.

Lahiri, S. and DeLaney, R.G. (1975) Stimulus interaction in the responses of carotid body chemoreceptor single afferent fibers. Respir. Physiol. 24(3), 249–266.

Lahiri, S., Maret, K. and Sherpa, M.G. (1983) Dependence of high altitude sleep apnea on ventilatory sensitivity to hypoxia. Respir. Physiol. 52(3), 281–301.

Nattie, E. (2000) Multiple sites for central chemoreception: their roles in response sensitivity and in sleep and wakefulness. Respir. Physiol. 122, 223–235.

Orr, J.A., Bisgard, G.E., Forster, H.V., Buss, D.D., Dempsey, J.A. and Will, J.A. (1975) Cerebrospinal fluid alkalosis during high-altitude sojourn in unanesthetized ponies. Respir. Physiol. 25(1), 23–37.

Pedersen, M.E., Fatemian, M. and Robbins, P.A. (1999) Identification of fast and slow ventilatory responses to carbon dioxide under hypoxic and hyperoxic conditions in humans. J. Physiol. 521(1), 273–287.

Przybylowski, T., Ashirbaev, A., Le Roux, J. and Zielinski, J. (2003) Sleep and breathing at altitude of 3800 m – the acclimatization effect. Pneumonol. Alergol. Pol. 71(5–6), 213–220.

Smith, C.A., Rodman, J.R., Chenuel, B.J., Henderson, K.S. and Dempsey, J.A. (2006) Response time and sensitivity of the ventilatory response to CO_2 in unanesthetized intact dogs: central vs. peripheral chemoreceptors. J. Appl. Physiol. 100(1), 13–19.

Solin, P., Roebuck, T., Johns, D.P., Walters, E.H. and Naughton, M.T. (2000) Peripheral and central ventilatory responses in central sleep apnea with and without congestive heart failure. Am. J. Respir. Crit. Care Med. 162(6), 2194–2200.

Topor, Z.L., Johannson, L., Kasprzyk, J. and Remmers, J.E. (2001) Dynamic ventilatory response to CO_2 in congestive heart failure patients with and without central sleep apnea. J. Appl. Physiol. 91, 408–416.

Topor, Z.L., Vasilakos, K. and Remmers, J.E. (2004) Interaction of two chemoreflex loops in determining ventilatory stability. Nonlin. Stud. 11, 527–541.

Topor, Z.L., Vasilakos, K., Younes, M. and Remmers, J.E. (2006) Model based analysis of sleep disordered breathing in congestive heart failure. Respir. Physiol. Neurobiol. May 4; [Epub ahead of print].

Weil, J.V. (1985) Sleep at high altitude. Clin. Chest Med. 6(4), 615–621.

Xie, A., Rutherford, R., Rankin, F., Wong, B. and Bradley, T.D. (1995) Hypocapnia and increased ventilatory responsiveness in patients with idiopathic central sleep apnea. Am. J. Respir. Crit. Care 152:1950–1955.

Young, T., Peppard, P.E. and Gottlieb, D.J. (2002) Epidemiology of obstructive sleep apnea: a population health perspective. Am. J. Respir. Crit. Care Med. 165(9), 1217–1239.

79
Ventilatory Response to Hypercapnia in Pre-menopausal and Post-menopausal Women

Chantel T. Debert[1], Kojiro Ide[2] and Marc J. Poulin[3]

1 Introduction

Women appear to have a lower incidence of sleep apnea, snoring, chronic mountain sickness and abnormal breathing than men, yet this beneficial effect appears to be lost with the decline in estrogen and progesterone seen during menopause (Leon-Velarde, Ramos, Hernandez, De Idiaquez, Munoz, Gaffo, Cordova, Durand and Monge 1997; Tatsumi, Pickett, Jacoby, Weil and Moore 1997). Further, although the ventilatory sensitivity to hypercapnia throughout the menstrual cycle in young women has been previously characterized, surprisingly few studies have compared resting ventilation ($\dot{V}_E$) and hypercapnic ventilatory responses in young women (PEMW) (Regensteiner, Woodard, Hagerman, Weil, Pickett, Bender and Moore 1989) to postmenopausal women (PSMW). Finally, little is known about the ventilatory sensitivity to hypercapnia in PSMW taking hormonal therapy (PSMW-HT).

The aim of the current study was to investigate the extent to which ventilatory sensitivity to hypercapnia (AHCVR) is altered in healthy PSMW compared with healthy PEMW. We also assessed the extent to which AHCVR is altered in PSMW on hormone therapy (HT, PSMW-PHT) compared with those who are not on HT (PSMW-noHT). We hypothesized that there would be a significant difference in the resting $\dot{V}_E$ and the AHCVR between PEMW and PSMW. As well, we theorized there would be a difference in the fast and slow components of the ventilatory response to hypercapnia between age groups.

[1–3]University of Calgary, Departments of Physiology & Biophysics and Clinical Neurosciences, Hotchkiss Brain Institute and Libin Cardiovascular Institute, Faculty of Medicine and Faculty of Kinesiology, poulin@ucalgary.ca

M.J. Poulin and R.J.A. Wilson (eds.), *Integration in Respiratory Control: From Genes to Systems*.

2 Methods

2.1 Subjects

Thirteen PSMW and ten PEMW took part. Of the PSMW, six were on HT and seven were not. Exclusion criteria included the occurrence of menses and smoking within the past year and pre-morbid respiratory or cardiovascular disease. Each woman was screened prior to testing with a pulmonary function test, a carotid screening and a 12-lead electrocardiogram. Subjects taking HT were taking the medication for at least one year. PSMW-noHT had never taken postmenopausal hormones. All PEMW were tested during the luteal phase. Exclusion criteria included the use of oral contraceptives, pregnancy, smoking and amenorrhea. This study was approved by the Conjoint Health Research Ethics Board**.**

2.2 Hypercapnic Protocol

The average barometric pressure for the study days was 663.8 ± 2.3 Torr (mean ± SD). The hypercapnia protocol lasted ~ 40 min. Briefly, the subject's normal end-tidal CO_2 ($P_{ET_{CO_2}}$) and end-tidal O_2 ($P_{ET_{O_2}}$) tensions were measured prior to the experiment, while the subject was sitting quietly and comfortably for approximately 10 min. The technique of dynamic end-tidal forcing was used to control $P_{ET_{CO_2}}$ and $P_{ET_{O_2}}$. The subjects sat quietly in the semi-supine position breathing through a mouthpiece with the nose occluded by a nose clip. The protocol started with a 10 min period when $P_{ET_{O_2}}$ was held constant at 88 Torr and $P_{ET_{CO_2}}$ was held 1.5 Torr above the subject's natural resting value on that day. After the initial 10 min period, $P_{ET_{CO_2}}$ was altered rapidly (over 1 or 2 breaths) to 8.5 Torr above the subject's normal resting value and maintained constant for 20 min. Finally, $P_{ET_{CO_2}}$ was returned to near-eucapnic values and maintained constant for 10 min.

2.3 Control of PET_{CO_2} and PET_{O_2}

The inspired and expired gases were sampled at a rate of 20 ml min^{-1} and analyzed by mass spectrometer for fractional concentrations of O_2 and CO_2. Respiratory volumes and flow information were obtained by using a pneumotachograph and differential pressure transducer (RSS100-HR, Hans Rudolph Inc., Kansas City, MO, USA). Respiratory flow direction and timing information were measured with a turbine volume transducer (VMM-400, Interface Associates, CA, USA). A computer sampled the experimental variables every 10 ms. Accurate control of the end-tidal gases was achieved using the technique of dynamic end-tidal forcing (BreatheM v2.07, University Laboratory of Physiology, Oxford, UK). A controlling

computer generated the inspired partial pressure of O_2 and CO_2 predicted to give the desired end-tidal partial pressures by using a fast gas mixing system (Ide, Eliasziw and Poulin 2003; Robbins, Swanson and Howson 1982).

2.4 Modeling Ventilation

Estimates of the ventilatory sensitivity to hypercapnia were obtained by fitting a dynamic mathematical model to the data. For hypercapnia, we assume the change in ventilation was proportional to the change in $P_{ET_{CO_2}}$. A deterministic mathematical model was fit to the data to separate the fast (peripheral) and slow (central) components of the ventilatory response to hypercapnia (Fatemian, Gamboa, Leon-Velarde, Rivera-Ch, Palacios and Robbins 2003). A standard algorithm for minimizing the sum of squares was used to fit these two models simultaneously to the data. Additional details of this model are given elsewhere (Fatemian *et al*. 2003).

2.5 Data Analysis

Statistical comparisons were undertaken by using analysis of variance (ANOVA SPSS V.11.0.1). When overall results from the analysis of variance were significant, a Duncan's multiple post-hoc analysis was employed. The overall level of significance was taken as $p \leq 0.05$.

3 Results

3.1 Resting PET_{CO_2}

The resting $P_{ET_{CO_2}}$ value for PSMW-HT, PSMW-noHT and PEMW were 35.4 ± 2.2, 38.3 ± 3.0 Torr and 35.0 ± 1.8 respectively. Eucapnic $P_{ET_{CO_2}}$ was significantly higher in PSMW-noHT compared to PSMW-HT and PEMW (ANOVA, $p < 0.01$).

3.2 Baseline Ventilation

The baseline $\dot{V}_E$ values for PSMW-HT, PSMW-noHT and PEMW were 9.33 ± 3.58, 6.39 ± 2.73 and 13.68 ± 3.47 l min^{-1}, respectively. PEMW had a significantly higher resting $\dot{V}_E$ compared to both PSMW-HT and PSMW-noHT (ANOVA,

$p < 0.001$). There was no significant difference in resting $\dot{V}_E$ between PSMW-HT and PSMW-noHT. However, there was a trend for PSMW-noHT to have lower baseline $\dot{V}_E$ than PSMW-HT.

3.3 Ventilatory Sensitivity to Euoxic Hypercapnia

The total chemoreflex sensitivity to CO_2 (G_{tot}) for PSMW-HT, PSMW-noHT and PEMW was 2.93 ± 1.71, 2.63 ± 0.65 and 4.11 ± 1.721 min^{-1} $Torr^{-1}$, respectively (not significant, NS). The peripheral chemoreflex sensitivity to hypercapnia (G_p) for PSMW-HT, PSMW-noHT and PEMW was 1.13 ± 0.73, 0.97 ± 0.17 and 1.90 ± 0.93, l min^{-1} $Torr^{1}$, respectively. The G_p was significantly lower in PSMW-noHT than in PEMW (ANOVA, $p = 0.04$). The central chemoreflex sensitivity to hypercapnia (G_c) for PSMW-HT, PSMW-noHT and PEMW was 1.81 ± 1.05, 1.66 ± 0.75 and 2.21 ± 1.181 min^{-1} $Torr^{-1}$, respectively (NS). The B, bias term which is equivalent to $P_{ET_{CO_2}}$ when ventilation is zero, for PSMW-HT, PSMW-noHT and PEMW was 31.4 ± 2.8, 34.8 ± 1.6 and 31.0 ± 1.6 Torr, respectively. The B term was significantly higher in PSMW-noHT compared with PEMW and PSMW-HT (ANOVA, $p = 0.003$).

4 Discussion

4.1 Resting $P_{ET_{CO_2}}$ and Baseline Ventilation

We found a significant increase in $P_{ET_{CO_2}}$ in PSMW-noHT compared to PSMW-HT and PEMW. In prior studies, PSMW have been shown to have higher $P_{ET_{CO_2}}$ values compared to PEMW (Leon-Velarde *et al*. 1997; Leon-Velarde, Rivera-Chira, Tapia, Huicho and Monge 2001; Regensteiner *et al*. 1989). Typically, $P_{ET_{CO_2}}$ has been shown to be approximately 9% greater in PSMW compared to PEMW in the luteal phase (Leon-Velarde *et al*. 2001; Regensteiner *et al*. 1989). Consistent with this, our group of PSMW-noHT had a 9.7% increase in $P_{ET_{CO_2}}$ compared to PEMW during the luteal phase.

The resting $\dot{V}_E$ was significantly higher in the PSMW-noHT compared with PEMW and PSMW-HT. There was no difference between PSMW-noHT and PSMW-HT. However, there was a trend for a lower baseline $\dot{V}_E$ in PSMW-noHT compared with PSMW-HT. Previous results have shown a significant decline in resting $\dot{V}_E$ in PSMW compared to PEMW (Leon-Velarde *et al*. 1997; Leon-Velarde *et al*. 2001; Regensteiner *et al*. 1989). Further, Regensteiner *et al*. (1989) found a significant increase in resting $\dot{V}_E$ with administration of progesterone plus estrogen and progesterone alone in PSMW. Our study, confirms these results.

4.2 Ventilatory Sensitivity to Hypercapnia

We found G_P to be significantly lower in PSMW-noHT compared with PEMW. Further, there was a trend for G_P to be lower in PSMW-noHT compared to PSMW-HT. Interestingly, there was no significant difference in G_c between groups.

One possible explanation to explain these findings is that ovarian hormones may selectively target the peripheral chemoreceptor response. Previous studies have proposed that estrogen and progesterone have both peripheral (carotid bodies) and central sites of action (Behan, Zabka, Thomas and Mitchell 2003; Regensteiner *et al*. 1989; Tatsumi *et al*. 1997). In contrast, others have suggested that progesterone acts primarily at peripheral sites, and estrogen only influences the central nervous system translation of carotid body activity into $\dot{V}E$ (Behan *et al*. 2003; Hayes, Moya Del Pino and Kaufman 2002; Tatsumi *et al*. 1997). Our study supports the theory that ovarian hormones influence ventilatory drive at the peripheral chemoreceptors, but not the central chemoreceptors.

A second possibility, at least in part, is the physiological changes that occur due to aging. Prior studies have suggested the decrease in ventilatory responses seen with aging can be contributed to a functional decline in the carotid body chemoreceptors (Conde, Obeso, Rigual, Monteiro and Gonzalez 2006).

It is evident that ovarian hormones and physiological changes seen with aging do contribute to the peripheral chemoreceptor responses to hypercapnia, but to what extent still remains unclear.

Acknowledgements This work was supported by the Alberta Heritage Foundation for Medical Research (AHFMR), Heart and Stroke Foundation of Alberta, NWT, & Nunavut, Canadian Institutes of Health Research and the Canada Foundation for Innovation. CTD was supported by an NSERC scholarship, and KI was supported by an AHFMR Postdoctoral Fellowship. MJP is a Senior Medical Scholar (AHFMR).

References

Behan, M., Zabka, A.G., Thomas, C.F. and Mitchell, G.S. (2003) Sex steroid hormones and the neural control of breathing. Respir. Physiol. Neurobiol. 136, 249–263.

Conde, S.V., Obeso, A., Rigual, R., Monteiro, E.C. and Gonzalez, C. (2006) Function of the rat carotid body chemoreceptors in ageing. J. Neurochem. 99, 711–723.

Fatemian, M., Gamboa, A., Leon-Velarde, F., Rivera-Ch, M., Palacios, J.A. and Robbins, P.A. (2003) Plasticity in Respiratory Motor Control: Selected Contribution: Ventilatory response to CO_2 in high-altitude natives and patients with chronic mountain sickness. J. Appl. Physiol. 94, 1279–1287.

Hayes, S.G., Moya Del Pino, N.B. and Kaufman, M.P. (2002) Estrogen attenuates the cardiovascular and ventilatory responses to central command in cats. J. Appl. Physiol. 92, 1635–1641.

Ide, K., Eliasziw, M. and Poulin, M.J. (2003) The relationship between middle cerebral artery blood velocity and end-tidal PCO_2 in the hypocapnic-hypercapnic range in humans. J. Appl. Physiol. 95, 129–137.

Leon-Velarde, F., Ramos, M.A., Hernandez, J.A., De Idiaquez, D., Munoz, L.S., Gaffo, A., Cordova, S., Durand, D. and Monge, C. (1997) The role of menopause in the development of chronic mountain sickness. Am. J. Physiol. .272, R90–R94.

Leon-Velarde, F., Rivera-Chira, M., Tapia, R., Huicho, L. and Monge, C. (2001) Relationship of ovarian hormones to hypoxemia in women residents of 4,300 m. Am. J. Physiol. 280, R488–R493.

Regensteiner, J.G., Woodard, W.D., Hagerman, D.D., Weil, J.V., Pickett, C.K., Bender, P.R. and Moore, L.G. (1989) Combined effects of female hormones and metabolic rate on ventilatory drives in women. J. Appl. Physiol. 66, 808–813.

Robbins, P.A., Swanson, G.D. and Howson, M.G. (1982) A prediction correction scheme for forcing alveolar gases along certain time courses. J. Appl. Physiol. 52, 1353–1357.

Tatsumi, K., Pickett, C.K., Jacoby, C.R., Weil, J.V. and Moore, L.G. (1997) Role of endogenous female hormones in hypoxic chemosensitivity. J. Appl. Physiol. 83, 1706–1710.

80
Oxidative Stress Impairs Upper Airway Muscle Endurance in an Animal Model of Sleep-Disordered Breathing

Mark Dunleavy[1], Aidan Bradford[1] and Ken D. O'Halloran[2]

Abstract Obstructive sleep apnoea is characterised by intermittent hypoxia due to recurrent obstructions of the pharyngeal airway during sleep. We have shown that chronic intermittent hypoxia impairs respiratory muscle function and CNS control of upper airway patency. In this study, we tested the hypothesis that disruption of an endogenous antioxidant defence system exacerbates the effects of intermittent hypoxia on upper airway muscle contractile function. Thirty-two male Wistar rats were placed in restrainers with their heads in hoods in which the ambient oxygen concentration could be modified by controlling the gas supply to the hoods. Sixteen rats were exposed to alternating equal periods of hypoxia and normoxia, twice per minute, 8 hours per day for 1 week. The remaining 16 animals were exposed to normoxia continuously under identical experimental conditions. In both groups, half the animals received daily injections of buthionine sulfoxamine (BSO), an inhibitor of the rate-limiting enzyme in glutathione synthesis. The other half received daily vehicle injections. At the end of the 1-week treatment period, the sternohyoid muscles were removed and fatigue characteristics were determined *in vitro*. Intermittent hypoxia was associated with a decrease in sternohyoid muscle endurance, an effect that was exacerbated by treatment with BSO. In separate experiments, daily treatment with the antioxidant N-acetyl cysteine blocked the deleterious effects of intermittent hypoxia on respiratory muscle function. We suggest that oxidative stress contributes to impaired upper airway muscle endurance in our animal model and that endogenous glutathione may be especially important in limiting free radical-induced muscle dysfunction. Our results may have particular relevance to respiratory disorders associated with recurrent hypoxia, such as the sleep apnoea/hypopnoea syndrome.

[1] Royal College of Surgeons in Ireland, Department of Physiology and Medical Physics, mdunleavy@rcsi.ie, abradford@rcsi.ie

[2] University College Dublin, School of Medicine and Medical Science, ken.ohalloran@ucd.ie

M.J. Poulin and R.J.A. Wilson (eds.), *Integration in Respiratory Control: From Genes to Systems*. © Springer 2008

1 Introduction

Sleep-disordered breathing is a common, often debilitating disorder. The condition is now recognised as a major public health problem with the cumulative effect contributing to cardiovascular and neurobehavioural morbidity and mortality. Obstructive sleep apnoea (OSA), a severe form of sleep-disordered breathing, is characterised by repetitive occlusions of the upper airway during sleep (Remmers, deGroot, Sauerland and Anch 1978). The causes of upper airway obstruction during sleep are likely multi-factorial, but there is evidence implicating upper airway muscle dysfunction in the pathophysiology of OSA. We have previously shown that chronic intermittent hypoxia, a feature of OSA due to recurrent apnoea, impairs pharyngeal dilator muscle endurance and recovery from fatigue and alters reflex regulation of upper airway EMG activity (Bradford, McGuire and O'Halloran 2005).

Recently, we have begun to explore the putative role of oxidative stress as a trigger of the maladaptive changes in upper airway muscle function that are seen in our animal model. Evidence is emerging that chronic intermittent hypoxia causes oxidative injury (Xu, Chi, Row, Xu, Ke, Xu, Luo, Kheirandish, Gozal and Liu 2004) and there is increasing evidence that OSA is, at least in part, an oxidative stress disorder (Lavie 2003). Although it appears that reactive oxygen species are required for optimum muscle function, excess free radical production is implicated in muscle dysfunction (Supinski 1998). Furthermore, pro-oxidant strategies exaggerate whereas antioxidant strategies retard the development of muscle fatigue under certain circumstances (Supinski 1998). In the present study, we sought to test the hypothesis that disruption of an endogenous antioxidant defence system exacerbates the effects of chronic intermittent hypoxia on upper airway muscle endurance.

2 Methods

Experiments were performed in 32 adult, male Wistar rats. Age and weight-matched animals were divided into two groups. On each experimental day, the rats were placed in restrainers with their heads surrounded by hoods in which the ambient O_2 concentration could be modified. Sixteen rats were exposed to alternating periods of normoxia and hypoxia, twice per min, for 8 h per day for 1 week. Briefly, using timed solenoid valves, N_2 was introduced into the hoods for 15 s reducing the ambient O_2 concentration to 6–8% at the nadir of the exposure followed by infusion of air for 15 s. Control animals were exposed to normoxia continuously. In both groups, half the animals received daily injections, beginning 1 day before the treatment period, of buthionine sulfoxamine (50 mg/kg *i.p.*), an inhibitor of the rate-limiting enzyme in glutathione synthesis. The other half received daily vehicle injections.

At the end of the 1-week treatment period, the animals were anaesthetized with Na^+-pentobarbitone (60 mg/kg *i.p.*) and the paired sternohyoid muscles were surgically removed. Longitudinal strips of muscle were prepared and suspended

vertically in physiological saline solution aerated with 95% O_2 and 5% CO_2 in water-jacketed organ baths at 30°C. The muscle strips were stimulated electrically via platinum electrodes located either side of the strip.

2.1 Protocol and Data Analysis

The tension-frequency relationship and fatigue characteristics of the muscle strips were measured in response to electrical field stimulation (supra-maximal stimulation). The tension-frequency relationship was determined by stimulating the muscle strips at 10, 20, 30, 40, 60, 80 and 100 Hz for 300 ms at each stimulus frequency allowing a 2 min interval between each stimulus. Fatigue was induced by stimulation at 40 Hz with 300 ms trains every 2 s for 5 min.

Specific tension was calculated in N/cm^2 of muscle strip cross sectional area. For the tension-frequency relationship, the values were normalised by expressing tension at each of the stimulation frequencies as a percentage of the maximum tetanic tension developed during the trial. For the fatigue protocol, the values were normalised by expressing the tension generated at 1, 2, 3, 4 and 5 min as a percentage of the value of the first pulse of the first train at 0 min. Absolute and normalised values for tension-frequency relationship and fatigue are expressed as mean ± SEM. Statistical comparisons were made between the four sub-groups by analysis of variance (ANOVA) and the Newman-Keuls *post hoc* test with $p < 0.05$ taken as significant.

3 Results

3.1 Intermittent Hypoxia Impairs Upper Airway Muscle Endurance

Chronic intermittent hypoxia caused a significant increase in sternohyoid muscle specific tension across a broad range of stimulus frequencies (Fig. 1; left panel). However, when data for the tension-frequency curves were normalised and expressed as a percentage of the peak tetanic tension developed during each trial there was no difference in the tension-frequency relationship (Fig. 1; right panel).

Data illustrating the fatigue characteristics of sternohyoid muscle strips from control and treated animals are shown in Fig. 2. Intermittent hypoxia increased the magnitude of fatigue compared to control animals.

3.2 Pro-oxidant Challenge Exacerbates the Effects of Intermittent Hypoxia on Muscle Endurance

Daily treatment with BSO, an inhibitor of endogenous glutathione synthesis, had no effect *per se* on sternohyoid muscle contractile and endurance properties

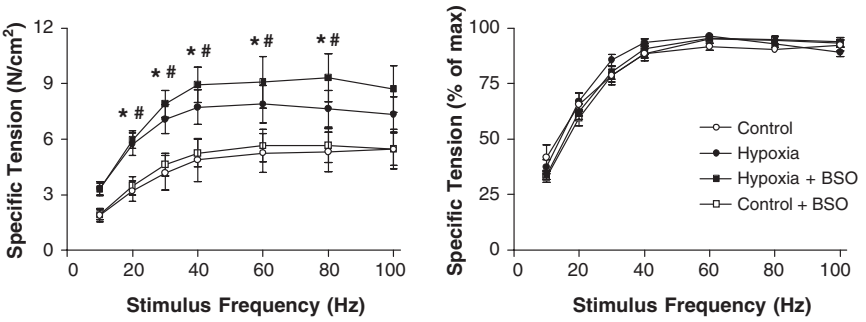

Fig. 1 Intermittent hypoxia and sternohyoid muscle tension
$p < 0.05$ control vs. hypoxia; * $p < 0.05$ control vs. hypoxia + BSO

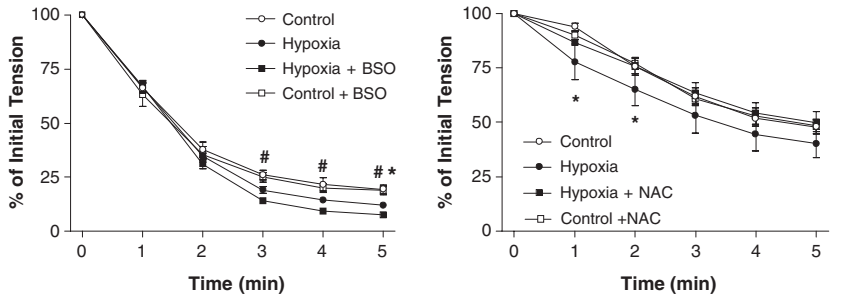

Fig. 2 Intermittent hypoxia and respiratory muscle fatigue
Left Panel: Sternohyoid * $p < 0.05$ control vs. hypoxia; # $p < 0.05$ control vs. hypoxia + BSO
Right Panel: Diaphragm * $p < 0.05$ control vs. hypoxia

(Fig. 1 and 2). However, in animals exposed to chronic intermittent hypoxia, BSO treatment exacerbated the deleterious effects of intermittent hypoxia on muscle endurance properties by further increasing the magnitude of sternohyoid muscle fatigue (Fig. 2; left panel).

3.3 Antioxidant Treatment Prevents the Effects of Intermittent Hypoxia on Muscle Endurance

In separate experiments in 16 animals, examining the effects of chronic intermittent hypoxia on muscle function, we observed that intermittent hypoxia for 1 week decreased diaphragm muscle endurance (Fig. 2; right panel) consistent with observations for the sternohyoid muscle. This effect was prevented by daily treatment with the antioxidant N-acetyl cysteine (NAC; 200 mg/kg *i.p.*).

4 Discussion

The upper airway dilator muscles play a pivotal role in the control and maintenance of upper airway patency. Fatigue of these muscles is implicated in obstructive airway conditions such as OSA. In this study, we have shown that 1 week of intermittent hypoxia decreases pharyngeal dilator muscle endurance. This is consistent with our previous observations of respiratory muscle dysfunction following several weeks of intermittent hypoxia (Bradford *et al*. 2005). On the basis of these observations, we speculate that in patients with OSA, intermittent hypoxia, a consequence of periodic airway occlusion, may in turn be responsible for progression of the disorder by virtue of impaired upper airway function leading to the establishment of a vicious cycle of further airway obstruction and hypoxic insult that over time exacerbates and perpetuates the condition.

With regard to the underlying mechanism of respiratory muscle dysfunction following chronic intermittent hypoxia, data from this study suggest that oxidative stress, resulting from the several thousand hypoxia/re-oxygenation cycles that the animals experience over the course of the week is a key mediator of impaired function in our animal model of sleep apnoea. We found that a pro-oxidant challenge exacerbates, whereas antioxidant treatment prevents, the deleterious effects of intermittent hypoxia on respiratory muscle contractile behaviour during repetitive activation. This implicates reactive oxygen species-dependent mechanisms that lead to increased vulnerability to fatigue. In BSO-treated animals the effect of intermittent hypoxia on muscle endurance was enhanced. In preliminary studies, antioxidant treatment blocked the deleterious effects of intermittent hypoxia on diaphragm muscle endurance. This requires further study and may have direct implications for treatment of OSA patients. Might antioxidant therapies yet prove beneficial as adjunct therapies in the treatment of sleep-disordered breathing in humans?

Acknowledgements This work was funded by the Health Research Board, Ireland (RP/2005/59). We are grateful to Julianne Hogan, MSc, for her contribution to this study.

References

Bradford, A., McGuire, M. and O'Halloran, K.D. (2005) Does episodic hypoxia affect upper airway dilator muscle function? Implications for the pathophysiology of obstructive sleep apnoea. Respir. Physiol. Neurobiol. 147, 223–234.

Lavie, L. (2003) Obstructive sleep apnoea syndrome – an oxidative stress disorder. Sleep Med. Rev. 7, 35–51.

Remmers, J.E., deGroot, W.J., Sauerland, E.K. and Anch, A.M. (1978) Pathogenesis of upper airway occlusion during sleep. J. Appl. Physiol. 44, 931–938.

Supinski (1998) Free radical induced respiratory muscle dysfunction. Mol. Cell. Biochem. 179, 99–110.

Xu, W., Chi, L., Row, B.W., Xu, R., Ke, Y., Xu, B., Luo, C., Kheirandish, L., Gozal, D. and Liu, R. (2004) Increased oxidative stress is associated with chronic intermittent hypoxia-mediated brain cortical neuronal cell apoptosis in a mouse model of sleep apnea. Neuroscience 126, 313–323.

81
Ventilatory and Blood Pressure Responses to Isocapnic Hypoxia in OSA Patients

Glen E. Foster [1], Patrick J. Hanly[2,4], Michele Ostrowski[2] and Marc J. Poulin[1,3,4,5,6]

1 Introduction

Obstructive sleep apnea (OSA) is a chronic medical condition resulting in chronic exposure to intermittent hypoxia (IH), which is correctable by continuous positive airway pressure (CPAP) therapy. Acute exposure to IH in healthy subjects affects respiratory control and vascular function (Foster, McKenzie, Milsom and Sheel 2005), but studies on the ventilatory response to hypoxia in OSA patients have yielded conflicting results and there have been few studies on the blood pressure response to hypoxia in this patient population. In addition, the effects of CPAP therapy on the blood pressure response to hypoxia have not been assessed. We hypothesized that the ventilatory and blood pressure response to hypoxia are enhanced in patients with OSA and that they are normalized following CPAP therapy.

2 Methods

2.1 Study Subjects

Patients with severe OSA who satisfied our inclusion criteria (non-smoker, BMI < 35 Kg m^{-2}, no history of cardio-respiratory disease, hypertension or treatment with CPAP) were recruited along with matched control subjects. The study protocol was

[1] University of Calgary, Faculty of Medicine, Department of Physiology and Biophysics

[2] University of Calgary, Faculty of Medicine, Department of Medicine

[3] University of Calgary, Faculty of Medicine, Department of Clinical Neurosciences

[4] University of Calgary, Hotchkiss Brain Institute

[5] University of Calgary, Libin Cardiovascular Institute

[6] University of Calgary, Faculty of Kinesiology
email: gfoster@ucalgary.ca; phanly@ucalgary.ca; poulin@ucalgary.ca

M.J. Poulin and R.J.A. Wilson (eds.), *Integration in Respiratory Control: From Genes to Systems*.

reviewed and approved by the local Ethics Board at the University of Calgary, and all subjects gave written informed consent to participate in the study.

2.2 Study Protocol

The acute hypoxic ventilatory response (AHR_{VE}) and blood pressure response (AHR_{MAP}) were measured. Subjects attended the laboratory on 3 occasions. The first visit involved subject familiarization with the experimental apparatus. The second visit involved the baseline measurement of the acute hypoxic responses. The following night, patients with OSA had overnight attended polysomnography in the sleep laboratory. Further details regarding the experimental protocol can be found elsewhere (Foster, Hanly, Ostrowski and Poulin 2007). During the first half of the sleep study, the severity of OSA was established. During the second half of the sleep study, patients were placed on CPAP, which was titrated to a level that controlled OSA. Following 4–6 weeks of effective CPAP therapy, which was confirmed by objective monitoring of CPAP use and overnight cardio-pulmonary monitoring while using CPAP at home, patients returned for follow-up measurement of the acute hypoxic responses. Control subjects also returned to the laboratory 4–6 weeks after their initial assessment for similar follow-up; however, they did not receive CPAP therapy.

2.3 Study Measurements

Home Cardio-pulmonary monitoring. Patients and control subjects were screened for OSA by continuous, overnight cardio-pulmonary monitoring at home (Remmers Sleep Recorder Model 4.2, Saga Tech Electronic, Calgary, Canada). An automated scoring algorithm calculated the respiratory disturbance index (RDI).

Polysomnography. The diagnosis and severity of OSA was further assessed by overnight, attended polysomnography (American Academy of Sleep Medicine 1999). All polysomnograms were scored manually by registered polysomnographic technologists according to established criteria (Rechtschaffen and Kales 1968).

CPAP Compliance. Following acclimatization to CPAP therapy, nightly use at the prescribed pressure was downloaded from the CPAP unit for four weeks prior to follow-up testing.

Acute Hypoxic Response. Accurate control of end-tidal gases was achieved using the technique of dynamic end-tidal forcing (BreatheM v2.38, University Laboratory of Physiology, Oxford, UK), as described previously (Ainslie and Poulin 2004). The experiment began with a 10-minute period during which the subject's resting end-tidal partial pressure of oxygen ($P_{ET_{O_2}}$) and carbon dioxide ($P_{ET_{CO_2}}$) were measured. After a 10-minute lead-in period of isocapnic euoxia ($P_{ET_{CO_2}}$= +1.0 Torr above resting values; $P_{ET_{O_2}}$= 88.0 Torr), the inspired gas was rapidly changed to a $P_{ET_{O_2}}$ of 50.0 Torr while $P_{ET_{CO_2}}$ remained constant at +1.0 Torr above resting values. Isocapnic hypoxia continued for 20 minutes, at which time the $P_{ET_{O_2}}$ was

rapidly returned to 88.0 Torr and maintained constant for a final 10 minutes. During the study, ventilation ($\dot{V}E$), mean arterial pressure (MAP; photoplethysmography) and SaO_2 (pulse oximetry) were recorded continuously.

A first order, dynamic mathematical model was used to fit the ventilatory response to isocapnic hypoxia as previously described (Liang, Bascom and Robbins 1997). This model provides a term for resting $\dot{V}E$, and for the sensitivity of the peripheral chemoreceptor to hypoxia (AHR_{VE}; expressed in l min^{-1} % $desaturaiton^{-1}$).

The AHR_{MAP} was calculated as the change in MAP from isocapnic euoxia to isocapnic hypoxia, divided by the change in SaO_2 (mmHg % $desaturation^{-1}$). For this measurement, SaO_2 was calculated from PET_{O2} based on the Severinghaus transform as previously described (Severinghaus 1979).

2.4 Statistical Analysis

Data were compared using repeated measures analysis of variance (v14.0, SPSS, Chicago, Illinois, USA). When significant F-ratios were detected, the simple effects test was applied *post hoc* to resolve differences. The level of significance was set at $p < 0.05$ for all statistical comparisons. All data are presented as mean ± SE.

3 Results

We studied 8 men with OSA and 10 healthy controls. The OSA and control groups were of similar age (41 ± 2 *vs*. 37 ± 3 years) and BMI (30 ± 1 *vs*. 28 ± 1 kg m^{-2}), respectively. Patients had severe OSA associated with significant nocturnal hypoxemia, confirmed both by home monitoring (RDI = 52 ± 10 events h^{-1}; mean

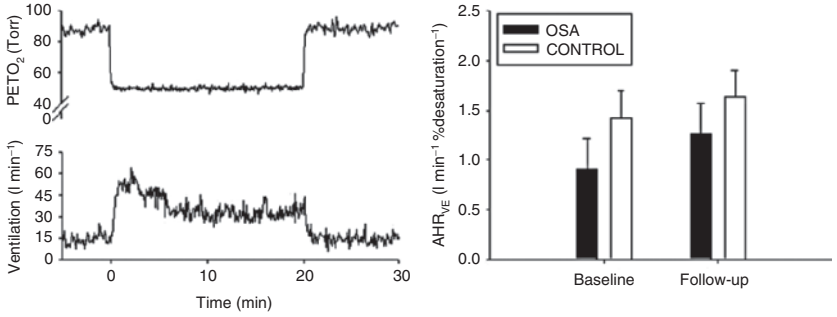

Fig. 1 Acute hypoxic ventilatory response. Left panel: Real-time recording of the AHR_{VE} from a control subject (ID# = 0091). Abbreviations: PET_{O_2} = end-tidal partial pressure of oxygen. Right Panel: The AHR_{VE} in OSA and control subjects at baseline and follow-up. Values are means ±SE. Differences are not statistically significant

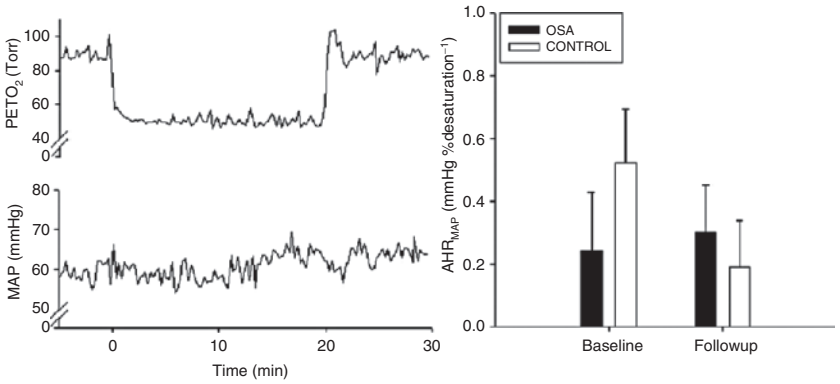

Fig. 2 Acute mean blood pressure hypoxic response. Left panel: Real-time recording of the AHR_{MAP} in one control subject (ID# = 0091). Abbreviations: $P_{ET_{O_2}}$ = end-tidal partial pressure of oxygen; MAP = mean arterial pressure. Right panel: The AHR_{MAP} in OSA and control subjects at baseline and follow-up. Values are means ± SE

SaO_2 = 88 ± 3%) and polysomnography (AHI = 101 ± 10 events h^{-1}; mean SaO_2 = 89 ± 1%), while control subjects had no evidence of OSA (RDI = 4 ± 2 events h^{-1}; p = 0.006) or nocturnal hypoxemia (mean SaO_2 = 93 ± 1%; p = 0.004). All OSA patients were successfully treated with CPAP, which was reflected by reduction in the RDI to normal (4 ± 1 events h^{-1}) and correction of nocturnal hypoxemia (94 ± 1%). All subjects were compliant with CPAP therapy, using it 5.1 ± 0.4 hours per night during the four weeks prior to their final assessment.

There were no differences in isocapnic euoxic $P_{ET_{O_2}}$, $P_{ET_{CO_2}}$, $\dot{V}_E$ or MAP between OSA patients and control subjects at baseline or follow-up (data not shown). In addition, the AHR_{VE} was not significantly different between OSA patients and control subjects at baseline or follow-up (Fig. 1). The AHR_{MAP} was not different between OSA and control subjects at baseline or follow-up and was not affected by CPAP therapy (Fig. 2).

4 Discussion

We studied patients with severe OSA and found that the ventilatory and MAP responses to hypoxia were not different from control subjects. In addition, CPAP therapy did not affect the ventilatory and MAP responses to hypoxia. These data suggest that in terms of AHR_{VE}, OSA patients acclimated to the effects of IH and in terms of AHR_{MAP}, that these patients, who were free from OSA-related cardiovascular disease, had not developed alterations in blood pressure control.

Acute exposure to IH in healthy humans increases the ventilatory response to hypoxia (Foster *et al*. 2005). However, we did not find a significant difference in AHR_{VE}

between OSA and control subjects at baseline or following CPAP therapy. Other reports of OSA patients indicate increased (Narkiewicz, van de Borne, Pesek, Dyken, Montano and Somers 1999), reduced (Osanai, Akiba, Fujiuchi, Nakano, Matsumoto, Ohsaki and Kikuchi 1999), or unchanged (Radwan, Maszczyk, Koziej, Franczuk, Koziorowski, Kowalski and Zielinski 2000) ventilatory responses to hypoxia.

OSA patients are reported to have elevated sympathetic activation and blood pressure responses to hypoxia (Narkiewicz *et al*. 1999). Our data indicate that the blood pressure response to hypoxia is not different from controls and is unaffected by CPAP therapy. We speculate that our contrasting results may be due to the fact that autonomic and vascular dysregulation were not present in our patients since we excluded those who were hypertensive, obese, or had cardiovascular and respiratory disease.

Finally, we speculate that the changes in AHR_{VE} previously observed in OSA may depend on a number of factors, including the severity of OSA, blood pressure status and the duration of OSA prior to diagnosis. However, this hypothesis requires further study.

5 Conclusion

Our study assessed the potential for chronic IH to affect the ventilatory and blood pressure responses to hypoxia in patients with OSA. We did not observe any differences in the AHR_{VE} and AHR_{MAP} in OSA patients compared to controls nor did we observe an effect of CPAP therapy.

Acknowledgements This project was supported by the Alberta Heritage Foundation for Medical Research (AHFMR), the Heart and Stroke Foundation of Alberta, NWT, & Nunavut, the Canadian Institutes of Health Research (CIHR) and the Canada Foundation for Innovation. GE Foster was supported by doctoral research awards from the AHFMR, HSFC and is a CIHR Strategic Training Fellow in TORCH (Tomorrow's Research Cardiovascular Health Professionals). MJ Poulin is an AHFMR Senior Medical Scholar.

References

American Academy of Sleep Medicine Task Force (1999) Sleep-related breathing disorders in adults: recommendations for syndrome definition and measurement techniques in clinical research. The Report of an American Academy of Sleep Medicine Task Force. Sleep. 22, 667–689.

Ainslie, P.N. and Poulin, M.J. (2004) Ventilatory, cerebrovascular, and cardiovascular interactions in acute hypoxia: regulation by carbon dioxide. J. Appl. Physiol. 97, 149–159.

Foster, G.E., Hanly, P.J., Ostrowski, M. and Poulin, M.J. (2007) Effects of continuous positive airway pressure on cerebral vascular response to hypoxia in patients with obstructive sleep apnea. Am. J. Respir. Crit. Care Med. 175, 720–725.

Foster, G.E., McKenzie, D.C., Milsom, W.K. and Sheel, A.W. (2005) Effects of two protocols of intermittent hypoxia on human ventilatory, cardiovascular and cerebral responses to hypoxia. J. Physiol. 567, 689–699.

Liang, P.J., Bascom, D.A. and Robbins, P.A. (1997) Extended models of the ventilatory response to sustained isocapnic hypoxia in humans. J. Appl. Physiol. 82, 667–677.

Narkiewicz, K., van de Borne, P.J., Pesek, C.A., Dyken, M.E., Montano, N. and Somers, V.K. (1999) Selective potentiation of peripheral chemoreflex sensitivity in obstructive sleep apnea. Circulation 99, 1183–1189.

Osanai, S., Akiba, Y., Fujiuchi, S., Nakano, H., Matsumoto, H., Ohsaki, Y. and Kikuchi, K. (1999) Depression of peripheral chemosensitivity by a dopaminergic mechanism in patients with obstructive sleep apnoea syndrome. Eur. Respir. J. 13, 418–423.

Radwan, L., Maszczyk, Z., Koziej, M., Franczuk, M., Koziorowski, A., Kowalski, J. and Zielinski, J. (2000) Respiratory responses to chemical stimulation in patients with obstructive sleep apnoea. Monaldi. Arch. Chest Dis. 55, 96–100.

Severinghaus, J.W. (1979). Simple, accurate equations for human blood O2 dissociation computations. J. Appl. Physiol. 46, 599–602.

82
Modeling of Sleep-Induced Changes in Airway Function: Implication for Nocturnal Worsening of Bronchial Asthma

Musa A. Haxhiu[1,2,3], Prabha Kc[1], Kannan V. Balan[1], Christopher G. Wilson[1] and Richard J. Martin[1]

Abstract Here we describe the model of sleep-induced worsening of airway function in patients with airway disorders. Our model is based on the noradrenergic pathways that link central neuronal structures responsible for alternating wakefulness and sleep with the neuronal networks regulating the activity of airway-related vagal preganglionic neurons (AVPNs). Our previous studies showed that cholinergic outflow to the airways depend on the activity of inhibitory inputs to AVPNs. Major inhibitory cell groups, regulating AVPNs discharge, include brainstem noradrenaline (NA)-containing cells receiving projections from the hypothalamic sleep-promoting neurons of the ventrolateral preoptic region (VLPO). When activated, VLPO cells, using GABA and/or galanin as mediators, downregulate the activity of inhibitory NA neurons projecting to AVPNs. Therefore, changes that occur during sleep lead to a shift from inhibitory to excitatory transmission of the AVPNs, thereby increasing cholinergic outflow to the airways. Our model, based on neuroanatomical and molecular studies, and physiology experiments, can be used to explain sleep-related worsening of bronchial asthma and might contribute to development of clinically meaningful treatment for patients with sleep-induced worsening of airway function and respiratory symptoms.

Keywords sleep-generating sites; noradrenergic neurons; nocturnal asthma; airway-related vagal preganglionic neurons

1 Introduction

In recent years, significant progress has been made in characterizing the chemical profile of reciprocally-connected cell groups entangled in the alternation of sleep states, wakefulness and sleep-induced respiratory changes (Saper, Chou and Scammell 2001). Here we describe a model of sleep-induced worsening of airway

Departments of [1]Pediatrics, [2]Medicine, and [3]Anatomy, Case Western Reserve University, Cleveland, Ohio 44106 USA; mah10@case.edu, kxp95@case.edu, kvb2@case.edu; cgw5@case.edu; rxm6@case.edu

M.J. Poulin and R.J.A. Wilson (eds.), *Integration in Respiratory Control: From Genes to Systems*.

function in patients with airway disorders. The model is based on the noradrenergic pathways that link central neuronal structures alternating wakefulness and sleep with the neuronal networks controlling the activity of AVPNs. This work extends the previous chapter on behavioral state control and airway instability.

Major inhibitory cell groups regulating AVPNs discharge, GABAergic, serotonergic and brainstem NA-containing cells (Haxhiu, Kc, Neziri, Yamamoto, Ferguson and Massari 2003; Moore, Wilson, Mayer, Acquah, Massari and Haxhiu 2004) receive projections from the hypothalamic sleep-promoting neurons (Saper *et al*. 2001) of the VLPO which, when activated, downregulate the activity of inhibitory neurons including NA-containing neurons projecting to AVPNs (Haxhiu *et al*. 2003). In a ferret asthma model, noradrenergic inhibitory influences are diminished. Therefore, changes that occur during sleep lead to a shift from inhibitory to excitatory transmission to the AVPNs, thereby increasing cholinergic outflow to the airways.

2 Cyclic Oscillations of Airway Conductivity

In asthmatics, sleep-related alterations in airway conductivity are enhanced (Sutherland 2005), causing decreases in arterial PO_2 that further reflexly worsens bronchoconstriction and breathing difficulties. Nocturnal changes are associated with accentuated bronchial hyperresponsiveness, worsening of airway function and asthma symptoms, leading to frequent arousals on a nightly basis (Turner-Warwick 1988). These nocturnal changes were thought to be caused by diurnal variations of circulating chemicals (Barnes, FitzGerald, Brown and Dollery 1980) and inflammatory mechanisms. However, later investigations showed that nocturnal worsening need not be related to humoral factors or any other known trigger, including airway inflammation, age, or treatment (Turner-Warwick 1988). A number of clinical studies suggested that nocturnal worsening of asthma is intimately related to changes in behavioral state and could be due to the sleep (Ballard 1999). Despite these findings, little effort has been made to characterize CNS determinants of sleep-related changes in lower airway function. A key conceptual reason for focusing on peripheral changes induced by circulating substances lies on complexity of the CNS and existence of the multiple levels of interplay between excitatory and inhibitory signaling pathways controlling AVPNs.

3 CNS Inhibitory Control of AVPNs

Parasympathetic vagal preganglionic neurons innervating lower airways arise mainly from the rostral nucleus ambiguus (rNA) and, to a lesser degree, from the rostral portion of the dorsal motor nucleus of the vagus (DMV) (Jordan 2001; Kc, Mayer and Haxhiu 2004). These cholinergic cells transmit cholinergic signals to the intrinsic tracheobronchial ganglia. Ganglionic neurons give rise to postganglionic fibers controlling specific effector targets (*i.e*., airway smooth muscle, mucous

glands and blood vessels). Recently, using conventional and transneuronal labeling techniques, ultrastructural and molecular approaches, we have identified three major inhibitory cell groups that project to the AVPNs: (1) noradrenaline (NA)-containing neurons, (2) serotonin (5-HT)-expressing cells, and (3) γ aminobutyric acid (GABA)-producing cells (Haxhiu *et al*. 2003; Moore *et al*. 2004). Here, we will focus on noradrenergic neurons and their role in control of the airways.

4 Noradrenergic Neurotransmitter System

The major noradrenergic inputs to the AVPNs arise from the A5 cell group, the locus coeruleus (LC; A6) and subcoeruleus region that are part of the arousal system. Double immunolabeling studies at the light and electron microscopic levels showed that, in the ferret, catecholaminergic terminals with frequent varicosities are present in close proximity to the identified AVPNs. Furthermore, using microdialysis and high performance liquid chromatography (HPLC), the basal extracellular NA level within the rNA was more than doubled following stimulation of the LC and subcoeruleus region. This led to a decrease in cholinergic outflow to the airways, via activation of α_{2A}-ARs, which are abundantly expressed by AVPNs. The responses were blocked by yohimbine, an α_{2A} adrenergic receptor blocker (Haxhiu *et al*. 2003).

5 CNS Circuits Regulating Sleep and Wakefulness

Brain regions controlling the onset of sleep and transitions from non-rapid eye movement (NREM) to rapid eye movement (REM) sleep, and from REM sleep to arousal, project to noradrenergic neurons (Aston-Jones and Bloom 1981; Saper *et al*. 2001). The VLPO is a major diencephalic NREM and REM sleep-promoting structure. Within the pontine field, one finds mesopontine REM-facilitating neurons and arousal-inducing monoaminergic cell groups that are inhibited by NREM and REM sleep-promoting neurons (Aston-Jones and Bloom 1981; Siegel 2000). Therefore, timing of sleep and wakefulness is determined by interconnected processes: a homeostatic regulatory operation that increases during waking and decreases during sleep, *i.e*., extracellular levels of adenosine that modulate VLPO neuronal activity.

Orexin-containing lateral hypothalamic area (LHA) neurons are important for maintaining wakefulness (Espana, Balso, Kelley and Berridge 2001). Sleep-active GABAergic neurons inhibit orexin-containing cells. The VLPO consists of neurons clustered just lateral to the optic chiasm, activation of which induce sleep. A majority of these cells express GABA and the inhibitory neuropeptide galanin.

After its onset, quiet sleep switches from light to deeper stages and, as it progresses, the amount of non-REM sleep decreases and REM sleep increases, being more frequent in the last third of the night. Recent studies suggest that the promotion and maintenance of REM sleep is partly associated with the activity of subsets of VLPO inhibitory cells. Lesions of these sleep active cells affect both

NREM and REM sleep. Hence, these results extend previous findings on the role of pontine acetylcholine-containing neurons in generating REM sleep (Lydic, Baghdoyan and Zwillich 1989; Siegel 2000).

6 A Simplified Model of Behavioral State-dependent Control of Airway Function

The model suggests that sleep unleashes the excitatory mechanisms that give rise to cholinergic outflow to the airways (Fig. 1). Hence, the sleep state decreases the discharge frequency of major inhibitory neurons that regulate the response of the

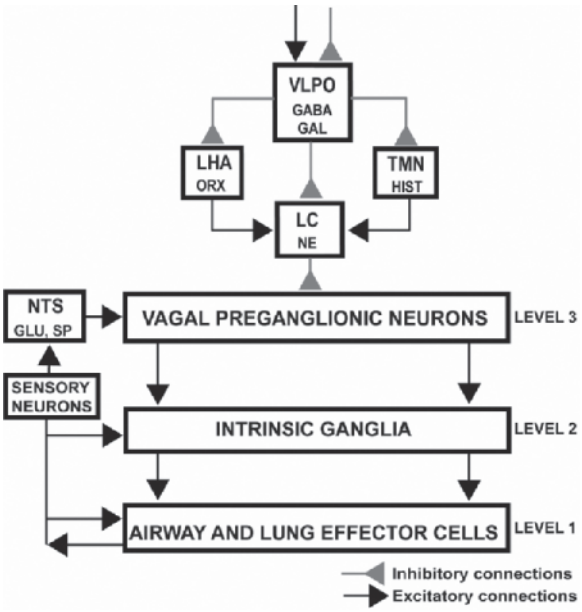

Fig. 1 Simplified diagram illustrating the organization of autonomic parasympathetic control of airway function and the pathways involved in sleep-induced airway narrowing. The AVPNs (level 3), as the final common pathway from the brain to the airways, transmit excitatory signals to the intrinsic tracheobronchial ganglia (level 2), controlling airway and lung effector cells (level 1). AVPNs are activated by sensory inputs from the airways and lungs through the NTS neurons using glutamate (GLU) and substance P (SP) as neurotransmitters. The response of the AVPNs to these excitatory inputs depends on the inhibitory inflow (level 4) to the AVPNs. Inhibitory cell groups projecting to the AVPNs are linked to the hypothalamic sleep-promoting region (VLPO). When activated, this cell group, using GABA and/or galanin as mediators, inhibits the histamine-containing neurons (HIST) of the tuberomamillary nucleus (TMN) and the orexin (ORX)-producing cells of the lateral hypothalamic area (LHA), causing withdrawal of excitatory inputs from TMN and LHA neurons to the Locus coeruleus (LC) noradrenaline (NA)-synthesizing cells. In addition, activation of VLPO neurons directly inhibits LC. Changes that occur during sleep, in both NREM and REM sleep stages, result in a shift from inhibitory to excitatory transmission to the AVPNs that could lead to worsening of airway function.

AVPNs to afferent inputs, resulting in a shift from inhibitory to excitatory transmission, a hyperexcitable state of the AVPNs and, consequently, an increase in cholinergic outflow that can predispose to and worsen bronchoconstriction.

Many features of sleep-induced worsening of airway functions, such as an increase in airway responsiveness, submucosal gland secretion, increase in bronchial blood flow, resistance of the lower airways or airway-parenchyma uncoupling in nocturnal asthma (Irvin, Pak and Martin 2000) could be due to withdrawal of inhibitory influences, as occurs with diminished noradrenergic inhibitory inputs to the AVPNs.

7 Summary

Recent studies elucidating fundamental mechanisms in rhythmic diurnal oscillations and alternation of sleep and wakefulness illuminate new concepts on state-dependent control of airway function. Furthermore, these findings, providing a deeper insight into the pathophysiology of sleep-related airway disorders, could reorganize our thinking and allow us to switch effortlessly to more complete and effective treatment of patients with sleep-enhanced airway dysfunction.

Acknowledgements This work was supported by the National Heart, Lung, and Blood Institute Grant HL-50527 (to M. A. Haxhiu).

References

Aston-Jones, G. and Bloom, F.E. (1981) Activity of norepinephrine-containing locus coeruleus neurons in behaving rats anticipates fluctuations in the sleep-waking cycle. J. Neurosci. 1(8), 876–886.

Ballard, R.D. (1999) Sleep, respiratory physiology and nocturnal asthma. Chronobiol. Int. 16(5), 565–580.

Barnes, P., FitzGerald, G., Brown, M. and Dollery, C. (1980) Nocturnal asthma and changes in circulating epinephrine, histamine and cortisol. N. Engl. J. Med. 303(5), 263–267.

Espana, R.A., Baldo, B.A., Kelley, A.E. and Berridge, C.W. (2001) Wake-promoting and sleep-suppressing actions of hypocretin (orexin): basal forebrain sites of action. Neuroscience 106(4), 699–715.

Haxhiu, M.A., Kc, P., Neziri, B., Yamamoto, B.K., Ferguson, D.G. and Massari, V.J. (2003) Catecholaminergic microcircuitry controlling the output of airway-related vagal preganglionic neurons. J. Appl. Physiol. 94(5), 1999–2009.

Irvin, C.G., Pak, J. and Martin, R.J. (2000) Airway-parenchyma uncoupling in nocturnal asthma. Am. J. Respir. Crit. Care Med. 161(1), 50–56.

Jordan, D. (2001) Central nervous pathways and control of the airways. Respir. Physiol. 125(1–2), 67–81.

Kc, P., Mayer, C.A. and Haxhiu, M.A. (2004) Chemical profile of vagal preganglionic motor cells innervating the airways in ferrets: the absence of noncholinergic neurons. J. Appl. Physiol. 97(4), 1508–1517.

Lydic, R., Baghdoyan, H.A. and Zwillich, C.W. (1989) State-dependent hypotonia in posterior cricoarytenoid muscles of the larynx caused by cholinoceptive reticular mechanisms. FASEB J. 3(5), 1625–1631.

Moore, C.T., Wilson, C.G., Mayer, C.A., Acquah, S.S., Massari, V.J. and Haxhiu, M.A. (20040) A GABAergic inhibitory microcircuit controlling cholinergic outflow to the airways. J. Appl. Physiol. 96(1), 260–270.

Saper, C.B., Chou, T.C. and Scammell, T.E. (2001) The sleep switch: hypothalamic control of sleep and wakefulness. Trends Neurosci. 24(12), 726–731.

Siegel, J.M. (2000) Brainstem mechanisms generating REM sleep. In: M.H. Kryger, T. Roth and W.C. Dement (Eds.), *Principles and Practice of Sleep Medicine*. Saunders, Philadelphia, pp. 112–133.

Sutherland, E.R. (2005) Nocturnal asthma: underlying mechanisms and treatment. Curr. Allergy Asthma Rep. 5(2), 161–167.

Turner-Warwick, M. (1988) Epidemiology of nocturnal asthma. Am. J. Med. 85(1B), 6–8.

83
The Effects of Wakefulness State on the Temporal Characteristics of Ventilatory Variables in Man

J. Ingemann Jensen[1], A.Varlese[2], S. Karan[3], W. Voter[4], L. Palmer[5] and D.S. Ward[6]

Abstract The effects of audiovisual stimulation on the temporal patterns of V_T, T_I, T_E were studied in 11 healthy subjects. 75 datasets of steady-state breathing each of eight minutes in duration were obtained during low wakefulness (lying still, eyes closed), low wakefulness with calibrated thermal pain stimulation and high wakefulness (playing a computer game). The analysis included removal of trend and mean, interpolation and re-sampling of the data to provide an equi-spaced time basis, test for normal distribution of datasets, power spectral estimation, estimation of the parameters of 1st and 2nd order autocorrelation models and estimation of the same parameters on the residuals following subtraction of the 1st or 2nd order models. All power spectra showed the highest power at the lowest frequencies; correspondingly the 1st order autocorrelation coefficients were significant at the 5% level except for T_E ($p = 0.12$). The 2nd order coefficients were non-significant for all series. The 1st order autocorrelation coefficients of the residuals (after subtraction of the 1st order autocorrelation component) were all non-significant. With 1st order autocorrelation coefficients averaging between .12 and .37 the non-random part of the variation explained by the 1st order autocorrelation structure is between 1.4% and 13.7% and independent of stimulation of breathing by thermal or mental stimuli.

1 Introduction

The temporal characteristics of ventilatory variables have been studied in awake subjects under various conditions, including eupnoea and combinations of hypercapnia, hypercapnia and hypoxia, and exercise (Ingemann Jensen 1987; Busso, Pei-Ji Liang and Robbins 1996). The pattern of temporal variation has consistently been that of a first-order autoregressive process (AR1), with a few percent of the seemingly random variation being explained by the AR1; thus the majority of variation remains random.

[1–6] Department of Anesthesiology, University of Rochester Medical Center, 601 Elmwood Ave., Box 604, Rochester, New York 14642, jens_ingemannjensen@urmc.rochester.edu

M.J. Poulin and R.J.A. Wilson (eds.), *Integration in Respiratory Control: From Genes to Systems*. © Springer 2008

It is an everyday observation that breathing and breathing patterns are influenced by voluntary interference and external stimuli, demonstrating that the processes governing breathing are connected to higher functions in the brain. These interactions and the difficulties of standardizing and measuring them have caused them to be studied much less than the chemoreflex regulation of breathing.

2 Methods

Eleven volunteers served as subjects. The protocol was approved by the local human subject protection committee.

Subjects were studied lying comfortably, breathing through a face mask. The inspired fractions of oxygen and carbon dioxide were manipulated through servo control to provide a well-defined step input of P_aO_2 into hypoxia (100 to 60 mm Hg) while P_aCO_2 was maintained at eucapnic levels during the transient as well as during the steady state. For a complete description of the methodology, see Karan *et al*. (2005) and Cartwright, Henson and Ward (1998).

Three conditions were compared:

- Low wakefulness: the subject was resting supine with eyes closed wearing headphones to prevent auditory stimulation (LWf);
- Low wakefulness with pain: as LWf, while thermal pain was applied to the forearm. The pain stimulus was applied using a calibrated thermode (PPS-3; Precision Pain Sources, Cygnus, Paterson, NJ) (Pain).
- High wakefulness: the subject was resting supine while playing a video game ("You Don't Know Jack – The Ride"; Berkely Systems, Jellyvision Inc., Chicago, IL) providing audio-visual stimulation (AVS).

Sequences of breath-by-breath recordings of tidal volume, V_T, inspiratory time, T_I, and expiratory time, T_E, were collected over eight-minute periods of steady-state breathing.

3 Analysis and Results

Basic statistics (Table 1) were calculated using STATA software (Stata Corp., College Station, TX). The time series analyses were performed with routines programmed in Matlab® (The Mathworks, Natick, MA).

For the time series analysis, the data had trends and means subtracted, were interpolated and re-sampled on an equi-spaced time basis; the analysis included estimation of power spectra and of the parameters of 1st and 2nd order autoregressive models. None of the resulting data series deviated significantly from normality at the 1% level.

Table 1 Basic statistics of the analyzed data series during the three different levels of wakefulness

	Statistic	V_T (l)	T_I (sec)	T_E (sec)
Low wakefulness	Mean	0.64	1.74	2.52
	Std. dev.	.015	0.32	0.46
	Coeff. Var.	0.22	0.18	0.18
	Trend (Breath^{-1})	$-1.8 \cdot 10^{-5}$	$-6.8 \cdot 10^{-4}$	$-4.7 \cdot 10^{-4}$
Pain stimulation	Mean	0.59	1.29	1.93
	Std. dev.	0.13	0.20	0.36
	Coeff. Var.	0.22	0.15	0.18
	Trend (Breath^{-1})	$-5.6 \cdot 10^{-5}$	$-1.7 \cdot 10^{-4}$	$2.1 \cdot 10^{-4}$
Audio-visual stimulation	Mean	0.60	1.56	2.28
	Std. dev.	.013	0.24	0.37
	Coeff. Var.	.020	0.16	0.17
	Trend (Breath^{-1})	$-2.7 \cdot 10^{-5}$	$-1.6 \cdot 10^{-4}$	$-0.37 \cdot 10^{-4}$

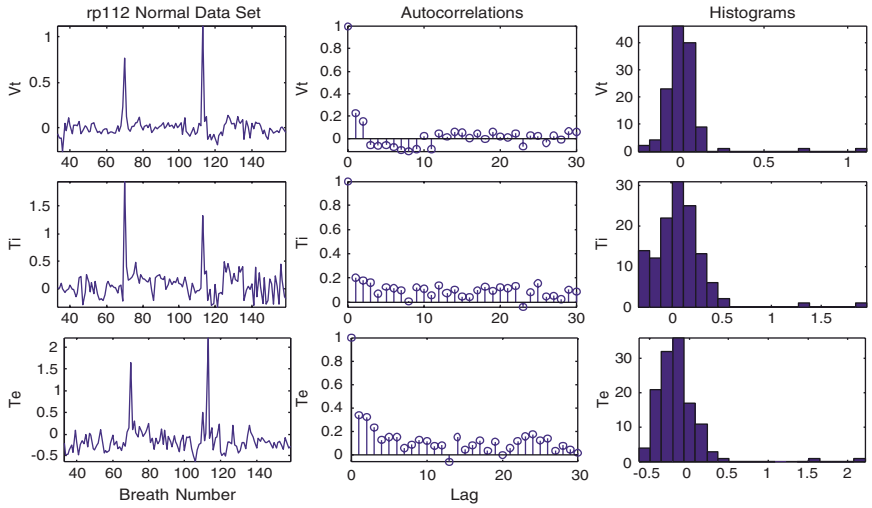

Fig. 1 Plots of data series after subtraction of the means and de-trending (left column), the corresponding autocorrelograms (middle column) and frequency distributions (right column) of V_T (top row), T_I (middle row), and T_E (bottom row) (see Color Plates)

Figure 1 shows time plots, autocorrelograms, and frequency distributions for three series, one for each of V_T, T_I, and T_E (after subtraction of the means and de-trending). The time plots illustrate that the data series appear to vary around zero. The frequency distributions show some skewness. The autocorrelograms show mainly positive coefficients with the first being larger than the rest of the coefficients; on the average, only the first one reached statistical significance. As the power spectrum is the Fourier transform or frequency domain representation of the autocorrelations (time domain), all power spectra exhibited the largest power at low frequencies.

Table 2 Autocorrelation coefficients for the three variables during the three levels of wakefulness

	Low wakefulness			Pain stimulation			Audio-visual stimulation		
	1st	1st	2nd	1st	1st	2nd	1st	1st	2nd
Order	$\acute{\alpha}_1$	$\acute{\alpha}_1$	$\acute{\alpha}_2$	$\acute{\alpha}_1$	$\acute{\alpha}_1$	$\acute{\alpha}_2$	$\acute{\alpha}_1$	$\acute{\alpha}_1$	$\acute{\alpha}_2$
V_T (l)	0.27	0.26	0.02	0.25	0.23	0.06	0.12	0.11	0.03
T_I (sec)	0.37	0.34	0.10	0.25	0.23	0.08	0.15	0.14	0.02
T_E (sec)	0.31	0.27	0.10	0.25	0.23	0.08	0.23	0.21	0.08

Table 2 shows the 1st and 2nd order autoregression coefficients. On average, none of the 2nd order coefficients reached statistical significance. A 1st order autoregressive process thus appears to best describe the temporal structure of the data. As the 1st order autocorrelation coefficients ranged from 0.12 to 0.37, it follows that the explained portion of the variance is between 1.4% and 13.7%.

In order to test the adequacy of the two models, the 1st and 2nd order autoregressive processes, these were subtracted from the data and the residual series were then analyzed in a similar manner.

The results of the analysis of the residual series after subtraction of both 1st and 2nd order autoregressive structures showed that the autocorrelation coefficients were close to zero, power spectra had less power at low frequencies and with no differences between the two sets of residuals. Thus, a 2nd order autoregressive process does not explain more of the variance than does the 1st order process.

4 Discussion

As already published by Karan *et al*. (2005), the present study demonstrated that the AHR is affected by audio-visual stimulation whereas pain had no such effect. The differences were mainly in T_I and in T_E, where they reached statistical significance, rather than in V_T for which the differences did not reach statistical significance. This paper provides further information on the pattern of breathing under these conditions.

The finding that a 1st order autoregressive process provides not only a simple but also sufficient statistical model of series of ventilatory variables demonstrates that this variability contains a larger random and a smaller non-random component, the latter anywhere between 1% and 14% in the current series.

In physiological terms, this means that there is inertia or a short-term memory in the system. Therefore, if one particular value is above the mean, the next breath is more likely than not also to be above the mean.

These results are qualitatively consistent with other studies done under other experimental conditions. The autocorrelation coefficients of the current series tend, however, to be slightly smaller than those of other series obtained under different conditions (Ingemann Jensen 1987, Busso *et al*. 1996).

One explanation for the possible quantitative differences between this and other studies may be that, in these series, the pain and wakefulness inputs to the respiratory controller supposedly are from centers higher in the brain while the chemoreceptor drive has been held constant. Other studies have manipulated the inputs from the two sets of chemoreceptors with or without an exercise stimulus. Even if the latter should turn out to originate in higher brain centers it makes no qualitative, but maybe a quantitative, difference compared to the inputs studied here. Changes in the 'wakefulness drive' may change the level of breathing and even moderate chemoreceptor sensitivity, but it has no effect on the variability or on the pattern of breathing.

Since this pattern of explained variability is remarkably consistent over different conditions, it is likely that this pattern is either a characteristic of the function of the respiratory controller or of the musculo-skeletal part of the respiratory system. No available experimental results allow a distinction between these two possibilities.

5 Conclusions

The results of the analysis of these series of ventilatory variables extend the observations previously made that the variability of such series contains a larger random and a smaller non-random component, the latter being best explained by a 1st order autoregressive process. Changes in the 'wakefulness drive' to breathing have no effect on the variability of the pattern of breathing even if such changes affect the sensitivity of the chemoreceptors.

Acknowledgements FAER Research Fellowship Grant to S. Karan and the Department of Anesthesiology.

References

Karan S., Voter W., Palmer L. and Ward D.S. (2005) Effects of pain and audiovisual stimulation on the opioid-induced depression of the hypoxic ventilatory response. Anesthesiology 103, 384–90.

Ingemann Jensen, J. (1987) An Analysis of breath-to-breath variability in steady states of breathing in man. Doctoral Thesis, University of Aarhus.

Busso, T., Pei-Ji Liang and Robbins, P.A. (1996) Breath-to-breath relationships between respiratory cycle variables in humans at fixed end-tidal PCO_2 and PO_2. J. Appl. Physiol. 81(5), 2287–2296.

Cartwright, C.R., Henson, L.C. and Ward, D.S. (1998) Effects of alfentanil on the ventilatory response to sustained hypoxia. Anesthesiology 89, 612–619.

84
Cerebral Blood Flow and Ventilatory Sensitivity to CO_2 Measured with the Modified Rebreathing Method

Jaideep J. Pandit[1], Ravi M. Mohan[2], Nicole D. Paterson[3] and M.J. Poulin[4]

Abstract The ventilatory response to carbon dioxide (CO_2) measured by modified rebreathing (SrVE) is closer to that measured by the steady-state method (SsVE) than is the response measured by Read's rebreathing method. Furthermore, the value estimated by the steady-state method depends upon the number of data points used to measure it. We planned to assess if these observations were also true for cerebral blood flow (CBF), as measured by steady-state (SsCBF) and modified rebreathing (SrCBF) tests. Six subjects undertook two protocols, one in the steady-state and one with modified rebreathing. SsVE depended upon the number of data points used to calculate it, and SsVE and SrVE were similar. However, this was not the case with SsCBF, and SsCBF was much higher than SrCBF. These findings are consistent with the notions that the specific CO_2 stimulus differs for CBF control as compared with ventilation (VE) control, and that prior hypocapnia has an effect on CBF and VE for longer than the duration of the hypocapnia.

1 Introduction

We have previously examined CBF sensitivities to CO_2: CBF sensitivity measured with Read's method was lower than that measured with the steady-state method (Pandit, Mohan, Paterson and Poulin 2003). This result is the opposite of the result for ventilation: ventilatory sensitivity to CO_2 is higher when measured with Read's method than with the steady-state technique (Mohan, Amara, Cunningham and Duffin 1999; Pandit *et al*. 2003; Pandit 2003). We previously concluded that these results

[1] University of Oxford, Nuffield Department of Anaesthetics, John Radcliffe Hospital, UK, jaideep.pandit@physiol.ox.ac.uk

[2] University of Oxford, Laboratory of Physiology, Parks Road, Oxford, UK, ravi.mohan@utoronto.ca

[3] University of Oxford, Laboratory of Physiology, Parks Road, Oxford UK, npate022@uottowa.ca

[4] Department of Physiology & Biophysics, University of Calgary, Canada, poulin@ucalgary.ca

M.J. Poulin and R.J.A. Wilson (eds.), *Integration in Respiratory Control: From Genes to Systems*.

suggest that brain tissue partial pressure of CO_2 (Pt_{CO2}), in contrast to its role in control of ventilation, may not be the ultimate determinant of the cerebral vasculature. Factors such as arterial or arteriolar wall PCO_2 may have a more important role (Pandit *et al*. 2003; Severinghaus and Lassen 1967).

'Modified rebreathing' is a technique introduced by Casey, Duffin and McAvoy (1987). It incorporates a period of voluntary hyperventilation just prior to the rebreathing, which is then undertaken according to Read's method (Read 1967). The technique is designed to lower the subject's PCO_2 below the central chemoreflex CO_2 threshold so that the method can be used to measure ventilatory responses above and below the threshold. The method can also incorporate computer-controlled flow of O_2 to the rebreathing bag, so that iso-oxia, hypoxia and hyperoxia, can all be examined. Using this method (Duffin, Mohan, Vasilou, Stephenson and Mahamed 2000), the ventilatory response is found to consist of two linear components during hypoxia (the break-point representing the central chemoreflex threshold and the second slope representing the combined peripheral and central CO_2 sensitivities), and just one linear component during hyperoxia (representing the central chemoreflex sensitivity).

Mohan *et al*. (1999) found that modified rebreathing in hyperoxia yielded values for central ventilatory CO_2 sensitivity in closer agreement with steady-state values than were those obtained using Read's rebreathing method. They speculated that the differing effects of the two methods (steady-state versus modified rebreathing) on CBF might be important. They also found differences between V_E-CO_2 slopes calculated using just two of the four steady-state points as compared with using all the steady-state data points. However, they did not ascertain if this was also the case with CBF-CO_2 sensitivity.

The purpose of this study was to compare CBF-CO_2 sensitivities with steady-state and modified rebreathing methods to assess if, as is the case with V_E-CO_2 sensitivities, the two methods are in good agreement. We also wished to investigate whether calculating steady-state sensitivities using different combinations of data points influences the comparison for both ventilation and CBF. Finally, we planned to compare and discuss our results for modified rebreathing with our earlier results for Read rebreathing we had obtained contemporaneously in the same group of subjects (Pandit *et al*. 2003).

2 Methods

2.1 Subjects and Apparatus

After ethical approval, six healthy subjects (five males, one female; age 21–35 years; weight 65–85 kg; height 167–180 cm) were studied.

The apparatus was as previously described (Pandit et al. 2003). A dynamic end-tidal forcing system was used to control end-tidal gases in the steady-state protocol. A 2 MHz pulsed Doppler ultrasound system measured Doppler signals from the middle cerebral artery. The mean velocity associated with the maximum frequency

of the Doppler shift (VP) was used as the index of CBF. Subjects rebreathed via a 6 L bag filled with 6.5% CO2 in O2.

2.2 Protocols

Subjects undertook two protocols. In the steady-state protocol, PET_{CO2} was held at 1.5 mmHg above normal (isocapnia) for 10 min, then raised to three levels of hypercapnia, (8 min each; 6.5, 11.5 and 16.5 mmHg above normal, separated by 4 min isocapnia). End-tidal P_{O2} was held at 300 mmHg. In the modified rebreathing protocol, subjects underwent 6 min of voluntary hyperventilation to PET_{CO2} 20–25 mmHg, and then rebreathed via a 6 L bag filled with 6.5% CO_2 in O_2 for at least 2 min or as long as they could tolerate it.

2.3 Data Analysis

For the steady-state protocol, we calculated the four hypercapnic steps generated four data points on the V_E-PET_{CO2} plot and on the CBF-PET_{CO2} plot, and we calculated the mean for all subjects of calculating the slope by linear regression using (a) the first 2 data points, (b) the middle 2 data points and (c) all 4 data points. This yielded mean group values for Ss_{VE} and Ss_{CBF}.

For the modified rebreathing protocol, V_E and separately CBF were plotted against PET_{CO2} for each experimental period. The point used as the start of rebreathing for purposes of calculation was identified as being (a) when PET_{CO2} changed from hypocapnia to hypercapnia (which was usually near-instantaneous), but (b) no sooner than the 7th minute after the start of hyperventilation (to allow for instabilities in the transition period between hyperventilation and rebreathing). Linear regression analysis was used to obtain the slopes of the V_E- PET_{CO2} and CBF-PET_{CO2} relationship. This yielded mean group values for Sr_{CBF} and Sr_{CBF}.

2.4 Calculation of x-Axis Intercepts

The calculated regression lines for SsVE, SrVE, SsCBF and SrCBF (data taken from all four data points) and SrVE were extended to the x-axis, and plotted on a graph.

2.5 Statistical Analysis

Analysis of variance (with *post hoc* t-tests) were used to assess the significance of the difference of values between steady-state and modified rebreathing protocols.

3 Results

Fig. 1 shows the ratio of VE-CO_2 and CBF-CO_2 sensitivities for the two methods. For ventilation, all methods for steady-state calculation were similar to SrVE but, within the steady-state methods, there were significant differences between taking the first 2 data points vs. the middle w points ($p < 0.05$). For CBF, SrCBF yielded a lower sensitivity than all steady-state methods of calculating SsCBF ($p < 0.05$), but there were no differences between the methods for calculating the latter.

Fig. 2 shows the x-axis intercepts for the two methods, as well as results from our previous study for Read rebreathing (Pandit *et al*. 2003). There were no significant differences between the x-axis intercepts for ventilation between steady state and modified rebreathing, but the x-axis intercepts between the two methods for CBF were highly significant ($p < 0.005$).

4 Discussion

Our findings for ventilation are generally in agreement with previous studies (Mohan *et al*. 1999). Based on our study of the Read rebreathing technique, we had previously suggested that the specific CO_2 stimulus governing CBF may not be the same as that governing V_E. The stimulus governing the latter is thought to be $PtCO_2$; the former may be arteriolar wall PCO_2 (Severinghaus and Lassen 1967). Our finding here that CBF-CO_2 sensitivity and x-axis intercepts yielded by

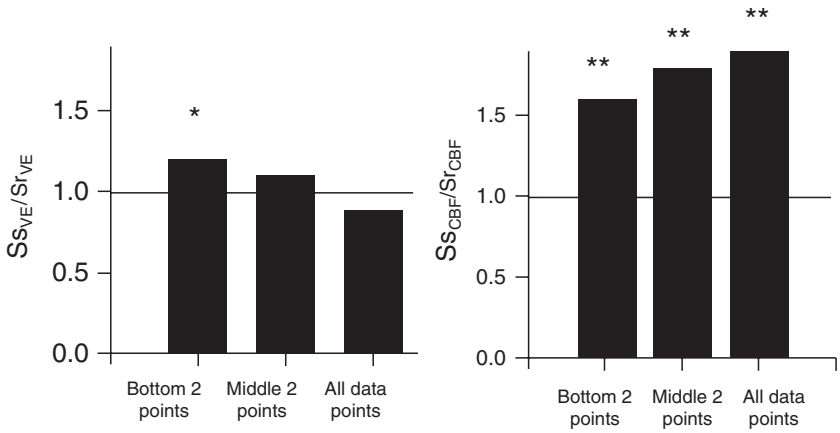

Fig. 1 Left panel: Ss_{VE}/Sr_{VE} values for each of the 3 methods of calculating Ss_{VE}. Right panel: Ss_{CBF}/Sr_{CF} values for each of the 3 methods of calculating Ss_{CBF}. The horizontal line is the line of unity. * = $p < 0.05$ vs. middle 2 points; ** = $p < 0.05$ vs. line of unity

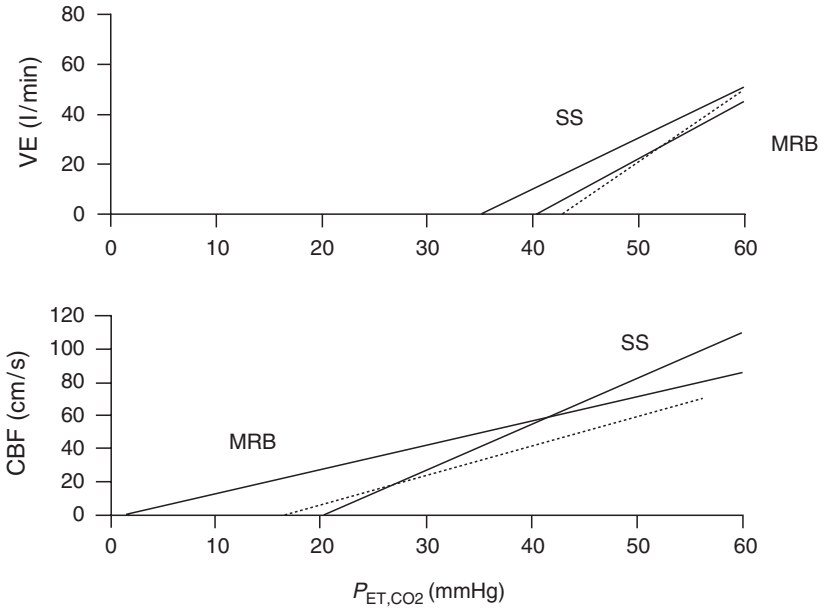

Fig. 2 Data plotted as lines and extended to the x-axis for VE (top) and CBF (bottom). Also shown (dashed lines) are results for Read rebreathing from our previous study (Pandit *et al*. 2003)

modified rebreathing are very different from that yielded by the steady-state method is consistent with this notion. Furthermore, the differences between modified rebreathing and Read rebreathing (Fig. 2) suggest that prior hypocpania with the former has ventilatory and CBF effects that last longer than the duration of the hypocapnia itself.

Acknowledgements This work was supported by grants from the Wellcome Trust, the Heart and Stroke Foundation of Ontario (Canada) and the Association of Anaesthetists of Great Britain and Ireland.

References

Casey, K., Duffin, J. and McAvoy, G.V. (1987) The effect of exercise on the central-chemoreceptor threshold in man. J. Physiol. 383, 9–18.

Duffin, J., Mohan, R.M., Vasilou, P., Stephenson, R. and Mahamed, S. (2000) A model of the chemoreflex control of breathing in humans: model parameters measurement. Respir. Physiol. 120, 13–26.

Mohan, R.M., Amara, C.E., Cunningham, D.A. and Duffin, J. (1999) Measuring central-chemoreflex sensitivity in man: rebreathing and steady-state methods compared. Respir. Physiol. 115, 23–33.

Pandit, J.J. (2003) Does Read's rebreathing technique overestimate the ventilatory response to CO_2? Anesth. Analg. 97, S–29.

Pandit, J.J., Mohan, R.M., Paterson, N.D. and Poulin, M.J. (2003) Cerebral blood flow sensitivity to CO_2 measured with steady-state and Read's rebreathing methods. Resp. Physiol. Neurobiol. 137, 1–10.

Read, D.J.C. (1967) A clinical method for assessing the ventilatory response to carbon dioxide. Aust. Ann. Med. 16, 20–23.

Severinghaus, J.W. and Lassen, N. (1967) Step hypocapnia to separate arterial from tissue PCO_2 in the regulation of cerebral blood flow. Circ. Res. 20, 272–278.

85
Naloxone Reversal of Opioid-Induced Respiratory Depression with Special Emphasis on the Partial Agonist/Antagonist Buprenorphine

Elise Sarton[1], Luc Teppema[2] and Albert Dahan[3]

Abstract Buprenorphine is relatively resistant to reversal by naloxone. We tested the effect of various doses and infusion schemes of naloxone on buprenorphine-induced respiratory depression and compared the data with naloxone-reversal of morphine and alfentanil-induced respiratory depression. Both morphine and alfentanil were easily reversed by low doses of naloxone (0.4 mg). Increasing doses of naloxone caused a bell-shaped reversal curve of buprenorphine with maximal reversal at naloxone doses between 2 and 4 mg. However, reversal was short-lived. The bell-shaped reversal curve may be related to the existence of two μ-opioid receptor subtypes, one mediating the agonist effects of opioids at low dose, the other mediating antagonistic effects at high dose.

1 Opioid-Induced Respiratory Depression: Buprenorphine

Buprenorphine (Fig. 1) is a semi-synthetic opiate derived from the morphine precursor thebaine, which has been used in clinical practice since 1979. It is a long-acting opiate and, as such, an important tool in the treatment of acute and chronic pain. Buprenorphine is 100 times more potent than morphine. It is an agonist at the μ-opioid receptor (MOR) and ORL_1-receptor and an antagonist at the κ-opioid receptor.

Just like all other opioids acting at the MOR, buprenorphine displays respiratory depression, a potentially life-threatening side effect of acute opioid treatment. The extent of opioid-induced respiratory depression is highly variable and depends on factors such as: the specific opiate/opioid give, the dose, the route of administration, concurrent medication, underlying disease, pain, arousal/sedation level and genetic factors (such as polymorphisms of the *OPRM1* gene) (Romberg, Olofsen, Bijl, Taschner, Teppema, Sarton, van Kleef and Dahan 2005). In both human and animal studies, buprenorphine, in contrast to full μ-opioid receptor agonists such as fentanyl, displays ceiling in respiratory depression with an apparent maximum in effect at IV

[1–3] Leiden University Medical Center, Department of Anesthesiology, 2300 RC Leiden, The Netherlands, e.y.sarton@lumc.nl; l.j.s.m.teppema@lumc.nl; a.dahan@lumc.nl

M.J. Poulin and R.J.A. Wilson (eds.), *Integration in Respiratory Control: From Genes to Systems*. © Springer 2008

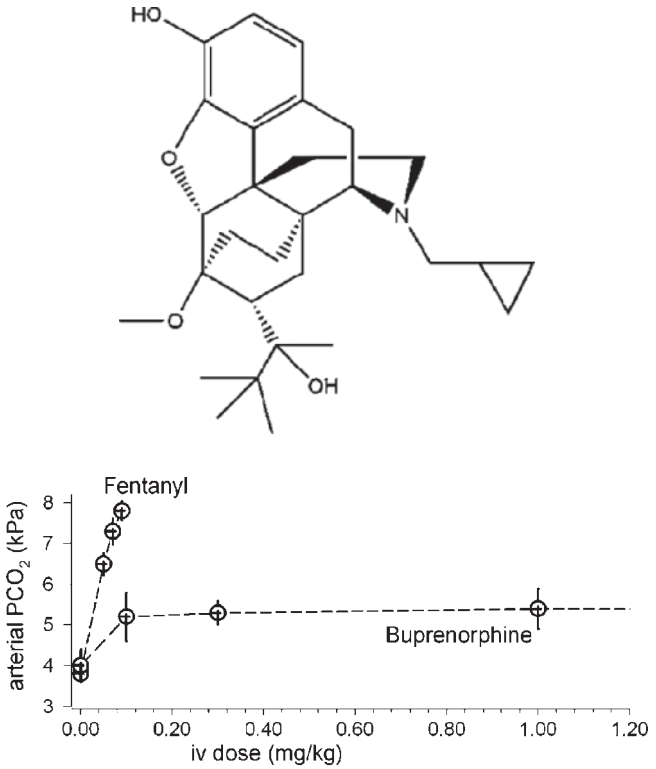

Fig. 1 Top: Chemical structure of buprenorphine. Bottom: Buprenorphine and fentanyl dose response curve in awake rats. In contrast to fentanyl, buprenorphine displays ceiling with a limited effect on arterial PCO_2. Data adapted from Dahan *et al*. (2005)

doses of 0.1 mg or greater (Fig. 1) (Dahan, Yassen, Bijl, Romberg, Sarton, Teppema, Olofsen and Danhof 2005). These observations suggest that buprenorphine has some advantage over other opioids with a limited respiratory depressant effect (Dahan, Yassen, Romberg, Sarton, Teppema, Olofsen and Danhof 2006). However, when buprenorphine is combined with sedatives/sleeping drugs, this advantage is rapidly lost and deaths related to the combination of buprenorphine and benzodiazepines are frequently described in the literature (see Dahan *et al*. 2005).

Because the occurrence of respiratory depression is unpredictable, the ability to induce rapid opioid reversal is of evident importance. There are some anecdotal data from the literature suggesting that reversal of buprenorphine is problematic and that large naloxone doses produce only limited reversal (see van Dorp, Yassen, Sarton, Romberg, Olofsen, Teppema, Danhof and Dahan 2006 and references cited therein). We tested the effect of naloxone on buprenorphine-induced respiratory depression and compared the data with naloxone reversal of morphine and alfentanil-induced respiratory depression. Both of these two opioids are full agonists at the μ-opioid receptor.

2 Protocols and Observations

All protocols were evaluated and approved by the local Human Ethics Committee. All studies were performed using the dynamic end-tidal forcing technique at a fixed end-tidal PCO_2 of 7 kPa (53 Torr) (Dahan, DeGoede, Berkenbosch and Olievier 1990).

2.1 Buprenorphine

In 24 subjects we tested, the effect the effect of increasing naloxone doses (0.5–7 mg, given over 30 min) on 0.2 mg buprenorphine induced respiratory depression. Subjects received 0.2 mg buprenorphine at t = 0 min, and 30 min later followed by one of the following doses of naloxone: 0 (placebo, n = 8), 0.5, 1, 2, 3, 4, 5, 6, 7 mg (each dose tested in two subjects). Buprenorphine was given as bolus (0.1 mg) followed by a 1 hr infusion (0.1 mg/h). Naloxone was given as bolus (half of the total dose) followed by a 30 min infusion of the remainder of the dose (*e.g.*, 2 mg naloxone: 1 mg bolus followed by 2 mg/h for ½ hr). All doses are per 70 kg.

Reversal (Φ) is expressed as follows:

$$\Phi(\rho) = [\text{Vnaloxone}(\rho) - \text{Vplacebo}(\rho)].[\text{Vbaseline} - \text{Vplacebo}(\rho)]^{-1} \quad (1)$$

where time period ρ ranges from t = 61 to t = 63 min (that is 1 min before to 1 min after the end of buprenorphine infusion); Vnaloxone(ρ) and Vplacebo(ρ) are the mean ventilations over time period ρ for the subjects receiving naloxoneand placebo, respectively; Vbaseline is pre drug baseline ventilation. Φ ranges from 0 (= reversal no better than placebo) to 1 (= full reversal reached with naloxone).

Next Φ was fitted to a sigmoid-Emax function (using the statistical program NONMEM) incorporating two opposing components: an increasing and a decreasing one:

$$\Phi = X_1^{\gamma} / (1 + X_1^{\gamma}) \,.\, [1 / (1 + X_2^{\gamma})] \quad (2)$$

where X_1 = dose/D_1, X_2 = dose/D_2, and γ is a shape parameter. D_1 is the naloxone dose causing 50% reversal, D_2 is the naloxone dose causing the return to 50% reversal after complete reversal was achieved.

Buprenorphine followed by placebo caused appreciable and long-lasting respiratory depression (baseline ventilation was reduced by 40% at t = 71 min). Low dose naloxone produced a dose dependent reversal of respiratory depression with Φ reaching 1 ± 0.2 at high naloxone doses of 2 mg or greater. However, increasing naloxone doses > 4 mg caused a significant decrease in level of reversal. D_1 (Φ = 50% or 0.5 in Fig. 2) was 0.95 ± 0.09 mg (medium value ± SE); Φ = 1 ± 0.2 at naloxone doses between 2 and 4 mg; D_2 (Φ = 50%) was 5.20 ± 0.94 mg (see also Fig. 2).

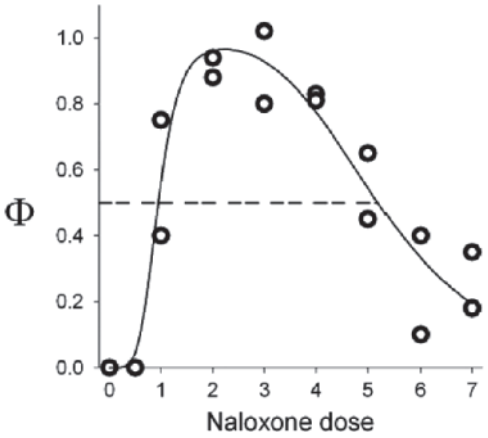

Fig. 2 Bell-shaped reversal of buprenorphine-induced respiratory depression with naloxone. The naloxone dose is in mg (per 70 kg). Φ is reversal ranging from 0 (reversal effect no greater than placebo) to 1 (complete reversal with naloxone achieved). Eight subjects received placebo (by definition Φ = 0), two subjects received each of the naloxone doses

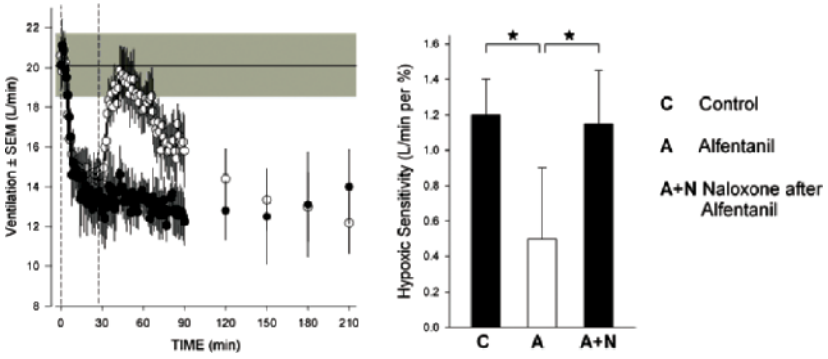

Fig. 3 Left: Morphine (0.15 mg/kg IV given at t = 0 min) followed by naloxone (open symbols, 0.4 mg IV given at t = 28 min) against morphine followed by placebo (closed symbols, given at t = 28 min). Right: Effect of 0.3 mg naloxone IV on alfentanil-induced depression the acute hypoxic ventilatory response. Star: $p < 0.01$ (one-way ANOVA)

2.2 Morphine and Alfentanil

Sixteen subjects received 0.15 mg/kg morphine IV at time $t = 0$. Eight subjects received 400 µg naloxone at time $t = 28$ min; eight other received placebo at time $t = 28$ min. Measurements continued for 4 hours (see Fig. 3). Morphine-induced respiratory changes were easily reversed with relatively low doses of naloxone (0.4 mg). This is a factor of about 10 smaller than the dose needed for full reversal after buprenorphine. Reversal of morphine effect was short lived with a rapid return (within the hour) to full respiratory depression.

Eight subjects received alfentanil by target-controlled infusion (TCI 30 ng/mL) after which hypoxic ventilatory responses were obtained (SpO_2 80% for 3 min). Next, 0.3 mg naloxone was given and hypoxic responses were repeated. See Fig. 3 for results (right panel).

3 Discussion

We observed that while reversal of morphine- and alfentanil-induced respiratory was relatively easy (although short lived), reversal of buprenorphine required high dose naloxone (> 2 mg). Furthermore, a peculiar observation is the recurrence of respiratory depression at higher doses of naloxone (> 4 mg). This results in a bell-shaped or inverse U-shaped naloxone dose-response curve (see Fig. 2).

The high dose naloxone needed to overcome buprenorphine respiratory depression is related to high affinity of buprenorphine for the μ-opioid receptor (K_D-values in the nanomolar range) (Yassen, Olofsen, Dahan and Danhof 2005; Yassen, Olofsen, Romberg, Sarton, Danhof and Dahan 2006). As a consequence, high doses of naloxone are required to compete successfully for the μ-opioid receptor. The short time of action of naloxone is related to the pharmacokinetics of naloxone itself and hence applies to all opioids. Its short elimination t½ (10 to 45 min) causes the rapid elimination from both the brain compartment and the body. As a consequence, long-term reversal is only possible with a continuous infusion of naloxone.

The inverse U-shaped curve of Fig. 2 was unexpected. However, buprenorphine has a long history of showing bell-shaped dose response curves for antinociception (all data from animals) (see Dahan *et al*. 2005; 2006; van Dorp *et al*. 2006). Our observation is best explained by a scenario of noncompetitive autoinhibition. In this hypothetical scenario there are two subsets of μ-opioid receptors, one mediating the agonistic effects of opioids at relatively low dose, the other mediating the antagonistic effects of opioids at relatively high dose. This same mechanism may explain opioid-induced hyperalgesia (increased pain sensitivity after high dose opioid treatment).

Finally, we cannot exclude that high dose naloxone affected other non-opioid receptor systems through which it may have affected, at least partly, our data. Further studies will need to focus on naloxone's behavior at high dose as well as possible gender differences and genetic implications (see Dahan, Sarton, Teppema and Olievier 1998; Sarton, Olofsen, Romberg, den Hartigh, Kest, Nieuwenhuijs, Burm, Teppema and Dahan 2000; Romberg *et al*. 2005).

References

Dahan, A., DeGoede, J., Berkenbosch, A. and Olievier, I.C.W. (1990) The influence of oxygen on the ventilatory response to carbon dioxide in man. J. Physiol. (Lond.) 428, 485–499.

Dahan, A., Sarton, E., Teppema, L. and Olievier, C. (1998) Sex-related differences in the influence of morphine on ventilatory control in humans. Anesthesiology 88, 903–913.

Dahan, A., Yassen, A., Bijl, H., Romberg, R., Sarton, E., Teppema, L., Olofsen, E. and Danhof, M. (2005) Comparison of the respiratory effects of intravenous buprenorphine and fentanyl in humans and rats. Br. J. Anaesth. 94, 825–834.

Dahan, A., Yassen, A., Romberg, R., Sarton, E., Teppema, L., Olofsen, E. and Danhof, M. (2006) Buprenorphine induces ceiling in respiratory depression but not in analgesia. Br. J. Anaesth. 96, 627–632.

van Dorp, E., Yassen, A., Sarton, E., Romberg, R., Olofsen, E., Teppema, L., Danhof, M. and Dahan, A. (2006) Naloxone reversal of buprenorphine-induced respiratory depression. Anesthesiology 105, 51–57.

Romberg, R.R., Olofsen, E., Bijl, H., Taschner, P.E.M., Teppema, L.J., Sarton, E.Y., van Kleef, J.W. and Dahan, A. (2005) Polymorphism of the μ-opioid receptor gene (*OPRM1:c.118A>G*) does not protect against opioid-induced respiratory depression despite reduced analgesic response. Anesthesiology 102, 522–530.

Sarton, E., Olofsen, E., Romberg, R., den Hartigh, J., Kest, B., Nieuwenhuijs, D., Burm, A., Teppema, L. and Dahan, A. (2000) Sex differences in morphine analgesia. Anesthesiology 93, 1245–254.

Yassen, A., Olofsen, E., Dahan, A. and Danhof, M. (2005) Pharmacokinetic-pharmacodynamic modeling of the antinociceptive effect of buprenorphine and fentanyl in rats: role of receptor equilibration kinetics. J. Pharmacol. Exp. Ther. 313, 1136–1149.

Yassen A., Olofsen, E., Romberg, R., Sarton, E., Danhof, M. and Dahan, A. (2006) Mechanism-based pharmacokinetic-pharmacodynamic modeling of the antinociceptive effect of buprenorphine in healthy volunteers. Anesthesiology 104, 1232–1242.

86
The Pulse Oxygen Saturation: Inspired Oxygen Pressure (SpO_2:P_IO_2) Diagram: Application in the Ambulatory Assessment of Pulmonary Vascular Disease

Neil M. Skjodt[1], Christian Ritz[2] and Dilini Vethanayagam[3]

Abstract *Background*: The inspired oxygen to pulse saturation (SpO_2:P_IO_2) curve mirrors the oxyhaemoglobin dissociation curve but is shifted to the right by the difference between inspired and alveolar oxygen fractions. Inspection of the curve has been used to discern changes in shunt. *Aims*: We aimed to demonstrate the SpO_2:P_IO_2 curve's quantification using readily available software, and its clinical utility in assessing ambulatory patients. *Methods*: Six normal and seven hereditary haemorrhagic telangiectasia (HHT) clinic patients have been studied. After measuring barometric pressure, seated subjects were monitored with finger probe pulse oximetry while breathing increasing fractions of humidified oxygen through a Venturi mask until either their SpO_2 or P_IO_2 was 100%. Resulting SpO_2 and P_IO_2 values were plotted, fitted, assessed for goodness-of-fit and compared using the free, open source nonlinear regression extension package *drc* for the R programming language whose accuracy was also tested against two NIST reference sigmoidal curve datasets. *Results*: All reference, individual and collected normal results were well fitted by the *drc* software with highly insignificant goodness-of-fit F tests. The laboratory normal curve was identically fitted by symmetrical Hill and asymmetrical Weibull functions. Although normal and negative HHT screening patient curves did not differ, there were significant differences between normal, pre-treatment (shunt fraction 9.44%), and post-treatment HHT curves. *Conclusion*: Nonlinear regression analysis of the SpO_2:P_IO_2 curve permits valid, simple, safe, noninvasive, sensitive and cheap estimation of shunt in ambulatory patients.

1 Introduction

The pulse oximetry saturation: inspired oxygen fraction (SpO_2:P_IO_2) curve runs in parallel but to the right of the sigmoidal oxygen-haemoglobin dissociation curve by exactly the difference between the inspired and alveolar oxygen fractions. In 1993,

[1]University of Alberta, Department of Medicine (Pulmonary), neil.skjodt@ualberta.ca

[2]Royal Veterinary and Agricultural University, Department of Natural Sciences, ritz@kvl.dk

[3]University of Alberta, Department of Medicine (Pulmonary), Dilini.Vethanayagam@ualberta.ca

M.J. Poulin and R.J.A. Wilson (eds.), *Integration in Respiratory Control: From Genes to Systems*.

Roe and Jones derived the SpO_2:P_IO_2 curve, and algebraically demonstrated shunt and ventilation (or more accurately resistance to alveolar oxygen diffusion) effects on the curve. Multiple applications of this method were then reported in pre-operative, various intra-operative, post-operative, inpatient, and normal control subjects (Andreassen, Egeberg, Schroter and Andersen 1996; de Gray, Rush and Jones 1997; Roe, Gadelrab, Sapsford and Jones 1997; Andreassen, Rees, Kjaergaard, Thorgaard, Winter, Morgan, Alstrup and Toft 1999; Jones and Jones 2000; Kjaergaard, Rees, Nielsen, Freundlich, Thorgaard and Andreassen 2001; Smith and Jones 2001; Rees, Kjaergaard, Perthorgaard, Malczynski, Toft and Andreassen 2002; Kjaergaard, Rees, Malczynski, Nielsen, Thorgaard, Toft and Andreassen 2003; Kjaergaard, Rees, Gronlund, Nielsen, Lambert, Thorgaard, Toft and Andreassen 2004; Rasmussen, Sollid, Rees, Kjaergaard, Murley and Toft 2006; Quine, Wong, Boyle, Jones and Stenson 2006). Despite this history, quantification of SpO_2:P_IO_2 curve has not been standardized with readily available software or been widely reported in ambulatory medical patients. The aims of our studies were therefore to: (a) validate fitting truncated sigmoidal curves using open source nonlinear regression software (Ritz and Streibig 2005), (b) construct a laboratory SpO_2:P_IO_2 normal curve, and (c) assess the clinical utility of shunt estimation using the SpO_2:P_IO_2 curve in ambulatory patients.

2 Methods

2.1 Experimental Procedure

The protocol was reviewed by a member of the IRB. Six normal, non-smoking adults (two males) served as controls. Seven patients referred for HHT screening undergoing shunt determination using the 100% oxygen breathing technique were tested. HHT screening patients had a room air blood gas performed. For each subject, the barometric pressure (P_B) was recorded. Seated subjects wore a simple mask through which humidified oxygen and air were delivered using a Venturi valve to obtain F_IO_2 values of 0.21, 0.24, 0.26, 0.28, 0.31, 0.35, 0.40, 0.50, and 1.0 until the SpO_2 via an Ohmeda Bioxx 3700 oximeter was stable for at least 3 minutes. When SpO_2 reached 100%, untested higher F_IO_2 values were assumed to have SpO_2 values of 100%. HHT patients were then left on 100% oxygen for 20 min before a second arterial blood gas was sampled to permit a shunt calculation.

2.2 Statistical Analyses

Two sigmoidal National Institute of Standards and Technology (NIST) Reference Statistical Datasets, mgh09 and thurber, were fitted using a Weibull model. P_IO_2

versus corresponding SpO_2 values were analyzed using the *drc* library (version 1.0–1) within the R statistical language (version 2.3.1, R Development Core Team 2006).

3 Results

3.1 Validation of Truncated Sigmoidal Curve Fitting Using NIST Nonlinear Regression Standard Datasets

There were no significant differences between drc and NIST reference equation results by: (a) visual curve comparisons and (b) the parameter estimates 95% confidence intervals as calculated from their standard deviations.

3.2 Construction of a Laboratory Normal Curve

The Hill (H) and Weibull (W) models fit the observed upper portions of collective normal data set well as judged from the highly insignificant lack-of-fit tests based on F-statistics ($F_H = 0.51$, $F_W = 0.51$, df = (9, 42), $p_H = 0.93$, $p_W = 0.93$).

3.3 Clinical Application

Illustrative SpO_2:P_IO_2 curves from: a clinic patient having no evidence of HHT, the grouped laboratory controls, a patient before incomplete endovascular coil ablation of her pulmonary arteriovenous malformations (100% oxygen breathing shunt fraction 9.44%) and the same patient after incomplete ablation are shown in Fig. 1. Using the Hill equation, the models had highly insignificant goodness-of-fit F test results ($p > 0.05$). Pairwise comparisons of the four curves' horizontal displacements, representative of shunt fraction, were all significantly different ($|t|_{min}$ = 2.63872, each df = 1, and $p_{max} = 0.0097$ for all four comparisons).

4 Discussion

The employed nonlinear regression software provided indiscernibly similar solutions to published reference datasets. Control data were fit equally well by the Weibull function and by the Hill logistic function traditionally employed to analyze related oxyhaemoglobin dissociation curves (Severinghaus 1979). Nonlinear

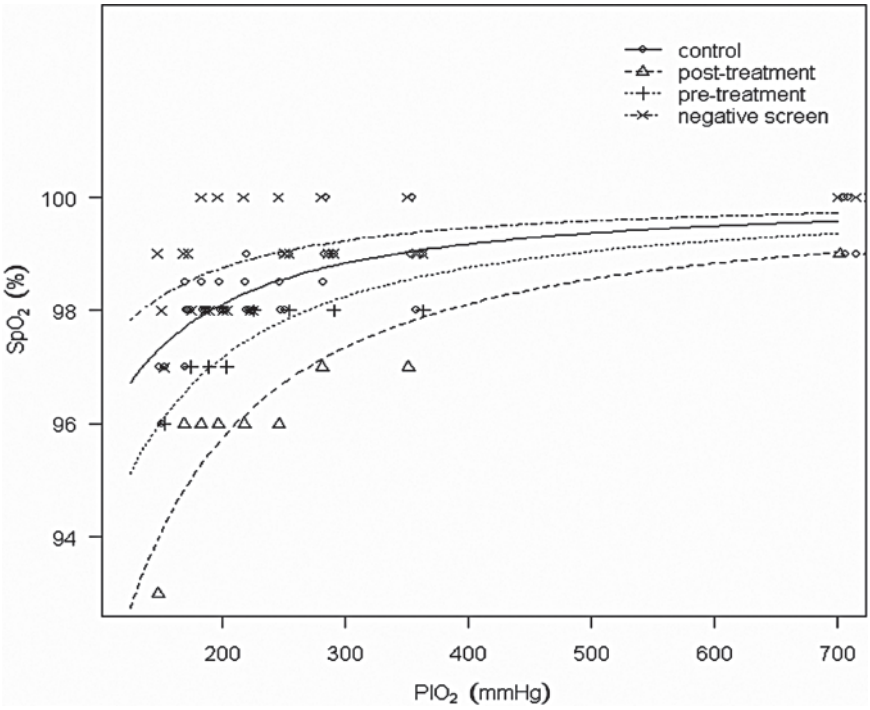

Fig. 1 Non-linear regression fitted curves for pulse saturation (SpO_2): inspired oxygen pressure (P_IO_2) data from progressively hyperoxic breathing in six normals, a subject with negative screening for HHT, and a subject with HHT before then after incomplete endovascular coil ablation of pulmonary arteriovenous malformations

regression results appropriately described of the SpO_2:P_IO_2 curve trajectories and distinguished between normal to moderately increased shunt fractions.

There are several potential limitations to our methods. First, hyperoxic breathing may worsen hypercarbia. Second, we used only one oximeter. Third, traditional expressions of shunt or ventilation are not reported. Fourth, factors other than shunt and resistance to alveolar oxygen diffusion effecting either the inspired-alveolar oxygen gradient or oxyhaemoglobin dissociation could skew interpretation of the SpO_2:P_IO_2 diagram. Such confounding factors are, however, usually absent in ambulatory subjects. Fifth, the SpO_2:P_IO_2 diagram does not anatomically localize shunt.

5 Conclusions

Assessing shunt using nonlinear regression of ambulatory SpO_2:P_IO_2 data is quick, relatively portable, easy, completely noninvasive, and, from preliminary results, quite sensitive to changes in moderate shunt.

References

Andreassen, S., Egeberg, J., Schroter, M.P. and Andersen P.T. (1996) Estimation of pulmonary diffusion resistance and shunt in an oxygen status model. Comput. Methods Programs Biomed. 51, 95–105.

Andreassen, S., Rees, S.E., Kjaergaard, S., Thorgaard, P., Winter, S.M., Morgan, C.J., Alstrup, P. and Toft, E. (1999) Hypoxemia after coronary bypass surgery modeled by resistance to oxygen diffusion. Crit. Care Med. 27, 2445–2453.

de Gray, L., Rush, E.M. and Jones, J.G. (1997) A noninvasive method for evaluating the effect of thoracotomy on shunt and ventilation perfusion inequality. Anaesthesia. 52, 630–635.

Jones, J.G. and Jones, S.E. (2000) Discriminating between the effect of shunt and reduced VA/Q on arterial oxygen saturation is particularly useful in clinical practice. J. Clin. Monit. Comput. 16, 337–350.

Kjaergaard, S., Rees, S.E., Nielsen, J.A., Freundlich, M., Thorgaard, P. and Andreassen, S. (2001) Modelling of hypoxaemia after gynaecological laparotomy. Acta Anaesthesiol. Scand. 45, 349–356.

Kjaergaard, S., Rees, S., Malczynski, J., Nielsen, J.A., Thorgaard, P., Toft, E. and Andreassen, S. (2003) Non-invasive estimation of shunt and ventilation-perfusion mismatch. Intensive Care Med. 29, 727–734.

Kjaergaard, S., Rees, S.E., Gronlund, J., Nielsen, E.M., Lambert, P., Thorgaard, P., Toft, E. and Andreassen S. (2004) Hypoxaemia after cardiac surgery: clinical application of a model of pulmonary gas exchange. Eur. J. Anaesthesiol. 21, 296–301.

Quine, D., Wong, C.M., Boyle, E.M., Jones, J.G. and Stenson B.J. (2006) Non-invasive measurement of reduced ventilation-perfusion ratio and shunt in infants with bronchopulmonary dysplasia; a physiological definition of the disease. Arch. Dis. Child. Fetal Neonatal Ed. 2006 Jun 27, [Epub ahead of print].

R Development Core Team. (2006) R: A Language and Environment for Statistical Computing. R Foundation for Statistical Computing. Vienna.

Rasmussen, B.S., Sollid, J., Rees, S.E., Kjaergaard, S., Murley, D. and Toft, E. (2006) Oxygenation within the first 120 hr following coronary artery bypass grafting. Influence of systemic hypothermia (32 degrees C) or normothermia (36 degrees C) during the cardiopulmonary bypass: a randomized clinical trial. Acta Anaesthesiol. Scand. 50, 64–71.

Ritz, C. and Streibig, C.J. (2005) Bioassay analysis using R.J. Stat. Software 12, 1–22.

Roe, P.G., Gadelrab, R., Sapsford, D. and Jones, J.G. (1997) Intra-operative gas exchange and post-operative hypoxaemia. Eur. J. Anaesthesiol. 14, 203–210.

Roe, P.G. and Jones, J.G. (1993) Analysis of factors which affect the relationship between inspired oxygen partial pressure and arterial oxygen saturation. Br. J. Anaesth. 71, 488–94.

Severinghaus, J.W. (1979) Simple, accurate equations for human blood O_2 dissociation computations. J. Appl. Physiol. 46, 599–602.

Smith, H.L. and Jones, J.G. (2001) Non-invasive assessment of shunt and ventilation/perfusion ratio in neonates with pulmonary failure. Arch. Dis. Child. Fetal Neonatal Ed. 85, F127–F132.

87
Hypocapnia and Airway Resistance in Normal Humans

Craig D. Steinback[1], William A. Whitelaw[2] and Marc J. Poulin[3]

Keywords hypocapnia, hyperventilation, airway resistance, asthma.

1 Introduction

Airway constriction causes an increase in airflow resistance and a breathing limitation. This constriction may be mediated by airway sensitivities to airborne allergens (Widdicombe 1983), cooling (Julia-Serda, Molfino, Califaretti, Hoffstein and Zamel 1996; Fontanari, Burnet, Zattara-Hartmann and Jammes 1996) or drying (Fontanari *et al*. 1996). Additionally, variations in carbon dioxide tension (PCO_2) have been implicated as a factor affecting airway tone, with both hypercapnia (Sterling 1969; Tashkin and Simmons 1972) and hypocapnia (Newhouse, Becklake, Macklem and McGregor 1964; Sterling 1968) causing an increase in airway resistance. However, in most experiments both of these conditions are accompanied by hyperventilation, which may itself result in airway drying and or cooling. To date, conclusive evidence of the specific role of CO_2 tension on airway tone has yet to be produced.

To look at the specific role of hypocapnia on the regulation of airway resistance in normal healthy subjects, we examined the separate effects of hyperventilation and hypocapnia on airway resistance while controlling air temperature and humidity.

2 Methods

Eight young, healthy volunteers (27 ± 5 yr; 2 females) participated. All subjects provided written informed consent. The study was approved by the Conjoint Health Research Ethics Board at the University of Calgary.

[1] University of Calgary, Department of Physiology and Biophysics, cdsteinb@uwo.ca

[2] University of Calgary, Department of Medicine, wwhitela@ucalgary.ca

[3] University of Calgary, Department of Physiology and Biophysics, poulin@ucalgary.ca

M.J. Poulin and R.J.A. Wilson (eds.), *Integration in Respiratory Control: From Genes to Systems*.

Subjects arrived at the lab having abstained from caffeine, alcohol and strenuous exercise for 12 hr prior to testing. They took part in three protocols in a random order, separated by 20 min rest periods.

Prior to each protocol, resting partial pressures of end-tidal O_2 ($P_{ET}O_2$) and CO_2 ($P_{ET}CO_2$) were measured for ~ 10 min. Respired gas was sampled at the mouth continuously (20 ml·min^{-1}) via a fine catheter and analyzed for PO_2 and PCO_2 by mass spectrometer (AMIS 2000, Innovision, Odense, Denmark). Values for PO_2 and PCO_2 were sampled by computer every 10 ms, and $P_{ET}O_2$ and $P_{ET}CO_2$ were identified and recorded for each breath using a computer and dedicated software (Chamber v2.10, University Laboratory of Physiology, Oxford, UK).

Respiratory volumes were measured using a turbine device (VMM-400, Interface Associates, Laguna Niguel, CA, USA); flow direction and timing were determined using a pneumotachograph and differential pressure transducer (RSS100-HR, Hans Rudolph, Kansas City, MO, USA).

Pleural pressure was determined using an esophageal balloon technique (Milic-Emili, Mead, Turner and Glauser 1964). A topical anesthetic (3 cc 2% Lidocaine, Pharmascience Inc., Montreal, Quebec, Canada) was applied intra-nasally to coat the mucous membranes. Following this, the esophageal balloon was passed nasally to the lower third of the esophagus and filled with ~ 0.5 mL of air such that the signal exhibited a negative deflection on inspiration and cardiac artifacts were minimized. The proximal end of the probe was fixed to one end of a differential pressure transducer (range ± 2 cmH_2O; MP45-1-871, Validyne Engineering, Northridge, California, USA), with the other end connected to the mouthpiece apparatus. Transpulmonary pressure (TPP) was determined as the difference between pleural and mouth pressure.

Accurate control of end-tidal gases was achieved using the technique of dynamic end-tidal forcing (Robbins, Swanson and Howson 1982; Robbins, Swanson, Micco and Schubert 1982) and dedicated software (BreatheM v2.35, University Laboratory of Physiology, Oxford, UK). Delivered gases were heated and humidified with respiratory humidifiers (HC150, Fisher and Paykel Healthcare, Auckland, New Zealand). Temperature of inspired and expired gases was measured using a digital thermometer with an analogue output (871A, Omega Engineering Inc., Laval, Quebec, Canada).

Each protocol began with a 10 min baseline period with the subject breathing normally through a mouthpiece with the nose occluded using a noseclip. Subjects were then asked to voluntarily hyperventilate by matching a tidal volume (V_T) of 2.5 L displayed on an oscilloscope and at a frequency (fB) of 20 bpm, resulting in a minute ventilation ($\dot{V}E$) of 50 L·min^{-1}. Hyperventilation was maintained for 20 min while $P_{ET}CO_2$ was controlled in one of three ways: (1) held constant at +1 Torr above resting values (ISO), (2) allowed to fall −8 Torr from resting values (M8) or (3) allowed to fall −15 Torr from resting values (M15). Following hyperventilation, $P_{ET}CO_2$ was returned to resting levels for an additional 10 min of recovery. $P_{ET}O_2$ was maintained at euoxic levels throughout testing (~ 88 Torr).

Continuous lung volume (V) and TPP signals were used to calculate airway resistance (R_{AW}) on a breath-by-breath basis using the methods described by Mead and Whittenberger (1953):

$$C = \Delta V / \Delta TPP \quad (1)$$

$$P_R = TPP - V / C \quad (2)$$

$$R_{AW} = \Delta P_R / \Delta F \quad (3)$$

Where C is compliance of the lung parenchyma, P_R is resistance pressure and F is flow. Breath-by-breath data were visually assessed, and deviant breaths were removed. To reduce inter-subject variability, C and R_{AW} values were calculated as a percentage of baseline. Breath-by-breath data were then averaged in 2 min bins.

All statistical analyses were performed using SPSS (v13.0, SPSS Inc.). Significance was set at $p < 0.05$. Data are expressed as mean ± SD, unless noted.

3 Results

Data during the M8 protocol were obtained in only seven subjects. Average end-tidals, breathing frequency, tidal volume, minute ventilation, lung compliance and airway resistance across all three protocols are illustrated in Fig. 1 with data and statistical comparisons for key time points shown in Table 1.

The confounding effects of temperature were avoided by maintaining the inspired gases at 30.7 ± 0.5° C during all three protocols. The same ventilatory rates were achieved between protocols (50.1 ± 7.6, 50.9 ± 6.2 and 50.2 ± 8.6 L/min during ISO,

Table 1 Ventilatory parameters during is ocapnic and hypocapnic hyperventilation

		Baseline	Hyperventilation	Recovery
V_E ($L \cdot min^{-1}$)	ISO	17.5±6.5	50.1±7.6[#]	22.6±7.9
	M8	16.5±7.3	50.9±6.2[#]	18.4±6.0
	M15	16.8±6.5	50.2±8.6[#]	22.7±8.8
P_ICO_2 (Torr)	ISO	18.0±9.8	28.3±7.1[*]	20.4±9.1
	M8	10.7±9.0	18.0±5.3[†]	15.1±9.6
	M15	11.2±9.5	10.7±4.7[‡]	20.9±14.9
P_ETCO_2 (Torr)	ISO	37.9±3.5	37.9±1.7	38.3±4.2
	M8	35.7±3.4	29.2±2.5[#,‡]	34.1±2.8
	M15	35.8±3.1	23.2±2.8[#,‡,§]	33.7±6.0
R_{AW} (%)	ISO	100.3±3.6	102.7±38.2	104.6±12.7
	M8	99.3±3.8	103.3±47.3	96.4±13.9
	M15	100.2±4.1	99.0±47.3	101.0±13.9

* $p < 0.05$, # $p < 0.001$ vs. Baseline. † $p < 0.005$, ‡ $p < 0.001$ vs. ISO. § $p < 0.001$ vs. M8.

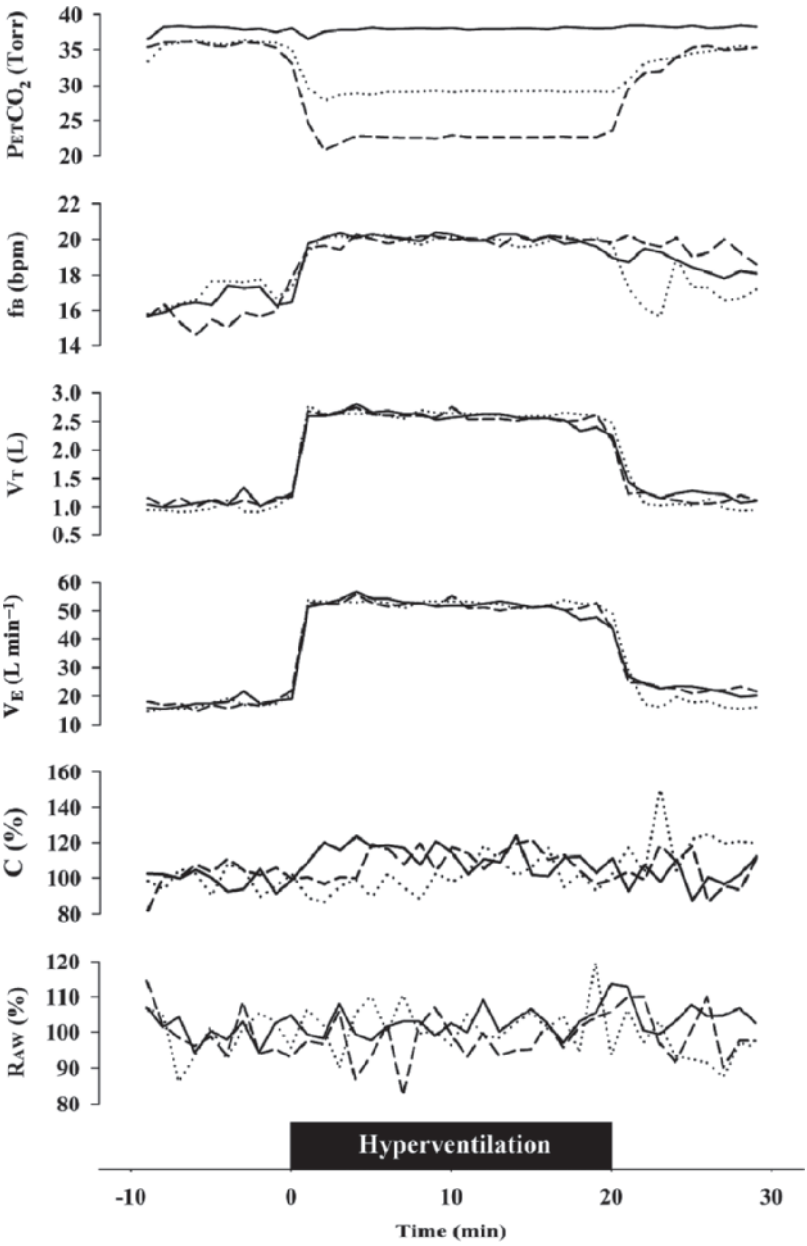

Fig. 1 Time courses of respiratory variables. ISO, solid; M8 dotted; M15 dashed

M8 and M15, respectively; Fig. 1 and Table 1), and maintained throughout the hyperventilatory phase. $P_{ET}CO_2$ was maintained at 37.9 ± 3.5, 29.2 ± 2.5 and 23.2 ± 2.8 Torr during the ISO, M8 and M15 protocols, respectively. This was achieved by altering the P_ICO_2 between conditions and protocols (Table 1). By controlling tidal volume, we also controlled for changes in lung compliance (Fig. 1).

Resistance data showed that isocapnic hyperventilation itself did not alter airway resistance. Further, there was no effect of altered $P_{ET}CO_2$ on airway resistance (Fig. 1 and Table 1). However, within this subject population a large inter-subject variability existed, as evident by the large standard deviation in responses (Table 1).

4 Discussion

In the present study we were able to assess the specific effects of hypocapnia on airway resistance by controlling confounding factors, such as air temperature and humidity, which are also known to affect airway tone (Fontanari *et al*. 1996). The use of dynamic end-tidal gas forcing provided a highly accurate means of controlling the amount of hypocapnia induced by hyperventilation and prevented hyperoxia from occurring during hyperventilation. Hyperoxia causes reflex airway constriction leading to increased airway resistance in normal subjects (Dewar, Smith, Spence and Ledingham 1972).

With these control measures in place, the present data indicate that hypocapnia does not systematically influence airway resistance in normal individuals, counter to previous investigations (Newhouse *et al*. 1964; Sterling 1968). Further, we are able to conclude that there is an absence of response to direct airway stimulation via variations in inhaled CO_2. This is evident when comparing data during ISO and M15. During ISO, arterial PCO2 is maintained while inspired CO2 is raised, whereas, during M15, arterial PCO2 falls while inspired CO2 is kept the same.

While we were unable to show changes in airway resistance in response to variations in inhaled or arterial PCO_2, a large inter-subject variability was seen. These data may indicate a stratification of the airway response to CO_2. In this way, individuals with heightened sensitivities may classify at one end of a spectrum, falling within an asthmatic population. This is in accord with previously reported heterogeneity of airway tone within asthmatic populations (Julia-Serda, Molfino, Chapman, McClean, Zamel, Slutsky and Hoffstein 1992). However, further research, strictly controlling for other confounding factors, is necessary before definitive conclusions can be made about inter-population differences.

We conclude that in healthy individuals alterations in PCO_2 do not systematically affect airway resistance. However, we are unable to account for possible stratifications in responses due to differences in airway sensitivities.

References

Dewar, K.M., Smith, G., Spence, A.A. and Ledingham, I.M. (1972) Effect of hyperoxia on airways resistance in man. J. Appl. Physiol. 32, 486–490.

Fontanari, P., Burnet, H., Zattara-Hartmann, M.C. and Jammes, Y. (1996) Changes in airway resistance induced by nasal inhalation of cold dry, dry, or moist air in normal individuals. J. Appl. Physiol. 81, 1739–1743.

Julia-Serda, G., Molfino, N.A., Califaretti, N., Hoffstein, V. and Zamel, N. (1996) Tracheobronchial constriction in asthmatics induced by isocapnic hyperventilation with dry cold air. Chest 110, 404–410.

Julia-Serda, G., Molfino, N.A., Chapman, K.R. *et al*. (1992) Heterogeneous airway tone in asthmatic subjects. J. Appl. Physiol. 73, 2328–2332.

Mead, J. and Whittenberger, J.L. (1953) Physical properties of human lungs measured during spontaneous respiration. J. Appl. Physiol. 5, 779–796.

Milic-Emili, J., Mead, J., Turner, J.M. and Glauser, E.M. (1964) Improved technique for estimating pleural pressure from esophageal balloons. J. Appl. Physiol. 19, 207–211.

Newhouse, M.T., Becklake, M.R., Macklem, P.T. and McGregor, M. (1964) Effect of alterations in end-tidal CO_2 tension on flow resistance. J. Appl. Physiol. 19, 745–749.

Robbins, P.A., Swanson, G.D. and Howson, M.G. (1982) A prediction-correction scheme for forcing alveolar gases along certain time courses. J. Appl. Physiol. 52, 1353–1357.

Robbins, P.A., Swanson, G.D., Micco, A.J. and Schubert, W.P. (1982) A fast gas-mixing system for breath-to-breath respiratory control studies. J. Appl. Physiol. 52, 1358–1362.

Sterling, G.M. (1968) The mechanism of bronchoconstriction due to hypocapnia in man. Clin. Sci. 34, 277–285.

Sterling, G.M. (1969) The mechanism of decreased specific airway conductance in man during hypercapnia caused by inhalation of 7 percent CO_2 . Clin. Sci. 37, 539–548.

Tashkin, D.P. and Simmons, D.H. (1972) Effect of carbon dioxide breathing on specific airway conductance in normal and asthmatic subjects. Am. Rev. Respir. Dis. 106, 729–739.

Widdicombe, J.G. (1983) Mediators and reflex bronchoconstriction. Eur. J. Respir. Dis. Suppl. 129, 65–94.

88
Disturbances of Breathing in Rett Syndrome: Results from Patients and Animal Models

Georg M. Stettner[1], Peter Huppke[1,3], Jutta Gärtner[1,3], Diethelm W. Richter[2,3] and Mathias Dutschmann[2,3]

1 Introduction

Rett syndrome (RTT) is a neurodevelopmental disorder caused by mutations in the X-linked gene *MECP2* (Amir *et al*. 1999). *MECP2* encodes the methyl-CpG binding protein 2 (MeCP2), which acts as a transcriptional repressor. The target genes regulated by MeCP2 are still subject to intensive research (Bienvenu and Chelly 2006). Besides mental retardation, most patients suffer from potentially life-threatening breathing arrhythmia during wakefulness (Kerr *et al*. 1997). Predominantly alternating periods of hyperventilation and apnoeas occur (Julu *et al*. 2001; Weese-Mayer *et al*. 2006). The availability of *Mecp2*$^{-/y}$ knockout (KO) mice (Guy *et al*. 2001), an animal model for RTT, now allows more detailed studies of the respiratory dysfunction. Plethysmographic investigations revealed a RTT like respiratory disorder in KO mice *in vivo* (Viemari *et al*. 2005). We recently linked the respiratory disorder of KO *in situ* preparations to an impaired control of postinspiratory activity (Stettner *et al*. 2007). In this book chapter we compare the respiratory phenotype of KO *in situ* preparations with our preliminary results from polygraphic investigations in RTT patients with severe respiratory phenotype.

2 Methods

The respiratory motor activity in KO mice (strain B6.129P2(C)-Mecp2^{tm1}–1Bird; Guy *et al*. 2001) was studied in comparison to wild type (WT) controls using the perfused working heart-brainstem preparation. We performed simultaneous

[1]Department of Pediatrics and Pediatric Neurology, Georg August University, Robert-Koch-Str. 40, 37075 Göttingen, Germany

[2]Department of Neuro and Sensory Physiology, Georg August University, Humboldtallee 23, 37073 Göttingen, Germany, mdutsch@gwdg.de

[3]DFG Research Center Molecular Physiology of the Brain (CMPB), Humboldtallee 23, 37073 Göttingen, Germany

M.J. Poulin and R.J.A. Wilson (eds.), *Integration in Respiratory Control: From Genes to Systems*.

recordings of phrenic and vagal nerve activities in all preparations (28 KO and 28 WT mice, postnatal age 40 ± 2 days) to analyse the three-phase motor pattern of breathing.

To analyse the breathing in RTT patients, we performed polygraphic recordings using a mobile sleep laboratory recorder (*SOMNOscreen PSG,* SOMNOmedics, Kist, Germany) that allowed us to monitor breathing activities in the home environment. Nasal-oral air flow, thoracic and abdominal movements, snore/phonation sounds, oxygen saturation, heart rate and ECG were recorded in three genetically-confirmed RTT patients with a severe breathing phenotype and analysed over a period of at least two hours during daytime wakefulness.

3 Results

3.1 Working Heart-Brainstem Preparation

The respiratory motor pattern of *Mecp2*$^{-/y}$ KO preparations was characterised by a disturbed postinspiratory activity (Fig. 1). In comparison to WT controls, the duration of the postinspiratory interval (T_{pi}) was prolonged ($p < 0.001$). Furthermore, the Tpi showed a significantly increased variance ($p < 0.001$), which correlated with arrhythmic respiratory activity and repetitive apnoeas. Consequently the enhanced postinspiratory activity led to a significantly shortened inspiratory ($p < 0.05$) and late expiratory phase ($p < 0.001$). The frequency of unprovoked

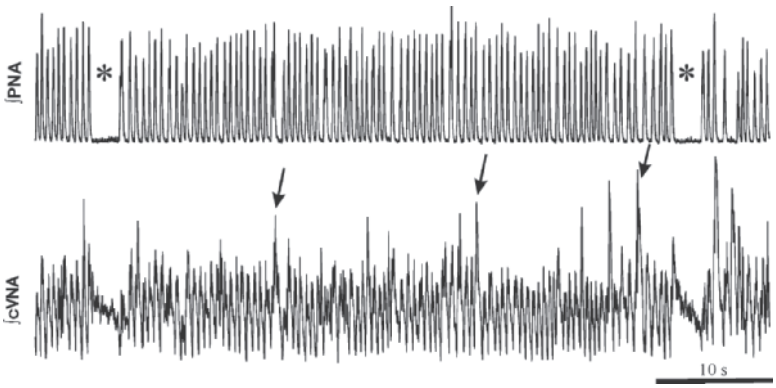

Fig. 1 Simultaneous recording of integrated phrenic (∫PNA) and central vagal nerve activities (∫cVNA) of a representative *Mecp2*$^{-/y}$ KO preparation. The figure illustrates the variability of vagal postinspiratory discharge as the characteristic feature of respiratory abnormalities in KO mice. Arrhythmic prolongation of the respiratory interval (T_{tot}) correlated with enhanced postinspiratory vagal discharge in terms of duration and amplitude (arrows). Repetitive spontaneous apnoeas (*) were accompanied by tonic vagal postinspiratory discharge

transient apnoeas in KO preparations was increased by 288% ($p < 0.001$) when compared to WT preparations. All apnoeas were accompanied by tonic postinspiratory vagal discharge.

3.2 Polygraphic Respiratory Recording

The breathing disorder in the investigated RTT patients was characterised by alternating episodes of apnoeas and hyperventilation (Fig. 2). Frequency and mean duration of apnoeas were variable between the patients: 10.5 apnoeas/h (apnoea duration 36 s, patient 1), 18.4 apnoeas/h (apnoea duration 59 s, patient 2), 60.0 apnoeas/h (apnoea duration 24 s, patient 3). The maximal apnoea duration was 89 s. All breathing pauses started from an end-inspiratory breathing position and evoked bradycardia that was followed sometimes by tachycardia (Fig. 2). Prolonged and repetitive apnoeas caused a drop in oxygen saturation (minimal SpO_2 76%).

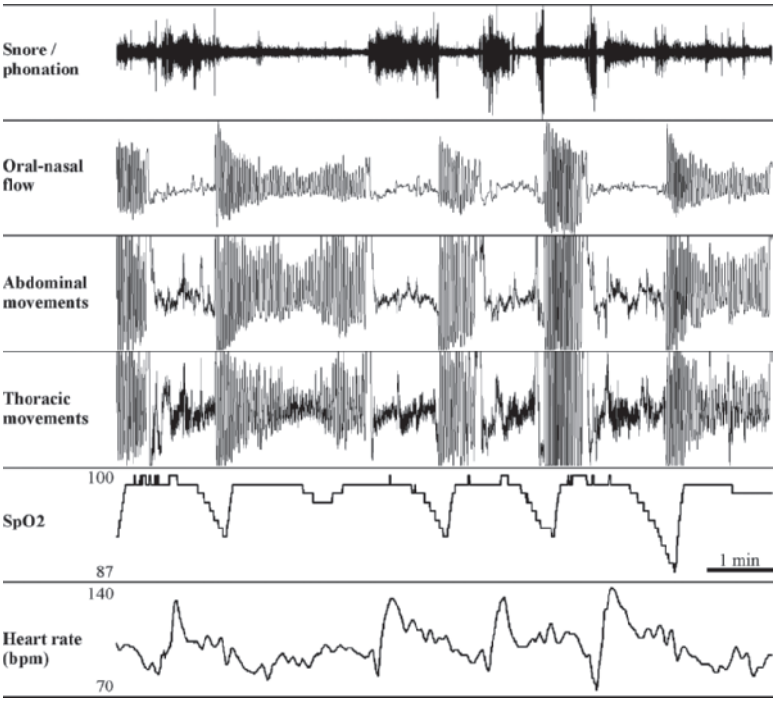

Fig. 2 Polygraphic recording of cardiorespiratory parameters during daytime wakefulness of a 23 year old RTT patient. Apnoeas alternate with periods of hyperventilation. Apnoea onset was accompanied by bradycardia. In this patient the initial bradycardia was followed by tachycardia most likely due to a reduced venous reflux because of high intrathoracic pressure (pressure phonation indicating Valsalva's manoeuvre)

Recording of phonation revealed a pressure phonation during most apnoeas probably due to laryngeal constrictor muscles activation. Timing of apnoeas within the respiratory cycle, initial bradycardic response and concomitant pressure phonation point to a postinspiratory nature of apnoeas in RTT.

4 Discussion

The pathomechanisms of RTT associated breathing disorders are still poorly understood. Plethysmographic investigations of the respiratory dysfunction of *Mecp2*$^{-/y}$ KO mice demonstrated that KO mice suffer from a RTT like breathing disorder (Viemari *et al*. 2005). Our analysis of the *in situ* respiratory motor pattern revealed an impaired control of the postinspiratory (PI) activity. The duration and amplitude of the PI vagal discharge in KO mice spontaneously fluctuated and caused unpredictable variations in the length of the expiratory interval leading to breathing arrhythmia and repetitive apnoeas. The overall picture of the respiratory dysfunction suggests an over-excitability of PI neurones within the ponto-medullary respiratory network. PI motor outputs specifically target laryngeal adductors in order to control upper airway patency during the breathing cycle (Dutschmann and Paton 2002a; Dutschmann and Herbert 2006), reflex adaptations (Shiba *et al*. 1999) or phonation (Farley *et al*. 1992). The impaired control of PI activity in KO mice could explain the upper airway symptoms in RTT, such as apnoeas with laryngeal closure, loss of speech and weak coordination of breathing and swallowing. Results from our polygraphic investigations of RTT patients also suggest a PI dysfunction. Apnoeas follow inspiration maintaining an end-inspiratory breathing position potentially due to PI laryngeal closure. The initial bradycardic responses to apnoeas described in our study and others (Julu *et al*. 2001; Weese-Mayer *et al*. 2006) might be another sign for PI- mediated activation of cardiac vagal motoneurones (Richter and Spyer 1990). It is also similar to the responses evoked by the diving reflex, which among other cardiorespiratory effects also lead to a PI-mediated apnoea and laryngeal closure in humans and rodents (Andersson *et al*. 2004; Dutschmann and Paton 2002b). The occasionally observed tachycardic response following bradycardia might be compensatory to reduced venous return due to increased intrathoracic pressure (Ferrigno *et al*. 1986). The spontaneous and unprovoked occurrence of respiratory arrhythmia and repetitive apnoeas resembles a severe autonomic dysfunction in RTT (Julu *et al*. 2001; Weese-Mayer *et al*. 2006). Clinical symptoms in RTT and results from the present study of *Mecp2*$^{-/y}$ KO mice imply a disturbance of the PI control within brainstem cardiorespiratory network circuitries. To find effective pharmacological therapies that specifically dampen the over-excitation of PI neurons will be a challenge for future investigations.

Acknowledgements The study was supported by the Rett Syndrome Research Foundation (RSRF) and the DFG Research Centre for Molecular Physiology of the Brain (CMPB).

References

Amir, R.E., Van den Veyver, I.B., Wan, M., Tran, C.Q., Francke, U. and Zoghbi, H.Y. (1999) Rett syndrome is caused by mutations in X-linked *MECP2*, encoding methyl-CpG-binding protein 2. Nat. Genet. 23, 185–188.

Andersson, J.P., Liner, M.H., Fredsted, A. and Schagatay, E.K. (2004) Cardiovascular and respiratory responses to apneas with and without face immersion in exercising humans. J. Appl. Physiol. 96, 1005–1010.

Bienvenu, T. and Chelly, J. (2006) Molecular genetics of Rett syndrome: when DNA methylation goes unrecognized. Nat. Rev. Genet. 7, 415–426.

Dutschmann, M. and Herbert, H. (2006) The Kölliker-Fuse nucleus gates the postinspiratory phase of the respiratory cycle to control inspiratory off-switch and upper airway resistance in rat. Eur. J. Neurosci. 24, 1071–1084.

Dutschmann, M. and Paton, J.F. (2002a) Inhibitory synaptic mechanisms regulating upper airway patency. Respir. Physiol. Neurobiol. 131, 57–63.

Dutschmann, M. and Paton, J.F. (2002b) Influence of nasotrigeminal afferents on medullary respiratory neurones and upper airway patency in the rat. Pflugers Arch. 444, 227–235.

Farley, G.R., Barlow, S.M. and Netsell, R. (1992) Factors influencing neural activity in parabrachial regions during cat vocalizations. Exp. Brain Res. 89, 341–351.

Ferrigno, M., Hickey, D.D., Liner, M.H. and Lundgren, C.E. (1986) Cardiac performance in humans during breath holding. J. Appl. Physiol. 60, 1871–1877.

Guy, J., Hendrich, B., Holmes, M., Martin, J.E. and Bird, A. (2001) A mouse *Mecp2*-null mutation causes neurological symptoms that mimic Rett syndrome. Nat. Genet. 27, 322–326.

Julu, P.O., Kerr, A.M., Apartopoulos, F., Al-Rawas, S., Engerström, I.W., Engerström, L., Jamal, G.A. and Hansen, S. (2001) Characterisation of breathing and associated central autonomic dysfunction in the Rett disorder. Arch. Dis. Child. 85, 29–37.

Kerr, A.M., Armstrong, D.D., Prescott, R.J., Doyle, D. and Kearney, D.L. (1997) Rett syndrome: analysis of deaths in the British survey. Eur. Child. Adolesc. Psychiatry 6 Suppl. 1, 71–74.

Richter, D.W. and Spyer, K.M. (1990) Cardiorespiratory control. In: A.D. Lowey and K.M. Spyer (Eds.), *Central Regulation of Autonomic Functions*. Oxford University Press, New York, pp. 189–207.

Shiba, K., Satoh, I., Kobayashi, N. and Hayashi, F. (1999) Multifunctional laryngeal motoneurons: an intracellular study in the cat. J. Neurosci. 19, 2717–2727.

Stettner, G.M., Huppke, P., Brendel, C., Richter, D.W., Gartner, J., and Dutschmann, M. (2007) Breathing dysfunctions associated with impaired control of postinspiratory activity in Mecp2-/y knockout mice. J Physiol. 579, 863–876.

Viemari, J.C., Roux, J.C., Tryba, A.K., Saywell, V., Burnet, H., Pena, F., Zanella, S., Bevengut, M., Barthelemy-Requin, M., Herzing, L.B., Moncla, A., Mancini, J., Ramirez, J.M., Villard, L. and Hilaire, G. (2005) *Mecp2* deficiency disrupts norepinephrine and respiratory systems in mice. J. Neurosci. 25, 11521–11530.

Weese-Mayer, D.E., Lieske, S.P., Boothby, C.M., Kenny, A.S., Bennett, H.L., Silvestri, J.M. and Ramirez, J.M. (2006) Autonomic nervous system dysregulation: breathing and heart rate perturbation during wakefulness in young girls with Rett syndrome. Pediatr. Res. 60, 443–449.

89
NHE3 in the Human Brainstem: Implication for the Pathogenesis of the Sudden Infant Death Syndrome (SIDS)?

Martin Wiemann[1], Stilla Frede[1], Frank Tschentscher[2], Heidrun Kiwull-Schöne[3], Peter Kiwull[3], Dieter Bingmann[1], Bernd Brinkmann[4] and Thomas Bajanowski[2]

Abstract Previous studies have demonstrated an inverse correlation between the degree of respiratory drive and NHE3 mRNA expression in the brainstem of awake rabbits. Here we show that the levels of NHE3 mRNA extractable from kryo-conserved tissue are highly variable also in the human brainstem. As an insufficient drive to breath may be a final event causing sudden infant death, we compared the expression of NHE3 mRNA in a collective of children who died from non-natural causes to an equal number of SIDS victims. Evaluation of signals from NHE3 RT-PCR showed higher values for the SIDS collective than for the control group. We suggest that the level of NHE3 expression in brainstem tissue may contribute to the vulnerability of infants for SIDS.

1 Introduction

Sudden infant death syndrome (SIDS) is currently believed to be triggered from a disturbed breathing control finally culminating in an insufficient drive to breathe. A widely-accepted hypothesis is the triple risk model (Rognum and Saugstad 1993) in which outside stressors act on a vulnerable infant being in a critical period of development. Neurobiological studies have focussed on finding significant alterations of cardiorespiratory areas within the brainstem to identify vulnerable structures and/or to describe abnormal development. Besides less specific alterations such as astrogliosis, or reduced muscarinc receptor densities, changes of the serotonin receptor binding (subtypes $5HT_{1A\text{-}D}$ and $5HT_2$) were found within brain regions involved in the control of cardiorespiratory functions

[1]University of Duisburg-Essen, Department of Physiology, martin.wiemann@uni-due.de

[2]University of Duisburg-Essen, Department of Forensic Medicine, thomas.bajanowski@uk-essen.de

[3]Ruhr-University Bochum, Department of Physiology, peter.kiwull@rub.de

[4]University of Münster, Department of Forensic Medicine, brinkma@uni-muenster.de

M.J. Poulin and R.J.A. Wilson (eds.), *Integration in Respiratory Control: From Genes to Systems*.

and arousal (Kinney *et al*. 2005; Sawaguchi *et al*. 2003). Serotonergic neurons are in part chemosensitive (Richerson 2004) and seem to be involved in the coordination of sighs and gasps (Tryba *et al*. 2006), the latter of which may be regarded as a last line of defence when eupnoic breathing had stopped. Prospective studies have found a positive correlation between frequency and/or duration of obstructive or mixed apnoea periods during sleep and the incidence of SIDS (Kahn *et al*. 1992; Sawaguchi *et al*. 2003) or an impaired response to CO_2 (Shannon *et al*. 1977). Together these results suggest that near-SIDS infants are prone to a disturbed respiratory drive.

Another system, which has been recognized to be involved in the control of breathing, is the sodium proton exchanger subtype 3 (NHE3). NHE3 acts as a regulator of the pHi of ventrolateral neurons in brainstem cultures, and NHE3 inhibition not only acidified and excited chemosensitive neurons but furthermore shifted the CO_2/H^+ response curve of rabbits to lower (setpoint) values (Wiemann *et al*. 1999; Kiwull-Schöne *et al*. 2001). With respect to the current investigation, it is most notable that alveolar ventilation in rabbits during wakefulness is inversely correlated with the amount of NHE3 mRNA expressed in the obex region of the brainstem (Wiemann *et al*. 2005). Thus, animals with low NHE3 mRNA expression exhibited a high alveolar ventilation along with a lowered $PaCO_2$ and vice versa. NHE3 expression within the brainstem, therefore, appears to be involved in determining the set point of normal breathing.

Based on these findings, we explored the variability of NHE3 expression also in the human brainstem. Moreover, we collected first data to test the hypothesis whether infants who died from SIDS expressed increased NHE3 levels as one might anticipate from the animal data.

2 Methods

Post mortem brainstem tissue was collected from a reference group of patients who underwent autopsy due to forensic examinations (for details see Fig. 1). Tissue from infants under the age of 1 year was collected from 1998–2001 during a national study (Bajanowski *et al*. 2005). All relatives or parents gave their informed consent; the study was approved by a local ethics committee. For analysis, 7 male infants who died from non-natural causes (5.1 ± 4.3 months) were compared to 7 male SIDS victims (4.42 ± 3.4 months). Brainstem tissue was kept frozen at −80° C until NHE3 mRNA was isolated and quantified by real time RT-PCR as described (Wiemann *et al*. 2005). PCR primers were adapted to the human gene sequence. Seize of the specific amplicon was 150 bp. Semi-quantitative analysis of NHE3 expression was carried out by measuring fluorescence intensity of ethidium bromide-stained PCR bands corrected for background fluorescence. The human renal carcinoma cell line RCC4 expressing NHE3 was used as a positive control.

3 Results

3.1 Brainstem NHE3 Expression in Young and Aged Individuals

Brainstem tissue of the medulla oblongata was sectioned into 4–6 transverse slices (termed (+2) to (−4) relative to the obex level) and analysed separately for NHE3 expression (Fig. 1A, 1B). NHE3-mRNA was found in all slices (Fig. 1B). The amounts of NHE3 mRNA in slices (+2) to (−4) from each brainstem are plotted vs. age in Fig. 1. While the maximum NHE3 expression was found in tissue of a 41 year-old patient (0.7–1.3 fg cDNA/µg RNA), the majority of patients (10/13) showed far lower values (from 0.1–0.2) with a range in longitudinal direction ((+2)–(−4)) being < 0.13 fg cDNA/µg RNA.

Three patients showed larger deviations. In these brainstems maximum values were found close to the obex within the (+1)- or (−1)-region. Male (n = 7) and female values (n = 6) were not significantly different (p = 0.44); there was no correlation of NHE3 expression with age in this collective (p > 0.15 in all regions). Values close to the obex level ((+1) and (−1) region) ranged from 0.04 – 1.3 fg cDNA/µg RNA.

3.2 NHE3 Expression in SIDS and Non-SIDS Infants

Brainstem tissue from male SIDS and male non-SIDS infants was taken from caudal regions ((−2) to (−3)) of the brainstem, as these parts of the brain had been

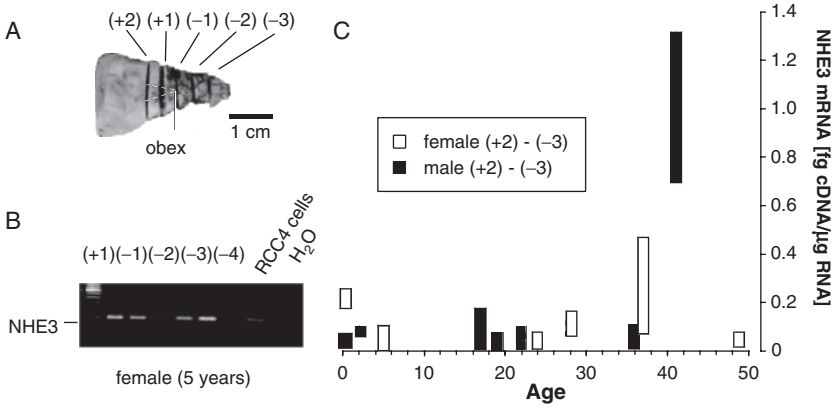

Fig. 1 Quantification of brainstem NHE3 mRNA by real time PCR. (A) Slices of the brainstem were named relative to the obex level. (B) NHE3 amplicons from the brainstem of a young female; signal from NHE3 expressing human RCC4 kidney cells served as positive control. (C) NHE3 mRNA plotted versus age in years. Each bar represents the values of all slices from one patient

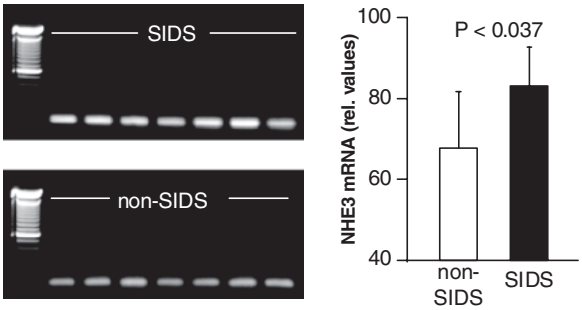

Fig. 2 Comparison of RT-PCR signals from 7 male SIDS and 7 male non-SIDS infants. Relative fluorescence intensity was quantified after background subtraction

collected in a previous investigation (Bajanowski *et al*. 2005). As is shown in Fig. 2, SIDS victims gave rise to more intense NHE3 mRNA PCR products, and quantification of the fluorescence signal revealed a significant difference.

4 Discussion

Data show that NHE3 mRNA is present in the brainstem of young and aged human individuals and that inter-individual expression levels vary by more than one order of magnitude. These differences in NHE3 mRNA expression were unlikely related to post-mortem intervals (< 48 h). The data from 13 patients did not substantiate a postnatal decrease of NHE3 mRNA, as has been found during the first weeks of life in rats (Ma and Haddad 1997). The fact that NHE3 expression varies in the longitudinal direction of the brainstem may point to a concentration of the exchanger within certain areas or nuclei. Its very low expression in brainstems of some patients suggests that NHE3 is not a common housekeeping exchanger. Rather, its expression may be influenced by individual factors (genetic, developmental and/or physiological), which may be involved in pathophysiology of SIDS and need to be further explored. With respect to the overall expression in brainstem, it may be deduced from Fig. 1 that if an individual exhibits an elevated expression (as seen in the 41 year-old patient), this encounters all regions down to the most caudal regions analysed. Based on this finding, we compared samples of the caudal medulla from SIDS and non-SIDS infants. First comparison of PCR products on a semi-quantitative level revealed a significantly higher level of NHE3 mRNA in male SIDS infants. Although the meaning of brainstem NHE3 expression for central chemosensitivity and respiratory drive is not yet known for humans, it is tempting to speculate that this exchanger, like in the rabbit, determines the set point of breathing (Wiemann *et al*. 2005). As has been shown by others, this set point together with the gain of the (central) respiratory controller is of ample importance for the stability of respiration during sleep (Khoo 2000; Dempsey *et al*. 2004).

Since NHE3 is a highly regulated antiporter (Orlowski and Grinstein 2004), we cannot exclude that elevated brainstem NHE3 expression is secondary to pathophysiological events, such as repeated hypoxia or hypercapnia which may have occurred in near-SIDS infants. However, chronic intermittent hypoxia *down-regulates* NHE3 in the mouse brain (Douglas *et al*. 2003), and hypercapnia has no influence on NHE3 expression in the rabbit brainstem (Kiwull-Schöne *et al*. 2003) suggesting that elevated NHE3 expression in SIDS victims is not a consequence of insufficient ventilation.

Thus, data suggest that enhanced brainstem NHE3 expression might be a causative factor for altered breathing control possibly involved in SIDS pathogenesis.

Acknowledgements Authors would like to thank Prof. Dr. A. Honig from the University of Greifswald, Germany, for his contribution to this work.

References

Bajanowski, T., Vennemann, M., Bohnert, M., Rauch, E., Brinkmann, B., Mitchell, E.A. and the GeSID Group (2005) Unnatural causes of sudden unexpected deaths initially thought to be sudden infant death syndrome. Int. J. Legal Med. 119, 213–216.

Dempsey, J.A., Smith, C.A., Przybylowski, T., Chenuel, B., Xie, A., Nakayama, H. and Skatrud, J.B. (2004) The ventilatory responsiveness to CO_2 below eupnoea as a determinant of ventilatory stability in sleep. J. Physiol. (Lond.) 560, 1–11.

Douglas, R.M., Xue, J., Chen, J.Y., Haddad, C.G. Alper, S.L. and Haddad, G.G. (2003) Chronic intermittent hypoxia decreases the expression of Na/H exchangers and HCO_3^- dependent transporters in mouse CNS. J. Appl. Physiol. 95, 292–299.

Kahn, A., Groswasser, J., Rebuffat, E., Sottiaux, M., Blum, D., Foerster, M., Franco, P., Bochner, A., Alexander, M. and Bachy, A. (1992) Sleep and cardiorespiratory characteristics of infant victims of sudden death: a prospective case-control study. Sleep 15, 287–292.

Khoo, M.C.K. (2000) Determinants of ventilatory instability and variability. Respir. Physiol. 122, 167–182.

Tryba, A.K., Pena, F. and Ramirez, J.N. (2006) Gasping activity *in vitro*: a rhythm dependent on 5-HT2A receptors. J. Neurosci. 26, 2623–2634

Kinney, H.C. (2005) Abnormalities of the brainstem serotonergic system in the sudden infant death syndrome: a review. Pediatr. Devel. Pathol. 8, 507–524.

Kiwull-Schöne, H., Wiemann, M., Frede, S., Bingmann, D., Wirth, K.J., Heinelt, U., Lang, H.-J. and Kiwull, P. (2001) A novel inhibitor of the Na^+/H^+ exchanger type 3 activates the central respiratory CO_2 response and lowers the apneic threshold. Am. J. Respir. Crit. Care Med. 164, 1303–1311.

Kiwull-Schöne, H., Wiemann, M., Frede, S., Bingmann, D. and Kiwull, P. (2003) Tentative role of the Na^+/H^+ exchanger type 3 in central chemosensitivity of respiration. Adv. Exp. Med. Biol. 536, 415–421.

Ma, E. and Haddad, G.G. (1997) Expression and localization of Na^+/H^+ exchangers in rat central nervous system. Neuroscience 79, 591–603.

Orlowski, J. and Grinstein, S. (2004) Diversity of the mammalian sodium/proton exchanger SLC9 gene family. Pflugers Arch. Eur. J. Physiol. 447, 549–565.

Richerson, G.B. (2004) Serotonergic neurons as carbon dioxide sensors that maintain pH homeostasis. Nat. Rev. Neurosci. 5, 449–461.

Rognum, T.O. and Saugstad, O.D. (1993) The fatal triangle in SIDS. Acta Paediatr. (Suppl.) 389, 852–854.

Sawaguchi, T., Patricia, F., Kadhim, H., Groswasser, J., Sottiaux, M., Nishida, H. and Kahn, A. (2003) The correlation between serotonergic neurons in the brainstem and sleep apnea in SIDS victims. Early Hum. Dev. 75 (Suppl.), S31–S40.

Shannon, D.C., Kelly, D.H. and O'Connell, K. (1977) Abnormal regulation of ventilation in infants at risk for sudden infant-death syndrome. N. Engl. J. Med. 297, 747–50.

Wiemann, M., Schwark, J.R., Bonnet, U., Jansen, H.W., Grinstein, S., Baker, R.E., Lang, H.J, Wirth, K. and Bingmann, D. (1999) Selective inhibition of the Na^+/H^+ exchanger type 3 activates CO_2/H^+-sensitive medullary neurones. Pflugers Arch. Eur. J. Physiol. 438, 255–262.

Wiemann, M., Frede, S., Bingmann, D., Kiwull, P. and Kiwull-Schöne, H. (2005) Sodium/Proton exchanger 3 in the medulla oblongata and set point of breathing control. Am. J. Respir. Crit. Care Med. 172, 244–249.

90
The Ventilatory Response to Exercise Does Not Differ Between Obese Women With and Without Dyspnea on Exertion

Helen E. Wood[1], Trisha L. Semon[2], Laurie A. Comeau[3], Belinda Schwartz[4], Rebecca M. MacDougall[5], Marilyn N. Klocko[6] and Tony G. Babb[7]

1 Introduction

Currently, over 30% of American adults are classified as obese (Body Mass Index, BMI ≥ 30) (Ogden, Carroll, Curtin, McDowell, Tabak and Flegal 2006). Obesity is a major public health concern since it is strongly associated with diabetes, heart disease, hypertension, stroke, sleep-disordered breathing, metabolic syndrome and some forms of cancer.

Although exercise is an important element in the prevention and treatment of obesity, many obese adults who are otherwise healthy cannot exercise due to dyspnea on exertion (DOE). Exertional dyspnea could be related to increased ventilation ($\dot{V}$) during exercise, associated with increased perception of work or effort to breathe or, alternatively, to decreased &Vdot;E during exercise, resulting in hypercapnia and sensations of 'air hunger.'

We have previously reported that the oxygen (O_2) cost of breathing is markedly increased in otherwise healthy obese women with DOE, compared with obese women without DOE. If $\dot{V}E$ during exercise is also increased, this could have an important impact on the overall O_2 demand and exercise capacity of obese women with DOE. In obese women, both O_2 uptake ($\dot{V}O_2$) and $\dot{V}E$ are increased, while $\dot{V}E/\dot{V}O_2$ is unchanged, compared with normal weight subjects, at levels of cycle exercise below the anaerobic threshold (Babb, Korzick, Meador, Hodgson and Buskirk 1991; Hulens, Vansant, Lysens, Claessens and Muls 2001; Salvadori, Fanari, Cavestri, Mazza, Baudo and Longhini 1991). To our knowledge, the ventilatory response to exercise has not been tested in obese women with and without DOE. The purpose of this study, therefore, was to determine whether the ventilatory response to exercise differed between obese women with and without DOE. We hypothesized that DOE could result from either an exaggerated response to exercise associated with greater sensations of respiratory effort or a blunted response associated with hypercapnia.

[1–7]Institute for Exercise and Environmental Medicine, Presbyterian Hospital of Dallas, and UT Southwestern Medical Center, HelenWood@TexasHealth.org

M.J. Poulin and R.J.A. Wilson (eds.), *Integration in Respiratory Control: From Genes to Systems*.

2 Experimental Design and Methods

Subjects were otherwise healthy obese ($30 \leq BMI \leq 45$) female volunteers. They were assigned to one of two study groups based on their rating of perceived breathlessness (RPB, Borg scale 0–10) (Borg 1982) during constant load cycling at 60W. Women with an RPB ≤ 2 were assigned to the Control group (n = 6) and those with RPB ≥ 4 were assigned to the DOE group (n = 7). Subjects scoring an RPB of 3 were disqualified from the study in order to differentiate between the groups. All subjects gave their written informed consent and the study was approved by our Institutional Review Board.

Pulmonary function testing and hydrostatic weighing were performed on each subject. The ventilatory response to exercise was determined during 6 min of constant load cycling at 60W. The response was defined as the slope of the relationship between $\dot{V}_E$ and carbon dioxide production ($\dot{V}_{CO_2}$) from rest to exercise. The O_2 cost of breathing was obtained from measurements of $\dot{V}_{O_2}$ and $\dot{V}_E$ at rest and during eucapnic voluntary hyperpnea at 40 and 60 L/min and defined as the slope of this relationship calculated in ml/L. The O_2 uptake of the respiratory muscles ($\dot{V}_{O_2}$RESP) at 60W was calculated from the O_2 cost multiplied by the $\dot{V}_E$ at this level. Values are given as mean ± SD. Variables were compared between groups by independent t-test and the relationship between variables was determined (for all subjects, n = 13) by regression analysis. Significance was assumed when $p < 0.05$.

3 Results

Age, height, weight, percent body fat and pulmonary function were similar between the two groups (Table 1). As previously reported (Babb, Semon, Comeau, Schwartz and Chwan 2005), the RPB during constant load cycling at 60W and the O_2 cost of

Table 1 Anthropometric Characteristics and Pulmonary Function

	Control (n = 6)	DOE (n = 7)	p value
Age (yr)	28 ± 7	34 ± 7	NS
Height (cm)	163 ± 6	160 ± 10	NS
Weight (kg)	89 ± 14	100 ± 11	NS
Body fat (%)	40 ± 3	44 ± 5	NS
FVC (% pred)	109 ± 13	95 ± 11	NS
FEV_1 (% pred)	102 ± 9	92 ± 10	NS
TLC (% pred)	97 ± 9	89 ± 11	NS
FRC (% TLC)	38 ± 4	38 ± 10	NS
RV (% pred)	65 ± 14	65 ± 12	NS
DL_{CO} (% pred)	76 ± 10	72 ± 6	NS

FVC, forced vital capacity; FEV_1, forced expiratory volume in one second; TLC, total lung capacity; RV, residual volume; DL_{CO}, diffusing capacity of the lung for carbon monoxide; % pred, percent of predicted value based on height, sex and age (mean ± SD)

Table 2 Ventilatory Response to Exercise and Oxygen Cost of Breathing

	Control (n = 6)	DOE (n = 7)	p value
RPB - 60W (BRS)	0.9 ± 0.6	5.1 ± 1.5	< 0.0001
O_2 cost (ml/L)	1.7 ± 0.4	3.0 ± 1.1	0.019
W^YE - 60W (L/min)	35.6 ± 9.1	37.8 ± 3.0	NS
VRE - 60W	30.3 ± 6.5	29.2 ± 3.8	NS
W^Yo2 RESP - 60W (ml/min)	60 ± 11	115 ± 44	0.016
V^Yo2 RESP - 60W (% of total V^YO2)	5.8 ± 1.0	9.9 ± 3.7	0.024

BRS, Borg Rating Scale 0–10; O_2 cost, oxygen cost of breathing; V^YE, ventilation; VRE, ventilatory response to exercise; V^Yo2 RESP, oxygen uptake of the respiratory muscles; V^Yo2, total oxygen uptake (mean ± SD)

breathing during eucapnic voluntary hyperpnea were significantly higher in the DOE than the Control group (Table 2). Ventilation during exercise and the ventilatory response to exercise at 60W were similar between the groups (Table 2). There were similar changes in breathing frequency, tidal volume and end-tidal PCO_2 from rest to exercise in both groups (data not shown).

$\dot{V}O_2$RESP was significantly higher in the DOE than the Control group at 60W, both when expressed in absolute terms and when expressed as a percentage of total $\dot{V}O_2$ (Table 2). RPB at 60W was significantly correlated with the O_2 cost of breathing during eucapnic voluntary hyperpnea ($r^2 = 0.72$, $p < 0.0005$) and with $\dot{V}O_2$RESP at 60W ($r^2 = 0.78$, $p < 0.0001$).

4 Discussion

The results of this study demonstrate that the ventilatory response to mild-to-moderate exercise does not differ between obese women with and without dyspnea on exertion (DOE). Hence, the DOE experienced by this group of women cannot be accounted for by either an exaggerated or a blunted ventilatory response to exercise.

Since the ventilatory response was not disproportionate in the obese subjects with DOE, this would suggest that the perceived effort required to achieve this level of ventilation was disproportionate. The American Thoracic Society's statement on dyspnea (1999) states that 'when ventilatory impedance increases, the level of central respiratory motor output required to achieve a given ventilation rises' and that 'when the respiratory effort expended in breathing is out of proportion to the resulting level of ventilation, dyspnea results.'

Changes in ventilatory impedance can be simulated in normal subjects by imposing external ventilatory resistive loads. A study in competitive male cyclists investigating the effects of respiratory muscle loading and unloading during exercise reported that $\dot{V}O_2$ and RPB were increased with respiratory muscle loading and decreased with unloading, and that these changes in respiratory discomfort and $\dot{V}O_2$ were closely correlated (Harms, Wetter, St Croix, Pegelow and Dempsey 2000). A similar study in normal, untrained subjects found that the addition of increasing

resistive inspiratory loads resulted in a progressive increase in the intensity of breathlessness at any given work rate, accompanied by small increases in $\dot{V}O_2$, consistent with an increasing metabolic load of the inspiratory muscles (El-Manshawi, Killian, Summers and Jones 1986).

In normal individuals, the O_2 uptake of the respiratory muscles is reported to be less than 3% of the total $\dot{V}O_2$ at rest (Robertson, Jr., Foster and Johnson, Jr. 1977a), and to increase exponentially with increases in the work of breathing (Robertson, Jr., Pagel and Johnson, Jr. 1977b). In obese subjects, $\dot{V}O_2$RESP has been found to be increased at rest (Kress, Pohlman, Alverdy and Hall 1999), and with increases in $\dot{V}E$ above baseline (Fritts, Jr., Filler, Fishman and Cournand 1959; Kaufman, Ferguson and Cherniack 1959). Here we report that during exercise $\dot{V}O_2$RESP is increased in obese women with DOE compared with Control obese women and that $\dot{V}O_2$RESP is highly correlated to perceived respiratory discomfort during exercise. This suggests that DOE is associated with an elevated O_2 uptake of the respiratory muscles in obese women.

In obese women with and without DOE, the O_2 cost of breathing is increased above that reported in normal subjects (Cherniack 1959). We believe this is related to the distribution of fat on the chest wall and abdomen. Our working hypothesis is that increased fat on the chest wall and abdomen imparts a mechanical load that requires a greater motor output and greater recruitment of respiratory muscles to achieve a similar ventilatory response to exercise. This results in an increased $\dot{V}O_2$RESP and a greater sensation of effort, which is perceived as respiratory discomfort, or DOE. Further research is required to test various aspects of this hypothesis.

References

American Thoracic Society. (1999) Dyspnea. Mechanisms, assessment, and management: a consensus statement. Am. J. Respir. Crit Care Med. 159, 321–340.

Babb, T.G., Korzick, D., Meador, M., Hodgson, J.L. and Buskirk, E.R. (1991) Ventilatory response of moderately obese women to submaximal exercise. Int. J. Obes. 15, 59–65.

Babb, T.G., Semon, T.L., Comeau, L.A., Schwartz, B. and Chwan, D.R. (2005) Exertional dyspnea in mildly obese women: association with an increased oxygen cost of breathing. 2005 American Thoracic Society meeting abstracts. Proceedings of the American Thoracic Society. Abstract #A72.

Borg, G.A. (1982) Psychophysical bases of perceived exertion. Med. Sci. Sports Exerc. 14, 377–381.

Cherniack, R.M. (1959) The oxygen consumption and efficiency of the respiratory muscles in health and emphysema. J. Clin. Invest. 38, 494–499.

El-Manshawi, A., Killian, K.J., Summers, E. and Jones, N.L. (1986) Breathlessness during exercise with and without resistive loading. J. Appl. Physiol. 61, 896–905.

Fritts, H.W., Jr., Filler, J., Fishman, A.P. and Cournand, A. (1959) The efficiency of ventilation during voluntary hyperpnea: studies in normal subjects and in dyspneic patients with either chronic pulmonary emphysema or obesity. J. Clin. Invest. 38, 1339–1348.

Harms, C.A., Wetter, T.J., St Croix, C.M., Pegelow, D.F. and Dempsey, J.A. (2000) Effects of respiratory muscle work on exercise performance. J.Appl. Physiol. 89, 131–138.

Hulens, M., Vansant, G., Lysens, R., Claessens, A.L. and Muls, E. (2001) Exercise capacity in lean versus obese women. Scand. J. Med. Sci. Sports. 11, 305–309.

Kaufman, B.J., Ferguson, M.H. and Cherniack, R.M. (1959) Hypoventilation in obesity. J. Clin. Invest. 38, 500–507.

Kress, J.P., Pohlman, A.S., Alverdy, J. and Hall, J.B. (1999) The impact of morbid obesity on oxygen cost of breathing (VO(2RESP)) at rest. Am. J. Respir. Crit. Care Med. 160, 883–886.

Ogden, C.L., Carroll, M.D., Curtin, L.R., McDowell, M.A., Tabak, C.J. and Flegal, K.M. (2006) Prevalence of overweight and obesity in the United States, 1999–2004. JAMA 295, 1549–1555.

Robertson, C.H., Jr., Foster, G.H. and Johnson, R.L., Jr. (1977a) The relationship of respiratory failure to the oxygen consumption of, lactate production by and distribution of blood flow among respiratory muscles during increasing inspiratory resistance. J. Clin. Invest. 59, 31–42.

Robertson, C.H., Jr., Pagel, M.A. and Johnson, R.L., Jr. (1977b) The distribution of blood flow, oxygen consumption and work output among the respiratory muscles during unobstructed hyperventilation. J. Clin. Invest. 59, 43–50.

Salvadori, A., Fanari, P., Cavestri, R., Mazza, P., Baudo, S. and Longhini, E. (1991) Relationship between body mass and tolerance to physical stress in obese patients. Respiration 58, 311–315.

Author Index

I

N

Subject Index